

# IDENTIFICATION AND DELINEATION OF MINING INDUCED SEISMIC RESPONSES

*By*

Kyle R. Woodward

*A thesis submitted for the degree of:*

DOCTOR OF PHILOSOPHY

*School of Civil and Resource Engineering*

*University of Western Australia*

2015



## **Abstract**

The phenomenon of seismicity is observed in many hard rock underground mines around the world. Seismic events pose a significant geotechnical challenge due to their potential to damage underground excavations. This translates to a risk to mining personnel, equipment, and infrastructure. The management of seismic hazard is an essential component in minimising the political, social, and economic risks associated with the mining industry.

The effective management of seismic hazard is underpinned by a sufficient understanding of the magnitude, spatial, and temporal characteristics of seismicity. Characteristics of seismicity are controlled by causative seismic source mechanisms that are associated with features such as rock mass stress and strength, excavations, geology, and geological features. The spatial dependency of seismic source mechanisms results in the spatial clustering of seismicity. The temporal traits of seismicity are ambiguously related to causative seismic source mechanisms. Temporal characteristics of event occurrence are generalised as time-dependent (seismic responses) or time-independent (background seismicity). Seismic responses are commonly observed following large events or routine blasting and comprise of time-dependent events that are spatially clustered.

The numerous interrelated factors that influence seismic event occurrence make it difficult to establish cause and effect correlations, and increase the importance of being able to quantify the spatial and temporal characteristics of seismicity. Developing the methods used to assess seismic characteristics improves the management of seismic hazard through an enhanced understanding of rock mass responses to mining and enables the quantification of seismic hazard. This thesis contributes a method of assessing spatial and temporal characteristics of seismicity through the identification and delineation of individual seismic responses. The methods and concepts established in this thesis enable improvements to be made to the management of seismic hazard.

## *Abstract*

Given the challenges of this type of analysis for mining seismicity, previous studies do not offer a comprehensive approach to identifying and delineating responses. Mining specific challenges require consideration to the following aspects:

- The spatial and temporal characteristics of seismicity must be considered independently of magnitude to ensure that the assessment of responses to blasting are not influenced by the chance occurrence of large events;
- The need to account for the superimposition of responses in space and/or time resulting from multiple routine blasts and responses to large seismic events;
- Response identification and delineation should perform consistently for a range of spatial and temporal event densities associated with various causative seismic source mechanisms; and
- The practical application of the method to a large dataset while minimising subjective decisions.

The development of a comprehensive approach is considered in three parts and focuses on the fundamental questions of identifying and delineating seismic responses while also addressing the challenges associated with a mining environment.

Identification of seismic responses: Where and when do responses occur?

This aspect is addressed through the development of an iterative framework that exploits the spatial and temporal characteristics of mining induced seismicity to identify the time and location of responses. This framework provides a subset of seismic events that are further refined by spatial and temporal modelling.

Spatial delineation of seismic responses: What is the extent of responses in space?

This aspect is addressed by modifying an established density-based clustering method. Modifications overcome the known shortcomings associated with existing clustering methods by utilising the initial information provided by iterative seismic response identification. The procedure developed within this thesis creates a subset of spatially related seismic events that are associated with the response identified by the iterative framework. Internal and external validation of this clustering procedure is achieved by assessing synthetic datasets with known spatial distributions. External validation is applied to the clustering of real data to optimise spatial clustering outcomes.

Temporal delineation of seismic responses: When do responses start and finish?

This aspect is addressed by developing a method to temporally delineate and quantify seismic responses from a subset of spatially clustered seismicity. This methodology employs a unique

### *Abstract*

approach to applying the Modified Omori Law that is specifically tailored to address the challenges associated with mining induced seismicity. A single quantitative metric is developed to combine modelling statistics that incorporate the additional information required to meet delineation objectives. This approach temporally delineates an optimal modelling interval by assessing the quantitative metric.

The developed iterative method is applied to identify and delineate seismic responses for the study of real datasets of mining induced seismicity. The objectives of this thesis are qualitatively evaluated in a number of practically orientated applications. Furthermore, the application of this method enables a number of novel analysis techniques. The application for the iterative method and complementary analysis enable the following case studies:

- Individual cases of seismic responses within the mining environment;
- The spatial and temporal relationship between seismic responses and blasting;
- The temporal evolution of response quantification and response-blasting relationships;
- The quantification of responses with respect to the mining environment; and
- The quantification of temporal changes in seismic hazard.

These case studies illustrate the contributions of this thesis and show the ability of the iterative method to assess seismic responses. The results from the successful application of this method provide insight into rock mechanics and seismic hazard associated with mining.



## **Acknowledgements**

I would like to acknowledge my supervisors, Prof. Yves Potvin and Dr. Johan Wesseloo for their invaluable time, assistance, and advice throughout this thesis. I am grateful for the experience and guidance that has been freely offered throughout my studies. I would like to express additional thanks to Prof. Yves Potvin in his capacity as the director and research coordinator of the ACG, and Dr. Johan Wesseloo as the leader of the Mine Seismicity and Rockburst Risk Management project. The research opportunities I have had at the ACG in the area of mine seismicity have significantly furthered my professional development by providing truly fascinating areas of undergraduate and postgraduate research.

Thanks to all the technical and administrative ACG staff. All assistance has been greatly appreciated, whether a small piece of formatting advice, a stationary order, or a lengthy technical discussion.

I would like to thank Paul Harris in his capacity as a software engineer whom has provided tutorage and support in the fundamentals of programming along with a ‘programmers’ insight into various aspects of this thesis. Often these valuable insights have set me on the right path, or less often, created a tangent path into the research abyss. I am grateful for always learning something valuable along the way!

I would like to extend a heartfelt thanks to my partner Stefania Almonte for her unconditional love and support. I am grateful for the daily things that make sure I remain fed and clothed along with the help, advice, tolerance, and eternal optimism throughout my studies. I would also like to thank family and friends whom have given support and encouragement over the years.

This research has been made possible by the past and present support from the industry. This research is part of the ACG’s Mine Seismicity and Rockburst Risk Management project and is sponsored by the following organisations.

Major project sponsors: BHP Billiton Olympic Dam, BHP Billiton Nickel West, Independence Gold (Lightning Nickel), LKAB (Luossavaara-Kiirunavaara AB), MRIWA (Minerals Research Institute of Western Australia), Perilya Limited, Broken Hill Mine, and Vale Inc.

Minor project sponsors: Agnico-Eagle Canada, BCD Resources (Tasmania Mine), Glencore Copper (Kidd Mine), Glencore Cosmos Nickel Australia, Glencore Nickel Rim South Mine Canada, Gold Fields St Ives Gold Operations, Hecla USA, Kirkland Lake Gold, MMG Golden Grove, Newcrest Mining, and Newmont Asia Pacific.



## Contents

Abstract.....	I
Acknowledgements.....	V
Contents.....	VII
1 Introduction .....	1-13
1.1 Background .....	1-13
1.2 Problem Definition.....	1-14
1.3 Objectives.....	1-15
1.4 Research Methodology.....	1-15
1.5 Organisation.....	1-16
1.6 Significance and Contribution.....	1-17
2 Literature Review .....	2-21
2.1 Introduction .....	2-21
2.2 Spatial Characteristics of Mining Induced Seismicity .....	2-22
2.2.1 Magnitude-Frequency Relationship.....	2-23
2.2.2 Seismic Source Mechanisms .....	2-27
2.3 Temporal Characteristics of Mining Induced Seismicity.....	2-29
2.3.1 Background Seismicity .....	2-31
2.3.2 Seismic Responses .....	2-34
2.4 Assessment of Spatially and Temporally Clustered Seismicity .....	2-40
2.4.1 Informal Assessment Approaches.....	2-47
2.4.2 Event Time and Location Assessment.....	2-48
2.4.3 Metric Assessment Approaches.....	2-49
2.4.4 Formal Models .....	2-60
2.5 Modified Omori Law .....	2-62
2.5.1 Applicability to Seismic Responses to Mining.....	2-64
2.5.2 Parameter Determination by Maximum Likelihood Estimation .....	2-67

## *Contents*

2.5.3	Suitability of Fit by Assessment of the Anderson-Darling Statistic .....	2-68
2.5.4	p-Parameter .....	2-69
2.5.5	K-Parameter .....	2-70
2.5.6	c-Parameter .....	2-72
2.5.7	Modelling Time Interval .....	2-74
2.6	Literature Review Conclusions .....	2-79
2.6.1	Spatial Characteristics of Mining Induced Seismicity .....	2-79
2.6.2	Temporal Characteristics of Mining Induced Seismicity .....	2-80
2.6.3	Analysis of Spatially and Temporally Clustered Seismicity .....	2-81
2.6.4	Modified Omori Law .....	2-82
2.7	Specific Issues Addressed in this Thesis .....	2-83
3	Iterative Approach to the Identification of Mining Induced Seismic Responses .....	3-85
3.1	Chapter Overview .....	3-85
3.2	Introduction .....	3-86
3.3	Seismic Response Identification using Spatial and Temporal Windows .....	3-89
3.4	Iterative Method for Seismic Response Identification .....	3-94
3.4.1	Practical Implementation .....	3-95
3.4.2	Iterative Mining Induced Seismic Response Identification .....	3-99
3.5	Considerations and Limitations of User Defined Parameters .....	3-101
3.5.1	Spatial Window .....	3-102
3.5.2	Temporal Window .....	3-104
3.5.3	Lower Count Threshold .....	3-106
3.5.4	Temporal Modelling Window .....	3-111
3.5.5	Response Scale Sets .....	3-114
3.6	Chapter Summary .....	3-118
3.6.1	Seismic Response Identification using Spatial and Temporal Windows .....	3-118
3.6.2	Iterative Method for Seismic Response Identification .....	3-118
3.6.3	Considerations and Limitations of User Defined Parameters .....	3-119

## Contents

4	Spatial Delineation of Mining Induced Seismic Responses.....	4-123
4.1	Chapter Overview .....	4-123
4.2	Introduction .....	4-124
4.3	Density-Based Clustering applied to Mining Induced Seismicity.....	4-129
4.3.1	Integration of Spatial Delineation and Seismic Response Identification.....	4-130
4.3.2	Density clustering core event tolerance .....	4-131
4.4	Spatial Clustering Procedure.....	4-134
4.5	Spatial Clustering Validation and Performance .....	4-139
4.5.1	Single Response Scenario.....	4-141
4.5.2	Multiple Response Scenarios .....	4-142
4.5.3	A Range of Multiple Response Scenarios.....	4-143
4.5.4	External Performance Measures.....	4-148
4.5.5	Internal Performance Measures .....	4-151
4.6	Base Cases for Mining Induced Seismic Response.....	4-158
4.6.1	Synthetic Responses .....	4-158
4.6.2	Mining Induced Responses .....	4-163
4.7	Chapter Summary .....	4-173
4.7.1	Density-Based Clustering Applied to Mining Induced Seismicity .....	4-173
4.7.2	Spatial Clustering Procedure.....	4-174
4.7.3	Spatial Clustering Validation and Performance .....	4-175
4.7.4	Base Cases for Mining Induced Seismic Response.....	4-177
5	Temporal Delineation of Mining Induced Seismic Responses .....	5-179
5.1	Chapter Overview .....	5-179
5.2	Introduction .....	5-180
5.3	Temporal Modelling of Mining Induced Seismic Responses .....	5-182
5.4	Modelling Mining Induced Seismic Response with the MOL.....	5-184
5.5	Critical Assessment of the Four MOL Modelling Models.....	5-188
5.5.1	Simple Seismic Response .....	5-191

## Contents

5.5.2	Seismic Response with Early Variation .....	5-195
5.5.3	Late Superimposed Seismic Responses .....	5-198
5.5.4	Early Superimposed Seismic Responses .....	5-202
5.5.5	Selecting the Optimal MOL Modelling Mode for Mining Induced Responses.....	5-206
5.6	Parametric and Statistical Selection of Modelling Interval.....	5-206
5.6.1	Relevant Parametric and Statistical Measures .....	5-207
5.6.2	Weighting of Parametric and Statistical Measures.....	5-208
5.7	Evaluation of the Weighted MLE Metric.....	5-212
5.7.1	Simple Seismic Response .....	5-212
5.7.2	Seismic Response with Early Variation .....	5-217
5.7.3	Late Superimposed Responses .....	5-222
5.7.4	Early Superimposed Responses .....	5-228
5.8	Iterative Functionality of Temporal Modelling .....	5-234
5.9	Performance Evaluation of Temporal Quantification and Delineation .....	5-237
5.9.1	Scope of Performance Evaluation.....	5-237
5.9.2	Errors Associated with Synthetic Data Generation.....	5-238
5.9.3	Seismic Response with Early Variation .....	5-245
5.9.4	Short Seismic Responses.....	5-251
5.9.5	Inclusion of Time-independent Seismicity .....	5-254
5.10	Chapter Summary .....	5-259
5.10.1	Temporal Modelling of Mining Induced Seismic Responses .....	5-259
5.10.2	Modelling Mining Induced Seismic Response with the MOL.....	5-259
5.10.3	Critical Assessment of the Four MOL Modelling Models.....	5-260
5.10.4	Parametric and Statistical Selection of Modelling Interval.....	5-261
5.10.5	Evaluation of the Weighted MLE Metric.....	5-262
5.10.6	Iterative Functionality of Temporal Modelling .....	5-263
5.10.7	Performance Evaluation of Temporal Quantification and Delineation .....	5-264

## Contents

6	Assessment of Mining Induced Seismic Responses .....	6-267
6.1	Chapter Overview .....	6-267
6.2	Scope of Application .....	6-267
6.3	Seismic Data used for Analysis.....	6-270
6.4	General Application as an Iterative Approach to the Identification and Delineation of Seismic Responses .....	6-271
6.4.1	Seismic Responses to Routine Blasting .....	6-271
6.4.2	Response to a Large Seismic Event .....	6-274
6.4.3	Complex Response to Mining .....	6-280
6.5	Seismic Responses and Blasting.....	6-284
6.5.1	Classification of the Relationship between Seismic Responses and Blasting .....	6-284
6.5.2	Responses Remote from Blasting .....	6-287
6.5.3	Responses Delayed from Blasting .....	6-288
6.5.4	Proportionality of Response Classifications.....	6-290
6.5.5	Temporal Evolution of Response Classifications.....	6-291
6.6	Evolution of Mining Induced Seismic Responses.....	6-293
6.6.1	General Response Assessment .....	6-293
6.6.2	Seismic Response and Undercut Blasting .....	6-294
6.6.3	Quantified Seismic Responses and Blasting Relationship.....	6-298
6.7	Seismic Response Hazard.....	6-303
6.7.1	Determination of Seismic Response Hazard .....	6-303
6.7.2	Retrospective Parameterisation of Responses .....	6-306
6.7.3	Current Seismic Response Hazard .....	6-311
6.8	Chapter Summary .....	6-316
7	Conclusions .....	7-317
8	Recommendations for Future Work .....	8-321
8.1	Recommendations for the Identification and Delineation of Seismic Responses .....	8-321
8.2	General Recommendations .....	8-323

## Contents

8.2.1	Seismic Source Mechanism.....	8-323
8.2.2	Time-Independent Rates of Seismicity .....	8-324
8.2.3	Comprehensive Seismic Hazard .....	8-326
9	References .....	9-327
10	Appendix .....	10-337
	Appendix A: Generation of Synthetic Seismic Responses .....	10-337
	Appendix B: Applying Hazard to Mining Induced Seismic Responses .....	10-341
	Appendix C: Complete List of Conclusions.....	10-343
	Chapter 2: Literature Review .....	10-343
	Chapter 3: Iterative Approach to the Identification of Mining Induced Seismic Responses .....	10-348
	Chapter 4: Spatial Delineation of Mining Induced Seismic Responses.....	10-351
	Chapter 5: Temporal Delineation of Mining Induced Seismic Responses .....	10-354
	Chapter 6: Assessment of Mining Induced Seismic Responses .....	10-360

# 1 Introduction

## 1.1 Background

The occurrence of seismicity is a historical and current geotechnical challenge affecting many hard rock mines around the world. This phenomenon can cause damage to underground excavations and can have a significant impact on both mining productivity and the health and safety of personnel (Cook 1976; Ortlepp 2005).

The spatial, temporal, and magnitude characteristics of mining induced seismicity are dependent on spatially controlled causative seismic source mechanisms with respect to features such as excavations and geology (Hasegawa, Wetmiller & Gendzwill 1989; Trifu & Urbancic 1996; Ortlepp 1999; Hudyma, Heal & Mikula 2003; Reimnitz 2004). The analysis of spatially clustered seismicity can improve insight into the rock mass response to mining and the sources of seismicity that underpin the seismic risk posed to mining operations (Hudyma, Heal & Mikula 2003).

The temporal characteristics of seismic events are challenging to evaluate and are utilised to provide insight into mining induced seismicity (Hudyma 2008). Temporal occurrence can be influenced by many factors that contribute to excitation and relaxation of rock mass processes (Mendecki & Lynch 2004). Furthermore, the interplay between the numerous factors that influence seismic event occurrence make it difficult to establish correlations between seismicity and underlying physical processes (Mendecki 2005). The temporal characteristics of mining induced seismicity can be considered as two broad categories. Firstly, strongly spatially clustered, time-dependent seismic responses, and secondly, weakly clustered, time-independent (or background) seismicity. The temporal traits of mining induced seismicity are linked to spatially dependent sources of seismicity (Hudyma 2008; Plenkens et al. 2010).

This thesis defines a seismic response as seismic events that are clustered in space and time. Events associated with a seismic response are observed to follow a consistent spatial distribution and a decaying rate of temporal occurrence.

Seismic responses are comparable to characteristics of earthquake mainshock-aftershock responses and are commonly observed following large events (Hills & Penney 2008; Kgarume, Spottiswoode & Durrheim 2010a; Vallejos & McKinnon 2010a), or after routine blasting within the mining environment (Heal 2007; Penney 2011). Literature indicates that the characteristics of seismic responses may vary significantly and are tenuously related to factors that influence sources of seismicity (Malek & Leslie 2006; Heal 2007; Eremenko et al. 2009; Kgarume, Spottiswoode & Durrheim 2010b; Penney 2011; Vallejos & McKinnon 2011).

Understanding the spatial and temporal characteristics of seismicity is essential as seismic responses and time-independent seismicity contribute to the characteristics of seismic hazard (Hudyma 2008; Cho et al. 2010). The spatial and temporal characteristics of seismic hazard ultimately impacts on the effectiveness of methods used to reduce seismic risks associated with different sources of seismicity, e.g., mine planning, dynamic ground support, and limiting workforce exposure (Hudyma 2008; Potvin 2009). The management of seismic hazard necessitates the assessment of spatial and temporal characteristics of seismicity and is the main motivation to identify and delineate individual responses.

## **1.2 Problem Definition**

The studies of mainshock-aftershock earthquake sequences and mining induced seismic responses are fundamentally similar when attempting to identify and delineate spatially and temporally clustered seismic events. Studies may utilise one or a combination of approaches that can be classified as informal, time and location, metric, or formal. The classification of these approaches and the related literature from each of these categories are discussed in Chapter 2.

A wide range of approaches is explored in the study of time-dependent earthquakes, many of which make assumptions that are not transferrable to mining induced seismicity. For mining induced seismicity, spatial and temporal characteristics are generally studied independently with limited attempts to quantify responses. These studies typically focus on determining appropriate criteria for limiting workforce exposure to time-dependent seismic hazard (re-entry protocols).

Due to the characteristics of mining induced seismicity, a comprehensive response identification and delineation method must consider the following challenges:

- The spatial and temporal characteristics of seismicity must be considered independently of magnitude to ensure that the assessment of responses to blasting are not influenced by the chance occurrence of large events;
- The need to account for the superimposition of responses in space and/or time, resulting from multiple routine blasts and responses to large seismic events;
- Methods for response identification and delineation should perform consistently for a range of spatial and temporal event densities; and
- The practical application to large datasets while minimising subjective decisions.

Furthermore, a comprehensive method must be able to address three fundamental questions for mining induced seismic responses:

1. Identification of seismic responses: Where and when do responses occur?
2. Spatial delineation of related seismicity: What is the extent of responses in space?
3. Temporal delineation of related seismicity: When do responses start and finish?

There is no comprehensive method for the spatial and temporal identification and delineation of individual mining induced seismic responses, or a transferrable counterpart from the study of earthquakes.

### **1.3 Objectives**

The objective of this thesis is to develop a comprehensive method that is capable of identifying and delineating mining induced seismic responses in space and time while taking into account the characteristics of seismicity that arise due to a range of rock mass failure processes caused by routine mining activities. The problem definition in Section 1.2 provides a list of considerations and fundamental questions that a comprehensive seismic response identification and delineation method must address. This method will define the time and location along with the spatial and temporal extents of seismic responses. Furthermore, this method aims to be generally applicable to datasets of seismic events associated with a range of mining environments.

### **1.4 Research Methodology**

The literature review focuses on developing an understanding of the spatial and temporal characteristics of mining induced seismicity. The review establishes the fundamental nature of time-dependent event occurrence that must be identified and delineated. To establish current practices, a comprehensive review of previous methods used to assess mining induced responses was conducted. The review is also extended to the study of earthquakes due to limited literature related to mining and the inherent parallels in the study of naturally occurring seismic responses. Due to the widespread application to the study of earthquakes, an exhaustive review of the application of the Modified Omori Law (MOL) is not practicable. As a result, the scope of the review was limited to the implications for the assessment of the temporal characteristics of seismic responses, the law's applicability to mining induced responses, existing approaches to modelling, and associated parameters.

The development of an appropriate method to assess seismic responses is considered in three parts. This segmented approach allows specific spatial and temporal components to be developed and for challenges to be clearly addressed before being integrated into a general approach. Individual chapters are related to the fundamental questions concerning seismic responses that address individual characteristics of mining induced seismicity:

- Chapter 3 addresses identification: Where and when do responses occur?
- Chapter 4 addresses spatial delineation: What is the extent of responses in space?
- Chapter 5 addresses temporal delineation: When do responses start and finish?

Chapter 6 applies the method to identify and delineate seismic responses to the study of real datasets of mining induced seismicity. The performance of the method in a number of typical applications is qualitatively evaluated against the objectives presented in Section 1.3. Furthermore, this chapter highlights the contribution of the method by assessing seismic responses using the analysis techniques enabled by this thesis. While the scope of the case studies is limited by the objectives of this thesis, these examples provide a context for this thesis' conclusions and recommendations for future work.

## **1.5 Organisation**

This thesis is organised into eight main chapters, references and two appendices. **Figure 1** illustrates the general flow of concepts within this thesis. Specifically shown are the sections of the reviewed literature utilised by Chapters 3, 4, and 5 along with the structure of these chapters within the assessment of responses.

Chapter 1 serves as an introduction to spatially and temporally clustered seismicity for underground hard rock mining. The chapter provides a definition of the problem, thesis objectives, research method, and organisation of the thesis. Additionally, this chapter summarises the significance and contribution of this thesis.

Chapter 2 examines the literature associated with the characteristics and assessment of mining induced seismicity clustered in space and time. This review establishes the motivation to assess seismic responses, the shortcomings of current methods, and the issues to be addressed within this thesis.

Chapter 3 establishes an iterative framework for the identification and delineation of seismic responses that is suitable for the challenges associated with the mining environment. This chapter establishes the requirements for the spatial and temporal delineation of seismic responses in the context of an iterative methodology.

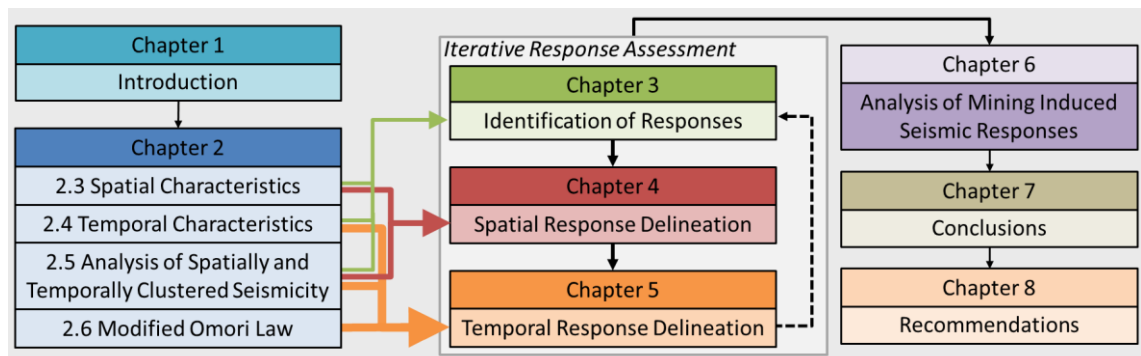
Chapter 4 adapts a density-based clustering method to develop a procedure able to delineate seismicity spatially. This chapter places emphasis on techniques to validate and quantify the performance of spatial clustering.

Chapter 5 is a detailed investigation of previous implementations of the established MOL. Based on the context of mining induced seismicity, the optimal implementation is established and a metric is developed to temporally delineate and quantify seismic responses.

Chapter 6 applies the iterative identification and delineation method to case studies of mining induced seismic responses. This chapter provides context for the outcomes and contributions of this thesis through the assessment of case studies that specifically examine the relationship between seismic responses and blasting.

Chapter 7 draws conclusions from the work presented within this thesis.

Chapter 8 proposes specific and general recommendations for future work.



**Figure 1** The organisation of the eight main chapters of the thesis.

## 1.6 Significance and Contribution

This thesis is significant due to the implications that seismicity has for mining operations around the world. The underlying motivation for this research is the potential for mining induced seismicity to be detrimental to political, social, and economic aspects of mining. This thesis focuses on the development of conceptual and practical approaches to the assessment of seismic responses that are associated with time-dependent rock mass failure processes induced by mining. This work is significant as it furthers the state-of-the-art assessment of seismic responses that enables an improved understanding of fundamental rock mechanics and seismic hazard associated with mining induced seismicity. These techniques are significant as they minimise subjectivity and increase the transparency of engineering decisions, whilst also improving the management of seismic hazard.

This thesis makes contributions through the review of literature, the development of an innovative method to assess seismic responses, and the practical application of the method to

provide insight into rock mechanics and seismic hazard associated with mining induced seismicity.

The literature review (Chapter 2) contributes a valuable summary of published work within the context of the problem defined by this thesis. Minor contributions are made by summarising the foundation of spatial and temporal characteristics of mining induced seismicity. A substantial contribution is the comprehensive review of the analysis techniques used to study mining induced seismic responses. This contribution is enriched by the review of selected studies from the field of earthquake seismology. An additional significant contribution is made by the detailed review of the MOL and focuses on the interpretation of its parameters, methods of implementation, and applicability to time-dependent mining induced seismicity. This review is also supplemented by relevant studies from the field of earthquake seismology. The most significant contribution of this chapter is the establishment of the fundamental concepts for assessing seismic responses given the inherent challenges associated with the mining environment and the shortcomings of existing methods.

The main contribution of this thesis is the development of a method for the identification and delineation of mining induced seismic responses and is made by the work presented in Chapters 3, 4, and 5, although, these chapters also result in additional contributions.

Chapter 3 contributes an iterative framework that exploits the spatial and temporal characteristics of mining induced seismicity to identify the time and location of responses within the mining environment. This framework provides a subset of seismic events that are further refined by spatial and temporal modelling. Delineation methods are modular components and in addition to achieving thesis objectives, this allows Chapter 3 to make a further important contribution by providing an interchangeable framework for future developments to spatial and temporal modelling.

Chapter 4 contributes a generalised method for the spatial delineation of mining induced seismic responses. This procedure modifies an established density-based clustering method to overcome the known shortcomings associated with existing methods. Shortcomings are addressed within the context of mining induced seismicity by utilising initial information provided by the iterative framework. The developed procedure creates a subset of spatially related seismic events that are associated with the response identified by the iterative framework. Chapter 4 makes additional contributions through the extensive work that validates this procedure and establishes a method to optimise clustering parameters objectively. These contributions pertain to the generation of synthetic datasets with known spatial distributions, the internal and external validation of clustering synthetic data, and the external validation of clustering real data to optimise outcomes.

Chapter 5 contributes a method to temporally delineate and quantify seismic responses from a subset of spatially clustered seismicity. This methodology employs a unique approach to applying the MOL that is specifically tailored to address the challenges associated with mining induced seismicity. The approach is a significant contribution for the study of time-dependent seismicity as it addresses challenges of selecting an appropriate modelling interval in addition to practically applying the MOL. This approach optimises the modelling interval by assessing the number of events and modelling statistics. Furthermore, a piecewise linear weighting function is applied to each modelling statistic to incorporate additional information required to meet thesis objectives, before being combined by a multiplicative function into a single quantitative metric. Additional contributions are made through the development of methods used to generate synthetic data to test temporal modelling under a number of scenarios relevant to the mining environment. These contributions pertain to methods of displaying modelling results, methods controlling the randomness associated with synthetic data to achieve effective testing, and quantifying errors associated with scenarios of mining induced responses.

Chapter 6 provides case studies that apply the iterative method for the identification and delineation of seismic responses. These case studies highlight the primary contribution of this thesis and make additional contributions by developing complementary assessment techniques that utilise results provided by the iterative method. Additional contributions are made by developing an objective understanding of the rock mass response to mining and associated seismic hazard in space and time. In summary, contributions are made by enabling and presenting the following case study assessments:

- Individual cases of seismicity within the mining environment;
- The spatial and temporal relationship between seismic responses and blasting;
- The temporal evolution of response quantification and response-blasting relationships;
- The quantification of responses with respect to the mining environment; and
- The quantification of seismic hazard.



## 2 Literature Review

### 2.1 Introduction

The inherent economic incentives of mining deeper deposits drives the need for the optimal management of geotechnical complexities associated with mining under high stress conditions. The occurrence of seismicity is one of these complexities and is a phenomenon that may significantly impact mining productivity and the safety of underground personnel (Cook 1976; Ortlepp 2005). Mining induced seismicity is defined by Cook (1976) as:

*“The incidence of seismic events caused by rock movements or failures resulting from changes in the state of stress in the rock near mine excavations brought about by the presence of those excavations.”*

Mining induced seismicity is experienced in a large number of underground operations around the world. Some selected examples of mining operations and regions where seismicity has influenced operations include:

- Australia - Beaconsfield (Hills & Penney 2008), Ridgeway (Hudyma & Potvin 2008), Mount Isa, Broken Hill and Northparkes (Ortlepp 2005), the Kalgoorlie district including Kanowna Belle (Varden & Esterhuizen 2012), Long Shaft (Sweby 2002), and Mount Charlotte (Hudyma, Mikula & Owen 2002);
- Canada - Kirkland Lake, Red Lake, Elliot Lake (Hedley & Udd 1989; Morrison, Blake & Hedley 2002), La Ronde (Heal, Hudyma & Vezina 2005), and numerous mines situated in the Sudbury basin (Hedley & Udd 1989; Larsson 2004);
- Chile - El Teniente (Dunlop & Gaete 2001);
- China - Twenty metallic and resources mines, mostly in Eastern China between Heilongjiang and Yunnan provinces (Li, Cai & Cai 2007);
- India - Kolar gold mining region (Arora et al. 2001);
- Indonesia - Big Gossan Mine (Arbi et al. 2012);
- Poland - Rudna and Mysłowic (Larsson 2004);
- Russia - Tashtagol mining area (Eremenko et al. 2009);

- South Africa - Numerous mines in the Witwatersrand, Klerksdorp, Carletonville, and Free State regions (Gibowicz 1990);
- Sweden - Kiirunavaara, Malmberget, and Kristineberg (Larsson 2004); and
- USA - Prominently the Coeur d'Alene district (Ortlepp 2005).

Mining induced seismicity exhibits spatial and temporal variation within any particular mine due to the varying contribution and complex interplay between the factors that contribute to an induced seismic response (Hudyma 2008). Furthermore, these contributing factors can vary significantly depending on the mining environment and include geology, geological structures, mining method, mining sequence, *in situ* stresses, and mining induced stresses. The literature discussing mining induced seismicity is reviewed with respect to the spatial and temporal characteristics of sources of seismicity that have been observed for a range of mining environments.

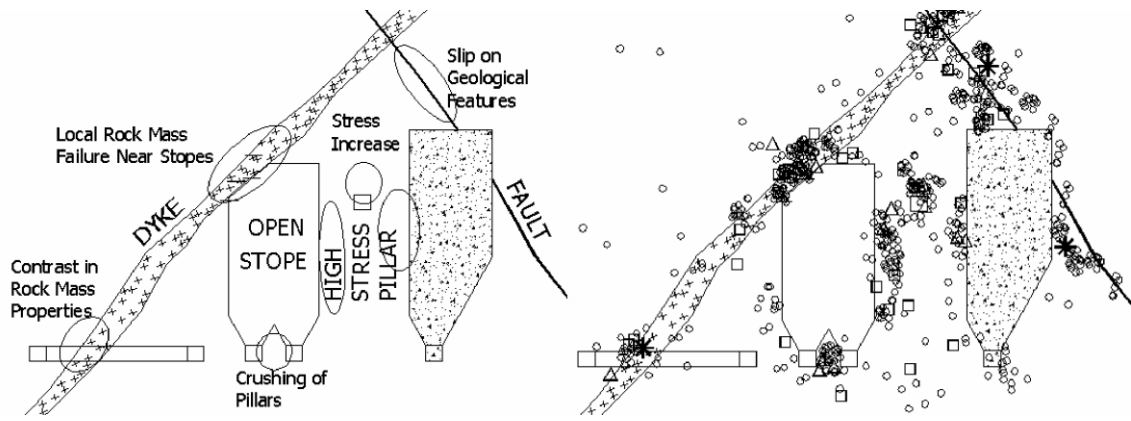
## 2.2 Spatial Characteristics of Mining Induced Seismicity

The general spatial characteristics of mining induced seismicity are controlled by the factors that influence the rock mass failure process. The mining induced rock mass failure manifests as a source of seismicity that generates a number of events over a range of magnitudes (Hudyma & Potvin 2010).

Multiple sources of seismicity may exist in close spatial proximity to mining excavations that contribute to an overall spatial seismic response to mining (Hudyma, Heal & Mikula 2003).

**Figure 2** shows a hypothetical open stoping operation that may experience seismicity generated by:

- Contrast in rock mass properties;
- Local rock mass failure near stopes;
- Crushing of pillars;
- Stress increase in pillars; and
- Slip on geological features.



**Figure 2** Hypothetic open stope mining environment showing sources of seismicity (left) and seismicity typically associated with these sources (right) (Hudyma, Heal & Mikula 2003).

Seismic source mechanisms can be determined by direct waveform techniques (moment tensor inversions and first motion analysis) along with inferred techniques. Direct waveform techniques are not applicable to a significant number of mines due to the high seismic monitoring resolution requirements needed to provide consistent solutions. As a result, this literature review focuses on broadly applicable inferred techniques (Hudyma 2008).

Inferred techniques investigate source mechanisms by statistically assessing various seismic event parameters for large quantities of seismic data. Confidence in characterising sources of seismicity is established by the implementation of complementing assessment techniques (Hudyma 2008). Inferred techniques require the selection of appropriate subsets of seismicity with the superimposition of multiple, contrasting source mechanisms indicated from bi and multi-nodal seismic relationships (Kwiattek 2004).

### 2.2.1 Magnitude-Frequency Relationship

The magnitude-frequency relationship is applied as an inferred technique to characterise distinct sources of seismicity. The first power-law relation for earthquake amplitudes was published by Ishimoto and Iida (1939). With the advent of consistent quantification of an earthquake's magnitude, Gutenberg and Richter (1944) suggested that the frequency of seismic event occurrence and the magnitude of seismic events follows a power-law relationship (**Equation 1** logarithmic form) and (**Equation 2** exponential form).

$$\log_{10}(N_M) = a - bM \quad \text{Equation 1}$$

And;

$$N_M = 10^{a-bM} \quad \text{Equation 2}$$

Where;

$N_M$ : Number of events having magnitude( $M$ ) or greater

$M$ : Event magnitude

$a, b$ : Constants

Kulhanek (2005) discussed the practical requirements to consistently evaluate the magnitude-frequency relationship in the context of the study of earthquakes:

- The dataset should comprise of events observed from a consistent monitoring period evaluated in uniform magnitudes scales and consistent observations over several orders of magnitudes;
- Seismicity above the magnitude of completeness should be used in the estimation of b-value and a/b estimates;
- The time period under consideration must be comparable or greater than the return period of the largest expected event;
- Geographic sub-regions should be treated separately; and
- Dataset should be free from foreshocks and aftershocks associated with large events.

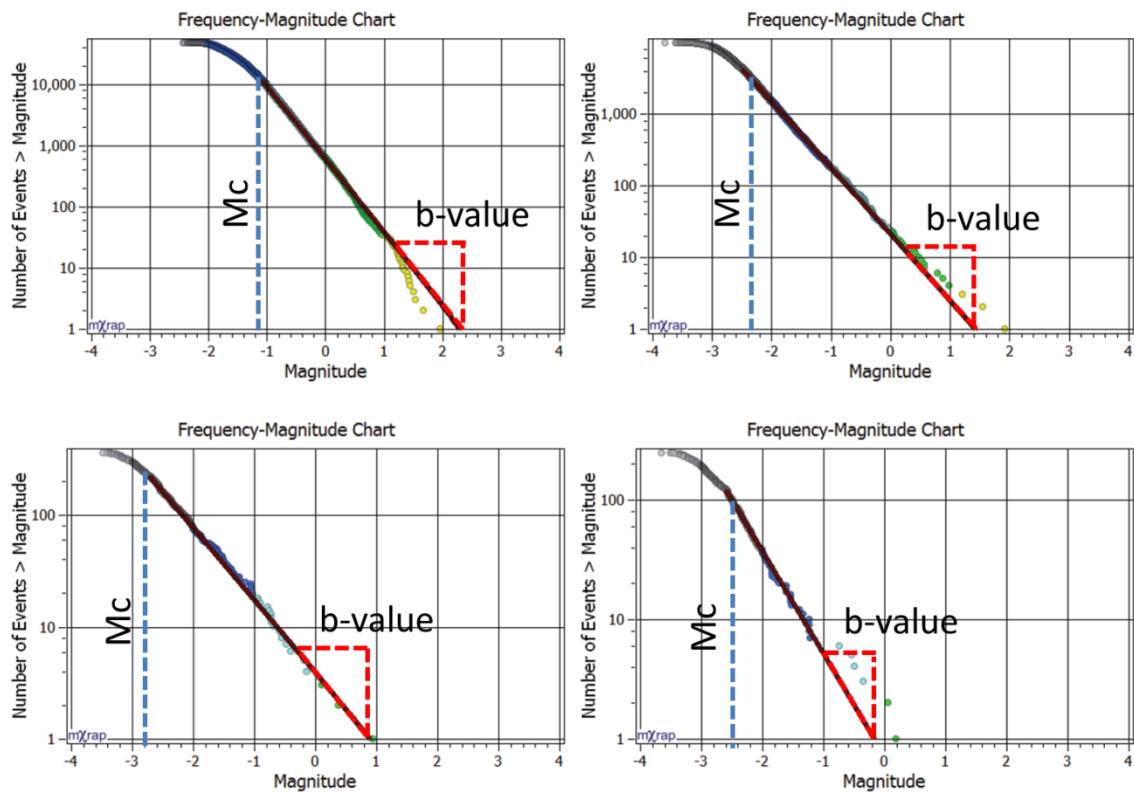
These points are generally applicable to mining induced seismicity. The delineation of geographic sub-regions and time-dependent seismicity is synonymous with the selection of seismicity that is self-similar in nature and is intrinsically linked to spatially and temporally controlled sources (Wesseloo 2014). Hudyma (2008) stated that the assessment of the magnitude frequency-relationship is an inferred technique and requires a significant amount of data before being reliable. He further discussed the potential for inconclusive analysis using this relationship if multiple sources of seismicity are considered in one population. This discussion reflects the requirements previously outlined by Kulhanek (2005).

The magnitude-frequency relationship is widely used in the investigation of earthquakes occurrence, e.g., identifying active magma bodies, spatial variation in tectonics, stress conditions, and material properties. Furthermore, this relationship is fundamental to the forecasting earthquake hazard (Reasenberg & Jones 1989; Utsu 1999; Wiemer & Wyss 2002). This relationship is also widely accepted and applied to the study of mining induced seismicity (Gibowicz & Kijko 1994; Mendecki, van Aswegen & Mountfort 1999; Gibowicz & Lasocki 2001;

Hudyma 2008) and plays an important role in the assessment of the rock mass response to mining and hazard assessment (Wesseloo 2014).

Two statistical properties of the power-law relationship are typically evaluated for mining induced seismicity (**Figure 3**):

- The diminished frequency of smaller events indicates the lower boundary of a complete dataset (blue dashed line). This is expressed by the lowest magnitude that has been reliably measured by the seismic monitoring system ( $M_c$ ); and
- The gradient of the magnitude-frequency distribution is given by the b-value and is typically related to seismic source mechanism (red dashed lines). The b-value is the relative proportion of smaller magnitude events to larger magnitude events.



**Figure 3** Four examples of magnitude-frequency relationships fitted to seismic datasets. Blue dashed lines highlight the magnitude completeness ( $M_c$ ), Red dashed lines highlights the gradient of magnitude-frequency relationship (b-value). Redrawn from Wesseloo (2014) .

The study of earthquakes established evidence that b-value is a function of material properties and stress conditions. The b-value quantifies the mean event magnitude of the magnitude-frequency distribution and has been assumed to be proportional to the mean crack length that initiates a seismic event (Wyss et al., 1997). The foundation of the current interpretation of b-value is based on the laboratory rock sample testing. While Mogi (1962)

showed that increasing heterogeneities resulted in higher b-values, Scholz (1968) suggested that the stress state plays a more significant role than rock mass properties. A number of studies have indicated that higher stress conditions result in lower b-values (Scholz 1968; Wyss 1973; Urbancic et al. 1992; Wyss, Shimazaki & Wiemer 1997). Moreover, seismicity generated from non-creeping fault zones has been related to the dimension of the fault and lower b-values, however, earthquake source length does not control the magnitude-frequency relationship on creeping fault systems (Amelung & King 1997). Earthquakes associated with volcanic structures have characteristically high b-values that are typically attributed to the increased crack density or increased stress conditions associated with magmatic intrusions (Wyss, Shimazaki & Wiemer 1997; Wiemer, McNutt & Wyss 1998).

Within mining induced seismicity, b-value is accepted to be related to the broad classifications of volumetric and shear rock mass failure mechanisms. High b-values are characteristic of seismicity occurring within a three-dimensional volume, while low b-values are characteristic of planar distributions of seismicity (Legge & Spottiswoode 1987).

In addition to the broad classifications of rock mass failure, the magnitude-frequency relationship has been evaluated for spatially confined sources of seismicity. In conjunction with a number of other inferred seismic analysis techniques, Hudyma (2008) assessed the spatial variation of b-value and characterises typical value ranges for common sources of seismicity:

- Faults (-0.6 to -1.0 M);
- Pillars (  $\approx$ -1 M);
- Stiff dykes (  $\approx$ -1 M);
- Caving(-1.0 to -1.3 M);
- Abutments (-1.1 to -1.3 M); and
- Orepass noise (-1.2 to -1.6 M).

Across a range of mining environments, the magnitude-frequency relationship supports the occurrence of spatially and temporally controlled source mechanisms and quantifies the lower magnitude limit of seismic monitoring.

### 2.2.2 Seismic Source Mechanisms

The terminology used for the discussion of seismic source mechanisms is varied depending of the context of the study. Definitions can be generalised into three categories based on the causative rock mass failure mechanisms (Ryder 1988; Duplancic 2001). These categories are:

1. Volumetric failure: Seismicity from this mechanism results from unstable failure of highly stressed rock near mining excavations, e.g., geometric features including pillars and abutments. This mode of failure may occur if no pre-existing fractures are available for slip. Failure is controlled by the stress and rock strength characteristics.
2. Shear failure: Seismicity from this mechanism results from the creation or continuation of unstable deformation on planes of weakness, e.g., bedding planes, existing shear zones, creation of new ruptures, and geological contacts. This mode of failure is controlled by stress magnitude and orientation with respect to discontinuity geometry and orientation. Failure may occur due to a reduction in minor principal stress, an increase in major principal stress, or a combination of both. Failure may also be induced by reducing effective normal stress or modifying the properties of the discontinuity.
3. Loss of confinement: Failure occurs due to the separation of discontinuities resulting from a reduction in confining stress, e.g., the undercutting a rock mass that caves into a pre-existing excavation. This mode is controlled by the occurrence of discontinuities and stress conditions. This mechanism is typically associated with caving rock mass failure under low stress conditions and is not considered to contribute to seismicity.

A range of studies discuss seismic source mechanisms in more depth with respect to mine excavations, geology, and geological features (Hasegawa, Wetmiller & Gendzwill 1989; Trifu & Urbancic 1996; Ortlepp 1999; Hudyma, Heal & Mikula 2003; Reimnitz 2004). Seismic source mechanisms discussed in this literature include:

- **Faulting:** Tension, normal, thrust, and shallow faulting whereby shear deformation occurs as renewed movement on a plane of weakness (Hasegawa, Wetmiller & Gendzwill 1989; Ortlepp 1999). The faulting mechanism can cause large seismic events as significant volumes of rock deforms relative to other sources mechanisms (Reimnitz 2004). Maximum magnitude seismic events can be in the range of 2.0 to 5.0 M (Hudyma, Heal & Mikula 2003). For this mechanism to occur, shear stress must exceed shear resistance (Ortlepp 1999).
- **Shear rupture:** Violent propagation of a shear fracture through an intact rock mass that results in maximum magnitude seismic events in the range of 2.0 to 3.5 M (Hudyma, Heal & Mikula 2003). For this mechanism to occur, the shear stress must exceed the shear strength of the rock (Ortlepp 1999).
- **Pillar burst:** Convergent forces act on a pillar cause (mostly) implosive rock failure (Hasegawa, Wetmiller & Gendzwill 1989; Ortlepp 1999). Maximum magnitude seismic events can be in the range of 1.0 to 2.5 M (Hudyma, Heal & Mikula 2003). For this mechanism to occur, stress must be greater than the rock mass strength of a destroyed volume (Ortlepp 1999).
- **Buckling:** Outward expulsion of large slabs that pre-exist parallel to the surface of an opening. Maximum magnitude seismic events range from 0 to 1.5 M (Hudyma, Heal & Mikula 2003). Requires a free surface (opening) (Ortlepp 1999).
- **Strain-burst:** Superficial spalling with violent ejection of fragments. Maximum magnitude seismic events are in the range of -0.2 to 0 M (Ortlepp 1999; Hudyma, Heal & Mikula 2003).
- **Collapse:** Rockburst (violent expulsion) or gravity driven collapse of mine ceiling. Gravity driven failure generates minimal seismic energy (Hasegawa, Wetmiller & Gendzwill 1989).
- **Coalescence of fracturing:** Failure of bridges between pre-existing discontinuities cause a coalescence of fracturing and rock mass damage (Trifu & Urbancic 1996).
- **Contrasting rock type:** Seismic events result from contrasting deformation due to a difference in rock mass stiffness (Hudyma, Heal & Mikula 2003).

Complementary discussion by Hudyma, Heal and Mikula (2003) provides an overview of two broad types of seismic occurrence with respect to source mechanisms and causative influences. These are:

- Type A: Seismicity caused by blasting induced stress changes and occurs over a relatively short period following a blast.
- Type B: Seismicity driven by stress changes on geological structures and are influenced by a number of factors that may vary over space and time. These factors include temporal and spatial dependence on blasting, characteristics of the geological feature, hydrology, and stresses.

Hudyma, Heal and Mikula (2003) provided additional context for the analysis of sources of seismicity. They suggested that seismic source characteristics remain consistent over time and develop a history of seismicity prior to the occurrence of large events. The regularity observed in sources of seismicity underpins quantification of the risk that seismicity poses to mining operations. They further discuss the pragmatic benefits of considering spatially clustered seismicity, outlining that considering relatively few significant sources of seismicity simplifies analysis and improves insight into the evolution of seismicity.

### **2.3 Temporal Characteristics of Mining Induced Seismicity**

Hudyma (2008) suggested that while the temporal aspect of seismicity is simple to quantify, this parameter is challenging to utilise and provide insight into mining induced seismicity. In a mining environment, seismicity is influenced by many factors that contribute to the excitation and relaxation rock mass processes (Mendecki & Lynch 2004). The interplay between the numerous factors that influence seismicity ensure that long-term correlations between seismicity and underlying physical processes are difficult to establish (Mendecki 2005).

The temporal characteristics of mining induced seismicity do not strictly fit a stationary or independent process. The lack of suitable mathematical concepts that completely model temporal seismic observations has resulted in a diverse exploration of concepts to model mining induced seismicity, e.g., chaotic dynamics, fluid dynamics, correlation lengths, reaction-diffusion models, and mode-switching models (Gibowicz & Lasocki 2001; Mendecki & Lynch 2004).

Gibowicz and Lasocki (2001) outlined that temporal characteristics of mining induced seismicity are not uniformly distributed in space or time. The temporal traits of mining induced

seismicity are intrinsically linked to the sources of seismicity and, therefore, are spatially dependent.

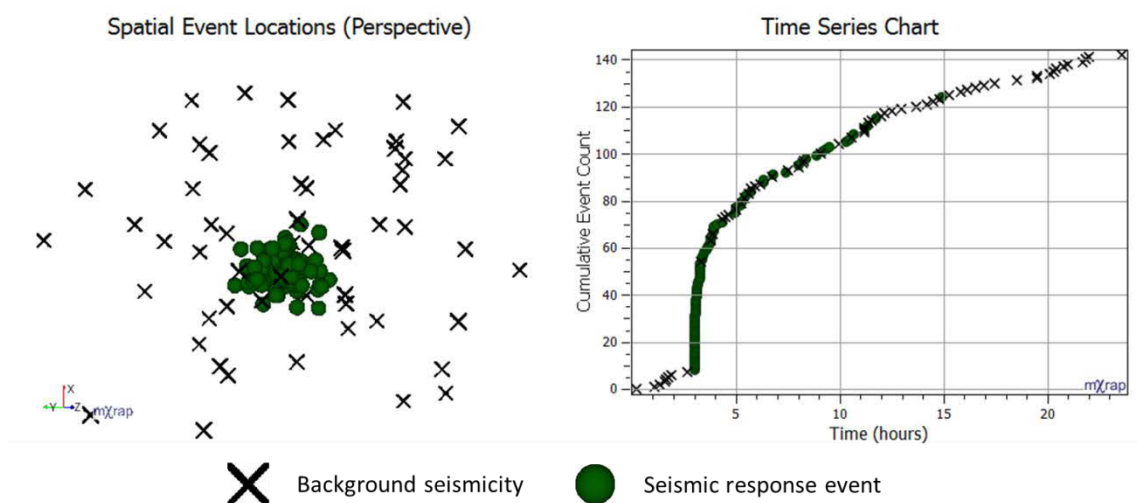
Analogous patterns of seismicity are commonly observed for earthquakes and mining induced seismicity. These patterns can be broadly classified in two categories (Kagan & Jackson 1991; Utsu 2002):

1. Earthquakes may exhibit short-term clustering in space and time. These processes are strongly time-dependent, e.g., seismic swarms and mainshock-aftershock responses.
2. Earthquakes may exhibit long-term weak spatial clustering. These events are approximately independent and uniform in time.

The temporal characteristics of mining induced seismicity are discussed further in the context of two broad categories that also unavoidably consider the spatial traits of seismicity:

1. Seismic Responses: Events are generated by sources of seismicity responding to transient conditions. Seismicity is interrelated throughout space and time.
2. Background or Time-independent Seismicity: Events are generated by sources of seismicity responding to long-term conditions. While events are not interrelated throughout time, spatial occurrence is controlled by the location and extent of the sources of seismicity.

These two broad classifications of seismicity can be synthetically reproduced in space and time. **Figure 4** shows a seismic response clustered in space and with a decaying event rate. This response has been superimposed with background seismicity sparsely located and uniformly distributed throughout time.

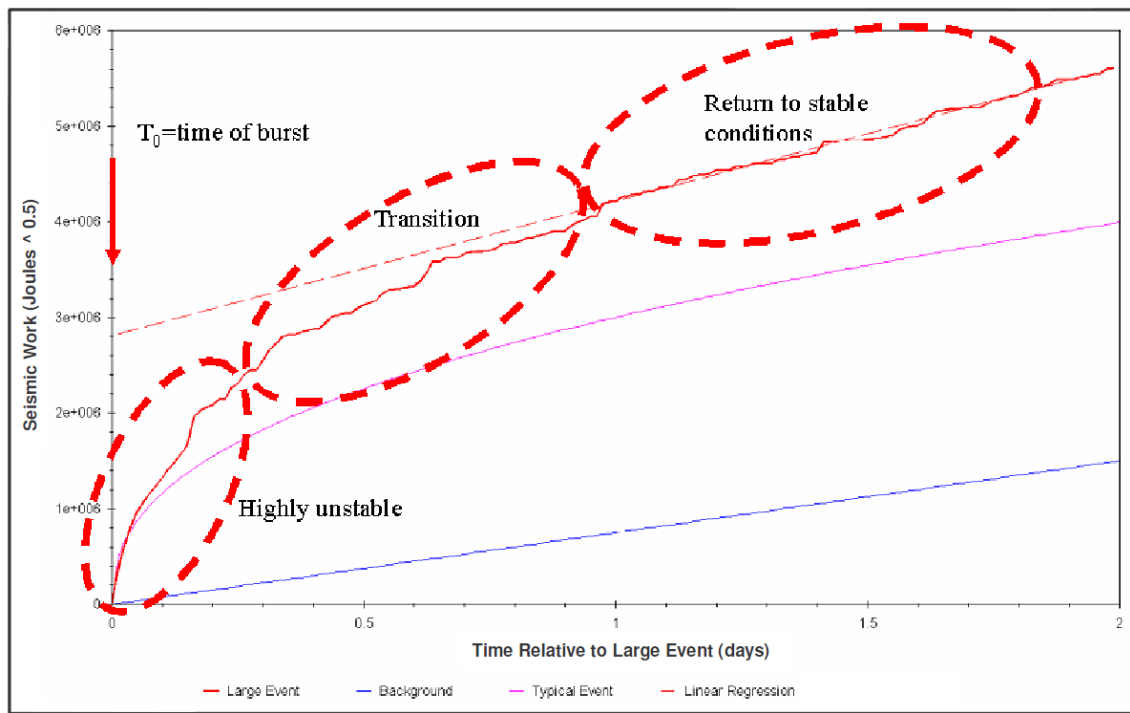


**Figure 4** A hypothetical seismic response superimposed with background seismicity. These events are shown in space by a 3D spatial perspective plot (left) and time series chart (right).

### 2.3.1 Background Seismicity

Although seismicity occurring over longer periods is difficult to clearly define within the mining context, these events are typically referred to as background or time-independent seismicity (Malek & Leslie 2006; Kgarume 2010). Background seismicity represents a portion of seismicity with a consistent rate and is not dependent on temporal influences (Vallejos & McKinnon 2008). While spatial and temporal variation can be observed in background seismicity, this type of seismicity is usually represented by a single rate parameter that is synonymous with a homogeneous Poisson model (Vallejos & McKinnon 2011). Similarly to the study of earthquakes, a homogeneous Poisson model is commonly utilised due to the simplicity of application as opposed to models requiring a larger quantity of data and model parameters (Anagnos & Kiremidjian 1988).

A major motivation for determining background rates of seismicity is to quantify a reference rate for assessing the length of seismic responses subsequently allowing inferences to be drawn concerning of rock mass behaviour. Malek and Leslie (2006) suggested that time-dependent behaviour of rock mass failure is indicative of critical phenomena and is evidence of unstable conditions. They considered seismicity returning to background rates as an indication that a non-critical rock mass response has been re-established. A return to background conditions forms the justification for lifting spatial and temporal restrictions designed to reduce workforce exposure to heightened seismic hazard. These restrictions imposed on the workforce are commonly referred to as re-entry protocols (Vallejos & McKinnon 2008). **Figure 5** provides an example of cumulative seismic work following an individual rockburst relative to a typical response and a predetermined background rate. Three periods have been inferred from the time series analysis: highly unstable, transition, and stable (Malek & Leslie 2006).



**Figure 5** Cumulative seismic work following an individual rockburst (red line) relative to a typical response (pink line) and a predetermined background rate (blue line). Three periods have been inferred from time series analysis: highly unstable, transition, and stable (Malek & Leslie 2006).

An additional motivation for the assessment of background seismicity is to quantify time-independent seismic hazard within the mining environment (Mollison, Sweby & Potvin 2003). Finnie (1999) highlighted that hazard associated with background seismicity may be misrepresented if the majority of events are related to stress changes associated with blasting. Conversely, if seismicity is predominately background events, then this represents seismic hazard that must be managed by using long-term strategies.

Mendecki (2008) asserted that mining induced seismicity is non-stationary over short periods, although, the random superposition of these processes over longer periods may conform to a stationary process. The applicability of assessing background seismicity without consideration to seismic responses depends on the seismic source mechanisms within the mining environment (Hudyma, Beneteau & Potvin 2012), e.g., seismicity caused by a caving rock mass will have a significantly larger background component in comparison to seismicity caused by stress changes from development blasting.

The characterisation of background seismicity without the significant influence of time-dependent responses is typically approached by assessing seismicity outside of blasting times. A common approach to this problem is to assess the cumulative number of events per hour of the day (diurnal chart). Background seismicity is then approximated by seismicity that

occurs outside of hours of the day that contain a high portion of seismic responses (Hudyma 2008; Vallejos & McKinnon 2008; Plenkers et al. 2010). A major consideration for this analysis is which hours contain a high portion of seismic responses. To remove subjectivity from this decision, Vallejos and McKinnon (2008) assumed that background seismicity is normally distributed throughout the day. A statistical method is then used to omit hours of high activity immediately following blasting times. An alternative approach is to assess seismicity following the blast over an extended time interval (Kgarume 2010; Penney 2011). For example, Penney (2011) determined background rates by fitting a linear regression relationship to a linear portion of cumulative event time series.

Additionally, background seismicity can be assessed during periods when no mining activities are undertaken. Background rate estimates without time-dependent processes related to blasting have been calculated during mine shutdowns (Mollison, Sweby & Potvin 2003; Malek & Leslie 2006). Mollison, Sweby and Potvin (2003) assessed seismicity during a care and maintenance period and concluded that a general decrease in seismic event frequency for the shutdown period occurred, with the exception of a caving stope. Malek and Leslie (2006) reiterated that background rates may be controlled by geological features and suggested background rates need to be established based on seismic source mechanism.

Malek and Leslie (2006) also determined rates of background seismicity during periods when mining had stopped. A minimum background seismicity rate was calculated from the shutdown period in addition to a maximum background rate calculated from a diurnal chart approach. To contrast these approaches, the maximum background rate was found to be six times greater than the minimum background rate.

While background seismicity may be approximated by a stationary process, the assessment of background seismicity over long periods will unavoidably include seismic responses and, therefore, will overestimate time-independent seismicity. Current methods used to estimate background rates during mining are likely to provide an over estimate of background seismicity as only the first hours of seismic responses following blasting have been excluded. Estimates of background seismicity will contain the portion of seismic responses that occur outside of these times. Additionally, this analysis will also consider any seismic responses that do not occur with blasting to be background seismicity. The large range in background rate estimates that are dependent on methodology highlights the potential for seismic responses to bias the estimation of background seismicity. Furthermore, the assessment of background rates highlights the influence of sources of seismicity on the variability of temporal characteristics of mining induced seismicity.

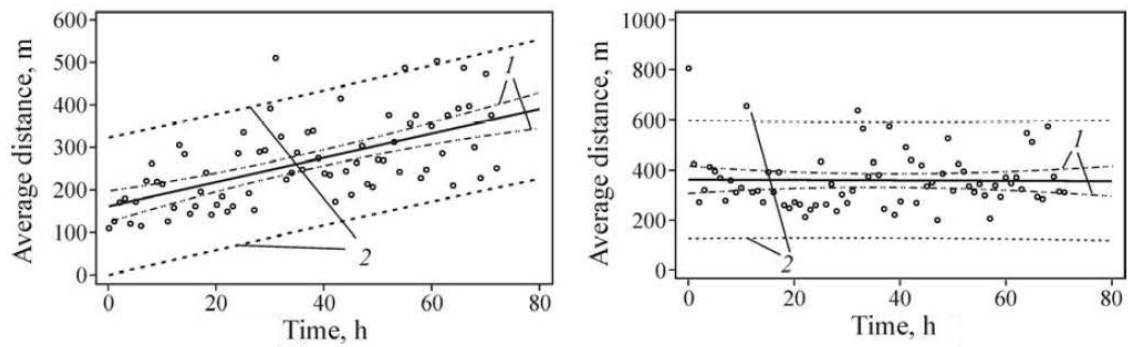
### 2.3.2 Seismic Responses

Seismic responses contribute to the timing, location, and magnitude of seismic hazard and, therefore, establishing an understanding of spatial and temporal characteristics of seismicity is fundamental for the effective management of seismic risk (Hudyma 2008; Cho et al. 2010). Spatial and temporal characteristics of seismic hazard impact on the effectiveness of strategic (e.g., mine planning and ground support) and tactical (e.g., minimisation of workforce exposure) methods used to manage the risk associated with different sources of seismicity (Hudyma 2008; Potvin 2009).

A theoretical foundation for time-dependent seismicity within a mining environment is not definitive and is tentatively addressed in studies. Malek and Leslie (2006) suggested that non-linear behaviour of rock mass failure is indicative of critical phenomena and is evidence of unstable conditions. This concept is discussed in detail by Mendecki and Lynch (2004) who gave a theoretical basis for system excitability as a model of self-organised criticality. It is postulated that the criticality (or state of the rock mass) can be monitored by pulse tests, otherwise described as taps (blasting) or self-taps (seismic events). Furthermore, it is suggested that seismic responses to these tests contain information concerning rock mass stability.

The spatial and temporal characteristics of mining induced seismicity following large events are comparable to characteristics of earthquake mainshock-aftershock responses (Hills & Penney 2008; Kgarume, Spottiswoode & Durrheim 2010a; Vallejos & McKinnon 2010a). Additionally, elevated rates of seismicity are observed after the routine practice of blasting within the mining environment and also exhibit similar characteristics to mainshock-aftershock responses (Heal 2007; Penney 2011).

Eremenko et al. (2009) assessed the relationship between timing and location of seismicity following blasting by considering the seismic response to a number of blasts. The average distance between events and blasting was found for a one-hour period over three days before and after blasting. A positive correlation of 0.61 was found between the distance from events to blasts and time after blasting (**Figure 6** left). There was no significant correlation (-0.01) for the period prior to blasting (**Figure 6** right). This study illustrates the interrelatedness of spatial and temporal clustering aspects of seismic responses within a mining environment.



**Figure 6** The average distance for events from blasting location for three days after blasting (left) and three days before blasting (right) with correlations of 0.61 and -0.01, respectively. Dashed lines indicate the mean distance between events and blasts. Dotted lines indicate the area of spatial distribution (Eremenko et al. 2009).

Plenkens et al. (2010) provided a case study at the South African Mponeng gold mine that substantiated the notion that distinct spatial and temporal responses are driven by specific sources of seismicity. The study evaluated high resolution monitoring of seismicity on a small scale with respect to the influence of geology and mining geometry. Patterns in seismicity were found to be consistent with phenomena observed on larger scale mine-wide monitoring systems. These are:

- Background seismicity: Spatial dispersed and relatively temporally consistent. Limited clustering occurrences were noted;
- Responses to blasting and large events: Strongly spatially clustered and closely related to sources of seismicity; and
- Seismic noise: Seismic waves generated by drilling, debris removal, and ore passes.

Literature indicates that seismic responses to blasting and large events can vary significantly and are at best tenuously related to factors that influence sources of seismicity (Malek & Leslie 2006; Heal 2007; Eremenko et al. 2009; Kgarume, Spottiswoode & Durrheim 2010b; Penney 2011; Vallejos & McKinnon 2011). The reviewed studies suggest that the variability associated with time-dependent seismic responses can be attributed to one or more of the following considerations:

1. Variations in natural and induced influences on seismicity over space and time, e.g., principal stress conditions, mining geometries, rock mass characteristics, and blasting practices etc.;
2. Inability to quantify factors that influence seismicity comprehensively, e.g., the use of depth as a proxy for *in situ* stress conditions and volume mined as a proxy for induced stress conditions; and
3. Insufficient understanding of the space and temporal variation in physical processes that result in seismic responses, e.g., quantifying the space-time relationship of stress transfer resulting in seismicity.

Discussion on the relative contribution of the first and second considerations is limited by the site-specific nature of these factors and falls outside the scope of this work. The third consideration warrants further detailed discussion as the topic is directly relevant to this thesis and is generally applicable to all mining environments.

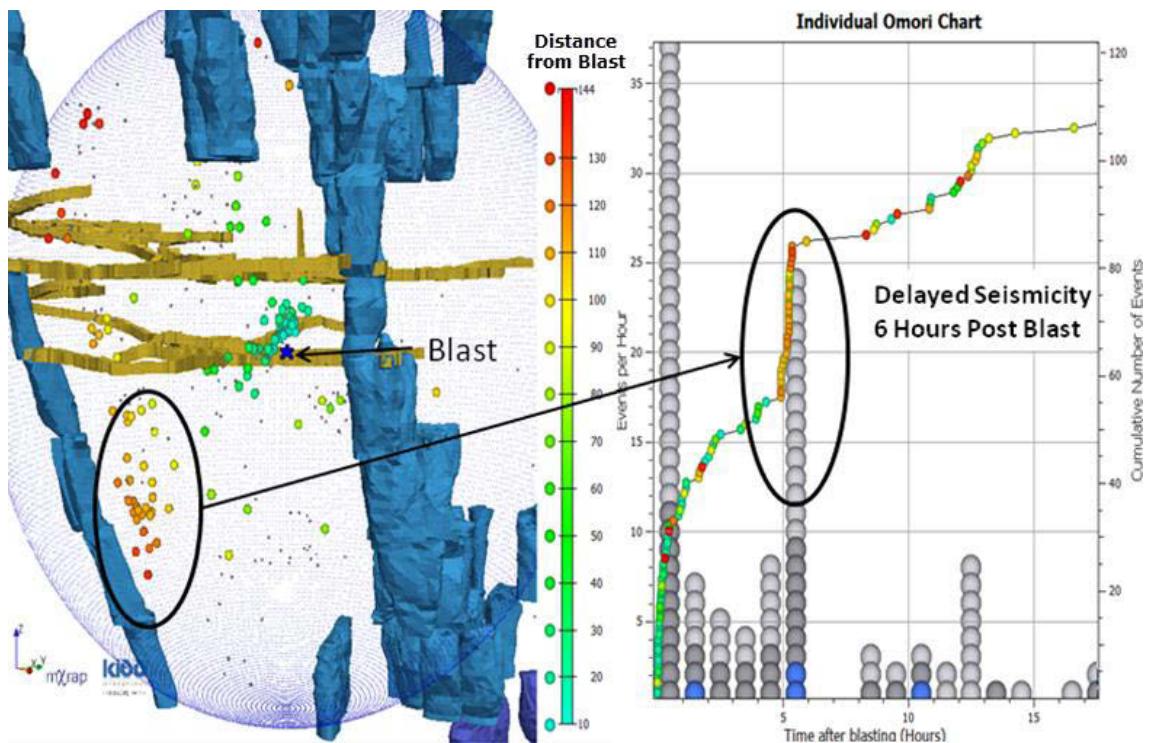
In order to discuss the stress transfer mechanisms that result in seismic responses, it is necessary to distinguish between causative modes of seismicity. Two general modes of seismicity are evident from the study of earthquakes and mining induced seismicity, these being induced and triggered seismicity (McGarr & Simpson 1997; McGarr, Simpson & Seeber 2002; Hudyma 2008).

The terminology “induced” and “triggered” are used in a broader sense for distinguishing between naturally occurring earthquakes and seismicity induced from human activities. Within the context of this thesis, induced and triggered modes of seismicity are defined as:

1. Induced seismicity: The causative stress changes are greater than, or proportional to, resultant seismic responses, e.g., localised response to blasting induced stress; and
2. Triggered seismicity: The causative stress changes are significantly less than the resultant seismic response, e.g., remote seismic response from geological features to stresses induced by blasting.

Induced seismic responses are commonly observed throughout a range of mining environments and are correlated closely with blasting and large events. This seismicity is directly related to the immediate and local re-distribution of stress to the surrounding volumes of rock mass (Hudyma 2008; Vallejos & McKinnon 2008; Eremenko et al. 2009; Kgarume, Spottiswoode & Durrheim 2010a). In addition to seismicity which is induced by a known causative process, there are numerous seismic responses that do not exhibit a strong spatial or temporal relationship to blasting (Urbancic & Trifu 1996; Hudyma, Heal & Mikula 2003; McKinnon 2006; Heal 2007; Potvin 2009; Vallejos & McKinnon 2010b).

Disley (2014) provided an example of a spatial and temporal dependent seismic response following blasting for the Canadian Kidd Creek Mine and illustrates the potential for an initial stress change (blasting) to result in a triggered seismic response. An immediate and local seismic response occurred closely with a small blast. A seismic response is observed along a potential seismic shear plane after a 6 h delay and 120 m from the new excavation (**Figure 7**).



**Figure 7** Left: Perspective three-dimensional view of seismicity occurring after a blast. Also shown are selected mine excavations, analysis search radius (blue sphere) and seismic events (coloured by distance from blast). Right: Time series chart for 24 h following blasting displays a histogram of hourly event occurrence (left axis) and cumulative event count (right axis). The remote and delayed seismic response is annotated on the 3D view and histogram. Redrawn from Disley (2014).

Kgarume (2010) assessed the reduced seismic response density following large seismic events in two mines. The distance dependent reduction in response density was well modelled by a

power law implemented from the study of earthquakes (Hill & Prejean 2007). The power law exponents found for this study support the concept that dynamic triggering may play a significant role in the generation of mining induced seismicity.

Despite triggered seismic responses being observed for a range of mining environments, there is a limited theoretical basis for the physical processes relating an initial stress change to remote or delayed seismic responses. The existing stress transfer mechanisms have been developed within the study of earthquakes (Felzer & Brodsky 2006; Hill & Prejean 2007). An unequivocally physical mechanism that accounts for induced and triggered responses has not been identified (Orlecka-Sikora 2010).

General stress transfer concepts have been applied directly and indirectly to the study of mining induced seismicity (Urbancic 1991; Urbancic & Trifu 1995; Butt, Calder & Apel 1998; Kgarume 2010) and can be summarised with respect to three fundamental mechanisms:

1. Static stress: Stress decays rapidly with distance and only extends short distances.
2. Quasi-static stress: Viscous relaxation extends to greater distances due to low viscoelastic propagation speeds and may contribute to remote/delayed events.
3. Dynamic stress: Amplitudes of seismic waves result in transient stress conditions that may trigger seismicity at significant distances from the initial stress change.

It is plausible that these three mechanisms of stress redistribution congruently contribute to time-dependent seismicity in a mining environment to create an induced and/or triggered seismic response. It is reasonable to expect the degree that each of these mechanisms contributes to seismicity depends on the pre-existing state of the rock mass in the locality and remote to an initial stress change.

Triggered seismic responses require sources of seismicity to be in a stress state that is sufficiently close to failure so relatively small transient changes in conditions may cause a heightened seismic response. Identifying and quantifying seismic responses that are not directly related to blasting or large events offered insight to the spatial and temporal nature of stress redistribution in the mining environment, in addition to information concerning the current state of sources of seismicity. A detailed discussion of triggered seismic response is provided due to the importance of assessing these responses and considers relevant parallels from the study of earthquakes to support this enigmatic topic.

The study of earthquakes indicates that the stress changes required to trigger seismicity can be a small fraction of the stress changes associated with resultant seismicity (McGarr, Simpson & Seeber 2002; Hill & Prejean 2007). This topic has important implications for human activities

that may cause seismicity if the rock mass is in a stress state close to failure, even if stress changes are relatively small. McGarr and Simpson (1997) provided the example of stress changes as small as 0.01 MPa due to reservoir impoundment, contributes to regional seismicity and highlights that while these observations are difficult to understand, there is growing body of evidence that triggered seismicity is a real and significant phenomenon.

The notion of triggered seismicity within mining literature is similar to the study of earthquakes with literature suggesting that relatively small stress changes due to seismicity or mining induced stress can contribute significantly to the seismic generation process (Kijko & Funk 1996; Hofmann & Murphy 2007; Hudyma 2008; Orlecka-Sikora 2010). There is evidence for an ambiguous causative relationship between seismicity and the stress changes for a rock mass close to failure (Kijko & Funk 1996; Mendecki & Lynch 2004; McKinnon 2006). Moreover, Hudyma, Heal and Mikula (2003) asserted that mining activities have the potential to trigger congruent responses from multiple source mechanisms. This cause and effect relationship between seismicity and major stress changes may not be obvious in a mining environment where several blasts occur simultaneously (Heal, 2007). Anomalous seismicity of this nature is typically discussed in the context of site-specific case studies.

The concept of triggered seismicity is illustrated by Naoi et al. (2011) through the observations of acoustic emissions following a large seismic event. While the majority (60%) of the 20,000 total events were spatially associated with the plane of mainshock rupture, several additional clusters were associated with excavations and geological features. The increase in seismic activity in the delocalised volumes was attributed to an increase in stress conditions relative to rock mass conditions.

Urbancic (1991) detailed an example of a systematic stress transfer on a mine-wide scale following a large seismic event in June 1988 at Strathcona Mine. Seismicity following the large event was observed to migrate from low to high stress conditions. The conclusion was drawn that stress changes within a rock mass may contribute to cascading stress changes and rock mass failure. He also noted that these observations required quantitative substantiation such as stress measurements.

The reviewed literature establishes the concept of background seismicity as being weakly spatially clustered and occurring over relatively long time scales. In addition, seismic responses are finite periods of seismicity clustered in space and time that occur due to induced or triggered changes in stress conditions. The spatial and temporal characteristics are controlled by sources of seismicity and are a result of pre-existing factors (e.g., rock mass properties and *in situ* stress), and mining factors (e.g., blasting parameters) and induced stress conditions. The

management of seismic hazard necessitates understanding and quantification of the spatial and temporal characteristics of seismicity and, therefore, it is necessary to identify and delineate seismic responses from background seismicity.

## 2.4 Assessment of Spatially and Temporally Clustered Seismicity

In the assessment of clustered seismic events, it is necessary to assume general spatial and temporal characteristics of seismicity. Reviewed literature supports the concept of seismic responses being finite periods of seismicity clustered in space and time that are superimposed with random background seismicity. This generalisation is applicable irrespective of the factors that contribute to rock mass failure. Molchan and Dmitrieva (1992) highlighted that it becomes impossible to completely separate background and response seismicity without error when assessing seismic responses.

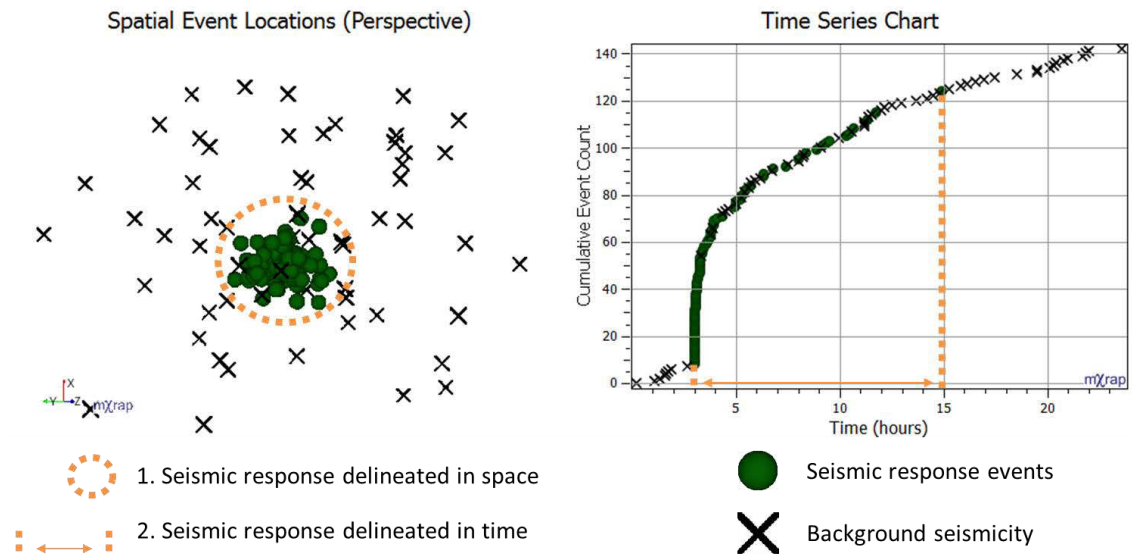
While the identification of events belonging to seismic responses is often ambiguous, this uncertainty does not typically detract from the study conclusions (Utsu, Ogata & Matsu'ura 1995). The reliability of detecting seismic responses depends on the contrast between a seismic response's spatial and temporal properties and background seismicity. The most appropriate solution for response delineation aims to maximise the number and completeness of the responses identified whilst minimising the number of background events that, by chance, form false responses (Molchan & Dmitrieva 1992). Response identification and delineation becomes increasingly involved when aiming to account for the variable cases in a mining environment (Heal, 2007). The spatial and temporal superimposition creates inherent challenges when identifying and delineating seismic responses. The mining practice of firing multiple blasts at designated times inevitably results in concurrently occurring seismic responses.

Literature that specifically addresses the identification and delineation of seismic responses in the mining environment is limited. In order to address relevant literature comprehensively, the scope of this review also considers studies that examine specific aspects of the problem. This review focuses on the study of mining induced seismicity or earthquakes, and addresses one or more of the following aspects associated with the identification and delineation of responses:

1. Identification of seismic responses: Where and when do responses occur?
2. Spatial delineation of related seismicity: What is the extent of responses in space?
3. Temporal delineation of related seismicity: When do responses start and finish?

The general concepts of identifying and delineating seismic responses are illustrated using synthetically generated seismicity. **Figure 8** shows a seismic response clustered in space with a

decaying event rate that has been superimposed with background seismicity sparsely located and uniformly distributed throughout time. The seismic response has been visually identified and delineated by considering the spatial and temporal extent of response events.



**Figure 8** A hypothetical seismic response superimposed with background seismicity. The seismic response has been visually identified and delineated by considering the spatial and temporal extent of response events.

The following discussion contains a complete review of literature that is directly related to this thesis. Relevant literature includes studies that identifies and delineates mining induced seismic responses in space and time.

To provide a broader and representative overview of the subject, a review of literature that is indirectly related to this thesis has also been selected. Further consideration is given to the study of the spatial and temporal characteristics of earthquakes due to the similar motivations that require seismic risk to be minimised through the management of time-dependent seismic hazard for both a mining and regional context. On a regional scale, the study of the spatial and temporal characteristics of earthquakes is required due to an elevated seismic hazard that is associated with an earthquake mainshock-aftershock response. Following a mainshock decisions are required concerning the provision of critical services (utilities, transport etc.), rescue operations, and reoccupation or use of infrastructure (Reasenbergs & Jones 1989). Managing earthquake aftershock hazard is congruent with the management of elevated seismic hazard following large seismic events and blasting within the mining context.

Despite an apparent range of approaches, studies of earthquakes and mining induced seismicity share similar fundamental approaches to identifying and delineating seismic responses. Studies may utilise one, or combination, of the following approaches:

- Informal approaches: Informal assessments that do not explicitly quantify the identification or delineation of seismicity responses. These methods rely on human interpretation to quantify spatial or temporal characteristics of seismic observations;
- Event time and location approaches: Methods that only assess event time and location to identify and delineate responses;
- Metric approaches: Metrics combine multiple aspects of seismic observation into a single measure to represent clustering. Metrics may comprise of various measures and combinations of the location, timing, and source parameters of seismic events; and
- Formal model approaches: This category considers studies that use statistical models to identify and delineate seismic responses. Models are formulated from empirical laws derived from the spatial and temporal characteristics of seismic responses.

The studies that form the focus of further discussion are summarised in **Table 1** (earthquake literature) and **Table 2** (mining literature). These tables provide an overview of the methods that have been implemented to identify and delineate seismic responses with major relevant considerations also noted. In addition to table summaries, graphical representations of studies that have used these fundamental approaches for seismic response identification and delineation are constructed for earthquake references (**Figure 9**) and mining references (**Figure 10**).

**Table 1** A summary of spatial and temporal analysis for the study of earthquakes.

Earthquake Reference	Response Identification	Spatial and Temporal Delineation	Additional Considerations
Gardner and Knopoff (1974)	Visual inspection of space-time clustering.	The extent of temporal and spatial response was defined based on empirical relationships to mainshock magnitude.	Study focused on the removal of aftershocks to assess temporal distribution of background seismicity.
Shilen and Toksöz (1974)	No method presented.	Presented a metric based on the time and distance between two events while also incorporating the normal rate of seismicity. If the metric fails a probabilistic threshold, the events were related in space and time.	Study focused on the removal of aftershocks to assess temporal distribution of background seismicity.
Knopoff, Kagan and Knopoff (1982)	Responses were identified by assessing the time and location of a mainshock.	Seismic responses were delineated with space-time windows that were defined using empirical relationships based on the magnitude of the mainshock.	Magnitude-frequency relationships were evaluated for responses. Events may belong to multiple responses.
Matsumura (1984)	Responses were visually identified from metric minimum.	Metric was based on the space-time distance derived from a Weibull distribution function. Patterns were classified according to the metric value as regular, completely random, or clustered.	Focus of the study was to identify patterns of seismicity to provide insight into the crustal stress state.
Reasenbergs (1985)	Responses were identified by assessing the time and location of a mainshock.	Aftershocks occur within an initially limited space-time window of the mainshock. Temporal extents of responses were determined by considering a probabilistic stochastic model. Spatial clustering was based on the space-time between events with consideration given to mainshock source dimensions.	The study aimed to assess background seismicity, identify aftershocks, spatial migration of aftershocks, and inter-dependency of aftershock responses.
Frohlich and Davis (1985)	For each event, the ratio of relative times for following and subsequent events was calculated. Responses were identified when the probability that events were generated by a Poisson process was small.	No method to delineate identified responses was presented.	The study focused on the identification of deep earthquake responses, i.e., response comprising of few events and few foreshocks and aftershocks.
Frohlich and Davis (1990)	Study implemented a Single-Link Clustering Method. Responses were identified by the removal of arbitrarily long space-time distance links.	A metric was constructed based on distance and time between events. Hierarchical clustering was implemented based on metric.	Metric assessment was used to identify space-time patterns of seismicity. Extensional studies include Davis and Frohlich (1991a) and Davis and Frohlich (1991b).

**Table 1 Continued**

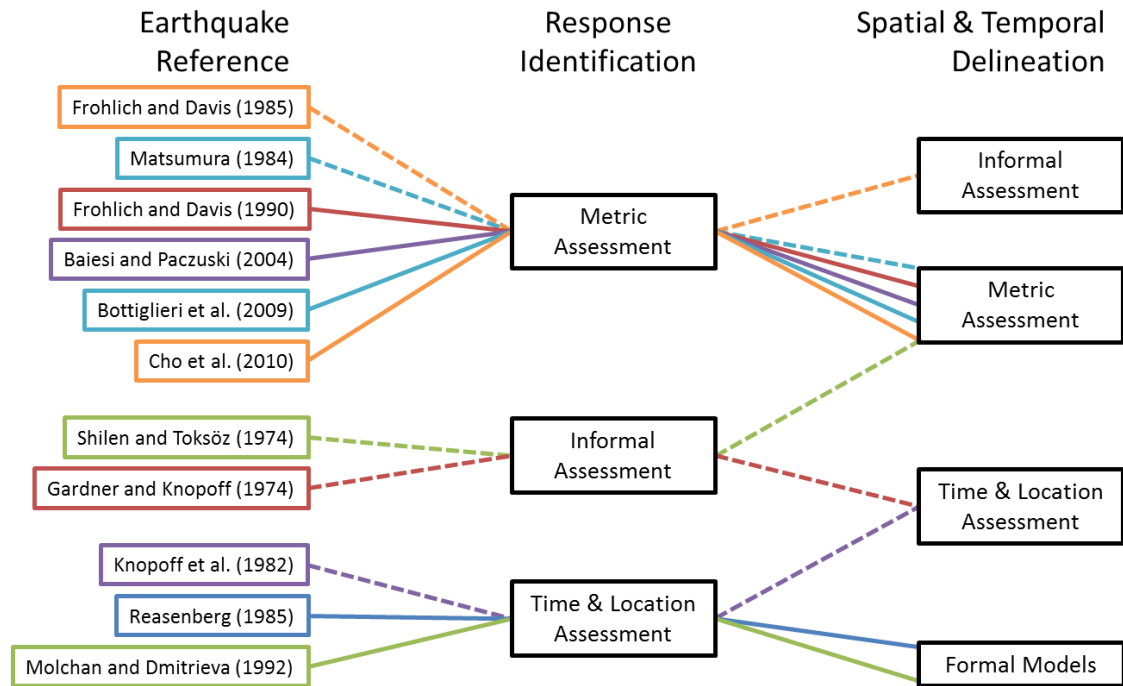
Molchan and Dmitrieva (1992)	Responses were identified by assessing the time and location of a mainshock.	Responses were modelled spatially by an elliptical area and temporally using the Modified Omori Law (MOL). An iterative approach refines initial parameters until aftershock rates become comparable to background rates.	This work focused on aftershock delineation.
Baiesi and Paczuski (2004)	Responses were identified from assessment of a metric that was constructed from number of events within a space, time, and magnitude.	Hierarchical clustering was based on this metric with a cut off selected to define responses. Each earthquake was linked to its most correlated predecessor.	This study focused on foreshock-mainshock-aftershock classification and assessed spatial and temporal characteristics of responses.
Bottiglieri et al. (2009)	Aftershock responses were identified when the proposed variability coefficient was based on inter-event times.	A seismic response ends when temporal occurrence rate falls below threshold.	The study aimed to delineate aftershock responses and estimate background rates. The study also investigated distributions of inter-event times and distances.
Cho et al. (2010)	Study implemented the Thirumalai-Mountain metric (Thirumalai & Mountain 1993). This metric was based on number of events within a time window and box of space.	Analysis conducted for a mesh of boxes assessing the spatial and temporal variance of the system. Seismic responses for the entire system were interpreted outside subsets of effective ergodic periods.	This study also assessed synthetic and mining induced seismicity. The method aimed to quantify spatial and temporal aspects of seismic clustering.

**Table 2** A summary of spatial and temporal analysis for the study of mining induced seismicity.

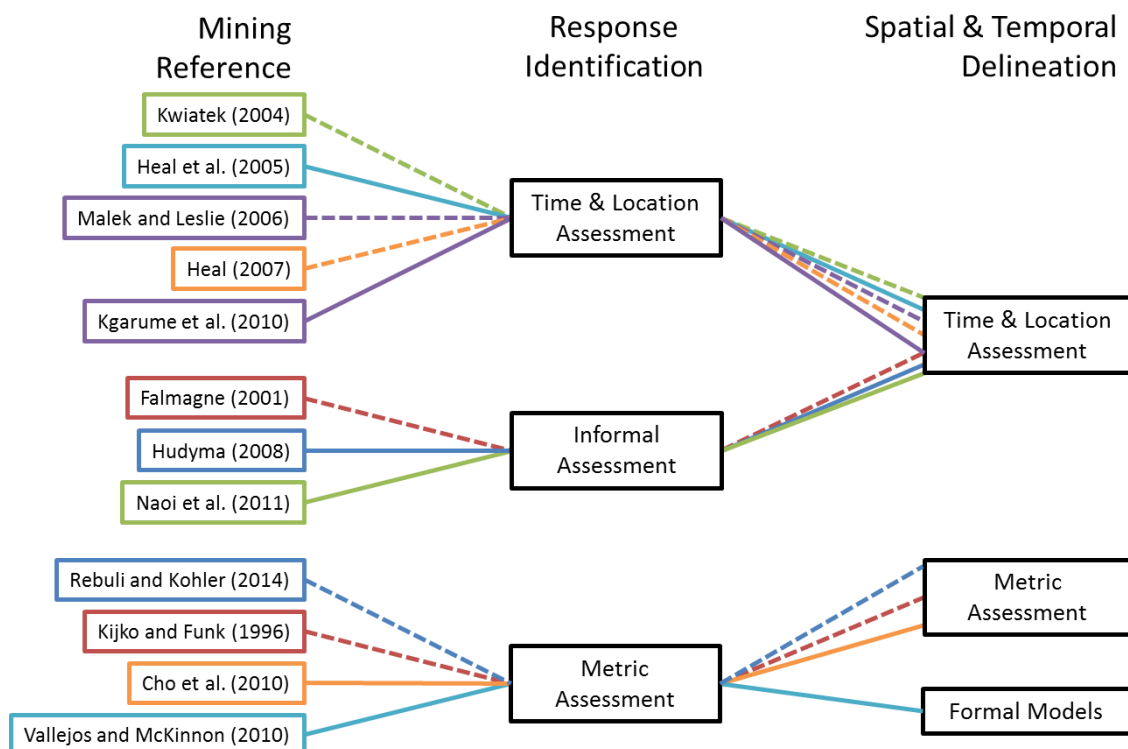
Mining Reference	Response Identification	Spatial and Temporal Delineation	Additional Considerations
Kijko and Funk (1996)	Implementation and adaption of the Single-Link Clustering Method (Frohlich & Davis 1990). Space-time distance link was formed if it was less than an arbitrary maximum.	Clustering was performed for a moving time window. Clusters were maintained until no events can be linked in a time window and were merged if centroids were closer than a minimum distance.	The study was a preliminary assessment of the interaction between identified clusters.
Falmagne (2001)	No method presented.	A metric was constructed from the distance between two events and seismic source radius. This metric was calculated for each event combination and summed for a seismic dataset.	The focus of this study is on approximating rock mass damage based on fracture coalescence.
Kwiatk (2004)	Responses were identified by assessing the time and location of mainshocks.	Space-time windows were used to delineate seismic responses surrounding mainshocks. Responses were temporally superimposed due to insufficient data.	Investigated time-dependent foreshock-mainshock-aftershock responses.
Heal, Hudyma and Vezina (2005)	Responses were identified by assessing the time and location of blasting.	Space-time windows were used to delineate a response following blasting.	This study aimed to characterise seismic responses to blasting.

Table 2 Continued

Malek and Leslie (2006)	No method presented.	Entropy metric was presented as a measure of spatial clustering. This metric was based on a normalised number of events within a clustering distance.	The study presented spatial clustering on a time series chart for a specific period of interest.
Heal (2007)	Responses were identified by assessing the time and location of blasting.	Space-time windows were used to delineate a response following blasting.	This study aimed to characterise seismic responses to blasting.
Hudyma (2008)	No method presented.	Study implemented a two-pass spatial clustering method. 1 <sup>st</sup> pass: CLINK clusters create a large number of small, spatially constrained clusters. 2 <sup>nd</sup> pass: Subjective grouping of CLINK clusters into SLINK cluster groups.	SLINK cluster-groups represent dominant sources of seismicity. The temporal characteristics of the CLINK clusters were considered when forming SLINK clusters.
Kgarume (2010)	Responses were identified by assessing the time and location of mainshocks.	Space-time windows were used to delineate seismic responses surrounding mainshocks. Due to insufficient data for individual response analysis, the responses were superimposed.	Responses investigated using MOL, magnitude-frequency relationship, and spatial aftershock density decay to estimate aftershock hazard.
Vallejos and McKinnon (2010a)	Responses were identified in the temporal domain by implementing the method of ratios (Frohlich & Davis 1985).	Seismic responses were temporally modelled by the MOL with parameters determined by a maximum likelihood method. The method constrains solutions using statistical criteria.	This analysis focuses on the temporal quantification of seismic responses considering a specific mining volume of interest.
Naoi et al. (2011)	Single case study assessing aftershocks following a large event.	A time window and spatial clusters of aftershocks manually defined in volume of interest.	The temporal decay of aftershocks was compared to the MOL without formal model fitting.
Rebuli and Kohler (2014)	Density clustering of a multi-parametric Euclidean metric.	DBSCAN clustering was applied to a space-time-source parameter metric.	Delineation of clusters associated with active mining panels aim to identify clusters of similar events.



**Figure 9** Diagrammatic representation of the interrelation between time and location, metric, and informal assessments for response identification and delineation used in the study of earthquakes.



**Figure 10** Diagrammatic representation of the interrelation between time and location, metric, and informal assessments for response identification and delineation for mining references.

It is evident from the reviewed literature that the study of earthquakes generally focuses on methods that utilise metrics, whilst mining induced seismicity studies focus on the assessment of the event time and location, and informal approaches. For the study of mining induced seismicity, formal models are not used to identify responses and are only used by Vallejos and McKinnon (2010a) to delineate responses. A comprehensive discussion is presented in the context of informal, event time and location, metric, and formal model approaches to seismic response identification and delineation. Further discussion considers the applicability of these approaches for the identification and delineation of mining induced seismicity. For a mining environment, approaches should consider:

- The spatial and temporal characteristics of seismicity independently of magnitude to ensure that the assessment of responses to blasting are not influenced by the chance occurrence of large events;
- The superimposition of responses in space and/or time, resulting from multiple routine blasts and responses to large seismic events;
- The consistent identification and delineation of responses for a range of spatial and temporal event densities; and
- The practical application of the method to large datasets while minimising subjective decisions.

#### **2.4.1 Informal Assessment Approaches**

Informal assessments of space and time characteristics refer to approaches that do not explicitly quantify the identification or delineation of seismic responses and instead rely on human interpretation to quantify spatial or temporal characteristics of seismic observations. These studies provide valuable perspective on the limits of informal approaches when considering response identification and delineation for mining induced seismicity.

In the study of earthquakes, visual inspection is not commonly implemented as a primary method to identify and delineate seismic responses. Manual processing has been used to construct lists of mainshocks and aftershocks (Gardner & Knopoff 1974). This approach is typically labour intensive and introduces an unavoidable degree of subjectivity, particularly for distant aftershocks (Molchan & Dmitrieva 1992). To address the shortcomings of informal techniques, Molchan and Dmitrieva (1992) have suggested that automated algorithms present an attractive option to extract information concerning timing and locations of seismic responses.

Naoi et al. (2011) used visual techniques to identify a single mainshock and to delineate the associated aftershock response. This informal method is more applicable to the study of individual responses as labour requirements and subjectivity can be minimised.

Studies of mining induced seismicity do not always consider formal response identification methodologies but instead focus on formal quantification of spatial characteristics of seismicity (Falmagne 2001; Hudyma 2008). These studies consider temporal occurrence of seismicity informally through the selection of the datasets and subsequent analysis techniques. Analysis techniques that complement spatial quantification are subjective and are typically labour intensive, e.g., the selection of a period for assessment and visual inspection of time series charts.

#### **2.4.2 Event Time and Location Assessment**

Assessment of event time and location is a broad category that includes methods that only consider event occurrence for the identification and delineation of responses. This category includes the use of time and location of mainshocks to identify and space-time windows to delineate seismic responses.

Earthquake studies that use approaches exclusively belonging to this assessment category are limited. Molchan and Dmitrieva (1992) provided a review on the use of the space-time window methods in the context of earthquake studies. The sizes of these windows are generally derived from empirical relationships related to the mainshock magnitude (Ogata, Utsu & Katsura 1996; Baiesi & Paczuski 2004). Baiesi and Paczuski (2004) suggested that while space-time windows can omit response events, the method generally performs well for large earthquakes.

In a significant number of mining induced seismicity studies, the identification of seismic responses considers the occurrence of large seismic events (Knopoff, Kagan & Knopoff 1982; Molchan & Dmitrieva 1992; Kwiatek 2004; Kgarume 2010) or blasting (Heal, Hudyma & Vezina 2005; Heal 2007). A simple methodology is to use the time and location of large events or blasts to determine the starting time and centre of seismic responses. This method is typically accompanied by the use of space-time windows to delineate seismic responses. This approach inherently assumes that seismic responses occur locally and concurrently with the identified initial stress changes. Spatial and temporal windows are arbitrarily selected based on the mining environment (Kwiatek 2004; Heal, Hudyma & Vezina 2005; Malek & Leslie 2006; Heal 2007; Kgarume 2010), rather than selected based on the seismic response characteristics.

The portion of captured response events depends on the size of the space-time window. Larger windows are more likely to include events that are not associated with the response,

and smaller windows are more likely to omit response events (Molchan & Dmitrieva 1992). Reasenber (1985) further discussed the drawbacks of implementing space-time windows. He points out that if these windows are defined to be large enough to delineate most events associated with seismic responses, this will overestimate responses due to the highly variable nature of time-dependent seismicity.

Seismic responses for this assessment category are identified using techniques that require a known cause (blast or large seismic event). As previously noted, identifying response causation can be an ambiguous task for mining seismicity due to both induced and triggered events occurring concurrently in space and time. Despite the uncertainty created by these different modes of seismicity, the reviewed studies have only attempted to identify seismic responses that are closely related to an initial stress change. Applying spatial and temporal windows centred on an assumed causation process inevitably excludes seismicity outside of these windows and, therefore, additional analysis is required to identify and delineate remote and delayed responses.

This approach for the assessment of mining induced seismic responses has some pragmatic limitations that need to be considered. Complete and accurate records of the space-time locations of blasting and large events are required for this method to be implemented. It may be impractical to reliably collect and validate the required information for the retrospective and routine analysis of mining induced responses that use blasts and large events for identification.

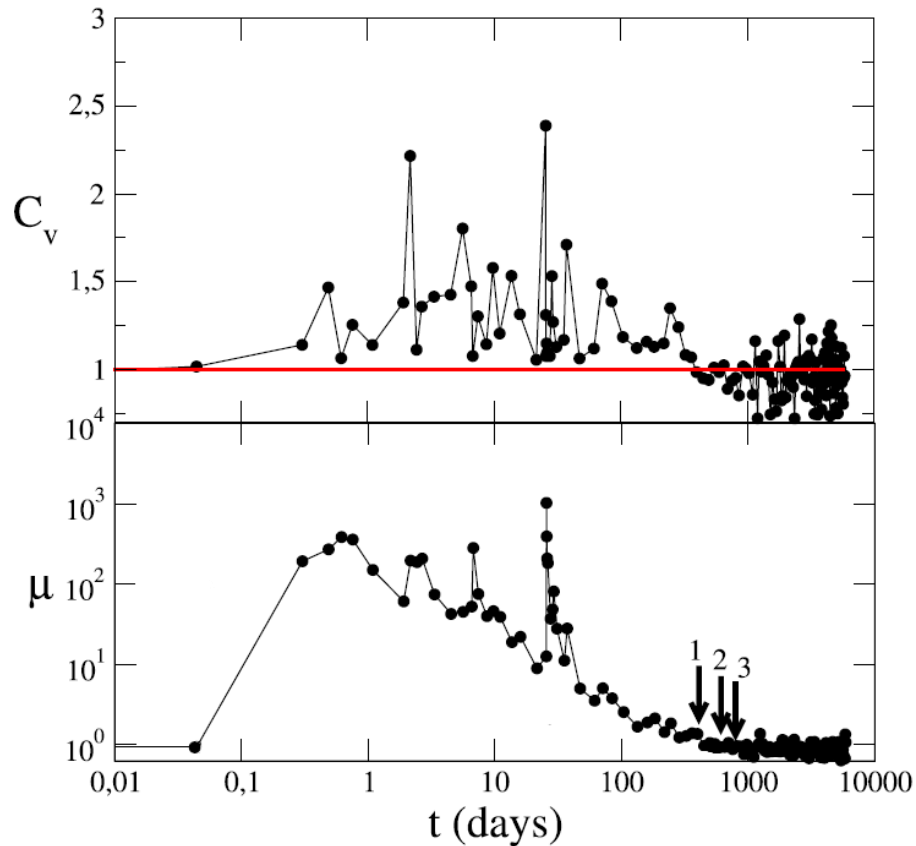
### **2.4.3 Metric Assessment Approaches**

Metric assessment methods combine multiple aspects of seismic observation into a single measure in order to represent spatial and temporal clustering. Metrics may be comprised of various measures and combinations of the location, timing, and source parameters of seismic events. Studies typically consider a metric to identify a seismic response, particularly for the study of earthquakes.

#### **2.4.3.1 Temporal Metrics**

The simple approach of identifying seismic responses is to consider the temporal observations of seismicity. The Method of Ratios was proposed by Frohlich and Davis (1985) to determine if a sequence of events is generated by a stationary Poisson process to a certain statistical confidence. For each successive event, this method determines the ratio between the event occurrence times for preceding and subsequent events. They suggested this method was optimal when there are very few preceding and subsequent events. Bottiglieri et al. (2009) implemented a similar temporal method by constructing a variability coefficient from the ratio

between standard deviation and average value of the successive inter-occurrence time within a non-overlapping temporal window. They distinguish between a periodic process, a Poisson process, and an exponential process. A response is identified when the metric exceeds a rate threshold and ends when the metric falls below a threshold. Furthermore, an iterative approach is implemented to improve the determination of when a response ends (**Figure 11**).



**Figure 11** Shown is a single aftershock response charting the variability coefficient versus time (top) and occurrence rate of earthquakes (bottom). The response end time has been delineated by the iterative method (arrows 1, 2, and 3). Reproduced from Bottiglieri et al. (2009).

#### 2.4.3.2 Spatial Metrics

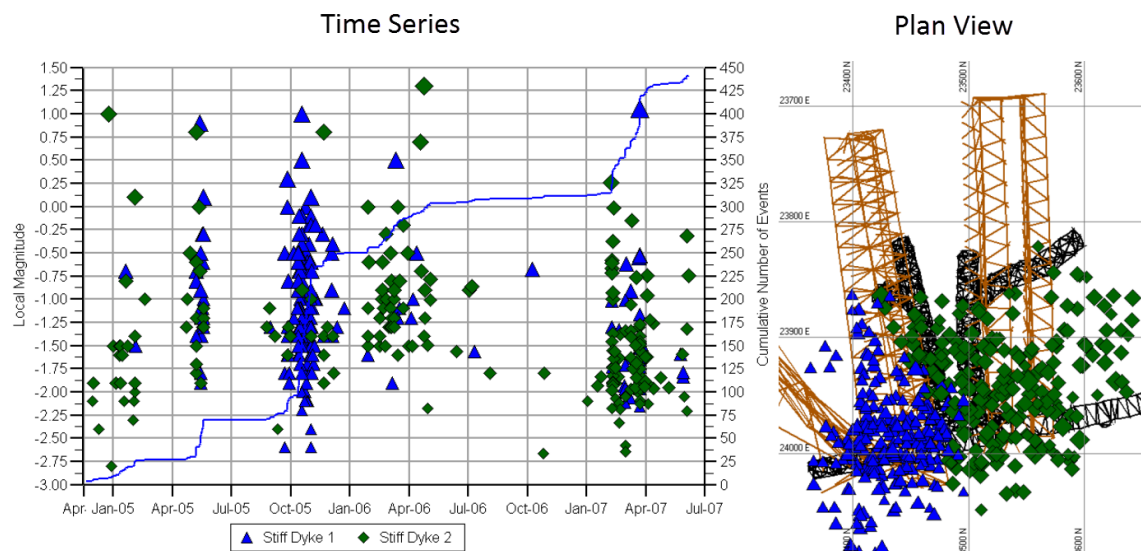
Approaches that consider spatial occurrence of seismicity have limited application when quantifying time-dependent responses. Over fifty publications have been listed by Hudyma (2008) which implement spatial clustering techniques in the assessment of mining induced seismicity. Hudyma (2008) asserted that very few studies attempt to use these methods to analyse seismic data. Due to the scope of this review, limited examples are selected to provide an overview of studies that utilise spatial approaches for the assessment of seismicity.

Falmagne (2001) focused on approximating rock mass damage from fracture coalescence by assessing a clustering metric that is constructed from the distance between two events and an effective seismic source radius. This metric is calculated for each event combination and

summed for all events within a dataset. In this study, the temporal occurrence of seismicity is indirectly considered by the selection of the seismic dataset time interval, e.g., assessment of changes to a spatial clustering parameter changes over two months.

Malek and Leslie (2006) also presented a method that adopts a spatial clustering approach which was complemented with time series assessment. They constructed normalised entropy metric representing the degree of spatial clustering for each event. Changes in this metric were assessed over time and focused on specific cases where seismic responses were evident, although, there was no formal consideration to response identification.

Hudyma (2008) introduced a two-pass, comprehensive spatial event clustering methodology. Firstly, CLINK clusters aim to combine a large number of small spatially constrained clusters. These clusters are created based on the distance between events, with new events being added to a group if they fall within a maximum distance from the centroid. Secondly, information of the mining environment and seismic analysis is used to subjectively group CLINK clusters into SLINK cluster-groups of similar, ideally distinct seismic source mechanisms. Similar to the spatial methods previously presented, the temporal characteristics are assessed qualitatively for a selected period of seismicity belonging to spatially constrained SLINK clusters (**Figure 12**).



**Figure 12** Analysis of two SLINK stiff dyke seismic clusters represented by blue triangles and green diamonds. Shown left is a time series analysis charting magnitude (left axis) and cumulative number of events (right axis) over time. Shown right is a plan view of events with respect to geology (brown frame) and excavations (black frame). Reproduced from Hudyma (2008).

Spatial approaches do not facilitate a quantitative approach to temporally identify or delineate seismic response. Spatial approaches required complementary assessment techniques to identify and delineate seismic responses in space and time. The reviewed literature indicates

that this analysis is typically manually conducted and, hence, labour intensive and inherently subjective. Additionally, spatial clustering of large or entire datasets is based on the final distribution of events in space. The distribution of events throughout space evolves with the progression of mining and, therefore, retrospective temporal analysis may be biased by the misallocation of events to spatial clusters.

#### 2.4.3.3 Space-Time Metrics

Space-time metrics are used to quantify the temporal occurrence of seismicity in combination with the spatial domain. Matsumura (1984) constructed an objective criteria based on the space and time distance between two adjacent earthquakes. No definitive criteria were presented for response identification using this metric. Visual assessment was undertaken of the clustering metric and activity rates to characterise periods of seismicity. Similarly, Shilen and Toksöz (1974) used a metric based on the distance and time between two events. The background rate of seismicity was also combined into this metric. The space-time-background rate metric formed the basis to discriminate probabilistically between independent and dependent events.

Similar measures of space-time distance have been used in hierarchical clustering. Single Link Clustering (SLC) utilises a simple metric to define a space-time distance between seismic events (Frohlich & Davis 1990) (**Equation 3**). Seismic responses are delineated by the removal of arbitrarily long (weak) space-time clustering links (**Figure 13**).

$$d_{ST} = \sqrt{d^2 + C^2\tau^2}$$

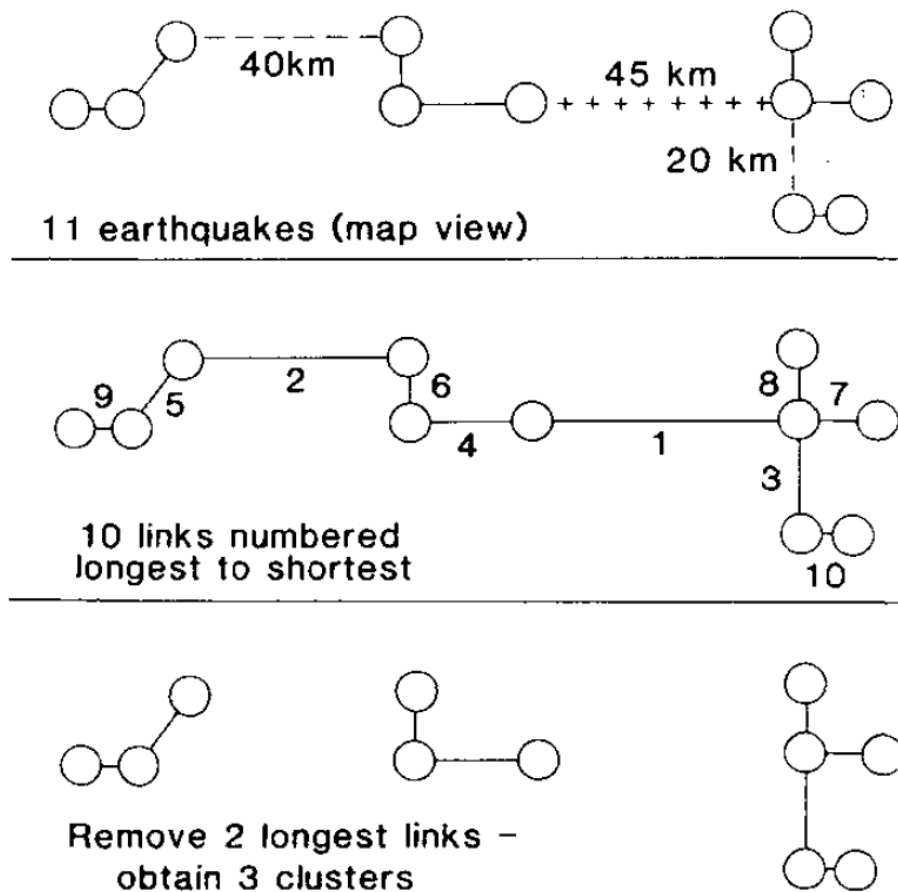
**Equation 3**

Where,

$d$ : Spatial separation of events

$\tau$ : Temporal separation of events

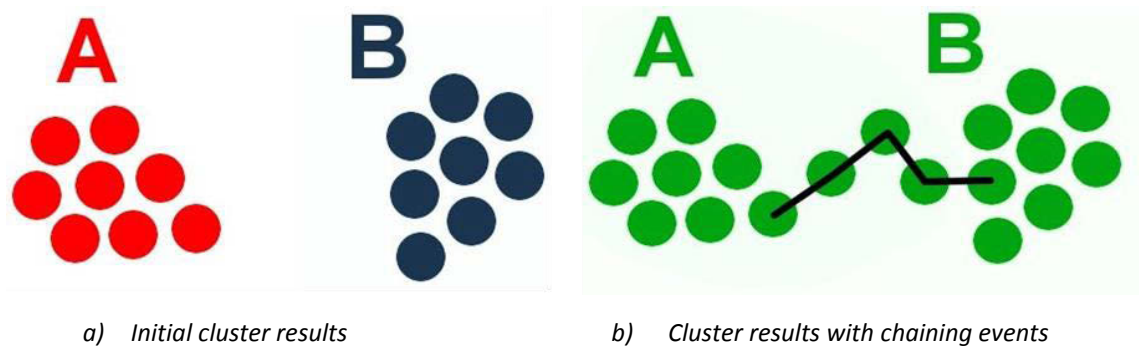
$C$ : Conversion constant relating the spatial and temporal separations



**Figure 13** An example of SLC by representing seismic events in space and time with circles. Groups are linked by the lines ---, +++, and / (top) which correspond the 1<sup>st</sup>, 2<sup>nd</sup> and 3<sup>rd</sup> longest links respectively (middle). Removal of these links result in three clusters in space and time (bottom) (Frohlich & Davis 1990).

Kijko and Funk (1996) applied the SLC method to mining induced seismicity based on the work of Frohlich and Davis (1990). Additionally, they adopted clustering for a moving time window approach based on the work of Matsumura (1984). Clusters are constructed from collections of events with short space-time links and maintained until no additional events can be linked in a time window. Clusters are then merged if centroids formed by these events are closer than a threshold distance.

A limitation associated with the SLC method is the occurrence of chaining which refers to the possibility of two clusters merging due to only a few events occurring in the parametric space between clusters (**Figure 14**). In the context of the previously considered hierarchical SLC, chaining is a result of the breakdown of the assumption that clusters will be separated by long distances in parametric space. As a result of the chaining limitation, clusters may be merged which contain significantly different attributes and, therefore, undermine the initial objectives of clustering (Rebuli & Kohler 2014).

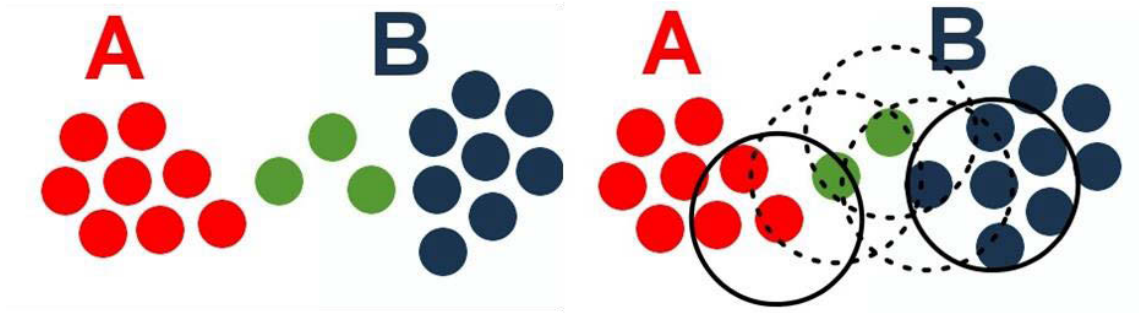


**Figure 14** An example of the chaining limitation for the SLC method. Two initial clusters (a) are merged after the introduction of three events which form a chain(b) (Rebuli & Kohler 2014).

The chaining limitation of SLC can be lessened by adopting an alternative approach to clustering data. Rebuli and Kohler (2014) applied a density clustering method to mining induced seismicity following the work of Ester et al. (1996) who provided the general framework for the DBSCAN algorithm. This method classifies elements by considering the number of neighbouring elements ( $N_e$ ) with respect to a user specified minimum number of neighbours ( $N_{MIN}$ ) within a search distance ( $D_s$ ). These classifications are:

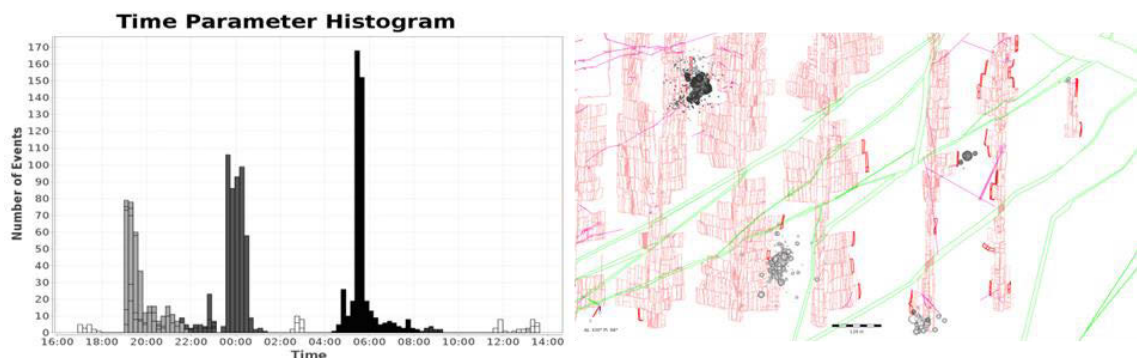
- Core elements: Within a search distance, there are more than the specified minimum neighbours ( $N_{MIN} \leq N_e$  within  $D_s$ ).
- Boundary elements: Within a search distance, there are less than the minimum specified neighbours and at least one core element ( $N_e < N_{MIN}$  and  $1 \leq N_{core}$  within  $D_s$ ).
- Noise elements: Within a search distance, there are less than the minimum specified neighbours and no core elements ( $N_e < N_{MIN}$  and  $N_{core} = 0$  within  $D_s$ ).

The algorithm creates clusters from core elements and their neighbours. Core events are recursively considered with the algorithm merging clusters if at least one core element is shared. Rebuli and Kohler (2014) illustrated the methods ability to address the chaining limitation by applying the algorithm to the previous example (**Figure 14**).  $N_{MIN}$  was set to five events and resulted in initial core elements forming two clusters, while three chaining events remain to be considered (**Figure 15 left**). Circles show the search distance ( $D_s$ ) considered for clustering which results in two events being classified as noise (green) and one as a boundary element of cluster B (**Figure 15 right**).



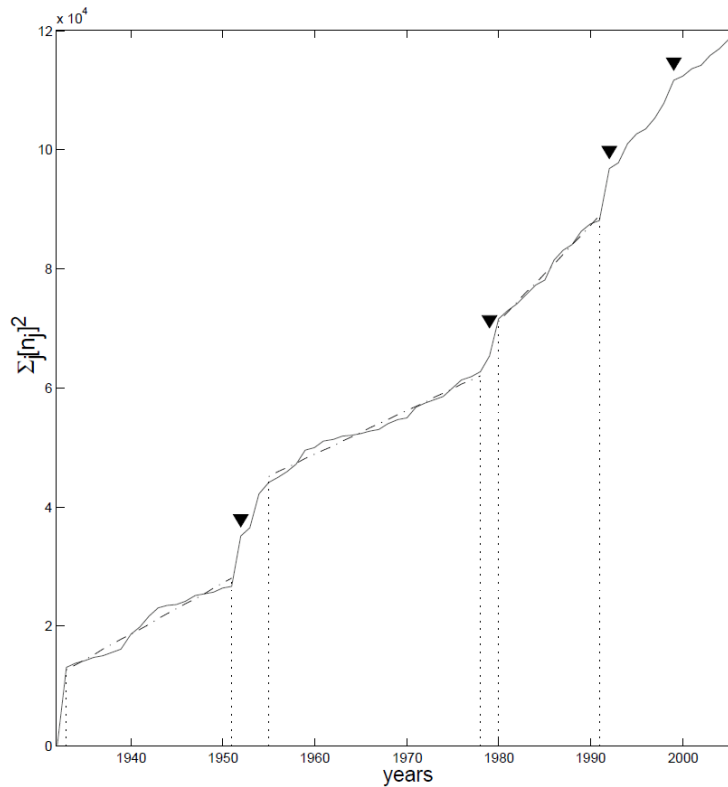
**Figure 15** Left: Results for partial clustering (formation of clusters A and B). Right: Clustering of chain elements resulting in two events classified as noise (green) and one as a boundary element of cluster B.  $N_{MIN}$  is set to five events with  $D_5$  shown by circles (Rebuli & Kohler 2014).

Rebuli and Kohler (2014) used standardised seismic parameters to form Euclidean metrics that assessed combinations of space, time, and seismic source parameters using the DBSCAN clustering algorithm. An example showed the results for the methods application to 24 h of seismic activity using a space-time metric. The clusters of seismicity identified gave insight when and where clusters occurred (**Figure 16**). The comparison to visually identified spatial clusters allowed for the identification of seismicity that did not exhibit temporal clustering.



**Figure 16** Space-time clusters have been identified for 24 h of seismicity using the DBSCAN method that considers a space-time metric. Each cluster is shown by specific grey scale shading on a daily histogram (left) and plan view (right) (Rebuli & Kohler 2014).

In order to incorporate spatial and temporal aspects of seismicity, Cho et al. (2010) implemented the Thirumalai-Mountain metric which was originally developed for the investigation of ergodic behaviour in liquids and glass systems (Thirumalai & Mountain 1993). The method aimed to identify periods of seismicity that follow a metastable equilibrium state, i.e., periods of seismicity that are similar in spatial and temporal attributes. This metric is adapted to consider the average inter-event time and spatial variation of seismicity for a mesh of discrete spatial cells. Seismic responses for the system are interpreted outside effective ergodic periods (time intervals of metastable equilibrium). An example of time series analysis using this metric is provided in **Figure 17**.



**Figure 17** An example of implementation of the Thirumalai-Mountain metric for the southern California dataset between 1932 and 2006. Three effective ergodic periods are identified, which are shown using linear regression dash-dot lines. Triangles indicate large earthquakes during this period.

#### 2.4.3.4 Space-Time-Magnitude Metrics

Space-time-magnitude metrics also consider seismic parameters. Baiesi and Paczuski (2004) constructed a metric by assessing the product of the distance and time between two events along with the magnitude of the first event. This metric focuses on correlating events with a limited number of preceding events. The correlation is achieved by combining relationships for the magnitude-frequency distribution and fractural dimension of earthquake epicentres. The space-time-magnitude parameters are combined into a metric that is the expected number of aftershocks for an event of a given magnitude and space-time window (**Equation 4**).

$$\bar{n} = C \tau r^{d_f} \Delta m 10^{-bm}$$

Equation 4

Where,

$\bar{n}$ : Expected number of aftershocks (events)

$C$ : Constant depending on seismic dataset

$\tau$ : Time interval considered

$r$ : Radius considered

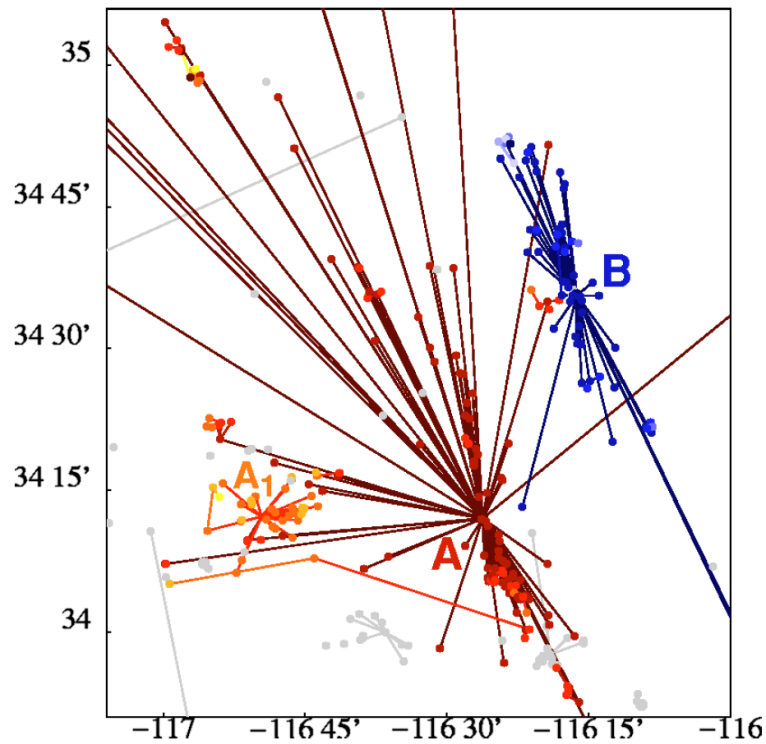
$d_f$ : Constant describing the fractal dimension relationship

$\Delta m$ : Observed magnitude range

$b$ : Constant describing the magnitude – frequency relationship

$m$ : Upper magnitude of expected events

The metric is used to determine each earthquake's correlation to its predecessors. A network of events is constructed by linking every earthquake to its most correlated predecessor. Baiesi and Paczuski (2004) applied this method to mainshock-aftershock responses from the southern California database (**Figure 18**).



**Figure 18** Earthquake network for the Landers (red cluster A) and Hector Mine (blue cluster B) mainshocks. The method also identifies a sub-cluster of the Landers earthquake (orange cluster A1) that was not directly linked to the mainshock.

The use of synthetic seismic data has been implemented in order to validate the identification and delineation of seismic responses (Bottiglieri et al. 2009; Cho et al. 2010). Davis and Frohlich (1991b) reviewed the success of four different aftershock identification schemes using synthetic data (Shlien & Nafi Toksöz 1970; Gardner & Knopoff 1974; Reasenbergs 1985). Davis and Frohlich (1991b) suggested that while these results had high failure rates due to the construction of the synthetic catalogues, they were generally comparable between the studies reviewed. They speculated that these schemes would identify more aftershocks than otherwise considered to be related in space and time by manual assessment.

#### **2.4.3.5 Metric identification and delineation of seismic responses**

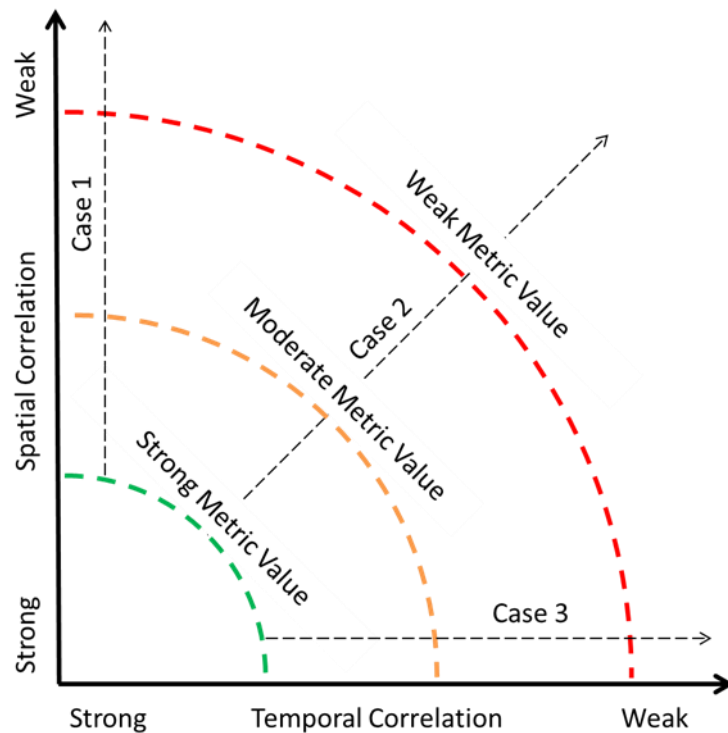
As mining induced seismicity exhibits spatial and temporal clustering, a metric that exclusively examines only one characteristic (spatial or temporal) will not be able to represent seismic responses adequately. Furthermore, in addition to mainshock-aftershock responses, time-dependent responses to blasting are commonly observed for mining induced seismicity.

Given the stochastic nature of seismicity, there is an inherent probability that two independent events will occur closely in space and time to result in a correlated metric score. While metric approaches have a small probability of correlating events erroneously, this probability diminishes for an increasing number of events forming responses and, therefore, is not a major consideration for the reviewed literature.

Metrics are able to identify seismicity that share similar characteristics, however, they will also quantify the following three cases equally:

1. Spatial correlation significantly weaker than temporal correlation;
2. Spatial correlation comparable to temporal correlation; and
3. Spatial correlation significantly stronger than temporal correlation.

This concept is represented graphically in **Figure 19**. The chart considers an arbitrary strongest to weakest range for spatial and temporal clustering shown on the left and bottom axis, respectively. The three cases are shown with black dashed lines over a range of arbitrary metric values.



**Figure 19** Arbitrary strongest to weakest clustering ranges for spatial (left axis) and temporal (bottom axis). Three equivalent cases are represented by black dashed lines over a range of arbitrary metric values: 1. spatial correlation significantly weaker than temporal correlation, 2. spatial correlation comparable to temporal correlation, and 3. spatial correlation significantly stronger than temporal correlation.

Metric approaches have the potential to correlate seismicity separate in space or time if events occur sufficiently close in the alternate metric component. While seismicity typically occurs in the same space and time following blasting, events can also occur in the same space but with some time offset, or they may occur at the same time in different spatial volumes. Consequently, mining induced seismicity may be falsely correlated despite being caused by discrete failure processes.

Metric approaches may assume conversion and threshold constants. These assumptions are suited to consistent seismic dataset source mechanisms, e.g., b-value for magnitude-frequency relationship or space-time conversion constants. In contrast to earthquake occurrence, mining induced seismicity is caused by diverse source mechanisms with contrasting spatial and temporal scales, e.g., seismicity triggered on a geological structure, in comparison to, seismicity induced by blasting related rock mass failure. These methodology limitations conflict with the objective of identifying and delineating mining induced seismic responses for a range of mining conditions.

The applicability of clustering techniques is improved by the DBSCAN method, which addresses the limitations of the SLC by considering a minimum number of neighbour elements and a search distance. This method requires the selection of clustering parameters that correspond to a specific and constant density tolerance that will cause the method to underperform when attempting to cluster variable space densities.

Mining induced seismicity may not be identified by large seismic events as seismic responses are also caused by stress changes induced and triggered by routine blasting. The occurrence and influence of blasting is not contained within seismic information. As a result, measures of magnitude in metric approaches are not optimal when describing a wider range of time-dependent responses, e.g., when using a space-time-magnitude metric, a seismic response will be identified and delineated differently if caused by a large seismic event in contrast to the exact same response caused by a blast.

#### **2.4.4 Formal Models**

The review of the statistical models to identify and delineate seismic responses considers established empirical laws. While the application of formal models in the identification and delineation of seismic responses is limited, it is important to highlight typical applications. This section focuses on methods that used formal models for the initial identification and delineation process. Formal models are more commonly used to assess time-dependent seismicity following an initial procedure to identify and delineate a seismic response. The application of formal models for the analysis of seismic responses is further addressed in this thesis. Section 2.5 provides a detailed discussion of the Omori Law, Modified Omori Law (MOL), and competing models.

Reasenberg (1985) considered aftershocks that occurred within a limited space-time window following large earthquakes. Subsequent assessment considered mainshock source dimensions, spatial clustering, and temporal occurrence to extend the definition of aftershocks. Spatial clustering is based on the space-time distance between aftershocks and seismic moment. Temporal extent of responses is determined by considering the time interval required to observe another event in the response and this is achieved with a probabilistic time-dependent Poisson model of aftershocks. Temporal event occurrence is assumed to follow OL and rewritten to describe the probability of observing earthquakes during the interval  $(t, t + \tau)$ . This formal model is used to determine the time interval that is required to observe one or more events given a specific probability (**Equation 5**).

$$\tau = \frac{-\ln(1 - P)t}{10^{2(\Delta M - 1)/3}}$$

**Equation 5**

Where,

$\tau$ : Time interval required to observe one or more events

$t$ : Time of event occurrence relative to the start of response

$P$ : Probability of observing event within give time period

$\Delta M$ : Observed event magnitude range

Molchan and Dmitrieva (1992) presented a Local Intensity Ratio method that is employed to identify and delineate mainshock-aftershock responses. The identification of seismic responses defines a mainshock to be the largest magnitude in the database. The delineation of the associated seismic response is determined iteratively and minimises the errors associated with the identification of time-dependent and time-independent seismic processes. The two processes are background seismicity that is modelled by a stationary Poisson process and aftershock seismicity, which is modelled by events that follow the MOL and is spatially dispersed over an elliptical area centred on a mainshock epicentre. After these events are removed, this identification and delineation process is repeated.

Similarly, Vallejos and McKinnon (2010a) used a combination of approaches to identify and delineate seismic responses. For a volume of mining induced seismicity, responses are temporally identified by utilising the Method of Ratios (Frohlich & Davis 1985). Temporal assessment of responses is achieved with a methodology utilising the MOL. Following the identification of a response, median inter-event times are calculated relative to all possible start and end times of the seismic response. For each possible start and end combination, the MOL is applied with solutions that are limited to consider only periods of seismicity with observed temporal occurrences conforming to power-law behaviour. From these limited solutions, the final solution is selected that maximises the ratio between the relative end and start time of the seismic response. Due the relevance of the MOL to this thesis, this method is discussed in detail in Section 2.5.

A limitation of implementing formal models is that inherent assumptions must be made concerning the spatial and temporal occurrence of seismicity. These assumptions must be validated during or following the identification and delineation procedure and are partially validated by quantification of the fit of the model to observations (Vallejos & McKinnon 2010a). More generally, the application of assessment techniques to synthetic data is an important process to validate the results and to quantify errors associated with the identification and delineation of seismic responses (Bottiglieri et al. 2009; Cho et al. 2010).

The use of formal models in mining seismology does not completely address the problem of seismic identification and delineation in space and time. Formal models, such as the MOL, are empirically derived from observed time-dependent seismic responses and attempt to represent temporal event occurrence. These models are not typically suited to identifying seismic responses and, therefore, to identify responses in space and time additional approaches must be used in conjunction with formal models.

Formal models applied to mining induced seismicity only assess the temporal domain. Similarly, earthquake studies also assess the temporal domain, although, may consider the spatial occurrence of seismicity through metric or space-time window approaches. Comprehensive procedures to delineate seismic responses require spatial aspects of seismicity to be congruently assessed with the temporal occurrence of seismicity. A spatial component is particularly relevant when applying formal models to quantify seismicity generated by a single failure process that is spatially constrained.

## 2.5 Modified Omori Law

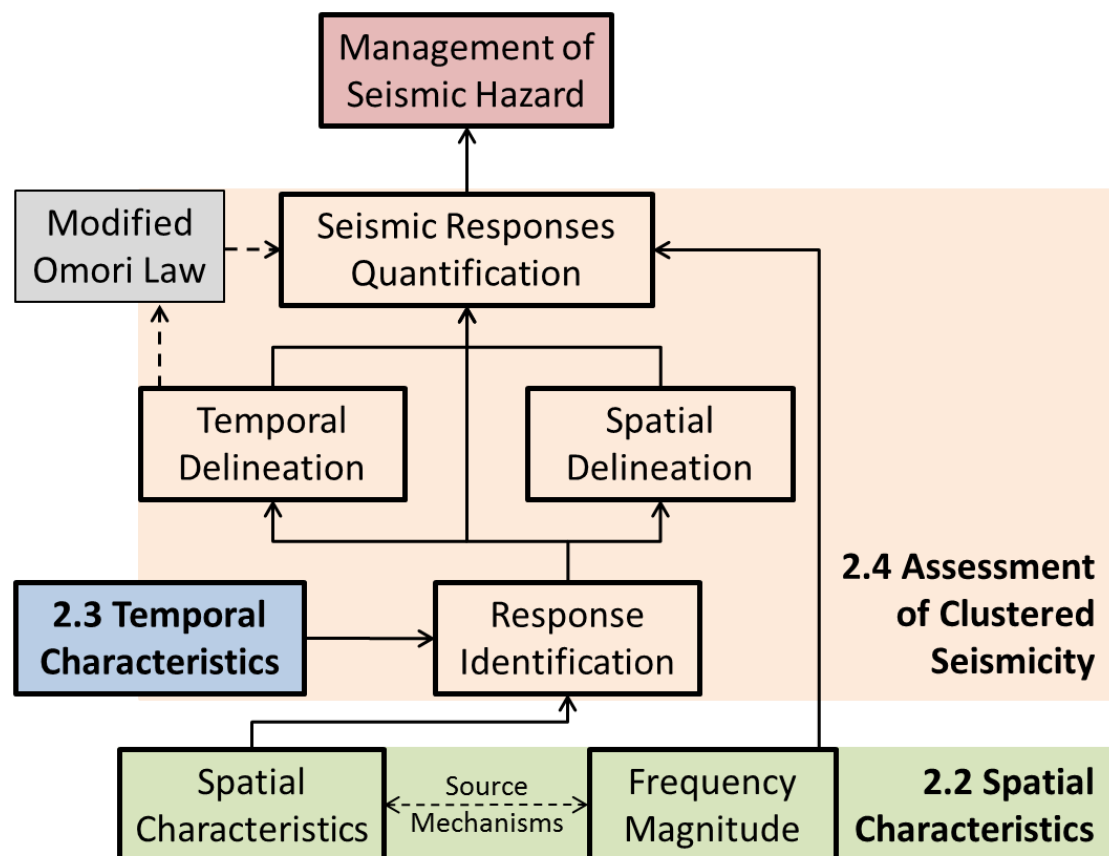
The management of seismic hazard is addressed on a fundamental level by considering the qualitative spatial and temporal characteristics of seismicity (Sections 2.2 and 2.3). The identification, temporal and spatial delineation of seismic responses (Section 2.4) enables the quantification of seismic responses. The quantification of seismic responses is an important component to shift managerial reliance from qualitative to quantitative seismic hazard. While a qualitative hazard assessment may provide exploratory insight and generalisations into prevailing trends in seismicity, a quantitative approach enables characteristics of the mining environment to be correlated to seismic responses and enables the optimisation of seismic hazard management. Establishing the answers to the previously presented research questions enables the quantification of seismic responses (**Table 3**).

**Table 3** A summary of research questions and the aspects of response quantification enabled by the analysis of seismic responses.

	Research Question	→	Response Quantification
Identification	Where and when do responses occur in space and time?	ENABLE	Time and distance from initial stress change, e.g., is a response local, remote, immediate, or delayed with respect to blasting.
Spatial Delineation	What is the extent of responses in space?		Distribution in space, e.g., density, geometry.
Temporal Delineation	When do responses start and finish?		Distribution in time, e.g., events productivity, occurrence decay rate.

The different aspects of seismic responses are not equally important with respect to the management of seismic hazard. The assessment of seismic responses generally assumes that seismicity occurs locally and immediately with an initial stress change. Typically, studies do not explicitly consider the identification or spatial extent of seismic responses. The temporal quantification of seismic responses is emphasised throughout the study of mining induced seismicity and, hence, relevant literature is subject to a detailed review.

The MOL is a widely accepted and is routinely applied to mining induced seismicity to describe time-dependent event occurrence. This law forms an essential link between the temporal delineation and the quantification of a response's productivity and rate of decay. The contribution of this law with respect to the quantification of seismic responses and previous sections of this chapter are shown diagrammatically in **Figure 20**. This chapter places particular emphasis on the MOL as this model commonly used to describe the temporal decay rate of seismic responses. This statistical law was developed for the study of earthquakes and, therefore, relevant literature is considered from mining induced seismicity and earthquake fields of research.



**Figure 20** Representation of the contribution of the MOL with respect to the quantification of seismic responses and previous sections of this chapter.

The Omori Law was first proposed to describe the decreasing frequency of aftershocks following Japanese earthquakes (Omori 1894a; Omori 1894b). In subsequent years, it has been applied to many other aftershock responses (Utsu, Ogata & Matsu'ura 1995). The law describes the frequency of aftershocks that occur for a time interval following a mainshock (**Equation 6**):

$$n(t) = K(t + c)^{-1} \quad \text{Equation 6}$$

Where,

$n(t)$ : Number of events per time interval at time  $t$

$K, c$ : Constants

Utsu, Ogata and Matsu'ura (1995) provided background literature to the development of models describing aftershock behaviour. Utsu (1957) noted that the decay rate of aftershocks was greater than estimated using the original Omori formula. The occurrence rate of aftershocks was shown to follow the Omori formula that also included a constant to describe the rate of decay. Utsu (1961) designated this equation the modified Omori formula and is referred to as the Modified Omori Law (MOL) throughout this thesis (**Equation 7**):

$$n(t) = K(t + c)^{-p} \quad \text{Equation 7}$$

Where,

$n(t)$ : Number of events per time interval, at time  $t$

$K$ : Constant (productivity)

$p$ : Constant (decay)

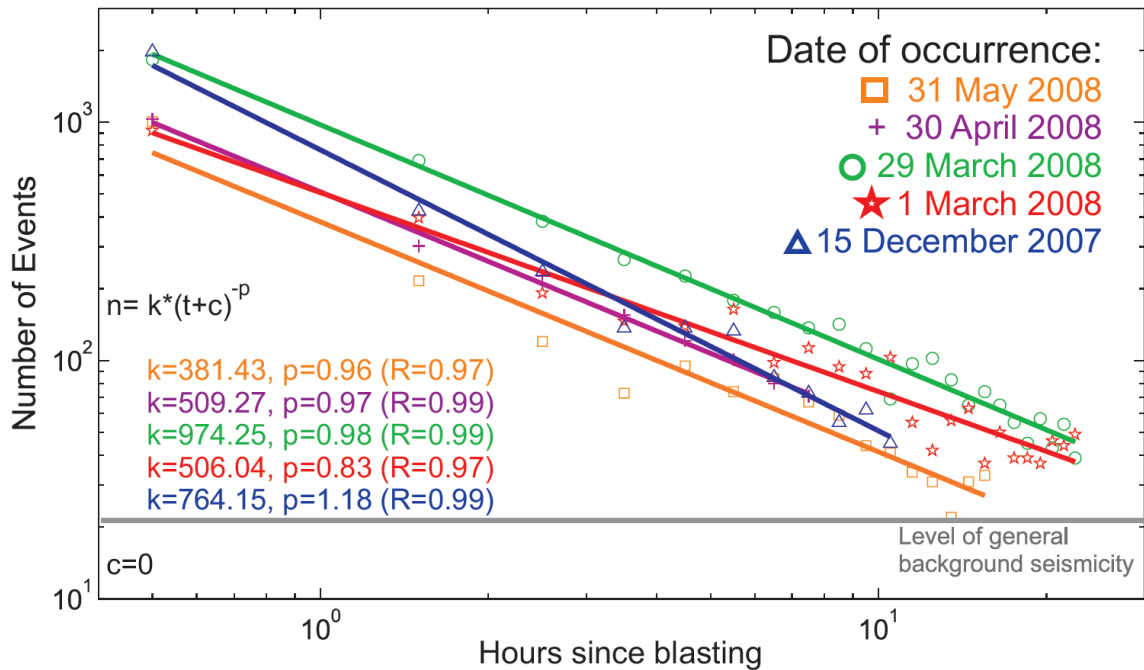
$c$ : Constant (time offset)

### 2.5.1 Applicability to Seismic Responses to Mining

Seismically active mines commonly experience increased event rates following large seismic events and blasting (Vallejos & McKinnon 2008). Despite being founded in the assessment of earthquake aftershocks, mining induced seismic responses are generally satisfactorily described by the MOL (Kgarume 2010; Vallejos & McKinnon 2010a). While Mendecki and Lynch (2004) agreed that seismic responses are well described by the MOL, they also note that some observed responses may not conform to this law.

Several case studies indicate the wide applicability of the MOL. Phillips et al. (1997) applied the MOL to seismicity following an induced collapse of a room and pillar mine situated 320 m below surface. The seismic response generated by the collapse was found to follow the law. In contrast to a shallow mine wide example, Plenkers et al. (2010) discussed findings from the joint Japanese-German Underground Acoustic Emission Research in South Africa (JAGUARS) project. The project focused on high resolution monitoring to detect seismic responses for a

limited section of the Mponeng Gold mine. Five acoustic emission responses following routine blasting were found to follow the MOL (**Figure 21**).



**Figure 21** The rate of acoustic emission is shown for five responses to blasting. The MOL has been fitted to each on these responses (coloured line). Modelling parameters are summarised on the chart along with an indication of background seismicity (Plenkers et al. 2010).

While the MOL has been found to be generally applicable to seismic responses, alternative approaches have been used to describe aftershocks. Literature exploring alternative rate models is derived from the studies of earthquakes along with limited applications to mining induced seismicity. Ogata (1983) discussed the temporal superimposition of responses and the use of multiple models to describe aftershock occurrence for a given time interval. The models evaluated by this study comprise of multiple MOL as opposed to a different fundamental relationship. The Tango earthquake (7.5 M) was given as an example of a double secondary aftershock model being statistically selected over a single aftershock model. This approach is similar to Vallejos and McKinnon (2010a) that assessed time intervals before and after a modelling period. An initial period was preferentially modelled by the MOL for 14% of assessed responses. This indicates that more than one response existed within the entire interval and is synonymous with secondary aftershock modelling.

Multiple responses within a time period have also been addressed by implementing an epidemic-type aftershock model (ETAS) (Kagan & Knopoff 1981; Kagan & Knopoff 1987; Ogata 1988; Saichev & Sornette 2007; Tiampo & Shcherbakov 2012). ETAS is a generalisation of the MOL based on the premise that all seismic events result in a number of aftershocks proportional to event magnitude. This application of the MOL assumes a branching model, i.e.,

each seismic event results from a single parent event (Helmstetter & Sornette 2002) and cannot consider non-seismic contributions in the generation of events. Within the mining environment, seismicity occurs due to a variety of seismic and non-seismic sources (e.g., blasting, removal of material etc.) and, therefore, branching models of this nature are not generally applicable. Despite varied implementations, all these applications utilise the MOL to model the temporal occurrence of seismicity.

While the MOL is widely used and accepted, there are additional models that are used to describe time-dependent seismic responses (Gross & Kisslinger 1994; Gasperini & Lolli 2009). Temporal models applied to responses are statistically selected by evaluating the number model parameters and the maximum log-likelihood estimate, e.g., assessment of the Akaike Information Criterion (Akaike 1974). Vallejos and McKinnon (2010a) considered individual, as well as, combinations of power law decay, exponential decay, and constant rate models for intervals before, during, and after a modelling period. Applying various models to initial periods provided no clear preferable alternative to the MOL. The models that included a constant rate expression were most representative following an initial modelling period.

Exponential functions have been found to describe a variety of physical systems and these models have been commonly compared to the MOL to improve modelling of aftershocks (Kisslinger 1993; Gasperini & Lolli 2009; Lolli, Boschi & Gasperini 2009). In a study of 29 earthquake aftershock sequences, Kisslinger (1993) found that the MOL is preferable in all cases unless the starting time of the response is delayed. The delay is required due to the inability of the exponential law to account for a deficiency in early aftershocks. After adjusting the modelling time interval, the MOL was preferable in approximately half of the cases. In an additional study of 14 earthquake aftershocks, Gross and Kisslinger (1994) found that the majority of responses were preferably modelled by the MOL, while variants of the stretched exponential model was found to be preferable for five responses. Gasperini and Lolli (2009) found that if the background rate of seismicity is determined correctly, in comparison to alternative models, the MOL is only preferable in 12 out of 24 responses.

The reviewed literature indicates that the most appropriate temporal model may vary. Furthermore, studies indicate that the selection of the modelling time interval and the proportional contribution between response and background seismicity may influence which model is deemed optimal. While the MOL may not be the optimal model for some seismic responses, this model is typically adequate for a range of applications in the study of earthquakes and mining induced seismicity. The use of a single model facilitates a consistent comparison between seismic responses and the conditions that contribute to mining induced seismicity. This thesis only considers the MOL for temporal modelling as no model is clearly

more representative of mining induced seismicity or earthquakes. Furthermore, the established nature of the MOL provides a basis for the interpretation of results and a consistent approach to temporal modelling.

### 2.5.2 Parameter Determination by Maximum Likelihood Estimation

Ogata (1983) provided a maximum likelihood method to estimate the MOL parameters ( $K$ ,  $p$ , and  $c$ ) and associated uncertainties ( $\sigma_K$ ,  $\sigma_p$ , and  $\sigma_c$ ) by assuming that seismic responses are distributed by a non-stationary Poisson process and are conditionally independent on the time interval  $[S, T]$ . The Maximum Likelihood Estimates (MLE) are obtained by maximising a log-likelihood function over an interval with event times relative to the time of a principal event  $[t_i; i = 1, 2, \dots, t_N; N]$  (**Equation 8**):

$$\ln L(K, p, c, S, T) = N \ln K - p \sum_{i=1}^N \ln(t_i + c) - KA(p, c, S, T) \quad \text{Equation 8}$$

Where;

$$A(p, c, S, T) = \begin{cases} \ln(T + c) - \ln(S + c) & \text{for } p = 1 \\ \frac{(T + c)^{(1-p)} - (S + c)^{(1-p)}}{(1 - p)} & \text{for } p \neq 1 \end{cases}$$

$S$ : Start of time interval

$T$ : End of time interval

$K$ : Constant (productivity)

$p$ : Constant (decay)

$c$ : Constant (time offset)

Ogata (1983) determined the asymptotic standard errors of the MLE of each parameter by using the Fisher Information Matrix  $J(K, p, c, S, T)$  (**Equation 9**). The standard deviation of the marginal error of each parameter can be determined from the square root of the diagonal elements of matrix  $J(K, p, c, S, T)^{-1}$ .

$$J(K, p, c, S, T) = \int_S^T \begin{bmatrix} K^{-1}(t + c)^{-p} & -p(t + c)^{-p-1} & -(t + c)^{-p} \ln(t + c) \\ * & Kp^2(t + c)^{-p-2} & Kp(t + c)^{-p-1} \ln(t + c) \\ * & * & K(t + c)^{-p} [\ln(t + c)]^2 \end{bmatrix} dt \quad \text{Equation 9}$$

Where;

$t$ : Interval time

$S$ : Start of time interval

$T$ : End of time interval

$K$ : Constant (productivity)

$p$ : Constant (decay)

$c$ : Constant (time offset)

### 2.5.3 Suitability of Fit by Assessment of the Anderson-Darling Statistic

Nyffenegger and Frohlich (1998) highlighted that low uncertainties in the determination of MOL parameters do not indicate if the observed seismicity is well described by the equation. An assessment of the absolute suitability of fit is achieved by assessing the non-parametric Anderson-Darling statistic ( $W^2$ ) (Anderson & Darling 1954; Lewis 1961) (**Equation 10**):

$$W_N^2 = -N - \sum_{i=1}^N \frac{(2i-1)}{N} [\ln(u_i) + \ln(1 - u_{N+1-i})] \quad \text{Equation 10}$$

Where;

$$u_i = \begin{cases} \frac{\ln(t_i + c) - \ln(S + c)}{\ln(T + c) - \ln(S + c)} & \text{for } p = 1 \\ \frac{(t_i + c)^{1-p} - (S + c)^{1-p}}{(T + c)^{1-p} - (S + c)^{1-p}} & \text{for } p \neq 1 \end{cases}$$

$t_i$ : Time of the  $i^{\text{th}}$  event

$S$ : Start of time interval

$T$ : End of time interval

$N$ : Number of events

$p$ : Constant (decay)

$c$ : Constant (time offset)

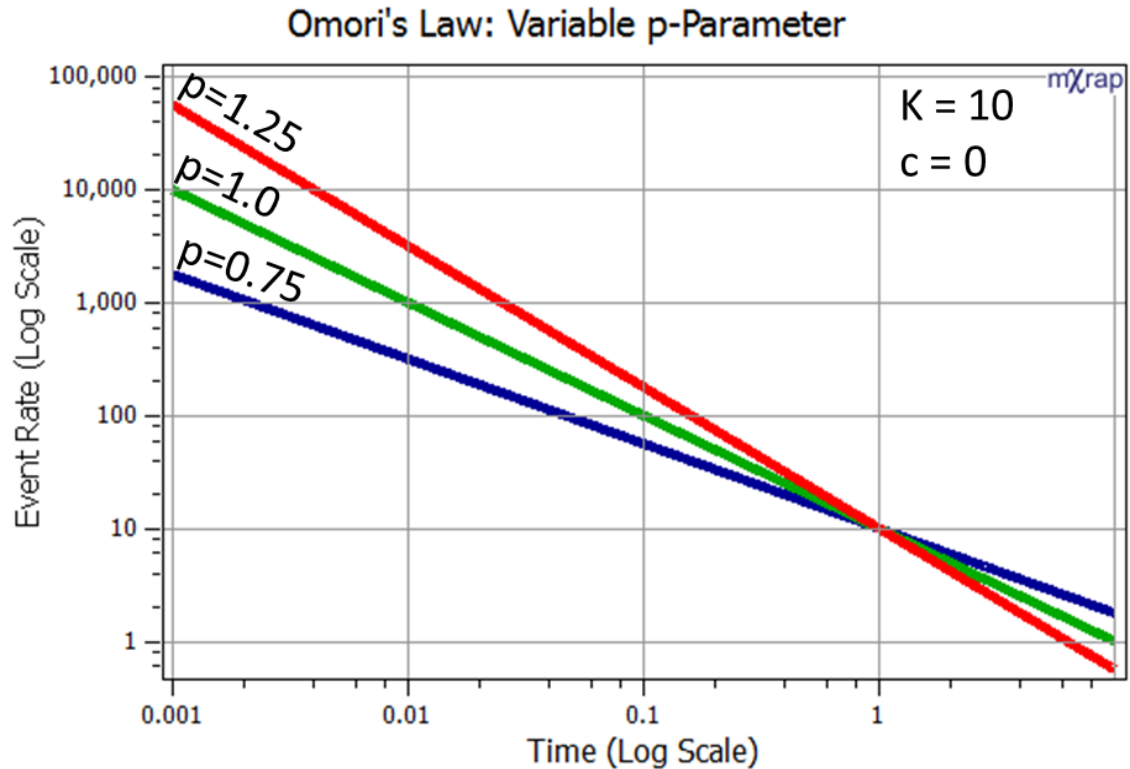
The distribution of  $W_N^2$  rapidly converges for  $N > 8$ , so for practical purposes, the asymptotic distribution is used. The Anderson-Darling statistic can be generalised by assessing the descriptive qualities that various studies have assigned to numerical values of  $W_\infty^2$  (Lewis 1961; Nyffenegger & Frohlich 1998; Nyffenegger & Frohlich 2000; Vallejos & McKinnon 2010a) (**Table 4**).

**Table 4** Descriptive qualities for values of  $W^2$  and confidence for distribution rejection.

$W_\infty^2$	Generalised Fit Description	Confidence for Distribution Rejection
$W_\infty^2 = 0$	Perfect	-
$W_\infty^2 \leq 0.5$	Excellent	25%
$W_\infty^2 \leq 1.0$	Good	64%
$W_\infty^2 \leq 2.0$	Acceptable	91%

### 2.5.4 p-Parameter

The p-parameter is proportional to the decay rate of event occurrence. **Figure 22** shows the impact that varying p-values have on the MOL event rate. Additional parameters are kept constant ( $K = 10$  and  $c = 0$ ) for a time interval between 0.001 and 10 (arbitrary units).



**Figure 22** The impact that varying p-values have on the event rate (log scale) given by the MOL. Additional parameters are kept constant ( $K = 10$  and  $c = 0$ ) for a time interval between 0.001 and 10 arbitrary time units (log scale).

Seismic responses within four Canadian mines were found to give p-values in the range of 0.4 to 1.6 (Vallejos & McKinnon 2010a), while p-values for South African mines ranged from 0.8 to 1.0 (Kgarume, Spottiswoode & Durrheim 2010a), and 0.64 to 1.10 (Spottiswoode 2000). These results are generally in agreement with earthquake p-values (0.5 to 1.5) (Dieterich 1994).

There are a number of factors that may influence the p-values observed for earthquake responses, e.g., fault heterogeneity, crustal stress, crustal temperatures, mainshock characteristics, faulting mechanisms etc. (Utsu, Ogata & Matsu'ura 1995). While all of these factors may influence aftershock decay rates to varying degrees, a significant factor is ostensibly regional crustal temperatures. The study of southern California aftershock responses suggested that greater temperatures at the hypocentre of mainshocks result in rapid decay rates (high p-values). These results do not exclude the influence of additional factors (Kisslinger & Jones 1991). This study concludes that regional crustal temperatures

control the average p-value, although, the decay rate of individual responses could be additionally influenced by local source conditions (Kisslinger & Jones 1991). A correlation between the high decay rate and high crustal temperatures is supported in the study of Japanese aftershock responses (Creamer 1994) and for seismic responses in proximity to volcanic regions (Klein, Wright & Nakata 2006). These studies conclude that high p-values may indicate higher crustal temperatures and an accelerated stress relaxation process.

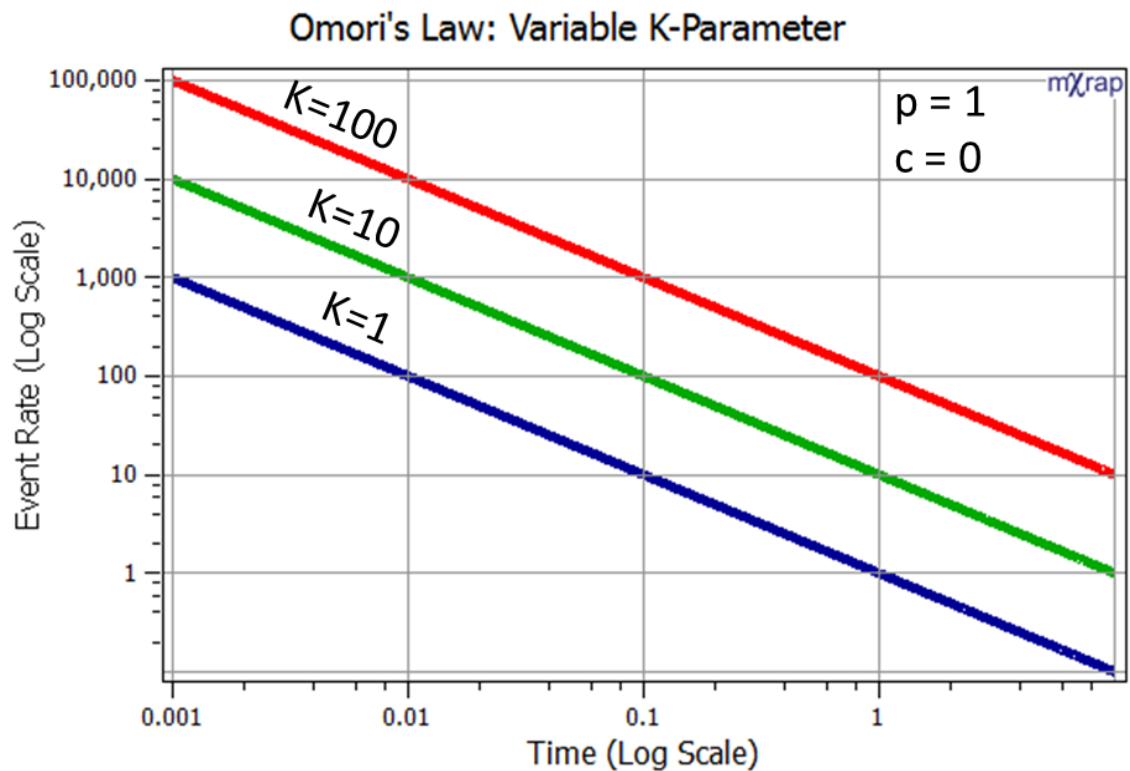
The most significant factors that control the decay rate of responses are not definitive for mining induced seismicity. While definitive conclusions were not made, Vallejos and McKinnon (2010b) suggested p-parameters were influenced by specific mining environments.

Dieterich (1994) considered an experimentally derived, numerical model of seismicity following a stress change on a fault system. The model developed provided a theoretical framework for interpreting the p-parameter. The fault system results in a  $p = 1$  if consistent stress and model parameters are used. Deviations of  $p < 1$  can be achieved by applying a non-uniform stress change. Various p-values may be observed if stress decreases with time.

Understanding the relationship between the decay rates of seismic responses has the potential to impact management of short-term seismic hazard and is a significant motivation to assess the relationship between the p-parameter and factors that influence mining seismicity. The factors that influence seismicity and the decay rate of responses may vary over space and time and, therefore, developing a method to identify and delineate seismic responses is essential to facilitate improvements to the quantification of seismic response hazard.

### 2.5.5 K-Parameter

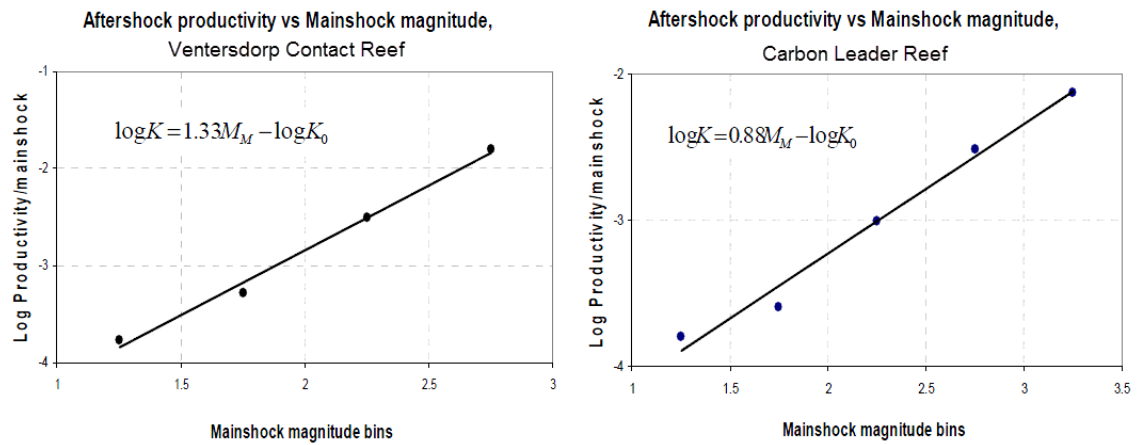
The K-parameter is proportional to the productivity of a seismic response. **Figure 23** shows the impact that varying K-values have on the MOL event rate. Additional parameters are kept constant ( $p = 1$  and  $c = 0$ ) for a time interval between 0.001 and 10 arbitrary time units.



**Figure 23** The impact that varying K-values have on the event rate (log scale) is given by the MOL. Additional parameters are kept constant ( $p = 1$  and  $c = 0$ ) for a time interval between 0.001 and 10 arbitrary time units (log scale).

The numerical values of the K-parameter are expressed on an arbitrary scale due to the site-specific nature of seismic monitoring. Vallejos and McKinnon (2010a) reported K-values between 0 and 80 for routine seismic monitoring, while Plenkers et al. (2010) report values that were between 380 and 760 for Acoustic Emission monitoring.

It is generally accepted that the mainshock magnitude significantly influences the productivity of an aftershock response (Reasenber 1985; Reasenber & Jones 1989). There are mixed observations for correlations between mainshock magnitude and the productivity of mining induced seismicity. Kwiitek (2004) found that no correlation existed for the analysis of responses to large events while also noting that there was a large degree of variation in responses for similar sized events. In contrast, a correlation was established between mainshock magnitude and aftershock productivity for two South African mines (Kgarume, Spottiswoode & Durrheim 2010b) (**Figure 24**).



**Figure 24** Scatter plot showing the correlation between aftershock productivity and mainshock magnitude for two South African mines. The best-fit relationship is shown on each plot.

There is some evidence to suggest that K-values may be influenced by mainshock magnitude for mining induced seismicity, although, many seismic responses cannot be attributed to a mainshock. The productivity of these responses will be controlled by alternative factors. In two South African mines, it was found that productivity was statistically correlated to mining factors by splitting responses into two populations based on the median distribution values of geology, stress, and strain conditions. Individually, these correlations were not strong enough to be considered as major influences (Kgarume 2010).

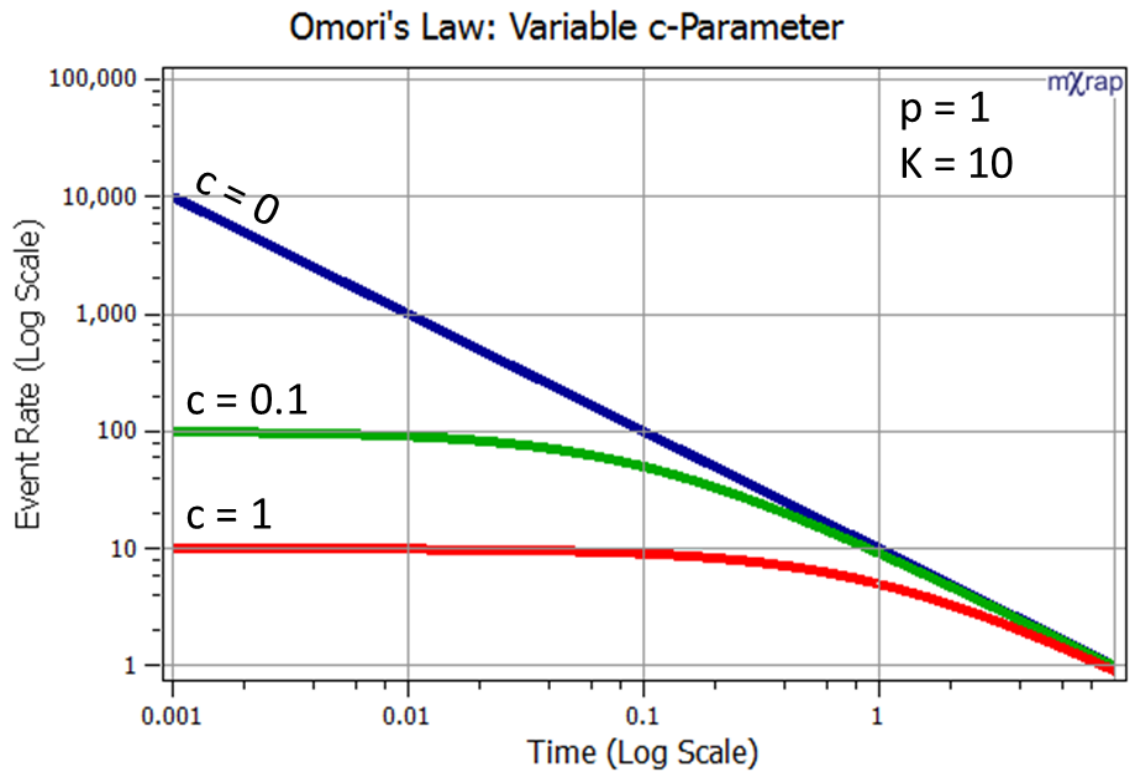
The cumulative number of events generated by a seismic response is related to the K-value by the modelling time interval, p-value, and c-value. For a study of Canadian mines, the K-values of 252 responses were proportional to the number of events for a seismic response (Vallejos & McKinnon 2011). This result indicates that the modelling period, p-value, and c-value can be represented by a constant. Additionally, Vallejos and McKinnon (2011) found that K-values are proportional to the volume blasted due to an increased stress change associated with larger blasts. Moreover, it was found that deeper mining increased seismic productivity and, therefore, indicated a dependency on *in situ* stress. They suggested that the variation observed in seismic responses productivity may be due to the influence of source mechanisms.

### 2.5.6 c-Parameter

The c-parameter has two roles: firstly, to avoid the divergence of the MOL when time is zero (Molchan & Dmitrieva 1992; Gross & Kisslinger 1994), and secondly, to account for less seismic events being observed during early time intervals (Utsu, Ogata & Matsu'ura 1995). The observation of proportionally less events soon after a mainshock is a phenomenon referred to as Early Aftershock Deficiency (EAD). There is a positive correlation between the c-parameter and p-parameter due to the interplay of these parameters within the MLE procedure

(Gasperini & Lolli 2006). It is important to understand and limit the influence of the  $c$ -parameter to minimise the potential for bias in the quantification of the  $p$ -parameter.

**Figure 25** illustrates the impact that varying  $c$ -values have on the MOL event rate. Additional parameters are kept constant ( $p = 1$  and  $K = 10$ ) for a time interval between 0.001 and 10 arbitrary time units.



**Figure 25** The impact that varying  $c$ -values have on the event rate given by the MOL. Additional parameters are kept constant ( $p = 1$  and  $K = 10$ ) for a time interval (log scale) between 0.001 and 10 arbitrary time units (log scale).

The deficiency in early seismicity is commonly attributed to two main causes. Firstly, EAD may be attributed to a breakdown in the power-law behaviour at times close to the initial earthquake rupture (Kagan 2004). Secondly, EAD may also be attributed to an inability to consistently record seismicity soon after a large seismic event due to overlapping waveforms along with additional monitoring constraints (Kagan 2004; Kagan 2006). Peng, Vidale and Houston (2006) considered the limitations to seismic monitoring soon after mainshocks to justify the selection of a modelling interval. Scrutinising mainshock coda resulted in the identification of additional aftershocks, although, subsequent assessment indicated that the frequency of events was not consistent with expected rates. This suggested the persistent EAD was a result of a physical process and not entirely a result of monitoring. It was concluded that an EAD might still exist irrespective of coda processing and monitoring limitations.

Enescu et al. (2009) did not support the notion that EAD is due to a physical process for a study of four moderate Japanese earthquakes. They conclude that commonly determined c-values greater than a few minutes are due to the incompleteness of seismic records and statistical variation. The c-parameter for southern Californian aftershock responses were attributed to the monitoring limitations and superposition of seismic records. Furthermore, the completeness of seismic records was empirically related to mainshock magnitude and the time after the mainshock (Helmstetter, Kagan & Jackson 2005) (**Equation 11**).

$$m_c(t, m_M) = m_M - a - b \log_{10}(t) \quad \text{Equation 11}$$

Where;

$m_c(t, m_M)$ : Magnitude of completeness

$m_M$ : Mainshock magnitude

$t$ : Time since mainshock

$a, b$ : Constants

For a study of mining induced aftershock responses, Kgarume (2010) suggested that the c-parameter has no physical significance and was an artefact of the seismic monitoring system. For seismic responses to large events within two South African mines, it took at most twenty seconds to re-establish seismic monitoring sensitivity (Kgarume 2010). Spottiswoode (2000) studied stacked aftershocks and blasting induced responses for four South African mines and also attributed EAD to monitoring limitations. For these responses, c-values were found to range from zero to six seconds with one exception of 20 seconds. These findings are supported by Vallejos and McKinnon (2010a) who were not consistently able to fit a rate model to the non-power behaviour observed at the start of time-dependent responses.

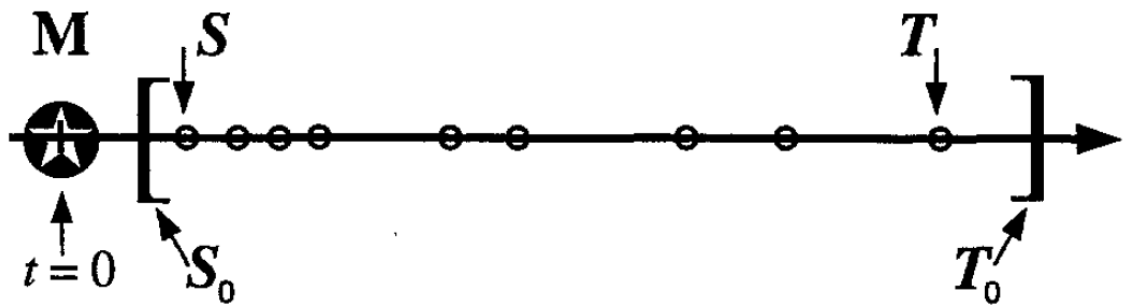
### 2.5.7 Modelling Time Interval

The selection of the modelling period is a decision of which events are well modelled by the MOL and has a significant impact on the quantification of MOL parameters. Due to the sensitivity of the MOL parameters to the modelling period, its selection is an important consideration when achieving consistent and representative results (Narteau, Shebalin & Holschneider 2002).

Determining the MOL parameters and their uncertainties is a simple process and is typically estimated through the maximisation of the log-likelihood function for a given modelling interval. Despite the ease that MOL parameters can be found, there is no best method for selecting the time interval for modelling a seismic response. Approaches to selecting this period vary between studies and can have a significant impact on the applicability of a power-law decay, the determination of the MOL parameters, and their uncertainties (Narteau,

Shebalin & Holschneider 2002). Nyffenegger and Frohlich (1998) provided a general framework for considering aftershock responses (**Figure 26**):

- A principal event is defined at time  $t = 0$ ;
- Aftershocks occur after a time delay from the mainshock over an interval  $[S_0, T_0]$ ; and
- Modelled events are delineated by the earliest and latest aftershock  $[S, T]$ .



**Figure 26** A mainshock occurs at  $t=0$  and events occur over the interval  $[S_0, T_0]$ . The modelling interval  $[S, T]$  is delineated by the first and last aftershock.

To test statistical models, Ogata (1983) considers the events which occur during a time interval  $[S, T]$  with respect to various time interval subsets and the assessment of the Akaike Information Criterion. The MOL parameters for the Niigata earthquake (7.5 M) are found to be nearly identical for the interval  $[0, 100]$  days in comparison to the interval  $[1/2, 100]$  days. In contrast, the selection of the time 'S' significantly influences parameter determination for the Fukui earthquake (7.3 M), particularly for c-values (**Table 5**). These findings introduce the concept that aftershock behaviour during early periods may be variable and may influence MOL parameters when excluded.

**Table 5** Changes to parameter determination for the Niigata earthquake (M7.5) 1964 based on the start of the time interval  $[S, T]$ . Reproduced from Ogata (1983).

Parameter	S = 1/2 day	S = 0 days
K	141.38±24.07	250.66±37.57
c	0.11±0.11	0.54±0.91
p	1.36±0.06	1.53±0.06

Selecting a modelling interval aims to address the complexities associated with a variable an EAD and attempts to ensure the interval can be appropriately modelled. Studies have taken different approaches to determine consistent and representative modelling parameters. These approaches typically focus on the selection of an appropriate modelling interval and manipulating the range of possible values of the c-parameter.

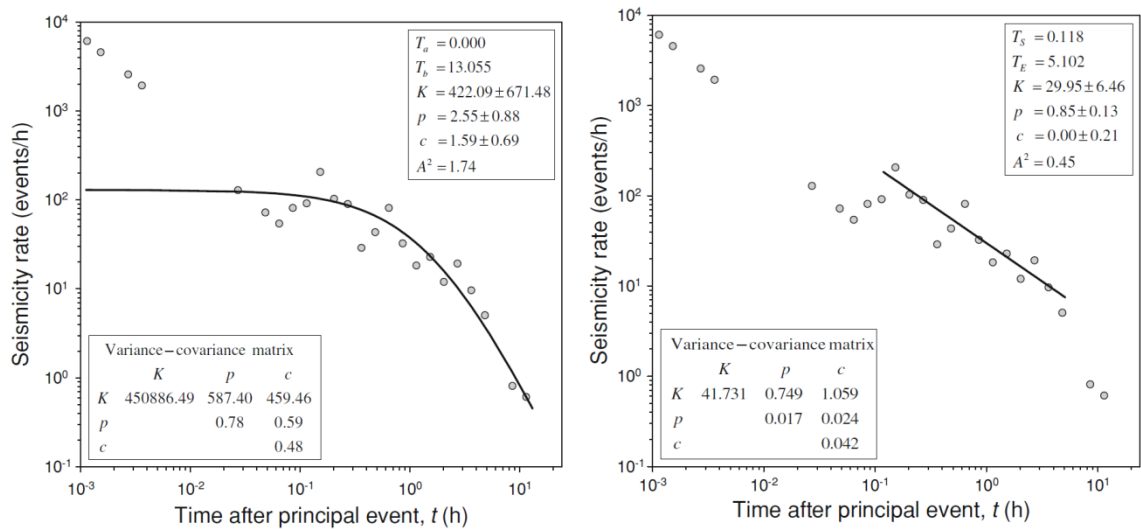
Davis and Frohlich (1991a) defined an arbitrary period after a mainshock based on a visual inspection and imposed a fixed c-parameter, e.g., a time interval for 0.1 to 20 days and a c-value of 0.003 days. In a similar approach, Bohnenstiehl et al. (2002) examined the early portions of earthquake responses and if a significant change in event rate was noted, the start of the response that provided the best relative fit was selected from a range of values. Nyffenegger (1998) cautioned against limiting the modelling interval of seismic responses without due consideration and highlighted these concerns are by modelling different intervals of synthetic responses. Nyffenegger (1998) also selected a time interval based on visual inspection of aftershock rates and considered solutions with c-values fixed at zero or, alternatively, allowed to vary. Based on the assessment interval and if the c-value was fixed or variable, it was found for different approaches that p-values differed by up to 0.77. While variation in p-values was reduced to approximately 0.1 by considering the Anderson-Darling statistic, variation was still significant in some cases (up to 0.4). These methods rely on qualitative visual inspection to validate modelling intervals for individual seismic responses.

Spottiswoode (2000) discussed a broad definition of mining induced responses for South African mining environments, noting the ambiguity in defining seismic responses. If any particular event is defined as a mainshock, then events preceding or following are considered foreshocks and aftershocks, respectively. This study assesses stacked foreshocks, aftershocks, and blasting induced responses from four similar mines. Kgarume, Spottiswoode and Durrheim (2010a) considers events greater than 2 M to be mainshocks and considers a stacked aftershocks assessment of events within a 24 h period. Events were modelled if they occur from fifteen seconds to one day after the mainshock.

In preliminary studies of mining induced seismicity, Vallejos and McKinnon (2010a) found that MOL parameters were impractically sensitive to the selection of the modelling interval. The study presented a method to exclude events at the start and end of the seismic response to achieve consistent estimates of parameters. Events could be eliminated to ensure only strict power-law behaviour was modelled ( $c$ -value = 0 and Anderson-Darling statistic  $\leq 1$ ). MOL parameters are determined for a time interval that is automatically selected for each seismic response that improves the fit of the MOL and significantly reduces parameter uncertainty. Their procedure of refining a time interval for modelling is summarised by the following steps:

1. Inter-event times define possible start and end times of the modelling interval  $[T_s, T_E]$ .
2. Considering modelling intervals that have solutions which have:
  - Anderson-Darling statistic  $\leq 1$ ;
  - $c$ -value = 0; and
  - A time of maximum curvature ( $T_{MC}$ ) within the interval  $[T_s, T_E]$ .
3. A reference time interval is set to be the solution that maximises  $T_{MC} - T_a$ .
  - Reference time interval is defined as  $[T_{ar}, T_{br}]$ ; and
  - Reference  $p$ -parameter is set as  $p_r \pm \sigma p_r$
4. The final solution interval  $[T_s, T_E]$  is selected that:
  - Maximise the ratio  $T_b/T_a$ ;
  - Has a  $T_a \leq T_{ar}$  and  $T_{br} \leq T_b$ ; and
  - A  $p$ -value within 95% confidence of the reference  $p$ -value.

Vallejos and McKinnon (2010a) provided an example of using this method to select a time interval for modelling. The MOL is applied to an initial modelling interval and results in high uncertainty in erroneous MOL parameters. The MOL adequately models seismicity according to an Anderson-Darling statistic, although, does not model aftershock behaviour during an initial short interval (**Figure 27** left). The modelling interval is refined to exclude events occurring at short and long time intervals. As a result, parameters are within previously reported ranges, there is a reduction to the uncertainty associated with MOL parameters, and the Anderson-Darling statistic is improved (**Figure 27** right).



**Figure 27** Left: MOL parameter determined from the interval  $[T_a, T_b]$ . Right: MOL parameter determined from the interval  $[T_s, T_E]$  by an algorithmic approach.

The MOL is well established and widely used to describe the temporal occurrence of earthquake aftershocks and mining induced seismicity. While the physical interpretations of the p-parameter are not conclusive, the decay rate of seismicity may relate to the rate of rock mass relaxation. The K-parameter is related to the productivity of a seismic response and is correlated to factors that drive seismicity. The c-parameter is an artefact due to the deficiency of early aftershocks most likely caused by seismic monitoring limitations. This parameter is deleterious to modelling due to its interdependency with the p-parameter. Typically, the c-parameter is minimised by selecting an interval that can be appropriately modelled by a power-law. The selection of the modelling interval has a significant impact on parameters, particularly when excluding early periods of events. Best practice has not been established when selecting a modelling interval for mining or earthquake responses.

## 2.6 Literature Review Conclusions

The following conclusions can be drawn from the review of the spatial and temporal characteristics of mining induced seismicity, the analysis of spatially and temporally clustered seismicity, and applicable scaling laws (Chapter 2). The reviewed literature provides a foundation for understanding the spatial and temporal characteristics of seismicity that is essential for the effective management of mining induced seismic hazard.

### 2.6.1 Spatial Characteristics of Mining Induced Seismicity

- Seismicity results from various rock mass failure mechanisms for mining environments.
- Rock mass failure mechanisms are broadly considered as seismic source mechanisms characterised by conditions resulting in seismicity.
- Classification schemes for seismic source mechanisms vary based on the scope and context of the studies, although, general source mechanism classifications are analogous throughout literature, e.g., volumetric and shear failure.
- Sources of seismicity are spatially controlled by factors including, but, not limited to:
  - Excavation geometry (development, stoping, pillars, abutments etc.);
  - Geological features (faulting, dykes, etc.); and
  - Rock mass properties (rock strength, frequency of discontinuities, etc.);
- Sources of seismicity are temporally influenced by factors that evolve over time such as stress conditions.
- The potential for large seismic events is controlled by failure mechanisms and, therefore, delineating sources of seismicity is an important component to understanding seismic hazard.
- Considering sources of seismicity has practical benefits by simplifying seismic analysis.
- Magnitude-frequency relationships are widely applicable to the mining environment and are consistent for distinct sources of seismicity.
- Magnitude-frequency relationships quantify the limits of seismic monitoring (magnitude of completeness  $M_c$ ) and the distribution of event magnitudes (b-value).
- b-values characterise sources of seismicity constrained in space and time.
- Consistent magnitude-frequency relationships support the spatial and temporal characteristics for self-similar sources of seismicity.

### 2.6.2 Temporal Characteristics of Mining Induced Seismicity

- There is significant uncertainty surrounding the factors that contribute to the temporal attributes of mining induced seismicity.
- Temporal characteristics of seismicity are analogous to the temporal characteristics of earthquakes and are considered with respect to two broad categories:
  - Time-independent seismicity (background) that typically follows a stationary Poisson process; and
  - Time-dependent seismicity (seismic responses) that typically follows a non-stationary Poisson process.
- No definitive theoretical foundation exists for the occurrence of background seismicity or seismic responses.
- Time-independent seismicity is considered as temporally independent and weakly spatially clustered.
- This seismicity is temporally represented by a single rate parameter that is synonymous with a stationary Poisson model.
- Accurate quantification of time-independent seismicity is important as these events are a major consideration for the management of seismic hazard with respect to:
  - Short-term re-entry decisions: When has a seismic response decayed to pre-existing conditions?
  - Long-term decisions: What portion of seismic hazard can only be managed using long-term strategies?
- Background seismicity is dependent on source mechanisms.
- Background seismicity is assessed by two general approaches:
  - The quantification of seismicity not associated with seismic responses. This method will typically result in an over-estimation of background seismicity due to the inability of current methods to delineate seismic responses.
  - The quantification of seismicity associated with periods of mining cessation. This method will typically result in an under-estimation of background seismicity as routine mining activities no longer influence stress conditions.
- The study and outcome of seismic responses in the mining environment is similar to earthquake mainshock-aftershock responses.

- Seismic responses contribute to the timing, location, and magnitude of seismic hazard and, therefore, are an important consideration in the management of seismic risk.
- There is significant variation in the characteristics of seismic responses following blasting or large seismic events.
- The spatial and temporal characteristics of seismic responses are related to sources of seismicity, although, only tentatively related to factors that contribute to rock mass failure.
- Isolated case studies show that time-dependent responses are intrinsically related to stress transfer mechanisms and can be generalised by two types of seismic responses:
  - Induced seismicity: A causative stress change is greater than or proportional to the observed seismic response.
  - Triggered seismicity: The causative stress changes are significantly less than the observed seismic response.

### **2.6.3 Analysis of Spatially and Temporally Clustered Seismicity**

- It is impossible to identify and delineate events that are associated with background or response seismicity without error.
- Routine activities in the mining environment may result in the spatial or temporal superimposition of seismic responses.
- There are limited studies that attempt to quantify temporal characteristics of spatially constrained responses and assess spatial and temporal relationships between responses and routine mining activities.
- The study of time-dependent seismicity comprises of three main components and aims to address three broad research questions:
  1. Response identification: Where and when do responses occur?
  2. Spatial delineation: Where do responses occur?
  3. Temporal delineation: When do responses start and finish?
- The outcomes of reviewed studies dictate if identification or delineation of responses is considered by assessing various combinations of the spatial, temporal, or magnitude attributes of time-dependent seismicity.

- The study of time-dependent earthquake occurrence explores a wider range of approaches. The majority of these methods employ assumptions that are not suitable for mining induced seismicity due to:
  - The reliance on magnitude of events for response identification;
  - Inability to account for superimposition of responses in space or time; or
  - The use of constants that inhibit the assessment of contrasting spatial and temporal densities associated with varied sources of mining induced seismicity.
- Quantification of mining induced seismic responses is limited, with the majority of studies focused on determining appropriate re-entry protocol criteria.
- For mining induced seismicity, temporal and spatial delineation are generally limited by arbitrarily defined space-time windows around blasting or large events. Methods have addressed aspects of response identification, temporal delineation, or spatial delineation.
- The temporal characteristics of mining induced seismicity are generally studied independently of spatial aspects and vice versa.
- Studies of mining induced seismicity do not provide a comprehensive method for the spatial and temporal, identification and delineation of mining induced seismic responses.

#### **2.6.4 Modified Omori Law**

- The MOL has been extensively applied to the study of earthquakes. Well-established methods exist to estimate the law's parameters and parameter uncertainty, and quantify the suitability of fit between the model and observations.
- A wide range of mining induced seismic responses has been modelled by the MOL.
- Other temporal models have been applied to mining induced seismicity and earthquake aftershocks. In comparison to the MOL, none of these models has shown to be consistently and significantly more representative of time-dependent behaviour.
- There is not a complete understanding of the relationship between MOL parameters and factors contributing to the occurrence of mining induced seismicity:
  - Decay rate (p-parameter): No clear relationships exist and are tentatively related to rate of rock mass relaxation.

- Productivity (K-parameter): Parameter has been related to mainshock magnitude, volume of blasted rock, and depth of mining.
- Time-offset (c-parameter): It is well accepted that the parameter is related to limitations of seismic monitoring and potentially related to the breakdown in power-law behaviour soon after response initiation.
- There is a range of approaches implemented for selecting a modelling time interval for mining induced seismicity and earthquakes.
- No single methodology is consistently applied to model spatially and temporally delineated seismic responses using the MOL.

## 2.7 Specific Issues Addressed in this Thesis

Literature that discusses the identification and delineation of seismic responses generally originates from the study of earthquakes. Comparable studies of mining induced seismic responses are limited due to the differences in the physical context and fields of research. Typically, the approaches developed for the assessment of seismic responses in the mining environment require the knowledge of the timing and location of blasting, or large seismic events and do not account for time-dependent seismicity that is not directly related to these causative processes. No single methodology exists that identifies and delineates seismic responses that address the five following requirements:

1. The identification of seismic responses using only spatial and temporal parameters to ensure all responses are captured independently of causation processes;
2. The spatial superimposition of responses due to spatially controlled rock mass failure;
3. The temporal superimposition of responses due to simultaneous causation processes;
4. Identification and delineation of responses for a range of spatial and temporal densities; and
5. Practical application to a large dataset while minimising subjective decisions.

This thesis will develop a comprehensive methodology to identify and delineate individual mining induced seismic responses while addressing the previously outlined challenges. To achieve this outcome, the assessment of time-dependent seismicity must be advanced through the creation, development, and integration of three fundamental research questions:

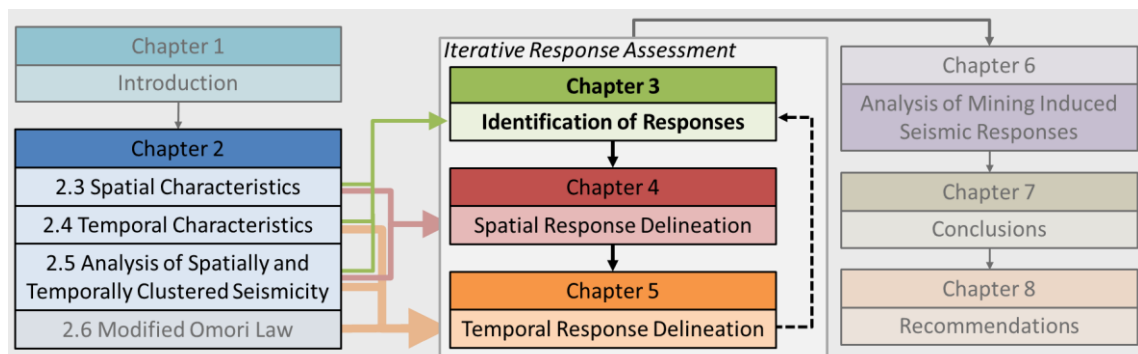
1. Identification of seismic responses: Where and when do responses occur?  
The identification of seismic responses is to be addressed through the creation of a methodology that identifies seismic responses in space and time, given the previously listed challenges specific to the mining environment;
2. Spatial delineation of related seismicity: What is the extent of responses in space?  
The spatial delineation of seismic responses is to be addressed through the development of a density-based clustering methodology that is appropriate for mining induced seismicity; and
3. Temporal delineation of related seismicity: When do responses start and finish?  
The temporal delineation and quantification of seismic responses is addressed through the development of methods that apply the MOL to mining induced seismicity.

An integrated methodology that identifies and delineates seismic responses facilitates statistical analysis of commonly observed source mechanisms throughout the mining environment. The assessment of the spatial and temporal characteristics of seismicity is a significant advancement in the quantification of seismic responses. This advancement provides an opportunity to develop an understanding of the cause and effect relationship between seismic responses, mining activities, and sources of seismicity. Developing an improved understanding of the characteristics associated with transient seismicity will ultimately improve the management mining induced seismic hazard.

### 3 Iterative Approach to the Identification of Mining Induced Seismic Responses

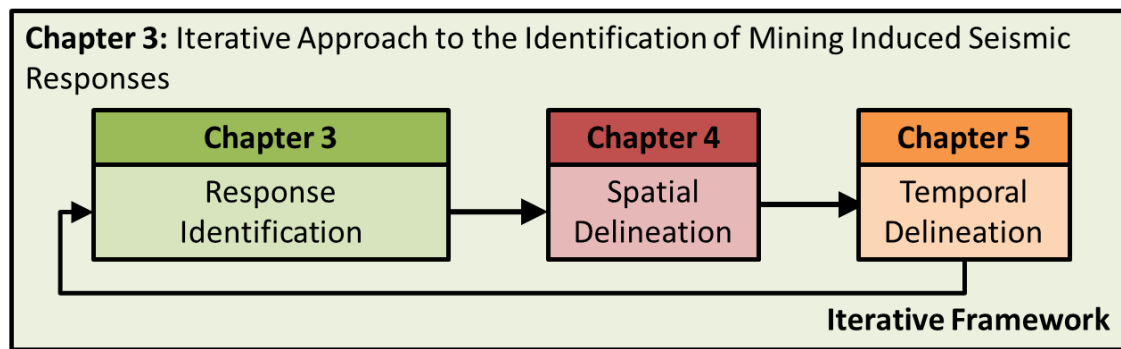
#### 3.1 Chapter Overview

This chapter formulates a generalised method for the identification of seismic responses that accounts for the spatial and temporal characteristics of mining induced seismicity while addressing the shortcomings of current methods. The identification method underpins the delineation of responses that is presented in Chapters 3 and 4 (**Figure 28**).



**Figure 28** The current chapter utilises findings from the literature review to develop a method to provide the identification of seismic response. This identification method underpins the spatial and temporal delineation of responses.

The identification of seismic responses has a number of components. Firstly, the procedure is required to evaluate when and where seismic responses occur. Secondly, once a response is identified, the method must delineate a subset of related events that can be refined by spatial and temporal modelling. Thirdly, the algorithm must provide a structured approach to identify seismic responses of various temporal and spatial scales. Fourthly, the method must be an iterative investigation of seismicity to delineate responses that are spatially or temporally superimposed. The focus of Chapter 3 is to provide the method and iterative framework for response identification. The following chapters address the spatial modelling (Chapter 4) and temporal modelling (Chapter 5) that is implemented within the iterative framework (**Figure 29**).



**Figure 29** The contribution of this chapter with respect to the iterative framework for response identification, spatial modelling, and temporal modelling.

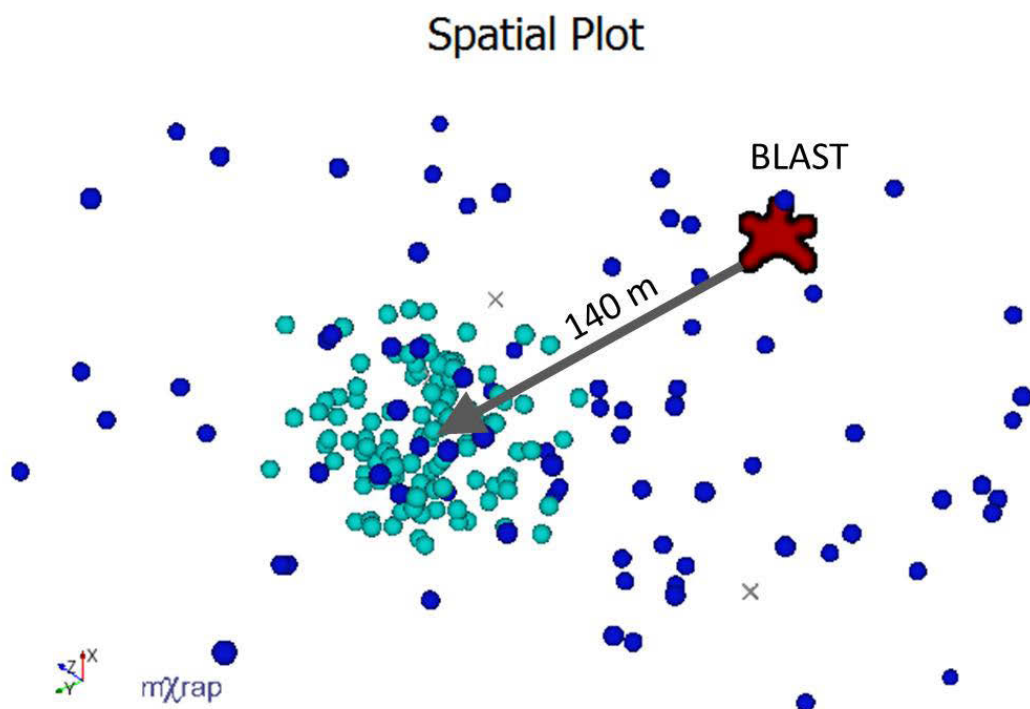
## 3.2 Introduction

The identification of seismic responses ideally provides the location and initiation time of seismic events that are spatially and temporally related. Literature reveals that the challenge of identifying seismic responses in the mining environment has been attempted with a number of approaches. These approaches include informal approaches, assessment of the time and location of blasting and large events, and the assessment of metrics. Additionally, these approaches are suboptimal for implementation into a generalised method to identify seismic responses on the basis that:

- They are labour intensive, potentially subjective, and manual analysis is required;
- The causation of seismic responses is assumed and there is a reliance on additional information, e.g., blasts and large seismic events;
- They fail to account for the spatial or temporal superimposition of seismicity; and
- A combination of seismic parameters is used together in a metric that reduces information describing the timing and location of a seismic response.

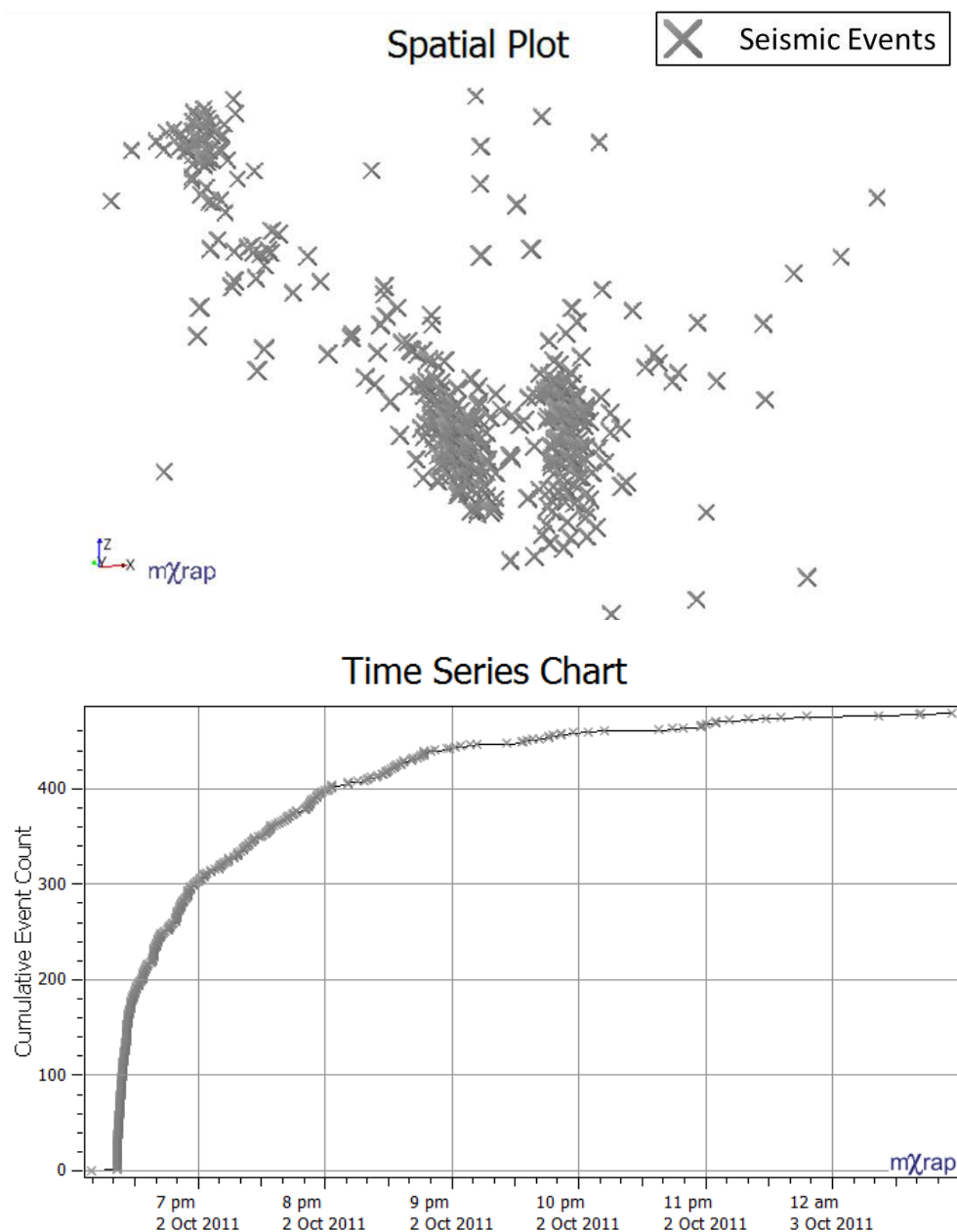
**Figure 30** provides an example of seismic responses to blasting within a mining environment. A seismic response (light blue) occurs immediately (within minutes of blasting), although, at a distance of 140 m away from the blast (red star). Another seismic response occurs on a larger scale and is relatively sparser (dark blue). Additionally, this sparse response is spatially superimposed on top of the dense response. This example illustrates two key requirements of seismic response identification:

1. Seismic responses may not be spatially related to localised stress changes. As a result, the identification of seismic responses should be conducted independently from non-seismic information. This consideration also addresses the pragmatic limitation of mine sites maintaining a complete and accurate blast database, particularly when trying to obtain and validate historical blast information for retrospective assessment.
2. Seismic responses may be superimposed in space and time whilst having very different spatial distributions. This configuration of seismic responses has an inherent component of ambiguity when trying to determine which specific seismic event belongs to which seismic response. If there is a clear difference in spatial distributions then the responses can be separated.



**Figure 30** A seismic response occurs immediately and 140 m away from blasting (light blue). An additional response is sparser and occurs on a larger scale (dark blue).

**Figure 31** builds on the concept that multiple seismic blasts may occur concurrently. This is an example of when one or more blasts have resulted in multiple seismic responses throughout the mine (**Figure 31** top). While three responses are clearly separate in space and relate to localised rock mass failure, an additional sparser response occurs on a mine-wide scale. These four responses have distinctive spatial distributions of varying geometries and densities and it is evident from the time series chart that these responses occur concurrently in time (**Figure 31** bottom). The identification of seismic responses is required to account for spatial and temporal superimposition while being insensitive to a range of spatial and temporal characteristics (e.g., geometries, densities, durations etc.).



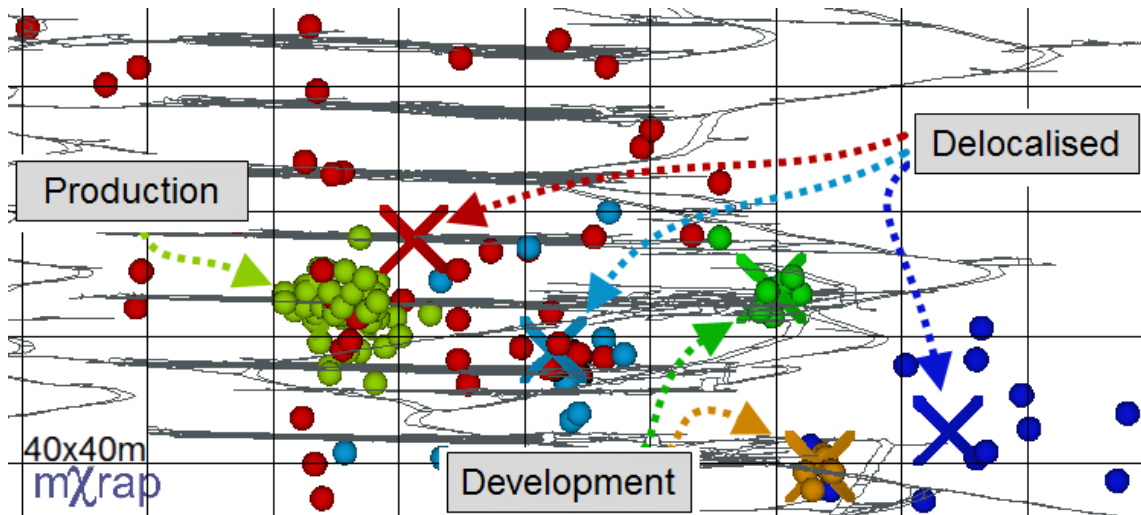
**Figure 31** Three responses are clearly separate in space and relate to localised rock mass failure throughout the mine. An additional response is sparser and occurs on a mine-wide scale (spatial plot). These responses occur concurrently in time (time series chart).

### **3.3 Seismic Response Identification using Spatial and Temporal Windows**

A new method is required to identify seismic responses while specifically addressing the challenges that are associated with mining induced seismicity. The approach should be as simple as possible while addressing the shortcomings of current methods.

The development of an appropriate method utilises existing concepts within the analysis of mining induced seismicity. A rudimentary technique is the implementation of spatial and temporal windows to partition seismic events. Spatial and temporal windows are commonly implemented in the assessment of mining induced seismicity around blasts and mainshocks to delineate responses. This simple approach has been successfully used for specific cases of seismic responses that are close, both spatially and temporally, to a known stress change, e.g., seismic responses locally and immediately induced by blasting. Whilst there are a number of drawbacks when using this method to delineate seismic responses, the fundamental concept of using spatial and temporal windows provides a basis for developing a method to identify seismic responses.

The applicability of spatial and temporal windows to identify seismic responses is linked to scales of occurrence for mining induced seismicity, e.g., localised rock mass failure associated with a 5 m x 5 m x 3 m development blast will typically occur on a spatial scale similar to the scale of blasting. For the scale of these rock mass failures, each event within the seismic response will have relatively more events close by in space and time than events that do not form part of this specific response. **Figure 32** provides an example of different scaled seismic responses that are related to the scale of their causative rock mass failure processes. This annotated figure shows seismicity occurring over 12 h and is related to development blasting ( $\approx 10$  m), production blasting ( $\approx 40$  m), and delocalised stress redistribution ( $>100$  m). For this example, three consistent scales are observable. Seismic events are coloured according to their spatial and temporal cluster while a cross illustrates the mean location of the cluster.



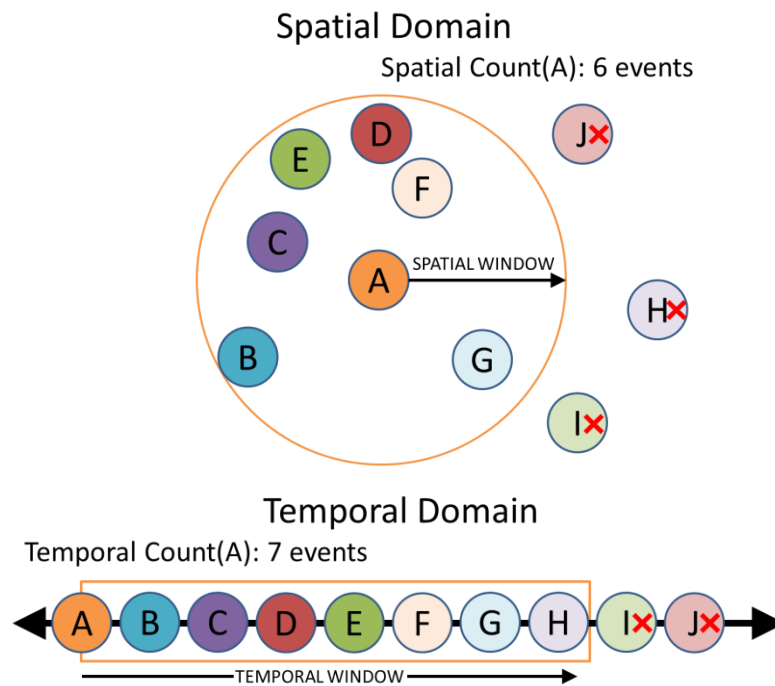
**Figure 32** Seismicity occurring over 12 h and is related to development blasting ( $\approx 10$  m), production blasting ( $\approx 40$  m), and delocalised stress redistribution ( $>100$  m).

When and where seismic responses occur on these scales is indicated by heightened rates of seismicity in space and time. A measure of the spatial and temporal rate of seismicity can be achieved by assessing the number of events that surround each event, i.e., for each seismic event find the number of subsequent neighbouring events. The definition of following neighbours is provided by using spatial and temporal windows that are characteristic of individual scales that exist within the mining environment, e.g., development blasting, production blasting, and delocalised processes. The site-specific configuration of the seismic monitoring network must be considered in order to limit analysis to only assess seismic events that are consistently and accurately observed.

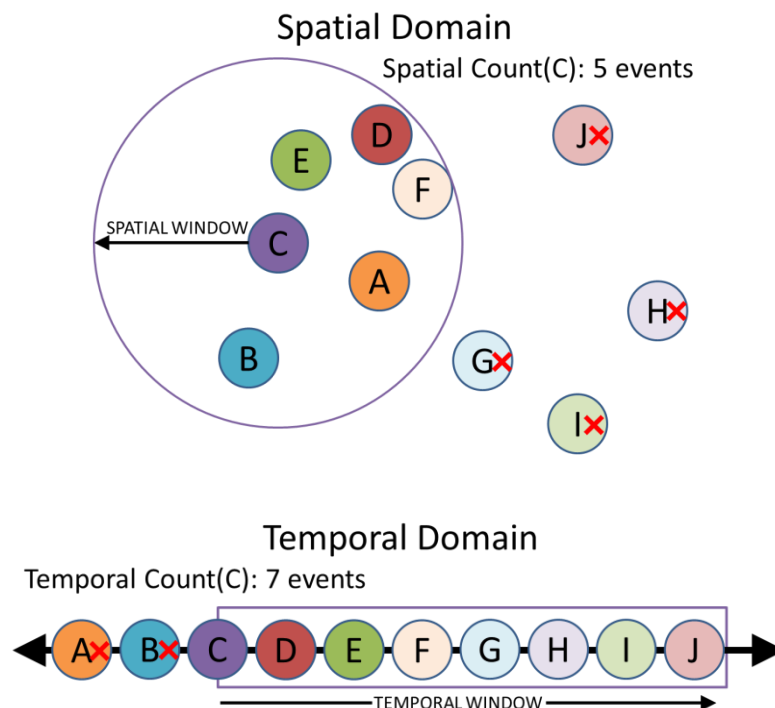
A simple method is used to assess the time and location of seismic events to determine a start of heightened seismicity in space and time. Response identification considers the density of event occurrence in space and time for every event with respect to three following parameters:

1. Spatial Window ( $S_W$ ): This parameter provides the Euclidean distance to define neighbouring events.
2. Temporal Window ( $T_W$ ): This parameter provides the period to define subsequent events.
3. Count Threshold ( $C_T$ ): This parameter provides the number of neighbouring and subsequent events required to define the beginning of a seismic response.

These three parameters are utilised by the fundamental approach of the method to count the number of neighbouring events occurring within a spatial window and subsequent events within a temporal window for every event in the dataset. Note that the order that events are considered does not influence the count of subsequent neighbours. An example of spatial and temporal counts, along with the resultant count of the intersection of the spatial and temporal criteria is shown in **Table 6**. This table also references figures representing the counts for Event A (**Figure 33** top: spatial and bottom: temporal) and Event C (**Figure 34** top: spatial and bottom: temporal). The start of a seismic response is identified if the intersection count is greater than the threshold count, with events being assessed in a reversed chronological order, e.g., first test  $N_J > C_T$ , then test  $N_I > C_T$  ... then test  $N_A > C_T$ . The test  $N_A > C_T$  is true and this event designates the start of a response. The time of this event and the mean location of successive neighbouring events provides an initial description of the seismic response.




**Figure 33** Top: Two-dimensional representation of counting neighbouring events in space. For Event A, six events are found within the spatial window and included in the spatial count. Bottom: Representation of counting subsequent events in time. Seven events are included in the temporal count for the temporal window following the occurrence of Event A.



**Figure 34** Top: Two-dimensional representation of counting neighbouring events in space. For Event C, five events are found within the spatial window and included in the spatial count. Bottom: Representation of counting subsequent events in time. Seven events are included in the temporal count for the temporal window following the occurrence of Event C.

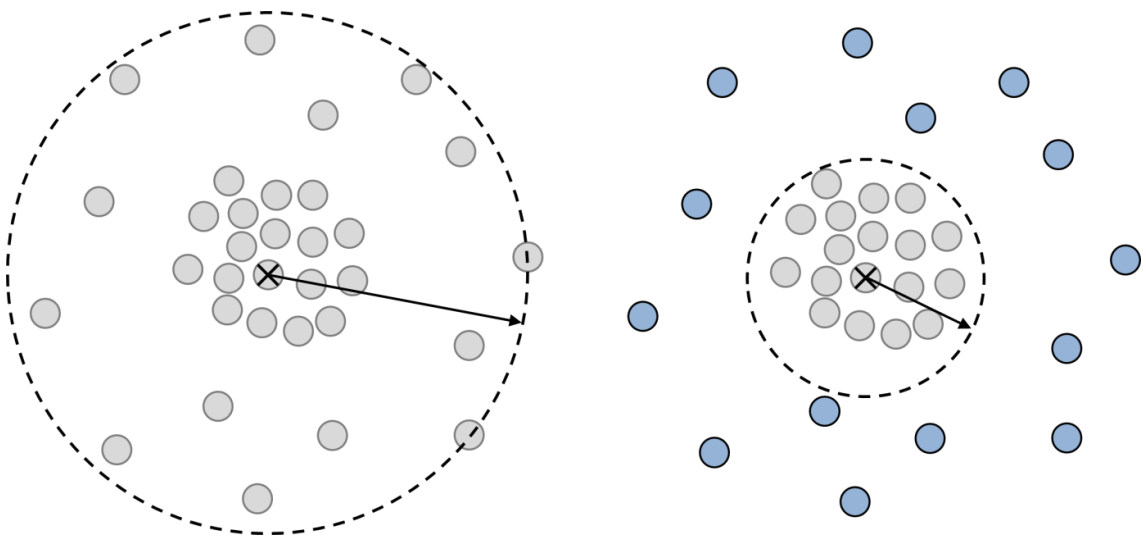
**Table 6** An example of the sequential spatial and temporal analysis of events to determine the beginning of a response. Search directions are given for the spatial component (3-D), temporal component (forwards), and response identification (backwards).

	Spatial Count If distance between $e_i$ and $e_{i+1..n-1} <$ spatial window	Temporal Count If time between $e_i$ and $e_{i+1..n-1} <$ temporal window	Intersection Count of the two criteria $N_i$	Response Identification count $N_i >$ count threshold	Search Direction reverse
<b>A</b>	6 (Figure 33 top)	7 (Figure 33 bottom)	6	<b>True</b>	
<b>B</b>	3	7	2	False	
<b>C</b>	5 (Figure 34 top)	7 (Figure 34 bottom)	3	False	
<b>D</b>	4	6	2	False	
<b>E</b>	4	5	1	False	
<b>F</b>	6	4	2	False	
<b>G</b>	4	3	2	False	
<b>H</b>	1	2	0	False	
<b>I</b>	3	1	0	False	
<b>J</b>	1	0	0	False	

While this information satisfies the initial objectives of identifying spatially and temporally dependent seismicity, additional methods must be employed to address all the challenges of identifying seismic responses. These challenges are addressed in the remainder of Chapter 3 by an iterative framework for the identification of additional seismic responses.

### 3.4 Iterative Method for Seismic Response Identification

The implementation of a complementary iterative technique is required to account for seismic responses of varying scales that may be superimposed spatially or temporally. It is inherently necessary to consider different scales of seismic responses to delineate the structure of varying densities. Furthermore, to ensure that spatially smaller, dense responses are not identified and modelled with significantly less dense, spatially larger responses, it is important to consider smaller dense spatial scales prior to large spatial scales. Spatial scales can be separated if smaller scales are identified and delineated first before considering larger spatial scales (**Figure 35**).



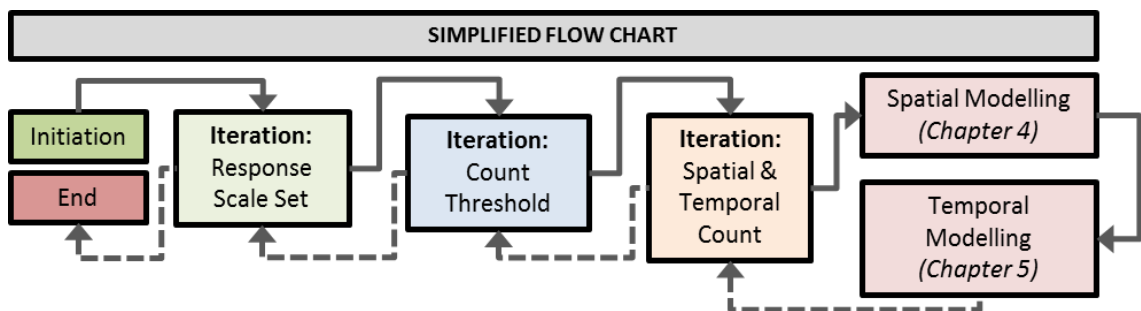
**Figure 35** Left: Small and large spatial scales are grouped together by assessing large spatial scales first. Right: Spatially smaller seismic responses can be identified within larger spatial scales if this scale is considered first.

This essential feature allows responses that are associated with sources of seismicity of different scales to be identified and delineated. For the previously presented example (**Figure 32**), three response scale sets would represent development blasting ( $\approx 10$  m), production blasting ( $\approx 40$  m), and delocalised stress redistribution ( $>100$  m). An iterative approach achieves structured response identification. These components are:

- Primary iteration (response scale set): Check sets of parameters that represent the scale of responses within the dataset. Consider the smallest to largest scale.
- Secondary iteration (count threshold): Check a range of count thresholds on the scale of responses defined in the primary iteration. Consider the most to least events; and
- Tertiary iteration (spatial and temporal count): For each event, check if the subsequent neighbour count surpasses the count threshold defined in the secondary iteration.

The primary and secondary iterations provide the structured approach that is required to assess responses of varying densities and scales. The tertiary iteration is the component that assesses the identification of seismic responses for each seismic event within a dataset. If a seismic response is identified (i.e., the tertiary iteration finds the number of subsequent neighbours is greater than or equal to the current count threshold) the seismic response is spatially and temporally delineated. Spatial and temporal delineation methods are presented in Chapter 4 and Chapter 5, respectively. The seismic response is removed from consideration by future iterations.

In summary, the algorithm comprises of three iterations. The primary iteration provides a spatial and temporal window that is characteristic of the response. The secondary iteration considers a range of count thresholds and is the criteria for identifying the initiation of a seismic response. A range of count thresholds are assessed before the scale of responses considered is increased by the primary iteration. The tertiary iteration assesses the number of subsequent neighbours for each event, with respect to the count threshold (provided by the second iteration) and scale window (provided by the primary iteration). The algorithm finishes once all response scale sets have been assessed for all count thresholds. The iterative functionality of this approach is illustrated by the simplified flow chart in **Figure 36**. A detailed flow chart is provided in **Figure 40** following a discussion of the practical implementation of the method.



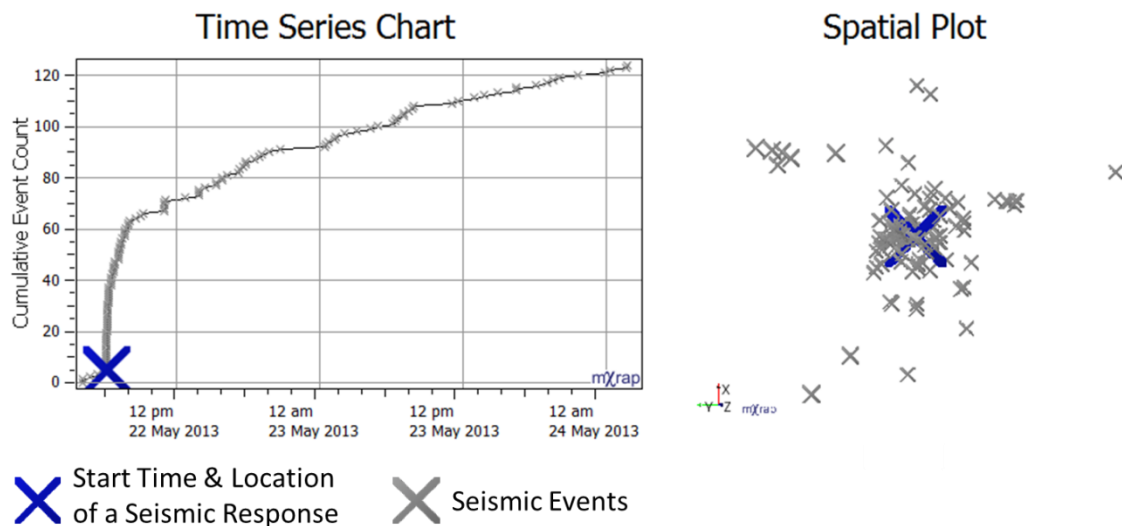
**Figure 36** Simplified flow chart of the interaction between response scale, count threshold, and spatial and temporal count aspects of seismic response identification. The initiation, modelling (Chapters 4 and 5), and end points of the algorithm are also represented.

### 3.4.1 Practical Implementation

As previously detailed, a temporal window ( $T_w$ ) and spatial window ( $S_w$ ) is required for the identification of seismic responses. Additionally, a count threshold is needed and is systematically manipulated during the count threshold iteration to preferentially model dense responses. The highest count threshold is found from initial assessment of the dataset, while the incremental change will only be a single event and, therefore, only the lowest count threshold ( $C_L$ ) is required. This parameter reflects the least number of events, on a particular

scale, that is tolerable to identify a seismic response. This parameter is set to ensure the identification of sufficiently strong seismic responses and is controlled by pragmatic considerations such as the time-independent portion of seismicity and the sensitivity of seismic monitoring.

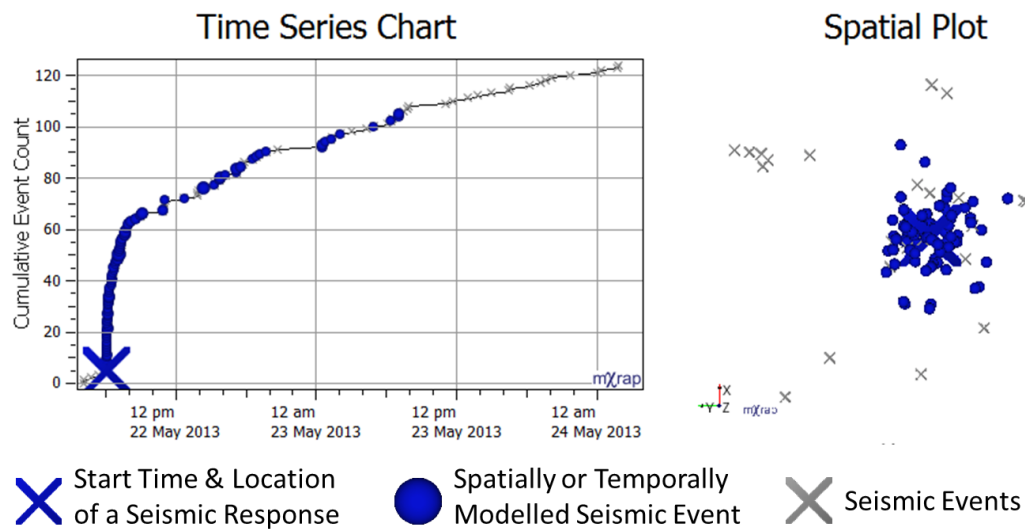
A number of shortcomings associated with other methods are addressed by implementing the seismic identification method using a decreasing lower count threshold. The method provides the location and initiation time of a cluster of related seismic events without the need for manual analysis, assumptions of causation, use non-seismic information, and the retention of spatial and temporal information describing the seismic response. This implementation of the method describes a seismic response by the time of the first event within a seismic response (**Figure 37** left) and the mean location of all subsequent neighbours of the first event (**Figure 37** right).



**Figure 37** Left: Time series showing the time that the response was identified (large blue cross) with respect to seismic events (grey crosses). Right: Spatial plot showing the mean location of the response (large blue cross) and events (grey crosses).

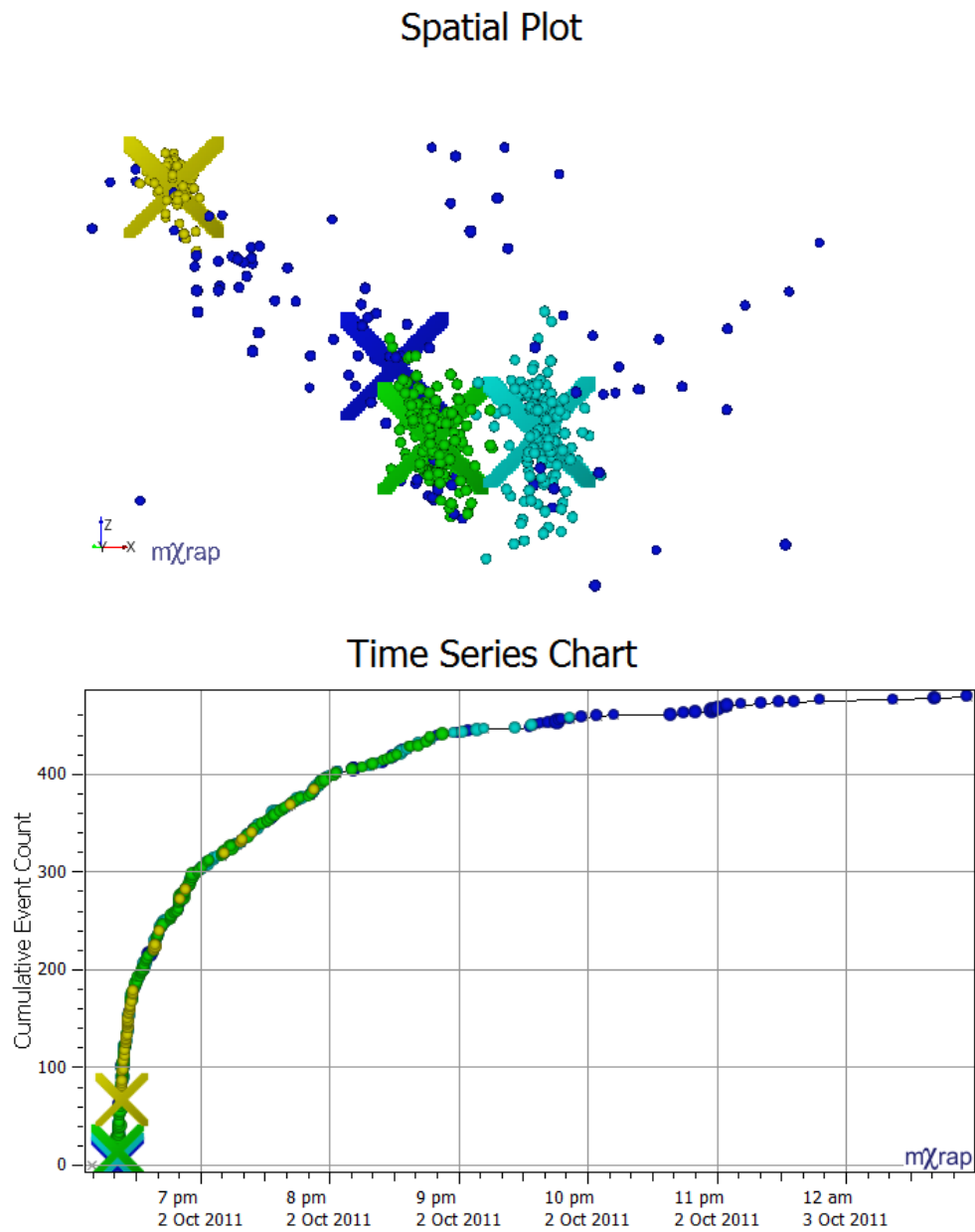
This approach provides the general information (timing and location of a seismic response) required to initiate spatial and temporal modelling. The delineation of a seismic response is a critical component to account for the spatial or temporal superimposition of seismicity on various scales. This is achieved by the modelling of events that follow the initiation of a seismic response and is enabled by the introduction of an additional temporal window. The temporal window ( $T_w$ ) that is used for response identification is relatively short, e.g., scale of minutes. In contrast, the additional temporal modelling window ( $T_M$ ) is required to conservatively reflect the observable length of seismic responses, e.g., scale of hours to days.

An iterative approach allows the accuracy of space and time identification of seismic responses to be improved by incorporating spatial and temporal modelling results. Spatial modelling identifies events that are spatially related to the response identified and contributes to a more representative refined mean location. Temporal modelling refines the initiation time of the response by determining an interval that is consistent with time-dependent event occurrence. The modelling results also delineate the seismic events that are spatially (**Figure 38** right) and temporally (**Figure 38** left) associated with the seismic response. This is a critical aspect of the method as the delineated events are removed from subsequent iterations that consider less dense responses over increasing spatial scales. The iterative removal functionality, in conjunction with the delineation of responses, accounts for the spatial or temporal superimposition of seismic responses on various scales.



**Figure 38** Left: Time series showing when the response was identified (large blue cross), the subsequently modelled events (blue spheres), and the events that have remained unmodelled (grey crosses). Right: Spatial plot of the mean location of the response (large blue cross), modelled events (blue spheres), and unmodelled events (grey crosses).

The seismic responses presented in **Figure 31** typify the need for identification to account for spatial and temporal superimposition on different scales. Implementing the iterative method as an automated algorithm results in three responses being identified and delineated from this dataset (light blue, green, and yellow spheres), along with a single sparse response (blue spheres) (**Figure 39** top). The initiation and mean location of these responses are represented with a cross of corresponding colour. The four seismic responses occur concurrently in time, although, do not initiate simultaneously and last for varying durations (**Figure 39** bottom).



**Figure 39** Top: Light blue, green, and yellow responses are separate in space and relate to localised rock mass failure. The dark blue response is sparser and occurs on a mine-wide scale. Bottom: Responses do not initiate simultaneously, although, occur concurrently, and last for varying durations.

### 3.4.2 Iterative Mining Induced Seismic Response Identification

A general description of the practical implementation of the complete iterative approach to response identification comprises of four main steps: Algorithm Initiation, Response Scale Set Iteration, Count Threshold Iteration, and Spatial and Temporal Count Iteration. This general description is supplemented by **Figure 40**, which provides a detailed flow chart of the algorithms iterative approach to seismic response identification.

#### **Algorithm Initiation**

- 1 Define  $U$  number of Response Scale Sets characteristic of seismic response and increasing in spatial scale. Each set comprises of:
  - a.  $S_W$  spatial window;
  - b.  $T_W$  temporal window;
  - c.  $C_L$  minimum number of events; and
  - d.  $T_M$  maximum response length.
- 2 Define the current response scale index as zero ( $u = 0$ ).
- 3 Define ( $n$ ) as the total number of events in the dataset.
- 4 **CONTINUE** to the Response Scale Set Iteration.

#### **Response Scale Set Iteration**

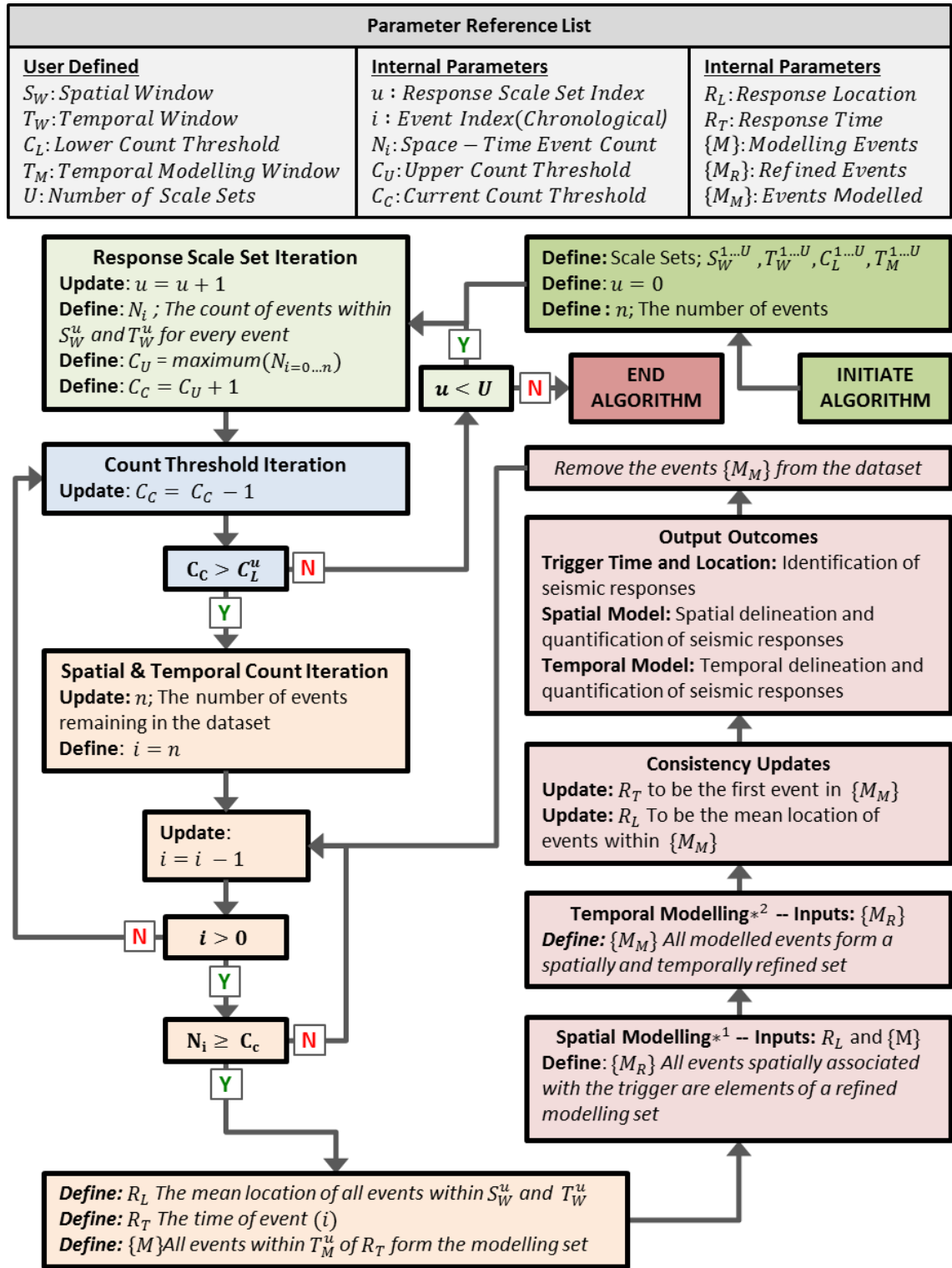
- 1 If the current response scale index is less than the total number of Response Scale Sets defined, **CONTINUE**, *otherwise* the algorithm **ENDS** (all scale sets have been checked).
  - a. Check the next response scale set ( $u = u + 1$ ).
  - b. Define the number of subsequent neighbours ( $N_i$ ) within  $S_W^u$  and  $T_W^u$  for every event ( $i$ ).
  - c. Define the upper count threshold ( $C_U$ ) as the highest subsequent neighbours count ( $N_i$ ).
  - d. Define the current count threshold ( $C_C$ ) as one more than the upper count threshold ( $C_C = C_U + 1$ ).
  - e. **CONTINUE** to the Count Threshold Iteration.

#### **Count Threshold Iteration**

- 1 Reduce the current count threshold by one ( $C_C = C_C - 1$ ).
- 2 If the current count threshold is greater than the lowest count threshold, **CONTINUE** to the Spatial and Temporal Count Iteration, *otherwise* **RETURN** to the Response Scale Set Iteration.

***Spatial and Temporal Count Iteration***

- 1 Update the number of events ( $n$ ) (events may have been removed in previous iterations).
- 2 Define the event index ( $i$ ) to be the last event in the dataset( $n$ ).
- 3 Evaluate the next Space-Time Event Count( $N_i$ ) in descending chronological order  $i = i - 1$ .
- 4 If this was not the last event in the dataset ( $i > 0$ ) **CONTINUE**, otherwise **RETURN** to Count Threshold Iteration.
- 5 If the count is greater than the current count threshold then **CONTINUE**, otherwise **RETURN** to Spatial and Temporal Count Iteration: Step 3 (evaluate the next ( $N_i$ )).
  - a. The event identifies a seismic response characterised by the time of the first event ( $R_T$ ) and the mean location of surrounding events( $R_L$ ).
  - b. All events within a modelling time window ( $T_M$ ) from the response ( $R_T$ ) are found and defined to be the set of modelling events  $\{M\}$ .
  - c. This initial set of events is  $\{M\}$  refined by:
    - i. Spatial modelling:  $\{M_R\}$  (Method detailed in Chapter 4).
    - ii. Temporal modelling:  $\{M_M\}$  (Method detailed in Chapter 5).
  - d. Events spatially and temporally modelled  $\{M_M\}$  are then removed from the dataset.
  - e. **RETURN** to Spatial and Temporal Count Iteration: Step 3 (evaluate the next ( $N_i$ )).



**Figure 40** Comprehensive flow chart detailing the iterative interaction between aspects of response identification. \*<sup>1</sup>Details of spatial modelling are presented in Chapter 4. \*<sup>2</sup>Details of temporal modelling are presented in Chapter 5.

### 3.5 Considerations and Limitations of User Defined Parameters

The limitations and considerations for the identification and delineation of responses using this method centre on the selection of appropriate parameters with respect to the attributes of the seismic dataset.

The identification of seismic responses utilises a simple approach requiring the user to define parameters that are relatable to the attributes of the data. The following discussion considers each parameter with respect to the:

- Influence of the parameter on assessment outcomes,
- Practical selection of parameter values,
- Approaches to reduce the sensitivity of assessment outcomes to the parameter; and
- Limitations associated with the parameter.

### **3.5.1 Spatial Window**

#### **3.5.1.1 Influence of the Parameter on Outcomes**

The spatial window is related to the physical scales of responses within the mining environment. To represent the spatial density of seismicity, the spatial window needs to be large enough to provide a sufficient sample given the scale of interest. If the spatial window is underestimated, then spatial variation will influence neighbouring event counts. Conversely, if the spatial window is overestimated then event counts become insensitive to localised changes in event density. Maintaining a contrast in event densities for different spatial scales is important to achieving meaningful and consistent seismic response identification.

The selection of an appropriate spatial window has the most influence of the identification and delineation of seismic responses. Seismic responses tend to share similar temporal scales and can have similar (minimum) event counts. As a result, the spatial scale is typically the most distinct feature of a seismic response. Due to a lack of distinction within the other aspects of seismic responses, the spatial scale becomes the most important consideration when attempting to separate superimposed responses.

The spatial window is also dependent on the ability of seismic monitoring to locate events accurately. Seismicity will be less well clustered for monitoring systems with poor location accuracy and, therefore, spatial windows will be relatively larger in comparison to accurate seismic monitoring.

### 3.5.1.2 Practical selection of parameter values

The selection of appropriate spatial windows focuses on two aspects of the spatial occurrence of events and relates to physical characteristics of the mining environment. These are:

- What scales are typical for this dataset? Spatial scales should provide a sample of seismicity on the typical dimension of typical rock mass failure. For example:
  - Localised responses to blasting: 10 m (development) or 40 m (production);
  - Geometric features: 30 to 50 m; and
  - Delocalised redistribution of stress: >100 m.
- What separation in scales should be expected to distinguish sources of seismicity? Scales should be different enough to ensure that each response scale is meaningful, e.g., selecting a scale of 15 m to capture responses to development blasting along with a 20 m scale to capture responses to production blasting will not provide a meaningful distinction given the inherent spatial uncertainties and inherent variation of event locations.

### 3.5.1.3 Approaches to Reduce the Sensitivity of Outcomes

The sensitivity of analysis to the selection of an appropriate spatial scale is reduced by the subsequent use of spatial modelling. The spatial window is only required to provide a sample of seismicity associated with a scale and, hence, the total extents of the seismic responses are inevitably underestimated. Spatial modelling of seismic responses allows the total extent to be delineated even if the spatial window does not accurately represent the spatial scale of identified. It is important to note that the leniency provided by spatial modelling is limited by considering small-scale responses first and only modelling similar spatial event densities. As a result, the propagation of the spatial model does not allow larger less dense responses to be modelled if responses are identified on a smaller scale. This important feature of spatial modelling enables the delineation of spatially superimposed responses.

### 3.5.1.4 Limitations associated with the parameter

Spatial scales of seismic responses can vary within a dataset as mining evolves over time. The optimal sets of spatial windows may not be the same for datasets as changes occur to spatial scales of rock mass failure. While this limitation is partially mitigated with the use of spatial modelling, the selection of suitable spatial windows are an important user defined parameters to achieve consistent and representative results.

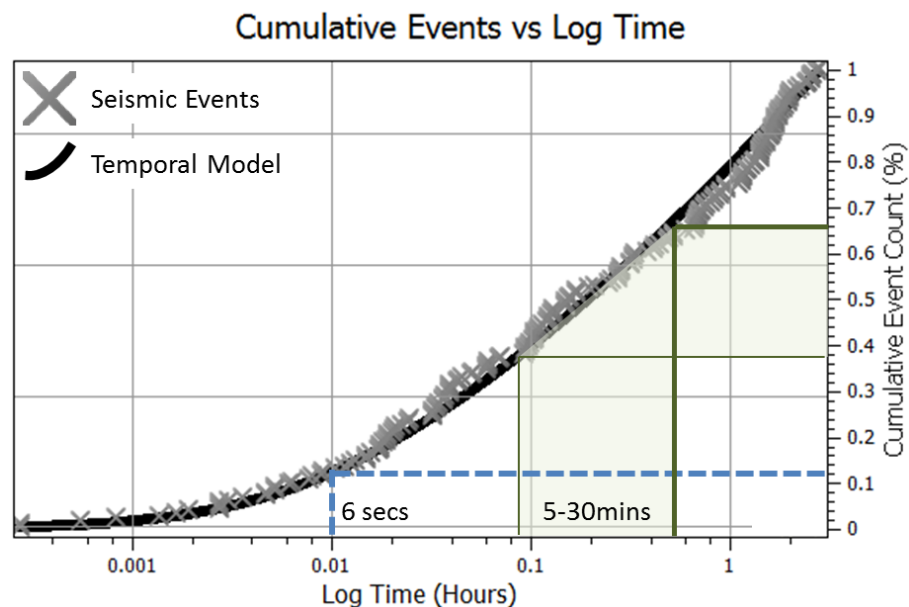
### 3.5.2 Temporal Window

#### 3.5.2.1 Influence of the Parameter on Outcomes

The selection of a temporal window is related to the time scale of seismic response initiation. The window needs to be large enough to provide a sufficient sample of subsequent events to represent the temporal density of a seismic response. If this window is underestimated, then subsequent event counts will be influenced by the variation in temporal event occurrence. Conversely, if the window is overestimated then the event counts will be insensitive to increases in the rate of seismicity.

#### 3.5.2.2 Practical Selection of Parameter Values

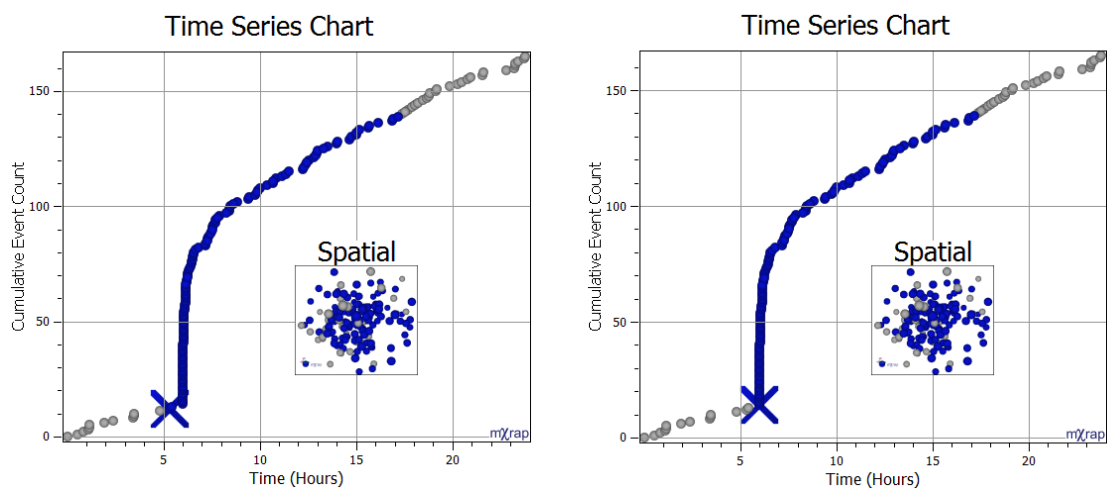
In contrast to the selection of the spatial window, analysis results are not sensitive to the selection of a temporal window. This is due to time-dependent seismicity typically following a power-law decay and, hence, the largest portion of seismicity occurs immediately after response initiation. A scale of minutes to tens of minutes is sufficient to represent an initial sample of the response. **Figure 41** illustrates the insensitivity of selecting a time window to capture a reasonable portion of a seismic response. Within a time window of 6 seconds from response initiation, 11% of events have occurred (blue dashed line) and may not be a sufficient sample. In contrast, using any time window between 5 and 30 minutes includes 40 to 65% of the response and captures a significant sample of the response (green lines and shaded area).



**Figure 41** Illustration of the insensitivity of selecting a time window to capture heightened rates of seismicity. Selecting a time window in the order of seconds provides a limited sample of seismicity (blue dashed lines). Increasing the time window to between 5 and 30 mins results in a significant portion of the response being sampled.

### 3.5.2.3 Approaches to Reduce the Sensitivity of Outcomes

The selection of a time window that is not long enough to provide a representative sample is not a major consideration due to the power law nature to temporal event occurrence. The inherent nature of temporal event occurrence does not safeguard against the selection of a time window that is too large. The use of a relatively large temporal window may result in the inclusion of events that have occurred before the response initiation. This occurs if the temporal attributes of the seismic response are similar to a chance temporal occurrence just prior to the initiation of the seismic response (**Figure 42** left). The temporal window can be adjusted (shortened) to account for chance occurrences of the events before response initiation. This will not assist in cases where the subsequent erroneous event occurs closer to the response. Instead, it is preferable to reduce the sensitivity of response identification to the selection of the temporal window. This is achieved by implementing temporal modelling that assesses which seismic events contribute to time-dependent behaviour and adjusting the response identification accordingly (**Figure 42** right).



**Figure 42** Seismic responses with a significant rate of time-independent seismicity. Left: Due to a large temporal window, the start of the seismic response has been found before the initiation of the response (large blue cross). Right: Temporal modelling adjusts the response start time to the initiation of the seismic response.

### 3.5.2.4 Limitations Associated with the Parameter

Due to the power law temporal behaviour of time-dependent seismicity and the built-in methods to mitigate potential errors, there are few limitations associated with the temporal window. The main limitation of the temporal window is the increased importance for temporal modelling to refine the initiation time of the response correctly. In addition, the selection of appropriate temporal windows may be hindered if seismic responses vary greatly with respect to temporal occurrence, particularly for early periods after a response initiation.

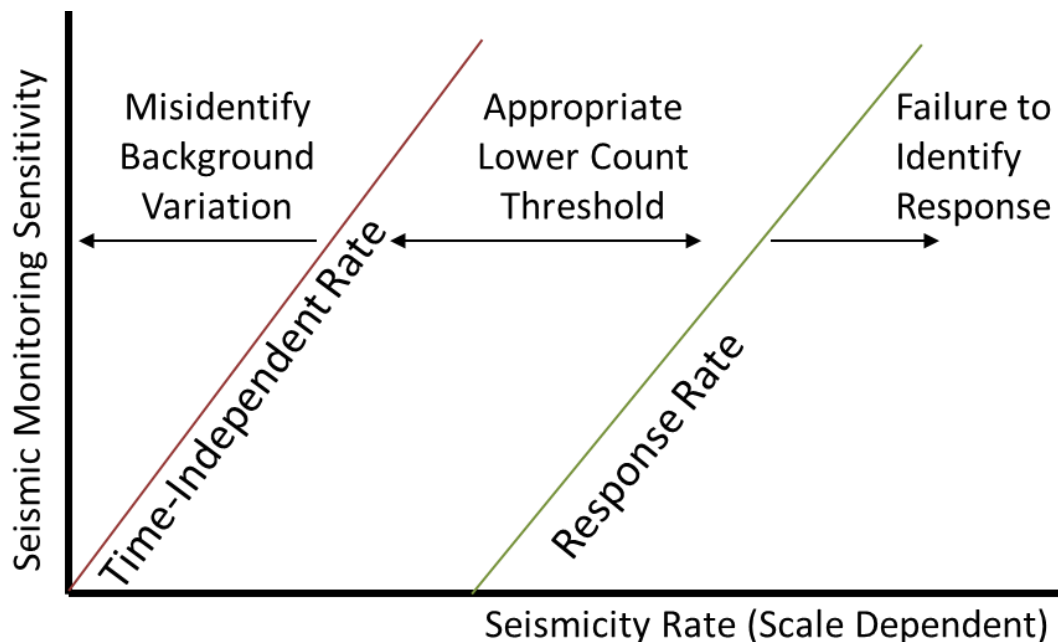
### 3.5.3 Lower Count Threshold

#### 3.5.3.1 Influence of the Parameter on Outcomes

The lowest count threshold represents the lowest spatial and temporal density that is required to form a response. The selection of the lower threshold aims to maximise the number of seismic responses identified and must ensure that responses are not falsely identified due to spatial and temporal variation.

#### 3.5.3.2 Practical Selection of Parameter Values

The selection of an appropriate lower count threshold is dependent on the sensitivity of the seismic monitoring system, time-independent rate of seismicity, and the rate of the seismic response (**Figure 43**). An appropriate lower count threshold is specified between the time-independent and response event rates. The lower count threshold may be higher or lower, based on the ability of seismic monitoring to observe responses. The sensitivity of analysis results, when selecting an appropriate lower count threshold, depends on the contrast between time-independent and response rates. As time-independent rates of seismicity become higher relative to the number of events associated with a seismic response, the temporal occurrence of a seismic response will be similar to variations in ambient seismicity.



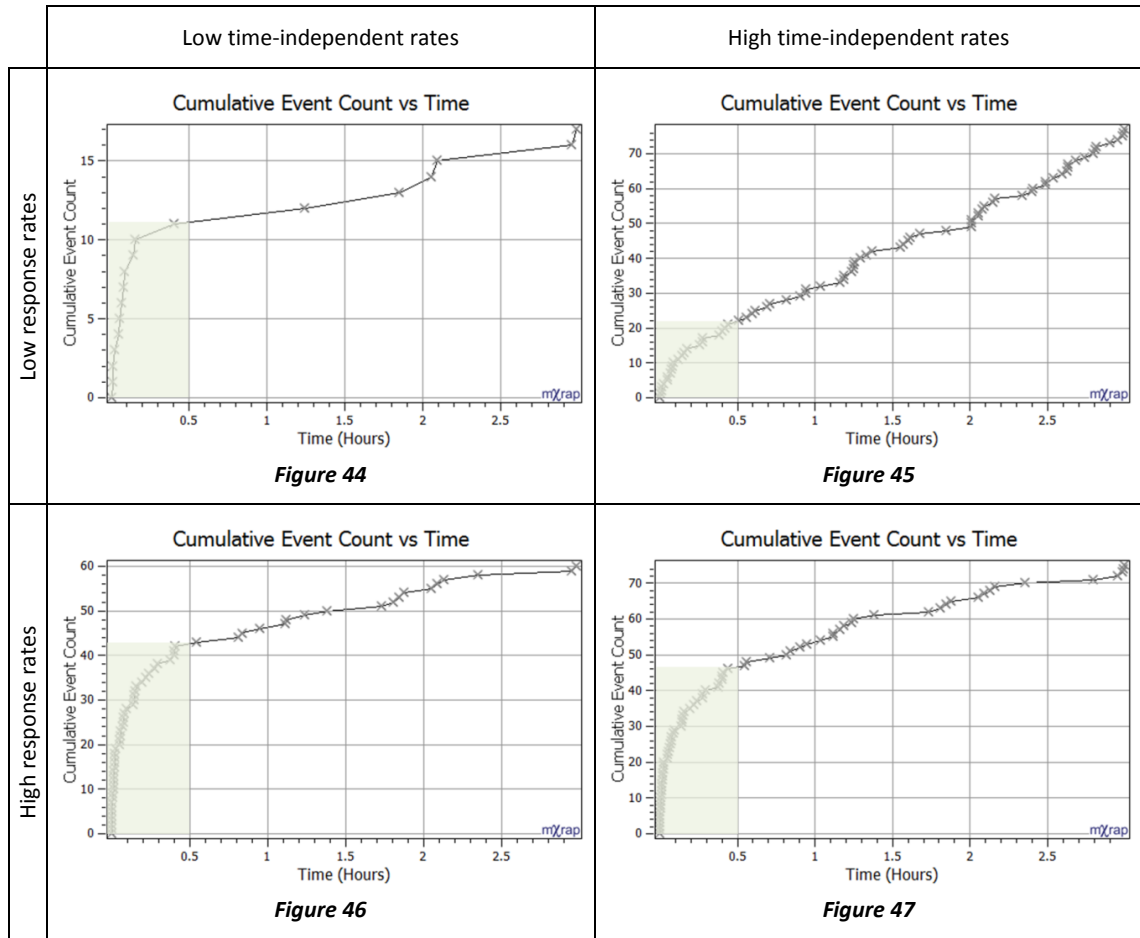
**Figure 43** Representation of the selection of the lower count threshold with respect to seismic monitoring sensitivity, time-independent rate, and response rate. Selecting an appropriate lower count threshold depends on the contrast between time-independent and response rates, along with the ability of seismic monitoring to observe seismic events.

To illustrate the considerations associated with the selection of a lower count threshold, a number of supplementary examples are provided in **Table 7**. These figures show low and high response rates that are temporally superimposed with low and high time-independent rates. The number of events within the time window is shown by shaded areas and is the lowest count threshold required to identify this response.

The lowest count threshold is selected based on considering three aspects of the seismic data set. These considerations are:

- What is the sensitivity of the seismic monitoring system?
  - Sensitive monitoring will increase response and time-independent rates of seismicity and lower count thresholds will have to be set relatively higher.
- For a given spatial and temporal scale, what is the minimum number of seismic events that will indicate the initiation of a seismic response?
  - Smaller responses require lower thresholds to be identified (e.g., **Figure 44**: 12 events), in comparison to larger responses (e.g., **Figure 46**: 42 events).
- What is the influence of the time-independent rate of seismicity likely to be for this spatial and temporal scale?
  - If time-independent seismicity is high on this scale then the lower count threshold must be relatively higher to ensure significant responses are identified (e.g., **Figure 44**: 12 events in comparison to **Figure 45**: 22 events). For increased response sizes the importance of time-independent rates relative to response rates have less impact on the count threshold (e.g., **Figure 46**: 43 events, in comparison to **Figure 47**: 48 events).

**Table 7** Supplementary examples for the comparison of different response time-independent rates. Note that the time window (0.5 h) and event counts that give the lowest count threshold required to identify this response are shown by shaded areas.

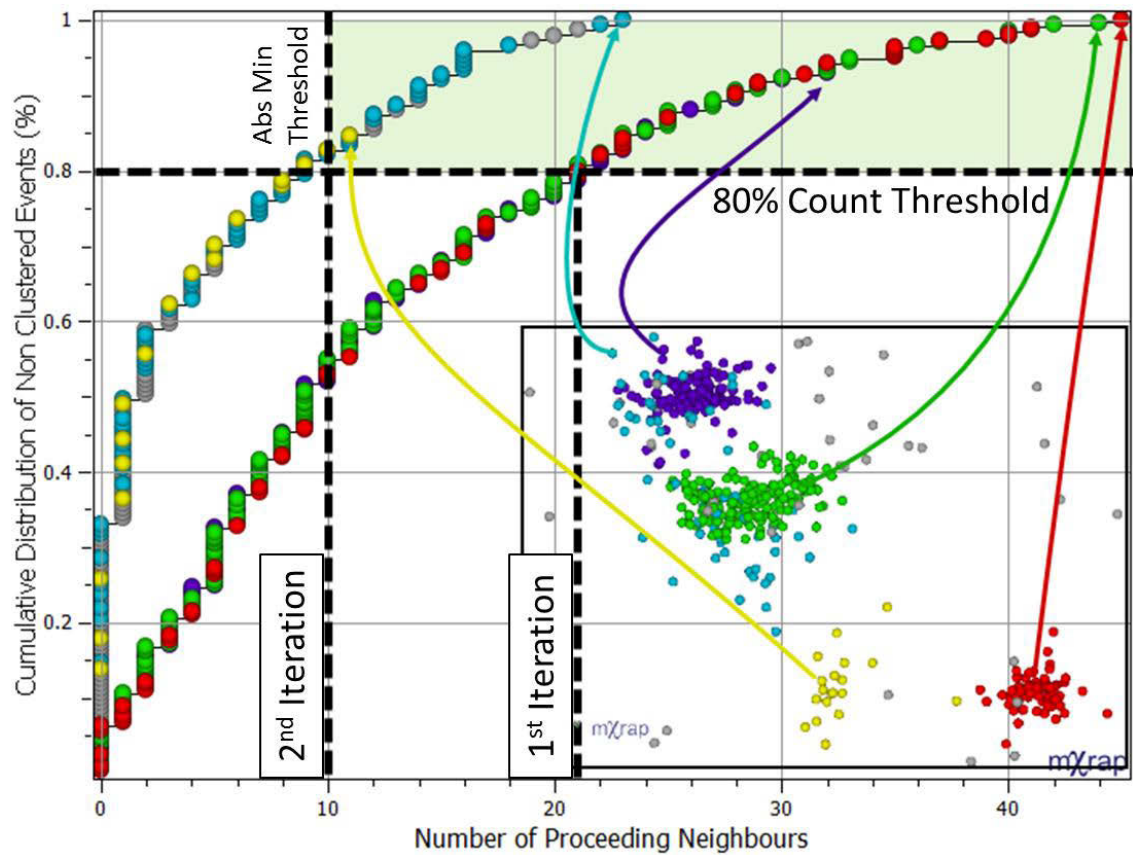


### 3.5.3.3 Approaches to Reduce the Sensitivity of Outcomes

The sensitivity of response identification to selecting an appropriate lower count threshold is reduced by the inherent temporal characteristics of mining induced seismicity. Firstly, different thresholds are set for different spatial and temporal scales. This functionality allows the lower count threshold to be raised for the scales that contain a greater portion of time-independent seismicity. Secondly, smaller responses are identified as the count threshold reduces during the iterative process. When additional seismic responses cannot be identified, only the smallest responses remain in the dataset. A small response may not be identified depending on the lower count threshold selection (**Figure 45**), although, a large response will be identified for with any reasonable lower count threshold (**Figure 47**). Failure to identify and delineate the smallest and most ambiguous responses from time-independent seismicity will have the least impact on analysis outcomes. Additionally, small responses may be falsely identified due to the stochastic nature of seismicity.

The lower count threshold can be difficult to set appropriately for a given scale due to the need to consider spatial and temporal attributes of event occurrence. To improve consistency in setting the lower count threshold for each response scale set, the distribution of the number of subsequent neighbours for each event can be considered to limit the identification of seismic responses. The original assumption that the lower count threshold is less than the number of subsequent neighbours at the start of response initiation is replaced with the assumption that response initiation is within the upper portion of events with the most subsequent neighbours for that specific scale. Specifying a portion of events instead of an absolute number has the benefit of considering different scales with the same proportional count threshold and is not reliant on the user considering the changes to the number of subsequent neighbours for different scales. An absolute minimum threshold is set to prevent the proportional lower count threshold falling below a reasonable value.

**Figure 48** provides an example of the functionality of using a proportional lower count threshold. During the first iteration, three seismic responses are found (red, green, and purple) by considering events that have a subsequent neighbour count within the top 20% of all events for this scale. The 80% count threshold corresponds to an absolute lower count threshold of 21 subsequent neighbours. A second iteration is considered after the removal of the events associated with the responses identified during the first iteration. The 80% count threshold corresponds to nine subsequent neighbours, although, the lower count threshold is limited to the absolute minimum threshold of 10 events. Blue and yellow responses are found during the second iteration, as these responses contain an event that has more than 10 subsequent neighbours.



**Figure 48** The functionality of using a proportional lower count threshold. The first iteration identifies the red, green, and purple responses by considering events that have the subsequent neighbour count within the top 20% of all events for this scale (21 subsequent neighbours). The second iteration identifies the blue and yellow responses by considering relative lower count threshold of 80% (nine events) but is limited by the absolute threshold of 10 events.

### 3.5.3.4 Limitations Associated with the Parameter

The limitations of using a constant lower count threshold are the same as those for constant spatial and temporal windows. The variation between response and time-independent rates influences the optimal lower count threshold, potentially failing to identify small responses or falsely identifying a response from spatial and temporal variation. Ultimately, the degree that this limitation can influence results depends on the contrast that exists between time-independent and response rates, and if there is enough difference in spatial and temporal counts to justify the identification. The most pragmatic example of a constant lower count threshold not being appropriate is when background seismicity varies significantly as mining progresses, particularly if time-independent seismicity is confined to the spatial scales that contribute to seismic responses.

### **3.5.4 Temporal Modelling Window**

#### **3.5.4.1 Influence of the Parameter on Outcomes**

The modelling time window is ideally the length of the duration of the seismic response. This ideal case requires the duration of a response to be known, despite the duration of any given seismic response being ambiguous, as there is no clear cessation of event occurrence. Furthermore, seismic responses are commonly interrupted due to additional responses being caused by routine blasting. The assessment of the duration of responses prior to temporal modelling is avoided due to additional methods and assumptions being required. Instead, the modelling time window is set to overestimate the duration of the seismic response significantly and relies on temporal modelling to select the ideal interval.

#### **3.5.4.2 Practical Selection of Parameter Values**

The length of responses is not directly correlated to the spatial, temporal, or count threshold and, therefore, it is not possible to set a modelling time window reliably for each response scale set. A response with a small spatial scale and few events is likely to be shorter than a larger more productive response, although, response durations are unknown and may vary for individual responses. As a result, constant modelling time windows are not set for specific sets of scale parameters and instead a single parameter is used for the entire dataset. There are two approaches to setting the temporal modelling window.

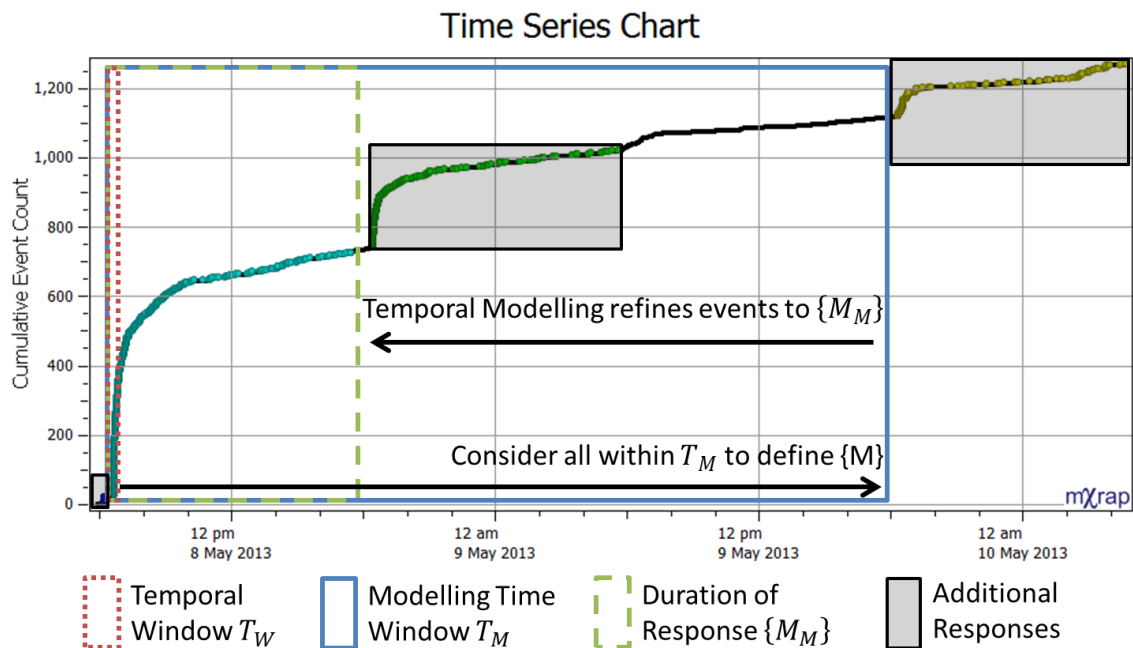
The first approach deals with specific types of seismic datasets. The modelling time window is set by considering mining methods with respect to seismic responses and time-independent seismicity. For mining environments where seismic responses are associated with routine blasting, then the modelling time window can be set to the period between blasts. While events associated with the seismic response after this period are excluded it is ensured that seismicity caused by subsequent blasts will not be considered as a single response. This option is appropriate for datasets with very little variation in seismic response length, or in datasets that contain a significant portion of time-independent seismicity, leading to durations being overestimated, e.g., responses associated with caving methods. This approach manages computational times associated with spatial and temporal modelling of long time windows that contain a large number of events not associated with the initially identified response.

The second approach specifies modelling times for datasets that contain varied lengths of seismic responses. This approach sets long modelling time windows and relies on the temporal modelling to delineate the seismic response. Modelling windows may be in the order of days for typical datasets. It is important to note that this method will delineate the response during this period that is associated with the best temporal model. If this response is not the original

response identified, identification outcomes are updated to match temporal modelling and the originally identified response is reconsidered during subsequent iterations.

### 3.5.4.3 Approaches to Reduce the Sensitivity of Outcomes

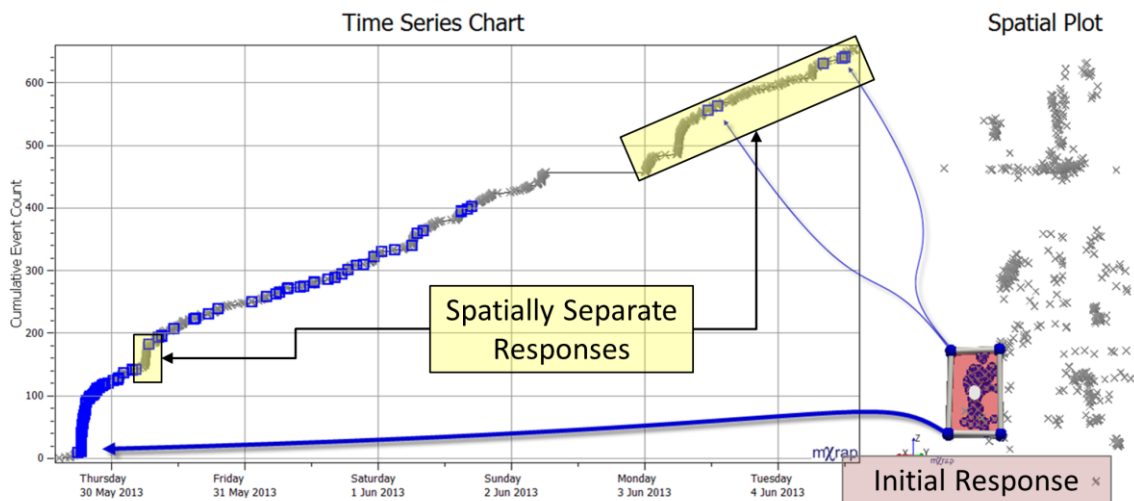
The sensitivity of analysis to this parameter is reduced by the process of spatial and temporal modelling. **Figure 49** provides an example of the functionality of implementing a modelling time window that intentionally overestimates response duration. The temporal window (red dot box) is relatively small to capture increases in the event rate associated with the response initiation. In contrast, the modelling time window (blue solid box) is significantly longer and intentionally overestimates the duration of the response to define the set  $\{M\}$ . This set of events is reduced to include only the duration of the dominant response in the period  $\{M_M\}$  (green dash box). Additional responses are identified and delineated during later response scale sets and count threshold iterations (grey boxes).



**Figure 49** The small temporal window (red dot box) captures event rate increases. The larger modelling time window (blue box) intentionally overestimates the duration of the response to define the set. Events are refined only to include the dominant response (green box). Additional responses are identified and delineated during later iterations (grey boxes).

The selection of the modelling time window does not greatly influence the identification and delineation of seismic responses. The spatial component of seismicity is considered before the adjustment of the response duration and, therefore, the events considered for temporal modelling are limited. The procedure considers the spatial and temporal components of seismicity, improving the distinction between different seismic responses and, hence, typically makes the choice of a modelling time window straightforward. **Figure 50** provides an example

of a seismic response that is spatially isolated (highlighted blue and contained within the pink box). Additional time-dependent and independent seismicity occurs during the following period (highlighted yellow). By limiting the area of interest to the volume of the initially considered response, seismicity is limited to three days after the initiation (up to Sunday 2<sup>nd</sup> June 2013), with the exception of five events occurring five days later (small blue arrows). Imposing spatial modelling improves consistency and the distinction in temporal characteristics despite the modelling time window overestimating response durations.



**Figure 50** An example of a seismic response that is spatially isolated (blue / pink box). Additional time-dependent and independent seismicity occurs during the following period (highlighted yellow). By limiting the area of interest to the volume of the initially considered response, seismicity is limited to three days after the initiation (up to Sunday 2<sup>nd</sup> June 2013), with the exception of five events occurring five days later (small blue arrows).

#### 3.5.4.4 Limitations Associated with the Parameter

This approach is inherently reliant on the removal of responses through spatial and temporal procedures before following iterations finds additional responses. Seismicity that does not follow spatial or temporal modelling assumptions may not be optimally delineated within the temporal modelling window. Additionally, including too many subsequent events will influence the spatial model that is constructed prior to temporal modelling. As a result, the spatial model may include events that are related in time but not in space. These additional later events act as a spatial link to include remote seismicity. A major pragmatic consideration is that computational times are related to the number of events are considered during spatial and temporal modelling. Considering longer modelling windows will contribute to longer computational times, the impact that the time window has on computational times will ultimately depend on the overall rate of seismicity within the mine.

### 3.5.5 Response Scale Sets

#### 3.5.5.1 Influence of the Parameter on Outcomes

Constructing response scale sets is one of the most important inputs to achieving consistent seismic response identification. While the selection of each individual parameter has been discussed, specifying scale sets provides two additional pieces of information. Firstly, the scale sets allow the user to control the absolute values of the scales that are considered and, secondly, sets specify how different the responses should be before they are identified and delineated on different scales.

The optimal number of scale sets is related to the number of significantly different spatial scales that exist within a mining environment. Clusters of seismic events will be merged or subdivided if the absolute values of the spatial scales do not represent the response intended for identification or if there is insufficient distinction between the spatial scales. The time window, temporal modelling window, and lower count threshold are not dependent on the spatial scale and, therefore, are typically set to be constant for all scale sets. In practice, the flexibility to modify these parameters is retained to allow for the assessment of specific cases.

#### 3.5.5.2 Practical Selection of Parameter Values

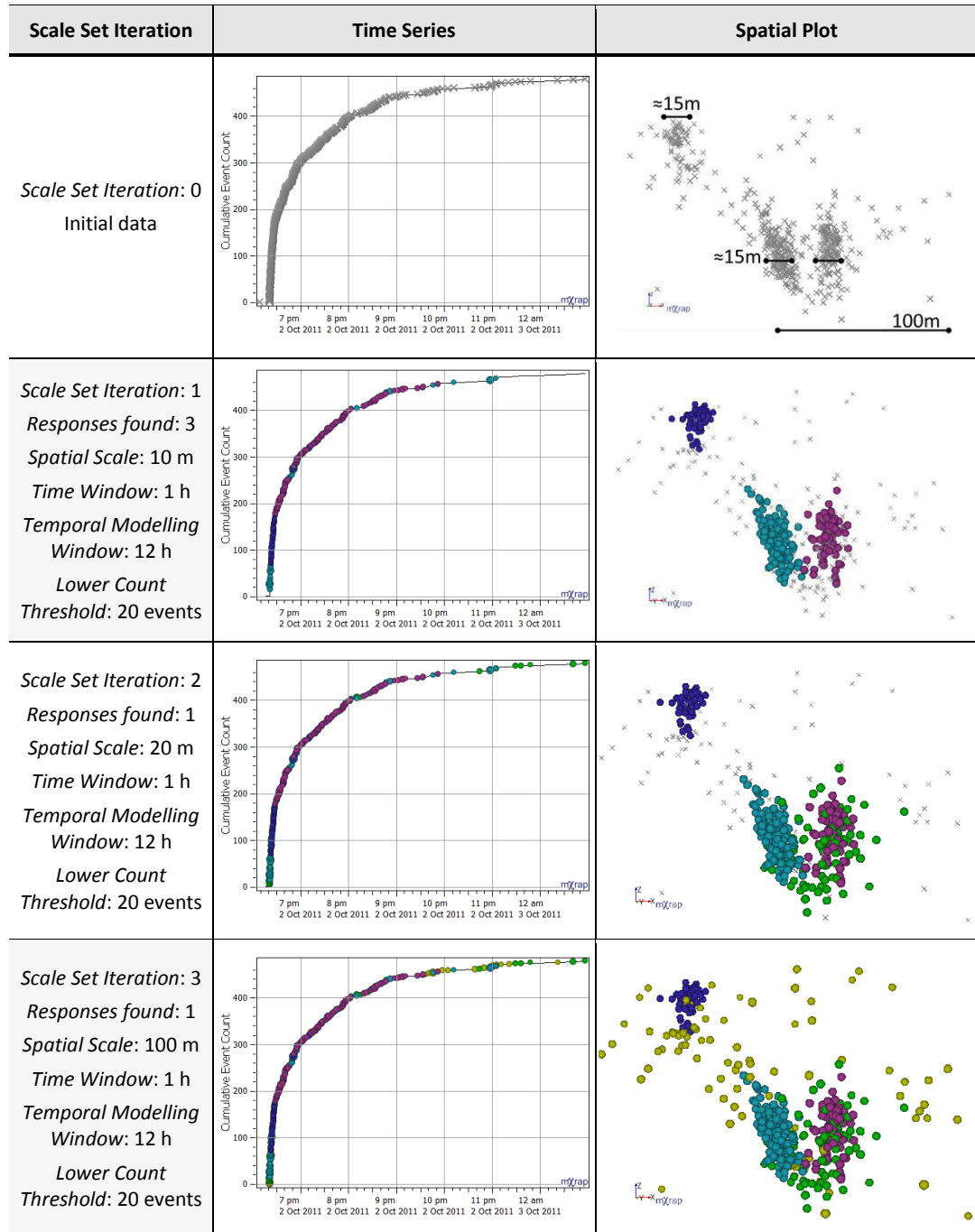
For general applications, the primary considerations for the selection of response scale sets are to maintain adequate confidence through the choice of a lower count threshold and accurate representation of the spatial scales present in the dataset. The spatial window, time window, and lower count threshold are interrelated with respect to a spatial and temporal event rate, i.e., number of events per period per spatial volume. A longer time window will result in a higher event count and, hence, the lower count threshold must be higher to result in the same identification. Setting the time window and lower count threshold to a constant for all response scale sets has the practical implication of ensuring that the spatial and temporal event rate is directly relatable to the spatial scale. Ultimately, two responses with similar temporal event rates are comparable even if they occur on different spatial scales. This comparison becomes important to assist with setting spatial scales and achieving consistency in the identification of seismic responses.

**Table 8** provides an example of the construction of three response scale sets for the analysis of seismic responses. In practice, all of these sets would be specified prior to analysis. For this example, each set is progressively applied to illustrate the process used to construct the sets. Each set uses a constant time window of 1 h, temporal modelling window of 12 h, and a lower count threshold of 20 events. The spatial window the only parameter manipulated to investigate the structure in the data.

First scale iteration: Three dense localised responses were found during this scale set iteration using a small spatial scale of 10 m (the approximate smallest dimension of these responses). The spatial and temporal clustering of these responses is unambiguous. Additional seismicity remains non-clustered, particularly surrounding the light blue and purple responses.

Second scale iteration: The spatial scale is increased to 20 m to capture additional seismic responses that have occurred on a larger scale, particularly surrounding the localised responses at the bottom of the window (green). The amount of seismicity that is spatially superimposed with the purple response indicates a significant portion of the green response occurred before and after the denser cluster of events. While there is less confidence that the green response is due to a separate process to that which generated the purple response, the distinction between the responses is valuable for exploratory analysis.

Third scale iteration: To investigate the temporal behaviour of the spatially non-clustered seismicity that occurs around the mine during this period, an additional set is specified with a spatial scale of 100 m. This scale set identifies the remaining seismicity as a seismic response (yellow) and implies this seismicity is time-dependent.

**Table 8** Constructing response scale sets to identify and delineate seismic responses.

### 3.5.5.3 Approaches to Reduce the Sensitivity of Outcomes

The previous example in **Table 8** considers a subset of data over the order of hours, although, a complete database may contain several years of seismicity. General parameters for the assessment of longer periods are found by the manual assessment of typical seismic responses to identify generally applicable response parameter sets.

This process is subject to the limitations that are common to using constant parameters over a longer period of seismicity, namely, changes in spatial and temporal scales will influence the optimal parameters for the identification and delineation. As a result, the validation of results

is essential to ensuring confidence in analysis results. Response scale sets used in analysis are refined if required and validated based on the following techniques.

Visual inspection aims to identify obvious errors, e.g., the merger of spatially or temporally separate seismic responses, and the subdivision of spatially and temporally clustered seismicity. This process focuses on blatant errors due to the use of poorly considered response scale sets. Modelling results allow for quantitative measures that identify when seismic responses identified did not result in expected modelling outcomes. Specific measures used are further discussed in Chapters 4 and Chapter 5. Examples of these measures include:

- **Spatial Assessment:** This focuses on the quantification of the effectiveness of spatial modelling by determining the variation in intra-cluster event density and inter-cluster separation of seismic responses.
- **Temporal Assessment:** This assessment quantifies the effectiveness of temporal modelling by determining how closely event occurrence follows the assumed model. Erroneous parameters may indicate responses that do not follow expected temporal behaviour, e.g., very slow decay of seismic event rates may indicate that a response is not time-dependent,

During the validation process, if poor results are found two actions can be taken to address errors. Firstly, if poor results are caused by the incorrect selection of response scale sets then these can be adjusted accordingly and the algorithm rerun. Secondly, if errors are due to the inherent natures of seismic data, then these results are not redundant as they provide information concerning the spatial and temporal behaviour of seismicity. Depending on the purpose of further assessment, the erroneous responses can be retained or excluded from further consideration.

#### **3.5.5.4 Limitations Associated with the Parameter**

The limitations of defined response scale sets are subject to the same limitations associated with each individual parameter. The main limitation to the use of discrete scale sets is the inherent assumption that seismic responses occur approximately on the specified scales. The approach may return suboptimal results if seismic responses occur on scales significantly different to those specified and does rely on the initial interpretation of parameters. The implementation of error mitigation measures for each user specified parameters and post analysis validation techniques increase the reliability of the identification and delineation of seismic responses.

### 3.6 Chapter Summary

This chapter presented a simple new iterative method to identify seismic responses that specifically addresses the challenges associated with mining induced seismicity and the shortcomings of existing methods. Three main sections of the chapter are summarised in the subsequent sections (Sections 3.6.1, 3.6.2, and 3.6.3).

In summary, the iterative method to identify seismic responses is able to:

- Evaluate when and where seismic responses occur;
- Delineate a subset of potentially related events to be refined by spatial and temporal modelling;
- Provide a structured approach to identifying seismic responses of various temporal and spatial scales; and
- Delineate responses that are spatially or temporally superimposed.

#### 3.6.1 Seismic Response Identification using Spatial and Temporal Windows

- Spatial and temporal windows are commonly implemented and are successful when responses occur on consistent spatial and temporal scales, and at the same time and place as a known stress change.
- The method presented identifies the time and location of responses by:
  - Defining a spatial window, temporal window, and count threshold.
  - Finding the number of subsequent and neighbouring events for every seismic event by searching within the spatial and temporal window.
  - Considering each event in a reverse chronological order and defining the beginning of a seismic response when the subsequent neighbours count is greater than the threshold count.
  - The time of this event and the mean location of neighbouring events provide initial information of the seismic response.

#### 3.6.2 Iterative Method for Seismic Response Identification

- As responses of varying scales may be superimposed spatially or temporally, smaller dense spatial scales are identified and delineated prior to large spatial scales.
- Identification parameters are introduced that are characteristic of individual scales within the mining environment (response scale sets).

- The method previously developed to identify the time and location of responses is applied within three layered iterations:
  1. Primary iteration: Check all response scale sets.
  2. Secondary iteration: Check all count thresholds for all events.
  3. Tertiary iteration: Check if the subsequent neighbours count is greater than the current count threshold for all events.
- Practical implementation of the method has the follow implications:
  - A range of count thresholds only requires a lower threshold to be defined and corresponds to the smallest number of events required to identify a response.
  - A temporal modelling window must also be introduced to delineate a subset of related events that can be refined by spatial and temporal modelling.
- The iterative identification of seismic responses requires the definition of one or more response scale sets that contain the following parameters:
  - $S_W$ : Spatial window;
  - $T_W$ : Temporal window;
  - $C_L$ : Minimum number of events; and
  - $T_M$ : Maximum response length.

### **3.6.3 Considerations and Limitations of User Defined Parameters**

The considerations and limitations for spatial windows are:

- Spatial window size is related to the physical scale of a response and is typically the most distinct feature.
- The parameter has the greatest impact on the identification and delineation of seismic responses.
- If underestimated, then counts are influenced by natural variation and if overestimated, then counts are insensitive to the rate of seismicity.
- Spatial windows are selected by considering typical scales associated with sources of seismicity within the mining environment.
- The sensitivity of analysis to the selection of an appropriate spatial scale is reduced by subsequent spatial modelling.

- Iterative assessment considers small-scale responses first and limits spatial modelling to only considering similar spatial event densities.
- Optimal spatial scales to identify seismic responses may vary as mining progresses.

The considerations and limitations for the temporal window are:

- Temporal window size is related to the time scale of response initiation.
- This window provides a representative sample of temporal event density.
- If underestimated, counts are influenced by natural variation.
- If overestimated, counts are insensitive to the rate of seismicity.
- The method is not sensitive to the selection of a temporal window due to the largest portion of events occurring immediately after initiation.
- A scale of minutes is general applicable.
- Sensitivity of analysis to the selection of this window is reduced by the ability of temporal modelling to adjust response identification.

The considerations and limitations for the lower count threshold are:

- The lowest count threshold is related to the lowest spatial and temporal density required to form a response.
- The selection of this number is dependent on the sensitivity of the seismic monitoring system, time-independent event rates, and the rate of the seismic response.
- Selection of values is based on the trade-off between identifying small responses and falsely identifying stochastic event occurrence.
- Analysis is not sensitive to this parameter as:
  - Large responses will be identified for any reasonable count threshold;
  - Failure to identify and delineate the small responses or the misidentification of small responses has the smallest impact on subsequent analysis outcomes.
  - The distribution of subsequent neighbour counts can be considered to limit select reasonable scale dependent values.
- Optimal lower count thresholds may vary over time, although, this limitation is partially mitigated by distribution analysis.

The considerations and limitations for the temporal modelling window are:

- The temporal modelling window is ideally the length of the duration of the seismic response.
- Duration of any given seismic response is ambiguous as there is no clear cessation of event occurrence.
- The length of responses is not directly correlated to spatial, temporal, or count thresholds.
- The temporal modelling window is either a significant overestimate of response temporal duration or the fixed period between known changes to stress conditions.
- The selection of this parameter is generally a significant overestimate of duration.
- The temporal modelling window can be fixed if: time-independent seismicity leads to the overestimation of responses, there is very little variation in response duration, or analysis is constrained by computational times.
- The selection of the modelling time window does not greatly influence the identification and delineation of seismic responses.
- Limitations associated with setting the temporal modelling window include:
  - A window too short will not capture the entire seismic response;
  - A window too long may cause unrelated events to influence the spatial model that is constructed prior to temporal modelling;
  - Longer window includes more events and increases computational times; and
  - A long modelling window increases the reliance of temporal modelling to delineate seismic responses.
- The sensitivity of analysis to this parameter and the potential influence of limitations are reduced by the distinction that generally exists between different seismic responses.

The considerations and limitations for the response scale sets are:

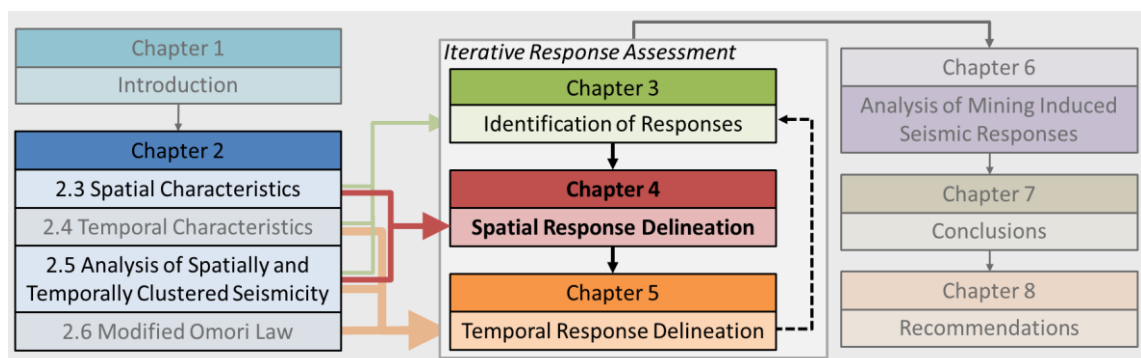
- The number of response scale sets specified is related to how many significantly different spatial scales exist within the mining environment.
- Response scale sets specify the absolute and relative values of the considered scales.
- Parameters within a response scale set are interrelated with respect to scale dependent event rates.

- Constant temporal windows and lower count thresholds across response scale sets are optimal to achieve consistent identification.
- Response scale sets are validated by visual inspection to identify obvious errors and quantitative measures of modelling outcomes.
- The limitation of response scale sets is the inherent assumption that seismic responses occur on the discrete scale sets specified.

## 4 Spatial Delineation of Mining Induced Seismic Responses

### 4.1 Chapter Overview

Chapter 4 formulates a generalised method for the spatial delineation of mining induced seismic responses. The method accounts for the spatial characteristics of mining induced seismicity (Chapter 2) and forms a component of the iterative approach applied to the identification of seismic responses (Chapter 3). Spatial delineation utilises the location of responses identified using the iterative framework and results in a subset of spatially clustered events that are considered by temporal modelling (Chapter 5). **Figure 51** illustrates the contents of this chapter, with respect to previous and subsequent chapters.

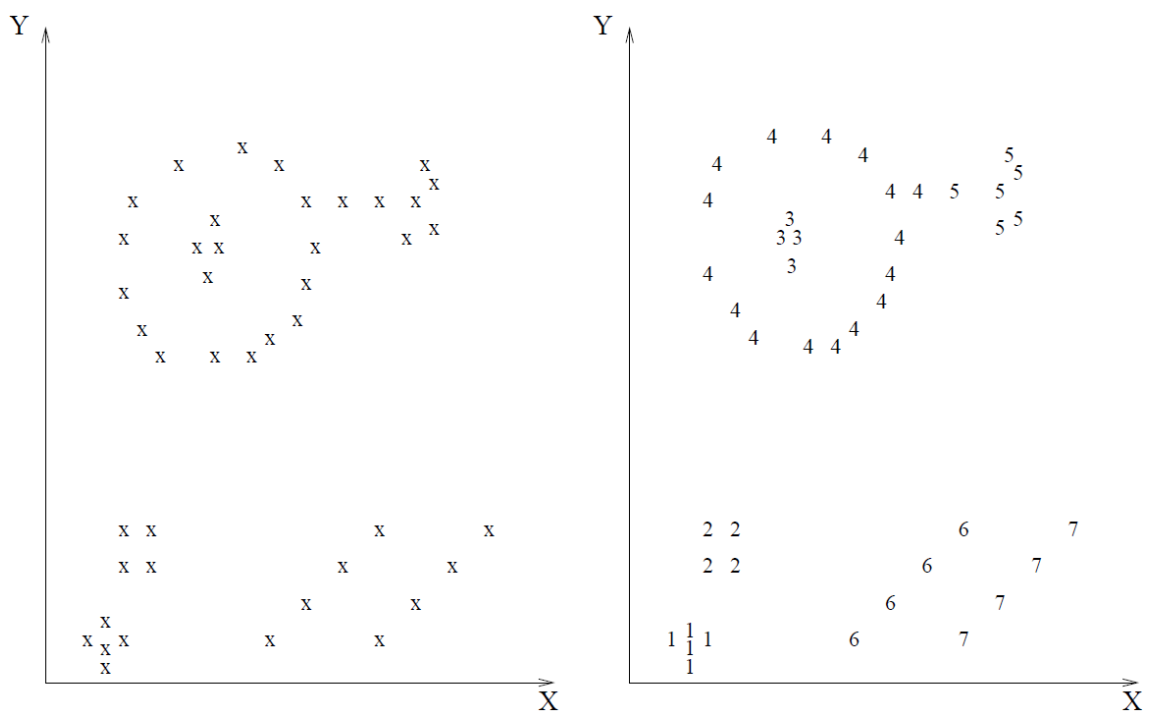


**Figure 51** Chapter 4 utilises the outcomes from concepts established in Chapter 3, and the spatial characteristics and analysis reviewed from literature. A method is developed that delineates the spatially clustered seismicity associated with a seismic response and results in a subset of spatially clustered events for temporal modelling in Chapter 5.

## 4.2 Introduction

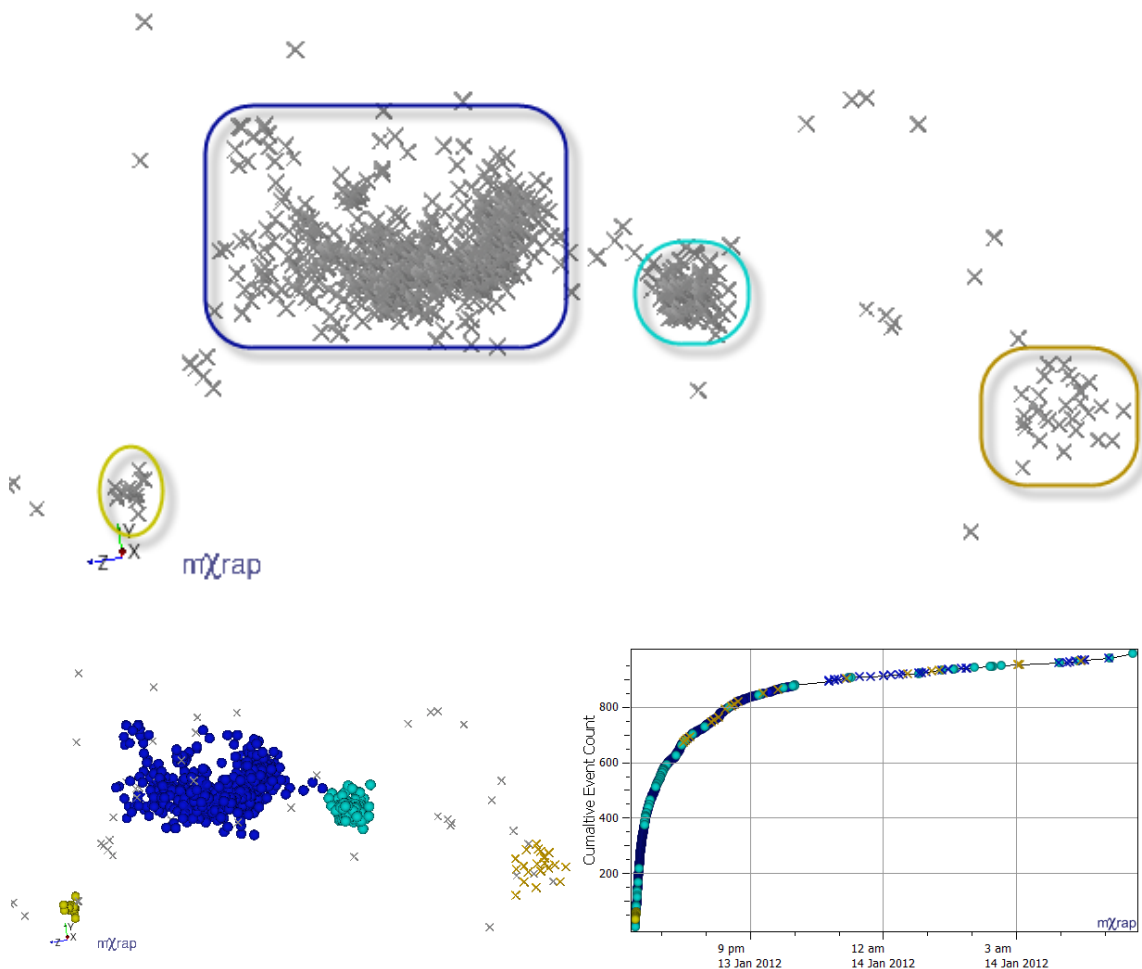
The spatial characteristics of mining induced seismicity are influenced by factors that controlled rock mass failure. These factors manifest in the mining environment as distinct spatial sources of seismicity and include features such as faulting, pillars, contrasting rock types, or localised stress changes. Assessing the spatial distribution of seismicity forms the basis for understanding and quantifying the seismic hazard associated with causative processes and is an essential component to the assessment of seismic responses.

The most fundamental aspect of clustering requires elements that share similar characteristics to be grouped together (Jain, Murty & Flynn 1999). This condition does not necessarily mean that closest elements cluster together and instead focuses on identifying the underlying structures present within a dataset. This philosophy underpinning clustering is illustrated by the grouping of elements that contribute to recognisable structures within a dataset (Figure 52).



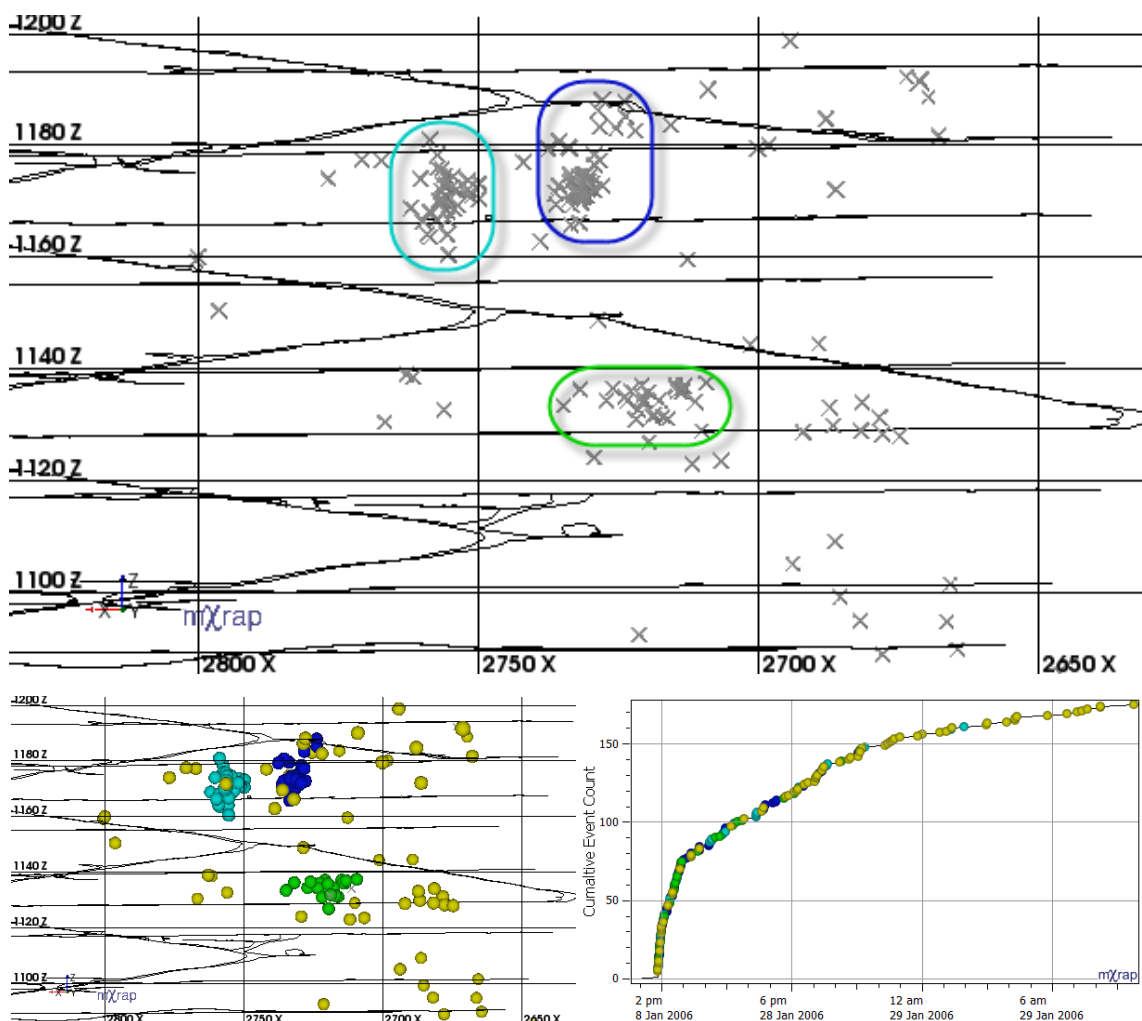
**Figure 52** The identifiable underlying structures in the  $[x,y]$  attributes of the data (left) is delineated into numbered clusters (right) (Jain, Murty & Flynn 1999).

Simple spatial analysis of mining induced seismicity aims to delineate clusters of events. These clusters vary in size, shape, and densities for any given period due to the spatially controlled factors that influence rock mass failure. An unambiguous example of spatial clustering is the occurrence of four clusters of seismicity superimposed with sparsely located events during the same period (**Figure 53**). These clusters can be visually identified (top) and delineated using automated spatial clustering (bottom left) so that events belong to one individual cluster. A time series of the cumulative number of events shows that the clusters of events occur concurrently (bottom right).



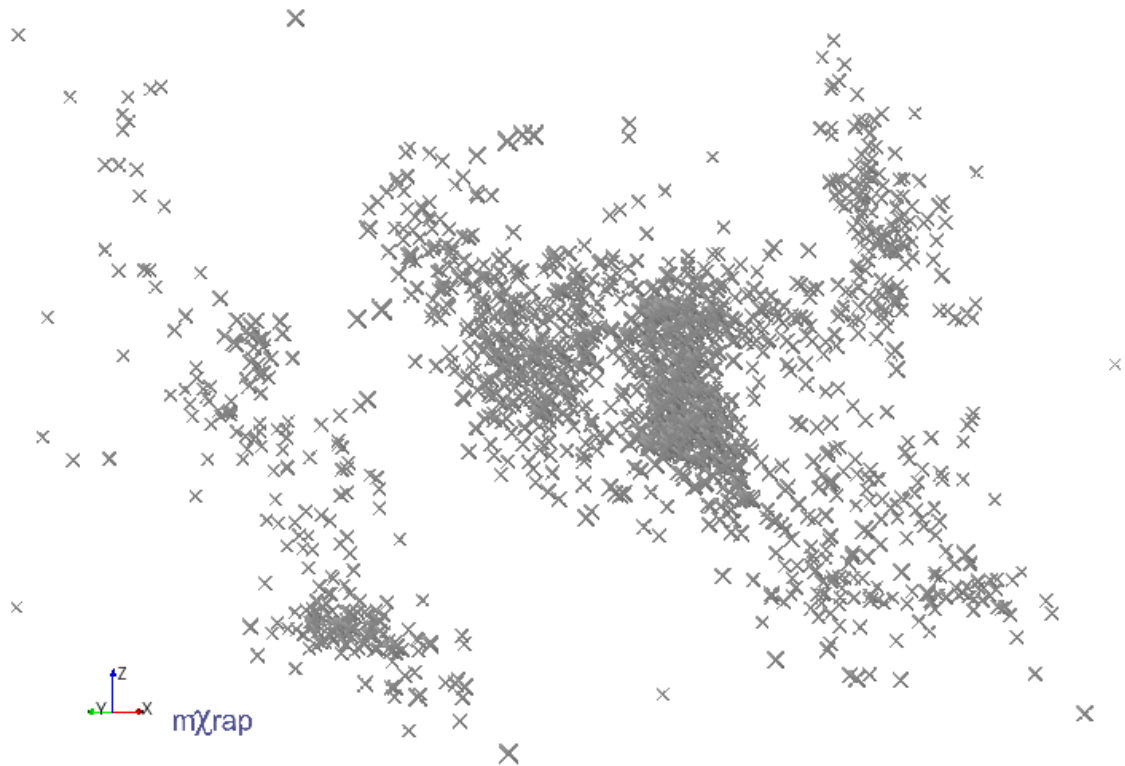
**Figure 53** Top: Four clusters of varying size, shape, and density are visually identified among sparsely distributed events. Bottom left: Clusters delineated by spatial clustering. Bottom right: Temporal chart showing the cumulative event count with event markers corresponding to the bottom left spatial plot.

In the previous example, clusters of spatially related events are delineated from sparse seismicity that was attributed to time-independent rock mass failure processes. Assuming that sparsely spatially distributed events are time-independent seismicity is not reasonable without assessment of the temporal occurrence of these events. To be able to test this assumption clustering methodologies must delineate superimposed spatial clusters of varying densities. **Figure 54** provides an example of three visually identified clusters along with sparsely located events that may be an additional, albeit weaker, seismic response to mining (top). These responses are spatially delineated (bottom left) and plotted with respect to a cumulative event count over time (bottom right).



**Figure 54** Top: Three clusters of varying size, shape, and density can be visually identified among sparsely distributed events. Bottom left: Dense clusters are delineated by spatial assessment along with a superimposed, sparsely distributed cluster. Bottom right: Temporal chart showing cumulative event count with event markers corresponding to the spatial plot. Note that the spatial figures are longitudinal sections of the mine, with the irregular black lines representing excavations as 2D floor strings.

In these two examples, decisions concerning clustered and non-clustered events have been unambiguous. An ideal clustering methodology offers the benefit of being less subjective in comparison to manual techniques and capable of deal with complex structures in seismic spatial occurrence, e.g., multiple superimposed clusters that exhibit distinguishable shapes and densities. **Figure 55** provides an example of a seismic response that has a complex underlying structure. While some areas of high-density and low-density are evident, the manual identification of clusters with similar spatial characteristics will be unavoidably subjective.



**Figure 55** An example of uncertain spatial structure within mining induced seismicity.

The ideal characteristics of clustering methods that spatially delineate seismic responses are not exclusive to this specific application, e.g., clustering elements with different densities and non-uniform geometries. Clustering methods are applied to a large number of practical and research applications and, hence, there is a significant amount of literature related to clustering techniques (Jain, Murty & Flynn 1999). In many of these applications, clustering is used to explore the structure of data without prior knowledge concerning its distribution and making as few assumptions as possible. This underlying philosophy is maintained for the clustering of mining induced seismicity.

Different discussions of clustering techniques vary based on the study in question (Jain, Murty & Flynn 1999; Xu & Wunsch 2005). For the purpose of this thesis, clustering is considered in two broad categories: parametric and non-parametric. Parametric approaches produce

clusters by the optimisation of a function that describes the likelihood of elements belonging to a set of assumed clusters. Examples of parametric clustering include, but are not limited to, Gaussian Mixture Models, C-Means Fuzzy Clustering, and K-Means Models. These approaches generally require underlying assumptions of the structure of the data and, hence, are not suited to the clustering requirements of this thesis.

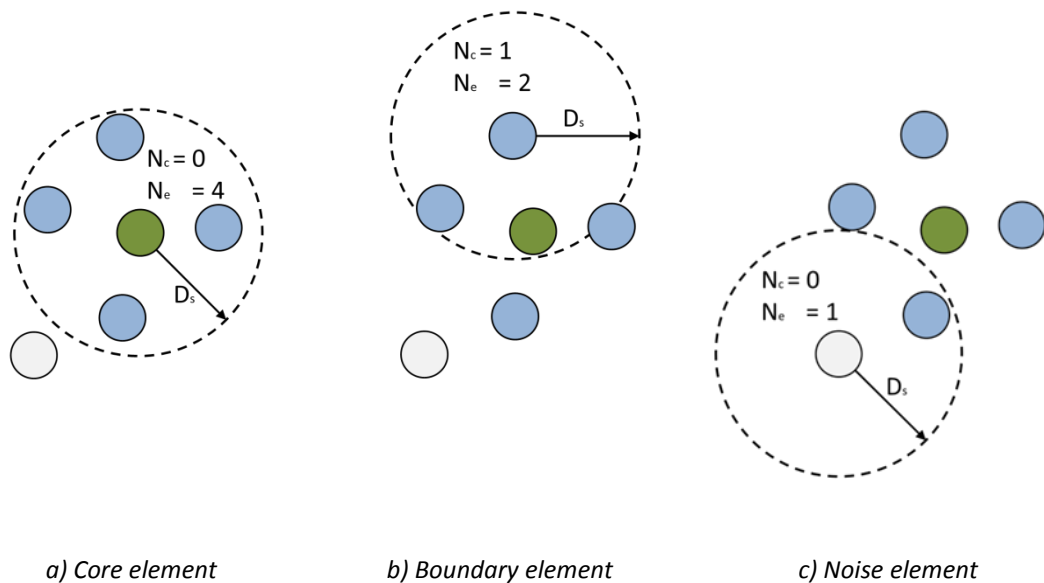
In contrast, non-parametric approaches do not require assumptions concerning data structure. Instead, non-parametric methods will group elements based on similarity (agglomerative) or disassociate elements based on differences (divisive). Examples of non-parametric clustering include, but are not limited to, Single Linkage, Centroid Linkage, and Hierarchical Clustering. Simple non-parametric approaches may perform poorly if clusters are inconsistent in size, density, or geometry (Xu & Wunsch 2005). Modified algorithms aim to address these issues while preserving the fundamental approach to non-parametric clustering. Density-based clustering is a non-parametric clustering method that is applicable to mining seismicity for the following reasons (Ester et al. 1996; Kriegel et al. 2011):

- Class identification: Seismic events should be allocated to one, unique cluster;
- Minimal requirements of existing dataset knowledge: Assumptions concerning spatial distributions are not likely to be generally applicable due to the variation in sources of seismicity and mining environment;
- Discovery of clusters with arbitrary shapes: Allows for various shaped seismic responses to be clustered as spatial distributions are controlled by sources of seismicity, e.g., planar faults, spherical stress changes, or cylindrical pillars; and
- Discovery of high-density clusters within low-density areas: Required for the identification of high-density responses superimposed with sparse responses.

### 4.3 Density-Based Clustering applied to Mining Induced Seismicity

Density-based clustering allows for the discovery of arbitrarily quantified, dense regions that are separated by low-density regions. A simple density-based method is Density-Based Spatial Clustering of Applications with Noise (DBSCAN) proposed by Ester et al. (1996) and provides the general framework for density-based approaches. DBSCAN classifies elements by considering the number of neighbouring elements ( $N_e$ ) with respect to a user specified minimum ( $N_{MIN}$ ) within a search distance ( $D_s$ ). Element classifications are:

- Core: If there are more than the specified minimum neighbours within the search distance ( $N_{MIN} \leq N_e$  within  $D_s$ ) (**Figure 56 a**);
- Boundary: If there are less than the minimum specified neighbours and at least one core element within the search distance ( $N_e < N_{MIN}$  and  $1 \leq N_{core}$  within  $D_s$ ) (**Figure 56 b**); and
- Noise: If there are less than the minimum number of specified neighbours and no core elements within the search distance ( $N_e < N_{MIN}$  and  $N_{core} = 0$  within  $D_s$ ) (**Figure 56 c**).



**Figure 56** The definition of core (green dot), boundary (blue dot), and noise elements (grey dot) for density-based clustering with  $N_{MIN}$  of four elements and an arbitrary search distance  $D_s$ .

The DBSCAN method creates clusters from core elements and their neighbours. Core events are recursively considered and merged if one or more core element is shared (Ester et al. 1996). While density-based methods are resistant to noise, they also have a number of shortcomings. These include finding a suitable density threshold, poor performance for datasets with varying element densities, and the sensitivity of clustering outcomes to clustering parameters. These are the main shortcomings when applying this spatial cluster

approach to mining induced seismicity. For general applications, these shortcomings are partly addressed by hierarchical methods (Kriegel et al. 2011).

Significant research efforts have been devoted to expanding the application of density-based methods to address the shortcomings of the initial approach by Ester et al. (1996). Publications of density-based clustering algorithms includes, but are not limited to, CURE (Guha, Rastogi & Shim 1998), DBCLASD (Xu et al. 1998), DENCLUE (Hinneburg & Keim 1998), GDBSCAN (Sander et al. 1998), OPTICS (Ankerst et al. 1999), Chameleon (Karypis, Han & Kumar 1999), SNN (Ertöz, Steinbach & Kumar 2003), DECODE (Pei et al. 2009), and DBCLUM (Fawzy et al. 2013). Many specialised density-clustering algorithms focus on aspects of clustering that are irrelevant to this thesis, e.g., clustering data with a large number of attributes (dimensions). Despite a large number of density-based methods, these approaches do not vary drastically. In general, these methods implement different definitions of element densities and connectedness (Kriegel et al. 2011).

While the underlying concepts of density clustering are generally applicable to the clustering of mining induced seismicity, the prevalence of specialised approaches indicate the need for algorithms to be tailored to address general and problem-specific limitations. The challenges associated with the implementation of density-based clustering to mining induced seismicity are distinct from existing applications due to restricted clustering outcomes. Only one cluster associated with a seismic response is extracted from a larger subset of the database, hence, there is no need to consider all spatial clusters within a time interval. In contrast, the clustering method is required to delineate seismic events that belong to one cluster with similar spatial locations and distribution characteristics.

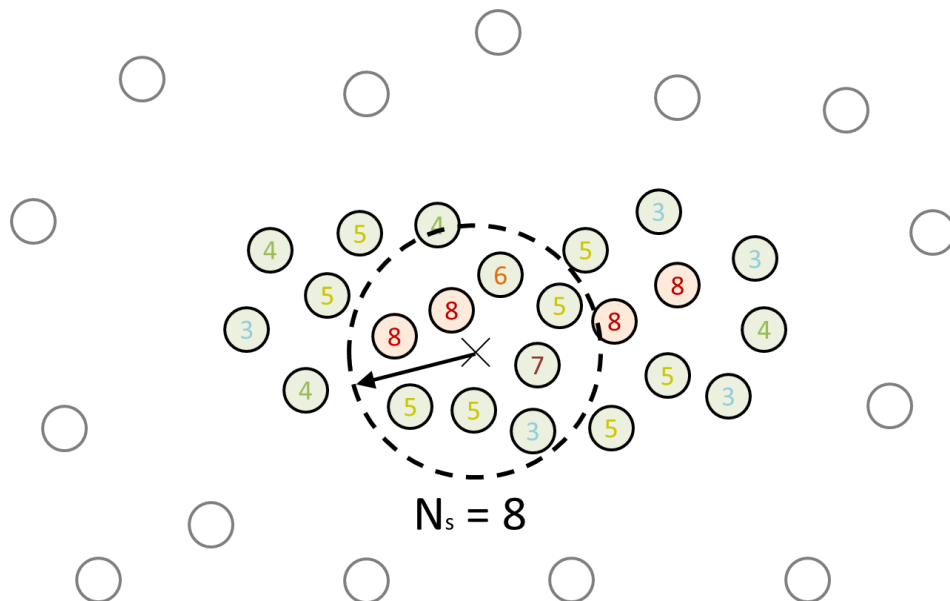
To be applied to mining induced seismicity, density-based methods need to address the clustering of datasets with varying densities and the sensitivity to clustering parameters. These limitations are addressed in Chapter 4 by further developing the DBSCAN approach presented by Ester et al. (1996). Desirable attributes of clustering methods include the improved determination and sensitivity of clustering parameters. Furthermore, spatial clustering methods must be able to be integrated with the iterative identification of seismic responses (Chapter 3) and temporal modelling (Chapter 5).

#### **4.3.1 Integration of Spatial Delineation and Seismic Response Identification**

In addition to developing the framework required for the spatial and temporal delineation of seismic responses, the work presented in Chapter 3 identifies seismic responses in space and time. The outcome from the identification of seismic responses provides valuable initial information concerning the distribution of the seismic response to be spatially delineated. The use of an iterative approach to seismic response identification has two important outcomes:

1. The approximate location of the seismic response is identified.
2. The spatial density of a seismic response can be estimated.

These outcomes can be used for the determination of clustering parameters and account for clusters of different densities and, therefore, specifically address the limitation of density-based clustering approaches. The method utilises an initial density estimate of a seismic response to address the limitations of a density-based approach. Figure 57 illustrates the delineation of a dense cluster within a sparse cluster by using initial triggering information to identify eight events within a search distance ( $N_s=8$ ). The sample of event density in the centre of the cluster provides an estimate of appropriate densities to delineate core events (shaded red), boundary events (shaded green), and noise events (unshaded circles). The number within a circle represents the number of surrounding events that are found within this same search distance. As discussed in Chapter 3, the use of an iterative clustering approach finds and removes dense clusters from the dataset before considering larger response scale sets, hence, subsequent iterations will identify and delineate the noise events (grey circles).



**Figure 57** The use of initial identification information to estimate appropriate clustering parameters. The event count ( $N_s$ ) within an initial search distance is representative of event density surrounding core events. The number within a circle represents the number of surrounding events that are found within this same search distance.

#### 4.3.2 Density clustering core event tolerance

The challenge of finding appropriate clustering parameters and the sensitivity of analysis to these parameters is partially addressed by initially sampling the cluster during the identification procedure. This approach will inevitably provide an upper estimate of event densities that are contained within the cluster. This is due to the response scale sets used in

the identification responses searching for progressively less dense and sparser seismic responses. As a result, the location for response identification centres on the densest section of a spatial cluster. In addition to being the highest density sample, the initial estimate has a component of inherent uncertainty associated with sampling event locations.

A variable tolerance is introduced to decrease the sensitivity of results to the clustering parameters. This tolerance allows for a percentage deviation in the neighbouring event count when considering the designation of core events and allows the cluster to propagate throughout space. The approach is distinct from the DBSCAN implementation of density-based clustering whereby core events are defined if neighbouring events exceed a specific number of events within a specified distance. The modification of allowing a tolerance for the number of neighbouring events to define a core event ensures that core events are not designated if the procedure considers regions of significantly different densities. This feature ensures that clustering is confined to regions of similar spatial characteristics to that initially identified, while allowing for a degree of variation that is consistent with the stochastic nature of event locations (**Figure 58**).

The tolerance is expressed as a percentage of the initially sampled density (**Equation 12**):

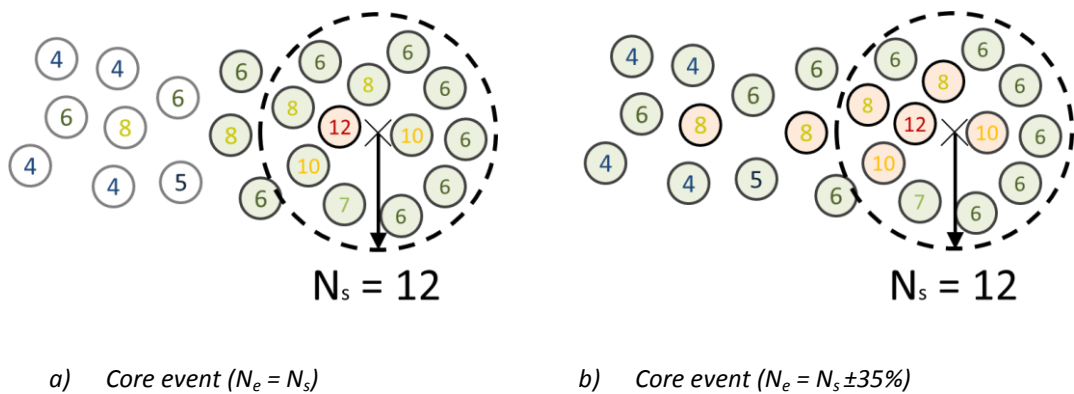
$$S_t = \frac{N_s - N_e}{N_s} \times 100\% \quad \text{Equation 12}$$

Where,

$S_t$ : Spatial density tolerance

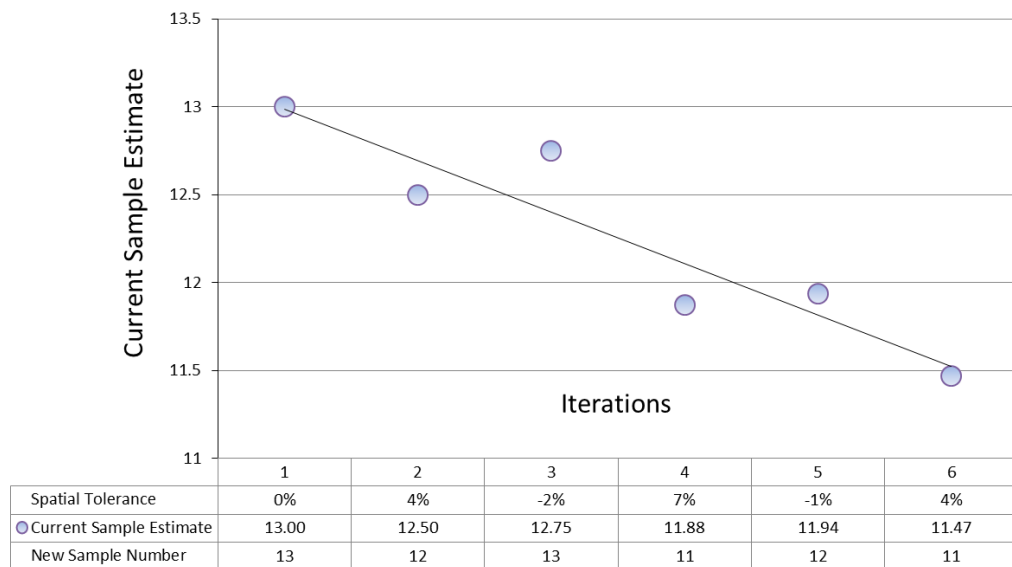
$N_s$ : Number of events within initial search distance

$N_e$ : Number of events within search distance of event



**Figure 58** Core events (red shade), boundary events (green shade), and noise events (no shade) are shown as circles that specify the number of surrounding events. a) Clustering results defining core events to be equal to initial density estimate. b) Clustering results defining core events allowing for 35% difference from the initial density estimate.

As the initial sample is an upper estimate of expected event counts and subject to variability due to sampling, additional measures can be taken to ensure that the expected event count is representative of the cluster. **Figure 59** illustrates an additional modification to refine the expected event count surrounding core events when additional information concerning the spatial characteristics of the core events becomes available. This is achieved by updating the sample number ( $N_s$ ) every time an event is designated as a core event. The updated sample number is an average between the current sample number ( $N_s$ ) and the number of events surrounding a newly discovered core event ( $N_e$ ).



**Figure 59** Adjustment of the current sample number for initialisation and each new core event discovered. The decreasing trend in the current sample number corresponds to the tabular values for iteration number (1 to 6), spatial density tolerance, and new samples numbers.

The selection of an appropriate spatial count tolerance depends on the spatial characteristics of the identified seismic responses. If the spatial density tolerance is underestimated, then variation in the spatial occurrence of seismicity will result in the cluster not being able to capture the events associated with the seismic response. Conversely, if spatial density tolerance is overestimated then the algorithm will include events that are not associated with the seismic response.

For datasets that contain clusters of consistent densities, an appropriate spatial count tolerance are small, e.g., 10%. If cluster densities vary, then the tolerance is set higher to enable the spatial modelling of these responses, e.g., >50%. Increasing the spatial density tolerance is typically required when modelling planar orientations of seismicity as sampling events with two-dimensional locations results in greater variation. In practice, the optimal

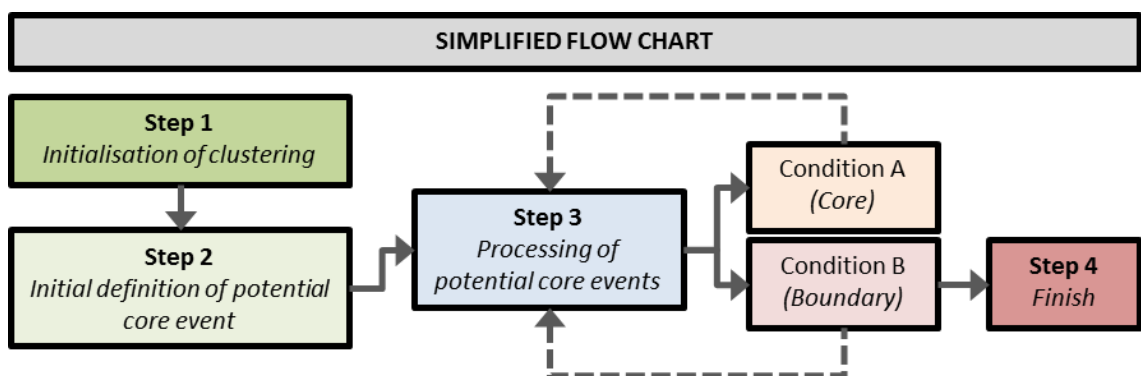
spatial count tolerance is dependent on the scale of the response and, therefore, the specification of this parameter occurs with the response scale sets (Section 3.5.5).

#### 4.4 Spatial Clustering Procedure

The method classifies elements by considering the number of neighbouring elements ( $N_e$ ) within a search distance ( $D_s$ ), with respect to an initially estimated number of events ( $N_s$ ) and a spatial density tolerance ( $S_t$ ). Element classifications are:

- Potential core ( $C_p$ ): An element within the search distance of initial response location or an unprocessed element within the search distance of a core element;
- Core ( $C_e$ ): An element previously designated as a potential core element and with a neighbouring element count within the tolerable range ( $N_s - S_t N_s \leq N_e$  or  $N_e \leq N_s + S_t N_s$  within  $D_s$ );
- Boundary ( $B_e$ ): An element previously designated as a potential core element and with a neighbouring element count outside the tolerable range ( $N_e \leq N_s - S_t N_s$  or  $N_s + S_t N_s \leq N_e$  within  $D_s$ ); and
- Noise elements: An element that is not a core element or boundary element.

Element classifications are utilised in the following four-step procedure to obtain a single spatial cluster within a dataset given an initial location. **Figure 60** provides a simplified flow chart of the clustering procedure that corresponds to the steps described in the subsequent lists. The procedural steps are also detailed in a comprehensive flow chart in **Figure 61**.



**Figure 60** Simplified flow chart outlining steps taken by the spatial clustering procedure.

**Step One      Initialisation of clustering**

- 1 Define a search distance ( $D_s$ ) that approximates the spatial scale of the response. This distance is set to be the spatial window used for iterative seismic response identification.
- 2 Define a spatial density tolerance ( $S_t$ ) that reflects the consistency in spatial response density for a given response scale set.

Explanatory notes: Prior to spatial clustering, the initial response identification finds the centre (response location) of the seismic response. The response scale set that was used to identify this response also specifies the search distance (equal to the spatial window used for the identification procedure) and the spatial density tolerance.

**Step Two      Initial definition of potential core event**

- 1 All events that occur within the search distance ( $D_s$ ) of the response trigger location are designated as potential core events.
- 2 The number of events within the search distance of response identification is found ( $N_s$ ).
- 3 The range of tolerable spatial count is defined from the previous count and the count tolerance ( $\pm S_t N_s$ ).

Explanatory notes: The events defined during this step initialise a list of potential core events that are recursively processed. An example is provided in **Figure 62** where six events are found with the search distance ( $N_s = 6$ ) and designated potential core events ( $+C_p$ ). Tolerable spatial count is  $6 \pm 2.4$  ( $N_s \pm S_t N_s$ ).

**Step Three      Processing of potential core events**

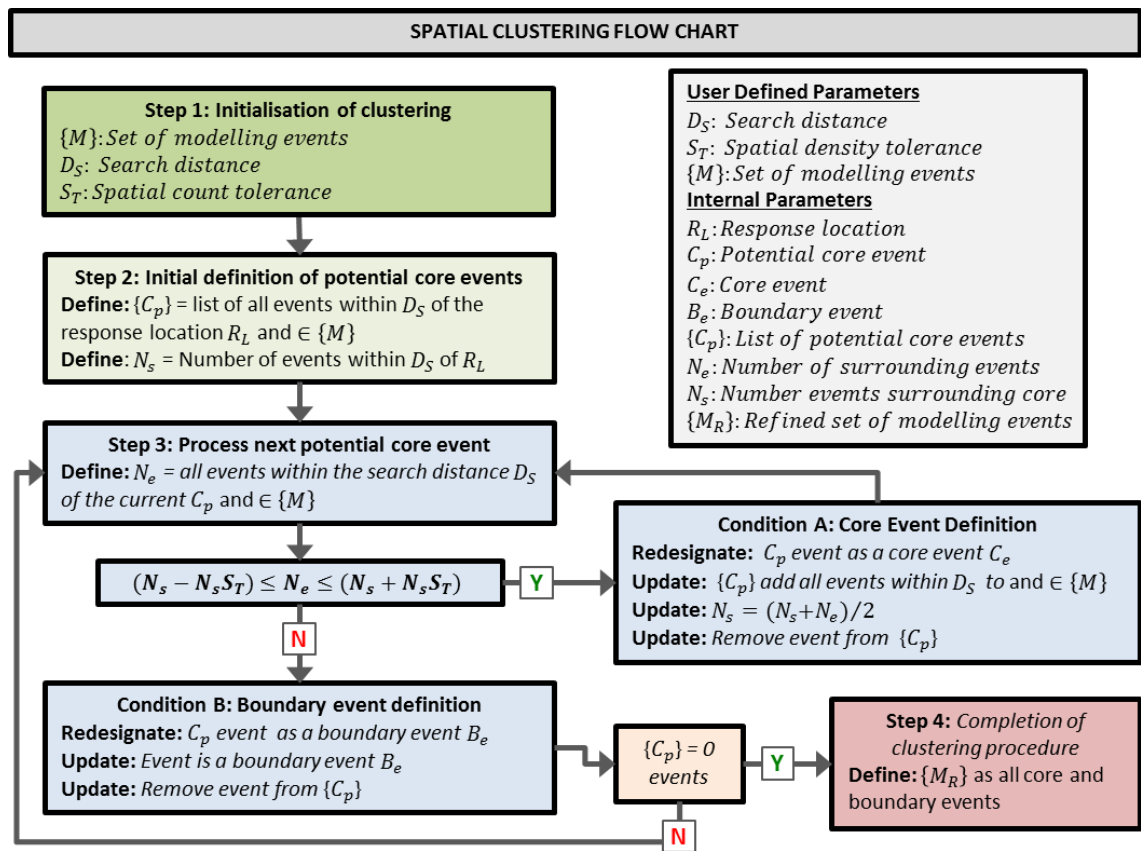
- 1 Count all events ( $N_e$ ) within the search distance ( $D_s$ ), for the next listed potential core event.
  - a. Condition A: If the number of events ( $N_e$ ) is within the tolerance ( $N_s \pm S_t N_s$ ) (**Figure 63**):
    - i. Then all events without a designation and within the search distance are designated potential core events ( $+C_p$ ).
    - ii. This event is redesignated as a core event ( $C_p \rightarrow C_e$ ).
    - iii. Update sample  $N_s$  to be an average of the sample and neighbouring events ( $N_e$ ).
  - b. Condition B: If the number of events ( $N_e$ ) is outside the tolerance ( $N_s \pm S_t N_s$ ) (**Figure 64**):
    - i. Then all events without a designation remain without a designation.
    - ii. This event is redesignated as a boundary event ( $C_p \rightarrow B_e$ ).

Explanatory notes: These steps will always result in an event being designated as a boundary or core events. Potential core events are only added if the count is within allowable tolerances.

**Step Four Completion of clustering procedure**

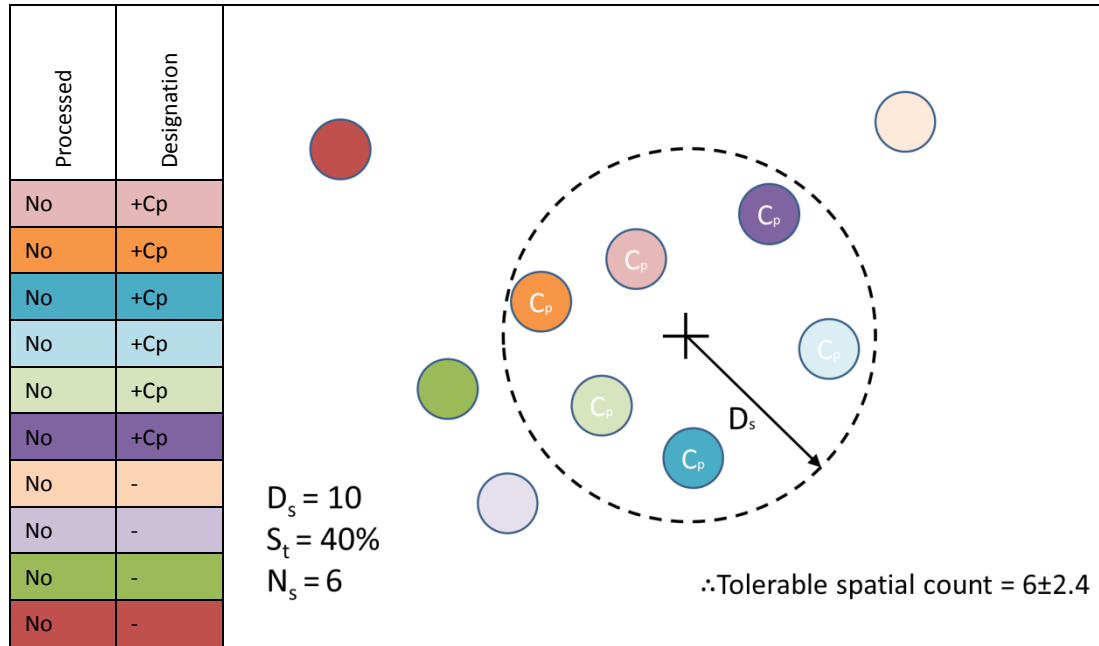
- 1 If additional potential core events remain in list then continue processing of potential core events (repeat Step Three).
- 2 If no additional potential core events remain to be processed then the output cluster is defined from boundary and core events.

Explanatory notes: This will result in a diminishing list of potential core events and cause the clustering algorithm to cease once no additional potential core events remain to be processed. An example of the stopping condition is provided in **Figure 65**.



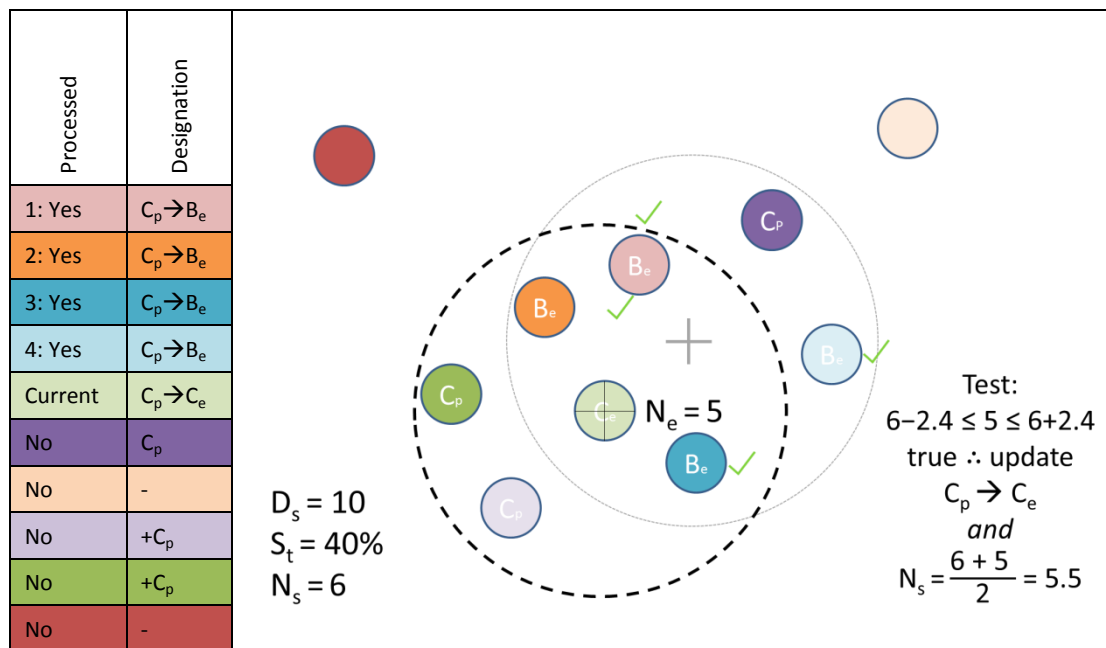
**Figure 61** A comprehensive flow chart are the procedural steps used to achieve spatial clustering of seismic responses.

## Step Two



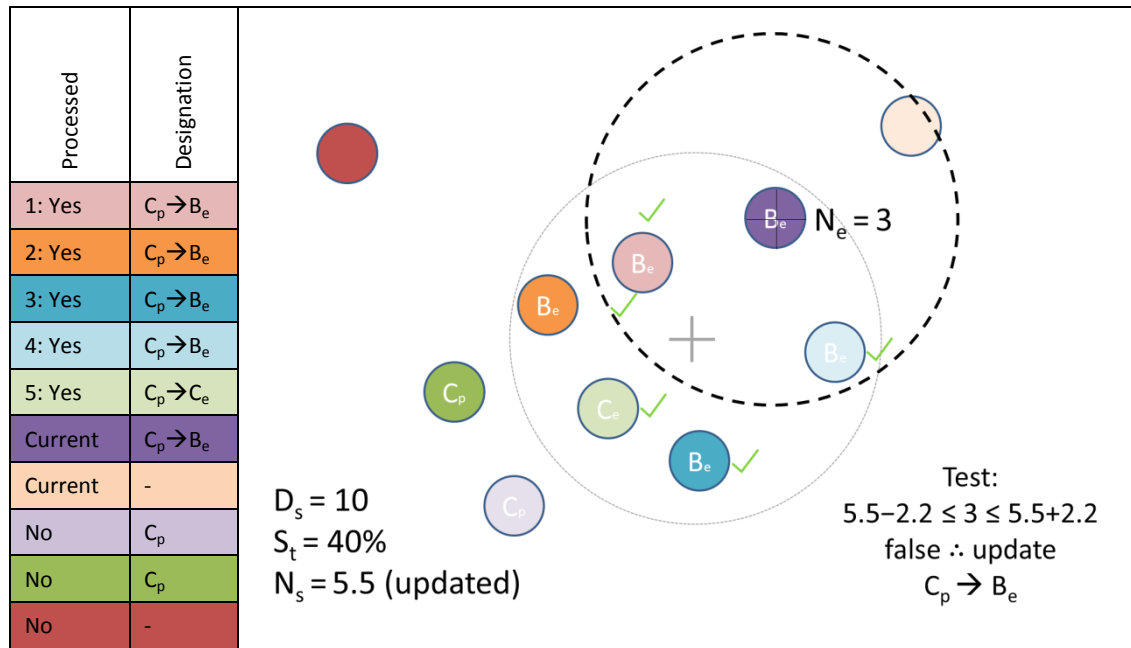
**Figure 62** Initialisation of clustering. Potential core events are all events that occur within  $D_s$  of the response trigger location (black cross). A list of processed events and designations are provided for reference to the clustering procedure (table left).

## Step Three: Condition A



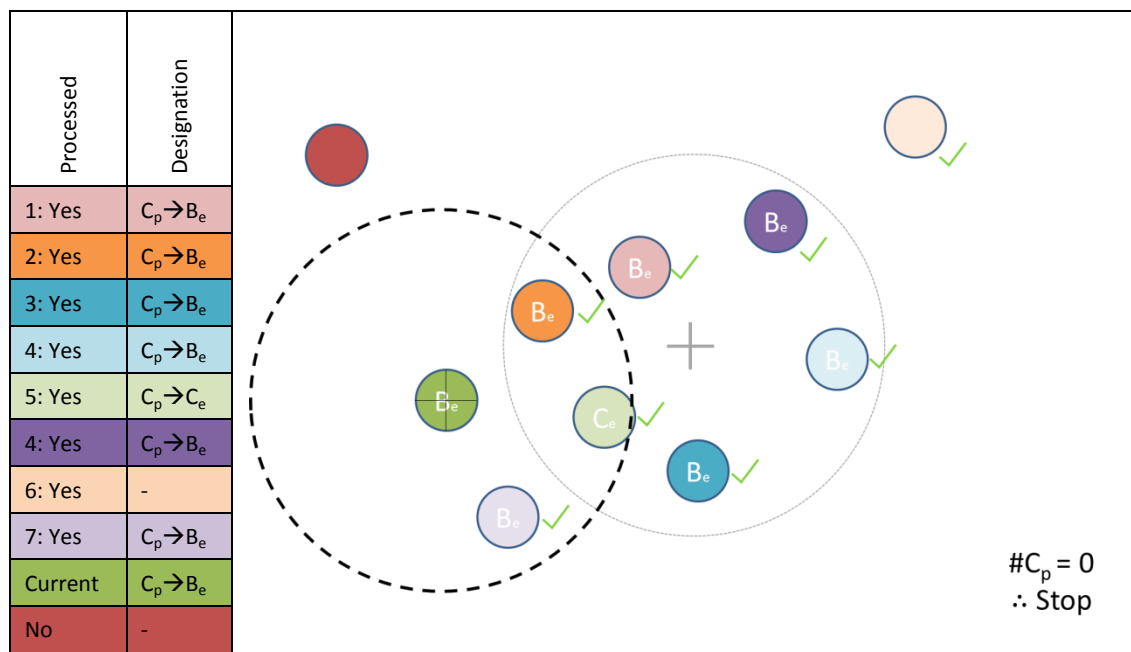
**Figure 63** Processing of a potential core event resulting in a core event designation as the count surrounding of neighbouring events is within the allowable tolerance. Search centre and limits are shown with dashed lines for the initial search (grey) and the search (black). A list of processed events and designations are provided for reference to the clustering procedure (table left).

### Step Three: Condition B



**Figure 64** Processing of a potential core event resulting in a boundary event designation as the event count surrounding potential core event is outside of the allowable tolerance. Search centre and limits are shown with dashed lines for the initial search (grey) and the search (black). A list of processed events and designations are provided for reference to the clustering procedure (table left).

### Step Four



**Figure 65** *If there are no additional potential core events remaining to be processed then clustering is complete. Search centre and limits are shown with dashed lines for the initial search (grey) and the final search (black). A list of processed events and designations are provided for reference to the general clustering procedure (table left).*

## 4.5 Spatial Clustering Validation and Performance

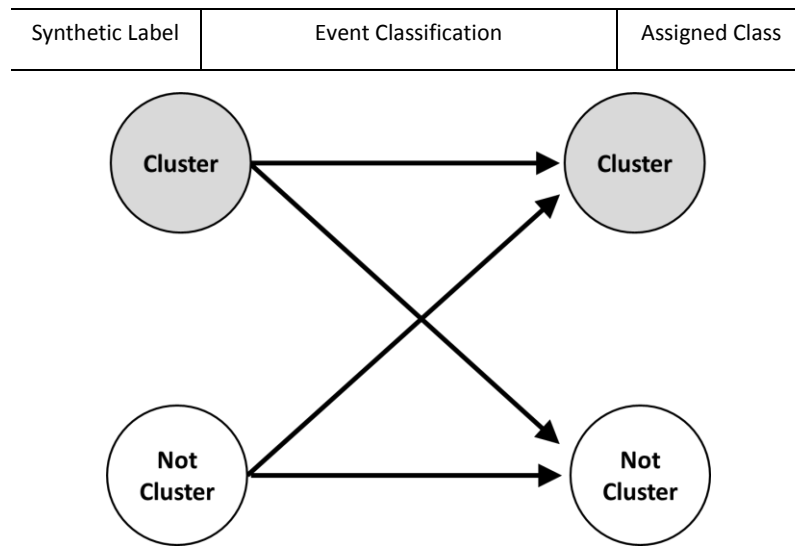
Assessment of clustering performance has not been addressed for mining induced seismicity despite relevant techniques having been developed and applied to numerous fields of science (Baldi et al. 2000; Aliguliyev 2009). Assessments of the performance of clustering methods is summarised by two broad categories. Firstly, external cluster validation uses prior knowledge of the dataset and focuses on truth class labels. Secondly, internal clustering validation assesses the cohesion (similarity individual cluster elements) and separation of clusters without prior knowledge of the element labels. The approach undertaken to understand the errors associated with spatial clustering of seismicity can be summarised in four steps:

1. Generation of synthetic scenarios (one or more seismic responses with realistic spatial distributions);
2. Applying spatial clustering to identify and delineate responses;
3. Synthetic responses and clustering outcomes are compared to quantified errors using an external cluster validation approach; and
4. Characteristics of clustering outcomes are assessed with an internal cluster validation approach.

Classification tasks assign labelled items to predefined classes. There are four general types of classification tasks (Sokolova & Lapalme 2009):

1. Binary classification assigns items into one of two non-overlapping classes.
2. Multi-class classification assigns items into one of 'n' non-overlapping classes.
3. Multi-label classification assigns items into multiple of 'n' non-overlapping classes.
4. Hierarchical classification assigns items into one class that is subdivided or grouped.

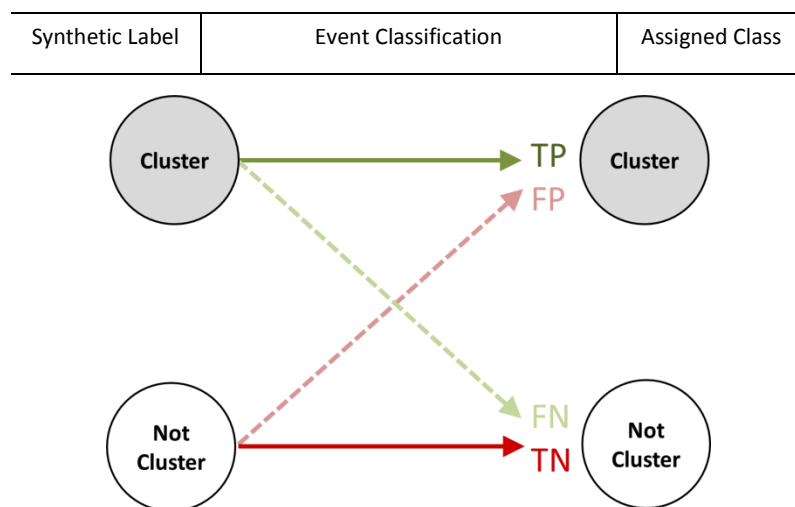
The binary classification of clustered synthetic seismicity compares the unique synthetic label of an element to a unique class assigned by the clustering procedure. This fundamental concept is illustrated in **Figure 66**. Binary classification is appropriate for this task and is a pragmatic selection due to the straightforward interpretation of classification results.



**Figure 66** Binary classification of seismic events. Synthetically generated element labels (cluster or not cluster) are classified as element classes (cluster or not cluster).

The performance of the spatial clustering algorithm is tested by examining a simple binary classification scheme. This analysis quantifies the types of errors that may result from clustering commonly observed distributions of seismic responses along with the sensitivity of analysis to input parameters.

The correctness of a classification can be evaluated by computing the number of class elements recognised correctly (true positives, TP) and incorrectly (false positives, FP), along with the number of non-class elements recognised correctly (true negatives, TN) and incorrectly (false negatives, FN). The derivation of item classifications is illustrated with respect to the binary classification of events in **Figure 67**. The four counts of item classifications constitute the confusion matrix shown in **Table 9**.



**Figure 67** Confusion matrix classifications (TP, FP, FN, and TN) are derived from of item classifications.

**Table 9** Confusion matrix derived from item classifications of synthetic label and assigned classes.

Outcome	Synthetic Label	
	Condition Positive	Condition Negative
Cluster True	True Positive	False Positive
Cluster False	False Negative	True Negative

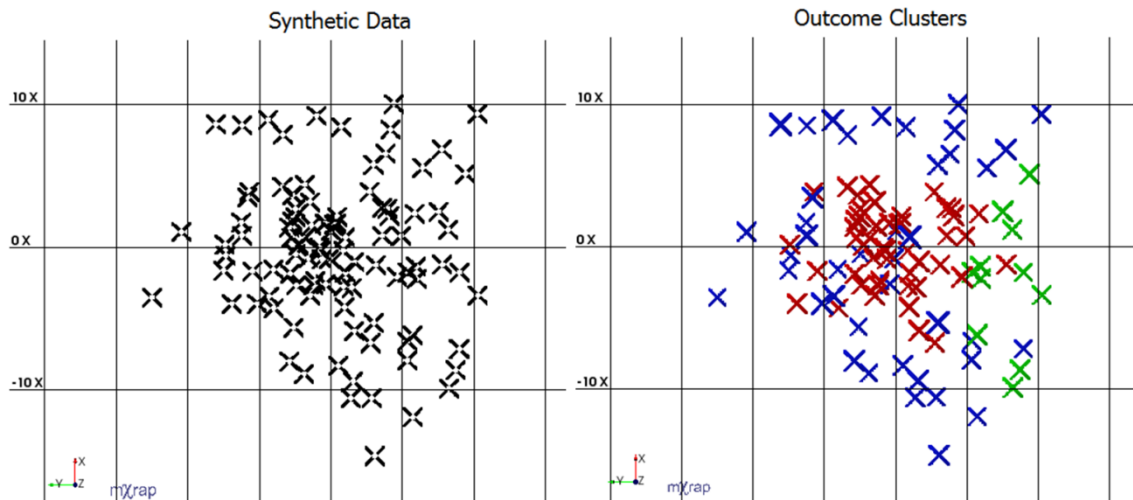
Generating synthetic seismic data that overlaps in space and time requires generalisations to determine assigned classes and item classifications with a consistent methodology. These decisions are based on which assigned class are associated with which synthetic label and become increasingly more complex when one or more assigned classes are delineated for a single synthetic label. It is paramount to establish a consistent framework so item classifications are comparable under different synthetic scenarios.

To ensure synthetic labels are assigned to classes consistently for each synthetic label, the class that contains the most elements of a synthetic label is considered as the positively assigned class. All other assigned classes are considered the false assigned class, e.g., given a case where two seismic responses (two synthetic labels) have been grouped into one cluster (one assigned class), the same cluster will be the positive classification for both of these responses. Conversely, if a seismic response (one synthetic label) results in delineation of three clusters (assigned classes), the cluster that captures the most of the synthetic response is considered the only correct outcome cluster.

#### 4.5.1 Single Response Scenario

A single response scenario is presented to illustrate the approach taken to allocate event classifications and to introduce the approach of synthetically generating spatial distributions of seismicity. Spatial clustering of a single synthetic response is the simplest case of classifying errors. A single response is constructed from 100 events with locations sampled from a normal distribution for each coordinate component. For example,  $\text{mean}[x,y,z] = \mu[0,0,0]$ ; and standard deviation  $[x,y,z] = \sigma[5,5,5]$ . The standard deviation of the normal distribution measures event dispersion throughout space and is referred to as the scale of the response. For illustrative purposes, this response is clustered using search distance equivalent to the spatial scale (5) and no spatial density tolerance. The use of suboptimal clustering parameters results in the erroneous classification of events. For the single synthetic label, **Figure 68** shows three assigned classes as a red cluster (47 events), a blue cluster (42 events), and a green cluster (11 events). This information can be summarised in a confusion table assuming that the largest cluster (red) is the true outcome, and the blue and green clusters are false outcomes

(Table 10). It is not possible for an event to have a negative synthetic label as there is only one synthetic label.



**Figure 68** Left: Synthetically generated events belonging to one cluster label. Right: Spatial clustering using erroneous parameters resulted in three outcome clusters (red, blue, and green).

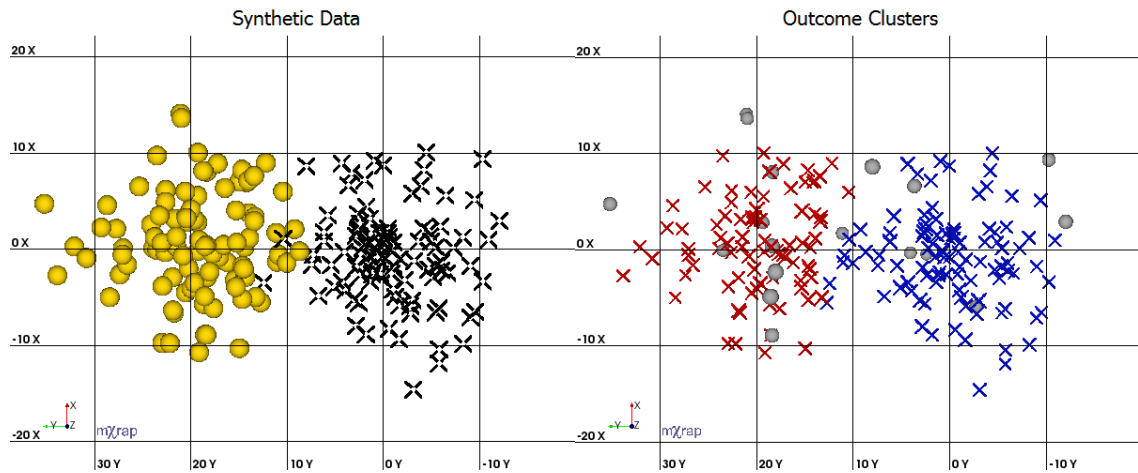
**Table 10** The confusion matrix for binary classification of a single synthetic response. The size of the cluster is intentionally underestimated by erroneous parameters.

Outcome	Synthetic Label	
	Black Cross	
	Condition Positive	Condition Negative
Cluster True	47	0
Cluster False	53	0

#### 4.5.2 Multiple Response Scenarios

A significant component of spatial clustering is the ability to delineate multiple seismic responses occurring during the same time and, therefore, error classification should consider scenarios where multiple synthetic labels are used. A simple scenario is to consider two responses synthetically generated containing one hundred events (per response) with locations sampled from normal distributions: Response one ( $\mu[0,0,0]$ ,  $\sigma[5,5,5]$ ) and Response two ( $\mu[0,20,0]$ ,  $\sigma[5,5,5]$ ). The distance between the mean of the two responses normal distribution provides a measure of separation. The synthetic label best represented by a cluster is considered the true outcome, e.g., the yellow label is clustered by the red outcome label, while the black label is clustered by the blue outcome label (**Figure 69**). A combined confusion matrix is constructed from these results by adding classifications for each synthetic label and normalising results by the total number of synthetic events. These results are summarised by the confusion matrix for each of the synthetic label classifications, along with a

combined matrix for the scenario (**Table 11**). This example is spatially clustered using a search distance twice as large as the response scale (10) and a spatial density tolerance of 10%.



**Figure 69** Left: Synthetically generated events belonging to two cluster labels (yellow spheres and black crosses). Right: Spatial clustering resulted in three outcome clusters (red, blue, and grey) of which, red and blue clusters are representative of the synthetic labels.

**Table 11** Confusion matrices for the two synthetic labels and generally accurate, corresponding outcome clusters. The confusion matrix for the combined synthetic labels and scenario outcome is derived from the combined corresponding cells from the two results.

Blue Cluster	Synthetic Label Black Crosses		Red Cluster	Synthetic Label Yellow Spheres			Synthetic Label Combined	
	Condition Positive	Condition Negative		Condition Positive	Condition Negative		Condition Positive	Condition Negative
Cluster True	94	9	Cluster True	75	1	Cluster True	$\frac{94+75}{200}$	$\frac{9+1}{200}$
Cluster False	6	91	Cluster False	25	99	Cluster False	$\frac{6+25}{200}$	$\frac{91+99}{200}$

### 4.5.3 A Range of Multiple Response Scenarios

Any one individual test of clustering performance represents a single scenario and is limited when assessing the performance of spatial clustering for a range of scenarios. To investigate how classification errors change over a range of conditions, numerous scenarios are synthetically generated with small incremental changes to the initial scenario parameters. The errors for each scenario are then determined and charted for the range of parameters.

A range of scenarios is constructed to explore the ability for spatial clustering to separate two responses that are a variable distance from each other. Similar to the example given in **Figure 69**, scenarios are constructed that comprise of two responses: Response one ( $\mu[0,0,0]$ ,  $\sigma[5,5,5]$ ) and Response two ( $\mu[0, 5+\Delta,0]$ ,  $\sigma[5,5,5]$ ). For each successive scenario, response two is moved away from response one by a small incremental change ( $\Delta$ ). A ratio is defined to

express the separation of two responses with the same spatial scale (**Equation 13**). An example of calculating the  $\Psi$  ratio value is provided in **Figure 70**.

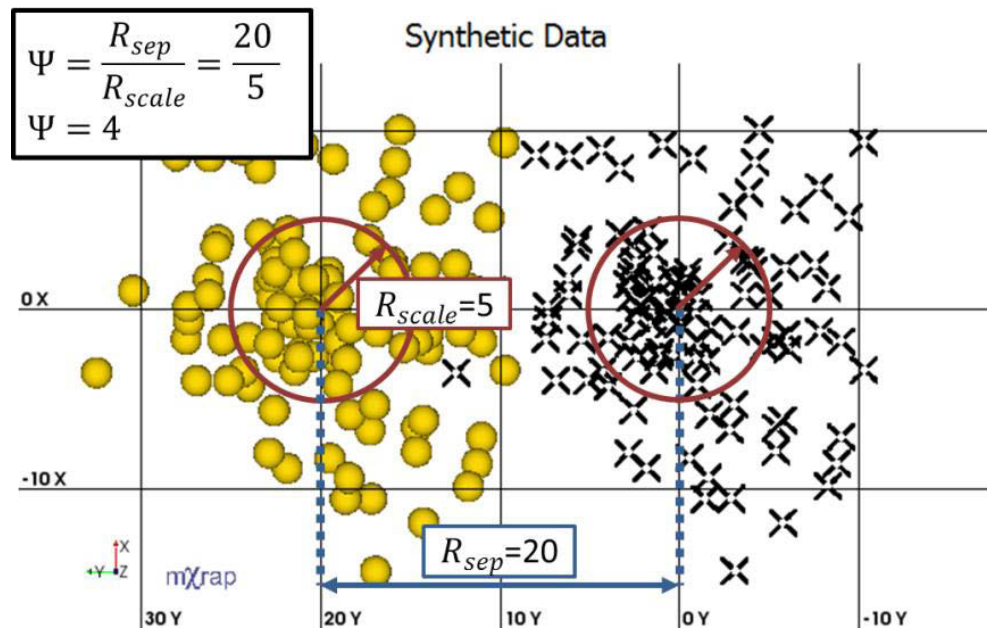
$$\Psi = \frac{R_{sep}}{R_{scale}} \quad \text{Equation 13}$$

Where,

$\Psi$ : Ratio between response separation and scale

$R_{scale}$ : Synthetic response scale (normal distribution standard deviation)

$R_{sep}$ : Separation between synthetic responses

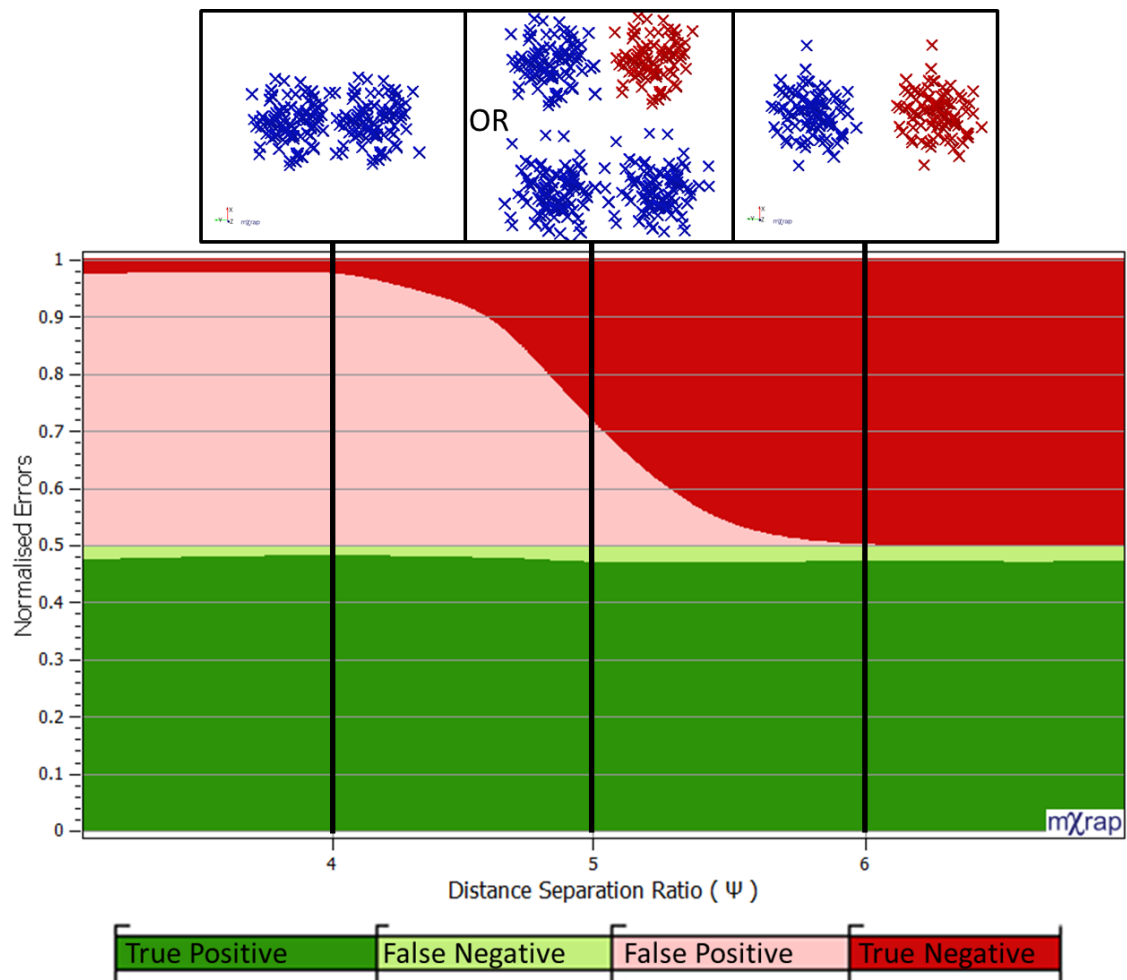


**Figure 70** An example of the determination of the ratio  $\Psi$  between response separation (blue annotation:  $R_{sep}=20$ ) and response scale (red annotation:  $R_{scale}=5$ ).

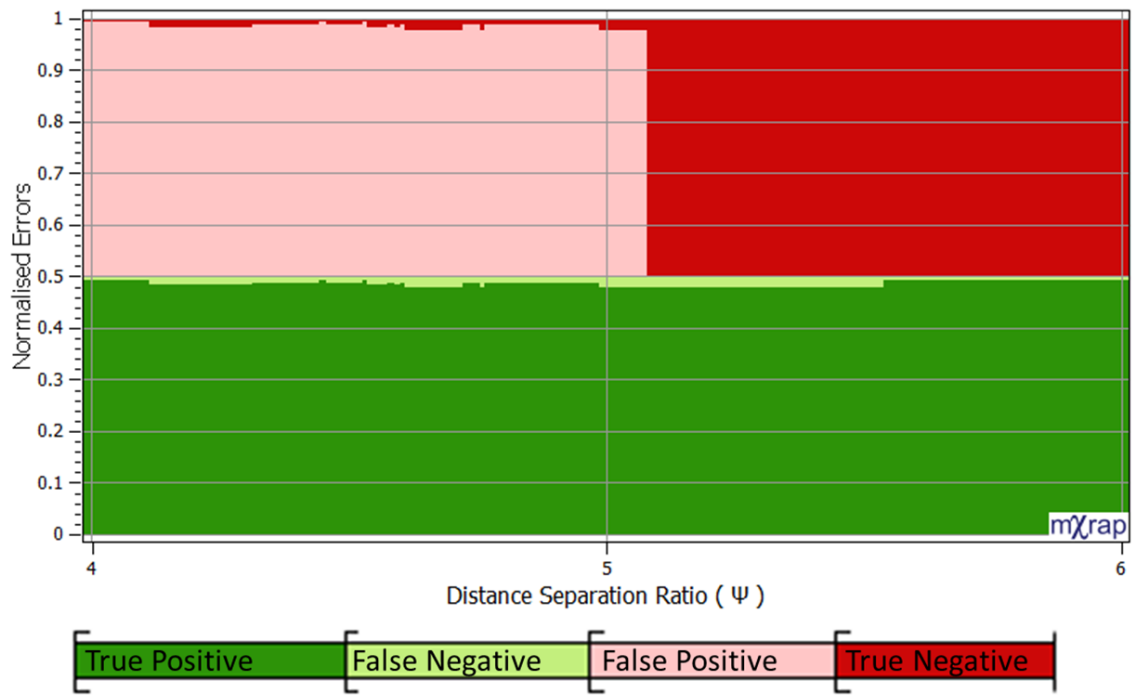
**Figure 71** shows the clustering results for a range of scenarios with an incremental separation increase. This assessment used a search distance twice as large as the response scale (10) and a spatial count tolerance of 10%. When the spatial separation between the two responses is relatively small ( $4\Psi$ ), analysis of these responses result in one cluster. A spatial plot excerpt for this result is shown at the top of the figure. The true positive classifications are high and show that almost all of the response events have been captured. This is shown by the y-axis indicating  $\approx 48\%$  (of the 50% available) are true positives, leaving  $\approx 2\%$  false negative errors. The false negatives are also high and show that clusters have also erroneously captured almost all events belonging to the other response. This is shown by the y-axis indicating  $\approx 45\%$  (of the 50% available) are false negatives, leaving  $\approx 5\%$  true negative classifications.

Increasing the separation between responses to  $5\Psi$  causes a 25% reduction in false negatives, with the same increase to true negative classifications. The false positive reduction at a separation of  $5\Psi$  is not due to responses being half clustered. Instead, this result is due to half

of the responses being clustered as a single response and the other half being delineated accurately. The distribution of errors is influenced by the random sampling of locations rather than inconsistencies in the spatial clustering method. **Figure 72** shows the distribution of errors for the same analysis presented in **Figure 71** without the resampling of event locations for each scenario, i.e., the relative event location is the same within an individual response. There is an immediate transition from clustering two responses as one, to accurate clustering of both responses for this sample of event locations. The distribution of errors in **Figure 71** is effectively the superimposition of the error distributions associated with many randomly sampled responses. **Figure 71** shows a further increase in separation to  $6\Psi$ , results in almost all true classifications and indicates that responses can be separated reliably, irrespectively of variation in event locations.



**Figure 71** The normalised errors (y-axis) for a range of scenarios of increasing response separations (x-axis). Separation is expressed as a ratio of the distance between distribution means and response scale, with excerpt spatial plots at  $4\Psi$ ,  $5\Psi$ , and  $6\Psi$  provided for reference.



**Figure 72** The normalised errors (y-axis) for a scenario of increasing response separation (x-axis). Note that event locations are not resampled for each new scenario.

Two responses are sampled from two normal distributions with the same mean location in order to examine the superimposition of dense and sparse synthetic responses. A ratio is defined to express the relative scales between a response with a constant scale and a response with a variable scale (**Equation 14**). **Figure 73** provides an example of calculating the  $\Phi$  ratio.

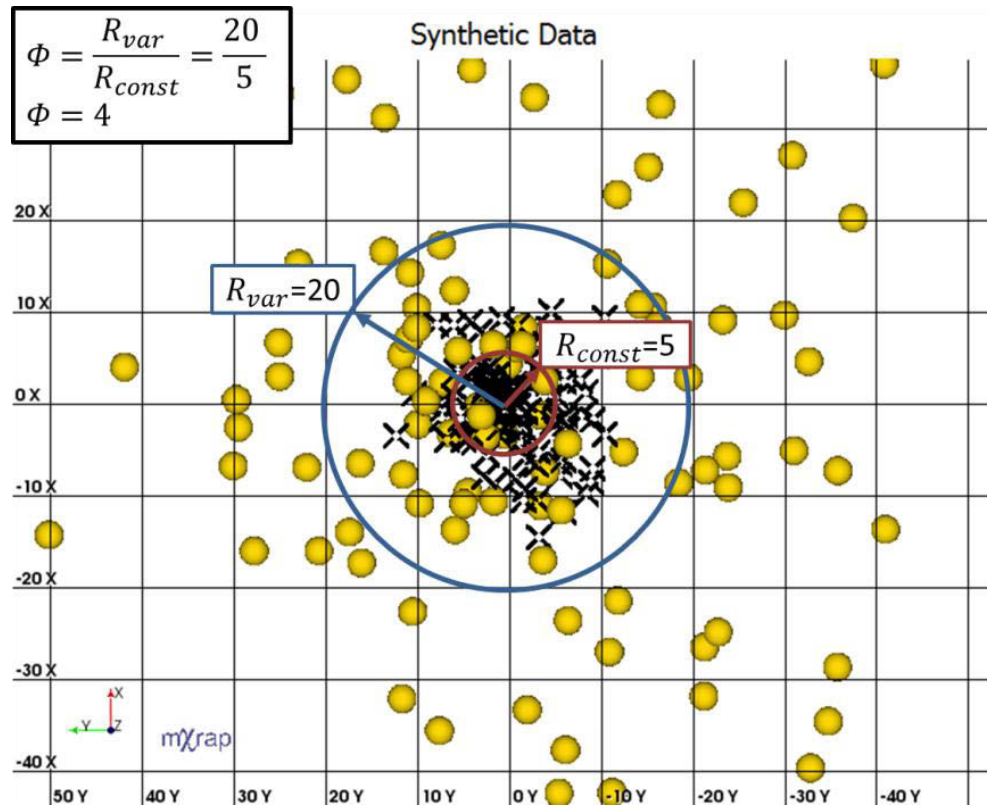
$$\Phi = \frac{R_{var}}{R_{const}} \quad \text{Equation 14}$$

Where,

$\Phi$ : Ratio between the variable response scale and constant response scale

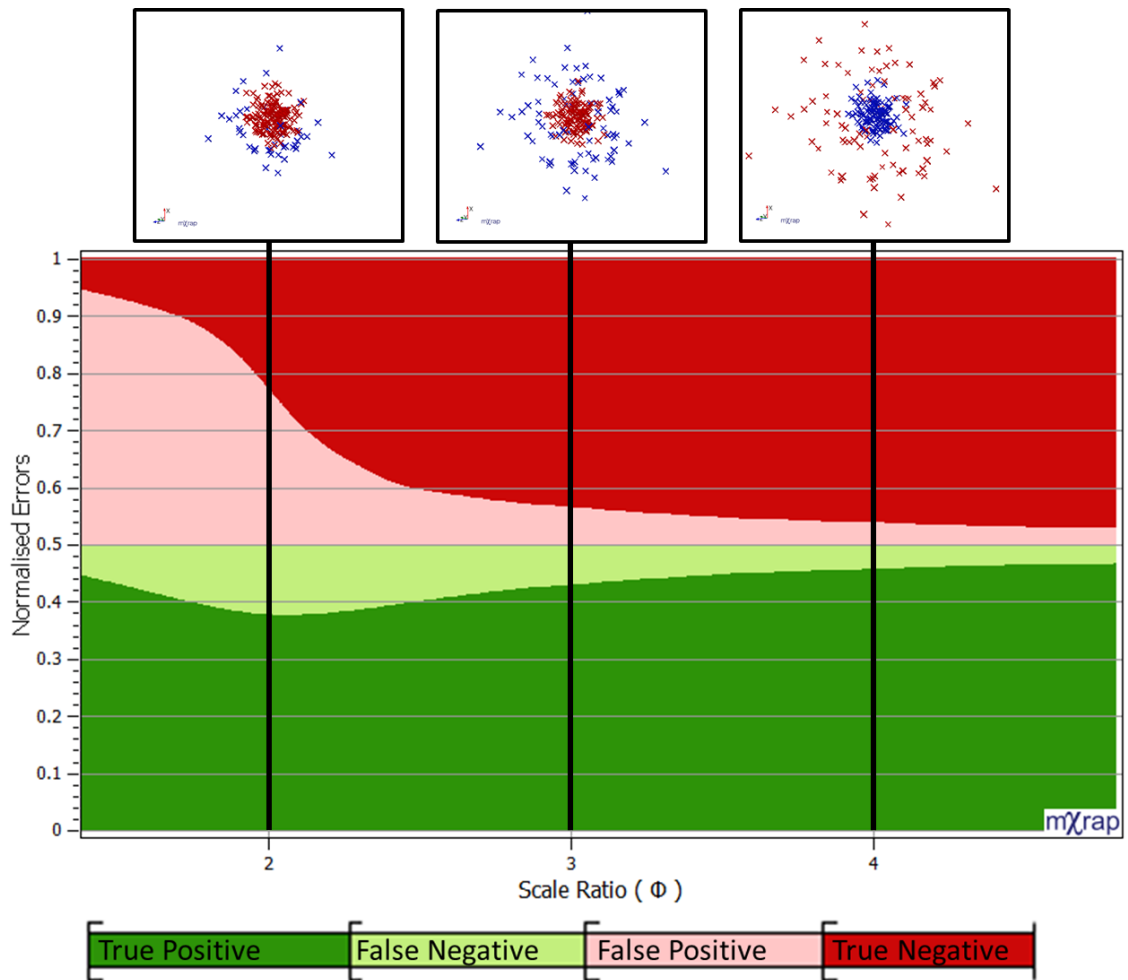
$R_{var}$ : Variable response scale (standard deviation of the normal distribution)

$R_{const}$ : Constant response scale (standard deviation of the normal distribution)



**Figure 73** Example of the determination of the ratio  $\Phi$  between a constant response scale (red annotation:  $R_{const}=5$ ) and a variable response scale (blue annotation:  $R_{var}=20$ ).

A range of scenarios is constructed to explore the ability for spatial clustering to separate superimposed responses with varying scales (**Figure 74**). Each scenario comprises of two responses that are synthetically generated from normally distributed event locations: Response one ( $\mu[0,0,0]$ ,  $\sigma[5,5,5]$ ), and Response two ( $\mu[0,0,0]$ ,  $\sigma[5+\Delta,5+\Delta,5+\Delta]$ ), where  $\Delta$  is a small incremental increase to the response scale. These scenarios are clustered using a search distance of twice as large the response scale (10) and a spatial count tolerance of 10%. Samples of spatial distributions of outcome clusters are shown by excerpts at the top of **Figure 74** for relative scale ratios of  $2\Phi$ ,  $3\Phi$ , and  $4\Phi$ . The number of false negatives is large when the scales of the two responses are similar ( $2\Phi$ ). As the relative scale ratio increases (3 and  $4\Phi$ ) there are less errors. It is impossible to separate superimposed responses perfectly despite a decrease in errors.



**Figure 74** An example of the distribution of errors associated with a scenario that examines increasing relative scale. The number of false negatives is large when scales are relatively similar ( $2\Phi$ ). The resultant errors decrease by increasing the relative scale ratio (3 and  $4\Phi$ ).

#### 4.5.4 External Performance Measures

The previous assessment examines the distribution of errors for a single search distance and spatial gradient. In practice, the optimal ideal clustering parameters are not known prior to assessment and, hence, it is desirable to consider the same range of scenarios using a number of clustering parameters.

In order to simplify the interpretation of when errors are minimised, the binary classifications can be combined into a measure that represent the success of clustering a scenario. Common measures of binary classifiers are expressed using terminology and definitions that can be specific to the field of study, e.g., medical, quality assurance, and computer science. While many measures of errors exist, their assessment depends on the focus and application of the classification system. Measures of errors should avoid assumptions concerning the distributions of errors while also avoiding the selection of measures that achieve improved performance by manipulating the definition of incorrect classifications (Parker 2011). For the

purpose of this thesis, the definition of combined performance measures are adopted from Sokolova and Lapalme (2009) and Matthews (1975). An overview of commonly implemented performance measures is provided in **Table 12**. This list is an overview and is not exhaustive.

**Table 12** Measures and the focus of binary classification errors. The equation for each measure is also detailed (Matthews 1975; Sokolova & Lapalme 2009).

Measure	Focus	Equation
Sensitivity (True positive rate)	The portion of correctly predicted positive elements - effectiveness to identify positive classes.	$\frac{TP}{TP + FN}$
Specificity (True negative rate)	The portion of correctly predicted negative elements - effectiveness to identify negative classes.	$\frac{TN}{TN + FP}$
F <sub>β</sub> -score	Relation between positive observed and predicted labels. β weights the importance of label classifications.	$\frac{(1 + \beta^2)TP}{(1 + \beta^2)TP + \beta^2FN + FP}$
Matthews Correlation Coefficient (MCC)	MCC is a correlation coefficient between the observed and outcome labels. The measure is a number between -1 (total disagreement) to 0 (random prediction), 1 (total agreement).	$\frac{(TP \times TN) - (FP \times FN)}{\sqrt{(TP + FN) \times (TN + FP) \times (TP + FP) \times (TN + FN)}}$

There are many measures of performance which have been employed to simplify the interpretation of external classifications results (Sokolova & Lapalme 2009). It is essential that the performance measure selected is able to represent the success of clustering by limiting the type of errors considered. While the F<sub>β</sub> score provides a measure of positive identification errors and is practical as a single measure of performance (Parker 2011), this measure does not include a measure of negative predictive performance. In order to represent the objectives of clustering seismic events with a single measure, it is required that the performance of positive and negative class identification is evaluated.

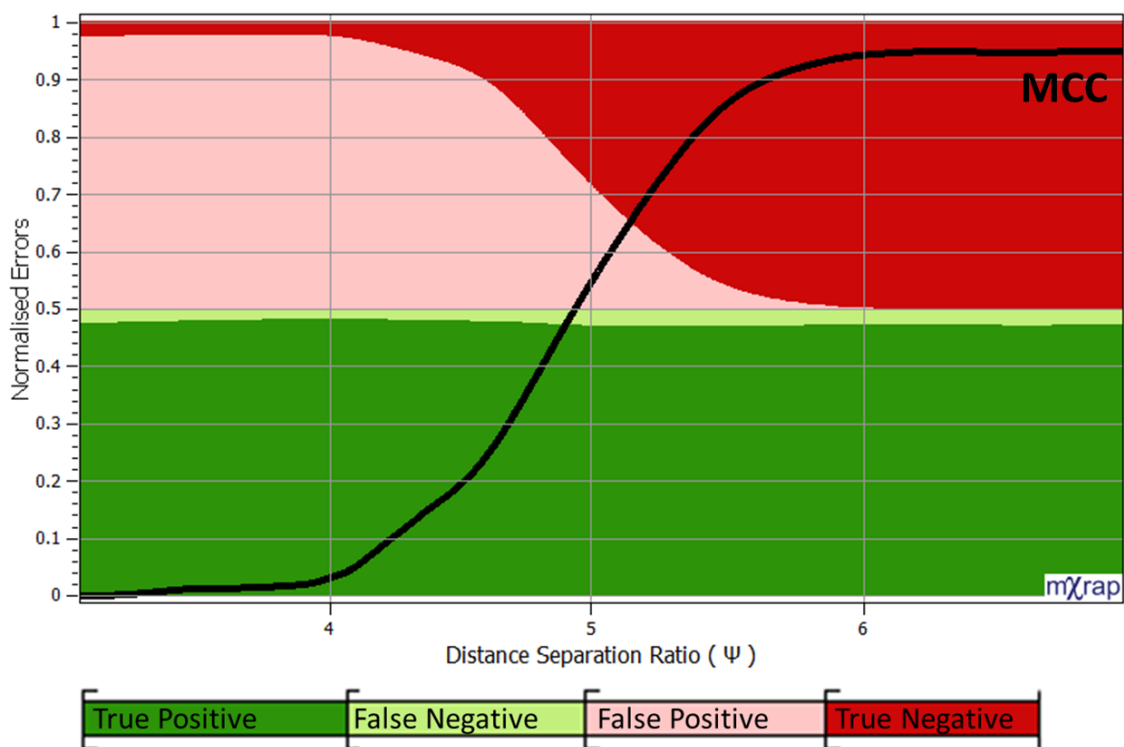
The Matthews correlation coefficient (MCC) is a measure of the performance between observed and outcome labels (Matthews 1975). MCC values indicate:

- -1: A perfect negative correlation, i.e., all observed labels were not outcome labels.
- 0: No correlation, i.e., random prediction.
- 1: A perfect positive correlation, i.e., all observed labels were outcome labels.

The MCC measure incorporates all four classifications discussed in **Table 9** and is generally balanced, although, may misrepresent error in specific cases. One example is, when relatively few true positive elements and few false positive elements exist (Baldi et al. 2000). The

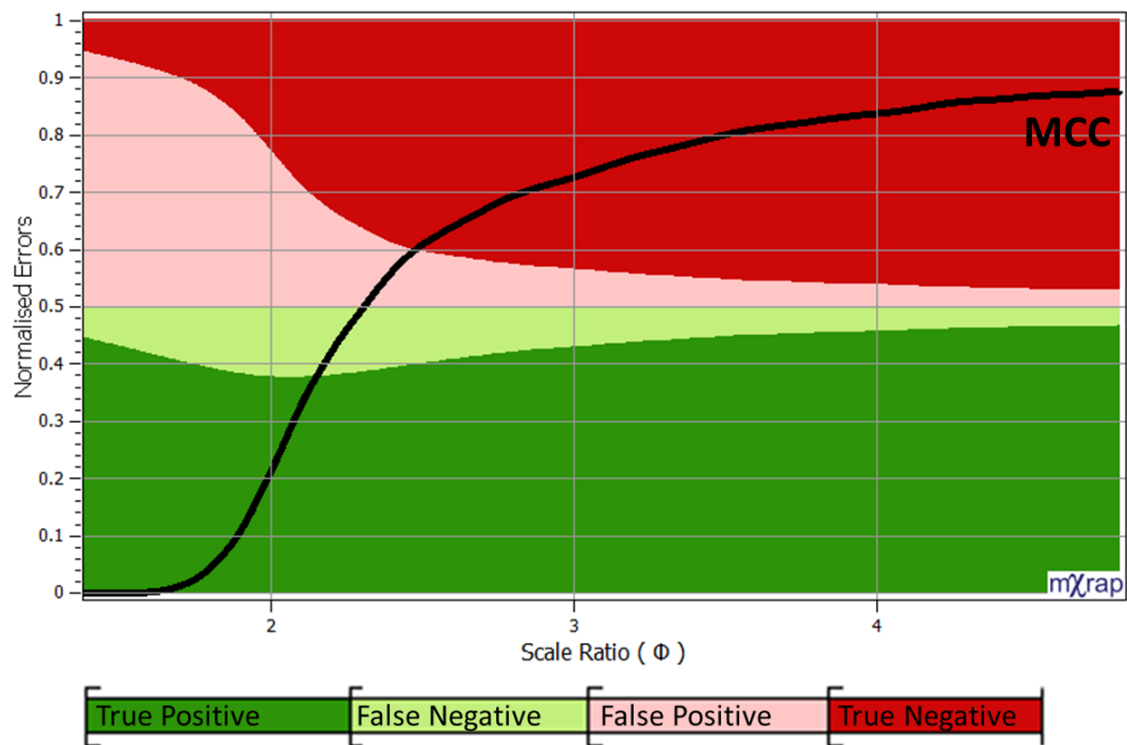
shortcomings associated with the use of the MCC occur during extreme cases and will be limited for realistic testing of seismic scenarios. The MCC is a coherent and general measure of performance (Parker 2011) and is adopted as it offers an interpretable summary of classification results.

The distribution of errors is summarised by trends in the MCC performance measure (**Figure 75**) for the range of scenarios with increasing separations previously presented in **Figure 71**. At low separations, the MCC indicates there is no correlation between synthetic labels and outcome clusters. The MCC increases as the correlation between synthetic labels and outcome clusters becomes stronger (4 to  $6\Psi$ ) before reaching a very strong positive correlation for separation greater than  $6\Psi$  response scale.



**Figure 75** An example of the distribution of errors and trends in MCC associated with a scenario that examines an increasing separation between responses. The MCC increases from no correlation ( $<4\Psi$ ) to a very strong positive correlation ( $>6\Psi$ ).

The distribution of errors is summarised by the MCC measure for scenarios with an increasing relative scale (**Figure 76**). At low relative scales, the MCC indicates there is no correlation between synthetic labels and outcome clusters. The MCC gradually increases as the correlation between synthetic labels and outcome clusters becomes stronger. The gradual increase in MCC reflects that relatively less of the sparse response is superimposed with the dense response as the relative scale ratio ( $\Phi$ ) increases.



**Figure 76** An example of the distribution of errors and trends in MCC associated with a scenario that examines an increasing relative scale. With an increasing relative scale, the MCC gradually improves as responses can be separated.

#### 4.5.5 Internal Performance Measures

Internal performance measures address the inability of external measures to quantify errors without prior knowledge of the dataset. Performance measures quantify the characteristics of clustered elements to determine optimal clustering parameters (Halkidi, Batistakis & Vazirgiannis 2002), e.g., the number of clusters for k-means clustering (Liu et al. 2010), or the cardinality and search distance for density-based clustering (Deborah, Baskaran & Kannan 2010).

Liu et al. (2010) provided an overview of eleven different internal validation measures that evaluate the similarity of elements within a cluster and distinctness of clusters from each other. With the aim to identify the correct number of clusters within synthetic datasets, this study assessed internal performance indicators with respect to various cluster characteristics. These characteristics were monotonic clusters, inclusion of noise, density variation, inclusion of sub-clusters, and skewedness (unequal number of elements in each cluster). Liu et al. (2010) showed that all methods have limitations with respect to these clustering characteristics with the exception of the SDbw validity index (SDbw) which found the true number of clusters in all tested cases. The details of this method are provided by Halkidi and Vazirgiannis (2001).

SDbw is found by the minimisation of two terms that are combined into a single internal performance measure:

1. Intra-cluster compactness (similarity of elements within a cluster) is assessed by evaluating the variance in densities of cluster elements.
2. Inter-cluster separation is assessed based on the premise that the density of cluster pairs should be greater than the density at the midpoint between the two clusters.

The definition of optimal clustering is specified by the measures that are considered by the SDbw. The applicability of these measures is underpinned by assumptions of the datasets general characteristics. SDbw is known to work well for compact and well-separated clusters and also performs well for non-standard shaped clusters (Deborah, Baskaran & Kannan 2010). The index is not applicable to complex geometrical structures (Halkidi, Batistakis & Vazirgiannis 2002; Deborah, Baskaran & Kannan 2010), e.g., ring-shaped or curved-shaped structures. Liu et al. (2013) extended the previous work by Liu et al. (2010) to address the shortcomings of previous methods, specifically, the approaches used to define inter-cluster separation. Previous methods use a single object to represent an entire cluster and, hence, reduce the geometrical information associated with the cluster. This method quantifies a CVNN index (**Equation 15**) that is a combination of measures of intra-cluster compactness (**Equation 16**) and inter-cluster separation (**Equation 17**).

**CVNN Index:**

$$CVNN(NC, k) = Sep_{norm}(NC, k) + Com_{norm}(NC) \quad \text{Equation 15}$$

Where,

$Sep_{norm}$ : Normalised separation index

$Com_{norm}$ : Normalised compactness index

Explanatory notes: The index is the normalised summation of measures of cluster compaction and separation. Preferable clustering results are indicated by lower CVNN index values.

**Intra-cluster Compactness:**

$$Com(NC) = \sum_i \left[ \left( \frac{2}{n_i} (n_i - 1) \right) \sum_{x,y \in C_i} d(x,y) \right] \quad \text{Equation 16}$$

Where,

$NC$ : Cluster number

$n_i$ : Number of elements within  $i^{th}$  cluster

$d(x,y)$ : Pairwise distance between elements belonging to  $C_i$

Explanatory notes: Summation of the pairwise distance between elements within a cluster and for all clusters within a dataset (scenario).

**Inter-cluster Separation:**

$$Sep(NC, k) = \max_{i=1,2,\dots,NC} \left( \left( \frac{1}{n_i} \right) \sum_{j=1,2,\dots,n_i} (q_j/k) \right) \quad \text{Equation 17}$$

Where,

$NC$ : Cluster number

$k$ : Number of nearest neighbouring elements considered

$n_i$ : Number of elements within  $i^{th}$  cluster

$q_j$ : Number of  $j^{th}$  nearest neighbour elements not belonging to the  $i^{th}$  cluster

Explanatory notes: For each element within a cluster, find if at least one of  $k^{th}$  nearest neighbours belongs to another cluster. Elements are weighted by the portion of  $k^{th}$  elements that do not belong to the cluster assigned to the element. The inter-cluster separation is the maximum average weighting for all clusters.

To assess the two internal measures of clustering, a comparative analysis is undertaken. SDbw and CVNN results are found for three scenarios of superimposed responses with varying relative scales, and three scenarios of responses with varying separations. These scenarios are the same as **Figure 71** and **Figure 74** but instead of assessing a range of scenarios, critical values for relative response scales and separations are selected for assessment. For each of these six critical values, five thousand scenarios are constructed following the previously detailed normal distributions.

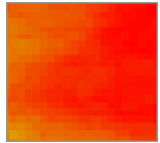

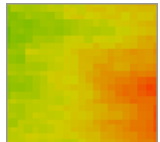



The six datasets (three scenarios of relative scales and three scenarios of separation) are clustered using a range of search distance and tolerance parameters. These ranges are a spatial search between one and four times the response scale and a spatial density tolerance from 0 to 25%.

Stochastic sampling is used to generate event locations to reflect reality. As a result, clustering outcomes may vary for two parametrically identical scenarios. Due to the variation for

individual scenarios, this analysis focuses on the identification of general trends in internal performance measures (SDbw and CVNN). The MCC external performance measure is also considered during this analysis to provide a true measure of clustering for these critical scenarios.

Parametric solution charts are created displaying combinations of search distance (x-axis) and spatial density tolerances (y-axis), with respect to normalised values of MCC, SDbw, and CVNN. The framework for the interpretation of the colour scales for these normalised measures is provided in **Table 13**. Results of parametric solution charts along with a plan view of synthetic responses are tabulated for each of the critical scenarios that have been previously presented. **Table 14** summarises the results for the three critical scenarios of two superimposed responses with varying scales. **Table 15** summarises the results for the three critical scenarios of two responses with varying spatial separation. The discussion of results focuses on the low, medium, and high critical values for scale ratios and separation.

**Table 13** The framework for the general interpretation of the MCC, SDbw, and CVNN colour scales with respect to normalised measures.

MCC	SDbw CVNN	Quantitative Measure	Qualitative Measure
		0.75<	Poor
		0.25 to 0.75	Medium
		<0.25	Good

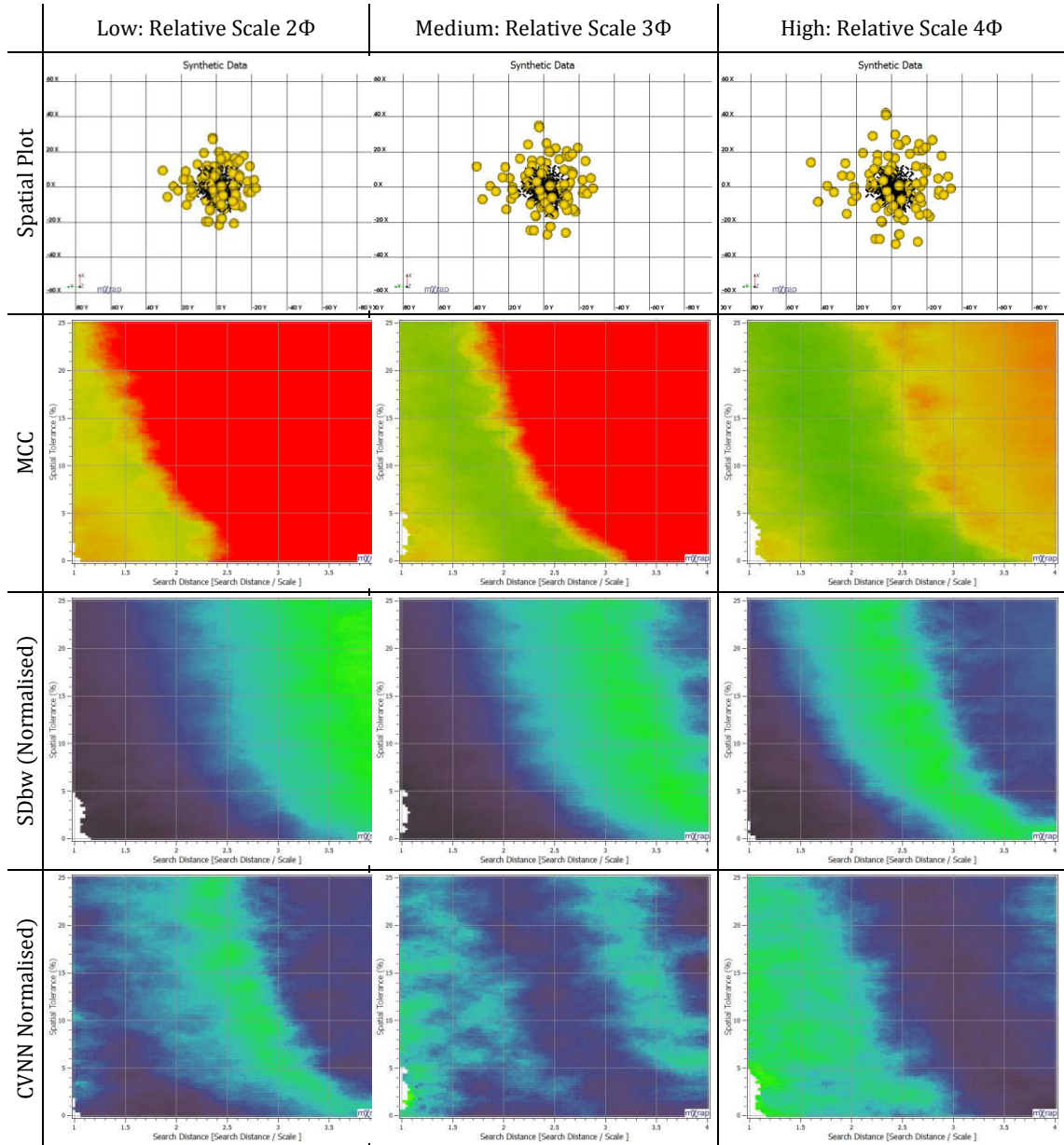
**Low scale ratios and separation:** Both internal indices indicate that parameter ranges that result in a single cluster are optimal. MCC indicates the highest correlation between synthetic labels and cluster outcomes are found when low search distances and tolerances are used. This is due to clustering only delineating a dense centre cluster. The dense cluster contains more of the constant scale response than the only slightly sparser response and, therefore, a relatively higher accuracy is found for these parameters. The relative low absolute accuracy (orange to red MCC) reflects the lack of distinction between the spatial characteristics of responses. Whilst this result is not correct with respect to the initial labels, given the similarity of synthetic responses, the range of parameters suggested by both internal indices result in reasonable cluster outcomes.

**Medium scale ratios and separation:** The two parametric regions are identified by the CVNN and only moderate accuracy is achieved by the MCC. This reflects the similar spatial characteristics for the two synthetic responses. MCC indicates that the most correct answers occur when the search distance is between 2 and 2.5 times the scale of the response. Additionally, an increase to the spatial density tolerance allows accurate clustering outcomes to be found with lower scale ratios. Assessment of both scenarios types using the SDbw results in the optimal parameters to be found when a single cluster is delineated. This is an unfavourable result as the scale and separation characteristics between the two responses are more distinctive. The CVNN index is minimised in the parametric area for a single cluster being identified, although, an additional parametric area is highlighted that represents the correct solution space shown through relatively better MCC values.

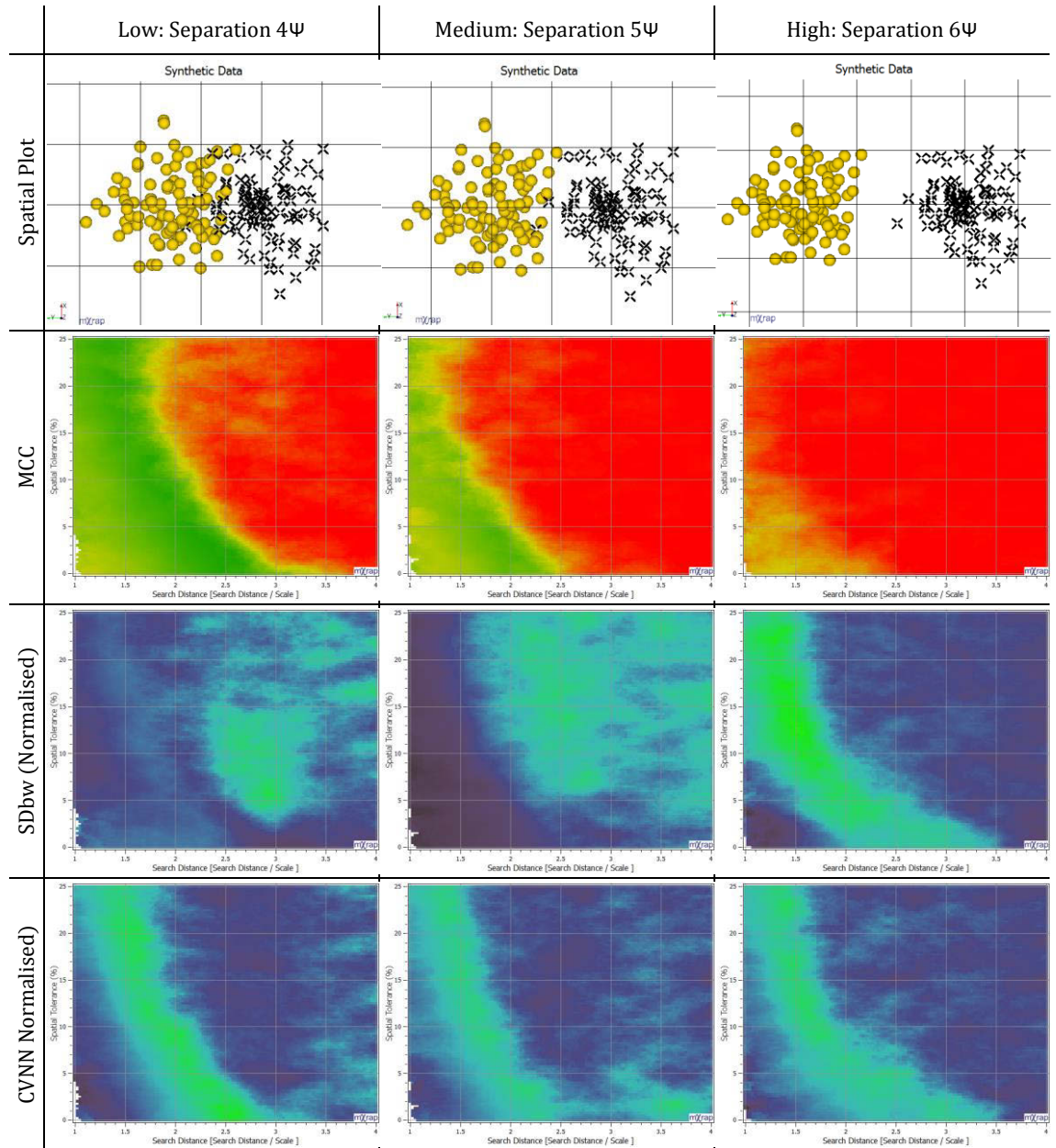
**High scale ratios and separation:** Strong correlations between synthetic labels and cluster outcomes are achieved by the MCC for search distances between 1.5 and 3 times the scale of the response. To a greater degree than the medium scale ratio and separation, increasing spatial density tolerance allows lower search distances to cluster the synthetic responses accurately. Trends in the SDbw and CVNN indices continue from the observations established from the low and medium scenarios. SDbw misrepresents the parametric space with high MCC values and only has a faint representation for the parametric space assessing responses spatially separated. In both cases, the CVNN index can reproduce the parametric space regions that result in highest accuracy clustering.

The CVNN can reproduce the known clustering accuracy quantified by the MCC for relatively high separations ( $4\Phi$  and  $6\Psi$ ), therefore, the CVNN index is preferable to the SDbw index at identifying appropriate search distances and count tolerance values. The CVNN index provides a good indication of appropriate clustering parameters for responses with distinctive spatial characteristics. Furthermore, these results are congruent with the parametric space with the highest correlation between synthetic labels and cluster outcomes, as indicated by the MCC.

**Table 14** Spatial plots and parametric spaces coloured by MCC, SDbw, and CVNN clustering validation measures for three critical scenarios. Each scenario evaluates two superimposed responses with different scales (ranging from 2 to 4 $\Phi$  relative response scale).



**Table 15** Spatial plots and parametric spaces coloured by MCC, SDbw, and CVNN clustering validation measures for three critical scenarios. Each scenario evaluates two responses with different spatial separations (ranging from  $4\psi$  to  $6\psi$  relative separation).

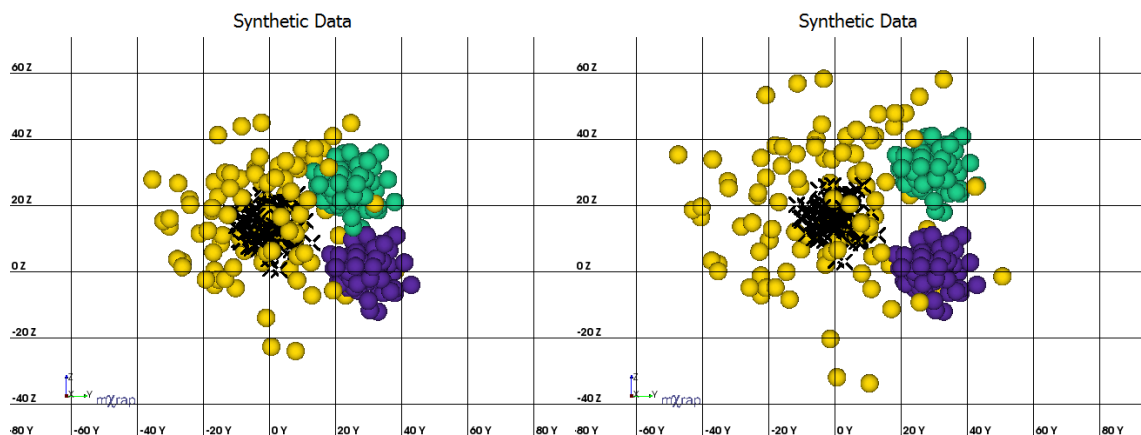


## 4.6 Base Cases for Mining Induced Seismic Response

The fundamental purpose of spatial clustering is to delineate significantly different superimposed or spatially separated seismic responses. In doing so, spatial clustering addresses two key requirements: firstly, the identification of responses independently of non-seismic information and, secondly, the identification of distinguishable responses that are superimposed in space.

### 4.6.1 Synthetic Responses

Given the fundamental purpose of spatial clustering, minimising the CVNN index represents search distance and tolerance parameters that find reasonable solutions. It is undesirable to separate the two responses associated with the cases of low relative scale ( $2\Phi$ ) and separation ( $4\Psi$ ). These responses should be clustered together due to the similarity of spatial distributions. Conversely, for the cases of high relative scale ( $4\Phi$ ) and separation ( $6\Psi$ ) it is warranted to separate these responses due to the difference in spatial distributions. A high relative separation ( $6\Psi$ ) and scale ( $4\Phi$ ) should be able to be separated with a range of parameters. Two relevant cases are constructed to test the ability of the algorithms' to delineate spatial clusters using a range of input parameters. A strict scenario is constructed comprising of two responses with a separation of  $5\Psi$  and two responses with a relative scale of  $3\Phi$  (**Figure 77** left). A lenient scenario is constructed comprising of a separation of  $6\Psi$  and a relative scale of  $4\Phi$  (**Figure 77** right).

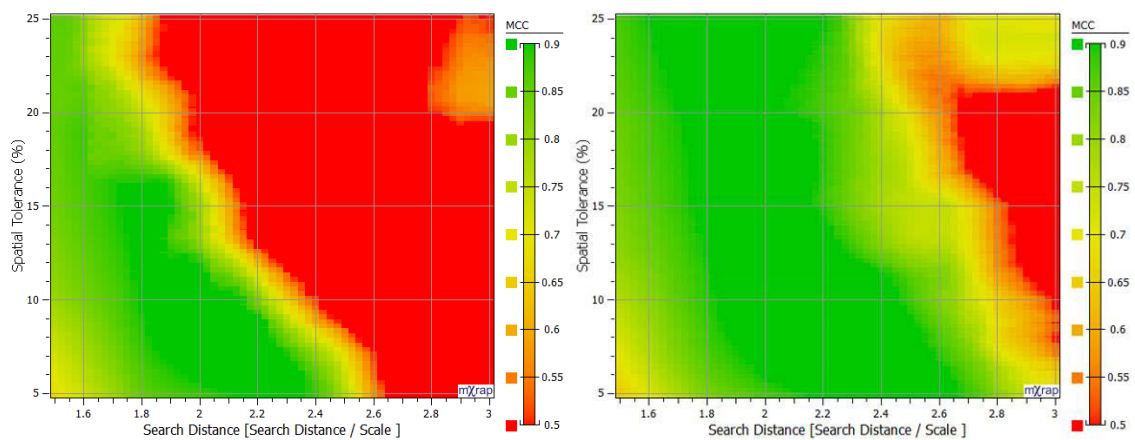


**Figure 77** Plan view comparison of the strict scenario ( $5\Psi$  separation and  $3\Phi$  relative scale) shown left, and the lenient scenario ( $6\Psi$  separation and  $4\Phi$  relative scale) shown right. Each colour corresponds to one of the four responses contained within the scenario.

Strict and lenient scenarios are investigated for a range of search distances (1.3 to 3 times the smallest response scale) and spatial density tolerances (5% to 25%). Five thousand scenarios

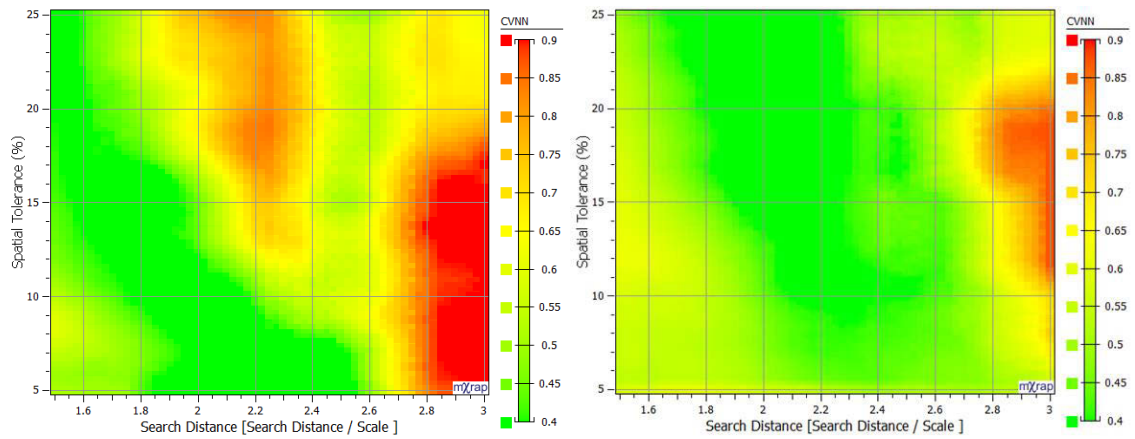
are assessed using unique combinations of the spatial parameters within these ranges. Response scale sets consider constant spatial density tolerances. Search distances are increased four times by discrete multiples of the initially defined search distance, e.g., an initial search distance of 1 and a spatial density tolerance of 10% results in response scale sets: [1, 10%] for the first iteration; [2, 10%] for the second iteration; [3, 10%] for the third iteration; and [4, 10%] for the fourth iteration. A constant lower count threshold of 20 events is used. A temporal modelling window is not used, as temporal modelling is not considered.

The external clustering validation (MCC) shows similar results for the combined scenarios compared to the results presented for the individual separation and relative scale responses (Section 4.5.5). For the strict scenario, there is a clear range of parameters that result in accurate solutions ( $MCC > 0.8$  darker green). This range is a search distance between 1.8 and 2.4 times the spatial scale. The accurate search distance range decreases with an increasing spatial density tolerance (**Figure 78** left). In comparison, the range of parameters is larger for the lenient scenario (1.8 to 2.8) with a weaker decrease in search distance for increasing spatial density tolerance (**Figure 78** right). These results confirm that the lenient scenario can be modelled with a wider range of parameters and, therefore, results are less sensitive to the user definition of the spatial parameters contained within iterative response scale sets.



**Figure 78** MCC results for combinations of search distances and spatial density tolerances attempted for the strict scenario ( $5\Psi$  separation and  $3\Phi$  relative scale) (left) and the lenient scenario ( $6\Psi$  separation and  $4\Phi$  relative scale) (right).

The internal clustering validation (CVNN) mimics the optimal parameters found by the MCC to cluster the strict (**Figure 79** left) and lenient (**Figure 79** right) scenarios. These two measures generally agree, although, there are some differences in trends associated with these solution spaces. In comparison to the MCC, the CVNN index indicates that relatively preferable solutions result from clustering the strict scenario using a search distance of 2.5 and any spatial gradient.

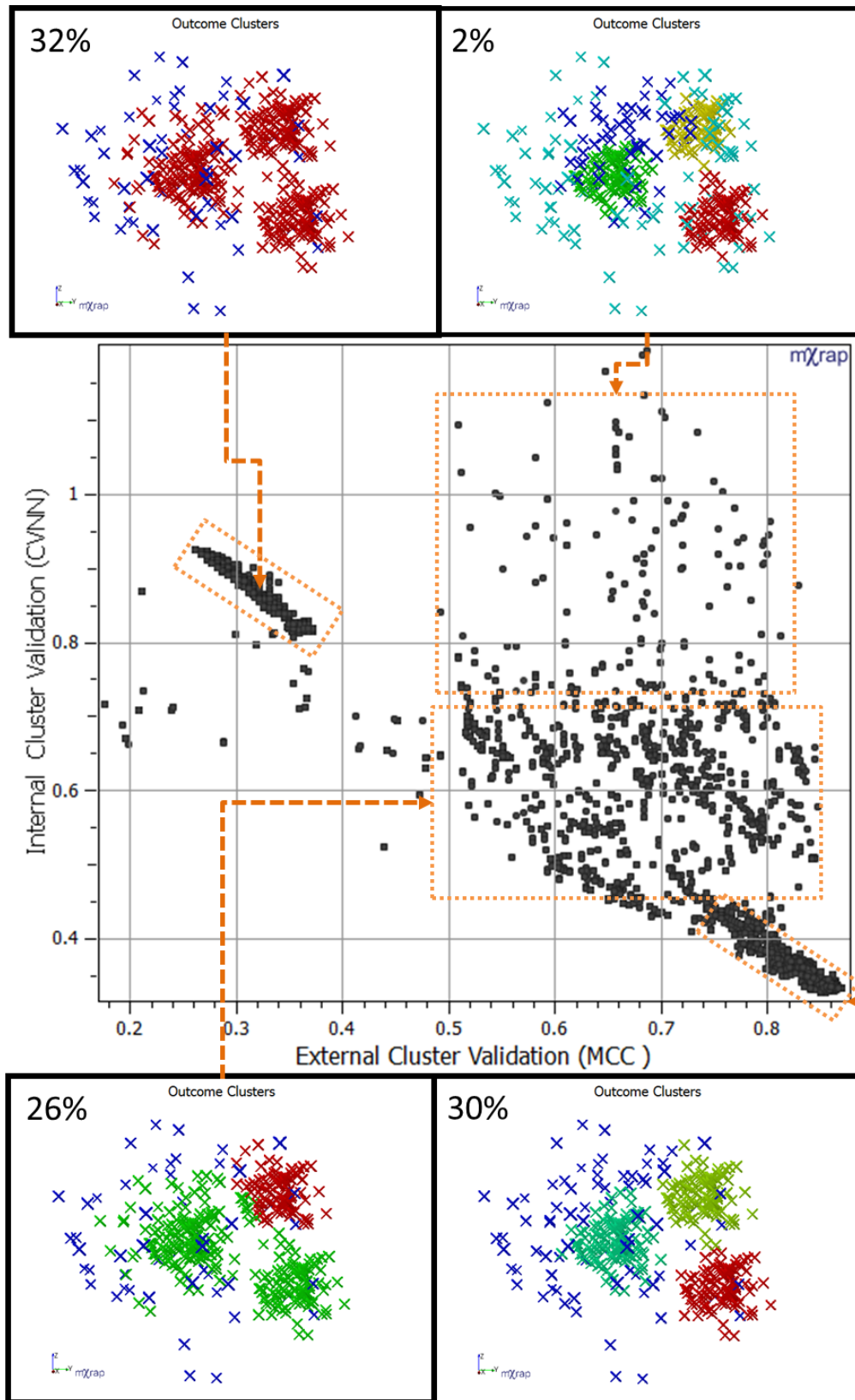


**Figure 79** CVNN results for combinations of search distances and spatial density tolerances attempted for the strict scenario ( $5\Psi$  separation and  $3\Phi$  relative scale) (left) and the lenient scenario ( $6\Psi$  separation and  $4\Phi$  relative scale) (right).

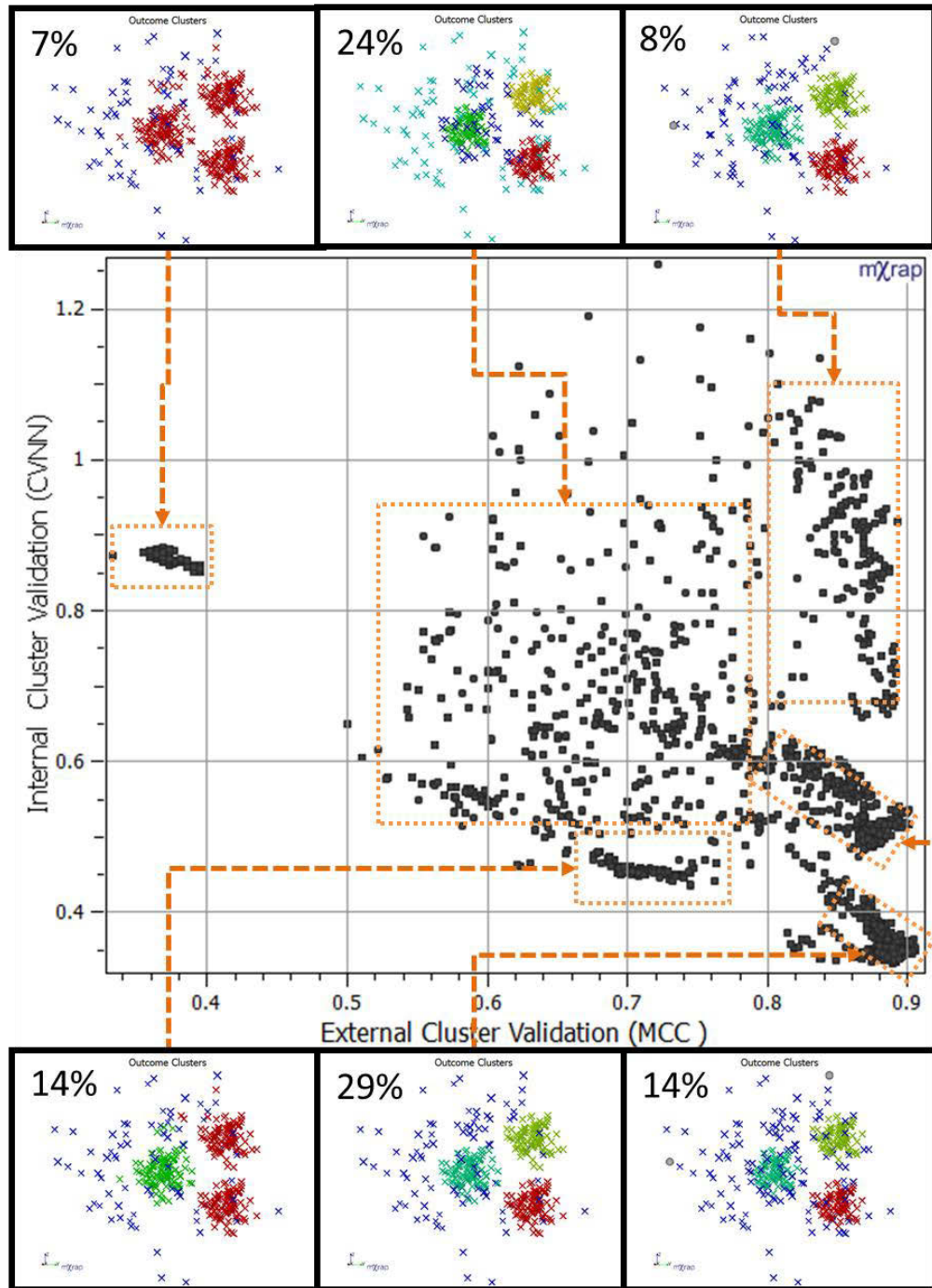
To investigate deviations in the relationship between internal and external cluster validation measures, the correlation of these two parameters is further considered by plotting the CVNN index measure against the MCC measure. If these two measures were in perfect agreement there would be a consistent relationship observed for these parameters for the strict and lenient scenarios. Instead of a consistent relationship between the CVNN and MCC measures, groups of solutions tend to form. Further investigation reveals that these distinct groups correspond to specific configurations of clustering solutions. A group of scenarios will form for solutions that model three clusters instead of four or if the four responses have incorrectly included or excluded events. This analysis is summarised in **Figure 80** for the strict scenario and in **Figure 81** for the lenient scenario. The following observations are made:

- MCC and CVNN measures agree on the group of optimal solutions;
- Optimal solutions represent a significant portion of scenarios (30% for strict and 29% for lenient scenarios) indicating that clustering is insensitive to parameter selection;
- MCC is comparatively better in cases when clustering has incorrectly included or excluded events. This results in a smaller decrease in MCC in comparison to penalties to the CVNN due to clustering of variable distributions; and
- The CVNN is comparatively better when responses have been erroneously clustered together. The CVNN does not completely account for the loss of accuracy indicated by the MCC due to the similarity of spatial distributions.

These observations support that the CVNN index is an applicable internal clustering validation measure. Furthermore, this measure emphasises the delineation of seismic responses of consistent spatial distributions and maximises spatial separation of clusters.



**Figure 80** The CVNN index plotted against the MCC measure index for the 5000 strict scenarios. Optimal solutions are found when MCC is maximised and CVNN is minimised (bottom right). Regions of the chart are annotated by their typical clustering solution along with the portion of solutions that fall within this region.



**Figure 81** Plotted is the CVNN index against the MCC measure index for the 5000 lenient scenarios. Optimal solutions are found when MCC is maximised and CVNN is minimised (bottom right of the chart). Regions of the chart are annotated by their typical clustering solution along with the portion of solutions that fall within this region.

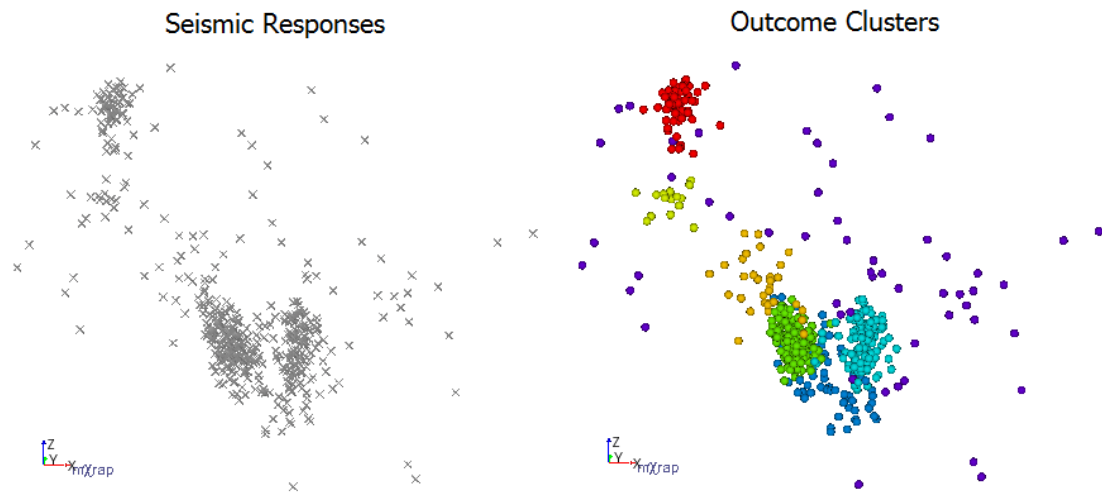
#### 4.6.2 Mining Induced Responses

Analysis can be extended to cases examining real seismic responses without the benefit of external cluster validation, given the confidence in the internal clustering validation established in the previous synthetic examination.

Mining induced responses are examined using a similar set of parameters to Section 4.6.1. Scenarios are assessed using unique combinations of search distances (5 to 20) and spatial density tolerances (0 to 25%). Search distances are in arbitrary units. Search distances are increased nine times by discrete multiples of the initially defined search distance, e.g., an initial search distance of 10 and spatial density tolerance of 10%, results in response scale sets of: [10, 10%] for the first iteration; [20, 10%] for the second iteration; and up to [90, 10%] for the ninth iteration. A wider range of response scale sets and a higher spatial density tolerance is used to reflect the lack of prior knowledge concerning the spatial dimensions and number of responses. In reality, these numbers can be refined for specific cases. This analysis reflects assessment of these responses within a larger dataset without prior manual consideration. A constant proportional lower count threshold of 80% is used (Section 3.5.3). A temporal modelling window is not used, as temporal modelling is not considered.

Three seismic responses are considered of varying geometries, densities, scales, and separations. Each seismic response is assessed 1000 times using the same response scale sets, using unique combinations of parameters. Results are presented as the cumulative distribution of CVNN results per scenario. Additionally, these distributions are annotated by 3D plots of spatial clustering that are typical of the CVNN values.

The first example contains 480 seismic events and is a reasonably difficult clustering problem due to the occurrence of multiple seismic responses of various densities in close proximity (**Figure 82** left). Despite the challenges of clustering these responses, the distinct spatial characteristics of responses result in relatively unambiguous clustering choices. Shown in **Figure 82** right is an example of outcome clusters. Seven clusters are found in total including three dense, localised responses (red, green, and light blue), with dense responses surrounded by sparser responses (dark blue and orange). In addition, there is a small-localised response (light green) and a significant amount of regionally distributed events (purple).

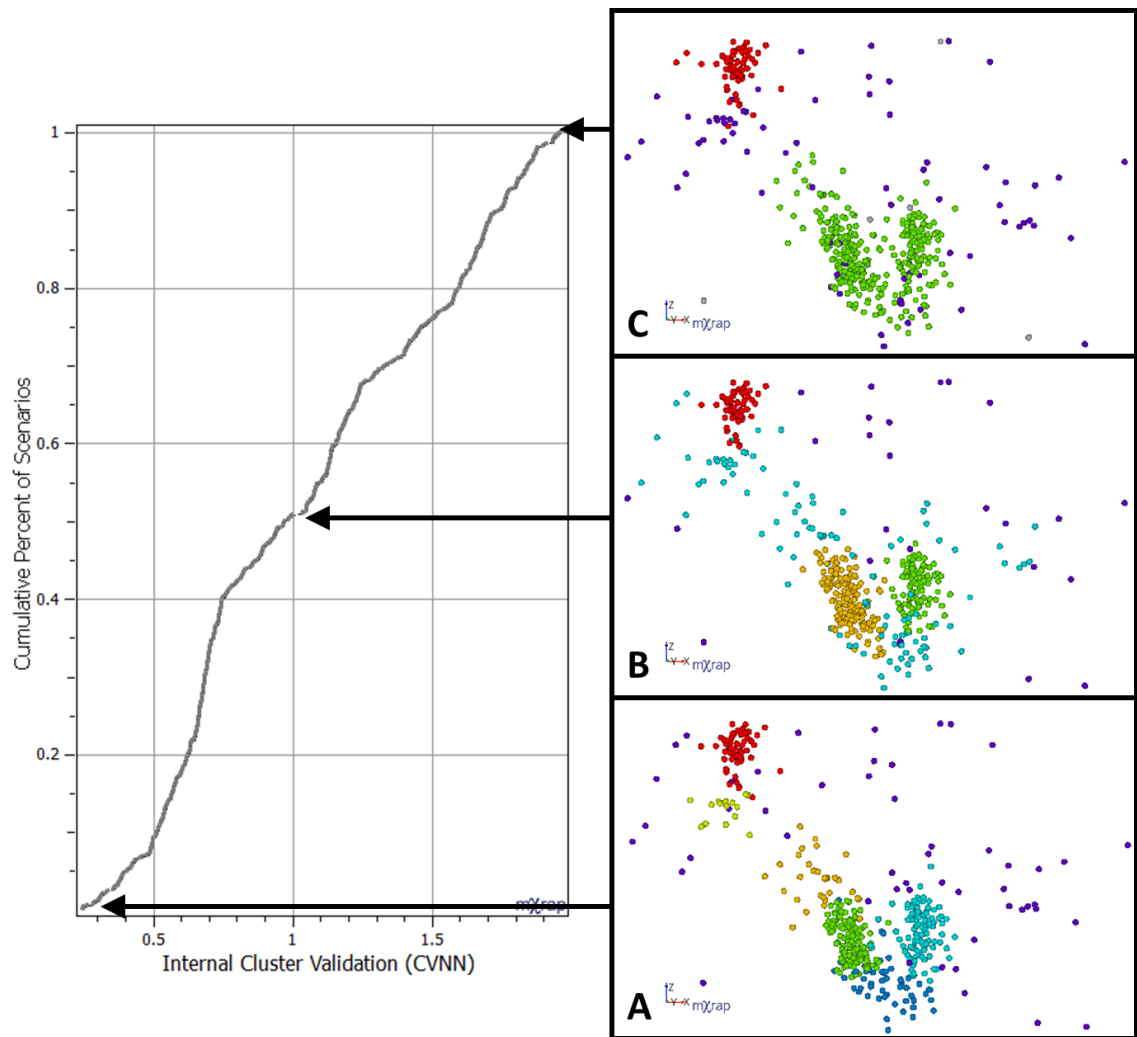


**Figure 82** Seismic responses related to multiple features within the mining environment. Non-clustered seismic responses (left) are spatially related by a number of distinct outcome clusters (right).

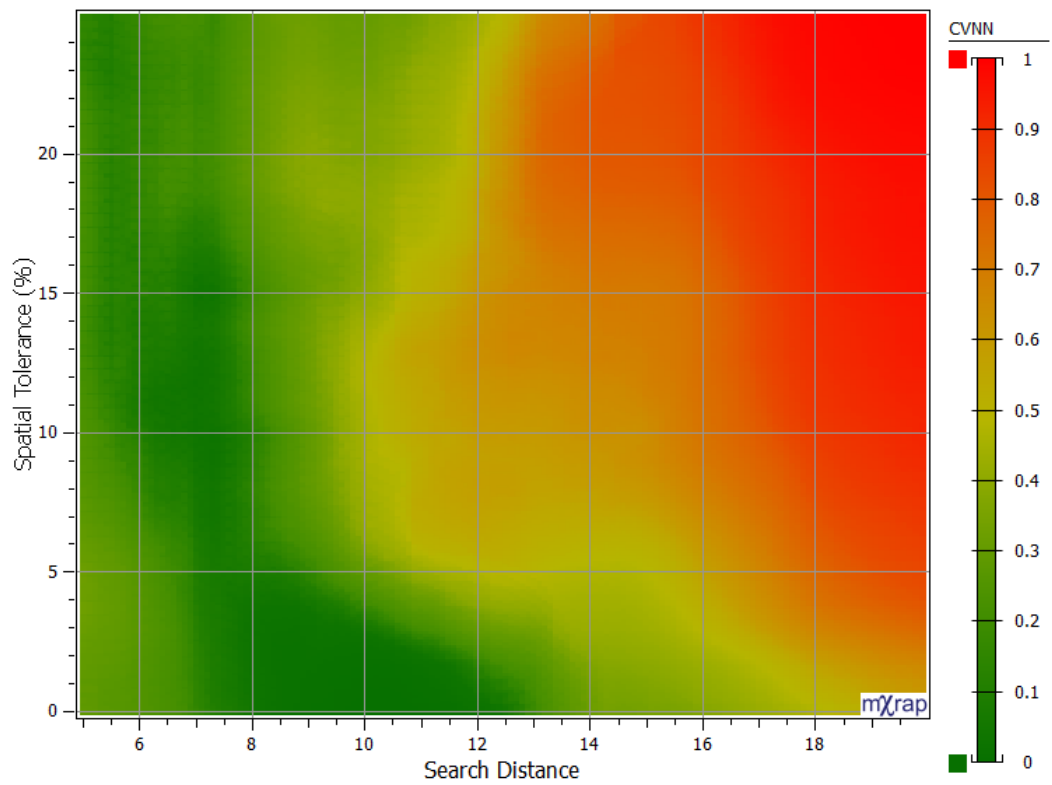
There is significant variation in the cumulative CVNN distribution due to the identification of three dense, distinct responses. A distinct change to the CVNN occurs when these responses are separated or clustered. Optimal cluster outcomes include the three dense clusters (red, light blue, and green), sparse responses (orange and dark blue), a small response (light green), and regional events (purple) (**Figure 83 A**). Optimal outcomes are found by using search distances (7 to 12) that represent the spatial scale of clusters ( $\approx 10$ ). If search tolerances are less than the spatial scale of clusters (5 to 9), a wide range of spatial density tolerances results in accurate clustering (**Figure 84**). While not apparent in this seismic response, the latter range of parameters is preferable (lower search distance and higher spatial density tolerance) as clustering will be allowed to spread into the various geometric shapes of other responses.

Less optimal solutions (**Figure 83 B**) still delineate three dense responses (red, green, and orange). These solutions cluster all sparse events surrounding dense responses into one response. The increased variation in intra-cluster density results in a lower CVNN index. The less optimal solutions cluster in inconsistent densities, e.g., **Figure 83 C** results in two dense clusters (red and green) and a sparse response (purple). These solutions result from overestimating search distances and spatial density tolerances (**Figure 84**).

Two aspects of internal validation provide insight into clustering these seismic responses by assessment of the CVNN index. Firstly, the distribution of values indicates how distinct clustering choices impact on the intra-cluster density and separation. Secondly, values indicate the most optimal solution with respect to the consistency and separation of clusters, and the range of response scales considered by clustering.

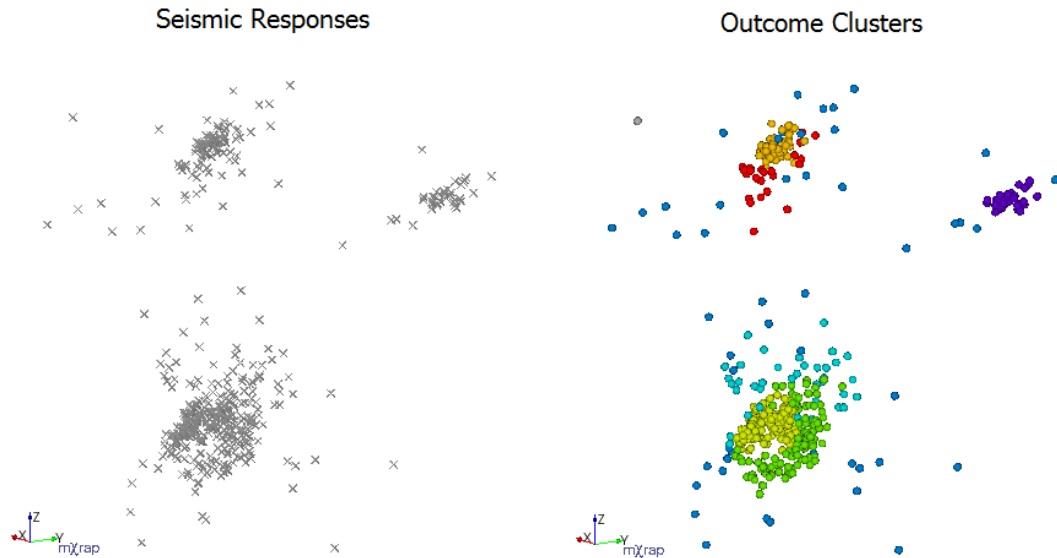


**Figure 83** Shown left is the cumulative distribution of CVNN values found for 1000 combinations of search distance and spatial density tolerance parameters. Shown right A) all responses found by the most optimal outcome clusters, B) less optimal solutions combine sparse responses, and C) least optimal results combine dense and sparse responses.



**Figure 84** Trends interval cluster validation (normalised CVNN index) for combinations of search distance (x-axis) and spatial density tolerance (y-axis). Optimal CVNN index values indicate accurate results and use search distances less than 12. A range of spatial density tolerances at smaller search distances results in accurate clustering.

The example in **Figure 85** highlights the inherently ambiguous decisions that may be associated with seemingly distinct clusters. This example contains 470 seismic events within three responses along with sparse seismicity. The three main responses are a dense response (orange) surrounded by sparse events (red), a dense response (yellow) surrounded by a planar, less dense clusters (green and light blue), a sparser cluster (blue), and a small cluster (purple).

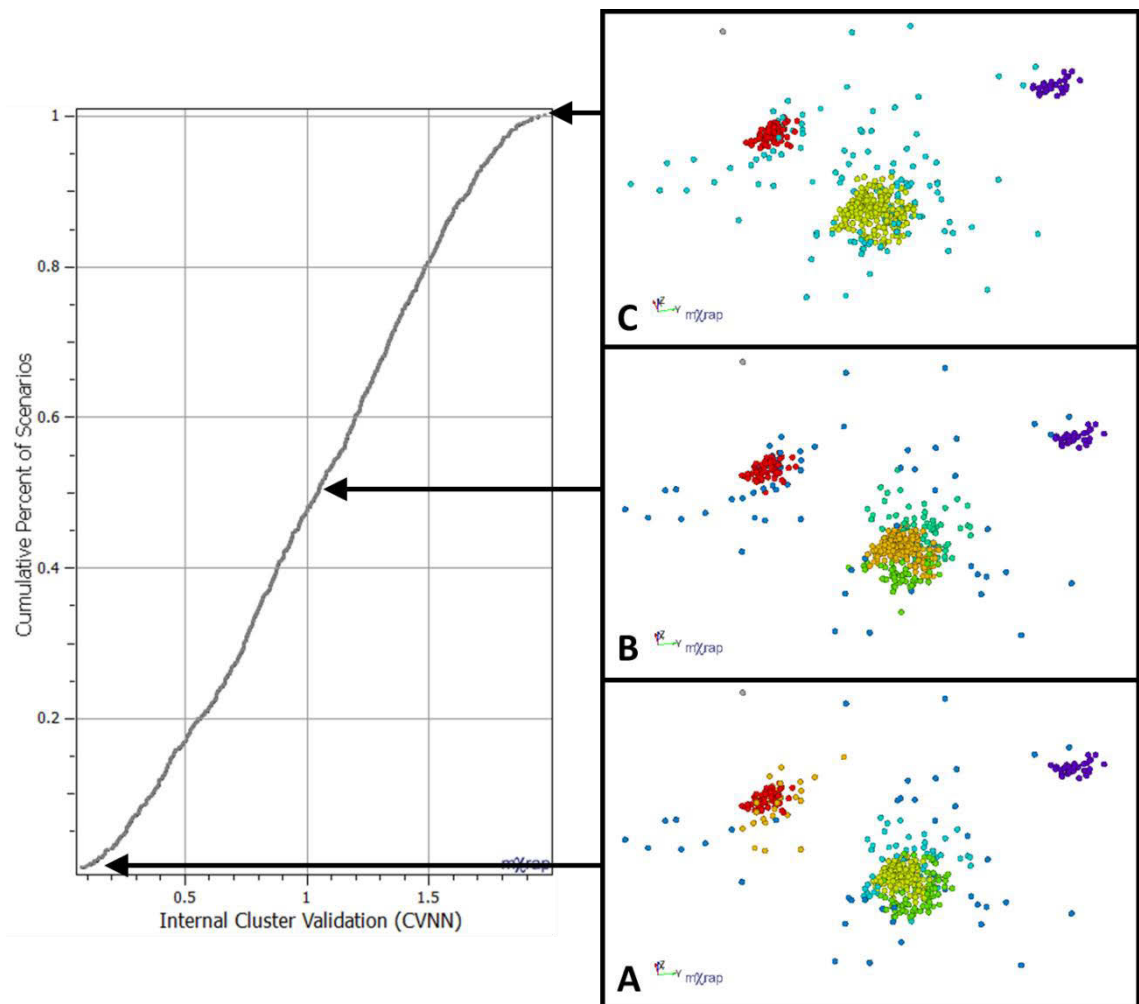


**Figure 85** Seismic responses related to multiple features within the mining environment. Non-clustered seismic responses (left) are spatially related by a number of distinct outcome clusters (right).

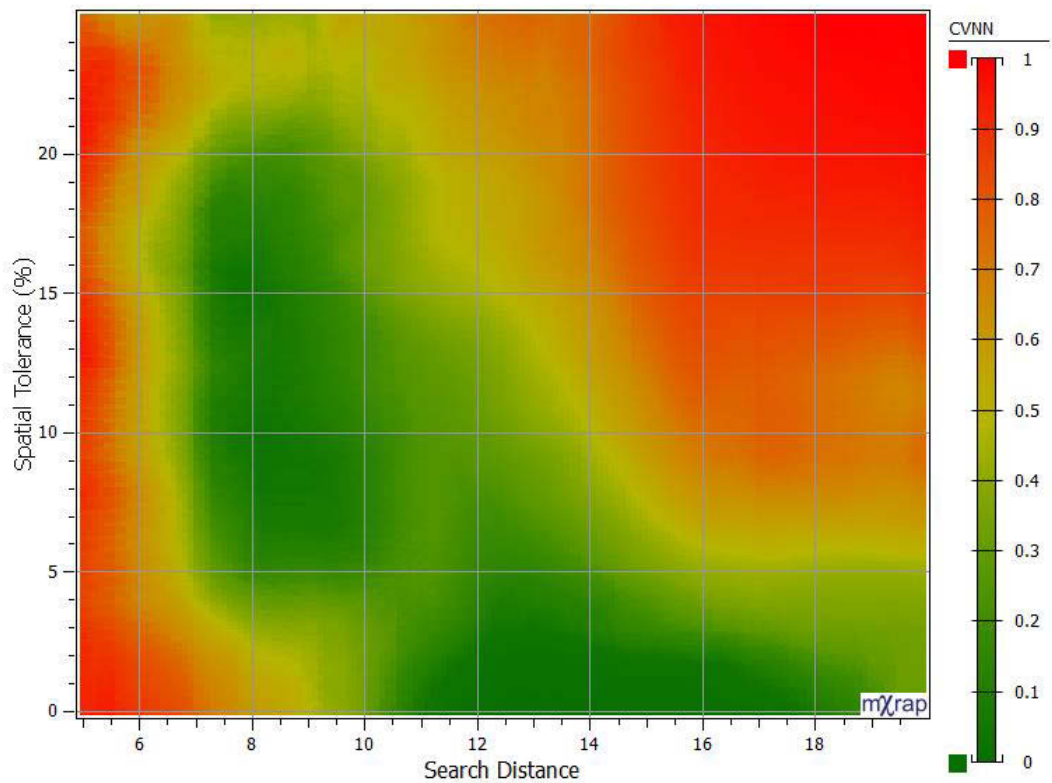
**Figure 86** (left) shows that there is no significant variation within the distribution of CVNN values. This indicates that at no point is there a distinct and major change to clustering outcomes as the search distance and spatial density tolerance change. Instead, there are small changes in spatial distributions of clusters rather than large jumps associated with the separation of distinct responses. The decision to delineate distinct spatial distributions is ambiguous due to the gradual transition in spatial clustering outcomes. This ambiguity can be partially addressed by internal clustering validation as the optimal CVNN index minimises variation in intra-cluster densities and maximises inter-cluster separation. The optimisation is scale dependent with densities that are more consistent for smaller clusters that include less variation. Ultimately, by specifying a relatively low search distance, it is assumed that this is the smallest cluster that can be meaningfully interpreted based on the location accuracy of seismic monitoring and the meaningfulness of this response scale in subsequent analysis.

**Figure 86** illustrates the effect of optimisation by using internal clustering validation with respect to a small spatial scale. The optimal clustering solutions are able to delineate the variations in densities surrounding seismic responses (**Figure 86 A**). Specific parameters result in optimal solutions if clustering is able to delineate responses on specific spatial scales present

in the dataset. **Figure 87** shows that a range of search distances (11 to 18) result in optimal clusters. An increase to the spatial density tolerance (>5%) makes relatively smaller search distances favourable. Less optimal solutions underestimated or overestimated spatial scales of interest and have a higher CVNN index as spatial variation increases within clusters (**Figure 86 B and C**). The suboptimal range of parameters includes search distances less than six for any spatial density tolerance or higher search distances for smaller spatial density tolerances (**Figure 87**). In practice, the less optimal clustering solutions may be more reasonable if there was less confidence in event locations or analysis focused on general quantification of seismic responses. This example serves to highlight that the CVNN index only provides guidance for the selection of optimal parameters within the context of the scales selected for assessment. Even though clustering parameters can be optimised, subjectivity is still associated with the inherently user based decision of defining a reasonable cluster.

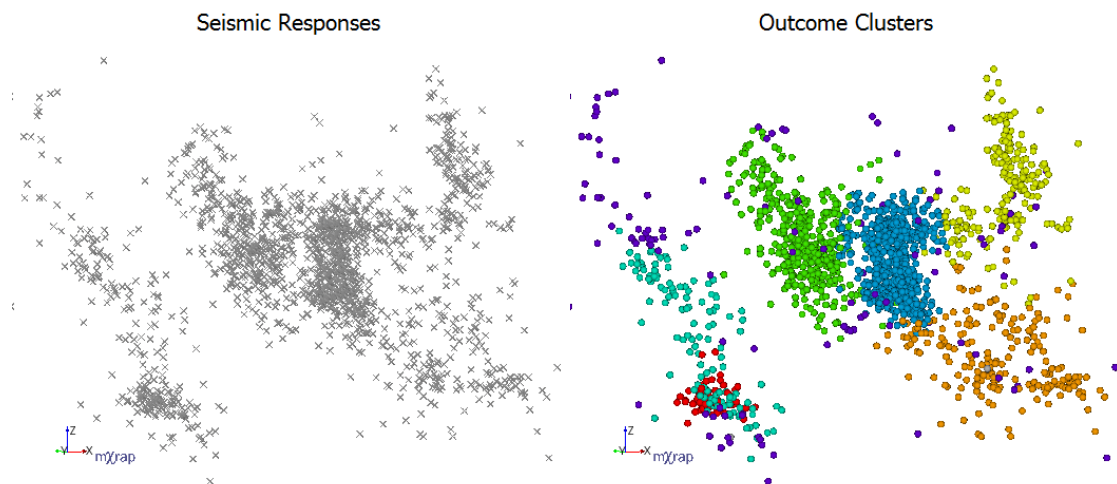


**Figure 86** Shown left is the cumulative distribution of CVNN values found for 1000 combinations of search distance and spatial density tolerance parameters. Shown right A) all responses found by the most optimal outcome clusters, B) less optimal solutions combine sparse responses, and C) least optimal results further combine responses.



**Figure 87** Trends in the normalised CVNN for combinations of search distance (x-axis) and spatial density tolerance (y-axis). Optimal values indicate that accurate results can be found using larger search distances at low tolerances or smaller search distances with higher tolerances.

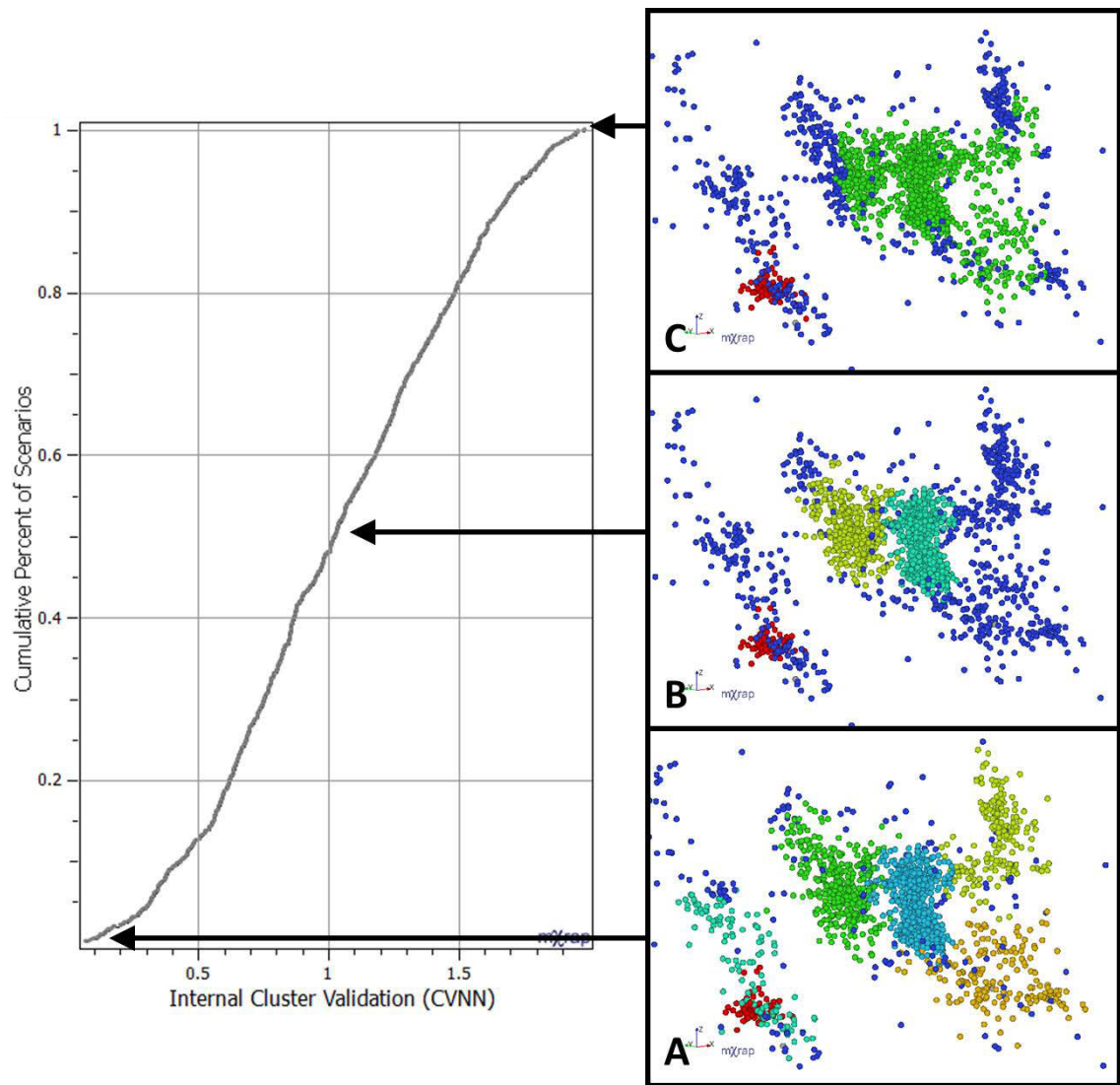
A complex example is presented in **Figure 88**, with 1,500 seismic events forming multiple seismic responses of various shapes, densities, and separations. Responses occur simultaneously and relate to a range of rock mass failure processes associated with blasting, geology, pillars, and abutments within the mining environment. An exception is a dense cluster that instead begins three hours after the other seismic responses (red cluster).



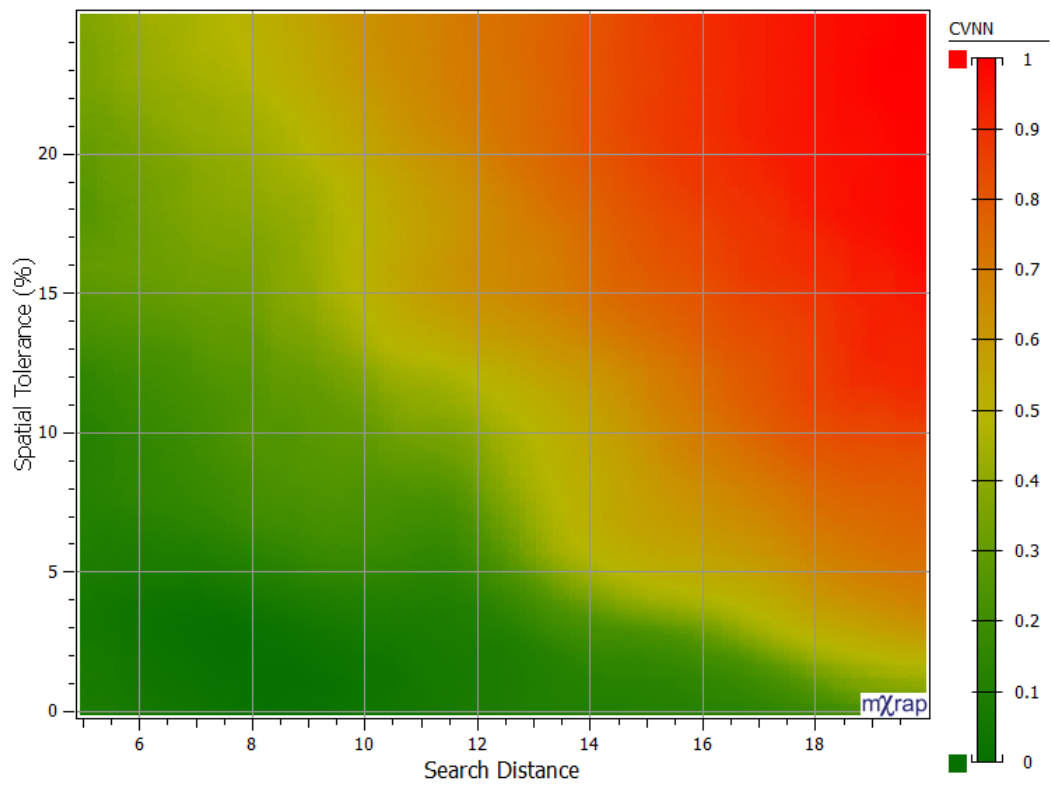
**Figure 88** Seismic responses related to multiple features within the mining environment. Non-clustered seismic responses (left) are spatially related by a number of distinct outcome clusters (right).

The task of spatially clustering seismicity is inherently difficult in cases where multiple seismic responses are sensitive to a stress change within the mining environment. Internal cluster validation becomes essential to measure the success of clustering outcomes in capturing the spatial attributes of the dataset, e.g. shapes, density, and separation. The cumulative CVNN distribution in **Figure 89** does not exhibit distinctive features due to a range of spatial attributes contained within the clustering outcomes. This is reflected by the gradual transition for different combinations of search distances and spatial density tolerances (**Figure 90**).

Given the context of scales selected for assessment, the CVNN index does provide clear guidance for the selection of optimal parameters. **Figure 89 A** shows optimal results with consistent and well-separated outcome clusters. **Figure 90** shows that optimal results are found using any search distance and low tolerance values, or by using wider range of spatial density tolerances when smaller search distances are used. The less optimal result in **Figure 89 B** has consistent and dense outcome clusters. Additionally, sparser seismicity has been erroneously clustered. **Figure 89 C** is an example of erroneous clustering primarily due to inconsistent intra-cluster densities. These results are the least optimal and occur due to high search distances and spatial density tolerances (**Figure 90**).



**Figure 89** Shown left is the cumulative distribution of CVNN values found for 1000 combinations of search distance and spatial density tolerance parameters. Shown right A) all responses found by the most optimal outcome clusters, B) less optimal solutions combine sparse responses, and C) least optimal results combine dense and sparse responses.



**Figure 90** Trends in the CVNN index for combinations of search distance (x-axis) and spatial density tolerance (y-axis). Optimal CVNN values indicate that accurate results can be found using a range of search distances at low tolerances. There is comparatively gradual transition between poor and optimal solutions due to the variable attributes of the clusters.

## 4.7 Chapter Summary

This chapter developed and validated a generalised method for the spatial delineation of mining induced seismic responses. The spatial delineation of responses forms a component of the iterative approach (Chapter 3) and creates a subset of spatially clustered seismicity that is required for the temporal modelling (Chapter 5). The main sections of chapter are summarised in Sections 4.7.1, 4.7.2, 4.7.3, and 4.7.4.

### 4.7.1 Density-Based Clustering Applied to Mining Induced Seismicity

- Spatial characteristics of mining induced seismicity are influenced by factors that controlled rock mass failure, e.g., faulting, pillars, contrasting rock types, or localised stress changes.
- Ideal clustering methodology introduces objective clustering that is able to group distinct shapes and densities of seismic events.
- Density-based clustering is a non-parametric method applicable to responses due to:
  - Class identification, i.e., one event allocated to one cluster;
  - Minimal existing knowledge requirements;
  - Discovery of arbitrary shapes; and
  - Discovery of high-density clusters within low-density clusters.
- DBSCAN is an example of density-based clustering. In summary, this method:
  - Considers the number of neighbouring elements ( $N_e$ ) with respect to a user specified minimum ( $N_{MIN}$ ) within a search distance ( $D_S$ ).
  - Classifies elements as core, boundary, or noise.
  - Creates clusters from core elements and neighbours. Events are recursively considered and clusters are merged if one or more core element is shared.
- Density-based methods have a number of shortcomings:
  - Difficult to find a suitable density threshold;
  - Poor performance for datasets with varying element densities; and
  - High sensitivity of clustering outcomes to clustering parameters.
- The prevalence of specialised approaches indicates the need to address problem-specific limitations of density-based clustering.

- Addressing limitations is simplified, as clustering only needs to delineate one spatial cluster at a time of a consistent event density.

The subsequent work within this section addresses these limitations in two subsections. Firstly, by the integration of spatial delineation and seismic response identification and, secondly, the introduction of a density clustering core event tolerance.

- The initial identification of a seismic response results in the approximate centre of the seismic response being known and allows the spatial event density to be estimated.
- This begins to address the limitation of finding a suitable density threshold.
- An initial estimate of density is an upper estimate, therefore, a user defined spatial density tolerance is introduced that allows for a percentage deviation in the neighbouring event count when considering the designation of core events.
- Core events are not designated if the procedure considers regions of significantly different densities. This ensures that clustering is confined to regions of similar spatial characteristics while allowing for a degree of variation within the cluster.
- The spatial event density is refined as additional information concerning the spatial characteristics of the core events becomes available. Every time an event is designated as a core event, the updated spatial event density redefined as the average between the current sample number ( $N_s$ ) and the number of events surrounding the newly discovered core event ( $N_e$ ).
- The definition of spatial density tolerance can be small for clusters of consistent densities or increased for greater variation in densities.
- The cluster is not able to capture the events associated with the seismic response if spatial density tolerance is underestimated or will include unrelated events if overestimated.

#### 4.7.2 Spatial Clustering Procedure

- The method implemented classifies elements by considering the number of neighbouring elements ( $N_e$ ) within a search distance ( $D_s$ ), with respect to an initially estimated number of events ( $N_s$ ), and a spatial density tolerance ( $S_t$ ).
- Spatial clustering is a four-step procedure to obtain a single cluster:
  1. Initialisation of clustering: Define a search distance ( $D_s$ ) that approximates the spatial scale of response. Define a spatial density tolerance ( $S_t$ ) that reflects the consistency in event density.

2. Initial definition of potential core event: Potential core events are events within  $D_s$  of identification location. Potential core events are counted ( $N_s$ ), and the range of tolerable spatial count is  $\pm S_t N_s$ .
3. Processing of potential core events: For the next potential core event, count events ( $N_e$ ) within ( $D_s$ ). If  $N_e$  is within  $N_s \pm S_t N_s$ : This event is a core event, all surrounding events without a designation are potential core events and updated  $N_s$ . If  $N_e$  is outside  $N_s \pm S_t N_s$ : All surrounding events are unchanged and this event is a boundary event.
4. Completion of clustering procedure: If additional potential core events remain, repeat Step 3. If no potential core events remain then the output cluster is boundary and core events.

#### 4.7.3 Spatial Clustering Validation and Performance

- Performance of clustering methods is either external cluster validation that uses prior knowledge of the dataset and truth class label, or internal clustering validation that assesses the similarity of individual elements and separation of clusters without prior knowledge of the element labels.
- The errors associated with spatial clustering are assessed by the generation of synthetically generated scenarios that are spatial clustered using the method developed. External validation compares synthetic and clustering outcomes by examining a binary classification scheme. Internal validation only examines clustering outcomes.
- Numerous synthetic scenarios are generated with small incremental changes to investigate how classification errors change over a range of conditions.
- $\Psi$  ratio defines the separation between two synthetic responses.
- $\Phi$  ratio defines the relative difference in scales between two synthetic responses.
- Matthews Correlation Coefficient (MCC) is a simplified interpretation of external binary classifications and results in values from -1 (perfect negative correlation) to 0 (no correlation), to 1 (perfect positive correlation).
- For simplified analysis of response separations, the MCC correlation increases as clustering begins to distinguish between clusters (4 to  $6\Psi$ ) before reaching a very strong positive correlation for separation greater than  $6\Psi$ .

- For simple analysis of superimposed responses with different scales, a gradual increase in MCC reflects that relatively less of the sparse response is superimposed with the dense response as the relative scale ratio ( $\Phi$ ) increases. Due to superimposition it is impossible to cluster these responses without errors.
- Internal performance measures address the inability of external measures to quantify errors without prior knowledge of the dataset by assessing intra-cluster variance in densities and inter-cluster separation.
- SDbw index is an established internal measure for compact and well-separated clusters and performs well for non-standard shaped clusters. A newer internal measure built on the same concepts is the CVNN index.
- Further analysis investigates the internal performance measures. Key aspects are:
  - Analysis allows for the comparison between the two internal measures;
  - The use of the MCC external validation can represent true errors;
  - Six datasets are constructed from critical  $\Psi$  and  $\Phi$  values;
  - The datasets are clustered with a range of search distance and spatial density tolerances; and
  - Parametric solutions spaces are created and display combinations of search distance and spatial density tolerances with respect to normalised values of MCC, SDbw, and CVNN.
- This analysis found for low scale ratios and separations:
  - Both internal indices indicate parameter ranges that result in a single cluster are optimal.
  - This reflects the lack of distinction between the responses spatial characteristics.
  - Clustering is not correct with respect to external measures, although, cluster outcomes are reasonable due to the lack of distinction in responses.
- This analysis found for medium scale ratios and separations:
  - SDbw index incorrectly indicates optimal parameters when a single cluster is delineated.
  - The two parametric regions identified by the CVNN reproduce the highest accuracy clustering.

- Moderate positive correlation is achieved by the MCC reflecting the similar characteristics of responses.
- This analysis found for high scale ratios and separations:
  - SDbw misrepresents the parametric solutions that result in optimal clustering.
  - Strong positive correlations are achieved by the MCC.
  - CVNN index can reproduce the parametric solutions that result in high clustering accuracy.
- CVNN index is comparatively better than the SDbw index at identifying appropriate search distances and spatial tolerance values.
- The CVNN can reproduce the known clustering accuracy quantified by the MCC for medium to high separations ( $4\Phi$  and  $6\Psi$ ).
- Minimising the CVNN index provides a good indication of appropriate clustering parameters for responses with distinctive spatial characteristics.

#### **4.7.4 Base Cases for Mining Induced Seismic Response**

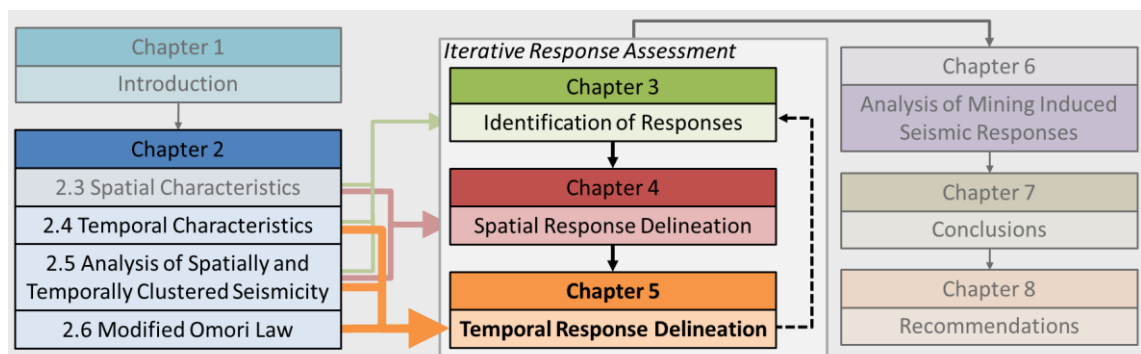
- Two relevant synthetic cases (strict and lenient), each comprising of four responses, are constructed to test the ability of the algorithm to delineate spatial clusters using a range of input parameters.
- The CVNN mimics the optimal parameters found by the MCC, despite some discrepancies. These deviations are further investigated by plots comparing the CVNN and the MCC measures. The following observations were made:
  - Solutions tend to form groups rather than a consistent relationship;
  - Distinct groups correspond to specific configurations of clustering solutions;
  - Both measures agree on the group of optimal solutions;
  - Accurate clustering is insensitive to parameter selection;
  - MCC is lower than the CVNN when clustering has incorrectly included or excluded events due to the CVNN penalising the clustering of variable distributions; and
  - CVNN is lower than the MCC when responses have been erroneously clustered together due to the similarity of spatial distributions.

- Analysis is extended to cases examining real seismic responses without the benefit of external cluster validation. This analysis considered three datasets containing a range of responses shapes, densities, and configurations.
- The real cases selected are nontrivial clustering problems due to the occurrence of multiple seismic responses of various densities in close proximity.
- CVNN indicates how clustering choices affects intra-cluster density and separation.
- Visually and with respect to CVNN values, there may be inherently ambiguous decisions associated with seemingly distinct clusters that results in subjectivity.
- CVNN index provides guidance for the selection of optimal parameters for the range of response scales considered by clustering.

## 5 Temporal Delineation of Mining Induced Seismic Responses

### 5.1 Chapter Overview

This chapter utilises the concepts established in Chapter 2 to develop a methodology to temporally delineate and quantify mining induced seismic responses. This method specifically accommodates the temporal characteristics of seismic responses (Section 2.3) and addresses the shortcomings of previous methods employed to assess mining induced responses (Section 2.4). This chapter applies the Modified Omori Law (MOL) to the temporal occurrence of seismic responses and refers to the reviewed literature concerning the implementation of the MOL, applicability to mining induced responses, and parameters associated with this law (Section 2.5). Moreover, temporal delineation forms a component of the iterative approach to the identification of seismic responses and, hence, this chapter considers temporal analysis with respect to the time of response initiation (Chapter 3), and the subset of spatially clustered seismic events (Chapter 4). **Figure 91** illustrates the contents of this chapter, with respect to previous and subsequent chapters.



**Figure 91** Chapter 5 utilises findings from the literature review along with outcomes derived from response identification and spatial delineation to develop a method that temporally delineates seismic responses.

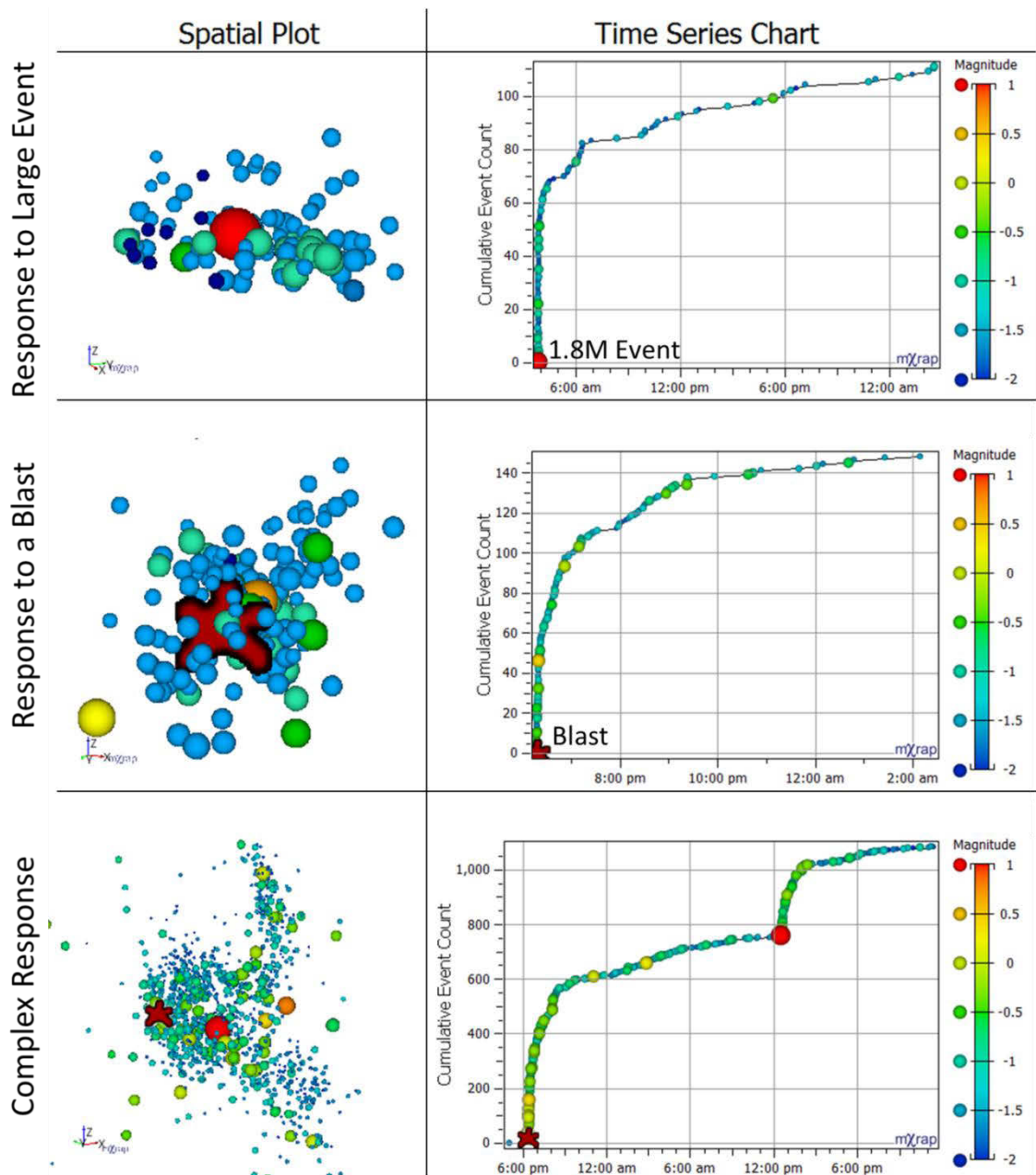
## 5.2 Introduction

Chapter 2 showed that mining induced responses are analogous to the temporal characteristics of earthquakes. Generally, the temporal characteristics of mining induced seismicity are comprised of relatively short duration responses following a non-stationary Poisson process and longer periods of events that follow a stationary Poisson process. This chapter showed that no definitive theoretical foundation describing temporal characteristics exists and highlighted the uncertainty surrounding the factors that contribute to the temporal occurrence of mining induced seismicity.

Mining induced seismicity is controlled by spatially and temporally varying factors that influence a possible range of rock mass failure mechanisms. The aspects that contribute to mining induced seismicity also have the potential to affect the productivity, rate of decay, and conformity to temporal power law behaviour of time-dependent event occurrence. Despite the range of influences on time-dependent seismicity, responses typically occur due to an abrupt stress change within the mining environment. Generally, time-dependent seismicity results from blasting or large seismic events. The dependency between a seismic response and stress changes may be ambiguous due to incomplete blasting records, the influence of pre-existing stress conditions, or rock mass strength conditions.

**Figure 92** provides examples of typical time-dependent seismicity:

- Top: Shown is a seismic response that follows a large seismic event (1.8M). The spatial (left) and a temporal (right) plots show a response containing 110 events, distributed in a planar orientation, and approximately following a power law decay.
- Middle: Shown is a seismic response to blasting containing 148 events and exhibits typical time-dependent characteristics of mining induced seismicity (right). This response follows a spherical spatial distribution (left).
- Bottom: Shown is a spatially and temporally complex seismic response to blasting and a large event. Time dependency is evident following the blast and the large event, along with a clear spatial structure to event locations. Spatial and temporal characteristics indicate that pre-existing stress and strength conditions significantly influenced seismic occurrence and this introduces ambiguity concerning the relationship between spatial and temporal occurrence.



**Figure 92** Examples of time-dependent seismic responses following a large event (top), blasting (middle), and ambiguous causation (bottom). A spatial plot (left) and cumulative events over time (right) are shown for each response. Markers are sized magnitude and are fixed relative to the spatial scale, i.e., top and middle responses are spatially smaller than the bottom response.

### 5.3 Temporal Modelling of Mining Induced Seismic Responses

The objective of the temporal modelling of seismic responses is to delineate and quantify time-dependent seismicity. Due to the complexity of the temporal delineation and quantification of seismic responses, there is a range of considerations that the temporal modelling methodology must address. These considerations include:

- The spatial and temporal superimposition of seismic responses;
- The applicability of the temporal model implemented;
- The need to quantify the errors associated with modelling;
- The delineation of responses based only on the temporal attributes of seismicity;
- The implementation of the c-parameter and time interval when modelling seismic responses with the MOL; and
- Integration with the iterative identification and delineation of seismic responses.

A significant portion of spatially and temporally superimposed responses can be delineated by the use of an iterative identification approach (Chapter 3) and spatial modelling (Chapter 4). Generally, distinct failure processes separated in space or time generate seismic responses due to inherent aspects of mining induced seismicity, such as the spatially confined sources of seismicity and routine blasting in different working mining volumes. The inherent causes of seismic responses do not completely ensure that multiple time-dependent responses do not exist within an initial modelling interval, e.g., seismic responses associated with caving, routine blasting in the same area of the mine, or additional responses to large events during time-dependent seismicity.

The inherent practice of blasting creates additional rock mass failure processes before previous processes have completely ceased. This inherent aspect of mining causes seismicity generated by time-dependent processes to be temporally superimposed. It is not possible to attribute individual seismic events to each response within a modelling interval, which inevitably reduces the modelling result quality. Considering this inherent limitation, the objective of temporal modelling is to delineate superimposed processes to allow for the most representative and consistent quantification practically possible.

In this thesis, the MOL is utilised to model responses due to the general applicability of this law to mining induced seismicity (Section 0). This model may not be optimal for all responses. In some cases, alternative models to the MOL can provide improved representation of temporal event occurrence. The use of multiple models requires the introduction of additional

parameters to delineate and quantify responses. This is undesirable as seismic responses within the same dataset become difficult to compare if they are delineated and quantified by different models. The use of multiple models limits subsequent analysis that relies on comparable results and reduces confidence when relating seismic responses to causative processes and conditions.

It is essential to quantify the quality of fit between the MOL and temporal observations. Appropriate measures of modelling quality allow the removal of poor results before additional analysis is undertaken. Additionally, optimisation is required between the quantification and delineation objectives of temporal modelling, i.e., the delineation of responses should not be significantly limited to marginally improve the suitability of modelling fit, or vice versa. To achieve this temporal modelling objective, there is a need to quantify modelling quality by evaluating the uncertainty in MOL parameters (Section 2.5.2) and the suitability of fit using the Anderson-Darling statistic (Section 2.5.3).

In the study of earthquake aftershocks, a distinctive large magnitude event is defined as the mainshock and the origin time of the aftershock response. Within the context of mining induced seismicity, this aspect of studying time-dependent seismicity is not transferrable as the mining processes can cause responses. Due to the uncertainty concerning the time of causation, the application of temporal modelling must only use temporal attributes to determine appropriate modelling intervals. Furthermore, limiting the selection of the modelling interval to temporal attributes allows the seismic response's causation to be tested independently of prior assumptions. This allows for the assessment of the possible causation of a seismic response that is temporally, although, not spatially related to blasting.

Methods of applying the MOL focus on the implementation of the c-parameter and the selection of a modelling interval. These are critical aspects to temporal modelling with the MOL (Sections 2.5.6 and 2.5.7). There is a need to consider these aspects of modelling due to a potential to bias and inconsistently influence MOL parameters. Specific areas to address are the interdependency between the p-parameter and c-parameter, and the selection of a consistent modelling interval that follows the MOL.

In summary, temporal modelling of mining induced responses must consider:

- The implementation of the MOL:
  - Selection of a modelling interval based only on temporal attributes;
  - Interdependency between the p-parameter and c-parameter;
  - Selection of a modelling interval following the MOL; and
  - Quantification of the quality of modelling results.
- The ability to delineate partially superimposed responses consistently.
- Optimisation of delineation and quantification objectives; and
- Integration with the iterative identification and spatial delineation of responses.

## 5.4 Modelling Mining Induced Seismic Response with the MOL

Modelling approaches are important to consider when seismic responses have a deficiency of events during times soon after the initiation of the response. The selection of a modelling interval is intrinsically linked to the impact of Early Aftershock Deficiency (EAD) due to the inclusion of early periods containing relatively fewer events. The MOL accounts for EAD by considering a time-offset (c-parameter). It is desirable to minimise the c-parameter due to interdependency with the decay rate (p-parameter). This is typically achieved by the removal of early response events, i.e., manipulation of the modelling interval, along with limiting the variation allowed in the c-parameter. A consistent selection of a modelling interval is required to achieve consistent MOL parameters and the delineation of seismic responses with consistent temporal behaviour.

When modelling seismic responses with the MOL, the selection of a time interval and the implementation of the c-parameter can have a significant influence on results. These two aspects of modelling need to be explicitly addressed to ensure an appropriate modelling interval is selected that minimises the interdependency between the p-parameter and c-parameter. Additional considerations are implicitly addressed by considering these three major aspects, namely, the selection of a modelling interval based on temporal attributes, selection of an interval following the MOL, and the quantification of the modelling result quality.

There are two approaches typically adopted in literature for defining event times. Both of these approaches require the definition of a principal event with the time of subsequent events being defined relative to the time of the principal event occurrence. One of these approaches does not change the definition of the principal event even if early time intervals

are excluded to avoid non-power law behaviour. For the purpose of this thesis, this approach is referred to as the principal event fixed (PEF) method. An alternative approach adjusts the definition of the principal event if early time intervals are excluded. In this case, the relative time of each event is redefined with respect to the adjusted principal event time. For the purpose of this thesis, this approach is referred to as the principal event adjusted (PEA) method.

A comparison of the PEF and PEA methods is shown in **Table 16** for 'N' sequential events. The first five events are excluded in this response. The PEF method defines all relative event times with respect to the first event in this response, i.e., principal event highlighted by blue shading. The modelled response over the interval  $(T_s, T_E)$  uses the relative times since the first event (0.41, 0.45, 0.51, ...,  $T_E$ ). In contrast, the PEA method redefines the principal event to be the first event during the modelled response (Event Index 5) and redefines the relative times of events (0.04, 0.10, ...,  $T_E$ ).

**Table 16** PEF and PEA methods of defining event times

	Excluded Events					$T_s$	Modelled Response			$T_E$
Event Index	0	1	2	3	4	5	6		...	N
Principal Event Fixed Relative Time	0	0.1	0.2	0.3	0.4	0.41	0.45	0.51	...	$T_E$
Principal Event Adjusted Relative Time	*	*	*	*	*	0	0.04	0.10	...	$T_E$

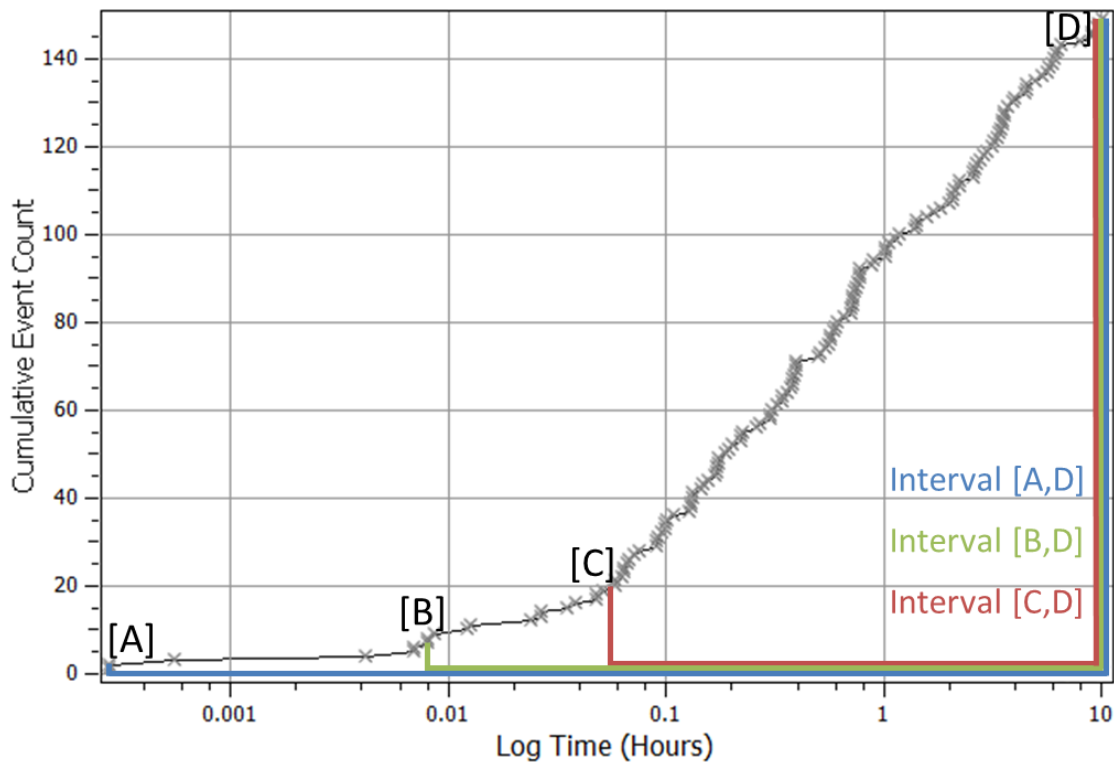
The use of a PEF method is reasonable when modelling a known causation process. A variable initiation time may be required when attempting to model responses without prior knowledge of the causation process, modelling responses with variation in temporal behaviour, or when response initiation has been misidentified.

In addition to the definition of event times, another major consideration for the implementation of the MOL is the limits placed on the c-parameter. For the original implementation of the law, the c-parameter is allowed to vary. In a number of reviewed studies (Sections 2.5.6 and 2.5.7) the c-parameter has been fixed to a constant value representative of a typical response, or set to zero. These studies remove an early portion of the response to ensure conformity to a power-law decay and ideally do not need the c-parameter to account for a deficiency in early aftershocks.

These approaches can be summarised by four modes of analysis, and are investigated further to evaluate methods of modelling mining seismic responses with the MOL:

- *Mode 1:* Principal Event Adjusted and a variable c-parameter (PEA  $c \geq 0$ );
- *Mode 2:* Principal Event Fixed and a variable c-parameter (PEF  $c \geq 0$ );
- *Mode 3:* Principal Event Adjusted and a c-parameter fixed to zero (PEA  $c = 0$ ); and
- *Mode 4:* Principal Event Fixed and a c-parameter fixed to zero (PEF  $c = 0$ ).

The application of the MOL to a real seismic response with variable early event occurrence is investigated in **Figure 93** and **Table 17**. This example shows the effect of the selection of a modelling interval, the definition of relative event times, and the use of the c-parameter with respect to MOL parameters, parameter uncertainties, and suitability of fit (Anderson-Darling statistic). **Figure 93** shows the cumulative event count for three modelling intervals that are defined to include a period of high  $EAD_{[A-B]}$ ,  $EAD_{[B-C]}$ , and consistent event occurrence [C-D] (modelling intervals [A,D], [B,D], and [C,D], respectively). These three time intervals are modelled using the four previously presented approaches. **Table 17** details the results for the 12 combinations of time intervals and approaches to modelling.



**Figure 93** Cumulative event count over time (log scale) for three modelling intervals that are defined to include a period of high  $EAD_{[A-B]}$ ,  $EAD_{[B-C]}$ , and consistent event occurrence [C-D]. The three modelling intervals are [A,D], [B,D], and [C,D], and corresponds to the rows in **Table 17**.

**Table 17** Four modes of modelling approaches applied to the three modelling intervals (**Figure 93**). The modelling index interval, MOL parameters ( $p$ ,  $K$ ,  $c$ ), and Anderson-Darling statistic are tabulated along with a graphical representation of these numbers.

	Index		Modelling Parameters							Anderson-Darling
	$T_s$	$T_E$	$p$		$K$		$c$			
Mode 1 PEA $c \geq 0$	0(A)	148(D)	$1.2 \pm 0.13$		$29.3 \pm 4.29$		$0.08 \pm 0.04$		0.31	
	7(B)	148(D)	$1.18 \pm 0.13$		$28.54 \pm 4.4$		$0.09 \pm 0.05$		0.29	
	20(C)	148(D)	$1.1 \pm 0.13$		$25.4 \pm 3.84$		$0.07 \pm 0.05$		0.27	
Mode 2 PEF $c \geq 0$	0	148	$1.1 \pm 0.13$		$25.4 \pm 3.8$		$0.07 \pm 0.05$		0.27	
	7	148	$1.18 \pm 0.13$		$28.54 \pm 4.4$		$0.07 \pm 0.05$		0.29	
	20	148	$1.1 \pm 0.13$		$25.36 \pm 3.82$		$0.07 \pm 0.05$		0.27	
Mode 3 PEA $c = 0$	0	148	$0.76 \pm 0.04$		$22.34 \pm 1.97$		$0 \pm 0$		5.76	
	7	148	$0.76 \pm 0.04$		$21.58 \pm 1.94$		$0 \pm 0$		4.99	
	20	148	$0.75 \pm 0.05$		$19.92 \pm 1.87$		$0 \pm 0$		3.5	
Mode 4 PEF $c = 0$	0	148	$0.76 \pm 0.04$		$22.34 \pm 1.97$		$0 \pm 0$		5.76	
	7	148	$0.94 \pm 0.08$		$23.2 \pm 2.35$		$0 \pm 0.01$		1.6	
	20	148	$1.06 \pm 0.12$		$24.32 \pm 3.34$		$0 \pm 0.04$		0.35	

The Anderson-Darling statistic indicates that *Mode 1* (PEA  $c \geq 0$ ) and *Mode 2* (PEF  $c \geq 0$ ) model the response suitably and result in similar parameters for all three intervals. Applying *Mode 3* (PEA  $c = 0$ ) to any of the modelling intervals does not result in the MOL being well fit to the response. When *Mode 4* (PEF  $c = 0$ ) is used, the MOL fit improves with the exclusion of early events. Additionally for this mode, the  $p$ -parameter and  $K$ -parameter increase to values typical of *Modes 1* and *2* as the model fit improves.

These results are congruent with the well-known properties of the MOL. The use of a variable  $c$ -parameter allows the influence of including the EAD intervals to be minimised. In this particular case, irrespective of a fixed or adjusted principal event, a variable  $c$ -parameter allows for consistent MOL results across a range of time intervals. This insensitivity to a specific time interval is a desirable characteristic for an algorithmic approach to applying the MOL.

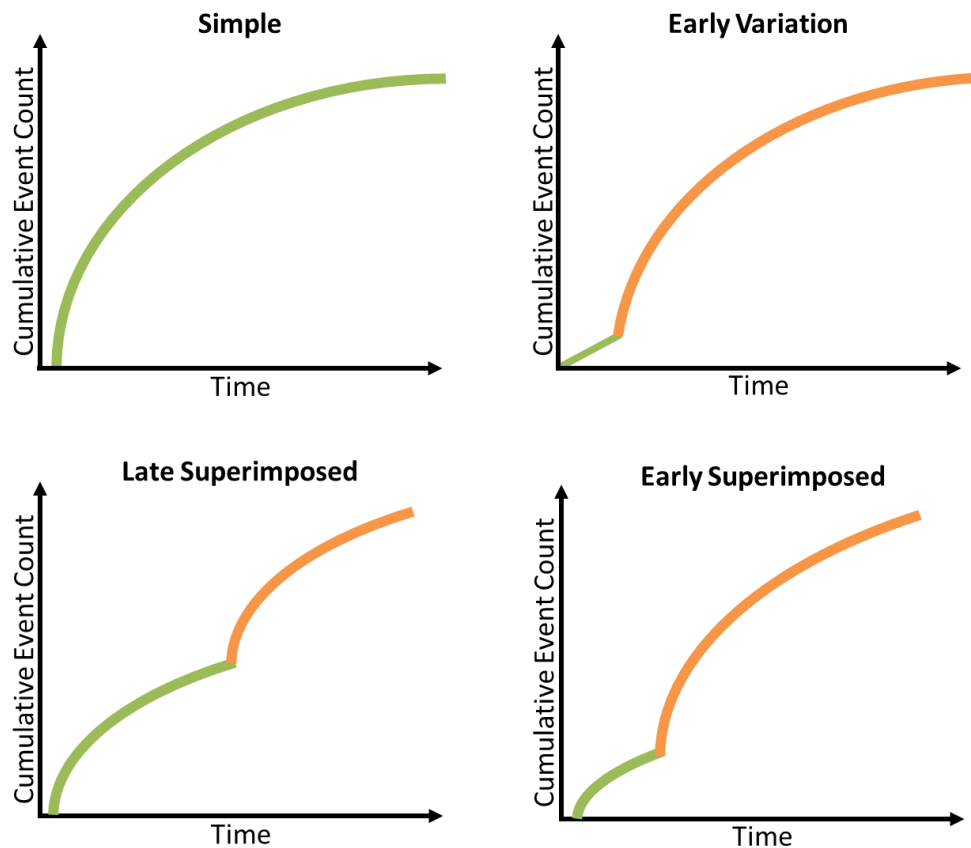
*Mode 4* is a reasonable approach if intervals of early temporal variation are excluded. *Mode 3* results in inaccurate modelling irrespective of the principal event selected. This is due to the adjustment of the relative event times that cause an unavoidable period of early variation that greatly influences results if the  $c$ -parameter is fixed at zero. This has an important implication for any approach that uses a  $c$ -parameters fixed to zero. If the initiation of the response was identified at index 20 instead of zero, then due to the definition of relative event times, applying *Mode 4* to this new scenario is the same as *Mode 3* for the original identification of the response. *Mode 4* requires the exclusion of early events to improve results. This suggests

that results from *Mode 4* are dependent on when the response is identified and the interval of events excluded. Interdependency is influenced by the stochastic nature of temporal event occurrence, the method used to identify responses, and the exclusion of early variation. Using a mode that is influenced by these indefinite factors is an undesirable characteristic for an algorithmic approach. The example presented in **Figure 93** and **Table 17** provides evidence that further investigation into the properties of the MOL application modes is required.

## 5.5 Critical Assessment of the Four MOL Modelling Models

This section investigates the previously presented MOL modelling modes with respect to four types of seismic response scenarios that are commonly observed in the mining environment. This is not a comprehensive list of possible scenarios, although, these responses are commonly observed for mining induced seismicity. A temporal modelling method that is applied to mining induced seismicity should be able to delineate and quantify these responses consistently. These four response scenarios are:

- Simple seismic response: a time-dependent seismic response that follows the MOL (**Figure 94** top left);
- Seismic response with early variation: a period of constant temporal rate of event occurrence is followed by a time-dependent response (**Figure 94** top right);
- Late superimposed response (shift blasting): a period of constant event rate occurs prior to a response. Another period of constant event rate and seismic response occurs hours after the first response (**Figure 94** bottom left); and
- Early superimposed responses (double aftershocks): a period of s constant event rate occurs prior to a seismic response. Another period of constant event rate and seismic response occurs soon after the first response (**Figure 94** bottom right).

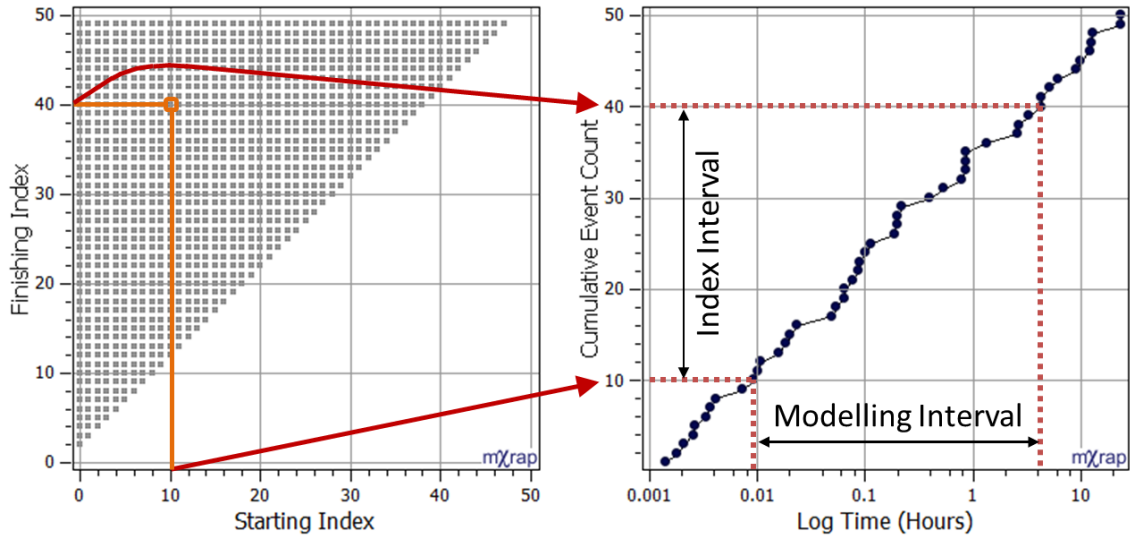


**Figure 94** The cumulative event count over time for four types of seismic response scenarios.

The analysis in this section evaluates the accuracy and reliability of the MOL parameters recovered for the four modelling modes. This is achieved by comparing temporal modelling results to known parameters associated with synthetically generated seismic responses. The method used for synthetic generation of seismic responses is detailed in Appendix A: Generation of Synthetic Seismic Responses. The determination of consistent modelling parameters allows methods to be developed that can delineate superimposed responses based on these results.

Charts referred to as solution spaces are used to evaluate the methods for obtaining the MOL parameters. The previously presented example assessed results for three visually identified time intervals (**Figure 93** and **Table 17**). The selection of modelling periods can be avoided by considering all positive time intervals for the response. To explore results that arise from evaluating all solutions, charts are constructed that represent every unique combination of start and end index within a seismic response. Each axis specifies a starting and finishing event index with each [x,y] point representing a solution. After imposing the restriction that intervals must be positive, each chart illustrates  $\frac{N \times N}{2}$  possible solutions. **Figure 95** provides an example of the representation of the solution space associated with a response containing 50 events. Shown right is a cumulative event count for this response. The solution for any particular

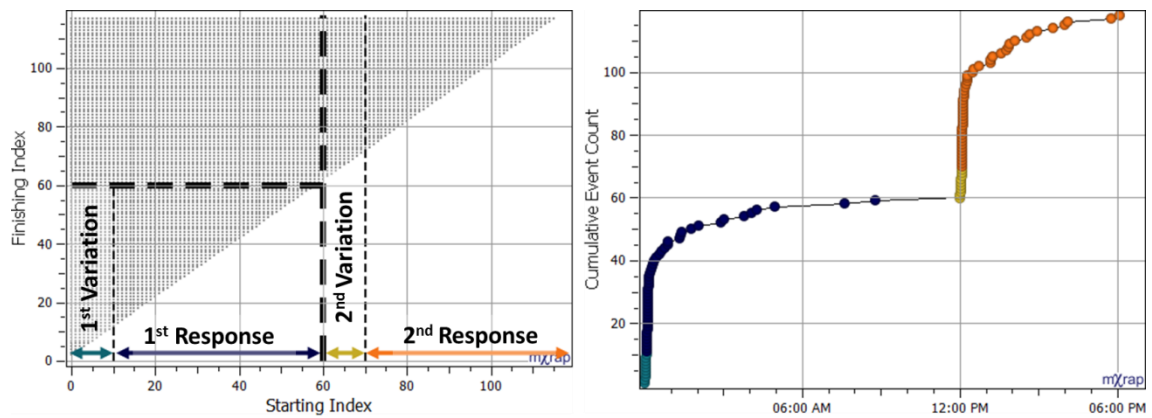
combination of starting and finishing index is represented by a single point on the solution space chart based on the start/finish events within a modelling interval (left). The example shown highlights the solution point for the interval starting at #10 and finishing at #40. These charts allow single parameters to be displayed for all possible index intervals.



**Figure 95** Derivation of the solution space associated with a response containing 50 events.

*Right: Cumulative event count over time (log scale). Left: Single points represent all combinations of starting and finishing index to form a solution space. The shown solution point (red arrows) uses an interval starting at #10 and finishing at #40 (red dash lines).*

In the case where solution spaces are generated by multiple seismic responses, for the start index (x-axis), a thin dashed line indicates the end of early variation and the start of the synthetic seismic response. For the starting index (x-axis) and finishing index (y-axis), thick dashed line indicates the end of the first response and the start of the variation before the second response. **Figure 96** shows an example of these lines on a solution space chart (left) and the cumulative event count over time (right). This example considers for two seismic responses preceded by 10 events of variation in temporal occurrence. The solution space chart is annotated with respect to the response associated with the start index. The response of a corresponding colour is shown on the time series chart.



**Figure 96** Left: A solution space chart annotated with respect to the response associated with the starting index. Right: Time series of responses correspondingly coloured.

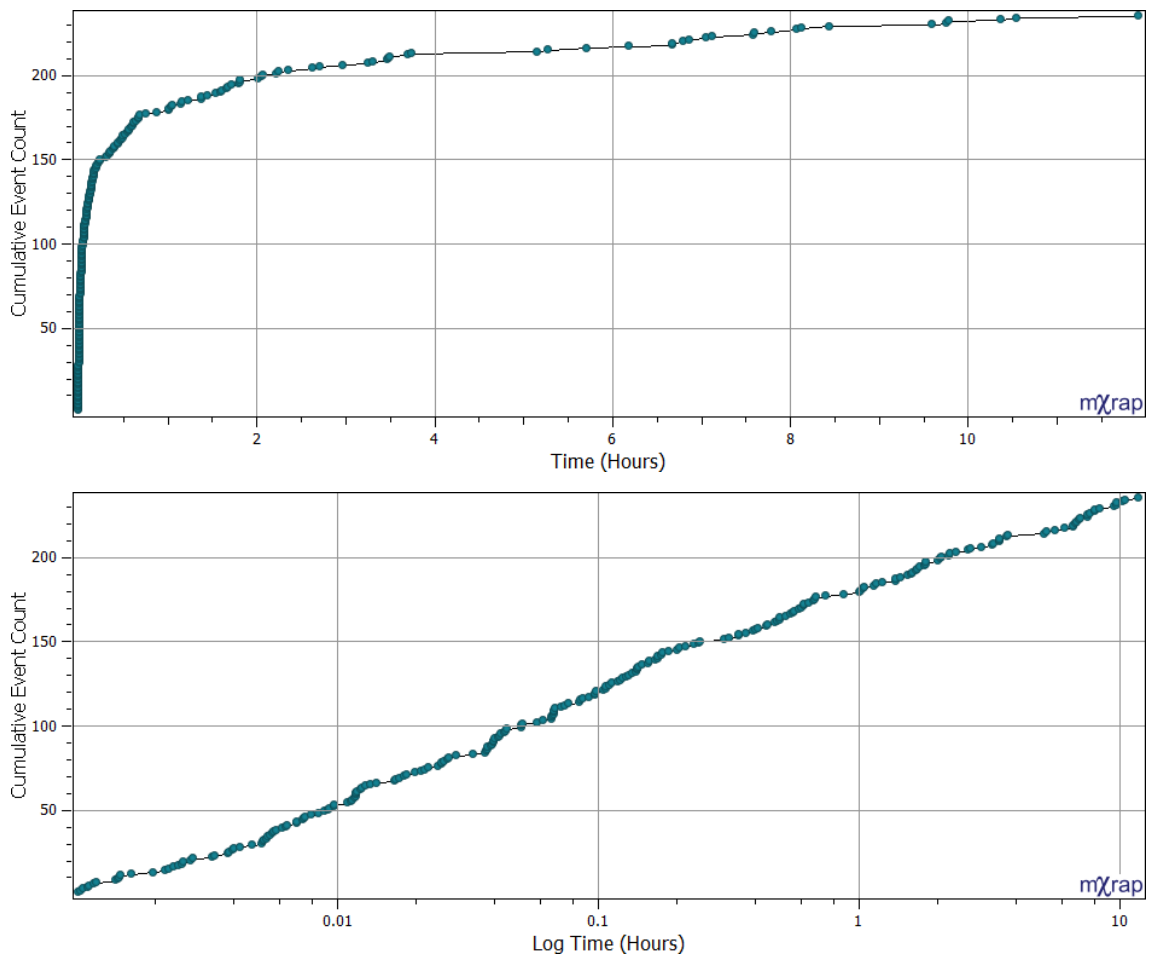
All possible index intervals of this seismic response are evaluated using the modes of applying the MOL. This assessment creates four solution spaces to display modelling results. An ideal solution will recover the parameters that were used to generate the response and delineate the majority of the response. These two objectives are represented by two features within the solution space. Firstly, grey solution points represent the intervals with results within 10% of the parameter that was used to generate the synthetic response. Secondly, an arbitrary area of the solution space is defined to capture the first 30 events of the starting index and the last 50 events of the finishing index. This area represents solutions that capture a significant portion of the response. The optimal mode will have the most representative parameters within the ideal index interval.

### 5.5.1 Simple Seismic Response

A simple seismic response represents typical time-dependent event occurrence for mining induced seismicity. The parameters chosen to generate the response are in the typical range reported in previous studies (**Table 18**) (Section 2.5). **Figure 97** illustrates the resultant response with two plots of cumulative event count over time (top) and log time (bottom).

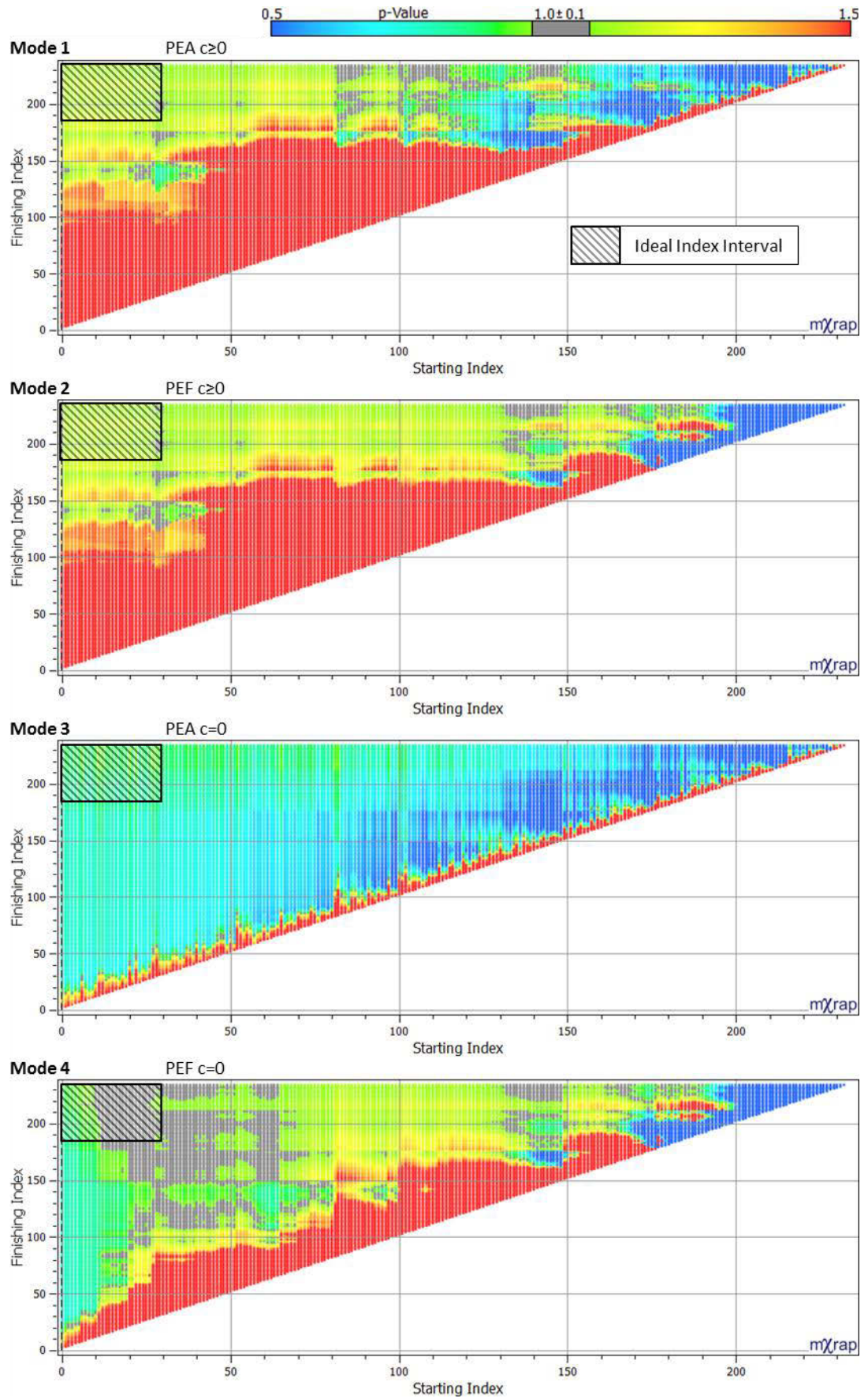
**Table 18** Parameters used to generate a simple, synthetic seismic response.

Response	Offset(h)	Var(h)	$T_s$ (h)	$T_E$ (h)	$p$	$K$	$c$
#1	0	0	0.001	12	1.0	25	0

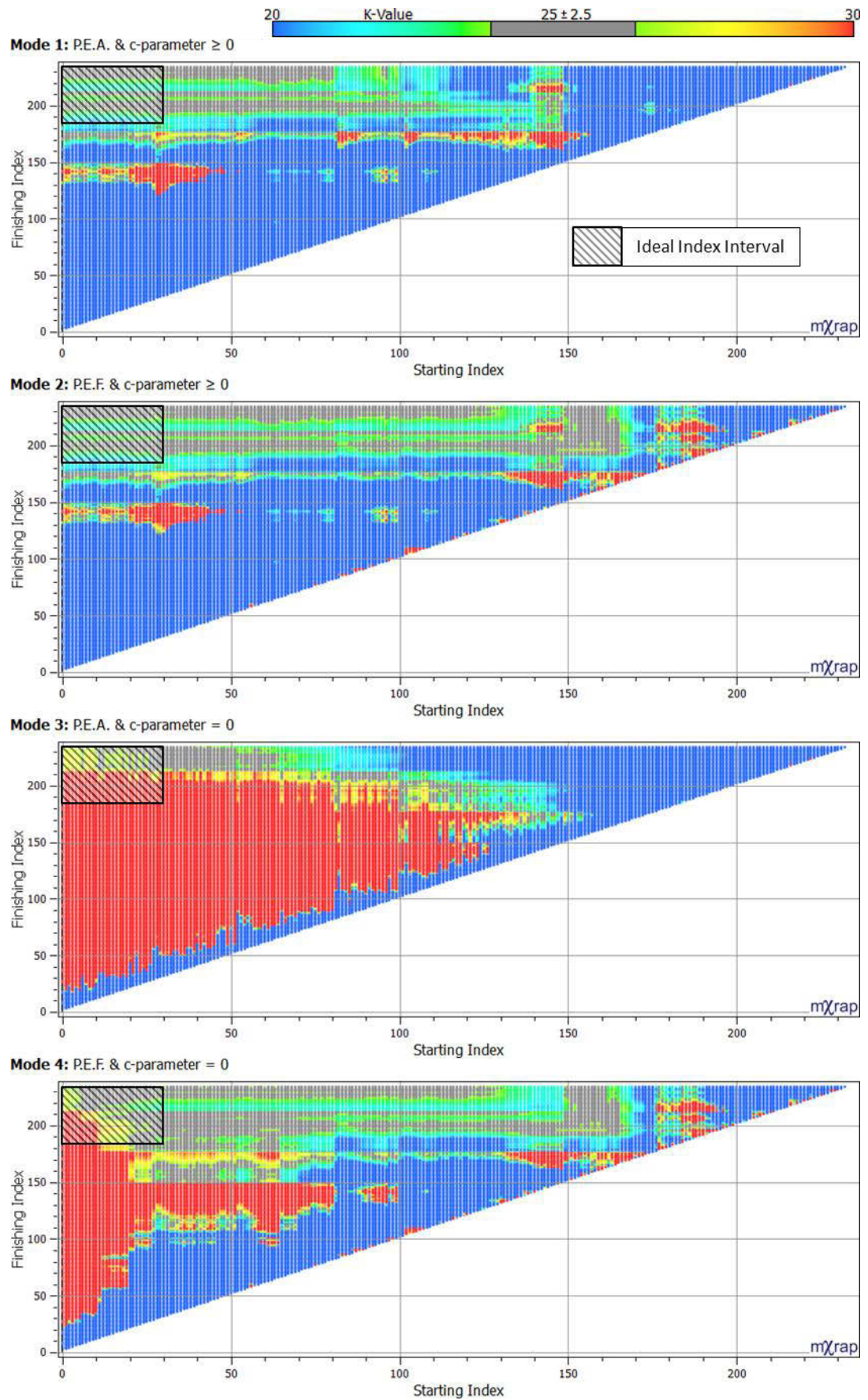


**Figure 97** A synthetically generated response typical of mining induced seismicity. Top: Cumulative number of events over time. Bottom: Cumulative number of events over log time.

The results from **Figure 98** and **Figure 99** are congruent with the previously presented real seismic response. *Mode 4* provides the best result with accurate parameter recovery within the ideal index interval, although, this mode does require the exclusion of early starting indices to achieve accurate results. *Mode 1* and 2 slightly overestimates the p-parameter, although, are consistent and identify accurate K-parameters for the majority of the ideal index interval. *Mode 3* results are erroneous for the vast majority of the solution space. The vertical streakiness of the solution space is due to the influence of a small number of events at the beginning of the response. The inconsistency of *Mode 3* is undesirable as the stochastic nature of temporal event occurrence has a significant influence on the modelling results. Furthermore, these results are generally inaccurate, particularly for the p-parameter.



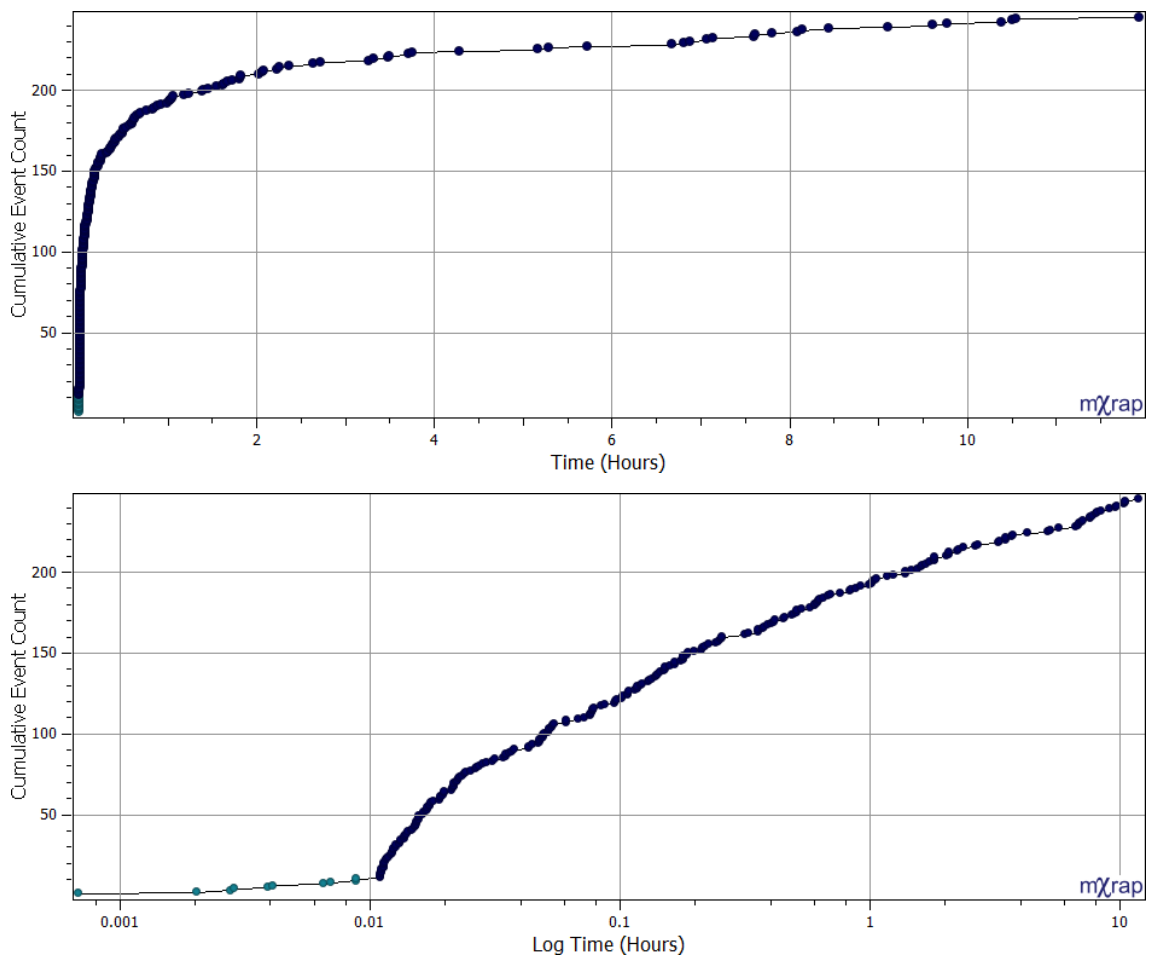
**Figure 98** *p*-parameter solution spaces for a simple response. Mode 4 performs optimally with accurate parameter recovery for the majority of the ideal index interval.



**Figure 99** K-parameter solution spaces for a simple response. Modes 1 and 2 perform optimally with accurate parameter recovery for the ideal index interval, followed by Mode 4, then Mode 3.

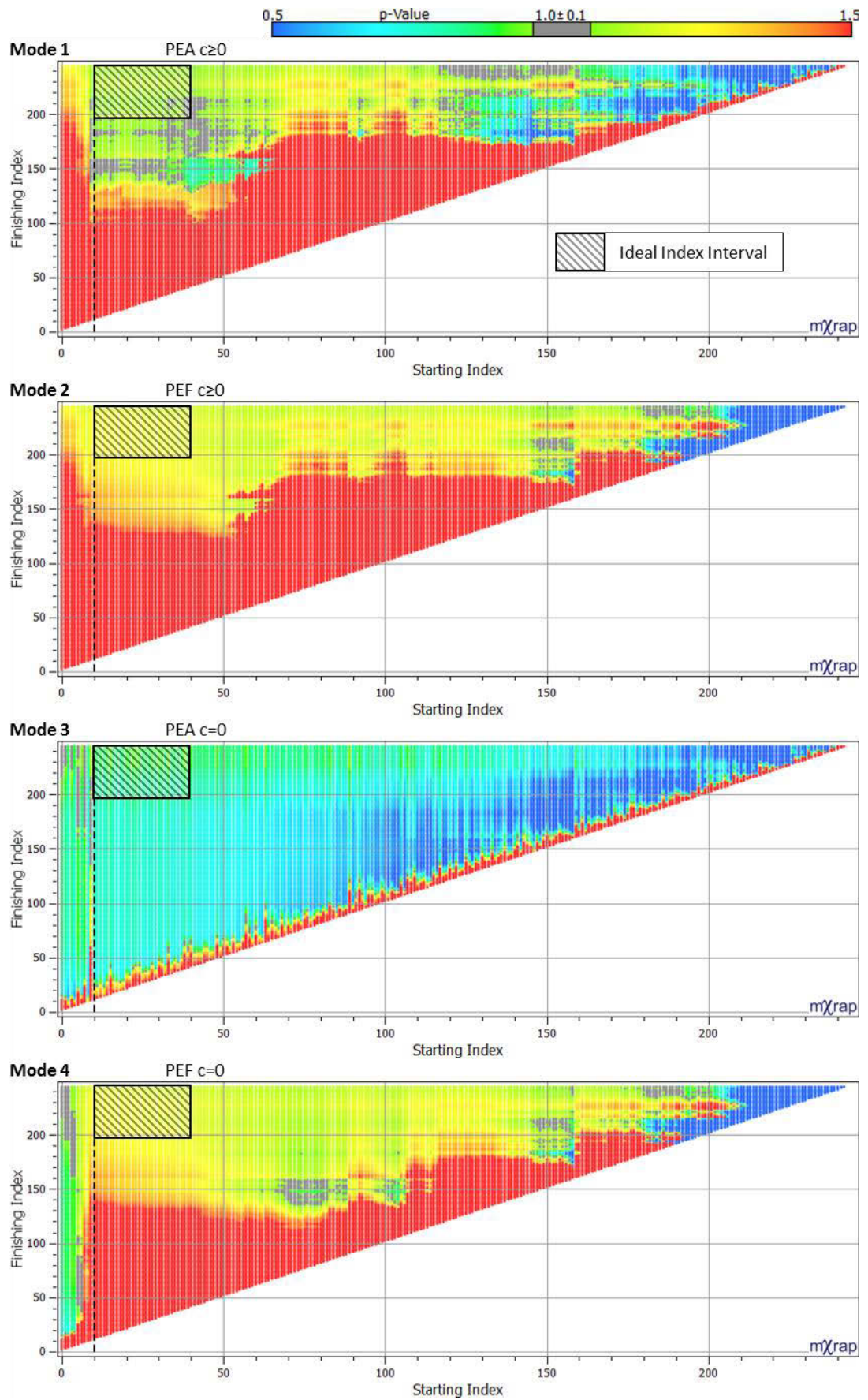
### 5.5.2 Seismic Response with Early Variation

The previous section examined a seismic response following the MOL and represented typical time-dependent event occurrence. This section examines the same response, although, with an early period of linear event occurrence that represents inconsistency due to an initial period deficient of aftershocks or the response being identified too early. The parameters that generate the seismic response are the same as Section 5.5.1. Also included in the dataset are 10 randomly sampled events over the initial 0.01 h. The resultant response is shown in **Figure 100** with a cumulative event count over linear time (top) and log time (bottom).

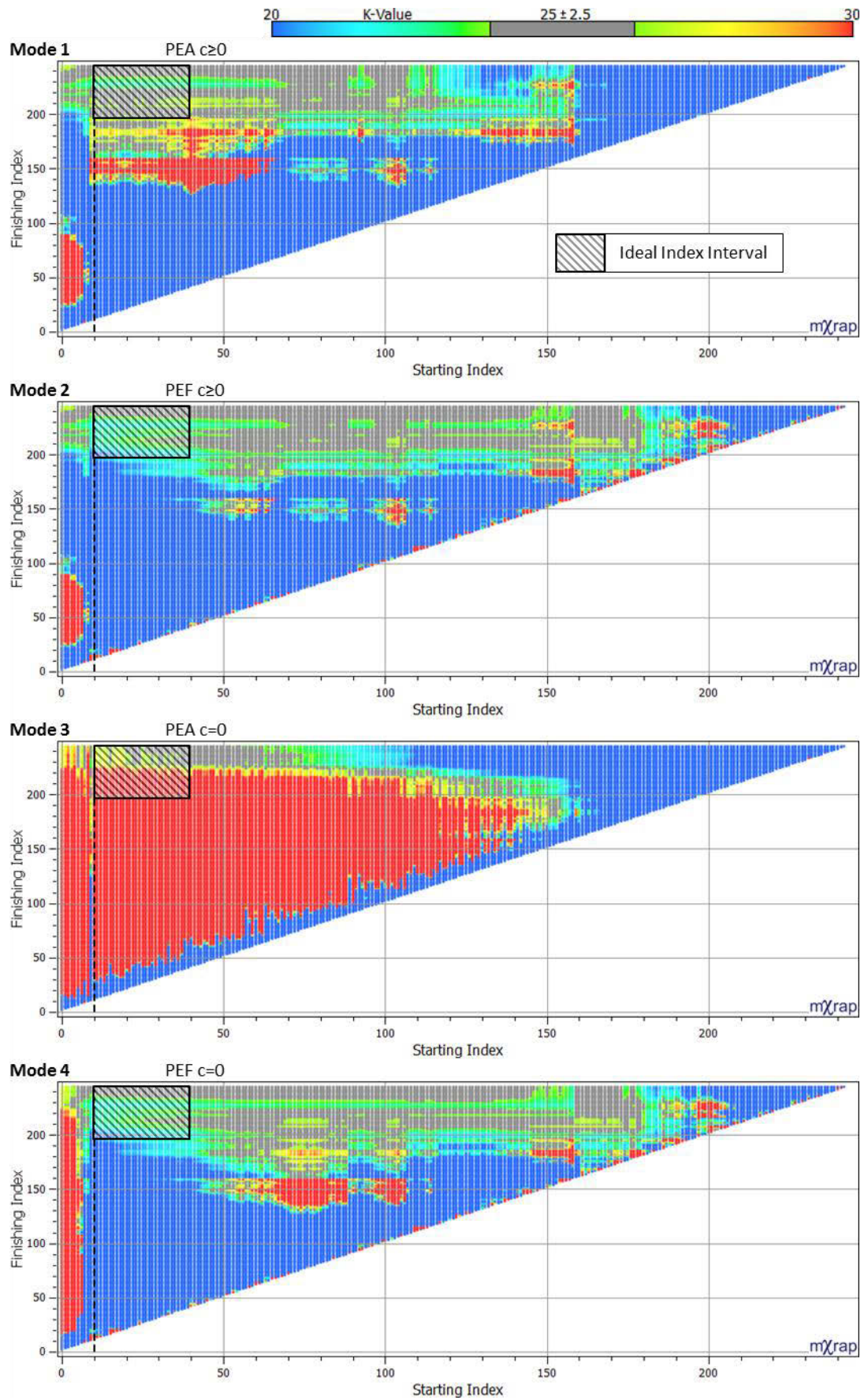


**Figure 100** Time series of a synthetic response with early variation in event occurrence. Charts show the cumulative number of events over time (top) and log time (bottom). Events are coloured by their generation procedure.

Resultant solution spaces are shown in **Figure 101** and **Figure 102**. *Mode 1* provides the most representative solution space for both p-parameters and K-parameters inside and outside of the ideal index interval. *Mode 2* and *4* overestimate p- parameters and have limited solutions with accurate K-parameters. This indicates that when there is early variation and the principal event is fixed there is a bias to p-parameters (overestimation). *Mode 3* results are erroneous for the vast majority of the solution space.



**Figure 101** Solution spaces for a single response with variation shaded by p-parameters. Mode 1 performs preferably with the most accurate p-parameters, followed by Mode 4, Mode 2, and then Mode 3.



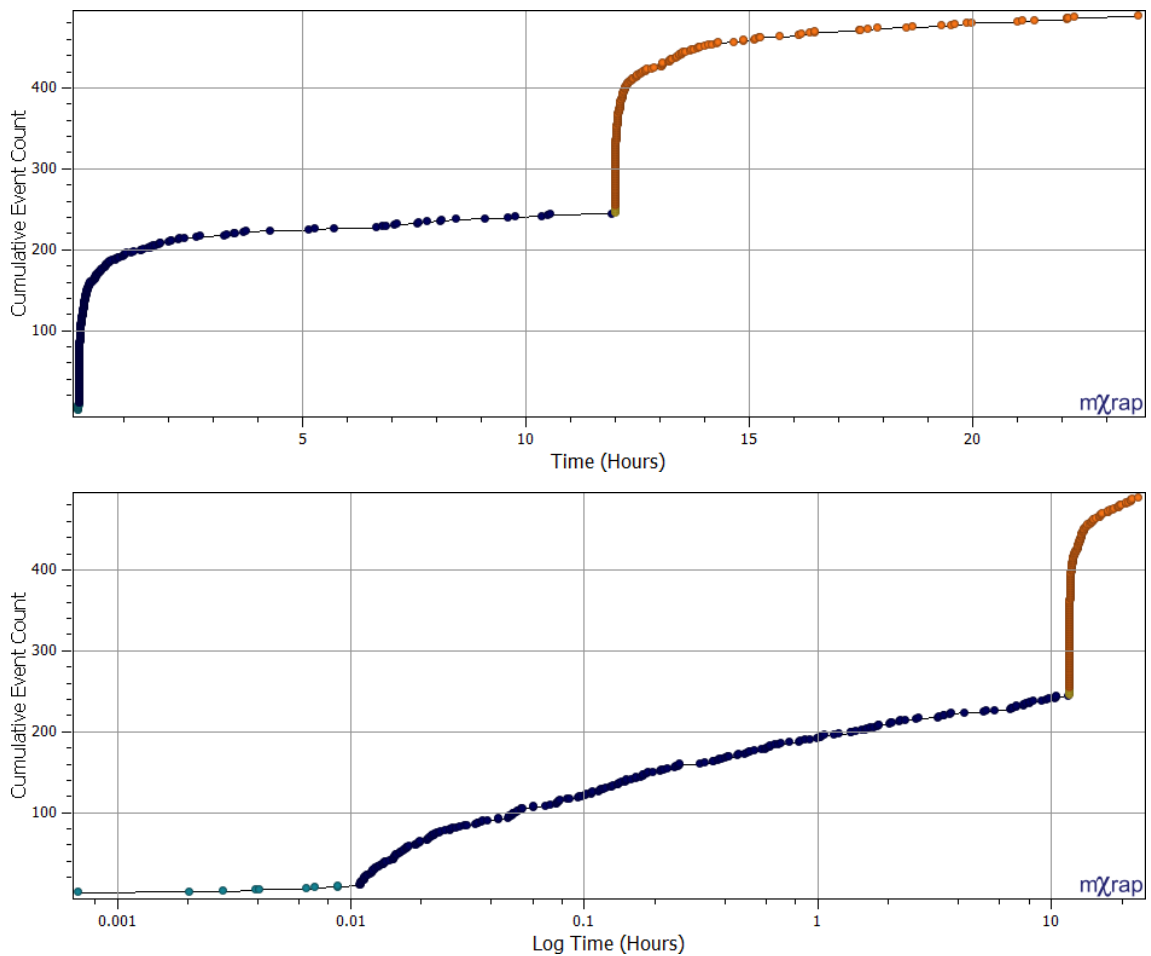
**Figure 102** K-parameters solution spaces for a single response with variation. Mode 1 performs optimally with a reasonable recover of K-parameters, followed by Mode 2, Mode 4, and then Mode 3.

### 5.5.3 Late Superimposed Seismic Responses

Late superimposed responses contain two responses following the MOL with an early period of variation. The second response is offset by a significant time interval, e.g., 12 h. The late superimposition of responses is representative of time-dependent seismicity induced by blasting in successive working shifts. The ability to find an appropriate modelling interval when multiple responses exist is a critical aspect of the iterative identification and delineation of seismic responses, particularly when composite models are not considered. The parameters chosen to generate the two seismic responses for this example are detailed in **Table 19**. The seismic responses are plotted showing the cumulative event count over time (**Figure 103 top**) and time on a log scale (**Figure 103 bottom**).

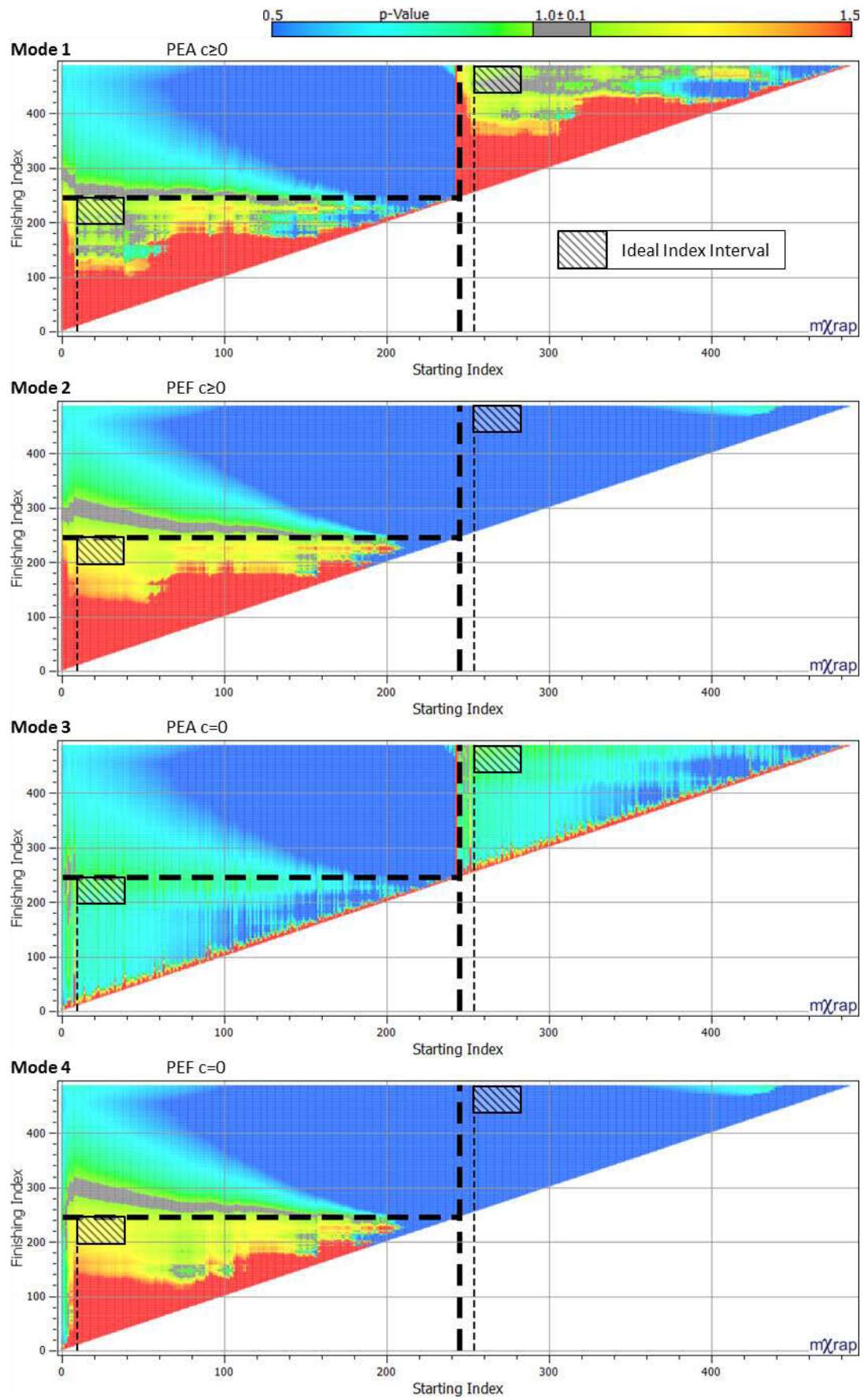
**Table 19** Parameters used to generate late, superimposed, synthetic seismic responses.

Response	Offset(h)	Var(h)	$T_s(h)$	$T_E(h)$	p	K	c
#1	0	0.01	0.001	12	1.0	25	0
#2	12	0.01	0.001	12	1.0	25	0

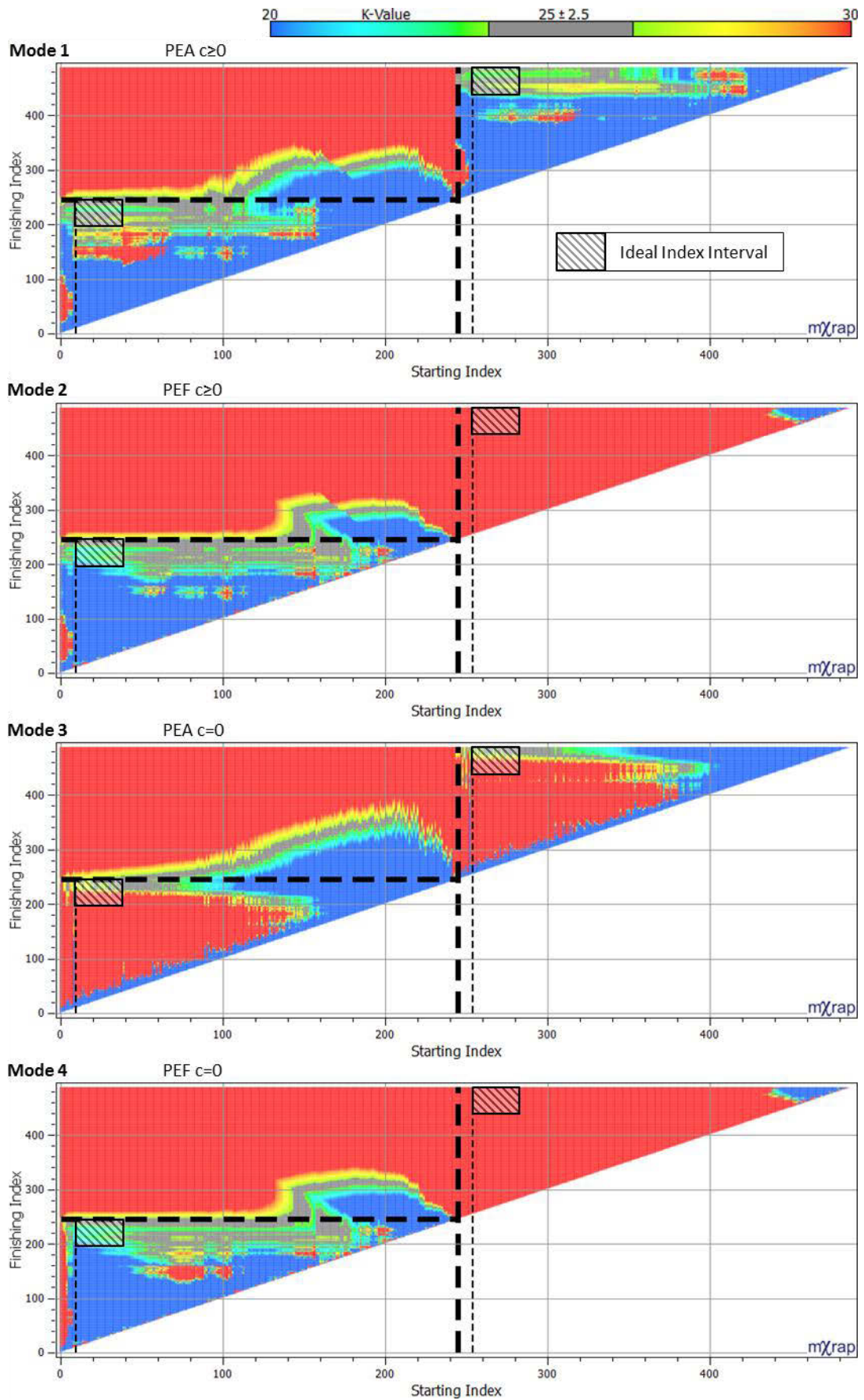


**Figure 103** Time series of two randomly sampled synthetic seismic responses, offset in time, and with early variations in event occurrence. Shown is the cumulative number of events over time (top) and log time (bottom). Events are coloured by their generation procedure.

Resultant solution spaces are illustrated by **Figure 104** and **Figure 105**. *Mode 1* is the optimal approach as parameters are recovered for a reasonable number of solutions within the ideal index intervals for both responses. When considering the parameter recovery for the first response, the results of *Modes 2* and *4* are the same for a seismic response with early variation (Section 5.5.2). These modes are not able to recover any reasonable parameters for the second response. This highlights that PEF methods are not able to recover parameters for a seismic response containing early variation or not identified precisely. Again, *Mode 3* has no reasonable solutions.



**Figure 104** Solution spaces for two responses with variation shaded by p-parameters. Mode 1 performs reasonably accurately and recovers parameters from both responses.



**Figure 105** Solution spaces for two responses with variation shaded by K-parameter. Mode 1 performs reasonably accurately for both responses.

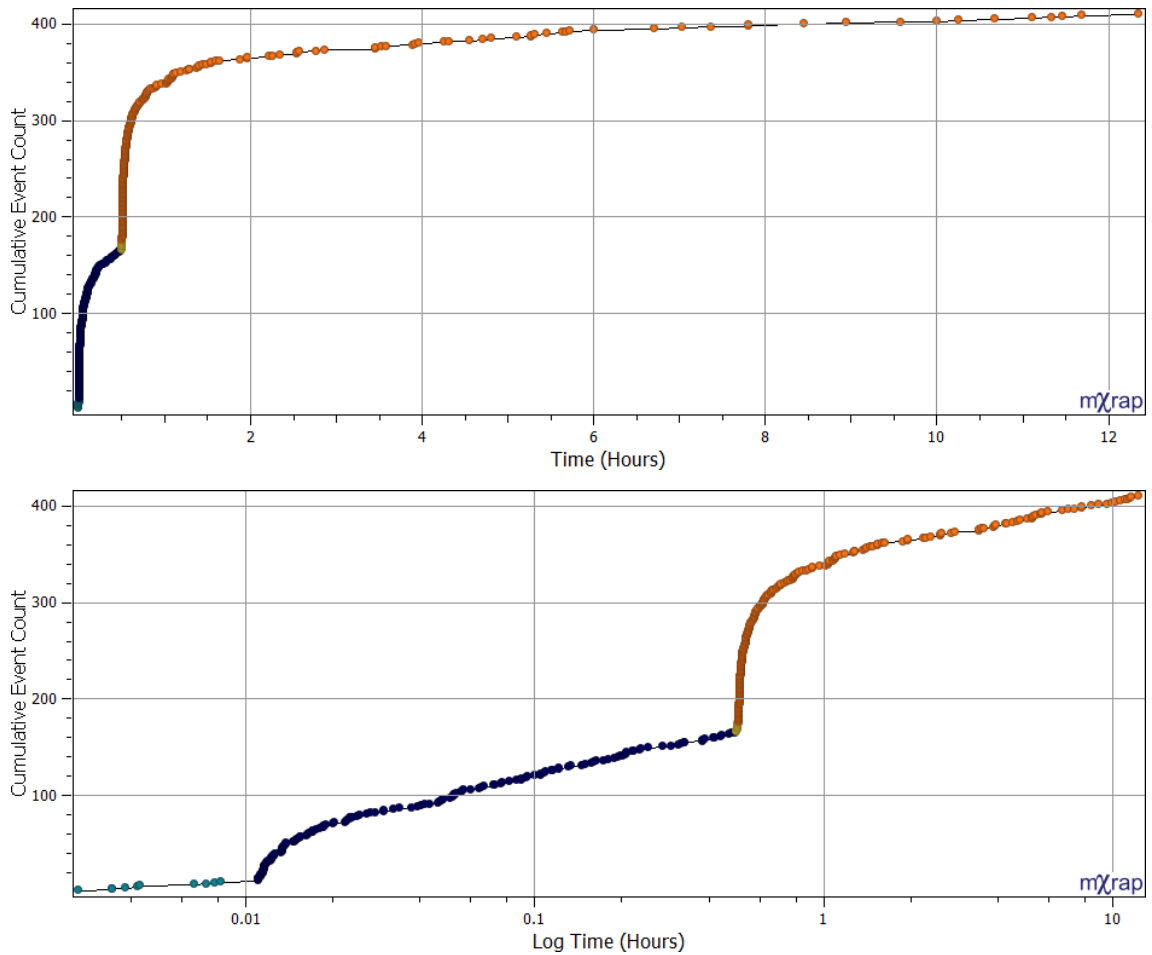
#### 5.5.4 Early Superimposed Seismic Responses

Early superimposed responses with variation represent successive responses that follow the MOL, although, the second response is offset by a short time interval. The late superimposition of responses is representative of a response initially occurring and a second response occurring due to an additional rock mass failure process, e.g., a large seismic event. This case is comparatively more complex than a late superimposition of a seismic response as there is more uncertainty in the parameters associated with the first seismic response. Furthermore, the initiation of the second response is more ambiguous due to a comparative similarity of event rates. As with the assessment of late superimposed responses (Section 5.5.4), the ability to find an appropriate modelling interval when multiple responses exist is a critical aspect of an iterative framework (Section 3.5.4).

The parameters chosen to generate the two seismic responses for this example are detailed in **Table 20**. The resultant seismic responses are plotted on two charts showing the cumulative event count over time (**Figure 106** top) and time on a log scale (**Figure 106** bottom).

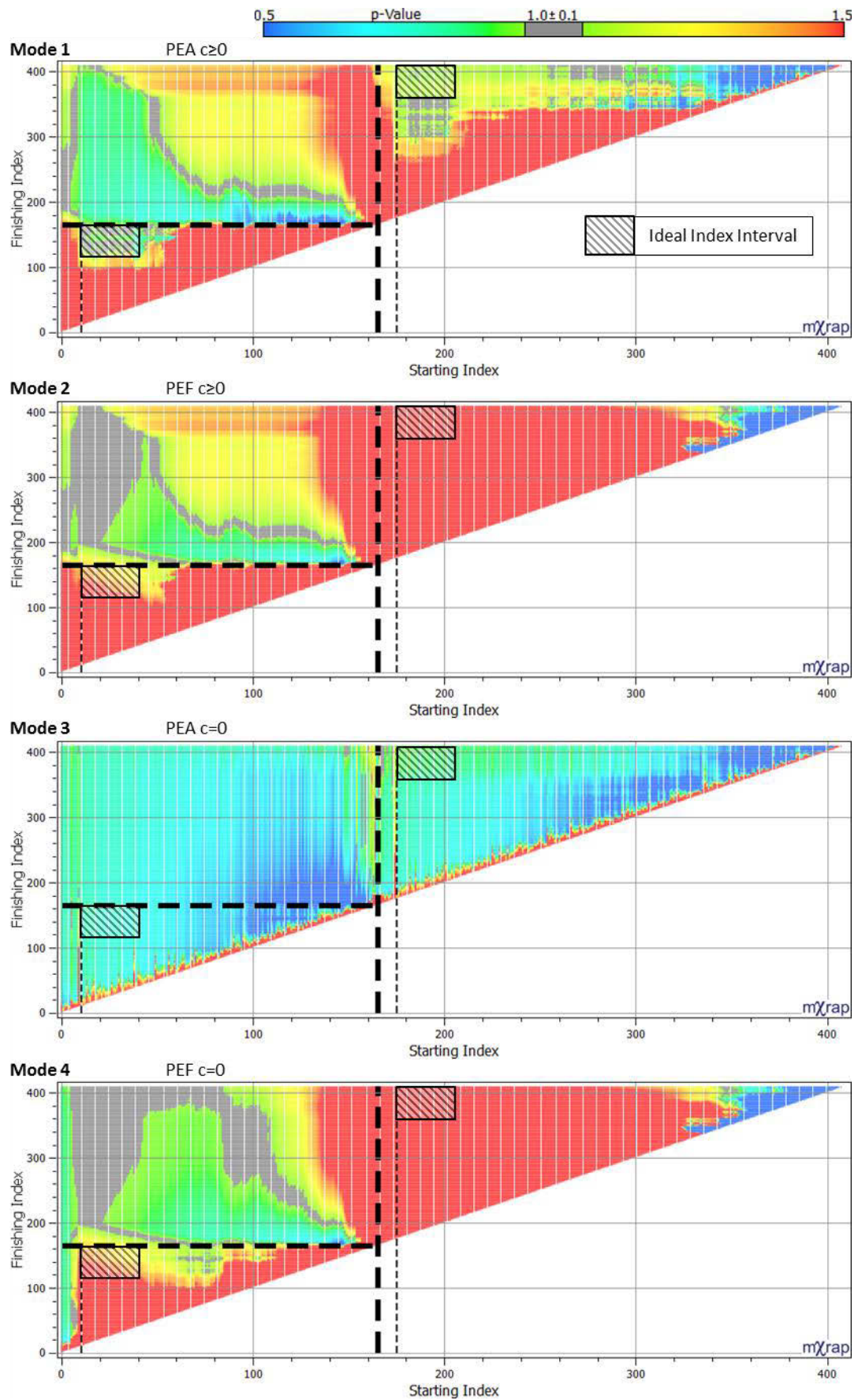
**Table 20** Parameters used to generate early, superimposed synthetic seismic responses.

Response	Offset(h)	EAD(h)	$T_s(h)$	$T_e(h)$	p	K	c
#1	0	0.01	0.001	0.5	1.0	25	0
#2	0.5	0.01	0.001	12	1.0	25	0

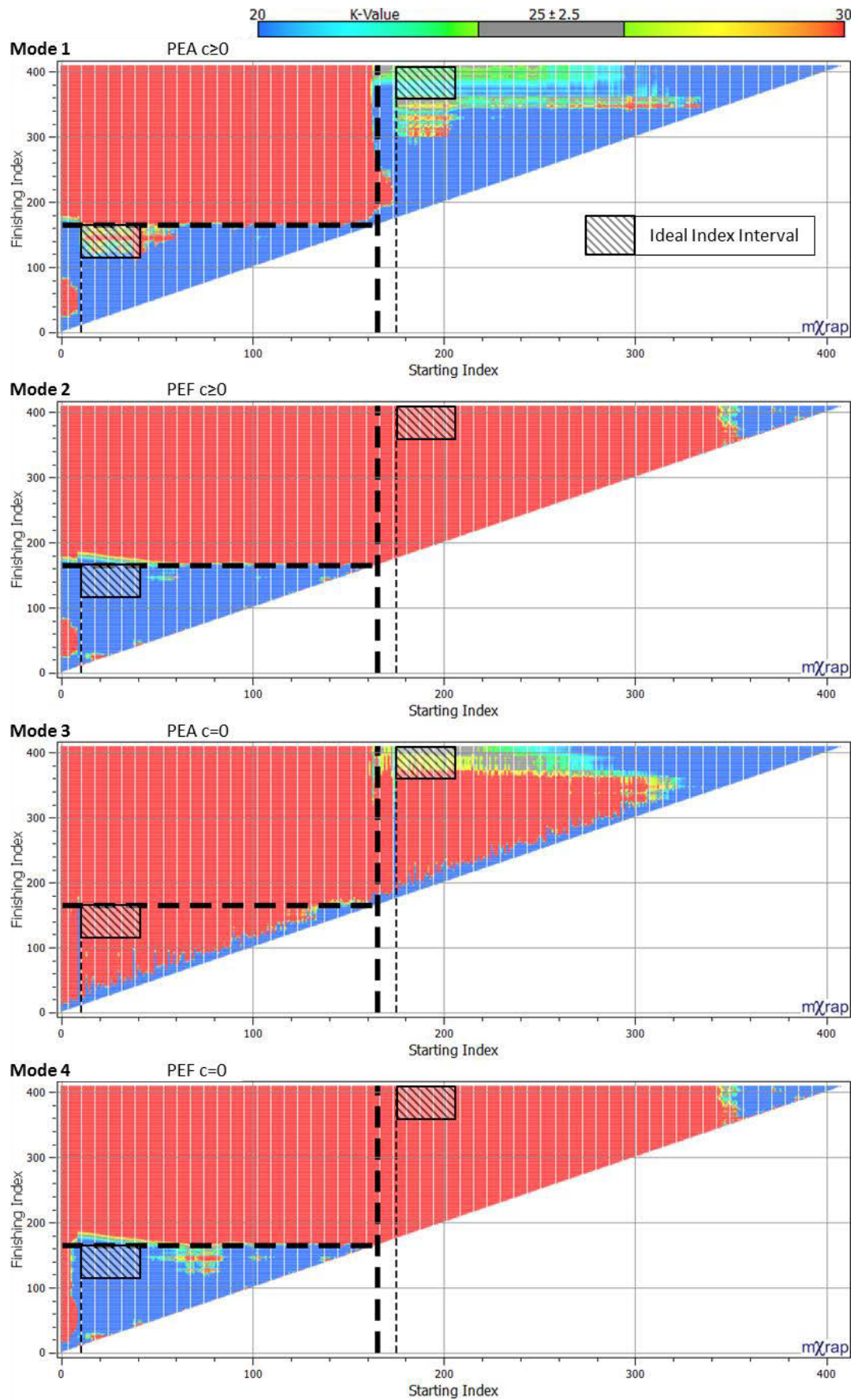


**Figure 106** Two synthetic responses with early variations in event occurrence. The second seismic response occurs 0.5 h after the initial response. Shown is the cumulative number of events over time (top) and log time (bottom). Events are coloured by their generation procedure.

Parameter solution spaces are shown in **Figure 107** and **Figure 108**. *Mode 1* is the only approach that can recover the MOL parameters that were used to generate any of the synthetic responses within the ideal index interval. In comparison to the other response scenarios, the K-parameters obtained by this mode tend to be more sporadic and reflect the uncertainty of recovering this parameter (event productivity) over short modelling intervals. *Mode 2*, *3*, and *4* perform poorly and are not capable of recovering the synthetic parameters within the ideal index interval. The K-parameters found by *Mode 3* for the second interval is arguably accurate (**Figure 108**), although, is not reliable due to the large influence of the events at the beginning of this response.



**Figure 107** Solution spaces for two responses with variation shaded by p-parameter. Mode 1 performs reasonably accurately for both responses. The other modes are generally inaccurate.



**Figure 108** Solution spaces for two responses with variation shaded by K-parameter. Mode 1 performs optimally whereas the other modes are generally inaccurate.

### 5.5.5 Selecting the Optimal MOL Modelling Mode for Mining Induced Responses

The previous analysis indicates that using a PEA approach with a variable c-parameter is optimal to delineate and quantify a range of mining induced seismic responses. The limitation of this approach is the need for a variable c-parameter that creates an inherent trade-off between the interdependency of p-parameter and c-parameter, as well as, achieving consistent quantification and delineation for a range of seismic responses.

The quantification of a seismic response using the MOL is sensitive to early time intervals when the c-parameter is fixed to zero. As such, events must be excluded to achieve accurate results even if the temporal occurrence of events follows a power law decay. The PEF method is unable to recover MOL parameters if the initiation of the response is not correctly identified or if there are subsequent responses. The aspects of using a c-parameter fixed to zero or a PEF approach conflict with the objectives of this thesis, specifically, the ability to consistently delineate and quantify a range of seismic response scenarios. Despite a variable c-parameter reducing the accuracy of p-parameter recovery by overestimating values, this parameter allows for the modelling of early seismic response intervals and consistent parameter solution spaces. Additionally, the PEA is not subject to the same shortcomings as the PEF method, which can recover the parameters of responses that are not associated with the principal event initially used to define a modelling period.

## 5.6 Parametric and Statistical Selection of Modelling Interval

The Maximum Likelihood Estimate (MLE) is the basis for statistical modelling selection (Section 2.5), either directly or in the form of an information criteria, e.g., Akaike (1974). The consideration of this measure alone can result in the unreliable optimisation, i.e., selection of a modelling interval if the temporal occurrence cannot be reproduced by the model applied to the seismic response. An unsuitable interval may be selected even if part of the seismic response could be suitably modelled. This section utilises the findings from Section 5.5 concerning the mode of MOL modelling and considers additional statistics associated with the MOL to optimise the selection of temporal intervals. Additional statistics are selected based on the ideal characteristics of modelling of a seismic response to construct a decision metric that optimises the quantification and delineation of seismic responses using the MOL. The parametric and statistical considerations to optimise the selection of a modelling time interval are the MLE, number of events modelled, c-parameter, parametric standard error, and Anderson-Darling statistic.

### 5.6.1 Relevant Parametric and Statistical Measures

Section 5.5 identified the PEA approach with a variable c-parameter to be optimal for a range of response scenarios. Using this method causes an inherent interdependency between the p-parameter and c-parameter that must be considered to minimise the introduced bias. This aspect of using a PEA approach with a variable c-parameter must be a priority of modelling interval selection with the c-parameter ideally being zero.

The suitability of a modelled interval is partially indicated by low uncertainty in MOL parameters (Section 2.5.2). The certainty for each parameter is represented by the standard deviation of the marginal error (standard error). These values are not an absolute measure of the parameter uncertainty required for a fair comparison between solutions and, hence, do not allow for the unbiased optimisation of the modelling time interval, e.g., there is relatively less certainty in a K-parameter of  $5 \pm 1$  in comparison to a K-parameter of  $50 \pm 1$ . The comparison of absolute parameter certainties for different intervals is achieved by calculating the portion of marginal error with respect to absolute values. While this approach is applicable to the p-parameter and K-parameter, the c-parameter is ideally zero to avoid interdependency with the p-parameter. As uncertainty may be associated with a zero c-parameter, the use of a simple percentage is not suitable. The modified value tends to infinity as the c-parameter approaches zero and is undefined when the c-parameter is zero, i.e.,  $\lim_{c \rightarrow 0} (\frac{c\sigma}{c}) = \infty$ . It is important to consider the complexity of the method used to adjust parameter certainties to an absolute measure. For an increasingly complex method of adjustment, the ambiguity of interpretation increases and the introduction of additional assumptions are also required. Additional information is not gained as high standard errors in the p-parameter and K-parameter will be accompanied by high uncertainty in the c-parameter.

The certainty in MOL parameters is represented by the average of the portion of p-parameter and K-parameter standard error (**Equation 18**).

$$SE_{pK} = \frac{1}{2} \left( \frac{\sigma p}{p} + \frac{\sigma K}{K} \right) \quad \text{Equation 18}$$

Where,

$SE_{pK}$ : Average portion of p – parameter and K – parameter standard error

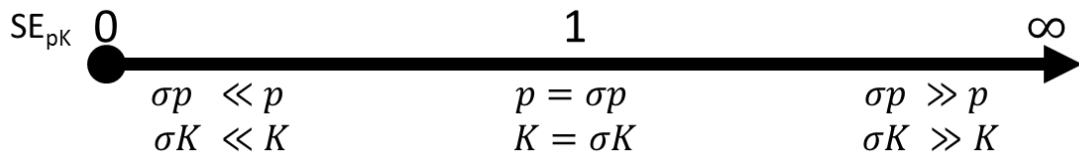
$\sigma p$ : Standard error of the p – parameter

$p$ : p – parameter

$\sigma K$ : Standard error of the K – parameter

$K$ : K – parameter

The measure capturing the average standard error will be small if standard errors are greatly less than parameter values, equal to one if standard errors and parameter values are equivalent, and approach infinity the greater standard errors (Figure 109).



**Figure 109** The relationship between standard errors and parameters with respect to  $SE_{pK}$ .

In addition to maximising the certainty of MOL parameters, the suitability of an interval also depends on the MOL achieving a statistically significant representation of a seismic response. The suitability of model fit is assessed by the Anderson-Darling statistic (Section 2.5.3) and is accompanied by guidelines relating the quality of fit and numerical values, e.g., 0: Perfect Fit, 1: Well Fit, and 2: Acceptable Fit.

### 5.6.2 Weighting of Parametric and Statistical Measures

The c-parameter, average portion of standard error, and Anderson-Darling statistic provide three measures that form the basis for the selection of an optimal modelling interval. An interval is optimised as these three measures approach zero, although, the parametric and statistical measures are relative and do not capture additional information concerning the acceptable range of parameter values, e.g., while a relatively smaller Anderson-Darling statistic is preferable, a response is not suitably modelled by the MOL if the statistic is still large.

Relative measures do not place emphasis on ideal solutions, limit poor solutions, or provide scaling within a range of marginal parameter values. As a result, solutions with low parameter values may be refined at the expense of other parameters despite both solutions representing a well-modelled interval, e.g., if the Anderson-Darling statistic is low for one solution, a solution with a slightly increased Anderson-Darling statistic is preferable if other parameters can be significantly improved. Additionally, if the parameter remains outside of reasonable value ranges then a relative reduction is not significant and the interval should be optimised using parameters within meaningful ranges. For these reasons, low parameter values are given a constant high weighting and vice versa. For parameters that are between optimally low and unreasonably high values, weightings are required to be proportional to the improvements to parameter values.

Absolute additional information associated with each relative parametric and statistical measure can be incorporated into the optimisation procedure by undergoing a piecewise transformation. A number of suitable transformations exist that can be applied to parameter values to achieve weighting objectives, e.g., logistic function. A continuous piecewise linear function is applied due to its simplicity in construction, application, and interpretation. Upper and lower limits for parameters and weightings are defined as two points  $[P_L, W_U]$  and  $[P_U, W_L]$  in the piecewise weighting function. The weighting function is defined with respect to  $P_L$ ,  $P_U$ ,  $W_L$ , and  $W_U$  in **Equation 19** and illustrated in Figure 110.

$$f(P) = \begin{cases} W_U & \text{for } P < P_L \\ \frac{W_U - W_L}{P_U - P_L} (P_L - P) + W_U & \text{for } P_L \leq P \leq P_U \\ W_L & \text{for } P > P_U \end{cases} \quad \text{Equation 19}$$

Where,

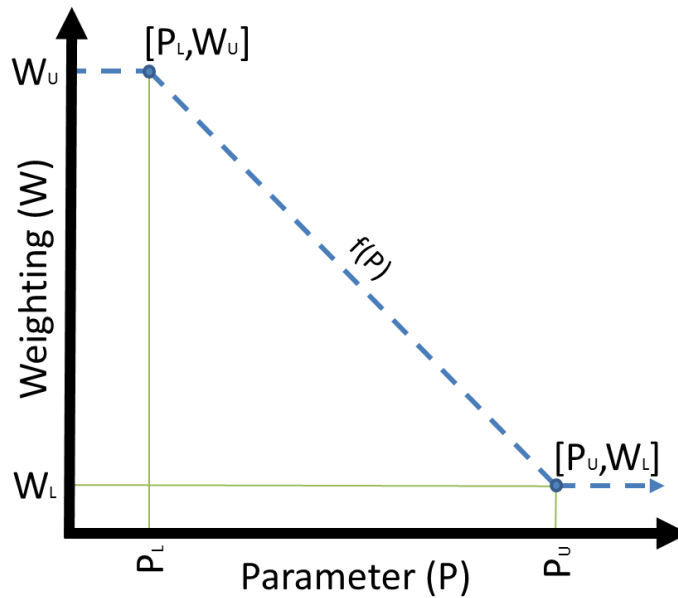
$f(P)$ : Piecewise linear parameter weighting function

$P_L$ : Lower parameter limit

$P_U$ : Upper parameter limit

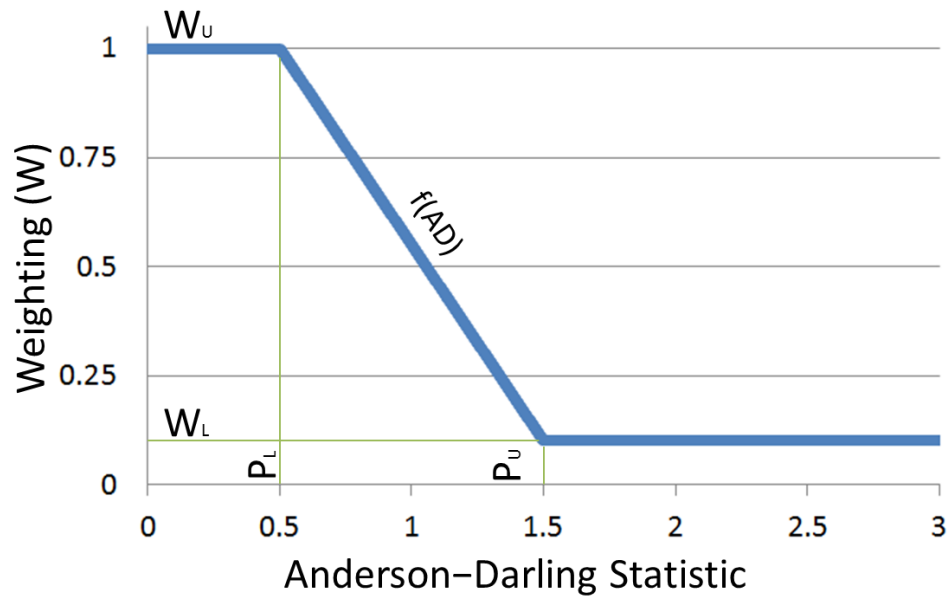
$W_L$ : Lower weighting limit

$W_U$ : Upper weighting value



**Figure 110** A graph of the piecewise linear weighting function that transforms parameters (x-axis) to weighting values (y-axis).

**Figure 111** provides an example of the piecewise linear weighting function applied to the Anderson-Darling statistic. This function is defined by the parameters  $P_L=0.5$ ,  $P_U=1.5$ ,  $W_L=0.1$ , and  $W_U=1$ . Parameter values below 0.5 are weighted equally as 1, values between 0.5 and 1.5 are assigned weightings linearly and inversely proportional to parameter values, and Anderson-Darling statistics above 1.5 are weighted equally as 0.1.



**Figure 111** The piecewise linear weighting function applied to the Anderson-Darling statistic.

Typical weighting values for the c-parameter, average standard error, and Anderson-Darling statistic (AD) are provided in **Table 21**. Weighting values are constrained between  $0.001(W_L)$  and  $1(W_U)$  in the decision metric. The use of a non-zero lower bound ensures that a solution may still be optimal even if one weighting is not ideal, and the use of an upper bound of one causes all optimal weights to be equivalent.

**Table 21** Typical piecewise weighting function values used for the weighting of parametric and statistical measures.

Weighted Parameter		$P_L$	$P_U$	$W_L$	$W_U$
Standard error	$SE_W$	10%	100%	0.001	1
Anderson-Darling statistic	$AD_W$	0.5	2	0.001	1
c-parameter	$c_W$	0	0.1 h	0.001	1

A holistic decision metric must consider delineation objectives along with the weighting factors used to optimise the quality of the MOL modelling. In addition to the MLE, that historically is the basis for statistical modelling selection, the number of events within each modelling interval is also introduced to emphasise delineation objectives along with modelling outcomes. This prevents the number of modelled events being dramatically reduced for marginal benefits to the weighting of modelling parameters.

A decision metric can be constructed using a number of approaches. The ideal solution will exhibit high parameter weightings for all aspects of modelling ( $SE_w$ ,  $c_w$ , and  $AD_w$ ) in addition to having a large number of events ( $N_{Events}$ ) and MLE. A simple combination of parametric and statistical measures is desirable as it offers pragmatic benefits in construction, application, and interpretation. Additionally, the function that combines measures must heavily penalise a solution if one or more of the parametric and statistical measures are small. A simple function that captures this attribute of interval selection is a multiplicative function (**Equation 20**).

$$MLE_w = SE_w \times AD_w \times c_w \times N_{Events} \times MLE \quad \text{Equation 20}$$

Where,

$MLE_w$ : Weighted maximum likelihood estimate metric

$SE_w$ : Standard error weight

$AD_w$ : Anderson – Darling weight

$c_w$ :  $c$  – parameter weight

$N_{Events}$ : Number of events within the modelling interval

$MLE$ : Maximum likelihood estimate

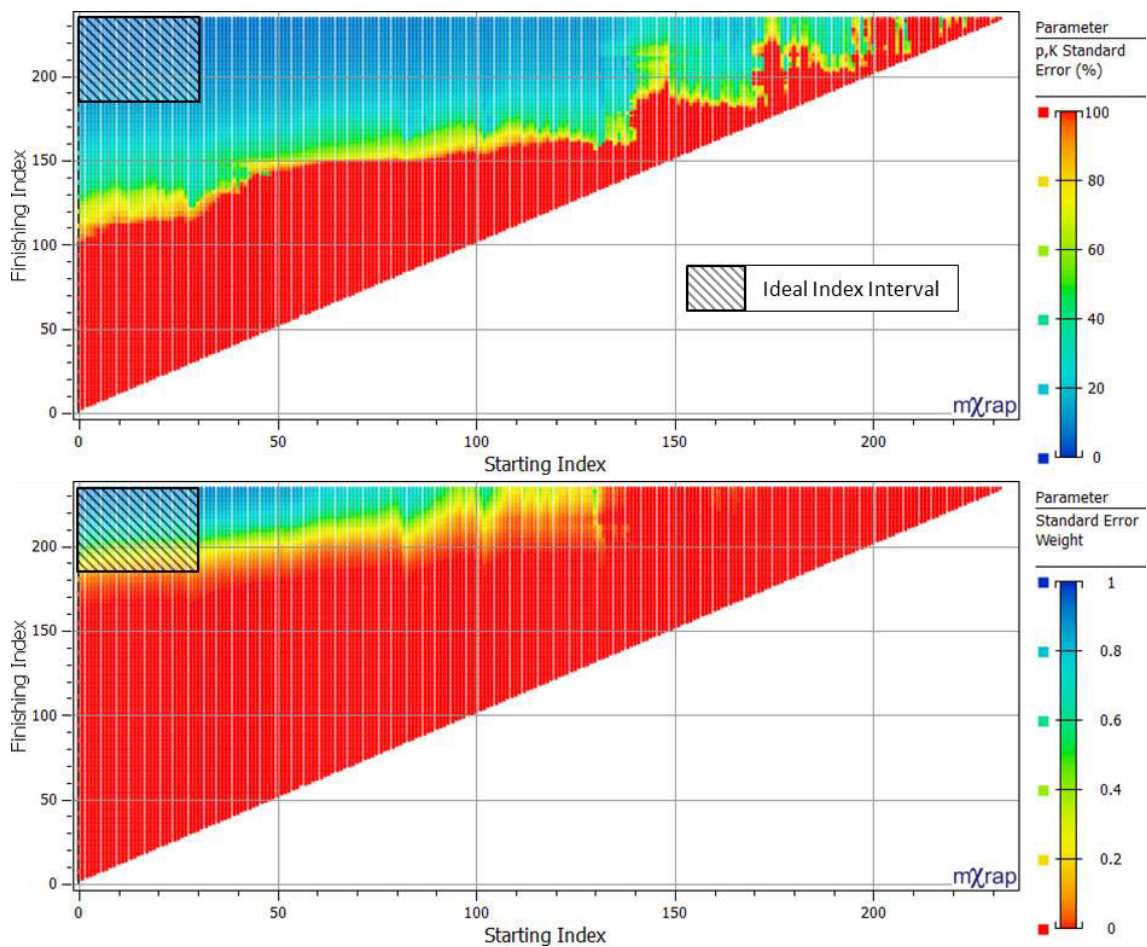
## 5.7 Evaluation of the Weighted MLE Metric

The application of the weighted MLE metric is examined within the context of the responses presented in Section 5.5. The same four seismic response scenarios are reassessed with respect to ideal index intervals along with the modelling weightings ( $SE_w$ ,  $c_w$ , and  $AD_w$ ). The delineation of responses and recovery of synthetic parameters is evaluated with respect to the optimal modelling interval found by the optimal weighted MLE metric and compared to the optimal MLE solution. The analysis uses the solution spaces introduced in Section 5.5.

### 5.7.1 Simple Seismic Response

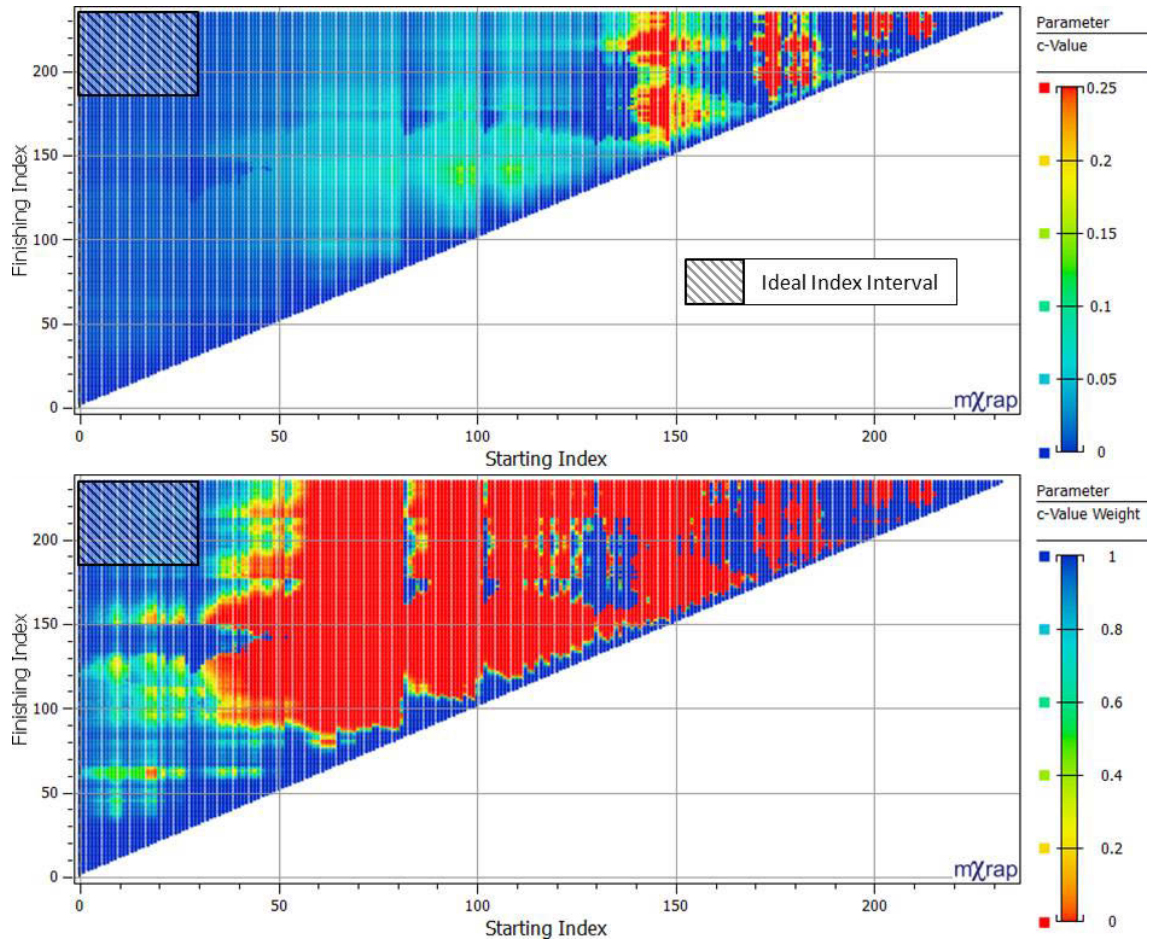
This application examines a simple response randomly sampled from the MOL (Section 5.5.1).

**Figure 112** shows solution spaces for the standard error (top) and the parameter weighted by the piecewise function (bottom). The weighting function does not drastically alter the average standard error, although, it does limit possible solutions. The weight improves the contrast between optimal and suboptimal solutions and closely corresponds to the ideal event index.



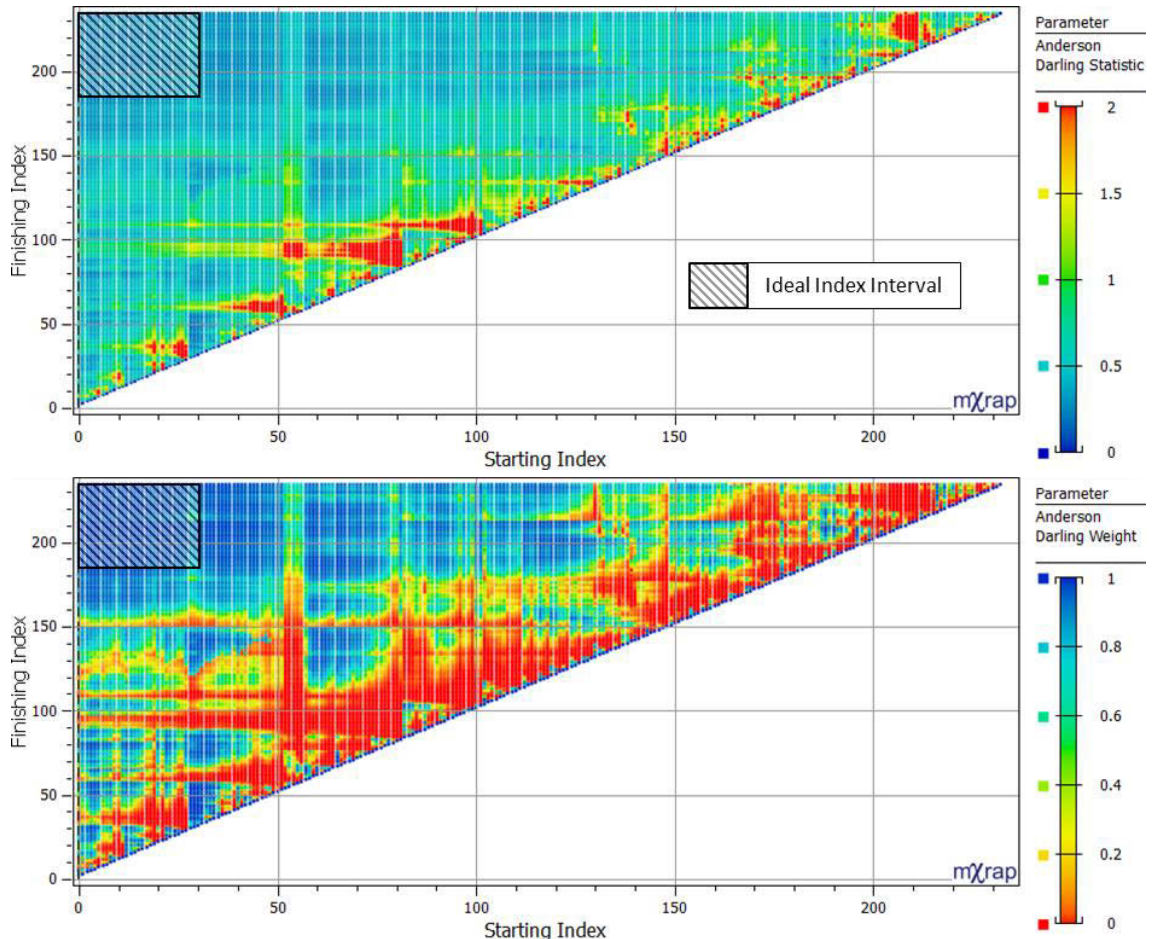
**Figure 112** The solution spaces for the average standard error (top) and the weighted parameter (bottom). The weighted solution space improves the contrast between solutions and corresponds more closely to the ideal event index.

**Figure 113** displays the c-parameter solution space (top) and weighted solutions (bottom). Solutions with an optimally weighted c-parameter capture the majority of the responses, despite high weightings also being observed in other regions. Weightings also improve the contrast between optimal and suboptimal c-parameters and shows that the ideal solution space contains very few modelling intervals with large c-parameters.



**Figure 113** Solution spaces for the c-parameter (top) and the weighted parameter (bottom). Weighting the parameter improves the contrast between better and worse solutions and limits reasonable solutions to the early intervals that capture the majority of the response.

**Figure 114** shows the Anderson-Darling statistic solution space (top) and the weighted parameter solution space (bottom). Similar to the c-parameter, weighting improves the contrast between better and worse solutions and shows that the ideal solution space contains intervals suitably modelled by the MOL. In addition to long responses that capture the majority of the events, there are also additional sporadic regions of low Anderson-Darling weights.



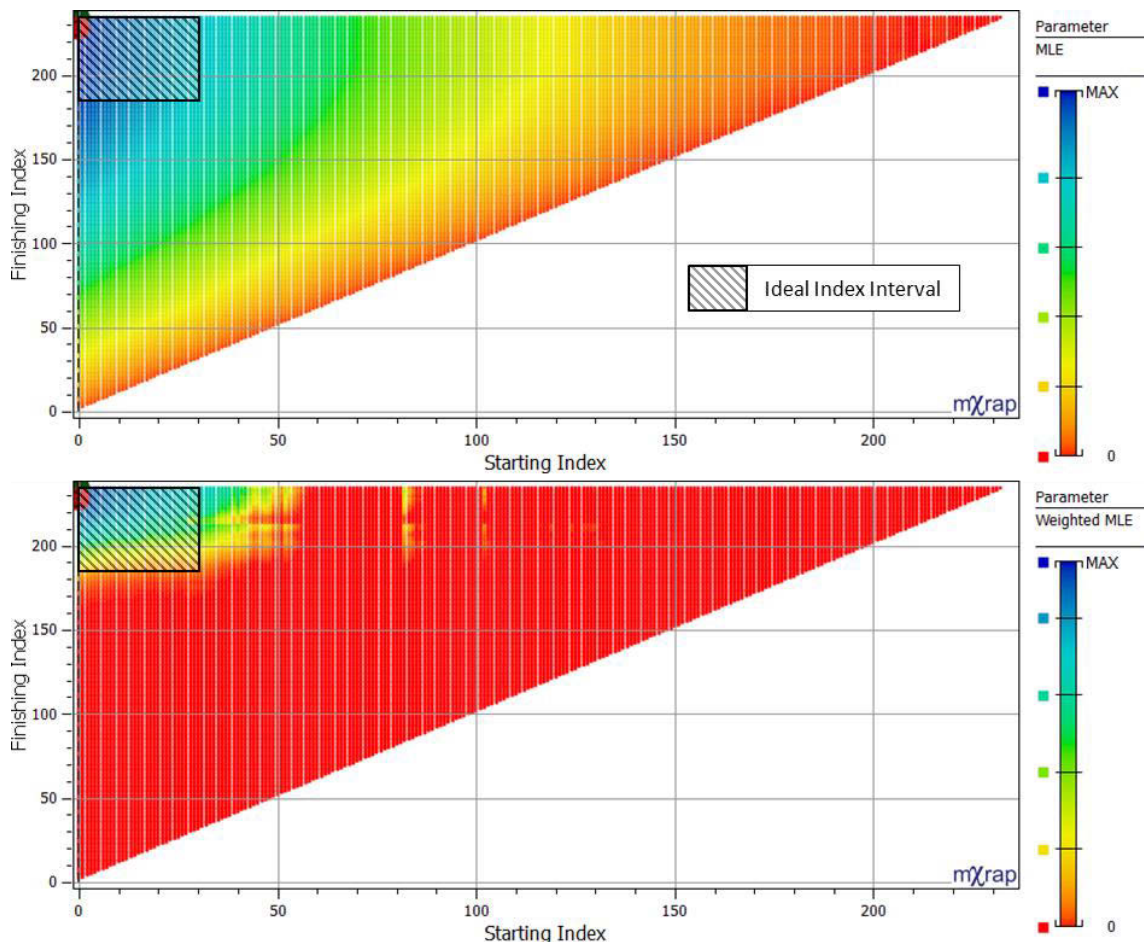
**Figure 114** Solution spaces for the Anderson-Darling statistic (top) and weighted parameter (bottom). Weighting identifies intervals that capture the majority of the responses and improves the contrast between better and worse solutions.

Modelling parameter weightings ( $SE_w$ ,  $c_w$ , and  $AD_w$ ) provide guidance for selecting a response within the ideal index interval that meets modelling quality objectives. Additional high weighting values for  $c_w$  and  $AD_w$  are sporadically distributed outside of ideal intervals. These solutions are penalised heavily by the multiplicative function if the other modelling parameter weightings are not also preferable. The role of modelling parameter weightings for this simple response is minimal as the MLE solution generally coincides with the weighted parameter and number of events. The parameters associated by the weighted and unweighted optimal solutions are similar to the synthetic values used to generate the response ( $p=1$ ,  $K=25$ , and  $c=0$ ) with low uncertainties, and an excellent suitability of fit (**Table 22**).

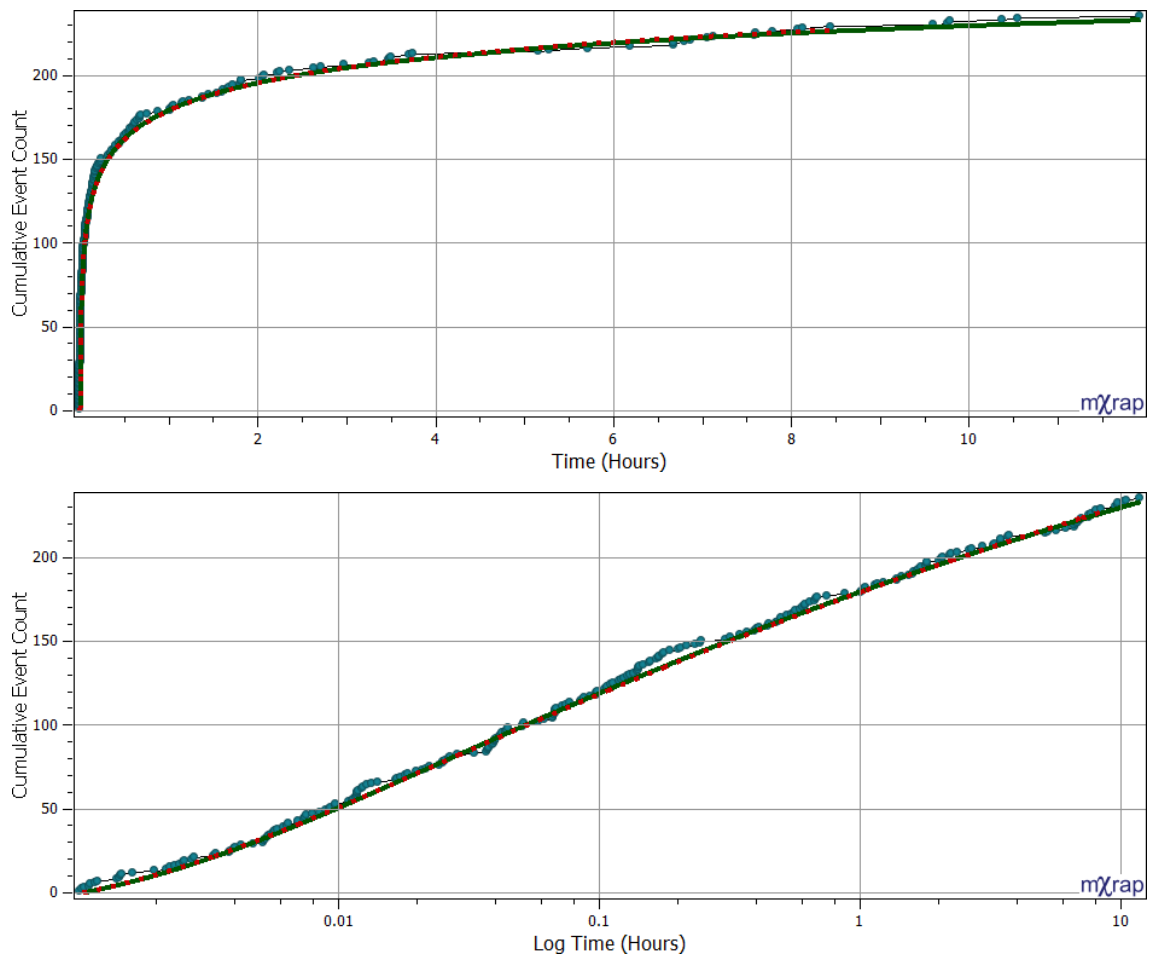
**Table 22** Starting and finishing indices along with MOL parameters and their standard errors found by the optimal MLE and weighted MLE solutions. Response parameters:  $p=1$ ,  $K=25$ , and  $c=0$ .

Solution	Start (i)	Finish (i)	p	p SE	K	K SE	c	c SE	AD
MLE	0	228	1.07	0.04	24.35	2.28	0.003	0.0011	0.3
Weighted MLE	0	234	1.08	0.04	23.99	2.12	0.003	0.0012	0.23

**Figure 115** shows the MLE solution space (top) and the weighted MLE solution space (bottom). The weighted maximum value (green dot) is not significantly different to the optimal unweighted solution (red dot) and both are found within the ideal event index. The solution space associated with the ideal index interval will have low standard errors, c-parameters, and Anderson-Darling statistics and, therefore, weight values close to or equal to one. Shown in **Figure 116** are the MOL solutions fitted to the time series of events. These charts show the cumulative event count over time (top) and log time (bottom) along with the MOL models for the weighted solution (green solid) and unweighted solution (red dash).



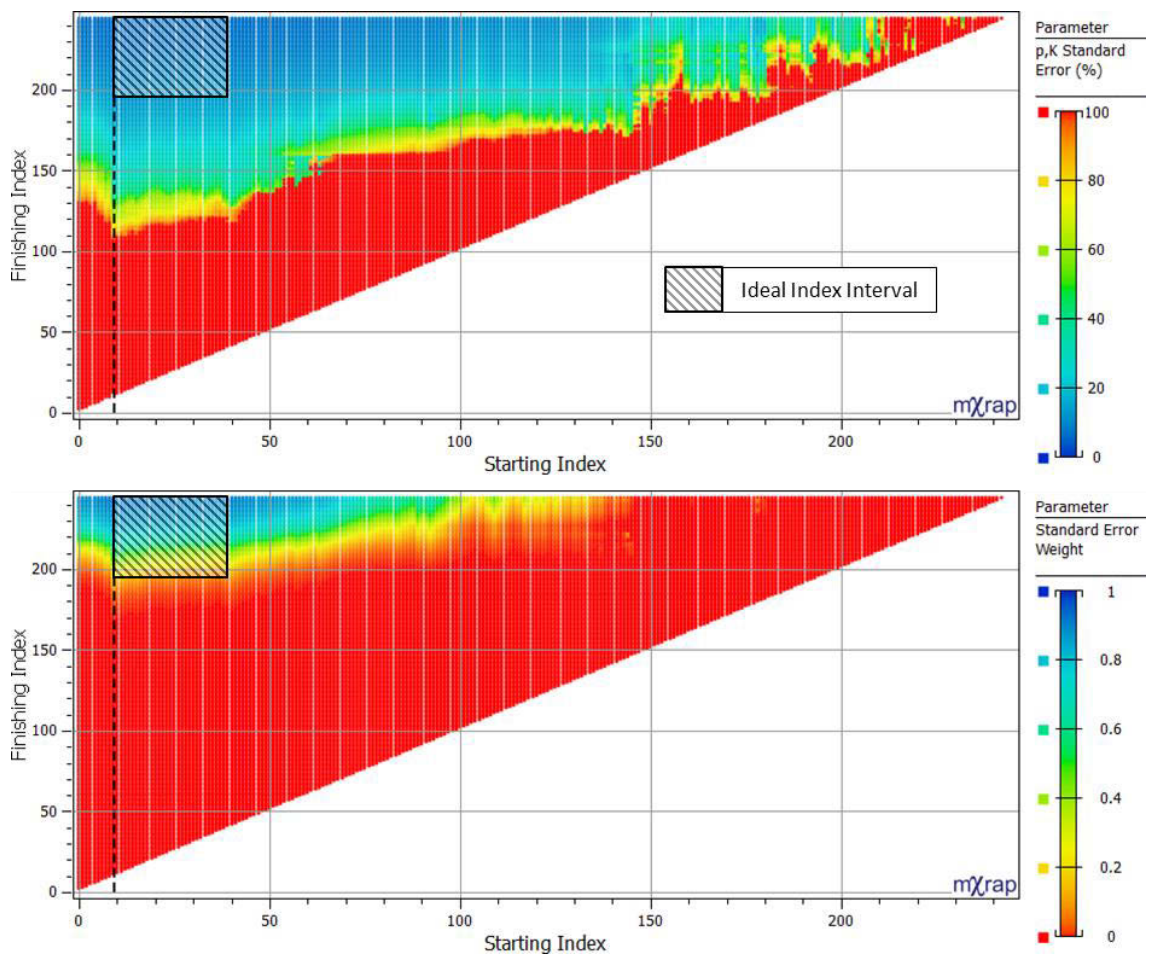
**Figure 115** The weighted MLE (bottom) is similar to the unweighted MLE solution space (top), although has been refined by considering measures of an optimal interval. The weighted maximum value (green dot) is not significantly different to the unweighted solution (red dot).



**Figure 116** Cumulative event count of a synthetic seismic response over time (top) and log time (bottom). The MOL solutions are plotted for the weighted (green solid) and unweighted (red dash) MLE solutions.

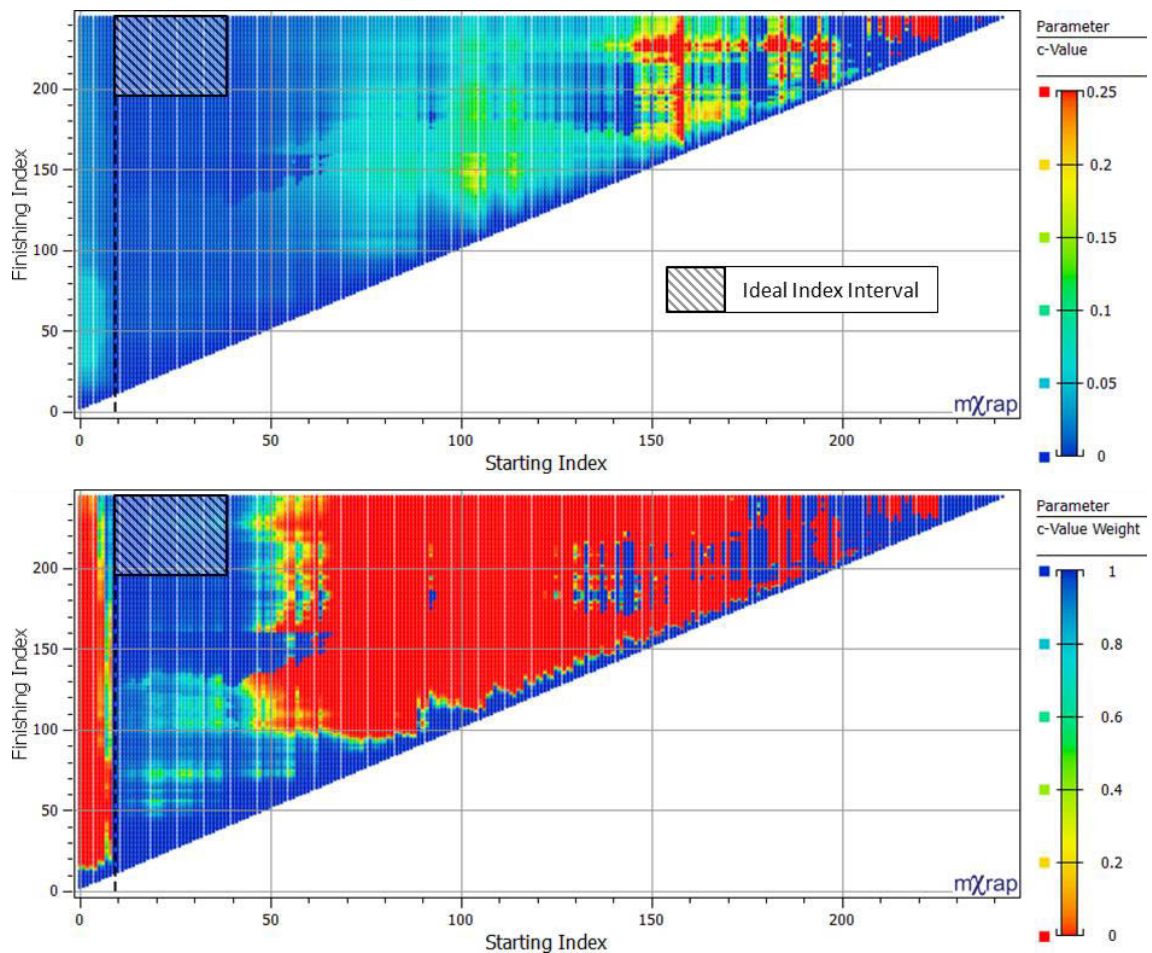
### 5.7.2 Seismic Response with Early Variation

A seismic response with early variation is generated using the same synthetic parameters as the previous example (Section 5.5.2). **Figure 117** shows the standard error solution space (top) and the weighting for this parameter (bottom) for this response. The weighting of this parameter reduces the appropriate solution space to a region approximately corresponding to the ideal index interval. The inclusion of early variation slightly reduces the weighting of late finishing indices, although, is not sufficient to influence the weighted MLE to ensure modelling intervals excludes early erroneous events.



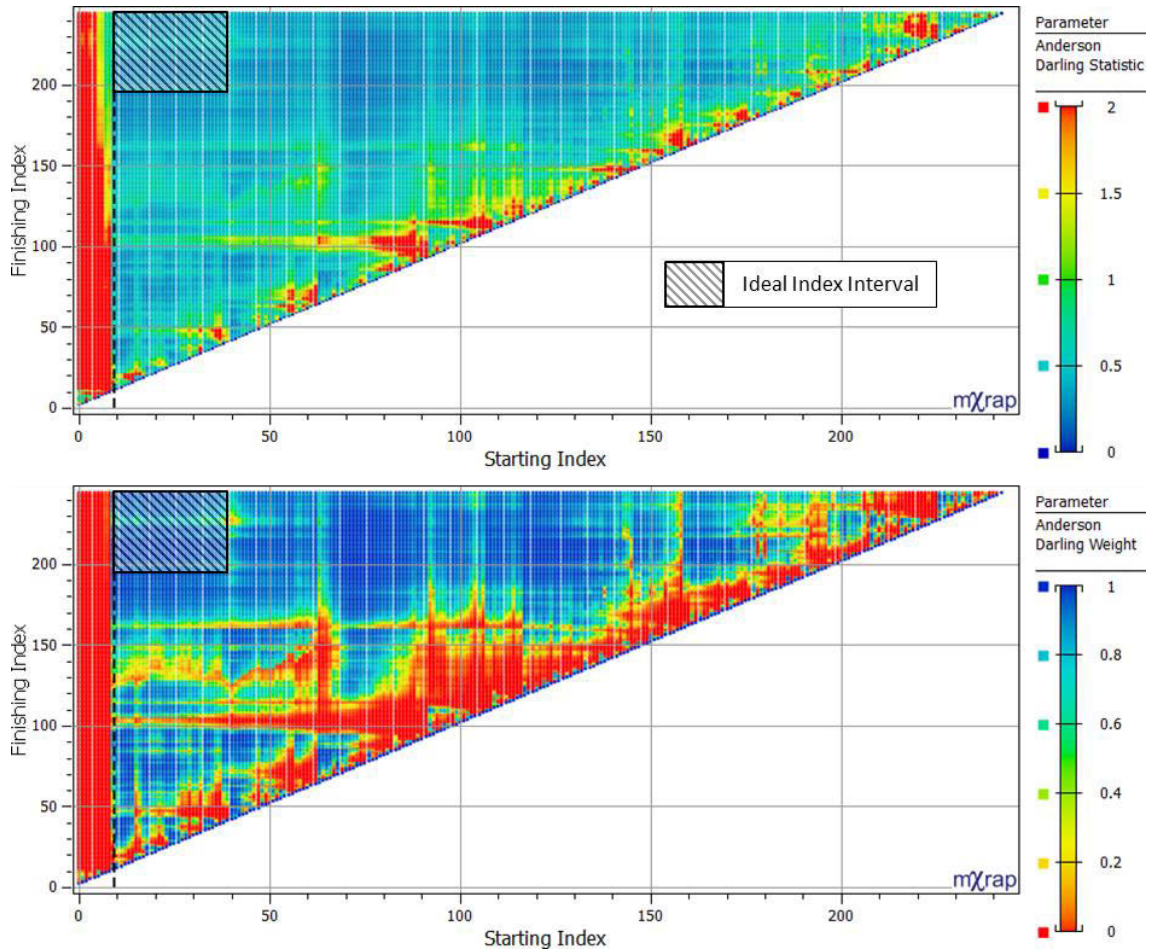
**Figure 117** The solution spaces for the standard error parameter (top) and weighted parameter (bottom). Early variation has a slight influence on the standard error weight solution space by reducing the range of appropriate finish indices.

**Figure 118** shows the c-parameter solution space (top) and the weighting for this parameter (bottom). The c-parameter weighting improves the contrast between values and favourably weighs the ideal index interval. In comparison to the standard error solution space (**Figure 117**), the c-parameter weighting clearly shows the influence of early variation. Modelling intervals that include variation events require higher c-parameters for modelling and result in low weighting values. The c-parameter weights are inconsistent for late starting and finishing indices that include early variation.



**Figure 118** Solution spaces for the c-parameter (top) and the weighted parameter (bottom). If the early variation is modelled, relatively higher c-parameters are required that result in low c-parameter weightings.

**Figure 119** shows the Anderson-Darling solution space (top) and the weighting for this parameter (bottom). While the weighted solution space improves the contrast between high and low values and favourably weighs the ideal index interval, the most beneficial aspect of this weight is that it reflects the non-conformity to the MOL when early variation is modelled.



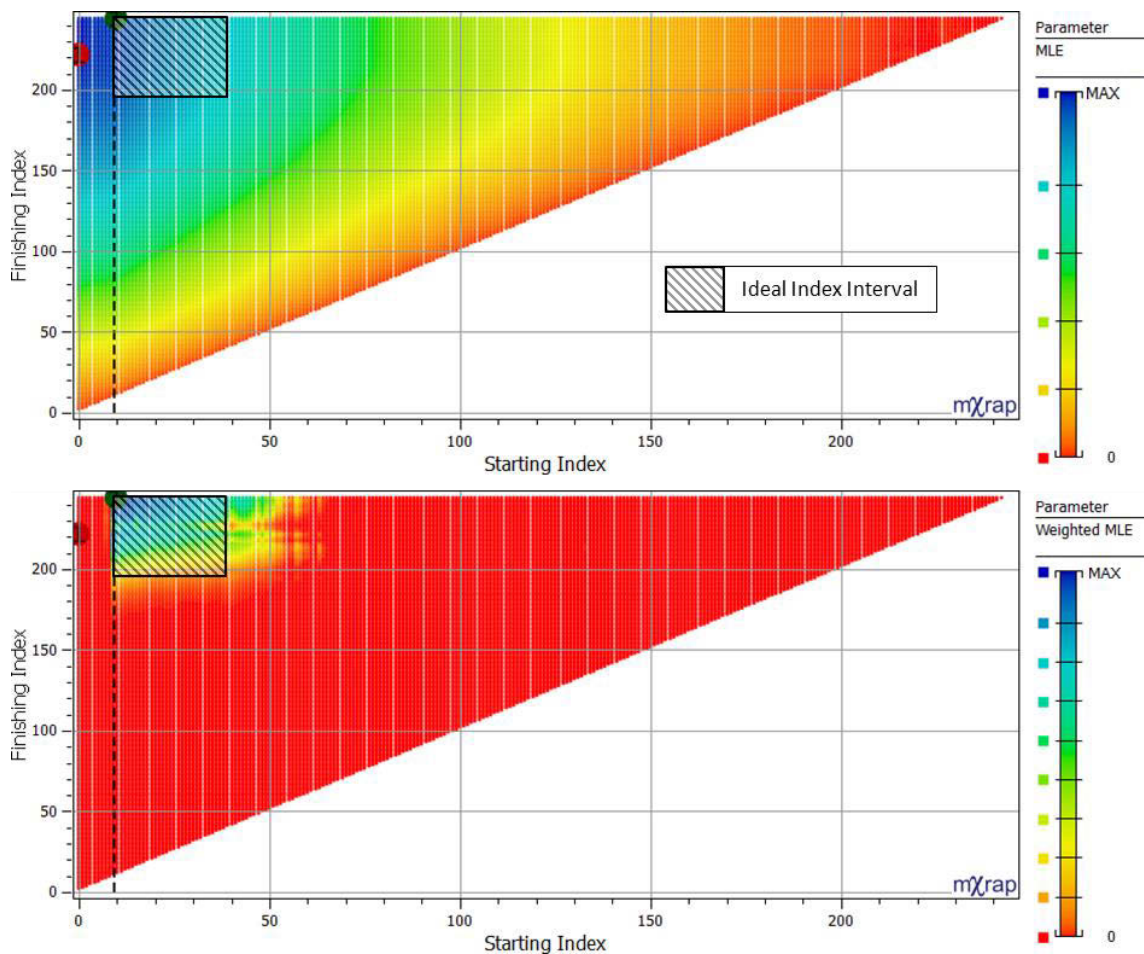
**Figure 119** Solution space for the Anderson-Darling statistic (top) and the weighted parameter (bottom). The Anderson-Darling weighting clearly reflects non-conformity to the MOL if the early variation is modelled.

The  $c_w$  and  $AD_w$  provide guidance in selecting a modelling interval that is within the ideal index interval, excludes early variation, and meets modelling quality objectives. While the  $SE_w$  modelling parameter does not assist with the exclusion of variation, it still contributes to selecting an ideal index interval that meets modelling objectives. The exclusion of early variation from the modelling interval has a significant influence on the MOL parameters recovered from the response. The MLE solution includes early variation and has a higher p-parameter, c-parameter, and Anderson-Darling statistic in comparison to the weighted MLE solution that excludes these events (**Table 23**). The MLE solution is only a marginally suitable model and is subject to the interdependency between the p-parameter and c-parameter.

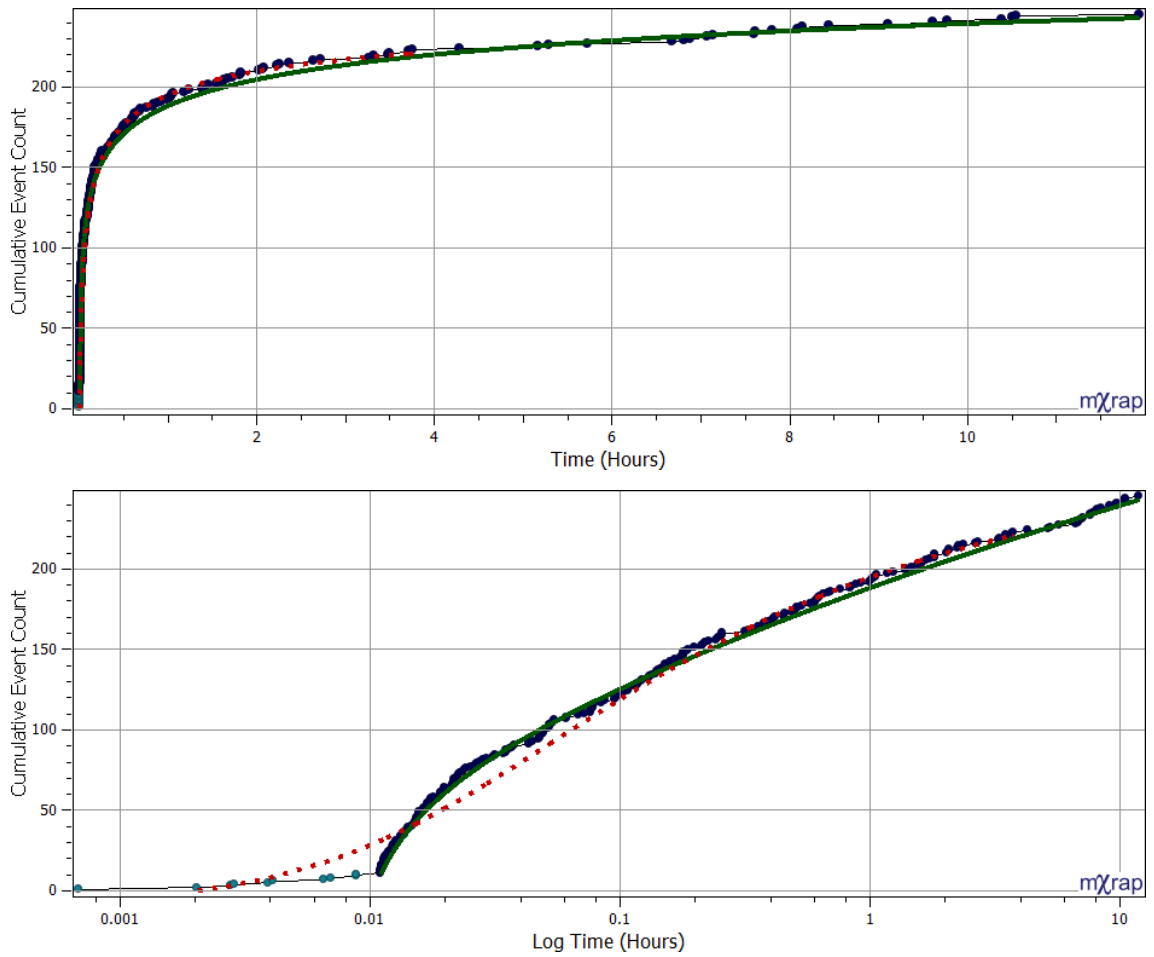
**Table 23** Starting and finishing indices along with MOL parameters and their standard errors found by the optimal MLE and weighted MLE solutions. Response parameters:  $p=1$ ,  $K=25$ , and  $c=0$ .

Solution	Start (i)	Finish (i)	p	p SE	k	K SE	c	c SE	AD
MLE	0	222	1.32	0.09	24.45	2.92	0.018	0.0069	2.12
Weighted MLE	10	244	1.08	0.04	24.13	2.12	0.0028	0.0011	0.27

Shown in **Figure 120** is the influence of weighting the MLE solution. Early variation has no obvious influence on the unweighted MLE (top). In contrast, the weighted solution penalises intervals that include these erroneous events. Weighting the MLE by  $N_{\text{Events}}$ ,  $SE_W$ ,  $c_W$ , and  $AD_W$  results in optimal solution spaces corresponding to the ideal event index. **Figure 121** shows a time series of events that have been modelled by the MLE (red dash) and weighted MLE (green solid). The MLE solution includes early variation and excludes the last eight hours of events. In comparison, the weighted solution excludes early variation and includes all later events. The weighted MLE clearly outperforms the unweighted solution by improved response delineation and parameter recovery.



**Figure 120** In contrast to the unweighted MLE solution space (top), the weighted MLE (bottom) considers additional measures of an optimal solution and excludes solutions that model early variation.

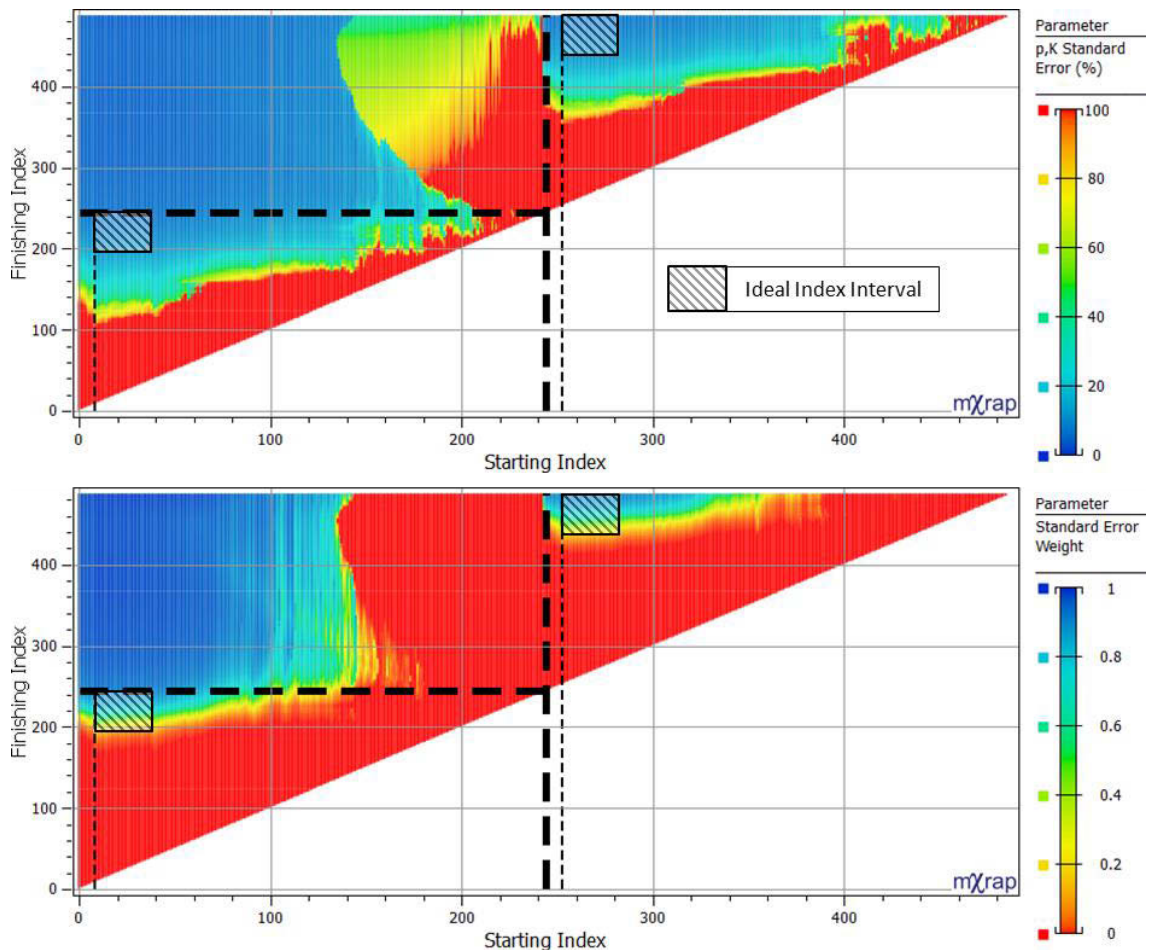


**Figure 121** Time series of the cumulative event count of a synthetic seismic response with early variation over time (top) and log time (bottom). The time interval modelled with the optimal weighted MLE excludes early variation and models the rest of the response. In comparison, the MLE solution includes the early variation and excludes the final eight hours of events.

### 5.7.3 Late Superimposed Responses

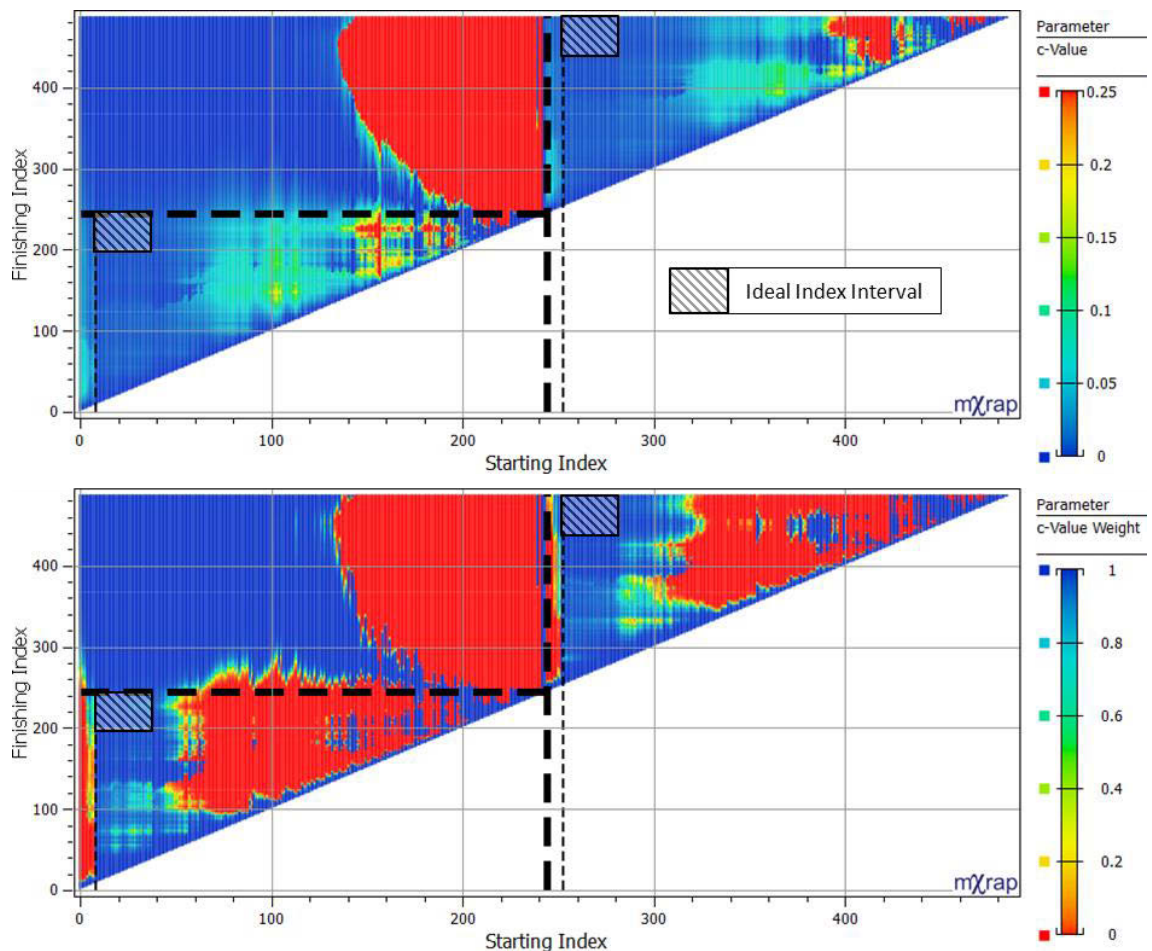
The late superimposed response scenario comprises of two seismic responses with early variation. The initiation of the second response is offset by 12 h. Two ideal index intervals are considered as the two seismic responses should be modelled separately.

**Figure 122** shows the standard error solution space (top) and the weighting for this parameter (bottom) for the complete time interval containing these two responses. These solution spaces display similar characteristics to a single response with early variation. In addition to the reduced preferable solutions associated with the ideal index interval, preferable standard error weightings can be achieved when the second response is modelled with the first response. As these solutions will positively weight erroneous modelling intervals, this characteristic of the solution spaces is not ideal. These intervals rely on the additional measures of modelling quality to reduce the weighting sufficiently to overcome relatively large values for the MLE and number of events associated with modelling both responses together.



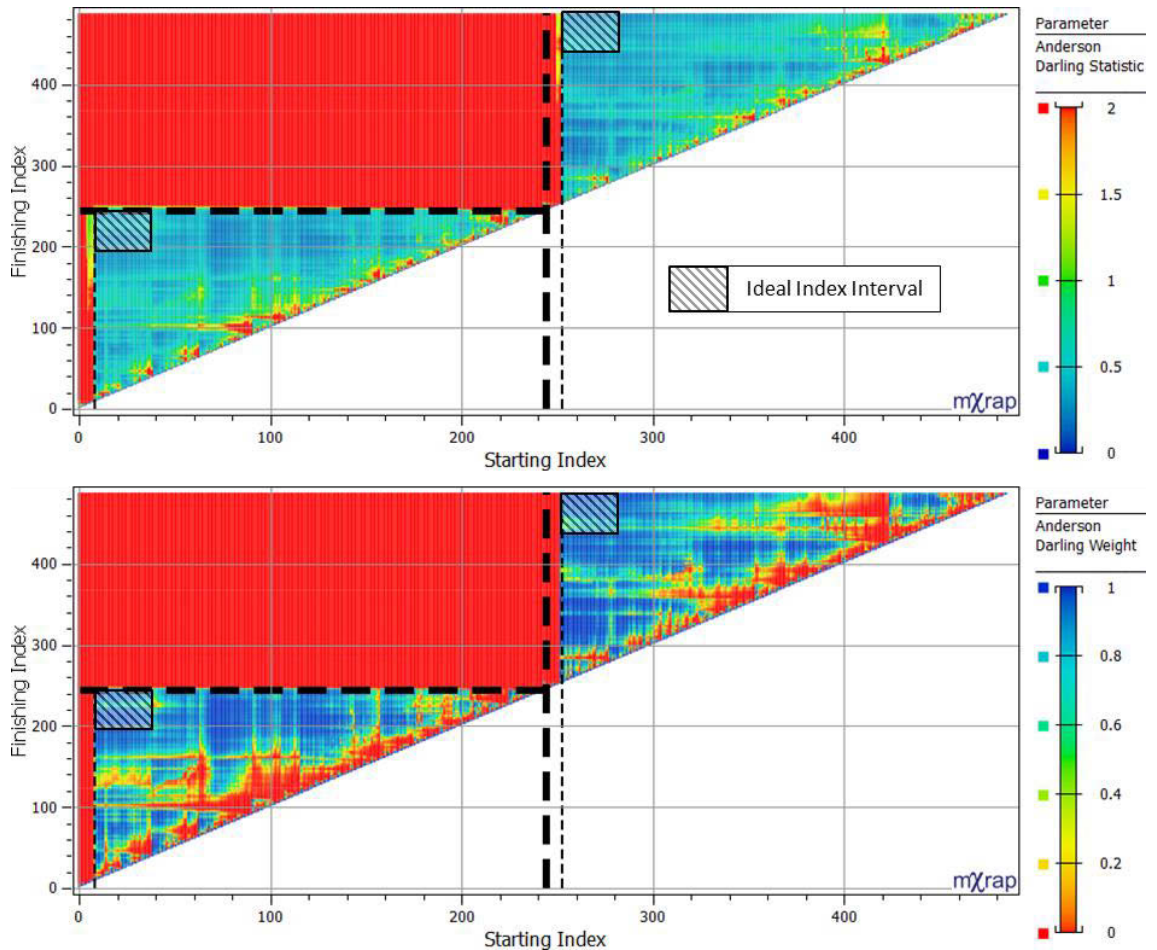
**Figure 122** Solution spaces for the standard error parameter (top) and the weighted parameter (bottom). Two regions of low standard errors capture appropriate responses. Modelling the first and second responses together also results in low parameters.

**Figure 123** shows the  $c$ -parameter solution space (top) and the weighting for this parameter (bottom). These solution spaces display similar characteristics to  $c$ -parameter solution spaces that model a single response with early variation. Similar to the weighting of standard errors, preferable weightings are found when the second response is modelled with the first response. These similarities increase the importance for the  $AD_w$  to reduce the weighted metric sufficiently in order to overcome relatively large values for the  $SE_w$ ,  $c_w$ , MLE, and the number of events associated with modelling both responses together.



**Figure 123** Solution spaces for the  $c$ -parameter (top) and weighted parameter (bottom). High  $c$ -parameter weightings are associated with the ideal index intervals and modelling the first and second responses together.

**Figure 124** displays the Anderson-Darling solution space (top) and the weighting for this parameter (bottom). The Anderson-Darling solution space and its weighted counterpart clearly indicate that long intervals, including the second response, are unsuitable to model with the MOL. The multiplicative weighting function ensures that these erroneous solutions are heavily penalised due to low Anderson-Darling weights, despite being relatively optimal in all other aspects. Both ideal index intervals are populated by high Anderson-Darling weights.



**Figure 124** The solution spaces for the Anderson-Darling statistic (top) and weighted parameters (bottom). Regions of highest Anderson-Darling weightings correspond to ideal index intervals despite some sporadically distributed low weightings.

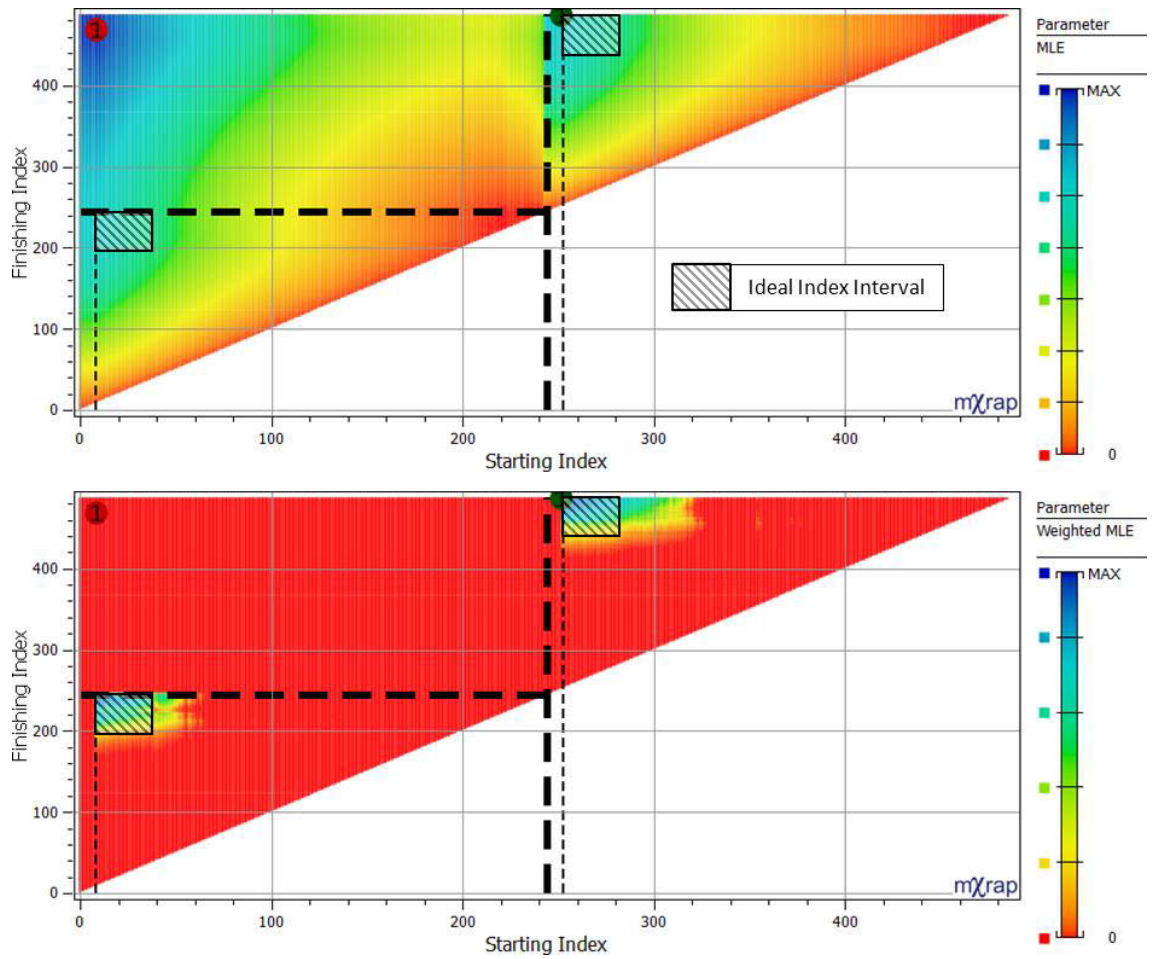
Section 5.5.3 showed that for late superimposed responses, parameters associated with solutions that modelled both responses together are not representative of individual responses. **Table 24** contains the parameters found for the MLE and weighted MLE solutions. The MLE solution models a significant portion of the second response despite excluding the early variation of the first response. The Anderson-Darling statistic indicates the solution is not suitable and that resultant parameters do not quantify the response adequately. The weighted MLE solution excludes early variations associated with the second response and recovers the synthetic parameters with reasonable accuracy.

**Table 24** Starting and finishing indices along with MOL and their standard errors found by the optimal MLE and weighted MLE solutions. Response parameters:  $p=1$ ,  $K=25$ , and  $c=0$ .

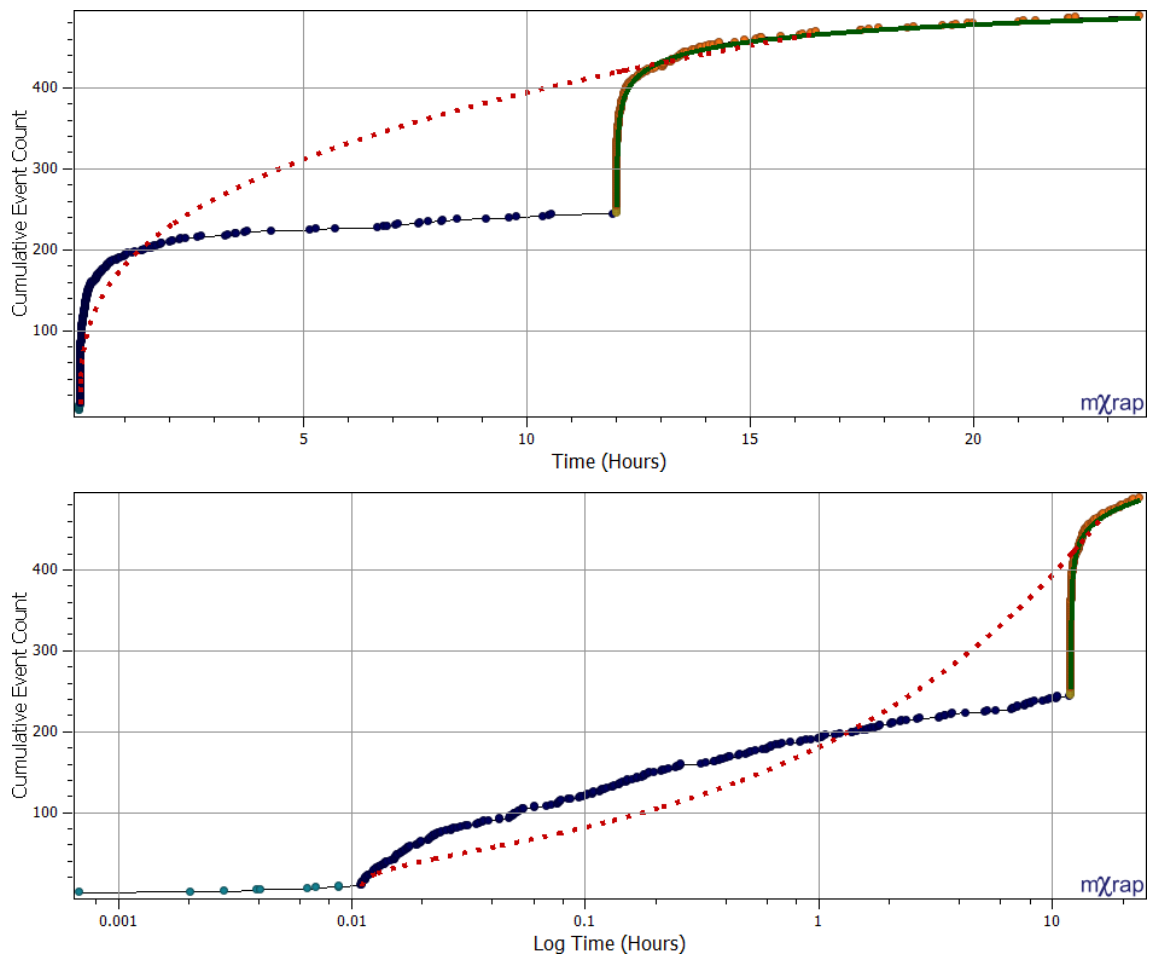
Solution	Start (i)	Finish (i)	p	p SE	K	K SE	c	c SE	AD
MLE	9	468	0.66	0.02	60.68	2.86	0	0	76.62
Weighted MLE	253	487	1.06	0.04	23.5	2.09	0.0018	0.0007	0.19

The two solution spaces that resulted in the optimal MLE (top) and weighted MLE (bottom) solutions being selected are shown in **Figure 125**. The contour in MLE shows some influence from the initiation of the second response. Modelling both of these responses within the same interval results in an improvement to the MLE and, therefore, the optimal MLE includes both responses (red dot). These responses cannot be adequately modelled solely by considering the MLE and would typically require consideration to alternative models. Additionally, modelling quality requires consideration to the suitability of modelling fit, which is not captured by parameter uncertainty or the c-parameter.

The weighted solution space (**Figure 125** bottom) limits the optimal solution spaces to the ideal index intervals. The weighted optimal solution will adequately model only one of the two responses (green dot). The unmodelled response will be captured during subsequent passes of the iterative approach to response identification (Section 5.8). **Figure 126** shows the capability of the weighted MLE solution (green solid) to identify an appropriate modelling interval that excludes early variation and models an entire response. The unweighted MLE (red dash) excludes early variation, although, the first response and a portion of the second response are included in the model.



**Figure 125** Solution spaces for the unweighted MLE (top) and weighted MLE metric (bottom). Weighting the MLE excludes intervals that model early variations, combine responses, and result in a significantly different optimal MLE (red dot) and weighted MLE solutions (green dot).

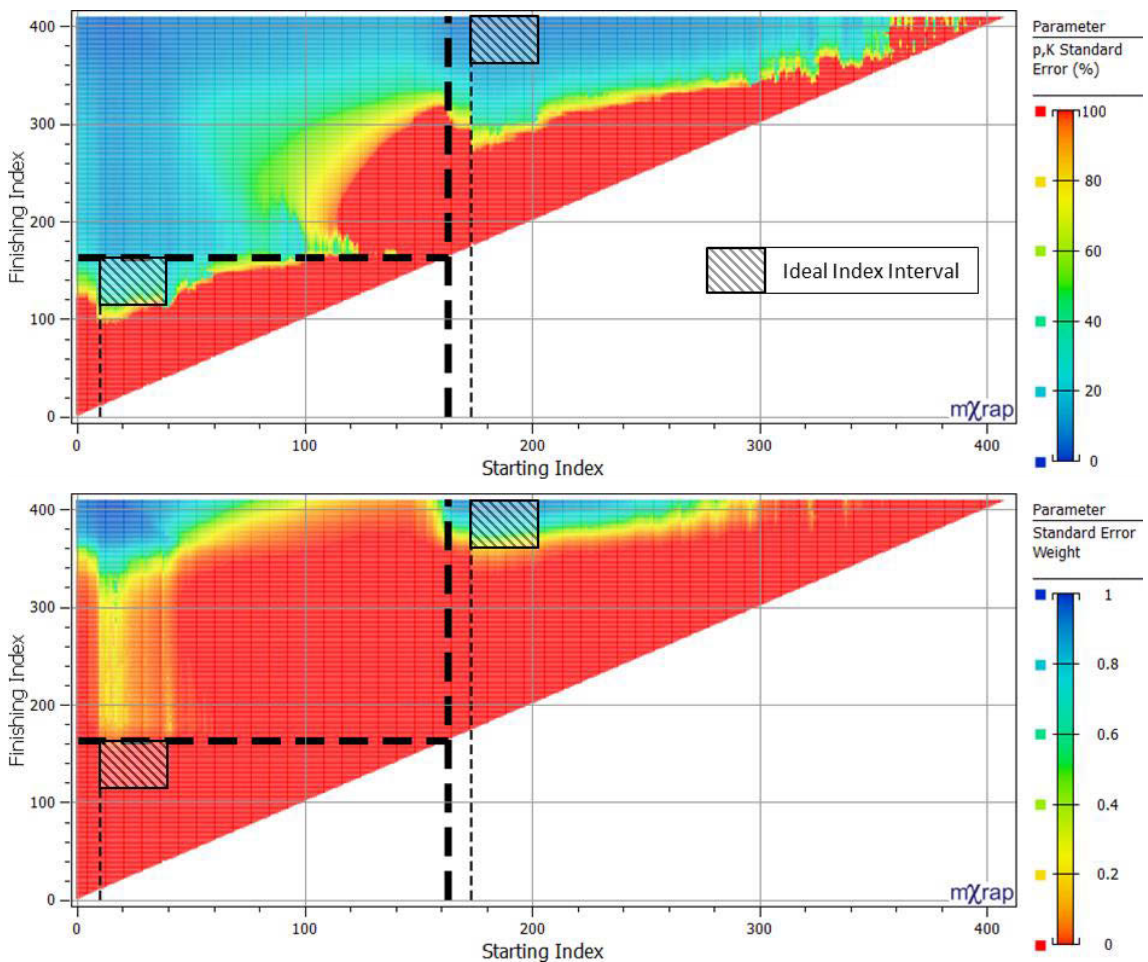


**Figure 126** Time series of two synthetic seismic responses and weighted (green solid) and unweighted (red dash) optimal MLE solutions. Shown is the cumulative event count over time (top) and log time (bottom). The second response is completely modelled with the optimal weighted MLE while the MLE solution is erroneous.

### 5.7.4 Early Superimposed Responses

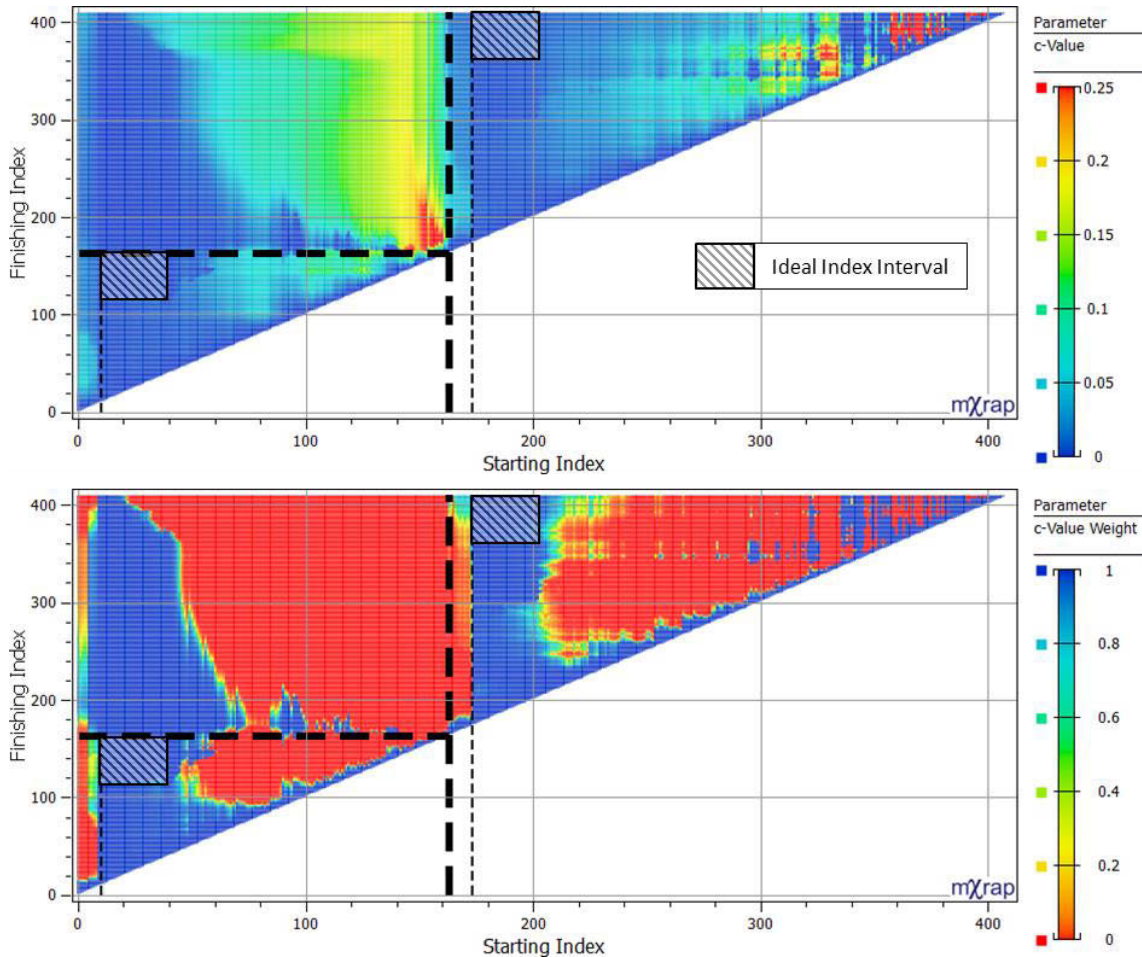
The early superimposed responses comprise of two seismic responses with early variation. The initiation of the second response is offset by 0.5 h. Delineation is more ambiguous in comparison to the late superimposition of responses. These two responses will ideally be modelled separately and this is represented by considering two ideal index intervals.

**Figure 127** shows the standard error solution space (top) and the weighting for this parameter (bottom). These results are congruent with the late superimposition of responses, with the exception that there is relatively high uncertainty in parameters associated with intervals that only model the first response. This is shown by the improved contrast provided by the standard error parameter weightings.



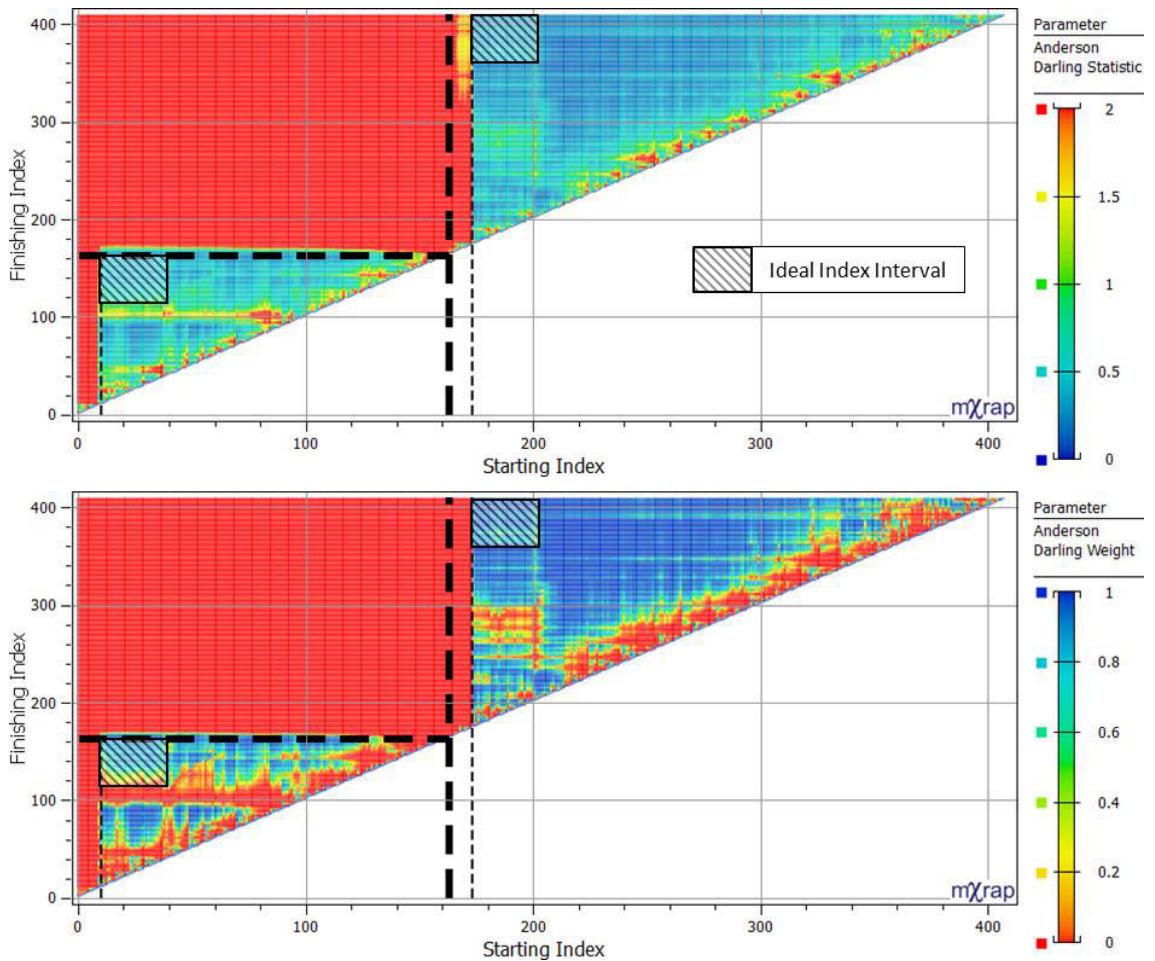
**Figure 127** Solution spaces for the unweighted (top) and weighted (bottom) standard error parameter. Low standard errors correspond to the ideal index interval of the second response. Low standard errors are also associated with modelling the first and second responses together.

**Figure 128** shows the c-parameter solution space (top) and the weighting for this parameter (bottom). These solution spaces are synonymous with the c-parameter weightings associated with the late superimposition of seismic responses. This parameter is influenced by event occurrence at early time intervals and, therefore, has little benefit in identifying time intervals that contain the early and late superimposition of responses.



**Figure 128** Solution spaces for unweighted (top) and weighted (bottom) c-parameter. Two regions of high c-weightings (low c-parameters) indicate appropriate modelling for intervals.

**Figure 129** displays the Anderson-Darling solution space (top) and the weighting for this parameter (bottom). Similar to the previously presented late superimposed responses, the Anderson-Darling statistic provides a clear indication of appropriate modelling intervals for early superimposed responses. Ideal index intervals are populated by comparatively high weighting values that contribute to the selection of an optimal temporal interval. This parameter assists in selecting optimal fits and contributes to reducing the weighting of unreasonable intervals.



**Figure 129** Parameter solution spaces for unweighted (top) and weighted (bottom) Anderson-Darling statistic. Regions of highest Anderson-Darling weightings correspond to ideal index intervals despite some sporadically distributed low weightings.

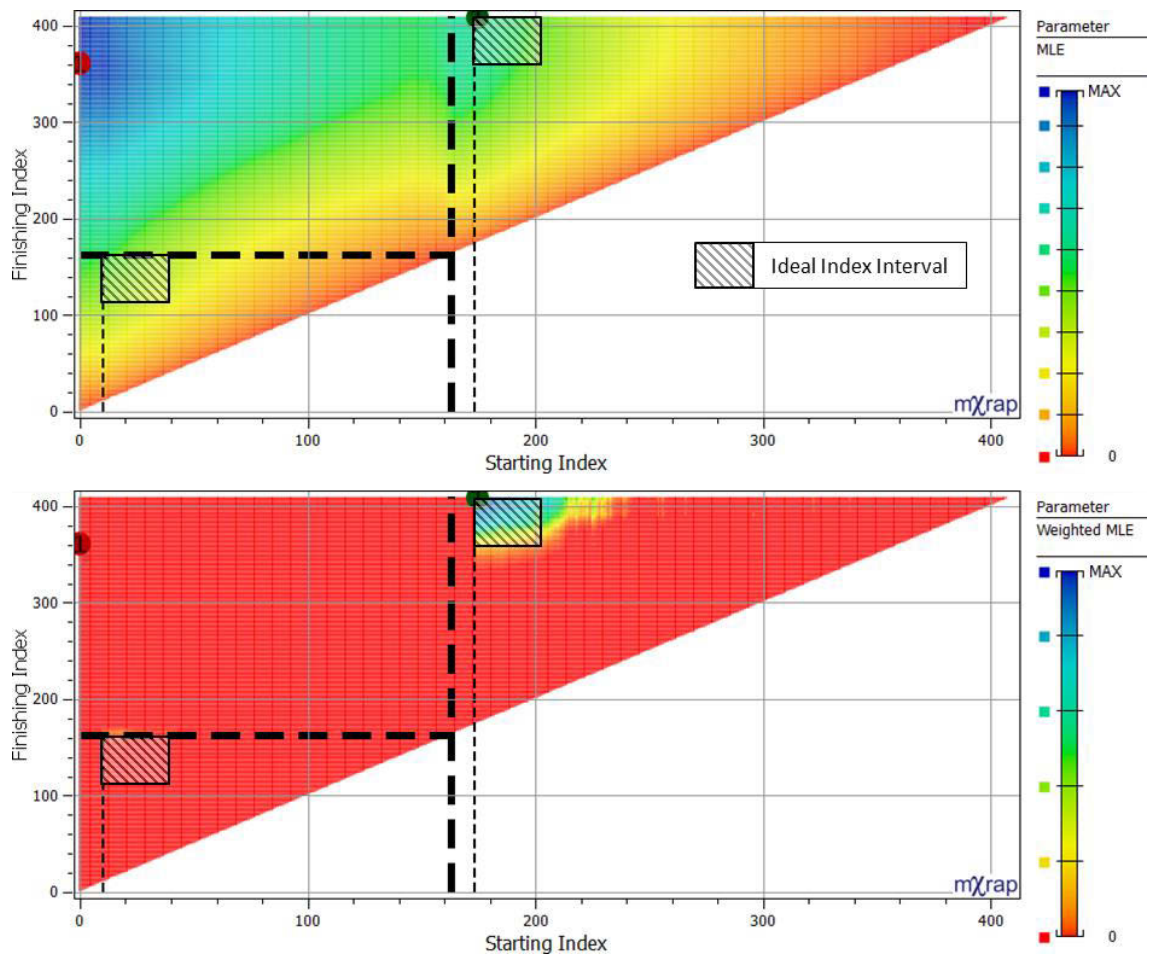
The MLE solution includes early variation and a significant portion of the second response. This is not a reasonable solution in terms of the parameters recovered or response delineated. In contrast, the weighted MLE solution delineates the second response and recovers synthetic parameters with reasonable accuracy (**Table 25**).

**Table 25** Starting and finishing indices along with MOL and their standard errors found by the optimal MLE and weighted MLE solutions. Response parameters:  $p=1$ ,  $K=25$ , and  $c=0$ .

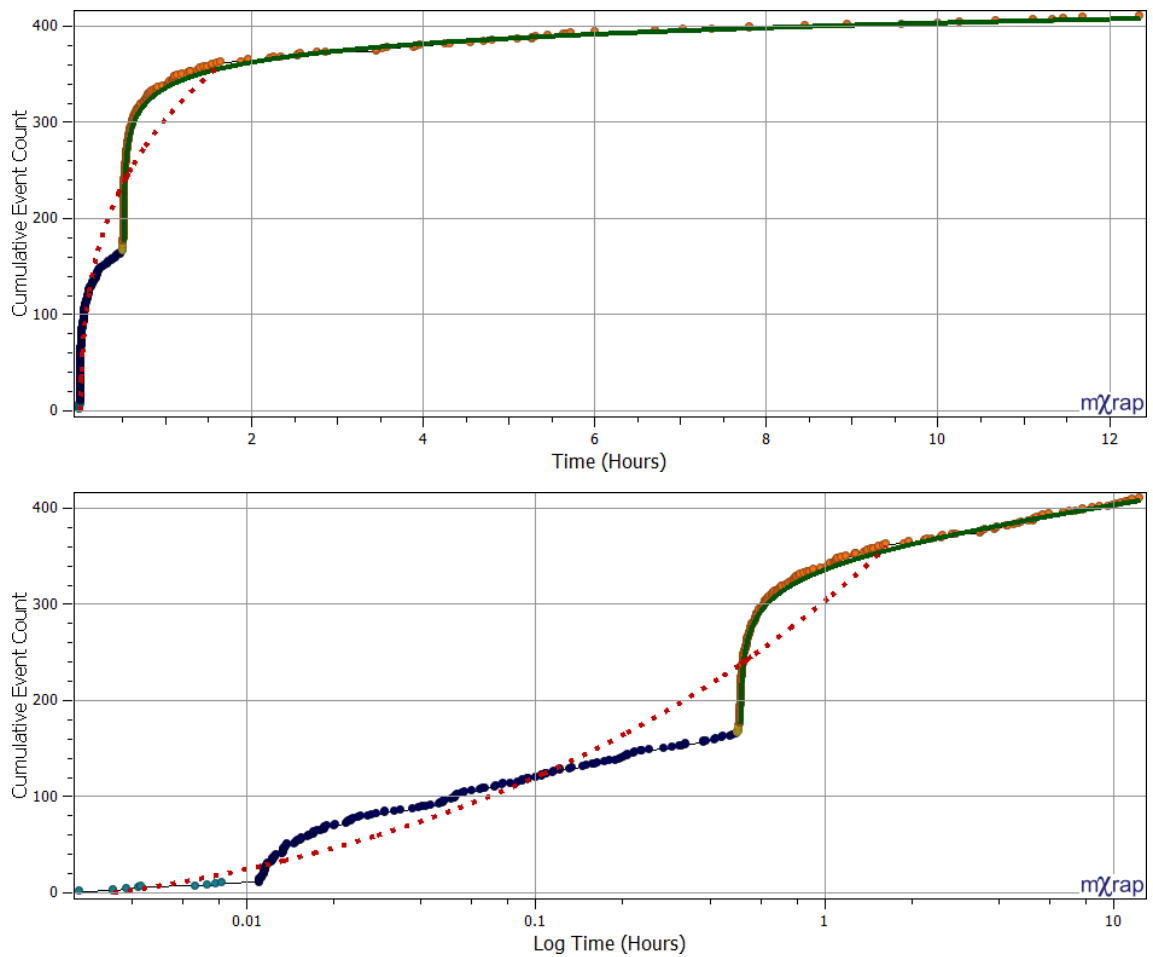
	Start(i)	Finish(i)	p	p SE	K	K SE	c	c SE	AD
MLE	0	361	0.73	0.06	106.88	8.74	0.004	0.0032	14.77
Weighted MLE	175	409	1.05	0.04	23.7	2.09	0.0018	0.0007	0.2

**Figure 130** shows the unweighted MLE solution space (top) and weighted MLE solution space (bottom). The optimal MLE solution (red dot) does not identify a reasonable time interval, while the weighted MLE solution (green dot) excludes early variation and completely models the second response. It is noteworthy that the weighted MLE solution space exhibits optimal values corresponding to the ideal index interval associated with the second response. There is not a corresponding preferable space associated with the first response. This is due to the first response containing fewer events and occurring over a shorter interval and, therefore, higher uncertainties are associated with modelling. Removal of the second response from consideration in subsequent iterations will cause the first response to become relatively preferable despite higher uncertainties.

**Figure 131** shows the weighted MLE solution (green solid) and the unweighted MLE solution (red dash) with respect to cumulative event count over time (top) and log time (bottom). These results are similar to the modelling time intervals found for late superimposed responses with the weighted solution excluding early variation and completely modelling the second response. The MLE solution erroneously includes early variation, the first response, and a portion of the second response in the modelling time interval.



**Figure 130** Solution spaces for the unweighted MLE (top) and weighted MLE (bottom). The MLE solution (red dot) combines early variation and responses, while the weighted MLE solution (green dot) excludes variation and delineates the second response.



**Figure 131** Shown is the cumulative event count over time (top) and log time (bottom) for the weighted (green solid) and unweighted (red dash) optimal MLE solutions. The second response is modelled with the optimal weighted MLE. In comparison, the MLE solution erroneously models early variation, the first response, and a significant portion of the second response.

## 5.8 Iterative Functionality of Temporal Modelling

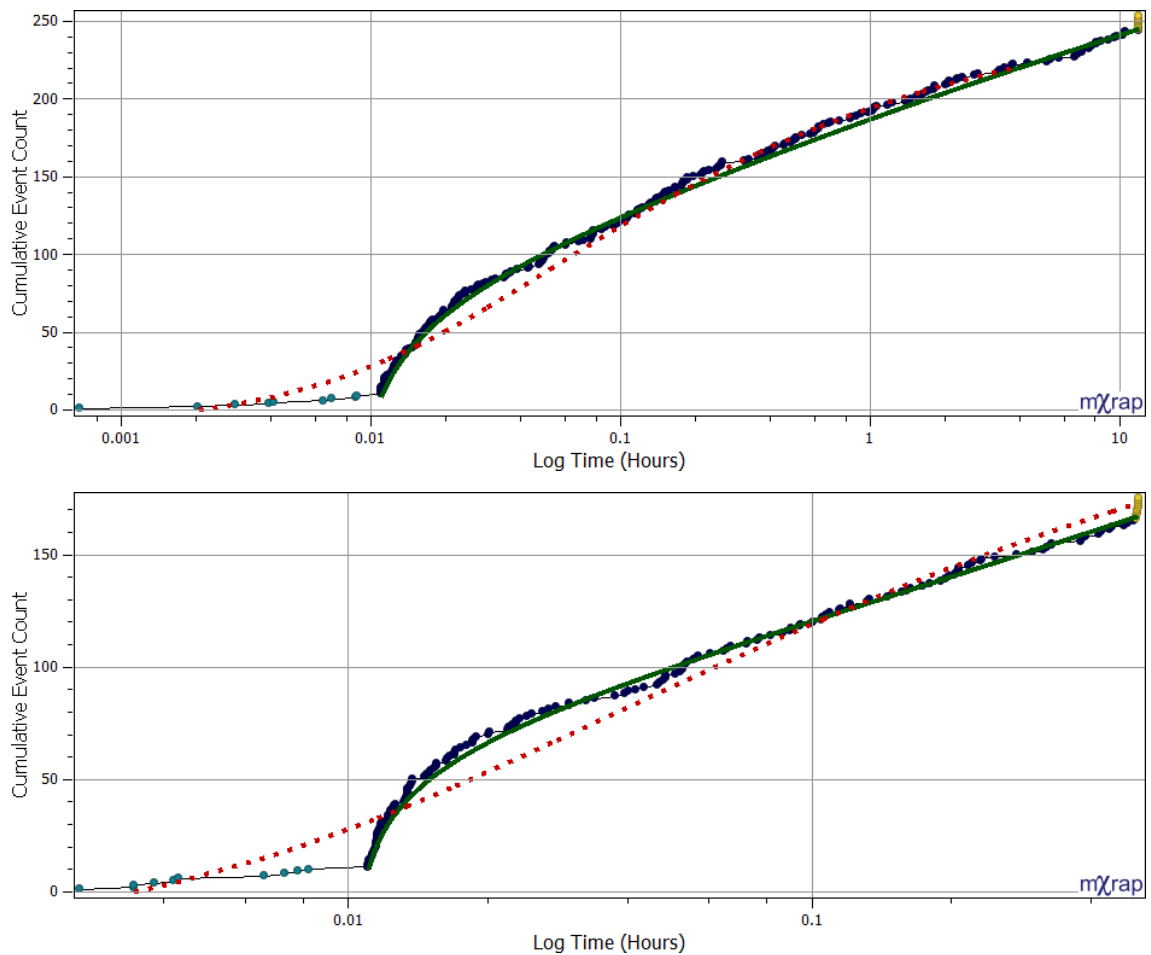
Temporal modelling plays a significant role in reducing the sensitivity of the identification and delineation of seismic responses (Temporal Window: Section 3.5.2 and Temporal Modelling Window: Section 3.5.4). The main features of temporal delineation aim to adjust misidentified responses by ensuring modelled intervals follow time-dependent behaviour and the refinement of an initially overestimated temporal modelling window by including only a single response. The application of the weighted MLE metric delineates the largest adequately modelled interval and meets the requirements for the iterative identification and delineation of seismic responses.

To illustrate the iterative functionality of using the weighted MLE metric approach for selecting a temporal modelling interval, analysis is reapplied to the late and early superimposed responses discussed in Section 5.7.3 and 5.7.4, respectively. The modelling intervals delineated by the initial application of the weighted MLE are removed from further consideration. The removal of seismic responses represents the seismic dataset after an initial iteration.

**Table 26** summarises the optimal weighted MLE solutions for the remainder of late and early superimposed responses. **Figure 132** shows the cumulative event count over log time for the reduced, late superimposed response (top) and early superimposed response (bottom). These solutions are plotted with respect to the weighted MLE solution (green solid) and the unweighted MLE solution (red dash). The second response contained within the solution is identified by both responses and is suitably modelled by the MOL. The parameters recovered by the delineation of the second late superimposed response are accurate. The parameters associated with the second, early superimposed response are less representative of the synthetic parameters used to generate the response. Decreased accuracy in the recovery of synthetic parameters associated with the shorter response (0.5 h) is expected due to the reduced certainty associated with a shorter modelling interval.

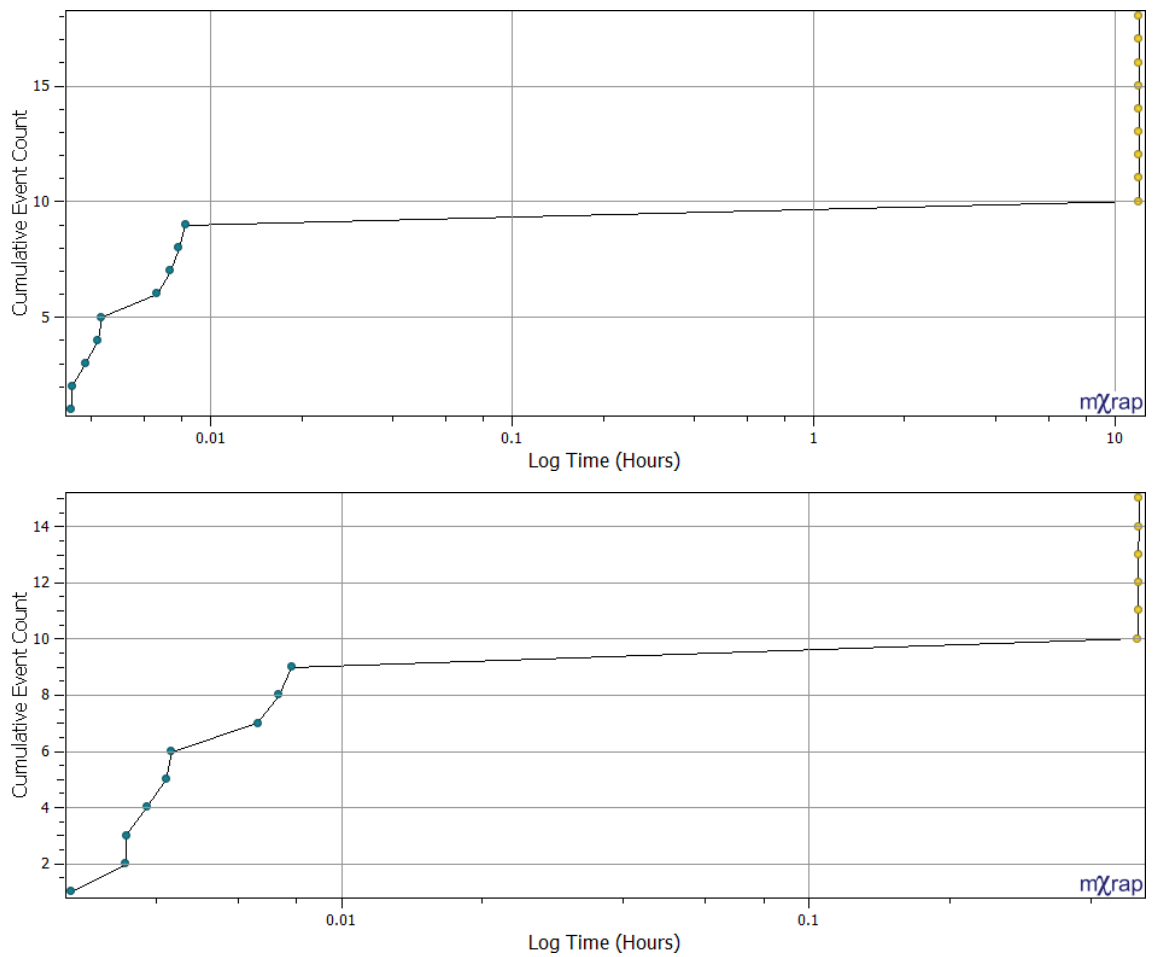
**Table 26** Starting and finishing indices along with MOL and their standard errors found by the optimal MLE and weighted MLE solutions. Response parameters:  $p=1$ ,  $K=25$ , and  $c=0$ .

Response	Start (i)	Finish (i)	p	p SE	K	K SE	c	c SE	AD
Late Superimposed	10	243	0.991	0.035	25.54	2.13	0.001	0.0005	0.53
Early Superimposed	10	168	0.940	0.07	30.04	6.52	0.0006	0.0004	0.48



**Figure 132** Time series of the cumulative event count over log time for the late superimposed response (top) and early superimposed response (bottom). Shown are the optimal weighted (green solid) and unweighted (red dash) MLE solutions.

**Figure 133** shows the remainder of the superimposed scenarios once the second responses are delineated and removed. These events consist of the variation remaining at the beginning of the late superimposed response (top) and early superimposed response (bottom). The two later superimposed responses have been accurately delineated from the early variation, although, a portion of the variation associated with the second response has been delineated with the first response for the early superimposed case. The tolerance of modelling to include these events reflects the inherent ambiguity of delineating the brief initial scenario. The choice of including versus excluding these events represents the trade-off between modelling quality and delineation that is controlled by the weighting metric. In this case, these events could be delineated with the response while not compromising modelling quality.



**Figure 133** The cumulative event count over log time for the remaining variation associated with the late superimposed response (top) and early superimposed response (bottom).

## 5.9 Performance Evaluation of Temporal Quantification and Delineation

### 5.9.1 Scope of Performance Evaluation

The reviewed literature provides guidance for the structural and parametric uncertainty associated with modelling mining induced seismic responses with the MOL (Section 2.5). A range of studies indicates that mining induced seismic responses are typically well modelled by the MOL by similar ranges of parameters. Confidence has been developed by reviewed literature that the MOL is applicable to mining induced seismicity and, therefore, the scope of performance evaluation and error analysis is able to focus on the uncertainty associated with temporal modelling. This section evaluates the error associated with temporal modelling by optimising the weighted MLE metric for a range of scenarios relevant to mining seismicity.

An additional consideration to modelling uncertainties are the inherent limitations of the seismic monitoring to observe seismicity, e.g., the capability to observe a range of event magnitudes and the ability to reliably identify and quantify seismic waveforms (Mendecki, van Aswegen & Mountfort 1999). These limitations manifest in the observed seismic data by characteristics such as the lowest magnitude that has been reliably observed by the seismic monitoring system (Section 2.2.1) and the need for the c-parameter in the MOL (Section 2.5.6). Given the inherent uncertainties concerning seismic monitoring and the stochastic nature of seismicity, there is a pragmatic limit to minimising temporal modelling errors.

Error analysis focuses on the accuracy and precision of the ability of temporal modelling to recover synthetic parameters used to generate seismic responses. See Appendix A: Generation of Synthetic Seismic Responses, for the general method used throughout this chapter. The accuracy of parameter recovery assesses how close parameters are to synthetic values while the precision of temporal modelling examines deviation of errors with respect to mean values. The accuracy and precision of temporal modelling is assessed with respect to epistemic (systematic) and aleatoric (random) errors associated with the generation of synthetic data and modelling procedures. The percentage error in the recovered parameters is quantified by the proportional difference between the synthetically generated parameter and the parameter found from modelling using the weighted MLE metric (**Equation 21**).

$$\theta_{\%} = \frac{\theta_{syn} - \theta_{MLE}}{\theta_{syn}} \times 100\% \quad \text{Equation 21}$$

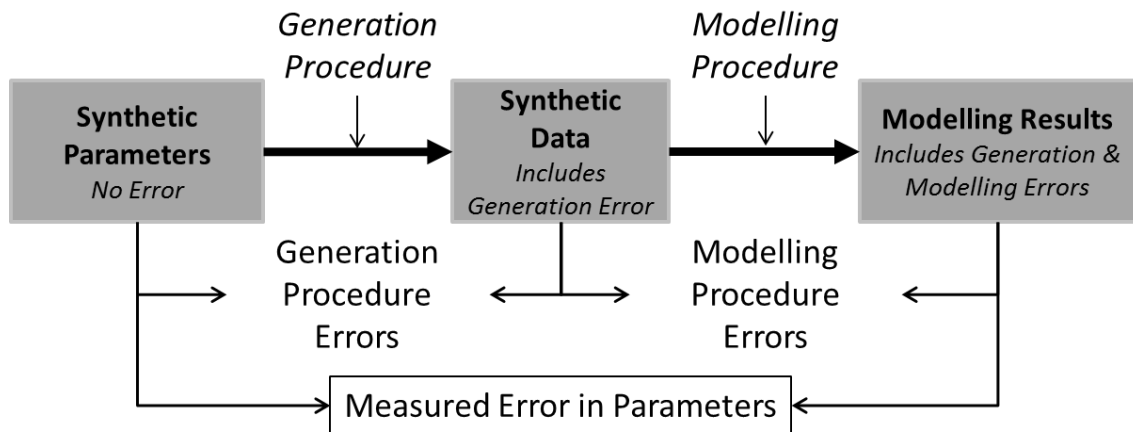
Where;

$\theta_{\%}$ : Percentage error in parameter

$\theta_{syn}$ : Synthetically generated parameter

$\theta_w$ : Modelled parameter from the weighted MLE metric

The errors induced during the generation of data from synthetic parameters are important in understanding the errors specifically associated with the modelling procedure as structural and parametric uncertainties are not known for practical applications. Algorithmic uncertainty is associated with the procedure of generating synthetic data, and the modelling procedure. Section 5.9.2 addresses the epistemic and aleatoric uncertainties of the generation procedure by assessing the errors that are associated with the construction of synthetic data. Given the errors associated with the generation of data, the remainder of Section 5.9 focuses on the uncertainties associated with the modelling procedure for a range of seismic response scenarios. **Figure 134** provides a diagrammatic representation of the process of generating and modelling synthetic data with respect to generation, modelling, and measured errors.



**Figure 134** Diagrammatic representation of the process of generating and modelling synthetic data and the generation, modelling, and measured errors.

### 5.9.2 Errors Associated with Synthetic Data Generation

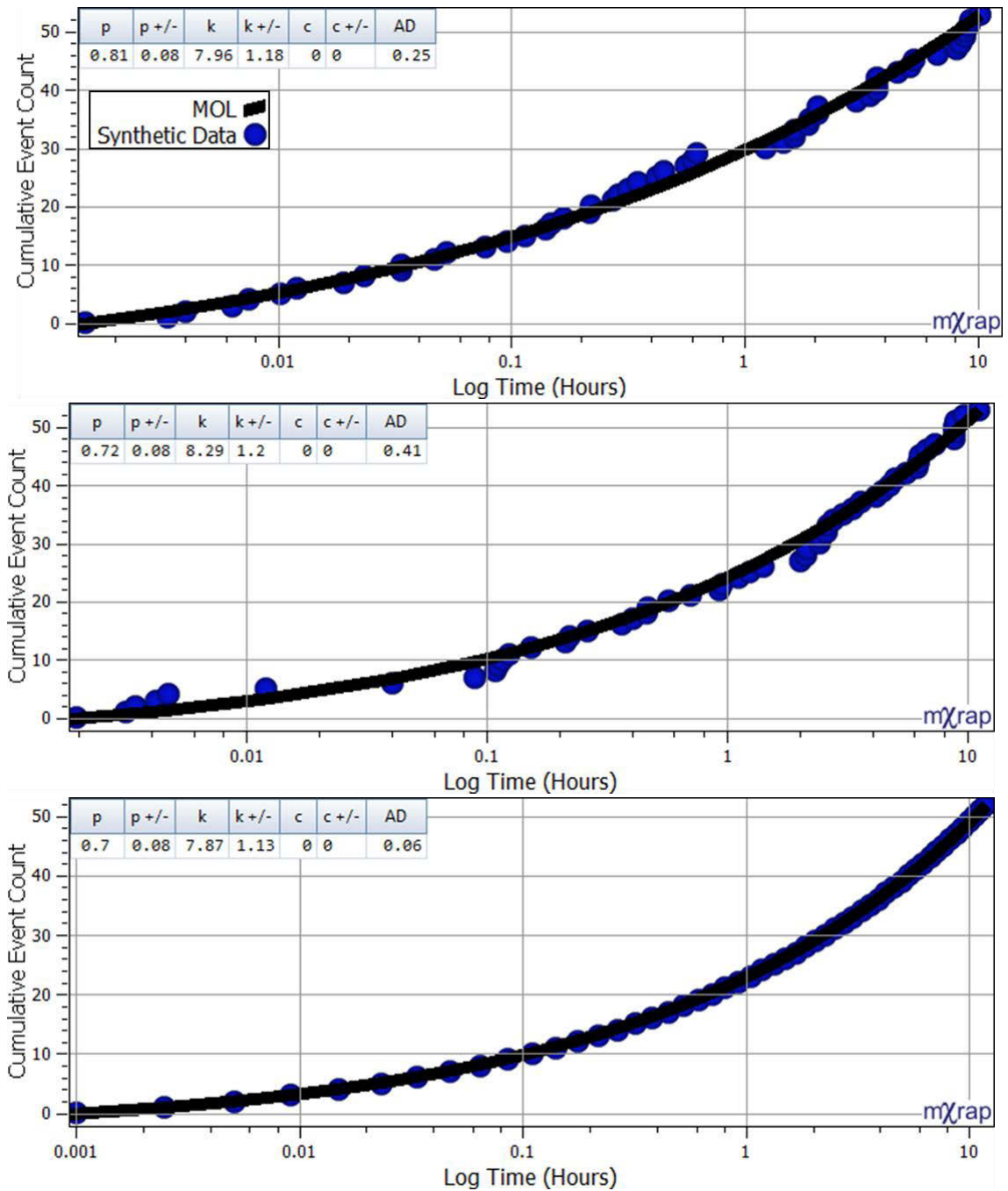
Guidance for the epistemic and aleatoric errors caused by the generation procedure of synthetic data is ascertained from seismic responses that are created using synthetic MOL parameters over known time intervals. The synthetic generation process will create randomness during short and long intervals due to sampling of the MOL cumulative event distribution. Inevitably, the seismic responses generated will not be perfectly representative of the synthetic parameters. The randomness during these times can have a significant influence on modelling results. Given the perfect time interval used to model the response, it is not

reasonable to expect the modelling precision and accuracy to surpass the uncertainties introduced during the generation of seismic responses.

An understanding of the distribution of inherent errors associated with data generation is investigated using three methods that capture different degrees of randomness:

1. Random Sampling: For  $N$  events, CDF values ( $u_i$ ) are randomly uniformly sampled from the interval  $[0,1]$  that specify relative event times ( $t_i$ ), on the interval  $[T_s, T_E]$ .
2. Quota Sampling: Subdivide the CDF  $[0,1]$  into a number of intervals. Randomly sample CDF values ( $u_i$ ) for the events that occur during each interval subdivision, e.g., for interval subdivisions of 20% and a response of 100 events, each interval contains 20 events and CDF values are sampled from  $[0, 0.2]$ ,  $[0.2, 0.4]$ , ..., and  $[0.8, 1]$ .
3. Non-sampled: Events have non-sampled CDF values, e.g., given a response of 100 events, CDF values are allocated  $[0, 0.01, 0.02, \dots, 1]$ .

**Figure 135** illustrates the three methods of synthetically generating event times. Three responses are generated from the same MOL distribution (blue spheres) and fitted using the MLE estimation of parameters over the entire interval (solid black line). Resultant parameters are tabulated on each time series. Charts show the cumulative event count over log time for randomly sampled events (top), quota sampled events (middle), and non-sampled events (bottom). The arbitrarily selected synthetic parameters used to generate the MOL distribution are  $p=0.69$ ,  $K=7.93$ ,  $c=0$  over the time interval  $[0.001, 12]$ . Fitting of the three synthetic responses reveals that randomness associated with synthetic data generation can have a significant impact on MOL results, particularly the  $p$ -parameter that is 0.81 for random sampling (-17.4% error), 0.72 for quota sampling (-4.2% error), and 0.7 for a non-sampled response (-1.4% error). Errors for the non-sampled response are significantly reduced, although, errors in  $p$ -parameter and  $K$ -parameter still exist. Additionally, the Anderson-Darling statistic indicates the fit is imperfect. These discrepancies are due to the selection of temporal intervals and the resolution of MOL parameters during modelling.



**Figure 135** Time series of synthetic seismic responses (blue spheres) fitted by the MOL (solid black line). Shown is the cumulative event count over log time for randomly sampled events (top), quota sampled events (middle), and non-sampled events (bottom).

The influence of random sampling is further investigated by assessing 5000 responses generated by uniformly sampled parameters ( $p[0.6,1.2]$  and  $K[5,20]$ ), a constant  $c$ -parameter ( $c=0$ ), and time interval  $[0.001, 12]$ . These responses have an absolute time offset of 12 h relative to the initiation of the preceding response. The MOL parameters selected reflect values observed in nature and the number of responses generated provides a significant sample while still being computationally practical. The trends in errors associated with the generation of a single response are also observed for the range of realistic  $p$ -parameter and

K-parameter. The tests examining the influence of random sampling are summarised in two figures. Each figure contains six individual charts examining errors for the K-parameter (left) and the p-parameter (right), along with the methods of generating synthetic data (top: randomly sampled, middle: quota sampled, and bottom: non-sampled). Quota sampling uses 20% CDF intervals. **Figure 136** presents a scatter plot of modelling results (x-axis) versus synthetic parameters (y-axis). Additionally, a linear trend has been fitted to each scatter plot (black line). **Figure 137** presents cumulative density functions for errors in the p-parameter and K-parameter. The results are summarised by error percentages for the mean, standard deviation, 10, 50, and 90% CDF values in **Table 27** (p-parameter) and **Table 28** (K-parameter).

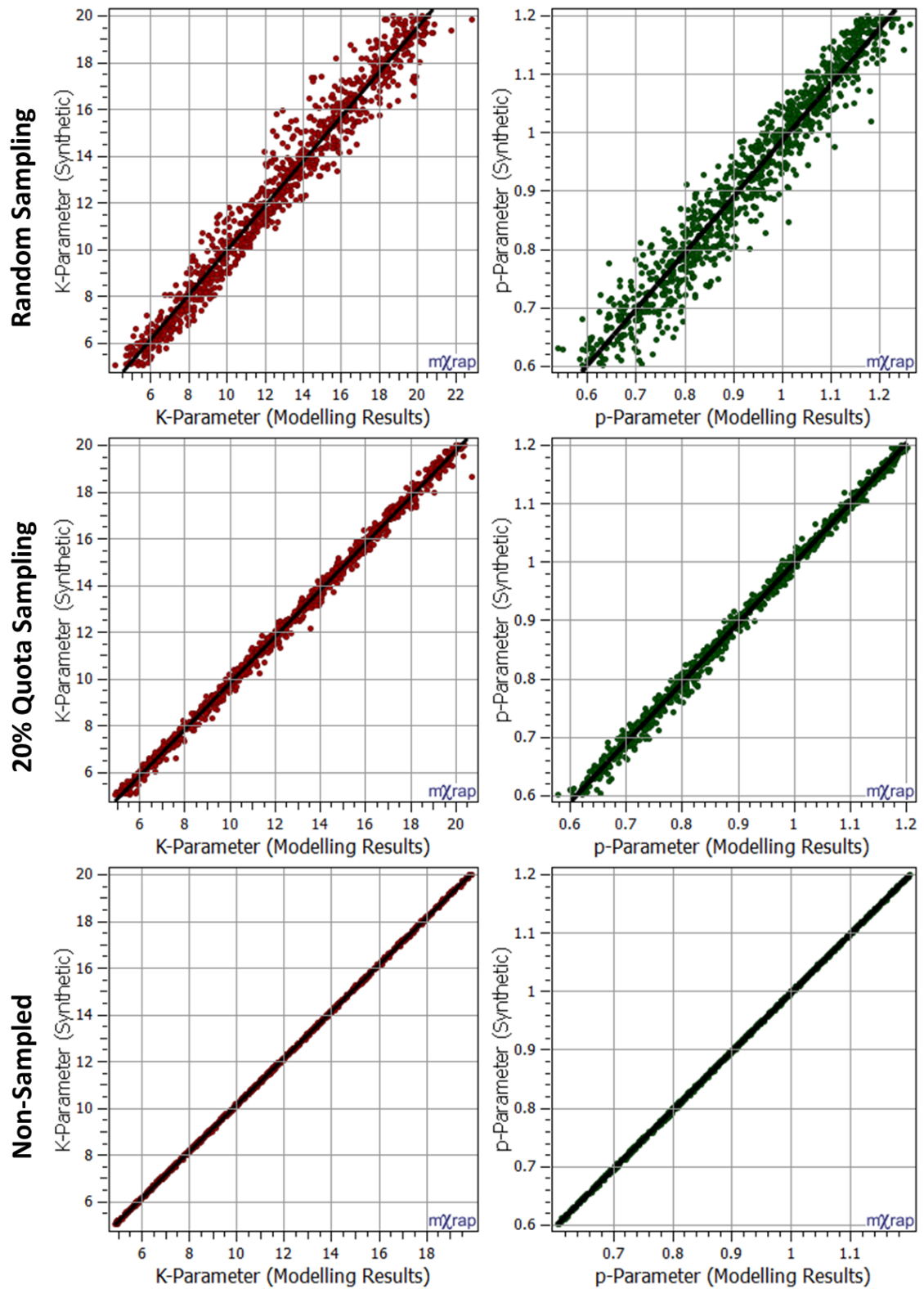
These two figures illustrate the relatively small degree of error when fitting the MOL to non-sampled synthetic data, and show that there is a systematic bias in this error to overestimate the p-parameter and underestimate the K-parameter. The positive bias in the p-parameter is observed in quota and random sampling methods (mean of 0.7 and 1.8%, respectively) and is accompanied by increased random errors (standard deviation of 1.4 and 5.8%, respectively). Non-sampled plots show that the K-parameter has been underestimated (mean error of -1.0%). Quota and randomly sampled responses overestimate this parameter (2.1 and 1.9%, respectively). Initial epistemic errors are due to the modelling interval selected and the modelling resolution. The overestimation of parameters is due to the sampling of the modelling interval, which inevitably reduces periods that are modelled as event times will not be generated exactly at the start and end of the response. Quota sampling partially addresses the influence of not sampling the time interval consistently by ensuring a portion of events is drawn from the beginning and end of the response. As a result, both epistemic and aleatoric uncertainties associated with the generation of synthetic responses decrease.

**Table 27** Tabulated result for the CDF of p-parameter errors.

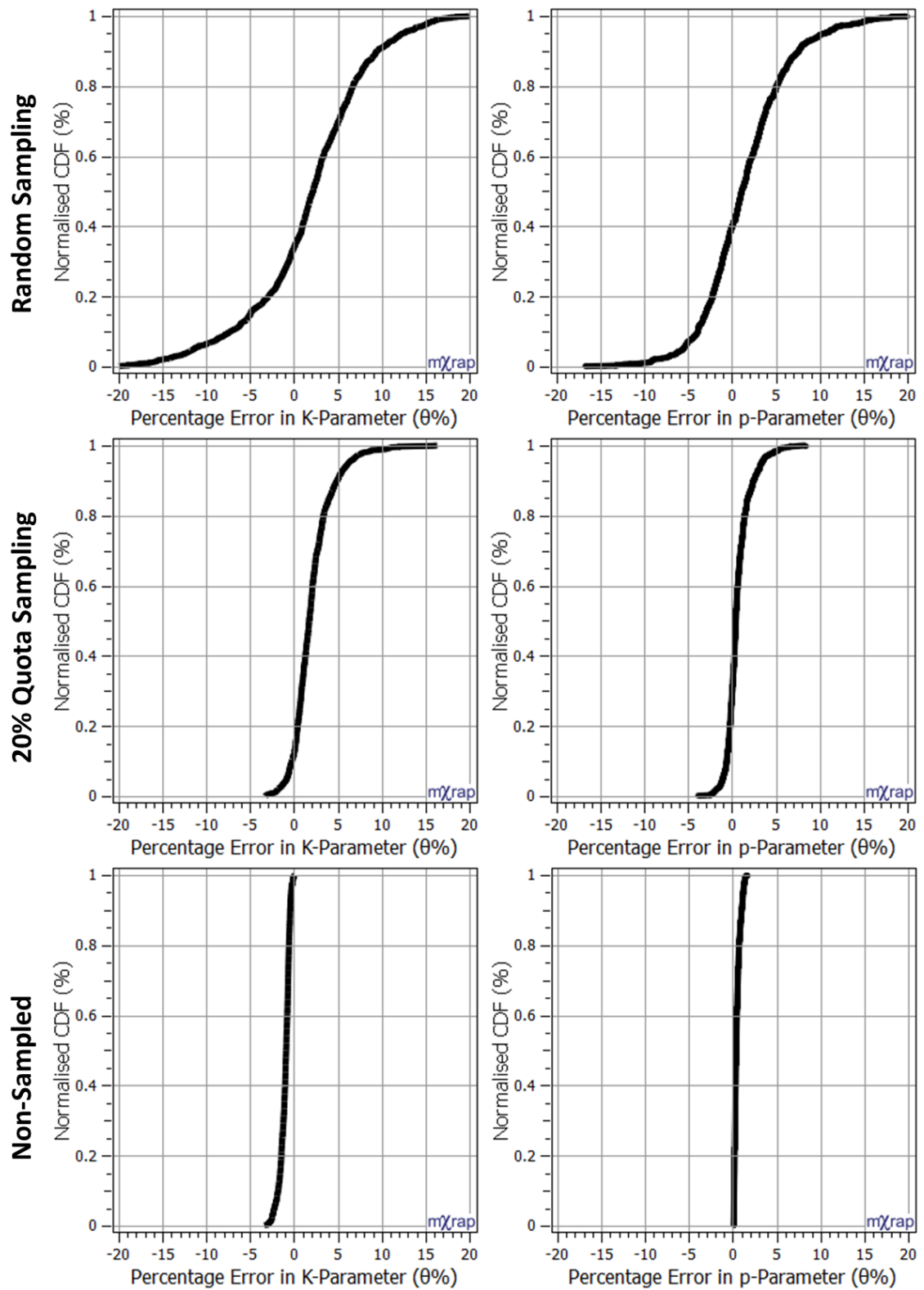
p-Parameter	Mean (Bias)	Standard Deviation (Variation)	Cumulative Distribution Function		
			10%	50%	90%
Randomly Sampled	1.8%	5.8%	-4.1%	1.1%	7.9%
Quota Sampled	0.7%	1.4%	-0.6%	0.4%	2.4%
Non-sampled	0.5%	0.3%	0.1%	0.4%	1.0%

**Table 28** Tabulated result for the CDF of K-Parameter errors.

K-Parameter	Mean (Bias)	Standard Deviation (Variation)	Cumulative Distribution Function		
			10%	50%	90%
Randomly Sampled	1.9%	7.8%	-7.6%	2.2%	10.5%
Quota Sampled	2.1%	2.3%	-0.2%	1.7%	4.9%
Non-sampled	-1.0%	0.6%	-1.8%	-0.9%	-0.4%



**Figure 136** Randomly sampled (top), quota sampled (middle) and non-sampled (bottom) methods of generating synthetic data, for synthetic and modelling results (Left: K-parameter Right: p-parameter). A black line shows the linear fit to the data.

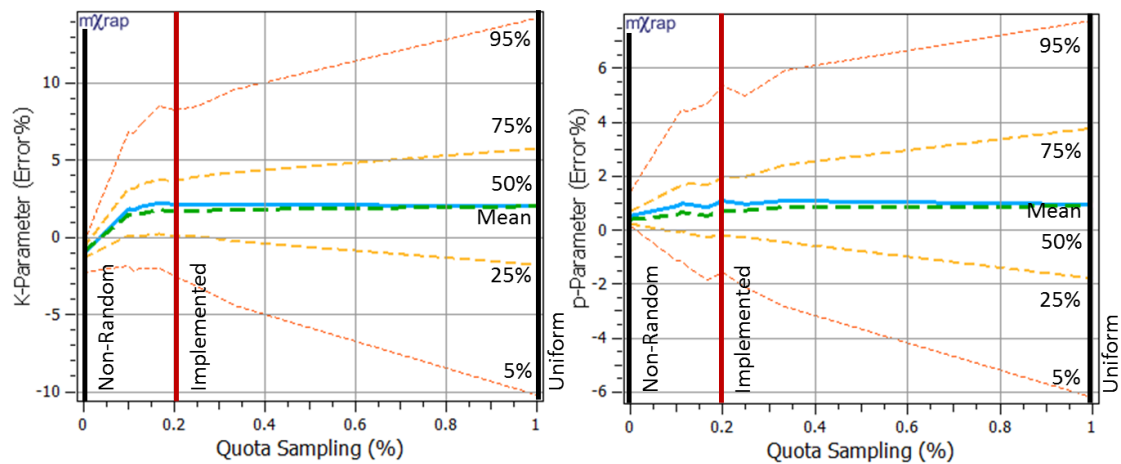


**Figure 137** CDFs for percentage errors when recovering K-parameter (left) and p-parameter (right) for randomly sampled (top), quota sampled (middle), and non-sampled (bottom) methods of generating synthetic data.

The stochastic nature of seismicity results in inherent aleatoric uncertainty that is congruent with the inherent errors associated with the generation of synthetic responses by uniform random sampling. While these errors may provide the best representation of the uncertainty, this method of generating synthetic data may not be preferable to quantify the error associated with the temporal modelling procedure. The aim of subsequent analysis is to evaluate the influence that various response scenarios have on the recovery of MOL parameters when using the weighted MLE metric developed in Sections 5.5, 5.6, and 5.7. To reflect reality, it is important to retain the stochastic nature of event occurrence. Additionally, it is also necessary to limit aleatoric uncertainty in order to retain confidence when assessing the influence of response scenarios on MOL parameter recovery.

For these reasons, quota sampling is used for the generation of synthetic data to test subsequent response scenarios. The inherent errors in the p-parameter and K-parameter for this data generation method have been quantified and are used as a comparative reference for further assessment of response scenarios (**Figure 136**, **Figure 137**, **Table 27**, and **Table 28**). In effect, error distributions found from response scenarios will be comparable to the inherent error distribution for quota sampling if the modelling procedure performs optimally and response scenarios do not influence the expected MOL parameters. For comparative purposes, these error distributions are referred to as generation errors. Additionally, the difference between modelling parameters and synthetic parameters is referred to as absolute errors for comparative purposes.

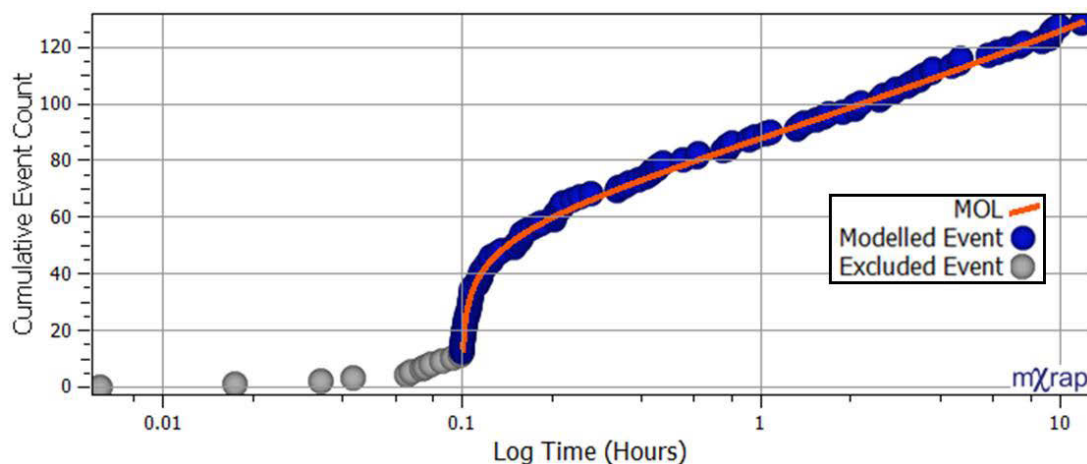
**Figure 138** shows the distributions of errors in p-parameters and K-parameter as the percentage size of quota sampling intervals increases. These distributions were constructed from analysis of 25,000 responses generated by uniformly sampled parameters ( $p[0.6,1.2]$  and  $K[5,20]$ ), a constant c-parameter ( $c=0$ ), and time interval  $[0.001, 12]$ . This assessment resulted in the selection of a Quota Sampling interval of 20%, as the interval represented a reasonable trade-off between representing inherent aleatoric uncertainty and allowing for modelling errors to be consistently assessed. Subsequent analysis in this chapter consistently uses 20% CDF intervals to generate seismic responses.



**Figure 138** The 5%, 25%, 50%, Mean, 75%, and 95% distributions of errors in  $p$ -parameters and  $K$ -parameter as the percentage size of quota sampling intervals increase. 0% quota sampling is equivalent to a non-random sample, 20% sampling is the implemented interval, and 100% is equivalent to uniform random sampling.

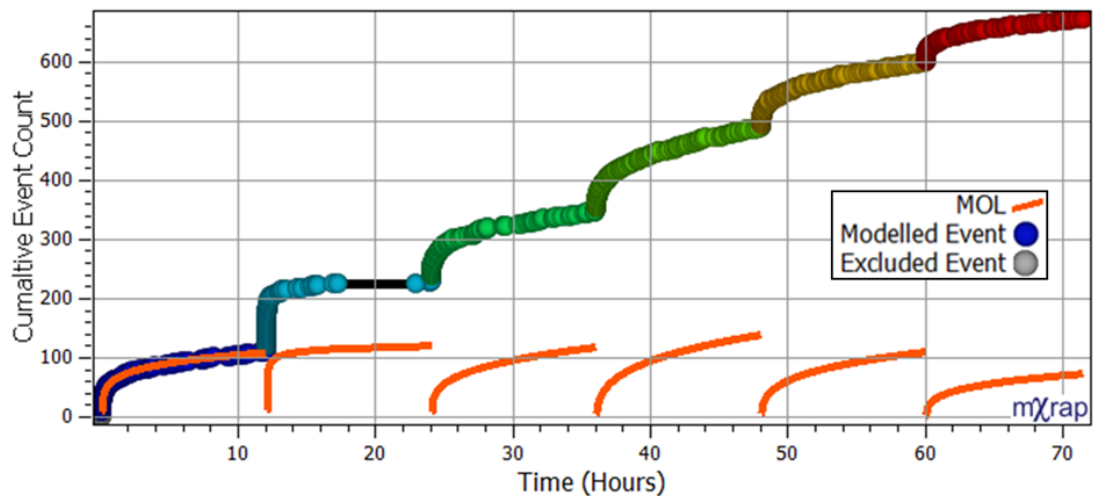
### 5.9.3 Seismic Response with Early Variation

Errors in the delineation and quantification of seismic responses with early variation are assessed by considering 5000 responses over an interval  $[0.001, 12]$  (hours), with an absolute time offset of 12 h, generated from uniformly sampled parameters ( $p[0.6, 1.2]$ ,  $K[5, 20]$ ), and a constant  $c$ -parameter ( $c=0$ ). The selection of parameters maintains representation of natural seismic responses to mining and ensures that the generation errors established in Section 5.9.2 are comparable. The introduction of early variation is achieved by uniformly sampling  $N[0, 20]$  events over an interval  $[0, 0.1]$  (hours). **Figure 139** provides a typical time series of cumulative event count over log time. The early variation before the response (grey events) is excluded from the optimal modelling interval (blue events) found by the weighted MLE metric (orange line illustrates the fitted MOL).



**Figure 139** A typical time series of cumulative event count over log time. The early variation (grey events) is excluded from the interval (blue events) that was modelled (orange line).

A continuous dataset is constructed by generating each subsequent response after a delay of 12.1 h since the initiation of the previous response. This feature is important to test the recovery of parameters when the modelling time window overestimates response length (Section 3.5.4). The temporal modelling window is set to 36 h for this analysis and captures three responses. The ability for the weighted MLE metric to identify and delineate the interval for each response within a continuous dataset is illustrated by **Figure 140**. A cumulative event count shows modelled responses over a 72 h period (distinct colours for each response). The MOL used to model each of the six responses generated during this interval is shown by relative cumulative event counts (orange lines).



**Figure 140** A cumulative event time series of modelled responses (coloured events) over a 72 h period. The MOL models are shown by relative cumulative event counts (orange lines).

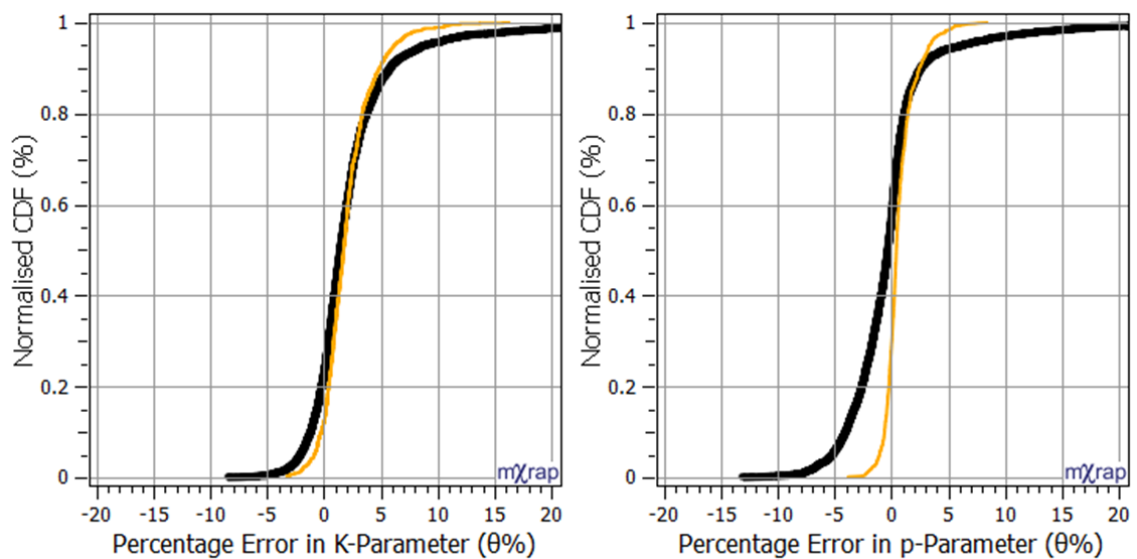
The CDF error results for 5000 synthetic responses with early variation are tabulated in **Table 29**. This table summarises the errors in recovering p-parameters and K-parameters for the mean, standard deviation, 10, 50, and 90% values for the error CDF. The difference between modelling results and generation parameters are calculated with the largest differences shown in bold. **Figure 141** shows the cumulative density functions for the errors in modelling results for p-parameters (right) and K-parameters (left). Percentage parameter errors for this assessment (black lines) are plotted along with the generation error CDF (orange lines). This figure and table provide a general comparison between modelling errors and the generation error distributions.

A two-sample Kolmogorov Smirnov test is used to provide context for the influence of the sample size. The null hypothesis that both error distributions are sampled from the same distribution is rejected at a relatively low confidence level of 0.1, if the Kolmogorov-Smirnov statistic ( $D$ ) is greater than a critical value. The statistics for the p-parameter ( $D_p = 0.348$ ) and K-parameter ( $D_p = 0.111$ ) are greater than the critical value ( $C_v = 0.024$ ) and, therefore, the null

hypothesis is rejected and this implies that these errors are sampled from different distributions. Due to the high number of samples, errors are due to fundamentally different distributions even though error distributions are similar in nature. Despite fundamentally different distributions, both may be accurate with respect to the inherent aleatoric and epistemic uncertainties associated with the synthetic generation of seismic response.

**Table 29** A summary of errors in recovering  $p$ -parameters and  $K$ -parameters. The largest differences between generation and modelling results are shown in bold.

	Mean	Standard Deviation	Cumulative Distribution Function		
			10%	50%	90%
p: Generation	0.7%	1.4%	-0.6%	0.4%	2.4%
p: Results	-0.2%	4.1%	-4.0%	-0.3%	2.6%
<i>Difference</i>	-0.9%	<b>2.7%</b>	<b>-3.4%</b>	-0.7%	0.2%
K: Generation	2.1%	2.3%	-0.2%	1.7%	4.9%
K: Results	2.2%	4.3%	-1.2%	1.4%	5.8%
<i>Difference</i>	0.1%	<b>2.0%</b>	-1.0%	-0.3%	0.9%



**Figure 141** CDFs for the errors in recovering  $p$ -parameters (right) and  $K$ -parameters (left). Plotted are distributions for generation (orange lines) and recovered errors (black lines).

Observations for p-parameter errors:

1. The absolute change in mean CDF values indicate that modelling is accurate with respect to errors (-0.2% absolute and -0.9% relative bias).
2. Standard deviation increases by 2.7% indicating that the range of errors increases but remain relatively precise in absolute terms (4.1% absolute and 2.7% relative variation).
3. The 10% CDF value decreases by 3.4% indicating p-parameters are underestimated.

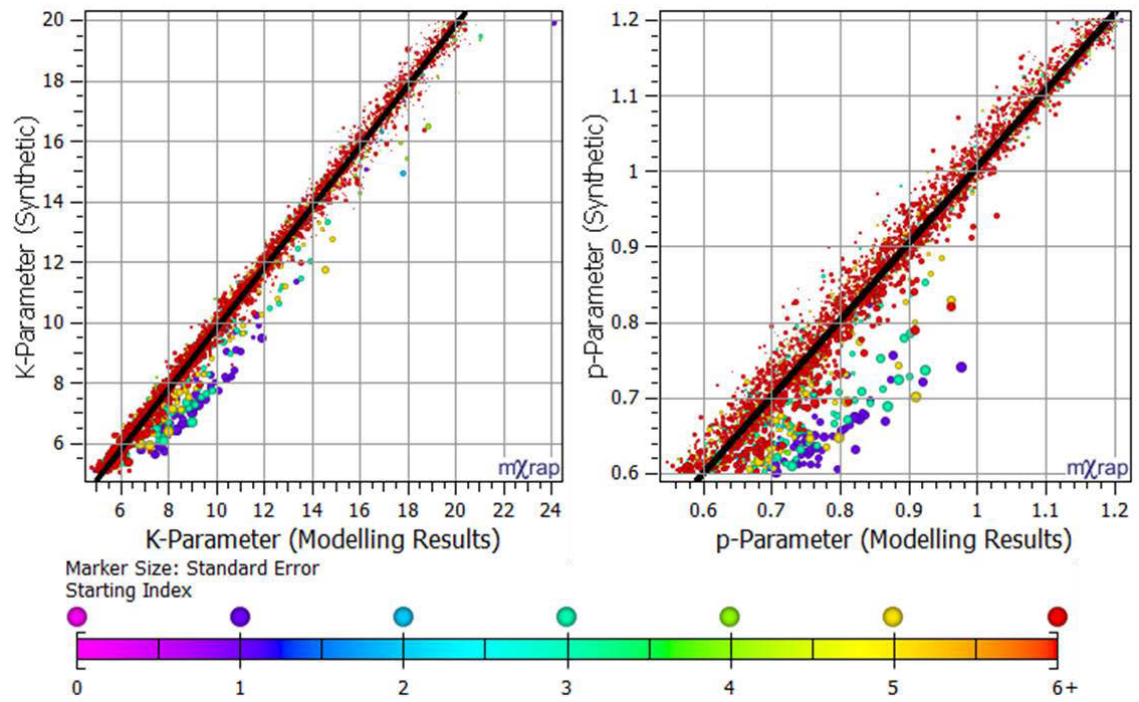
Observations for K-parameter errors:

1. The absolute change in mean CDF values indicates that modelling is accurate with respect to errors (0.1% absolute and 2.2% relative bias).
2. Standard deviation in K-parameter errors increases, although remains relatively precise (4.3% absolute and 2.0% relative variation).

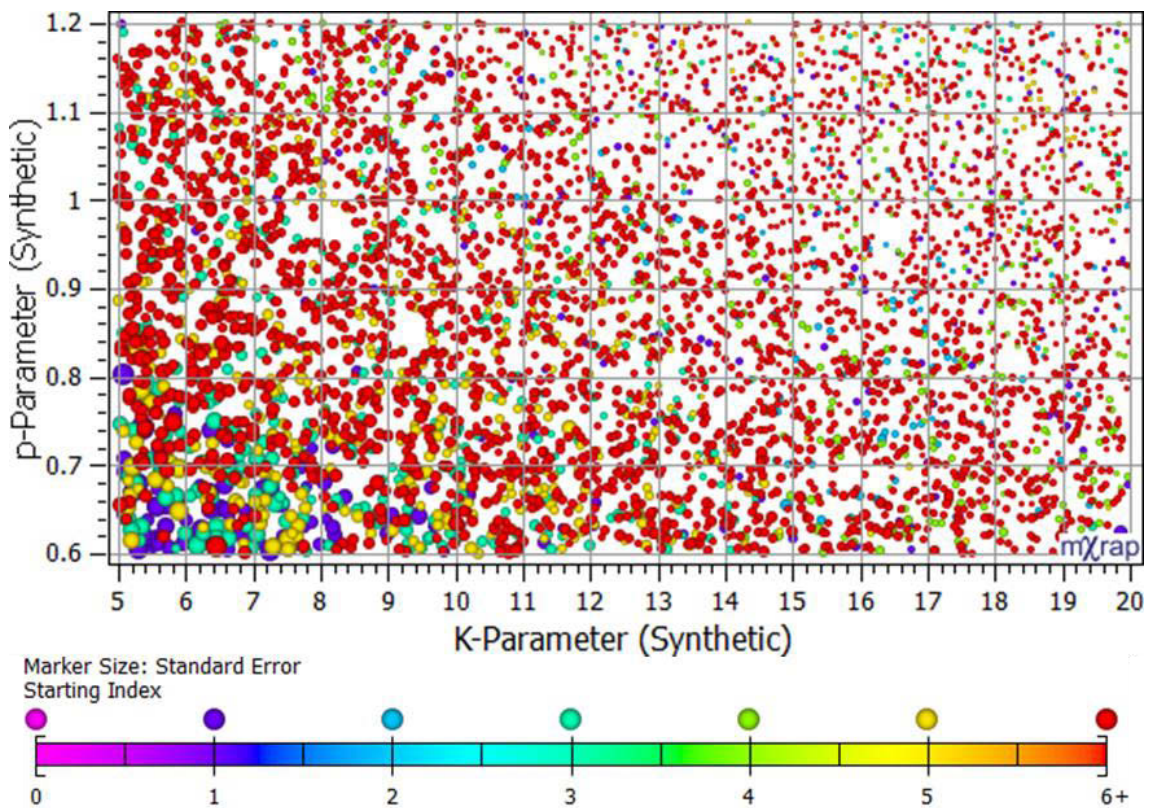
Increased error standard deviations and the underestimation of some p-parameters with respect to generation errors indicate a decrease in modelling accuracy. This decrease in accuracy is investigated by plotting synthetic parameters against modelling results for K-parameters (**Figure 142** left) and p-parameters (**Figure 142** right). Furthermore, the markers on these charts are coloured by the starting index used to define the modelling interval and are sized based on the standard error associated with MOL parameters (smaller markers indicate higher certainty).

The vast majority of these results are plotted by small, red markers that indicate that they have excluded some or all of the early variation. A small population of responses have low starting indices and high uncertainties in modelling parameters ( $\approx 200$  or  $\approx 4\%$  of all responses). These responses are generated by low p-parameters ( $< 0.75$ ) and low K-parameters ( $< 10$ ). **Figure 143** shows a systematic increase in uncertainty for smaller synthetic p-Parameter and K-parameters (larger markers). Lower parameters are accompanied by an increased likelihood that the initiation of the response will be misidentified and is a cause of significant errors in parameter recovery.

These responses have insufficient contrast to distinguish between the linear variation at the start of the response, and response events. This leads to p-parameters and K-parameters being underestimated as well as being accompanied by higher uncertainty in parameters. While the MLE metric weightings can manipulate the occurrence of these errors, they are unavoidable when there is insufficient contrast between processes. There is a small overall impact on analysis quality given that these errors are associated with a small portion of responses containing relatively few events and distinguishable by high uncertainty in parameters.



**Figure 142** Synthetic versus modelling results for K-parameters (left) and p-parameters (right). Markers are coloured by the starting index of the optimal modelling interval and sized by parameter standard error (smaller markers indicate higher certainty).

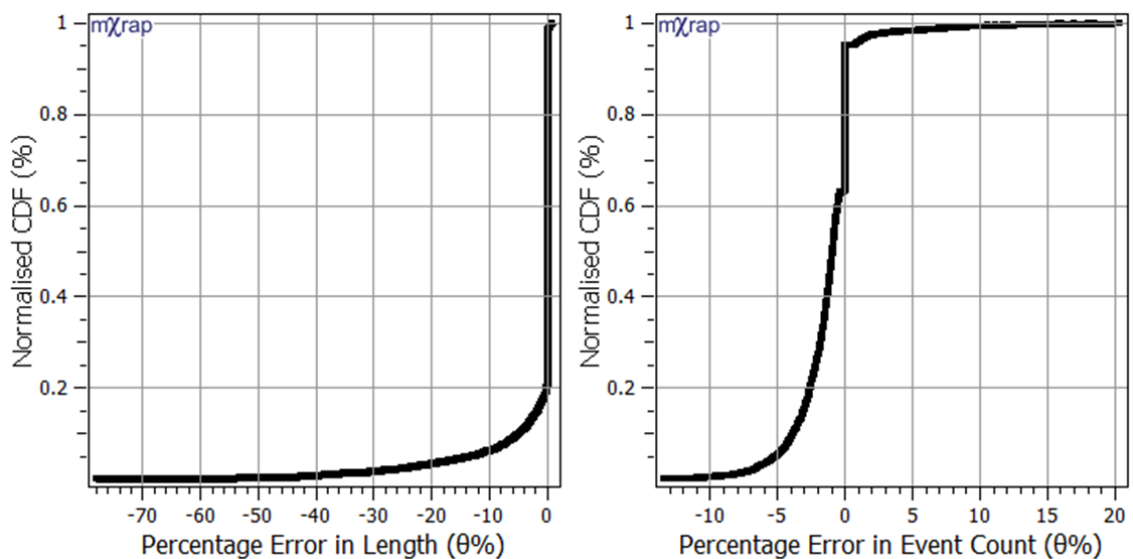


**Figure 143** Synthetic p-parameters vs. synthetic K-parameters coloured by the starting index of the optimal interval and sized by standard error (smaller markers indicate higher certainty).

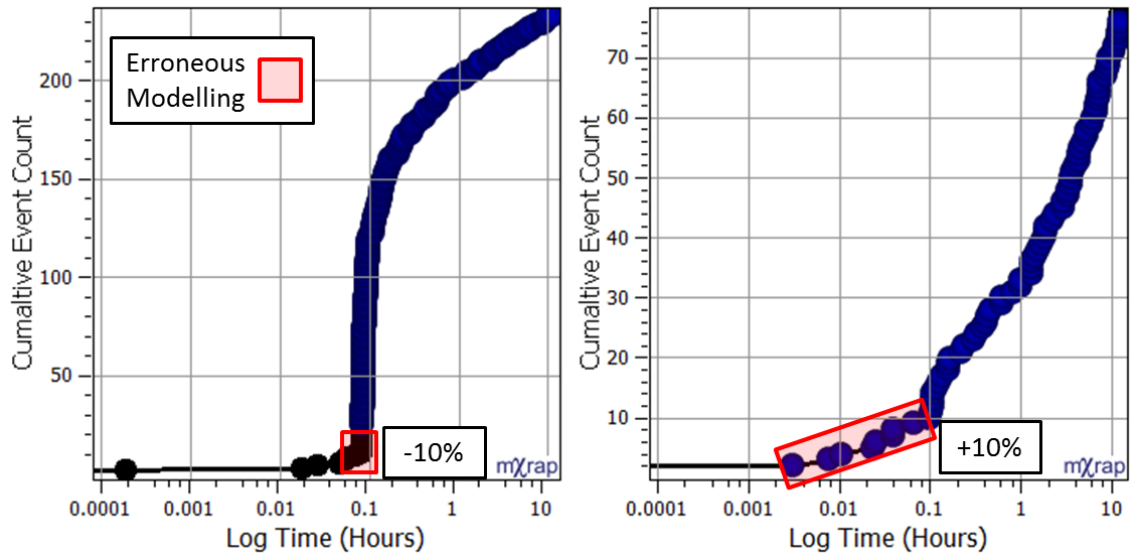
In addition to the accurate quantification of synthetic responses, it is also desirable to delineate the number of events and length of the seismic response accurately. **Figure 144**

provides the CDF for the percentage errors for recovering the number of events (right) and time interval (left) associated with the response. The recovered length of the response is generally accurate with 80% of responses completely delineated. The nature of a decaying event rate results in the response length being sensitive to a small portion of events that comprise late time intervals. Large range of underestimations is associated with 20% of responses, while a very small portion of responses overestimate lengths.

Temporal errors become significant if the temporal modelling excludes a portion of later times. These errors are insensitive to the inclusion or exclusion of early variation. The percentage error in event counts is more representative of the misallocation of individual seismic events. Errors in event counts are well constrained with  $\approx 95\%$  of responses between  $-5$  and  $5\%$  error. The inclusion of early variation occurs for  $\approx 10\%$  of responses (count error  $>0\%$ ) while  $\approx 65\%$  of responses have a portion (typically less than  $7.5\%$ ) of the events excluded. The linear transitions at  $75$  and  $95\%$  are caused by the relatively coarse resolution of the event count. **Figure 145** illustrates cases of underestimated response counts ( $-10\%$  error) (left) and overestimated response counts ( $+10\%$  error) (right).



**Figure 144** CDFs for the errors in recovering the response interval (left) and number of events (right).



**Figure 145** Examples of temporal modelling that result in the underestimation (left) or the overestimation of counts (right). Erroneous modelling is highlighted in a red box.

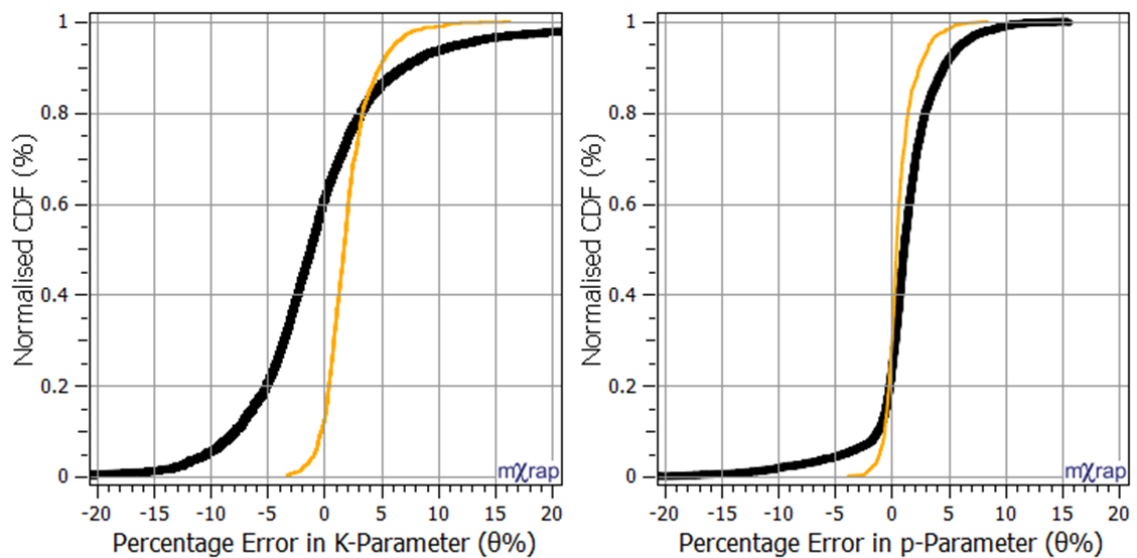
#### 5.9.4 Short Seismic Responses

The use of the weighted MLE metric readily delineates the largest seismic response within a modelling interval (Section 5.7.4), although, preferential delineation can result in a short response remaining to be modelled. Error analysis examines the influence of limiting the length of the seismic response. Similar to previous assessments, 5000 responses are generated by uniformly sampling parameters ( $p[0.6,1.2]$ ,  $K[5,20]$ ) and using a constant  $c$ -parameter ( $c=0$ ). While the start of the time interval is kept constant (0.001 h), the end of the time interval is uniformly sampled [0.1 to 2 h].

The CDF error results for the 5000 synthetically generated short seismic responses are tabulated in **Table 30**. This table is a summary of errors in recovering  $p$ -parameters and  $K$ -parameters that specifies the percentage error for the mean, standard deviation, and 10, 50, 90% CDF values. The difference between modelling and generation errors are calculated with the largest differences shown in bold. **Figure 146** shows the cumulative density functions for the errors in modelling results for  $p$ -parameters (right) and  $K$ -parameters (left). Percentage parameter errors for this assessment (black lines) are plotted along with the generation error CDF (orange lines). This figure and table provide general comparison of modelled and generation error distributions.

**Table 30** A summary of errors in recovering p-parameters and K-parameters. The largest differences between generation and modelling results are shown in bold.

	Mean	Standard Deviation	Cumulative Distribution Function		
			10%	50%	90%
p: Generation	0.7%	1.4%	-0.6%	0.4%	2.4%
p: Results	1.8%	2.3%	-0.4%	1.3%	4.7%
<i>Difference</i>	1.1%	0.9%	0.2%	0.9%	<b>2.3%</b>
K: Generation	2.1%	2.3%	-0.2%	1.7%	4.9%
K: Results	-1.6%	5.1%	-7.9%	-1.6%	4.4%
<i>Difference</i>	<b>-3.7%</b>	<b>2.8%</b>	<b>-7.7%</b>	<b>-3.3%</b>	-0.5%



**Figure 146** CDFs for the errors in recovering p-parameters (right) and K-parameters (left). Plotted are distributions for generation (orange lines) and recovered errors (black lines).

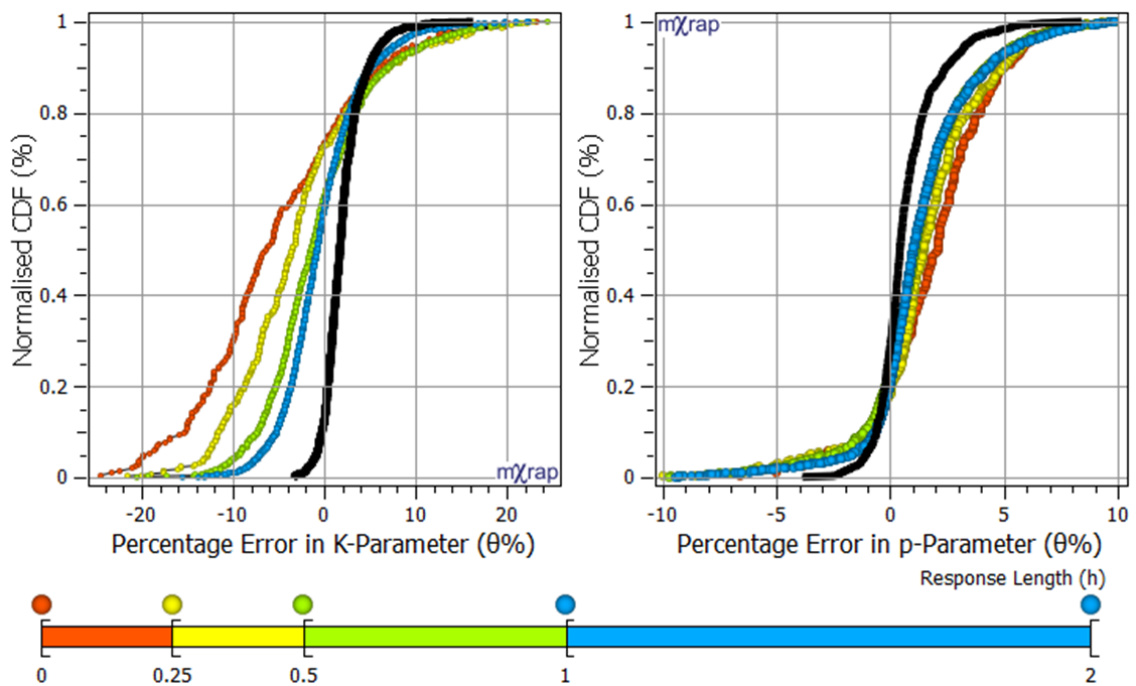
Observations for p-parameter errors:

1. CDF errors are generally consistent with the distribution of generation errors and indicate that modelling is accurate with respect to generation and true errors.
2. There is increased error for the 90% CDF value that indicates some p-parameters are overestimated.

Observations for K-parameter errors:

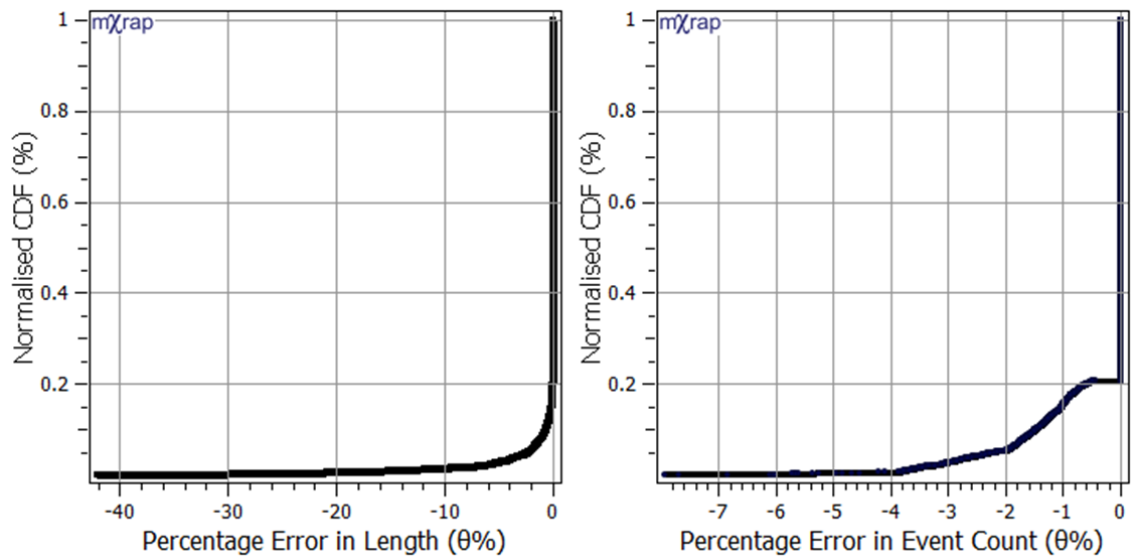
1. The portion of highest overestimated errors is relatively unchanged in comparison to a significant portion of K-parameters that are underestimated.
2. There is an increase in the standard deviation of K-parameter errors.

The error CDF previously presented in **Figure 146** shows response errors irrespective of the response duration. **Figure 147** provides further insight into the causation of the overestimation of the p-parameter and the underestimation of the K-parameter by constructing four error distributions for responses with similar temporal lengths. The four groups of response durations are lengths less than 0.25, 0.25-0.5, 0.5-1, and 1-2 h. The K-parameter error distributions show that underestimation of the K-parameter significantly decreases for increasing response durations. The p-parameter error distribution shows that overestimation of parameters decreases for longer durations. Furthermore, the recovery of p-parameters is less sensitive to the length of response durations.



**Figure 147** CDFs for the errors in recovering p-parameters (right) and K-parameters (left). Distributions are coloured by response duration groups (<0.25, 0.25-0.5, 0.5-1, and 1-2 h) with response to generation errors (black lines).

The CDFs presented in **Figure 148** summarise recovery errors of response lengths (left) and the number of events (right). Both of these distributions indicate that the vast majority of events and response lengths have been recovered, although, the weighted MLE metric has resulted in the optimal time interval excluding some initial events or final events. In comparison to Section 5.9.3, the exclusion of relatively few events and short intervals indicates that the weighted MLE metric is less likely to exclude events for shorter responses. The linear transition at 20% is caused by the relatively coarse resolution of the event count.



**Figure 148** Error cumulative density functions for the recovery of length (left) and event count (right).

### 5.9.5 Inclusion of Time-independent Seismicity

An additional consideration for the temporal modelling of seismic responses is the inclusion of seismicity that is generated by rock mass failure processes over longer time scales. This seismicity is characterised as a time-independent rate of events and are typically spatially dispersed (Section 2.3.1). Events that are associated with delocalised time-independent seismicity are excluded from analysis due to the spatial clustering component of the iterative approach to response assessment. The exclusion of events generated from these alternative processes is not ensured for mining environments that have sources of seismicity that generate time-dependent responses and spatially clustered time-independent seismicity. Additionally, seismic responses may superimpose in space and time. The later periods of a response are not strictly time-independent in behaviour, although, these events can be practically indistinguishable from time-independent processes given the uncertainty of the influence that routine blasting has on altering rock mass and stress conditions.

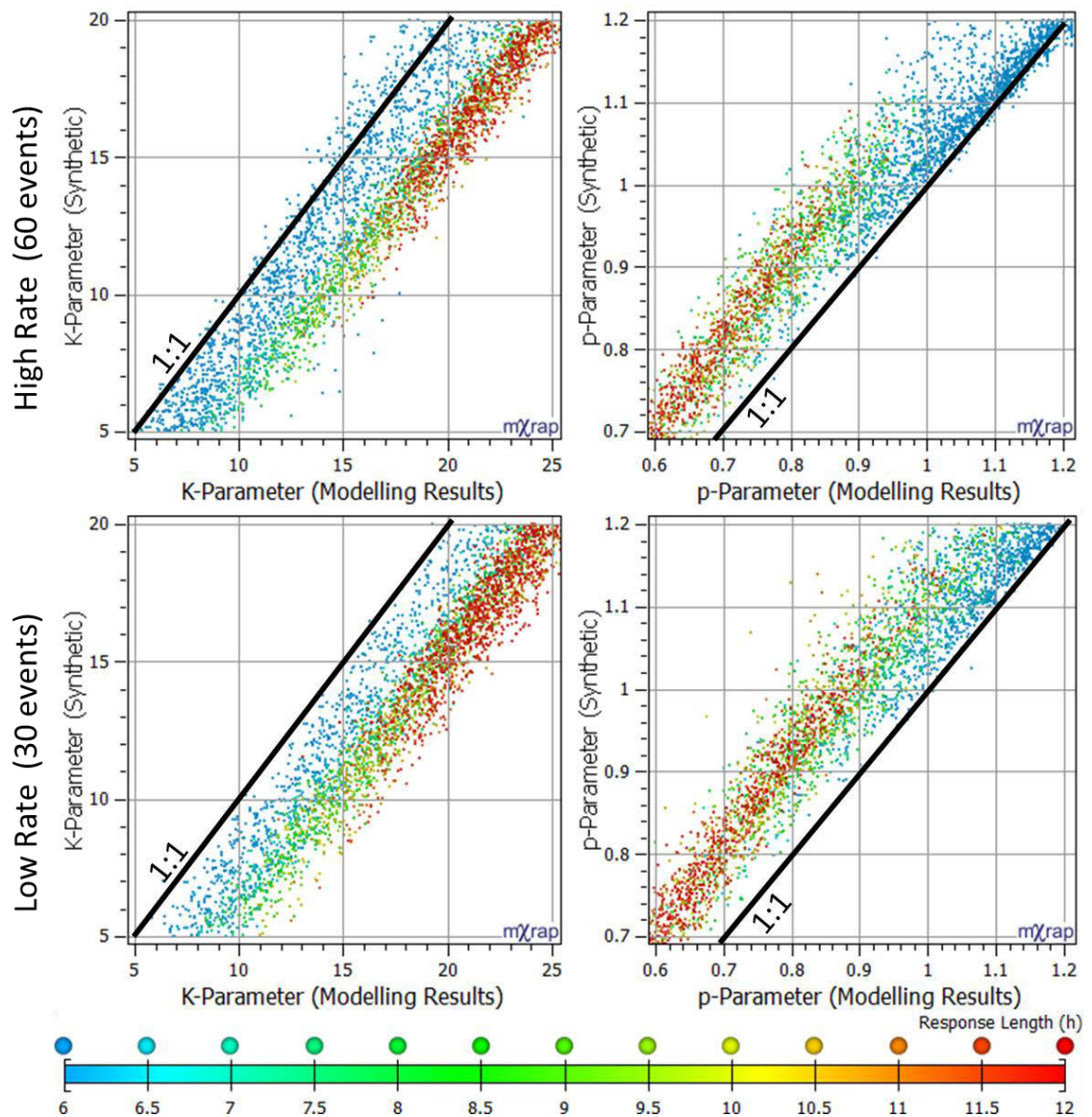
Due to the possibility of including time-independent events, it is important to assess:

- The influence of including a time-independent process on the determination of p-parameters and K-parameters;
- The ability of the weighted MLE metric to recover parameters despite the inclusion of time-independent processes; and
- The errors in temporal delineation are indicative of the inclusion of time-independent processes.

The concept of errors induced by the insufficient contrast between processes was introduced when early variation was included with a seismic response (Section 5.9.3). The influence of the insufficient contrast was limited as the processes were temporally separate and generally statistically different. The analysis of the inclusion of time-independent processes focuses on the effects of having insufficient contrast and, hence, temporally superimposes events to maintain a realistic representation of seismicity. Due to events being combined temporally, generation errors cannot be achieved by modelling these responses.

Similar to previous assessments, 5000 responses are generated over an interval [0.001, 12], with an absolute time offset of 12 h, uniformly sampling parameters ( $p[0.6,1.2]$  and  $K[5,20]$ ), and a constant  $c$ -parameter ( $c=0$ ). The introduction of a time-independent process is achieved by uniformly sampling 60 events over the modelling interval [0.001, 12]. A comparative scenario represents a lower rate of time-independent seismicity and instead samples 30 events over the modelling interval. Given the variable range of  $p$ -parameters and  $K$ -parameters, synthetic responses comprise of between 15 to 65% time-independent events for the high rate case and between 7.5 to 32.5% independent events for the low rate case. These portions represent a significant challenge for temporal modelling to quantify and delineate responses.

**Figure 149** shows that when time-independent seismicity is included, temporal modelling with the MOL causes the  $p$ -parameter to be consistently underestimated and  $K$ -parameter consistently overestimated (solutions compared to the 1:1 lines). This result is expected as increasing the number of events increases the modelled productivity ( $K$ -parameter). Additionally, the superimposition of infinitely slower event decay, i.e., constant, reduces the modelled event decay rate ( $p$ -parameter). Additionally, bifurcation occurs for the relationship between synthetic and modelled  $p$ -parameter when the synthetic  $p$ -parameter is high. This split population of results is related to the modelled length of responses ( $<6$  h: blue markers) and is more apparent for higher rates of time-independent seismicity. These two populations of results are not strongly apparent for the synthetic versus modelled  $K$ -parameter charts, as these solutions do not underestimate the  $K$ -parameter as severely. The bifurcation in results indicates that temporal modelling reduces the length of the modelling intervals for high synthetic  $p$ -parameters and results in more accurate parameters recovery.



**Figure 149** Synthetic versus modelling results for K-parameters (left) and p-parameters (right). Markers are coloured by the modelled response length (h).

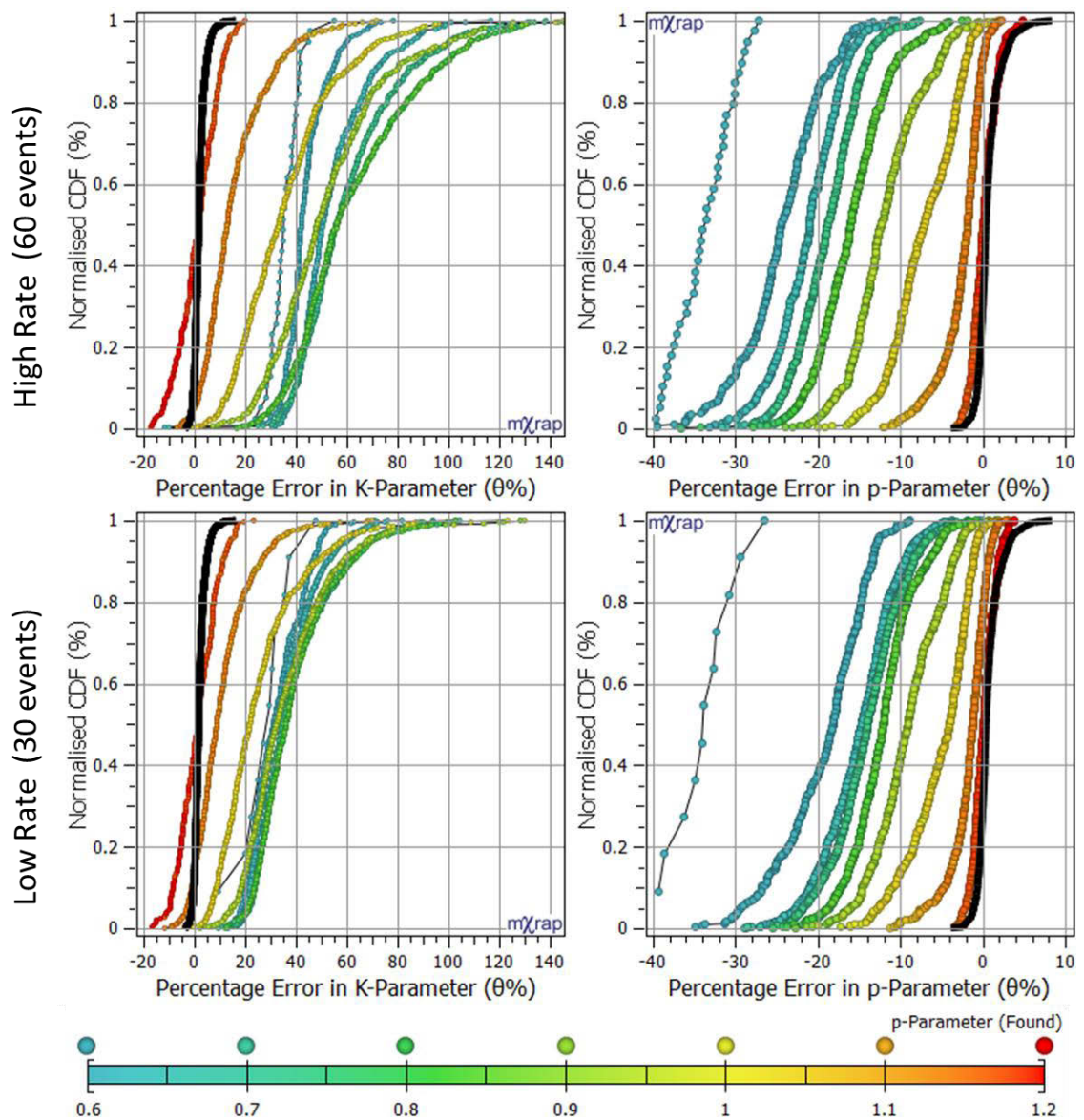
**Figure 150** investigates the accuracy of synthetic p-parameter and K-parameter recovery with respect to the modelled p-parameter. The influence of the modelled p-parameter is examined by constructing error CDFs for groups of modelled p-parameters (group intervals of 0.1). These distributions are constructed for combinations of recovery errors in p-parameter (right), K-parameter (left), high rates (top), and low rates (bottom).

The following observations are made for p-parameter errors:

1. p-parameters are always underestimated proportionally to the modelling p-parameter.
2. p-parameter errors are higher for a higher rate of time-independent seismicity.
3. If the modelled p-parameter is high ( $>1$ ), p-parameter errors are generally low ( $<10\%$ ).

The following observations are made for K-parameter errors:

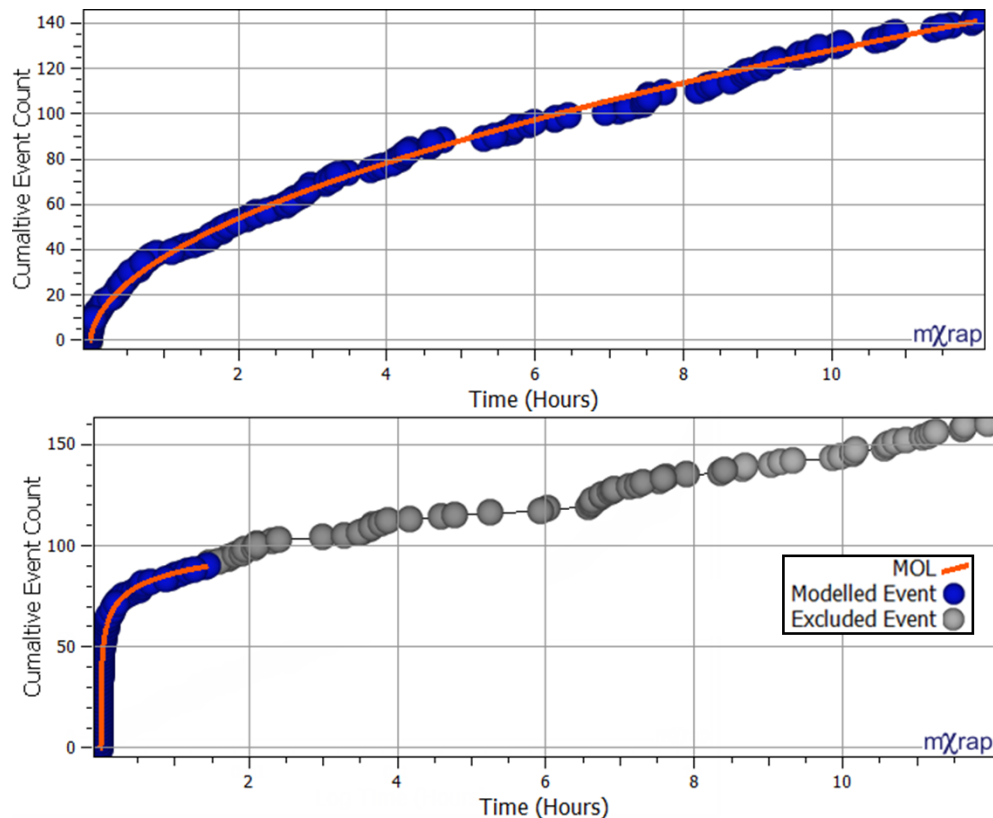
1. The recovered error in the K-parameter is greater than p-parameter errors and is related to the modelled p-parameter.
2. K-parameter errors are fairly consistent for modelled p-parameters below 0.9.
3. A decrease in K-parameter errors is associated with high p-parameters ( $\geq 0.9$ ).
4. K-parameter errors are larger for high rates of time-independent seismicity (40-100%) in comparison to low rates (20-60%) for low p-parameters ( $< 0.9$ ).



**Figure 150** CDFs of percentage errors in the recovery of modelling parameter for the p-parameter (right), K-parameter (left), high rates (top), and low rates (bottom).

The CDFs of parameter errors indicate a dependency between the recovered decay rate and the accuracy of modelling parameters. To model responses accurately, the observed dependency directly relates to the temporal contrast between seismic generation processes, i.e., high  $p$ -parameters are associated with high decay rates that provide sufficient contrast to time-independent processes. The use of the weighted MLE metric to exclude the later portion of responses is controlled by the Anderson-Darling statistic that measures how suitably the MOL models event occurrence. The application of the weighted MLE metric in Section 5.7.3 and 5.7.4 showed that this statistic is crucial to modelling a single response following the MOL when multiple processes are observed within a single modelling time window.

If the temporal contrast is sufficient then the weighted MLE metric can identify when the time-dependent process ceases to dominate event generation and transitions to a time-independent process. The need for temporal contrast is illustrated by two time series that show cumulative event counts and modelling results (**Figure 151**). Shown top is a response generated by a low  $p$ -parameter with a visually and statistically indistinguishable transition to a time-independent dominated process. Shown bottom is a response generated by a high  $p$ -parameter with a distinct transition to a time-independent process.



**Figure 151** Time series showing cumulative event counts and modelling results. Top: A response generated by a low  $p$ -parameter with an indistinguishable transition to a time-independent process. Bottom: A response generated by a high  $p$ -parameter with a distinct transition to a time-independent process.

## 5.10 Chapter Summary

This chapter developed and tested a methodology to temporally delineate and quantify mining induced seismic responses. This method forms a component of the iterative approach presented in Chapter 3 and utilises the subset of spatially clustered seismicity found in Chapter 4. The seven main sections of this chapter are summarised in the subsequent sections.

### 5.10.1 Temporal Modelling of Mining Induced Seismic Responses

In summary, temporal modelling of mining induced responses must consider:

- Selection of a modelling interval based only on temporal attributes;
- Interdependency between the p-parameter and c-parameter;
- Selection of a modelling interval following a power law event rate decay; and
- Quantification of the quality of modelling results.
- The ability to delineate responses that are partially temporally superimposed.
- The optimisation of delineation and quantification objectives.
- The integration with the iterative identification and delineation of seismic responses.

### 5.10.2 Modelling Mining Induced Seismic Response with the MOL

- The MOL is utilised to model responses due to the general applicability of this law.
- It is essential to quantify the quality of fit between the MOL and the observed seismicity by evaluating the uncertainty in MOL parameters and the suitability of fit using the Anderson-Darling statistic.
- Methods applying the MOL focus on the implementation of the c-parameter due to the interdependency between parameters. Additionally, methods focus on the selection of a modelling interval due to the need to select an interval that follows a power law decay in event rate.
- The two approaches typically adopted in literature for defining event times requires the definition of a principal event, i.e., mainshock, with the time of subsequent events defined relative to the time of the principal event occurrence:
  - Principal Event Fixed (PEF): If events are excluded, relative times are defined with respect to the same principal event; and
  - Principal Event Adjusted (PEA): If events are excluded, relative times are redefined with respect to a new principal event corresponding to the interval start.

These approaches can be summarised by four modes, and are investigated further to evaluate methods of modelling mining seismic responses with the MOL:

- *Mode 1*: Principal Event Adjusted and a variable c-parameter ( $PEA \geq 0$ );
- *Mode 2*: Principal Event Fixed and a variable c-parameter ( $PEF \geq 0$ );
- *Mode 3*: Principal Event Adjusted and a c-parameter fixed to zero ( $PEA = 0$ ); and
- *Mode 4*: Principal Event Fixed and a c-parameter fixed to zero ( $PEF = 0$ ).

### 5.10.3 Critical Assessment of the Four MOL Modelling Models

- This section investigates the four previously presented modes with respect to four types of seismic response scenarios that are commonly observed in the mining environment.
- These four response scenarios (synthetically generated) are: a simple response, simple response with early variation, late superimposed response, and early superimposed response.
- The following observations are made with respect to modelling models for a simple seismic response:
  - While *Mode 4* requires the exclusion of early events, it provides the most accurate parameter recovery within the ideal index;
  - *Mode 1* and *2* slightly overestimate p-parameters, although, are consistent and identify accurate K- parameters for the majority of the ideal index interval; and
  - *Mode 3* results are erroneous.
- The following observations are made with respect to modelling models for a seismic response with early variation:
  - *Mode 1* provides the most representative solution space for both p-parameters and K-parameters inside and outside of the ideal index interval;
  - *Mode 2* and *4* result in similar solution spaces that overestimate p-parameters and have limited solutions with accurate K-parameters; and
  - *Mode 3* results are erroneous.
- The following observations are made with respect to modelling models for a late superimposed response:
  - *Mode 1* is the optimal approach as parameters are recovered for a reasonable number of intervals within the ideal index intervals for both responses;

- The results of *Mode 2* and *4* are the same for a seismic response with early variation. These modes not able to recover any parameters for the second response; and
  - *Mode 3* results are erroneous.
- The following observations are made with respect to modelling models for an early superimposed responses:
  - *Mode 1* is the only approach that can recover the MOL parameters; and
  - *Mode 2, 3, and 4* perform poorly.
- These are commonly observed configurations of responses with mining induced seismicity, although, is not a comprehensive list of possible scenarios.
- The PEA approach with a variable c-parameter is optimal to delineate and quantify mining induced seismic responses given the occurrence of seismic responses proceeded by early variation and early/late superimposed responses.
- Using a variable c-parameter helps to achieve consistent quantification and delineation for a range of seismic responses, despite creating an inherent trade-off between the interdependency of p and c parameters.

#### 5.10.4 Parametric and Statistical Selection of Modelling Interval

- MLE is the historical basis for statistical modelling selection and can results in the unreliable optimisation of a modelling interval.
- Additional statistics are selected based on the ideal characteristics of modelling of a seismic response to create a decision metric that optimises the quantification and delineation of seismic responses using the MOL.
- Parametric and statistical considerations to optimise the selection of a modelling time interval are the MLE, number of events modelled, c-parameter, parametric standard error, and Anderson-Darling statistic.
- An interval is optimised as c-parameter, parametric standard error, and Anderson-Darling statistic approach zero, although, does not capture additional information concerning the acceptable range of parameter values.
- Relative measures do not place emphasis on ideal solutions, limit poor solutions, or provide scaling within a range of marginal parameter values. This has a number of implications:

- If a parameter is outside of reasonable value ranges then a relative reduction is not meaningful and, therefore, the interval should be preferentially optimised using parameters within meaningful ranges; and
- Solutions with low parameters may be refined to the detriment of other parameters.
- This additional information is incorporated by the implementation of the piecewise linear weighting function.
- Modelling quality objectives are optimised by weighting factors: c-parameter, parametric standard error, and Anderson-Darling statistic. Delineation objectives are considered in a holistic decision metric by the MLE and number of events modelled.
- A simple combination of parametric and statistical measures is desirable as it offers pragmatic benefits in construction, application, and interpretation. A multiplicative function captures these attributes.

#### **5.10.5 Evaluation of the Weighted MLE Metric**

- The weighted MLE metric is assessed with respect to commonly observed responses.
- The evaluation examines the quantification and delineation outcomes associated with the optimal weighted MLE metric in comparison to the optimal MLE solution.
- The following observations are made with respect to modelling models for a simple seismic response:
  - Weightings ( $SE_w$ ,  $c_w$ , and  $AD_w$ ) provide guidance in selecting a response within the ideal index interval that meets modelling quality objectives; and
  - The metric has little impact as MLE solution generally coincides with the weighted parameters and number of events.
- The following observations are made with respect to modelling models for a seismic response with early variation:
  - The  $c_w$  and  $AD_w$  excludes early variation and optimises quality objectives;
  - While the  $SE_w$  modelling parameter does not assist with the exclusion of variation, it still contributes to delineation objectives;
  - Exclusion of early variation from the modelling interval has a significant influence on the MOL parameters found from the response;

- Weighting the MLE by  $N_{\text{Events}}$ ,  $SE_W$ ,  $c_W$ , and  $AD_W$  results in optimal solution spaces corresponding to the ideal event index; and
  - MLE solution represents a marginally suitable model that includes early variation and excludes the last eight hours of events.
- The following observations are made with respect to modelling models for a late superimposed response:
  - $AD_W$  provides a clear indication of appropriate modelling intervals optimising quality and delineation objectives.
  - Weighted solution space limits optimal solutions to the ideal intervals, excludes variation, models an entire response, and recovers synthetic parameters accurately.
  - Modelling both of these responses within the same interval improves the MLE.
  - The optimal MLE solution excludes early variation of the first response and also includes a significant portion of the second response.
- The following observations are made with respect to modelling models for an early superimposed responses:
  - Weighted solution space limits optimal solutions to the ideal intervals, excludes variation, models an entire response, and recovers synthetic parameters accurately.
  - The MLE solution includes variation and a significant portion of the second response.

#### **5.10.6 Iterative Functionality of Temporal Modelling**

- This section illustrated two main features of temporal delineation to:
  - Adjust temporally misidentified responses to ensure seismicity is time-dependent; and
  - Refine an overestimated modelling window to model only one response.
- The weighted MLE metric delineates the largest adequately modelled interval and meets the requirements for the iterative identification and delineation of seismic responses.
- Optimal weighted MLE solutions for the remainder of late and early superimposed responses to mimic the iterative assessment process.

- The second response contained within the remainder of both late and early superimposed responses examples is identified, delineated, and well modelled by the MOL.
- The events that are not modelled are variation.

#### **5.10.7 Performance Evaluation of Temporal Quantification and Delineation**

- Mining induced seismic responses are typically well modelled by the MOL by similar ranges of parameters and, therefore, there is relatively high confidence in the inherent structural and parametric uncertainties associated with the MOL.
- Error analysis focuses on the accuracy and precision of the ability of temporal modelling to recover synthetic parameters used to generate seismic responses synthetically.
- Performance evaluation focuses on the algorithmic uncertainty associated procedure of modelling synthetic seismic responses using the weighted MLE metric along with the procedure of generating synthetic data.
- Synthetic generation process creates randomness during short and long intervals due to sampling the MOL cumulative event distribution.
- The randomness during these times can have a significant influence on modelling results.
- The errors associated with synthetic data generation are investigated by methods that capture different degrees of randomness (Random, 20% Quota, and Non-sampled).
- The stochastic nature of seismicity is congruent with the inherent errors associated with the generation of synthetic responses by uniform random sampling.
- Uniform random sampling may not be preferable to quantify the error associated with the temporal modelling procedure as random errors prevent reliable assessment of modelling errors, particularly for challenging scenarios.
- Non-sampled synthetic data indicates that small errors associated with fitting the MOL to non-sampled data are due to interval selection and the modelling resolution.
- Quota sampling reduces random errors by sampling the time interval consistently and ensuring that the beginning and end of the response is sampled. This method retains a degree of randomness to represent the stochastic nature of event occurrence.
- Twenty percent quota sampling is a reasonable trade-off between representing inherent uncertainty and consistent assessment of modelling errors.

- Three scenarios are assessed to evaluate the performance of temporal modelling:
  1. Seismic responses with early variation that include uniformly sampled  $N[0,20]$  events over an interval preceding the response of  $[0, 0.1]$ ;
  2. Short responses that have uniformly sampled end times  $[0.1, 2]$ ; and
  3. Inclusion of seismic independent seismicity by uniformly sampling 60 (high rate case) or 30 (low rate case) events over the response interval  $[0.001, 12]$ .
- These scenarios shared the following characteristics:
  - Continuous datasets of 5000 responses;
  - Uniformly sampled  $p[0.6,1.2]$  and  $K[5,20]$  parameters;
  - Constant  $c$ -parameter ( $c=0$ ); and
  - Constant time interval  $[0.001, 12]$  (except short responses).
- The following observations were made for performance analysis of response with early variation:
  - Using an overestimated temporal modelling window (36 h) the weighted MLE metric can delineate the interval for each response within a continuous dataset.
  - Increased error standard deviations for parameters along with the underestimation of some  $p$ -parameters, with respect to generation errors, show a small inclusion of errors due to temporal modelling.
  - A small population of responses ( $\approx 4\%$ ) have:
    - Low starting index;
    - High uncertainties in modelling parameters;
    - Low  $p$ -parameters ( $<0.75$ ); and
    - Low  $K$ -parameters ( $<10$ );
  - These responses have insufficient contrast to distinguish between the linear variation and response events. The start of the response is misidentified and cause of significant errors.
  - There is a small overall impact on analysis quality given the small portion of responses containing relatively few events and distinguishable by high uncertainty in parameters.

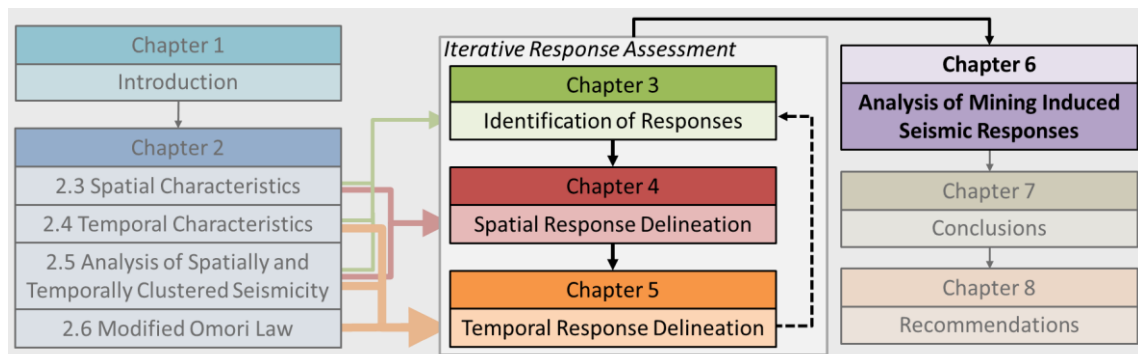
- The recovered length of the response is generally accurate with 80% of responses completely delineated. Underestimated length is sensitive to missing small portion of events that comprise late time intervals.
- Percentage error in event counts is more representative of the misallocation of individual seismic events. Errors in event counts are well constrained with  $\approx 95\%$  of responses between -5 and 5% error.
- The following observations were made for performance analysis of short responses:
  - Short durations cause the overestimation of the p-parameter and the underestimation of the K-parameter.
  - In comparison to the K-parameter, the recovery of p-parameters is less sensitive to the length of response durations.
  - Errors in parameter recovery significantly decrease for increasing response durations.
  - Length and event count distributions indicate that the vast majority of events and response lengths have been recovered.
- In summary, the following observations were made for performance analysis of responses including time-independent seismicity:
  - The portion of time-independent seismicity represents a significant challenge for temporal modelling to quantify and delineate responses. The portion of time-independent events is 15 to 65% of for the high rate case and 7.5 to 32.5% for the low rate case.
  - Temporal modelling time-independent seismicity causes the p-parameter to be consistently underestimated and K-parameter consistently overestimated.
  - Bifurcation occurs when the synthetic p-parameter is high. The two populations are related to the modelled length of responses and are more apparent for higher rates of time-independent.
  - To model responses accurately there must be sufficient temporal contrast between seismic generation processes.
  - If the temporal contrast is sufficient then the weighted MLE metric can identify when the time-dependent process ceases to dominate event generation and transitions to later times dominated by a time-independent process.

## 6 Assessment of Mining Induced Seismic Responses

### 6.1 Chapter Overview

This chapter applies the iterative assessment method developed in Chapter 3 (identification in space and time), Chapter 4 (spatial delineation), and Chapter 5 (temporal delineation) to investigate mining induced seismic responses. This chapter refers to the method established in the previous chapters as the STIDSR (spatially and temporally, identified and delineated, seismic responses) method.

This chapter provides context for the contribution of this thesis to academia and practical outcomes that can be utilised by the mining industry. This is achieved by application of the STIDSR method and additional analysis of the methods outcomes (**Figure 152**). While there is a wide scope of potential applications that utilise the outcomes of the STIDSR method, this chapter will focus on the relationship between seismic responses and routine blasting for a range of mining environments due to the wide applicability of the topic.



**Figure 152** Chapter 6 utilises the iterative assessment developed in previous chapters to spatially and temporally identify and delineate mining induced seismic responses.

### 6.2 Scope of Application

The topic of time-dependent seismicity and routine blasting is selected to demonstrate the capability of the STIDSR method to achieve the objectives (Section 1.3) and problem (Section 1.2) defined by this thesis. This chapter provides geotechnical discussions within the context of the qualitative and quantitative result of the STIDSR method. A comprehensive and robust geotechnical discussion is outside the scope of this thesis and requires consideration of additional seismic and non-seismic information (e.g., seismic source parameters, seismic moment tensors, numerical modelling, non-seismic monitoring, geological information, and geotechnical information).

Additionally, this chapter contributes to the practical approaches that can be utilised to evaluate the relationship between seismic responses and routine blasting to improve the management of seismic hazard.

This area of study has significant implications for mining operations that experience seismic events of sufficient magnitude to cause damage to excavations. Ultimately, the potential for seismicity to cause excavation failure translates to a workforce and operational hazard. The potential for seismic risk to adversely affect mining operations and the requirement for the mining industry to continually improve the management of seismic hazard is illustrated by the 2006 Anzac Day event at Beaconsfield Gold Mine (Hills & Penney 2008). In addition to significant economic loss, this event resulted in the loss of one life and a 14-day operation to rescue two trapped miners. The extensive review following this tragedy highlighted the importance of understanding the rock mass response to mining, changes to stress conditions, and mining induced seismicity. Furthermore, the review called for the refinement of methods that are used to manage short-term seismic hazard using re-entry protocols (Melick 2007).

The reviewed literature in Chapter 2 highlighted that a large number of studies attempt to develop re-entry protocol criteria without the quantification or delineation of mining induced seismic responses in space and time. Furthermore, the majority of these studies do not examine seismicity independently of causation processes. These studies do not allow for the evaluation of the space and time relationship between time-dependent seismicity and likely causation processes.

An additional consideration for the evaluation of seismic responses and their relationship to blasting is the role that site experience plays in the management of seismic hazard. Hudyma (2008) suggested that subjective decisions based on local experience form the basis of workplace closure and re-entry practices. Larsson (2004) discussed that most standard re-entry procedures require the contribution of experience from ground control engineers and management to make final decisions. In a survey of 18 seismically active mines, Vallejos and McKinnon (2008) found that re-entry protocols in over 70% of these mines were based on local experience due to large variation in seismic responses for a range of mining environments. Penney (2011) noted that site experience is used to extend minimum requirement set by re-entry protocols derived from retrospective analysis.

Although valuable insight is gained through site experience is important in managing seismic hazard, there are clear dangers associated with relying too heavily on unquantified personal impressions and interpretations. Mendecki (2008) discussed this topic in a broader context, suggesting that the use of human judgment to reduce complexities in the assessment of the

probabilities associated with seismic hazard may be subject to limitations of experience, interpretation, and motivational biases. The identification and delineation of seismic responses offers a methodology to prevent overreliance on subjective approaches evident throughout the mining industry.

A significant contrast exists between the management of a low seismic hazard response, e.g., development blasting resulting in few events associated with localised failure, and a high seismic hazard response, e.g., production blasting resulting in many events generated by geological structures. The seismic hazard of the former response may be effectively managed by a limited re-entry protocol and typical ground support. The latter response may require increased spatial and temporal exclusions to account for higher seismic hazard following blasting. Additionally, the hazardous response may also have broader implications for mining operations, including the management of future mining sequences that may result in similar seismic responses, planning of operations to account for longer re-entry restrictions, and optimising ground support requirements.

The contrast between these cases illustrates the need for a clear understanding of the characteristics of seismic responses. Identification and delineation of seismic responses allows the quantitative understanding of time-dependent seismic hazard to be developed. The quantitative component of seismic hazard is an essential aspect of analysis that removes subjectivity, increases the transparency of engineering decisions that may result in significant positive and negative political, social, and economic implications for the mine and associated stakeholders.

The assessment within this chapter is driven by the need for improvements in assessment of spatially and temporally dependent seismicity. The STIDSR method contributes to improving the understanding of the characteristics of seismic responses by achieving the objectives and addressing the problem defined by this thesis. The identification and delineation of seismic responses provides insight into two areas of interest:

- 1 Fundamental rock mechanics associated with mining induced seismicity:
  - a. Stress-strength state of the rock mass; and
  - b. Stress transfer mechanisms.
- 2 Seismic hazard associated with time-dependent rock mass failure:
  - a. Timing and location of seismic responses; and
  - b. Temporal quantification of seismic responses.

### 6.3 Seismic Data used for Analysis

The analysis in this chapter examines bulk and selective mining methods including caving, sub-level caving, and open stoping. These examples use seismic data obtained using seismic monitoring systems that range from average to excellent in quality with respect to sensitivity (i.e. range of consistent magnitude observation) and sensor placement (i.e. unbiased and accurate event location). The minimum local magnitude that is consistently observed for these systems ranges from -1.5M to -3M. Furthermore, these arrays all have sensors distributed in three dimensions and do not experience event location artefacts that may be associated with planar arrays (e.g. planar distribution of events or inverted locations perpendicular to the array orientation). The seismic data is used from both accelerometers and geophone monitoring systems. The specific configuration of these monitoring systems does not affect the selection of STIDSR parameters due to approaches taken to reduce the sensitivity of outcomes (previously discussed in Chapter 3.5).

The data presented in these examples has been filtered to exclude seismic events that fail general quality tests, e.g., very high uncertainty in locations, undetermined source parameters, and erroneously small or large source parameters. In addition to general quality filtering, events that are smaller than the minimum local magnitude that can be consistently observed are also excluded. These routine filtering practices are nonbiased in their application and are essential to achieving consistent and nonbiased analysis of a seismic dataset.

Due to the generalised nature of filtering, erroneous events may still be present in the database. The identification and delineation of seismic responses is not sensitive to these events due to their unique spatial and temporal characteristics. Seismic noise resulting from routine mining activities is commonly misidentified as seismic events, e.g., crusher operation or ore pass noise. Seismic noise may result in time-independent seismicity, although, these events may also be identified as very short seismic responses. Seismic noise is not considered further as it has a negligible impact on the interpretation of seismic responses. This is due to sources of noise being spatially confined to known locations and the implementation of quality filtering to remove seismic responses that are unreasonably short, modelled by erroneous parameters, or unsuitably modelled by the Modified Omori Law (MOL).

The results presented in this chapter have been sterilised to meet privacy requirements. When required, this includes the removal of coordinates systems, distinctive features of mining operations, and the discussion of site-specific details. Seismicity and blasting information has not been altered.

## 6.4 General Application as an Iterative Approach to the Identification and Delineation of Seismic Responses

### 6.4.1 Seismic Responses to Routine Blasting

The example presented in this section illustrates the ability of the STIDSR method to quantify seismicity associated with routine blasting for open stoping mining. Furthermore, this example discusses the practical aspects of implementing the iterative approach where seismicity is generally time-dependent and spatially clustered near development and production blasting. **Table 31** specifies the STIDSR parameters used for the analysis of seismic responses to routine blasting over three days. The temporal window, temporal modelling window, and lower count threshold are typical values used for most applications for the STIDSR method. The spatial window and tolerance is selected based on the extent and spatial distribution of events and are optimised by considering the CVNN index (Section 4.7.4). Typical weightings are used for selection of the temporal modelling interval (**Table 21**).

**Table 31** Identification and delineation parameters used for the analysis of responses to routine blasting.

Identification and Delineation Parameters	Initial Value	Iteration Increment
Spatial Window (m)	15	+15
Spatial Density Tolerance (%)	10	Constant
Temporal Window (h)	0.25	Constant
Lower Count Threshold (proportional method)	80% and >10 events	Constant
Temporal Modelling Window (h)	48	Constant

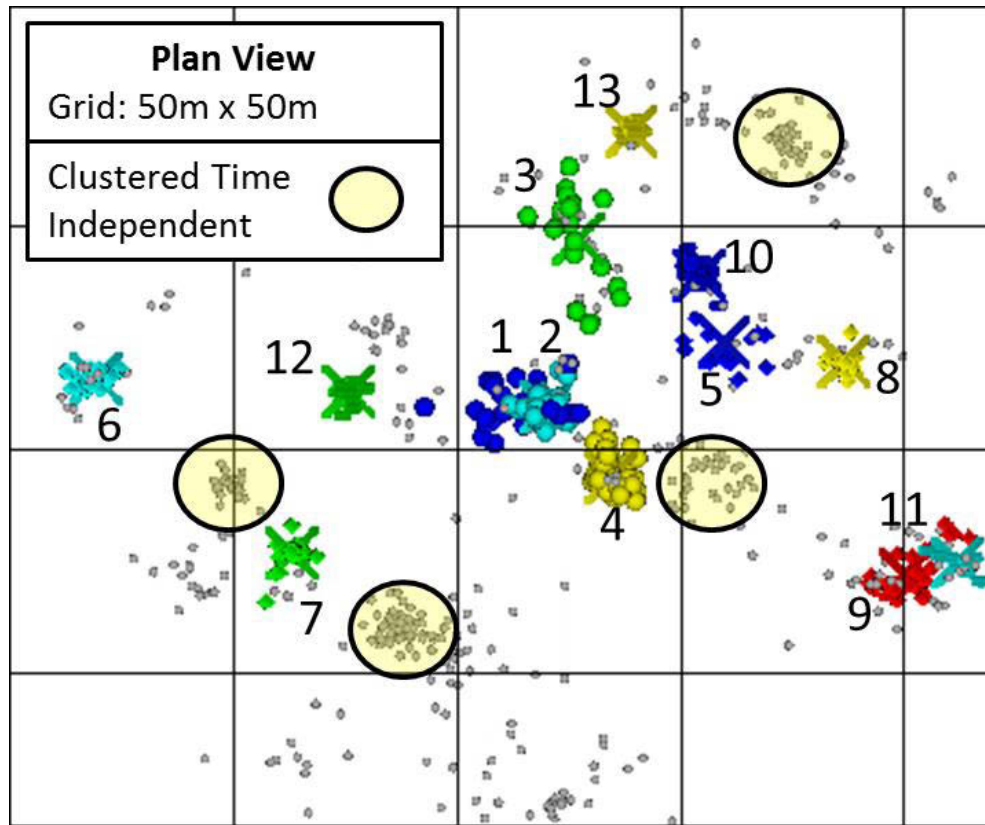
The algorithm first identifies and delineates densely clustered responses occurring on the scale of a space-time window, 15 m and 0.25 h, respectively. Using the same temporal parameters, the subsequent iterations identify seismic responses associated with failure processes occurring over larger spatial scales (30 then 45 m). While one to three responses occur during each shift (temporally superimposed), this analysis is insensitive to the temporal modelling window and spatial density tolerance parameters as there are very few subsequent spatially related events. As a result, delineation components do not capture unrelated seismicity unless extreme values are implemented. The optimisation of the CVNN index, in conjunction with manual assessment, ensures that responses are related to the scale of causation, i.e., scale of rock mass responses to blasting.

This assessment results in the identification and delineation of 13 seismic responses. Parameters found by the temporal quantification of responses and the corresponding iterative thresholds are detailed in **Table 32**, are spatially plotted in **Figure 153** (plan view), and shown on a cumulative event count over time in **Figure 154**. Responses are designated an ID in the table based on temporal order and are annotated by their corresponding ID in the spatial and temporal charts. Blasting occurs at the end of each 12 h shift for this mine (a specific blasting history is unavailable). For this example, a 12 h blasting periodicity correlates closely with the initiation time for all the seismic responses (6:00 and 18:00).

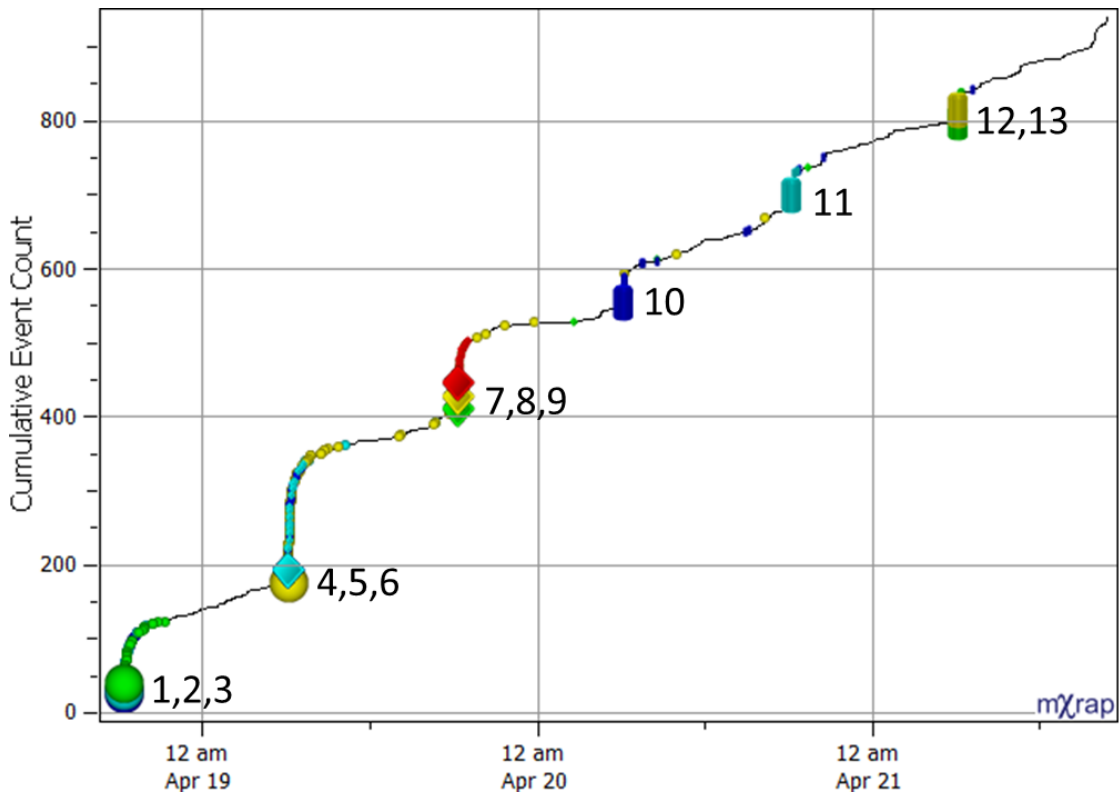
The responses are all suitably modelled by the MOL ( $AD < 1.5$ ). Four responses (ID 8, 11, 12, and 13) are very short ( $< 0.25$  h) and two of these responses (ID 8 and 13) have very high uncertainty in MOL parameters. These are examples of responses that are excluded to ensure only consistent parameters are considered for subsequent analysis. The final decision on acceptable response quality is guided by previous error analysis (Section 5.9) and the intended use of results. After the removal of these four responses from further consideration, quality responses are quantified by p-parameters within previously reported ranges (0.6-1.28) (Section 2.5.4), a range of K-parameters (0.7-10.3), and c-parameters equalling zero (except one response where  $c = 0.01$ ).

**Table 32** Quantification of MOL results and iterative thresholds for the 13 seismic responses identified. The chronological response ID corresponds to the spatial and temporal charts.

ID	Time	$T_S$	$T_E$	$p(\pm)$	$K(\pm)$	$c(\pm)$	AD	N	$S_T$	$C_T$	Iter.#
1	18/04 18:24:16	0.0001	0.9	0.84(0.13)	4.3(1.9)	0.00(0.00)	1.0	22	30	10	8
2	18/04 18:24:30	0.0044	35.5	1.28(0.12)	3.9(0.8)	0.01(0.01)	0.9	44	15	23	4
3	18/04 18:25:11	0.0037	2.9	0.74(0.17)	6.3(1.5)	0.00(0.01)	0.5	28	45	11	10
4	19/04 06:12:05	0.0001	34.1	1.16(0.06)	8.3(1.1)	0.00(0.00)	0.4	108	15	64	1
5	19/04 06:12:10	0.0005	0.9	0.66(0.17)	7.3(3.0)	0.00(0.00)	0.6	21	45	12	9
6	19/04 06:12:11	0.0003	1.0	0.96(0.12)	5.1(1.9)	0.00(0.00)	0.4	35	15	25	3
7	19/04 18:22:45	0.0001	25.1	1.20(0.09)	0.9(0.4)	0.00(0.00)	0.4	29	15	22	5
8	19/04 18:22:51	0.0002	0.1	1.72(222)	1.7(1508)	0.01(0.87)	1.0	13	15	11	7
9	19/04 18:23:02	0.0020	0.7	0.80(0.20)	10.3(4.5)	0.00(0.00)	0.5	34	15	15	6
10	20/04 06:12:06	0.0001	25.1	1.10(0.07)	2.3(0.6)	0.00(0.00)	1.1	39	15	29	2
11	20/04 18:19:39	0.0001	0.2	1.22(0.30)	0.7(0.8)	0.00(0.00)	1.0	13	15	15	6
12	21/04 06:10:50	0.0001	0.2	1.12(0.13)	1.3(0.9)	0.00(0.00)	1.4	24	15	22	5
13	21/04 06:10:55	0.0003	0.1	1.72(107)	1.3(580)	0.00(0.36)	0.2	15	15	15	6



**Figure 153** Spatial plot (plan view) showing 13 identified and delineated responses. Responses are plotted by marker styles corresponding to the time series chart and are annotated by ID. Strongly clustered, time-independent events are circled.



**Figure 154** Cumulative event count over time for clustered and non-clustered data. Each identified and delineated seismic response has the marker associated with the response ID.

The quantification of responses allows the development of an objective seismic history to blasting along with the identification of naturally occurring time-independent seismicity (or seismic noise). While these seismic responses are conceptually simple (immediate and localised stress redistribution), the development of characteristic seismic responses to known failure processes allows for seismic hazard associated with routine operations to be quantified. These responses provide an important contrast for future mining operations when seismicity can be associated with alternative rock mass failure processes. Seismicity caused by alternative processes may exhibit different spatial and temporal characteristics and may have a potentially higher seismic hazard. As a result, the quantification of seismic responses in space and time is important to identify when and where increased management of seismic hazard may be required to maintain acceptable levels of seismic risk.

This example shows the ability of the STIDSR method to address the problem defined by this thesis (Section 1.2) through achieving the required objectives (Section 1.3). The STIDSR method assesses seismic responses using only the time and location of seismic events. In this example, the occurrence of up to three responses following blasting during an individual shift shows the ability of the method to assess responses superimposed in time. Furthermore, responses 9 and 11 provide an example of seismic responses superimposed in space, although, offset in time. Responses 1 and 2 provide an example of responses superimposed in space and time, although, separated due to a sufficient difference in event density. The analysis is not sensitive to STIDSR parameters that have been selected based on the characteristics of mining and quantitative measures, e.g., CVNN index and temporal modelling outcomes.

#### **6.4.2 Response to a Large Seismic Event**

This example illustrates the ability of the STIDSR method to evaluate seismicity prior to a large seismic event and potential aftershocks. **Table 33** specifies the parameters used for identification and delineation of seismic responses for 12 h before and 36 h after the occurrence of a relatively large event. The algorithm parameters are consistent with the previous example (Section 6.4.1), with the exception of an increased spatial scale to capture larger seismic responses. Spatial parameters were optimised by considering the CVNN index.

**Table 33** Identification and delineation parameters used for the analysis of seismicity before and after a large seismic event.

Identification and Delineation Parameters	Initial Value	Iteration Increment
Spatial Window (m)	25	+25
Spatial Density Tolerance (%)	10	Constant
Temporal Window (h)	0.25	Constant
Lower Count Threshold (proportional method)	80% and >10 events	Constant
Temporal Modelling Window (h)	48	Constant

This assessment results in the identification and delineation of four seismic responses. These results are summarised in one table, a temporal figure, and a spatial figure:

- **Table 34:** Quantification and corresponding iterative thresholds for the seismic responses. A chronological ID is specified in this table and used in proceeding figures;
- **Figure 155:** Cumulative event counts over time for non-clustered (top) and clustered seismic events (bottom). Responses are coloured by magnitude (top). Events are coloured by response ID. Response initiation is represented by a cross; and
- **Figure 156:** Section and plan views for non-clustered events coloured by magnitude (top), and identified and delineated seismic responses (bottom). Seismic responses are coloured by ID and a cross indicates the mean location of the response.

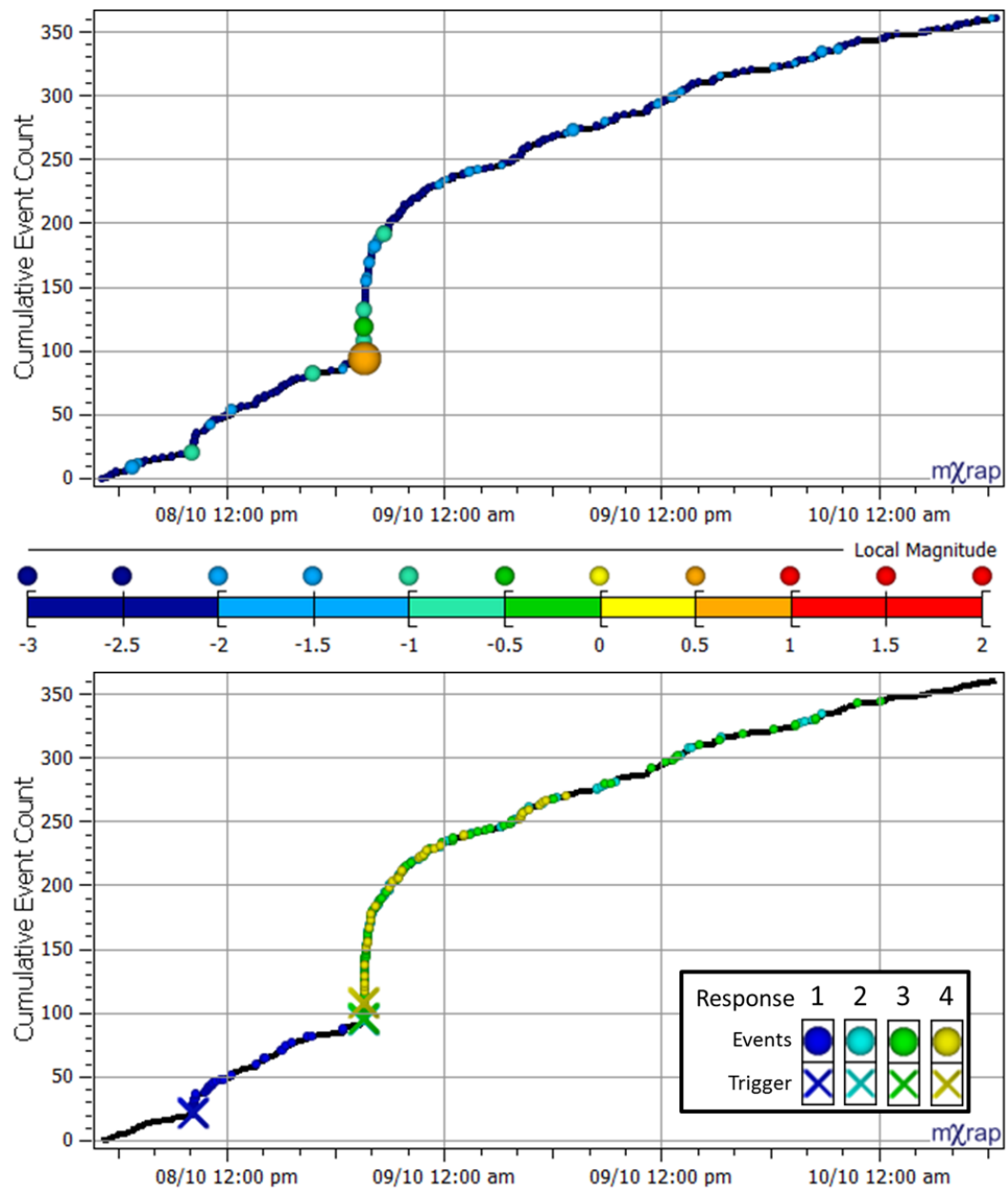
The four responses are populated by a significant number of events over long modelling intervals. MOL parameters are within expected ranges and the Anderson-Darling statistic indicates that responses are suitably modelled in time. These findings are reflected by the suitable temporal and spatial delineation apparent in **Figure 155** and **Figure 156**, respectively.

The first response to occur is a confined, relatively weak response (few events with a slow temporal decay). This response occurs in an approximately planar orientation within a region of relatively higher stress conditions associated with a rib pillar and the footwall abutment of the primary orebody. After approximately 9 h, a relatively large event ( $0.6M_L$ ) is immediately followed by two responses with very similar temporal characteristics. These two responses occur in the same planar orientation and occur within high stress conditions surrounding the primary and auxiliary orebodies. Additionally at this time, a seismic response (yellow) over a larger spatial scale (125 m) is observed. The centre of the seismic response (yellow cross) is located above the main responses due to additional events occurring throughout the wider area that are not shown in **Figure 156**.

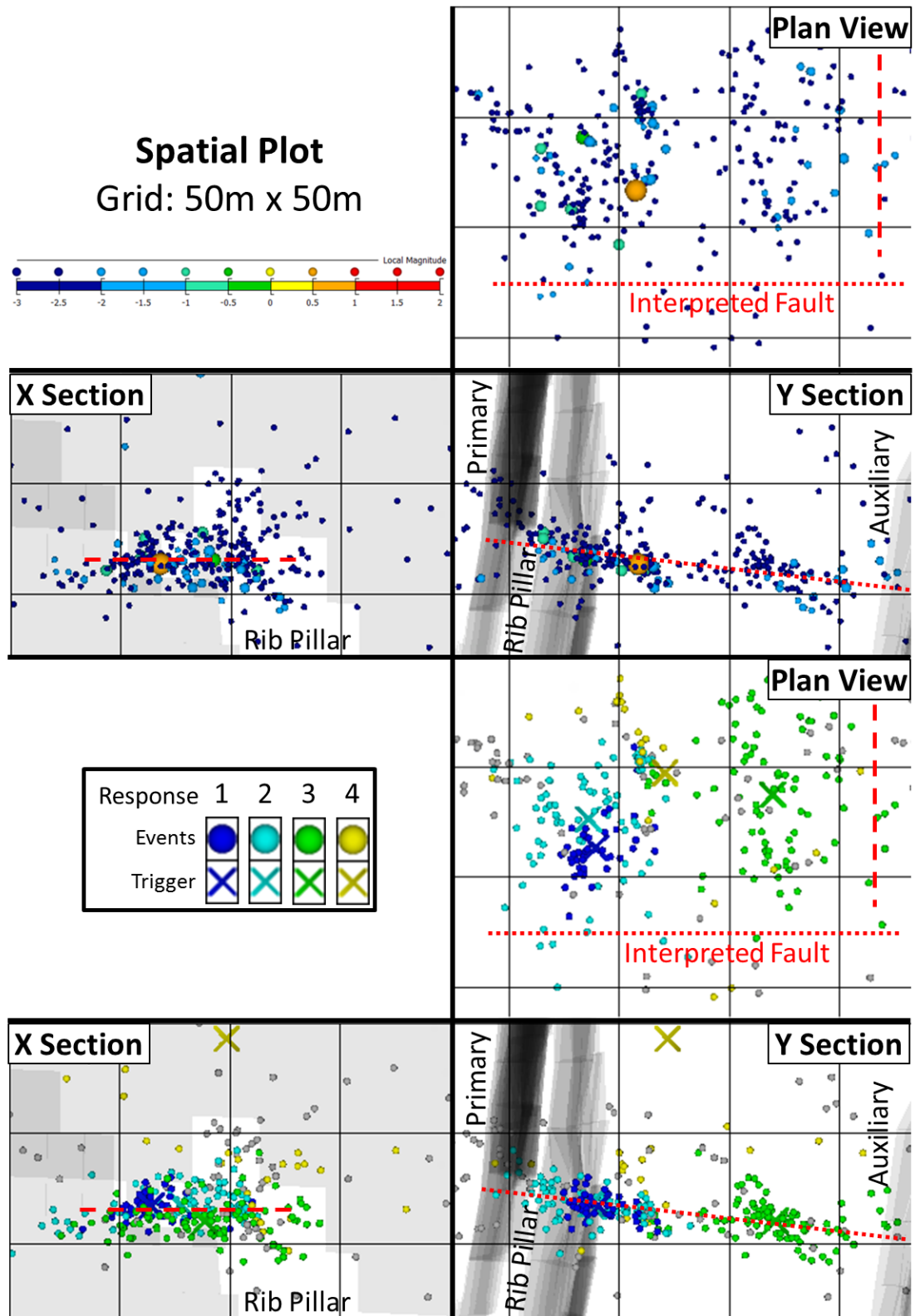
A single fault is interpreted to be the cause for the first three responses (dark blue, light blue, and green) due to the similar orientation and spatial scale (25 m) of this time-dependent seismicity. Seismicity also appears to be influenced by localised stress conditions associated with mining. Furthermore, the chance occurrence of an event of  $0.6M_L$  is not likely the sole cause of such a strong, large-scale, aftershock response. This assertion is largely dependent on the site-specific, historical quantification of responses proceeding similar magnitude events. The occurrence of a response (dark blue) shortly before this event supports the notion of time-dependent deformation recently occurring along this fault.

**Table 34** Chronological ID, quantification, and corresponding iterative thresholds for the seismic responses before and after a large seismic event.

ID	Time	$T_S$	$T_E$	$p(\pm)$	$K(\pm)$	$c(\pm)$	AD	N	$S_T$	$C_T$	Iter.#
1	08/10 10:08:50	0.0006	9.4	0.74(0.09)	5.9(1.0)	0.00(0.00)	0.4	39	25	14	2
2	08/10 19:35:40	0.0003	25.3	0.86(0.09)	10.9(1.7)	0.02(0.02)	0.5	78	25	14	2
3	08/10 19:35:42	0.0003	28.5	0.86(0.05)	10.1(1.1)	0.00(0.00)	0.5	91	25	15	1
4	08/10 19:35:55	0.0122	11.1	0.66(0.14)	5.9(1.2)	0.00(0.03)	0.7	37	125	5	3



**Figure 155** Cumulative event counts over time for non-clustered (top: coloured by magnitude) and clustered events (bottom: coloured by response ID). The initiation of a response is represented by crosses coloured by response ID.



**Figure 156** Section and plan views for non-clustered events (top), and identified and delineated seismic responses (bottom). Grey shapes represent production and mining excavations (not shown on plan view). Crosses represent the response centre and are coloured by response ID.

The identification, delineation, and quantification of these responses provide insight into the fundamental rock mechanics associated with the time-dependent deformation of this fault and the surrounding area. The identification of a response prior to a large event indicates this fault was seismically active and undergoing time-dependent deformation. It is important to distinguish that this behaviour is not considered as a predictive precursor to a large event. Responses following the large event provide a clear temporal and spatial quantification and delineation of seismicity created by the subsequent local stress redistribution. Furthermore, the observation of an additional, delocalised response suggests that after this event an additional, minor stress redistribution process occurs throughout the mining environment.

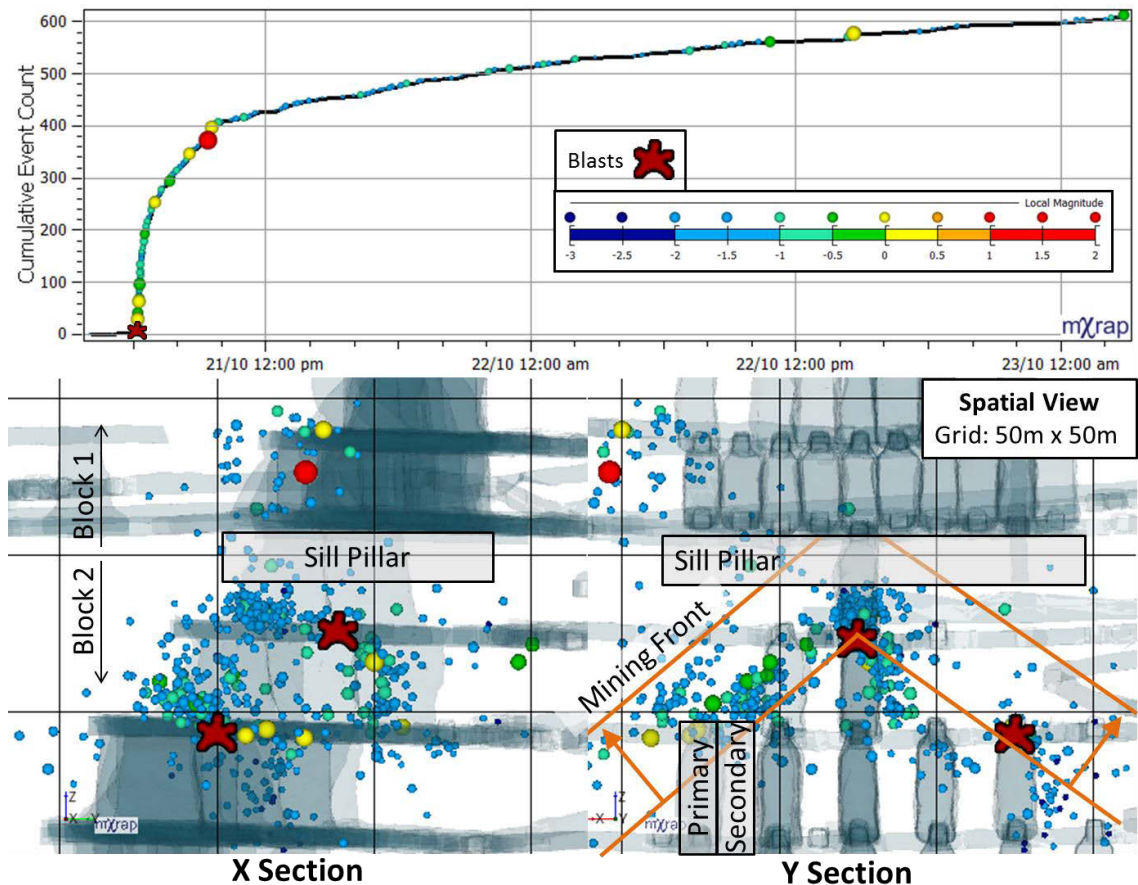
The identification and delineation of these seismic responses has important implications for fundamental rock mechanics and the management of seismic hazard during this period:

- Prior to the large event, an elevated rate of seismicity associated with the initial response indicates an elevated time-dependent seismic hazard in the area; and
- The following responses indicate further elevated time-dependent seismic hazard that is closely associated with the faulting causation process, and more ambiguously associated with stress redistribution throughout the mine.

The STIDSR method enabled the analysis of seismic responses before and after a large event by only evaluating the timing and location of events and being capable of delineating spatially and temporally superimposed seismicity of varying densities. It is acknowledged that some subjectivity remains in parameter selection, particularly the spatial clustering component, although, being able to optimise the spatial input parameters by evaluating the CVNN index reduces the degree that subjectivity can influence outcomes.

### 6.4.3 Complex Response to Mining

This example illustrates the ability of the STIDSR method to evaluate a complex response to mining. The example contains two blasts and a large seismic event that simultaneously created seismic responses in a number of spatial clusters. **Figure 157** provides a general overview of this example. Shown top is the cumulative event count over time following two blasts in this area of the mine. During the productive seismic response, a large event occurs that also appears to influence seismic event rates. Shown bottom is the spatial plot of seismicity during this period (coloured and sized by magnitude) and mining excavations. This example examines the mining of a chevron primary-secondary stoping sequence. Stresses are concentrated in the crown and abutment of stopes, and increase as the upper most primary stopes influence the sill pillar that separates mining blocks. A significant amount of time-dependent seismicity is commonly observed within these volumes of high stress conditions, when additional stress changes are induced, e.g., blasting.



**Figure 157** A cumulative event count over time following two blasts (top) and a spatial plot of seismicity during this period (coloured and sized by magnitude) and annotated mining excavations (bottom).

**Table 35** specifies the identification and delineation parameters used for the analysis of the two-day period following the initiation of a complex response. The algorithm parameters are the same as the first (Section 6.4.1) and second example with the exception of the spatial window (Section 6.4.2).

**Table 35** Identification and delineation parameters used for the analysis of a complex response.

Identification and Delineation Parameters	Initial Value	Iteration Increment
Spatial Window (m)	15	+15
Spatial Density Tolerance (%)	10	Constant
Temporal Window (h)	0.25	Constant
Lower Count Threshold (proportional method)	80% and >10 events	Constant
Temporal Modelling Window (h)	48	Constant

This assessment results in the identification and delineation of six seismic responses in space and time. **Table 36** provides the quantification of responses and corresponding iterative thresholds for each seismic response. **Figure 158** shows the temporal occurrence over time (top) and spatial occurrence with respect to blasting and the large event (bottom).

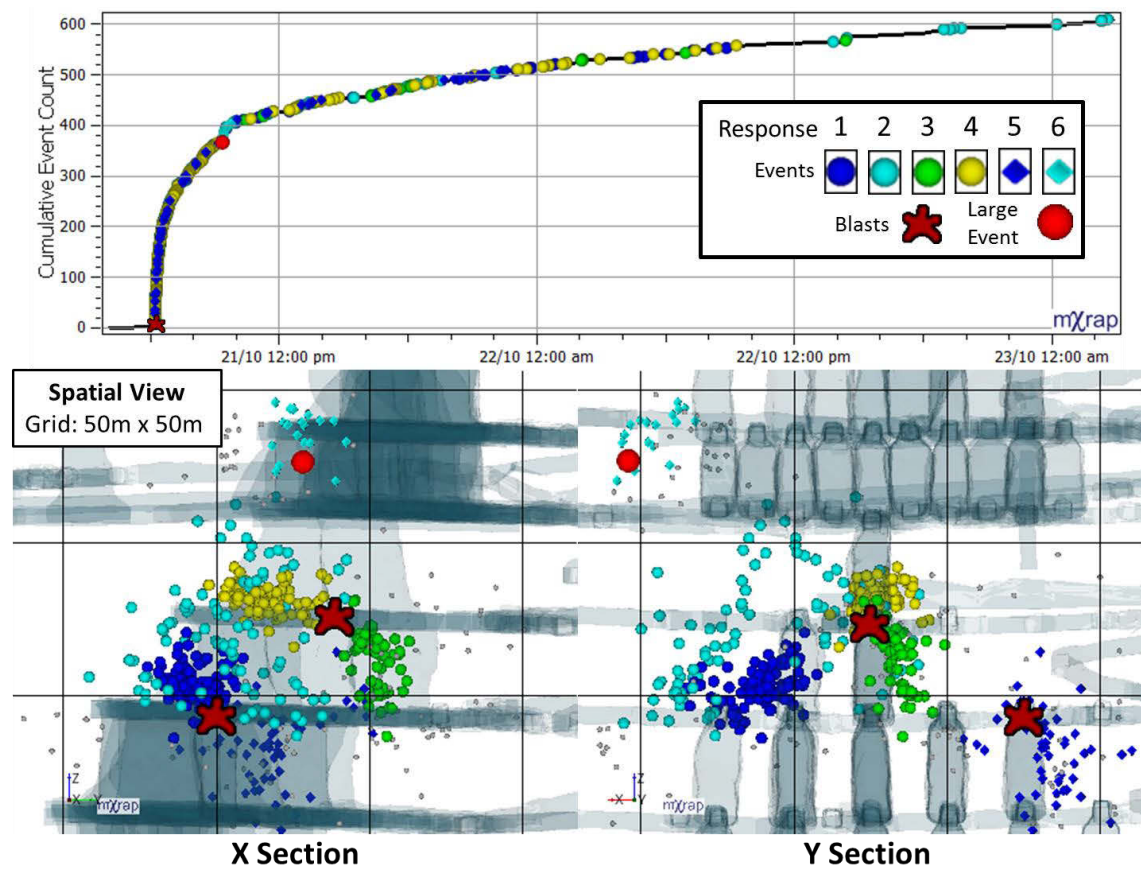
All responses are suitably modelled by the MOL ( $AD \leq 1.1$ ). The responses that were temporally related to blasting (at  $\approx 6:15$  am) share similar decay ( $0.9 \leq p \leq 1.18$ ) and productivity ( $10.5 \leq K \leq 19.9$ ), with the exception of Response 5 that was less productive ( $K=8.1$ ), exhibited a slower decay ( $p=0.78$ ), and identified on a relatively sparser spatial scale (30 m).

Response 2 (light blue sphere) also occurred on a sparser spatial scale (30 m) and is associated with the more widespread redistribution of stress along the chevron profile as opposed to a localised failure process (e.g., Responses 1, 3, and 4). While this response occurs on a different spatial scale, the temporal quantification of this seismicity is not significantly different to parameters associated with the dense spatial responses.

The response following a large event later in the period is interpreted to be associated with the abutment of the shallower mining block. While this short response (0.4 h) was suitably modelled by the MOL ( $AD=0.9$ ), there were higher uncertainties associated with parameters. The increased parameter uncertainty is due to the short duration and relatively few events associated with the response. This is an important feature of quantification as it provides a measure of confidence in results.

**Table 36** Chronological ID, quantification, and corresponding iterative thresholds for each seismic response for a complex example.

ID	Time	$T_S$	$T_E$	$p(\pm)$	$K(\pm)$	$c(\pm)$	AD	N	$S_T$	$C_T$	Iter.#
1	21/10 06:14:52	0.0002	26.6	0.90(0.05)	11.9(1.3)	0.00(0.00)	0.6	100	15	33	1
2	21/10 06:15:00	0.0019	46.5	0.92(0.06)	10.7(1.3)	0.01(0.01)	0.8	94	30	12	4
3	21/10 06:15:01	0.0001	32.2	1.18(0.10)	10.5(1.7)	0.04(0.02)	1.1	77	15	33	1
4	21/10 06:15:07	0.0040	27.1	0.96(0.08)	19.9(3.0)	0.05(0.04)	0.5	128	15	33	1
5	21/10 06:15:16	0.0030	16.3	0.78(0.11)	8.1(1.4)	0.01(0.02)	0.9	55	30	15	3
6	21/10 09:25:18	0.0012	0.4	1.04(0.31)	2.9(2.5)	0.00(0.00)	0.9	19	15	11	2



**Figure 158** Cumulative event count over time following two blasts (top) and a spatial plot of mining excavations and seismicity during this period (bottom). The events for each response are coloured and shaped corresponding to their chronological ID.

The benefits of the identification and delineation of seismic responses are congruent to Sections 6.4.1 and 6.4.2. This example presented a period containing multiple responses that are ambiguous to delineate spatially and temporally. In addition to being temporally superimposed, these responses have small spatial separations and small differences in relative spatial scales. This analysis allows for the spatial and temporal relationship between blasting, large events, and seismic responses to be consistently assessed. These responses provide

insight into the rock mass failure processes that are related directly and indirectly to causation processes and, hence, insight into the stress redistribution process associated with blasting during this period. The seismicity associated with each of these individual processes has been quantified and can be translated to short-term seismic hazard.

The STIDSR method enabled the separation of individual responses through its ability to assess temporally superimposed responses of different spatial distributions. The examples presented in Sections 6.4.1 and 6.4.2 are relatively unambiguous to spatially cluster and, therefore, not sensitive to spatial parameters. These parameters are the most subjective aspect of the STIDSR method. This section's example has a less clear spatial distribution of events and, hence, there is an increased potential for subjective spatial clustering to influence outcomes. The ambiguity also means that it is harder to preconceive what spatial clusters should be delineated and, therefore, there is an increased reliance on optimising the CVNN index to determine appropriate responses. Quantifying the internal performance of spatial delineation is important to validating spatial parameters for simple responses and plays a critical role in guiding the selection of appropriate parameters for complex spatial distributions. The STIDSR method acts to minimise the subjectivity associated with assessment in both simple and complex cases and, thus, contributes to achieving thesis objectives (Section 1.3).

## 6.5 Seismic Responses and Blasting

Analysis of the spatial and temporal occurrence of seismic responses can be combined with sources of additional information to achieve further insight into the causation of seismicity. Information may include the seismic database, e.g., magnitude of the event preceding a response, or information pertaining to mining operations, e.g., blasting records or volume mined. Analysis of seismic responses makes an essential contribution to the management of seismic hazard through an improved understanding of the conditions that may result in time-dependent seismicity. This section focuses on the relationship between seismic responses and blasting in a mining environment. The STIDSR method enables the identification of seismic responses independently of blasting by using only spatial and temporal seismic parameters. In addition, this section shows the ability of the method to identify spatially or temporally superimposed responses allowing for the classification of the relationship between individual responses and blasting. This is important as multiple distinct sources of seismicity may respond to a single blast. Furthermore, rather than the examples presented in Section 6.4 that assessed small datasets, e.g., 3 days, this analysis uses seismicity that occurs over years of mining. This shows the applicability of the STIDSR method to large datasets that contain responses with a range of spatial and temporal characteristics.

### 6.5.1 Classification of the Relationship between Seismic Responses and Blasting

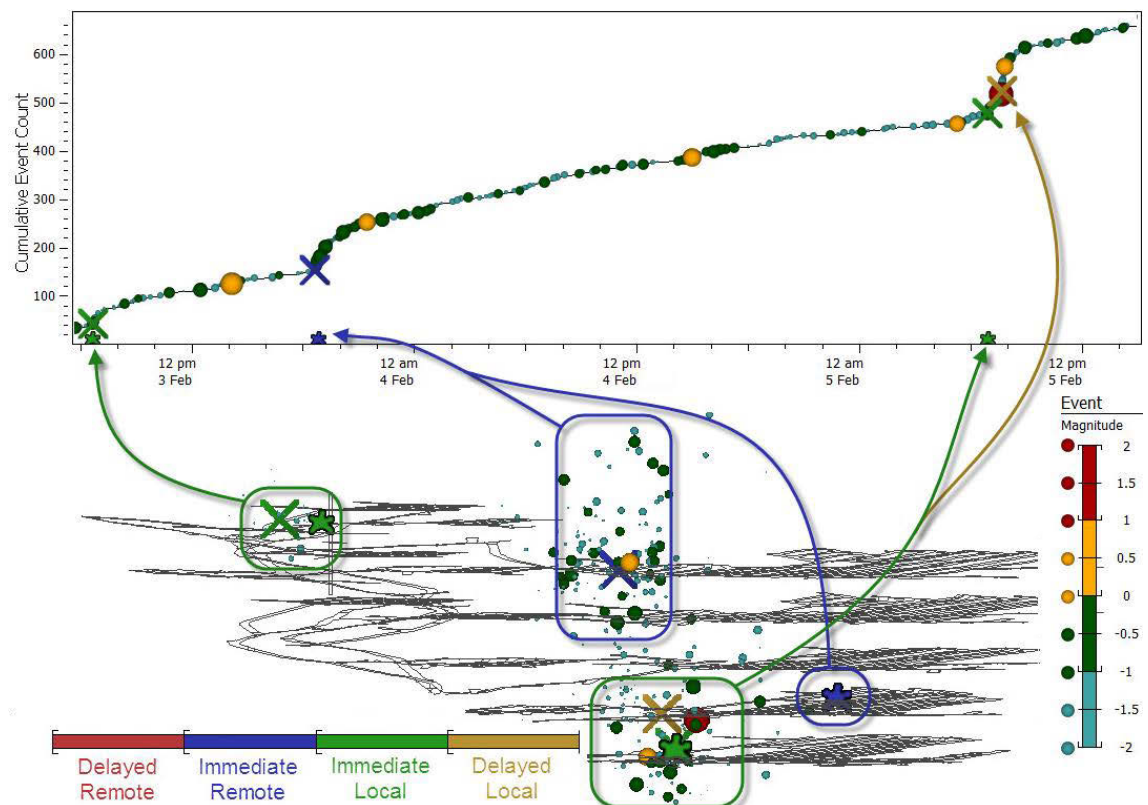
A classification scheme is proposed to enable the consistent assessment of the spatial and temporal relationship between seismic responses and blasting. This scheme uses four generalised cases defined to characterise the spatial and temporal relationship between responses and blasting (**Table 37**). While multiple blasts and responses may occur concurrently, these spatial and temporal relationships are limited to consider one blast and one response. Relationships are found by assessing the closest historical blast in space and time for every response. The closeness is defined from a simple additive measure of absolute time units (hours) and space units (metres). Classification of the relationship between responses and blasts are defined by considering the spatial influence of blasting, scale of sources of seismicity in the mining environment, the timing, and location accuracy of blast records, and the performance of the seismic array. A response's closest blast is not necessarily the blast's closest response as multiple responses can occur at the same time. For this reason, the spatial and temporal relationship for blasts requires the assessment of the closest subsequent response in space and time. The plots within this chapter show the relationship for each response's closest blast, or each blast's closest response. Note that blasts cannot be allocated a *remote and delayed* relationship. In addition to this section, the classification scheme is also used in Sections 6.6 and 6.7.

**Table 37** Four cases characterising the spatial and temporal relationship between a response and blasting in the temporal (top diagram) and spatial (bottom diagram) domain. The diagrams show a blast (orange), initial response (red), and delayed/remote response (green).

Case	Description	Conceptual Diagram
<b>Local and Immediate</b>	<p><b>Case</b> An immediate seismic response is limited to the volume subjected to initial stress change.</p> <p><b>Cause</b> Typical case of induced seismicity associated with blasting and large seismic events.</p>	
<b>Remote and Immediate</b>	<p><b>Case</b> Seismicity has increased in a volume remote to the initial blast.</p> <p><b>Cause</b> Volumes of rock mass close to failure respond to a remote blast resulting in a triggered response.</p>	
<b>Local and Delayed</b>	<p><b>Case</b> Seismicity has increased abruptly after some delay in the volume of rock mass subjected to blasting.</p> <p><b>Cause</b> Superimposition of time-dependent stress redistribution processes. Stress redistribution due to large seismic events within a local and immediate response.</p>	
<b>Remote and Delayed</b>	<p><b>Case</b> Response occurs in a volume that is remote and delayed to blasting.</p> <p><b>Cause</b> It is not possible to relate the response to a stress change with any significant confidence.</p>	

An example of response classifications is shown in **Figure 159** that displays cumulative event count over time and a perspective view of seismicity for a three-day period. Response classification uses arbitrarily defined spatial and temporal thresholds. Responses more than 50 m away from a blast are remote (up to 200 m) and responses 1 h after a blast are delayed (up to 6 h). Responses are assigned as *remote and delayed* if they occur outside of the upper 200 m or 6 h limits, although none occur during this period. Three distinctly different responses are shown in the figure:

- **Local and immediate response:** A response occurs on February 3<sup>rd</sup> at 6:30 am (green arrow and markers). This response is closely related to blasting.
- **Remote response:** The following shift (12 h later), a response occurs on February 3<sup>rd</sup> at 6:30 pm (blue arrows and markers). This remote response is identified at the same time, although, 130 m away from this shifts blasting. This response is associated with rock mass instability remote to blasting.
- **Delayed response:** A delayed response occurs with a large event (brown arrow and markers) following a *local and immediate* response to blasting (green arrow and markers) associated with blasting on February 5<sup>th</sup> at 6:30 pm. The occurrence of a delayed response indicates further stress redistribution.



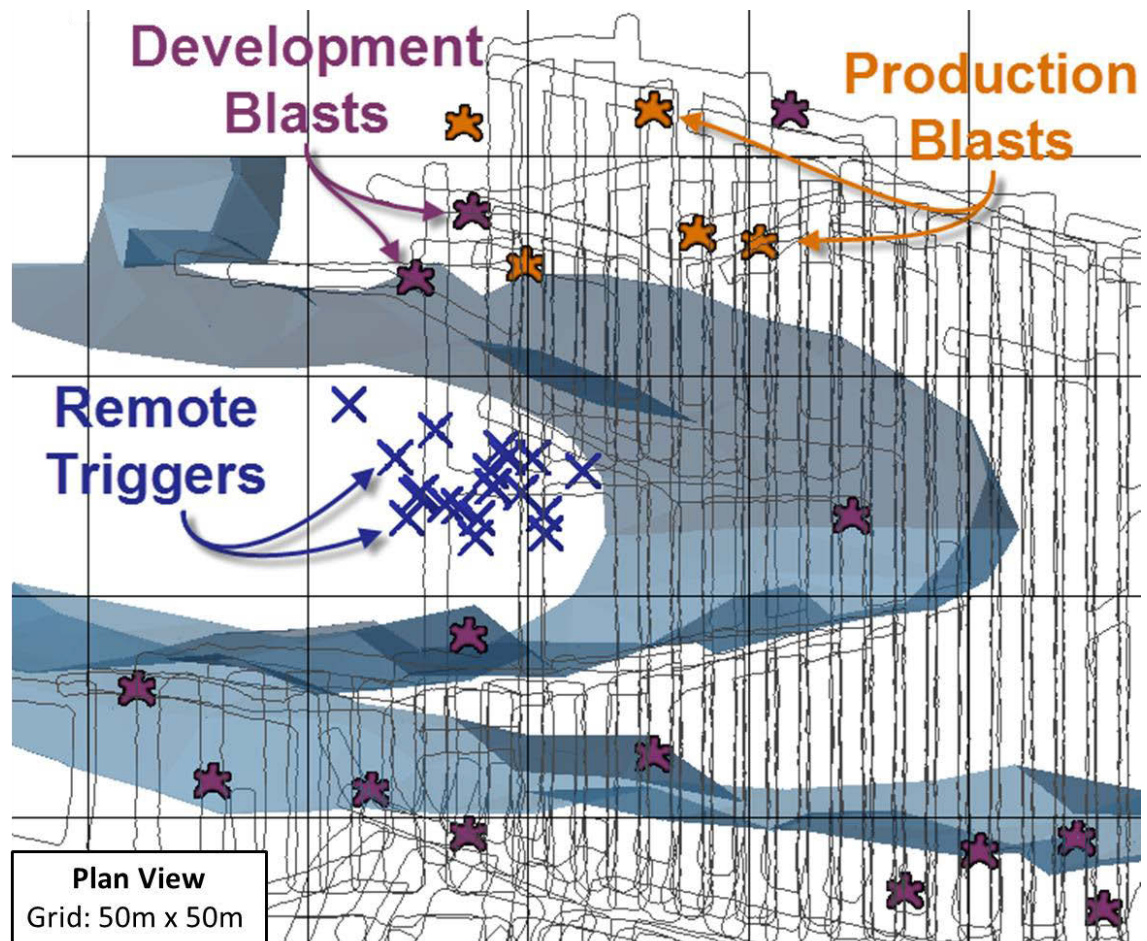
**Figure 159** A cumulative count plot (top) and a spatial view of seismicity (bottom). A 3-day period illustrates the variable spatial and temporal relationship between responses and blasting.

### 6.5.2 Responses Remote from Blasting

Seismic responses that remotely respond to blasting are associated with significant uncertainty due to the poorly understood, indirect causation of rock mass instability. Retrospective assessment allows for increased confidence in the observation of specific response relationships with respect to the mining environment. Consistent occurrence in space and time of *remote and immediate* responses reduces the probability that *remote and delayed* responses have been misidentified. Furthermore, consistency allows for increased confidence in the conditions that may result in specific seismic responses. Volumes of rock mass that respond remotely to blasting are particularly important for further consideration if the source is associated with high seismic hazard, e.g., a fault in close proximity to active workings. The management of remote responses should be emphasised when sources of seismicity exhibit signs of experiencing a stress state close to failure, e.g., strong seismic responses to blasting along with high rates of time-independent seismicity.

**Figure 160** illustrates spatially concentrated *remote and immediate* responses that are associated with production and development blasting. A significant number of these responses consistently centre on a volume of rock mass devoid of blasting and is spatially constrained by a geological contact (blue transparent surface) and mining geometry (black survey outlines). This volume of rock mass also experiences high rates of time-independent seismicity along with *remote and delayed* responses (not shown in the figure). The occurrence of responses and high time-independent rates indicates that the volume of rock mass experiences a stress state close to failure. The observation of *remote and immediate* responses highlights the potential for blasting to influence the stability of this source of seismicity. Responses that occur within the rock mass indicate that stability is sensitive to stress changes 50 to 200 m away, irrespective of whether the response is associated with development (350 t) blasts or larger production blasts (1,000 t to 10,000 t).

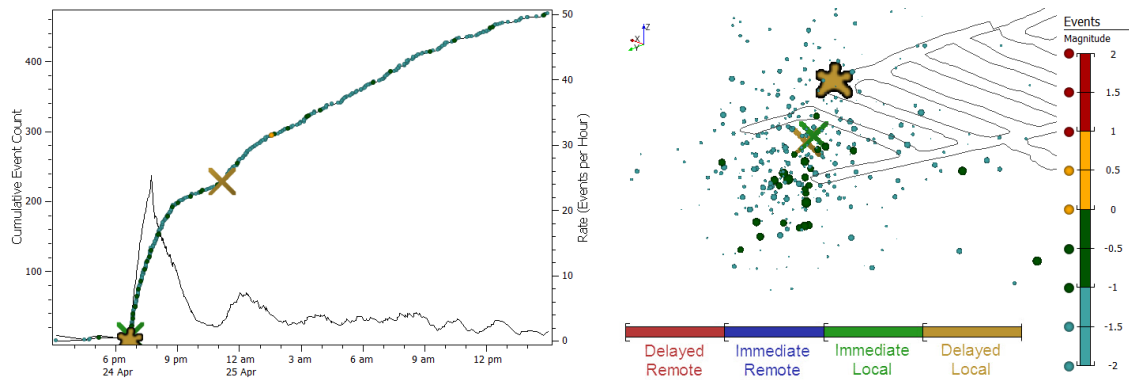
The STIDSR method enables the objective analysis of seismic responses and allows increased confidence to be developed in unexpected results. Remote triggering is a contentious issue due to the uncertainty surrounding the mechanism of stress transfer that creates rock mass instability. Although not the focus of reviewed literature, the STIDSR method provides the most definitive examples known to the author of the remote triggering of mining induced seismicity. These observations are enabled by the STIDSR method achieving thesis objectives (Section 1.3).



**Figure 160** Plan view of remote responses (blue) associated with a geological and geometrical defined source of seismicity. Also shown are production (orange) and development blasts (purple).

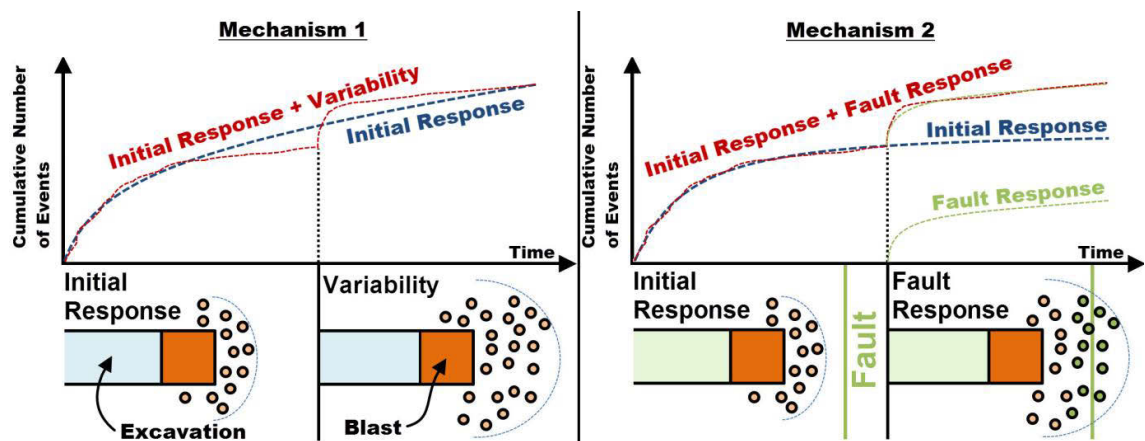
### 6.5.3 Responses Delayed from Blasting

Seismicity that is clustered in space and increases abruptly after a time delay from blasting is identified to be a delayed response. Delayed responses do not occur without an initial *local and immediate* seismic response to blasting. **Figure 161** provides an example of a delayed seismic response. An initial response is located close to blasting in space and time (green cross). A new response occurs after 4.5 h that is located close to the first response (green and brown cross). This second response is considered a *local and delayed* response.



**Figure 161** Cumulative events count, event rate, and time of response identifications (left). Modelled events and mean response location are shown with surveys and blasting (right).

The renewed elevated rates of seismicity associated with a delayed response correspond to renewed heightened seismic hazard if the underlying rock mass failure mechanism remains consistent. In the absence of an observable causation process, two hypothetical physical mechanisms of rock mass failure are proposed that may result in the occurrence of a delayed response following blasting. The first physical mechanism may result from a single time-dependent rock mass failure process that contributes to a population of self-similar seismic events. The variability in the generation of seismicity may arise due to further stress redistribution associated with additional events, and/or the stochastic nature of time occurrence (**Figure 162** left). The second physical mechanism requires the time-dependent initiation of a failure process in addition to the initial time-dependent rock mass failure (**Figure 162** right). The identification of a delay response has significant implications for the management of seismic hazard if the second process is relatively more or less hazardous.



**Figure 162** Two physical mechanisms illustrated using theoretical cumulative event counts for mechanism 1 (variability of one response) and 2 (superimposition of two responses).

Similar to the observation of remote responses in Section 6.5.2, delayed responses are also contentious due to uncertainty surrounding stress transfer mechanisms. The objective analysis of seismic responses enabled by the STIDSR method allows delayed responses to be evaluated consistently. This is achieved by incorporation of the suitability of fit to decide if the variability observed is too great to be associated with an initial response. Furthermore, validity of this classification of response is developed by allowing similar scenarios to be identified and is enabled by retrospectively applying the STIDSR method to large datasets.

#### 6.5.4 Proportionality of Response Classifications

The assessment of the response classification proportionality determines what percentage of identified responses fall into each classification and provides an indication of the sources of seismicity that may be present in a particular mining environment.

**Table 38** provides the proportional counts of response classifications for two mines. At Mine 1 (narrow vein stoping), the significant majority (78%) of all responses occur *locally and immediately* after blasting with low proportions of *remote or delayed* responses to blasting. In comparison, Mine 2 (sublevel caving) only experiences 32% of all responses *locally and immediately* after blasting, indicating that responses are influenced by relatively more complex stress conditions. This interpretation is supported by 16% of all responses occurring *remotely and immediately* after blasting (compared to none for Mine 1) and indicates that volumes of rock mass close to failure may be influenced by remote blasting.

Mine 1 experienced 18% of responses *remote and delayed* to blasting in comparison to Mine 2 that experienced 47% of responses outside of blasting times and locations. The causation processes associated with this type of time-dependent seismicity are unknown and, therefore, determining when re-entry protocols may be ambiguous and inevitably less effective. The practical management of seismic hazard associated with *remote and delayed* responses requires an increased emphasis on other management approaches and, therefore, it is essential to develop an understanding of the location and proportions of these responses.

**Table 38** Proportional counts of response classifications for two contrasting mining environments.

Case	Local and Immediate	Remote and Immediate	Local and Delayed	Remote and Delayed
Mine 1	78%	0%	4%	18%
Mine 2	32%	16%	5%	47%

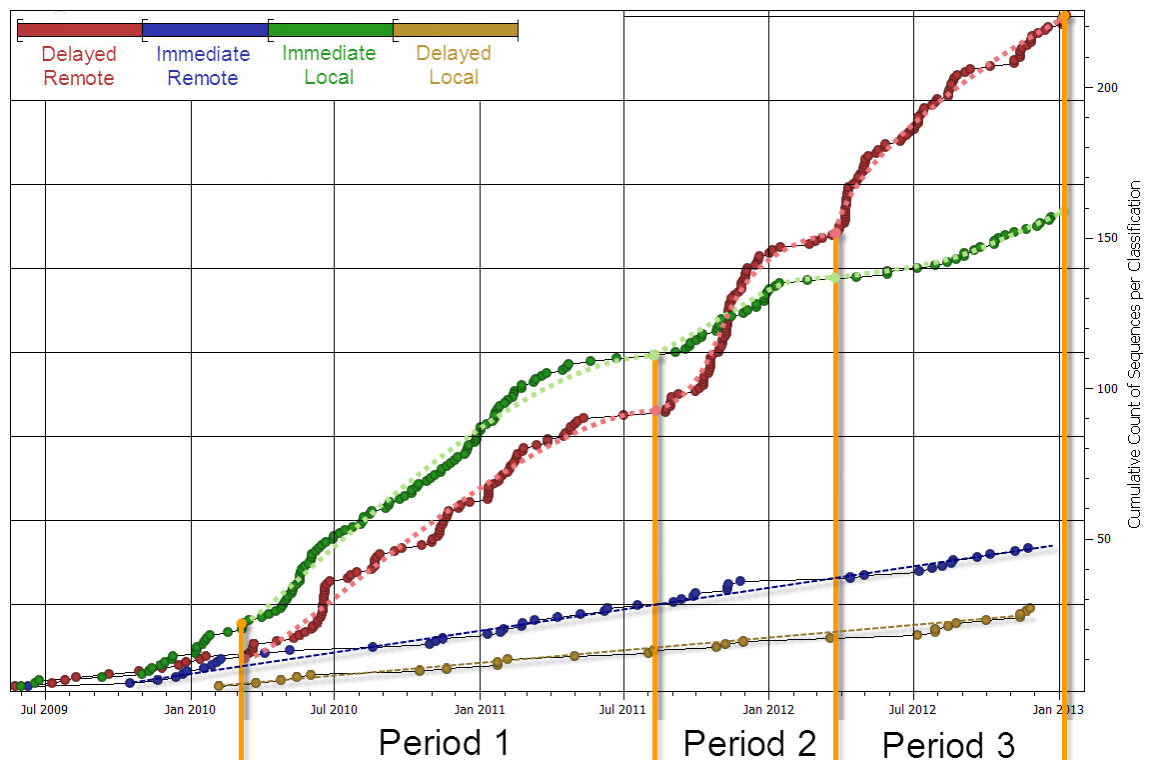
The proportional measure of the responses provides an indication of the spatially and temporally clustered seismicity that is closely related to blasting and, therefore, can be expected to be captured using traditional approaches to re-entry protocols. Responses that are

not directly related to blasting require additional re-entry exclusions and complementary management approaches. The underlying seismic hazard associated with *remote/delayed* responses may be similar to *local and immediate* responses. The seismic risk associated with *remote/delayed* responses will inevitably be elevated if these cases are not considered in the management of time-dependent hazards. Furthermore, proportional representation indicates the degree to which different stress redistribution mechanisms may influence time-dependent seismicity within a mining environment.

Assessment of the proportionality of seismic responses relationships is enabled by the STIDSR method achieving thesis outcomes. While achieving all thesis outcomes is required for this assessment, the results specifically highlights the analysis methods possible by only considering spatial and temporal aspects of seismic responses, and introduces the application of the STIDSR method to a large dataset.

### 6.5.5 Temporal Evolution of Response Classifications

The progressive influence of mining can be examined through the accumulation of individual responses over time based on response classifications. **Figure 163** shows trends in the relative rate of occurrence between response classifications. *Remote and immediate* and *local and delayed* responses occur consistently over the period considered, although further consideration is restricted due to the limited number of responses.



**Figure 163** Cumulative count of each response classification over time. Trends are drawn for periods of occurrence rates for local and immediate (green) and remote and delayed responses (red).

*Local and immediate*, and *remote and delayed* responses are characterised by three periods that are related to the progression of mining:

1. **Period 1:** Mining of the established regions resulting in proportional generation of seismic responses closely related to blasting (green) and independent responses (red).
2. **Period 2:** Several new headings are mined which are oriented perpendicular to the major principal stress direction and in close proximity to geological features. There is a strongly disproportional generation of seismic responses with significantly more independent responses (red) occurring relative to those related to blasting (green).
3. **Period 3:** The headings mined in the previous period continue to be developed deeper in the mine. The disproportional generation of seismic responses that was evident from the previous period resumes with more independent responses (red) occurring relative to those related to blasting (green). The discrepancy between the number of independent and blasting related responses is not as large as the previous period.

Trends in the spatial and temporal relationship between responses and blasting infer how the rock mass is evolving to the progression of mining. This relationship is essential to understanding how well time-dependent seismic hazard can be managed. Furthermore, this information may prove valuable in developing long-term management strategies that seek to control future mining conditions that contribute to sources of *remote and delayed* responses, as workforce exposure to this type of time-dependent seismicity typically cannot be limited.

Congruently to Section 6.5.4, the analysis of the temporal evolutions in seismic responses relationships is enabled by the STIDSR method achieving thesis outcomes. This section introduces retrospective analysis by defining seismic responses from only spatial and temporal attributes from a large dataset.

## 6.6 Evolution of Mining Induced Seismic Responses

The assessment of the evolution of seismic responses is challenging due to the difficulty in quantifying mining conditions (influence of geology, existing and induced stress conditions etc.). Seismicity associated with a block caving mining method provides structure to the evolution of mining conditions as the progressive nature of undercut blasting results in a systematic increase in stress conditions. While variation in conditions still exists, the block caving mining method creates distinct rock mass failure mechanisms associated with undercut blasting and the caving process. Block caving offers a structured seismic dataset to examine the quantification of seismic responses and their relationship to blasting.

This section shows the practical application of the STIDSR method to a large dataset containing seismic responses that range in attributes, and reiterates the ability of the STIDSR method to address thesis outcomes (Section 1.3) by specifically considering:

- Spatial and temporal parameters for the identification of responses;
- Superimposition of responses in space and/or time;
- Identification and delineation of responses for a range of event densities; and
- Practical application to a large datasets while minimising subjective decisions.

This section further shows the capability of the STIDSR method by considering the temporal quantification of responses with respect to blasting. This analysis is preliminary with a limited scope, although, the ability to quantify responses that are relatable to known rock mass failure processes highlights that the STIDSR method can consistently achieve thesis outcomes (Section 1.3) and addresses the problem defined by the thesis (Section 1.2).

### 6.6.1 General Response Assessment

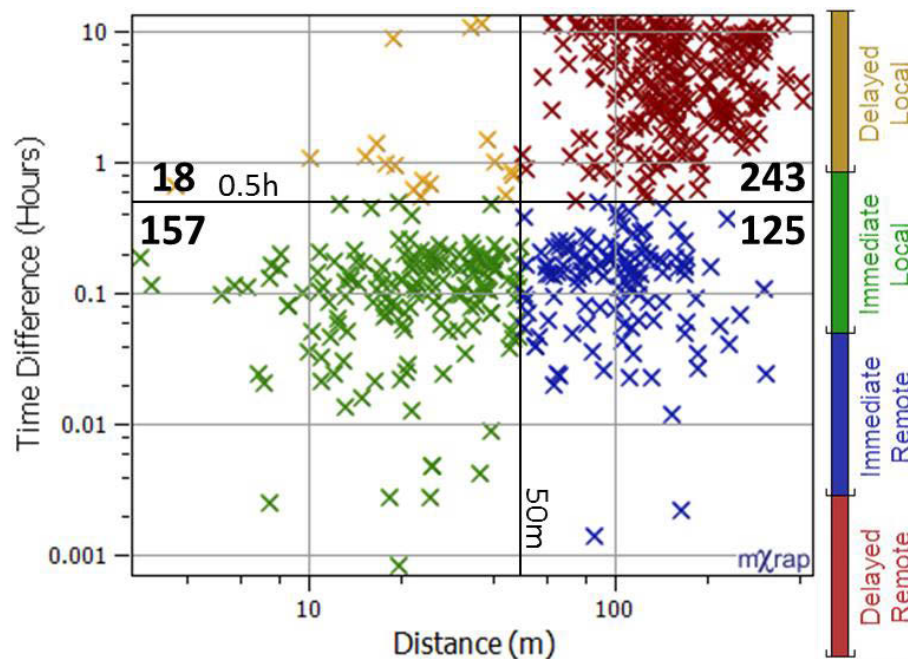
Response assessment investigates the evolution of time-dependent seismicity as mining conditions systematically change for an extensive seismic dataset. The STIDSR method is applied to a dataset containing 270,000 events using the parameters specified in **Table 39**. These parameters were calibrated by assessment of 3-day intervals of typical seismicity associated with undercut blasting and responses within the caving back. As a result, 1,067 responses were found that contained 73,000 events ( $\approx 25\%$  of all events). To improve the confidence in subsequent analysis, responses were excluded if unsuitably modelled by the MOL, unreasonably short, had high uncertainty in parameters, or had high c-parameters. This filtering removed 4,500 events in 142 responses from further consideration.

**Table 39** Identification and delineation parameters used for the analysis of seismic responses.

Identification and Delineation Parameters	Initial Value	Iteration Increment
Spatial Window (m)	15	+15
Spatial Density Tolerance (%)	10	Constant
Temporal Window (h)	0.25	Constant
Lower Count Threshold (proportional method)	80% and >10 events	Constant
Temporal Modelling Window (h)	12	Constant

### 6.6.2 Seismic Response and Undercut Blasting

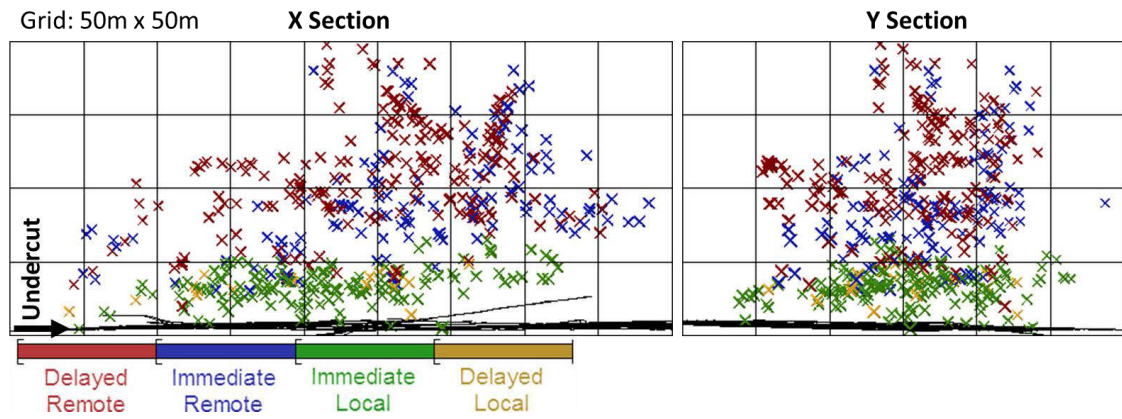
The classification scheme for defining the relationship between seismic responses and blasting is discussed in Section 6.5.1. A distance threshold of 50 m is used to define the threshold between local and remote, while a time difference threshold of 0.5 h is used to define immediate and delayed responses. **Figure 164** shows the blasting space-time relationship for each response coloured by classification. This figure is annotated with the number of responses found for each classification.



**Figure 164** Each response's distance to its nearest blasting for time (y- log axis) and distance (x- log axis). The number of responses within each category is also provided.

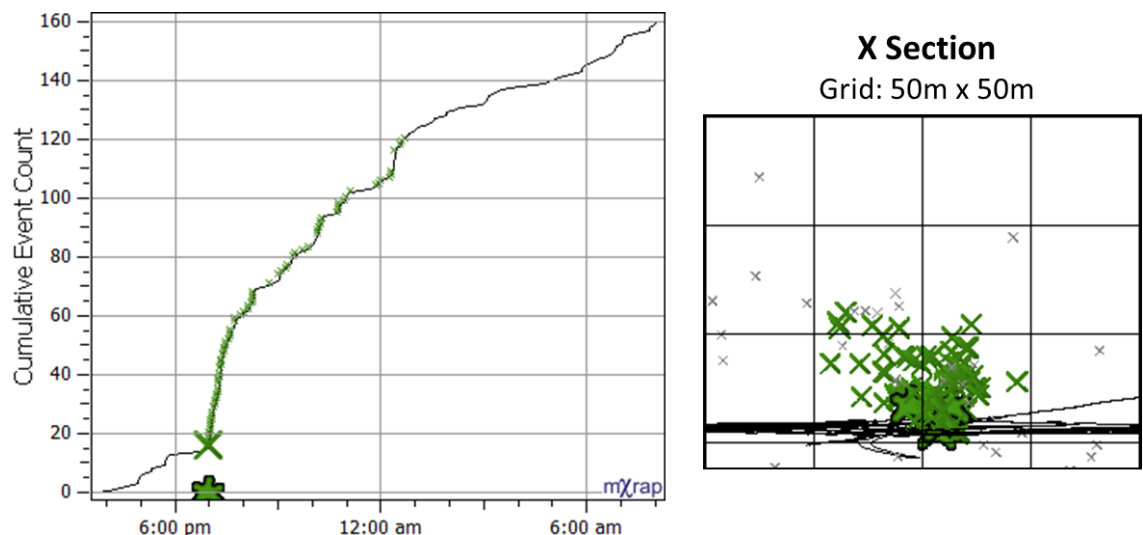
The spatial location of the responses with respect to their classifications and undercut development is shown in **Figure 165**. These two figures indicate that while the temporal transition between *immediate* and *delayed* responses is relatively clear, the spatial transition between *local* and *remote* responses is less clear. *Remote* and *immediate* responses (blue)

exhibit a similar distribution to *remote and delayed* responses (red). There is not a clear spatial separation between responses local and remote to undercut blasting due to the progression of the cave back over time. The cave back initiates slightly above the influence of blasting and over time it progresses through to the previously caved volumes. The cave back controls the spatial location of responses and contributes to remote responses throughout this process.



**Figure 165** Spatial plots of seismic responses with respect to the level of undercutting (Right: X section, Left: Y section). Responses are crosses coloured by space-time relationship.

Seismic responses to blasting during the early undercutting processes are *local and immediate*, and are consistent with the localised redistribution of stress associated with blasting. **Figure 166** shows a typical *local and immediate* response (green crosses) to blasting (green stars) with a cumulative temporal event count and a spatial plot. There are no temporal or spatial irregularities with this response, indicating the caving process has not been initiated.

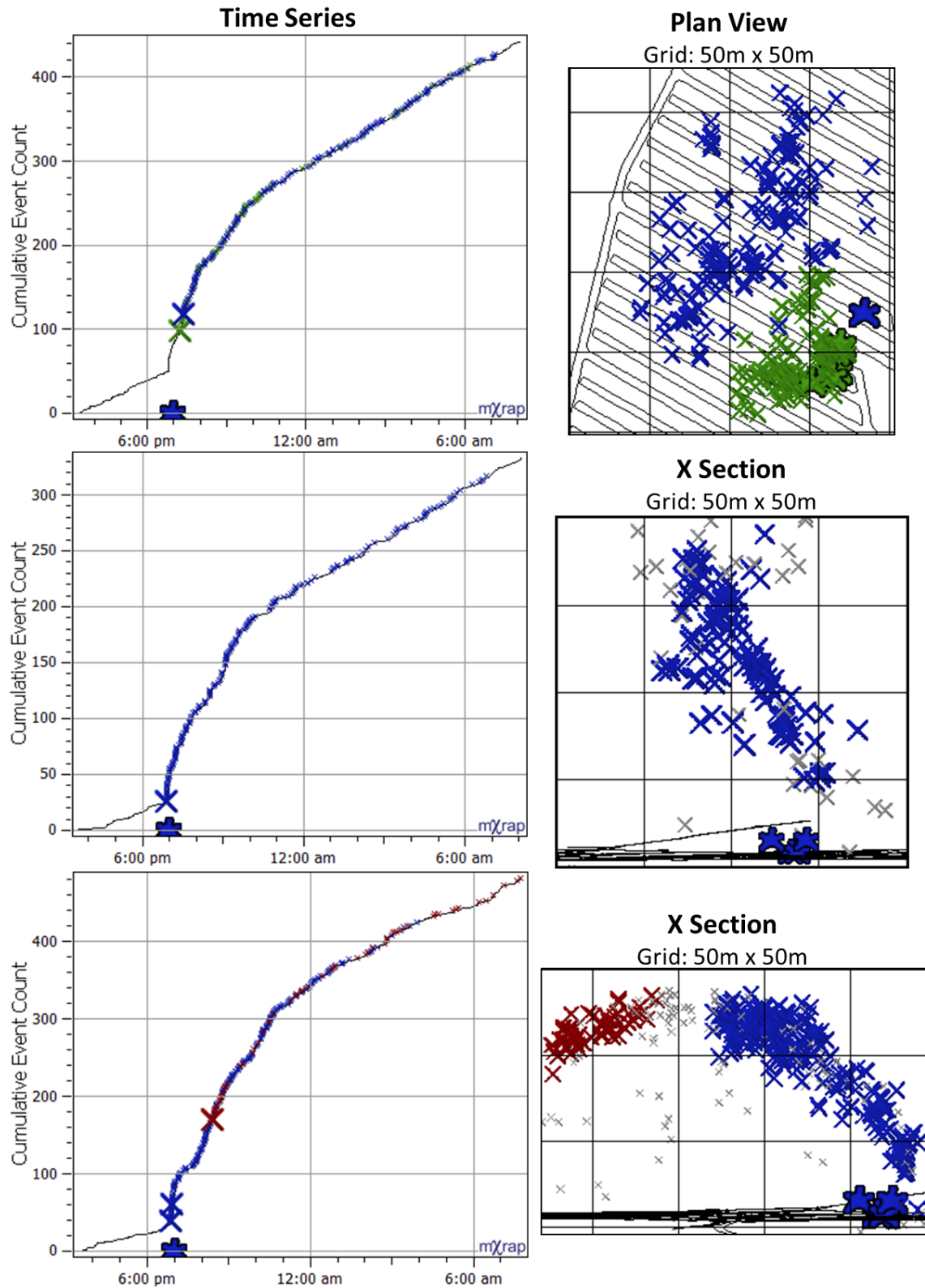


**Figure 166** Local and immediate seismic response (green cross) is shown on a cumulative event count over time (left) and a spatial plot (right), with respect to undercut blasting (green star).

Seismicity associated with the cave back becomes evident as undercut blasting continues and results in various combinations of spatially separate but temporally superimposed seismic responses. **Figure 167** provides typical examples of these seismic responses to blasting. Blasts and responses are shown on a time series (left) and spatial plot (right). Blasts and events are coloured by spatial and temporal relationships:

- Top: A *local and immediate* response occurs with undercut blasting, in addition to a *remote and immediate* response within the caving back. This indicates that this volume is sufficiently close to failure and that time-dependent seismicity can be caused by blasting despite being a significant distance away (>50 m).
- Middle: Routine blasting under the current caving arch results in a *remote and immediate* response above the expanded undercut. The spatial orientation of the response is controlled by the caving rock mass, although, there is high confidence that the immediate, strongly time-dependent response was caused by blasting.
- Bottom: Similar to the response in the middle example, a pair of *remote and immediate* responses occurs within the caving arch above blasting (spatial separation is perpendicular to the viewing plane). A *remote and delayed* response occurs in the opposite caving back. This response cannot be attributed directly to blasting with confidence, as the time delay falls outside of the 0.5 h threshold. These responses may provide insight into the time-dependent redistribution of stress over large distances ( $\approx 200$  m) if enough similar cases are observed.

While not considered in this thesis, it is acknowledged that remote or delayed responses may be more closely related to alternative causation processes, e.g., the extraction of caved material. The identification and delineation of seismic responses, independently of blasting information, allows the alternative hypothesis to be tested.



**Figure 167** Scenarios of remote and immediate responses (blue) with respect to blasting (stars).

*Top: Seismic response induced in the cave back above undercut blasting;*

*Middle: Seismic response induced locally with blasting and in the crown of the cave; and*

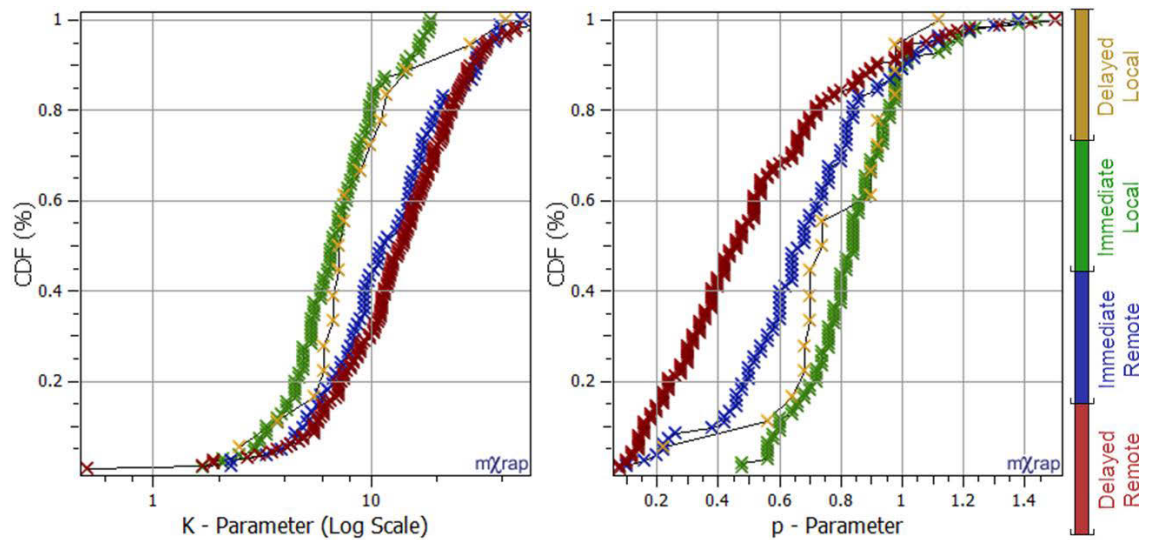
*Bottom: Remote response and a remote and delayed response in the opposite cave back.*

### 6.6.3 Quantified Seismic Responses and Blasting Relationship

Section 6.5 focused on the space-time relationship between blasting and seismicity irrespective of response parameters (aside from quality filtering). This assessment shows the thesis objectives achieved by the STIDSR method through the characterisation of individual responses associated with the localised redistribution of stress following blasting and time-dependent rock mass failure associated with caving. Furthermore, this assessment aims to delineate the point where undercutting is sufficiently extensive to initiate a caving rock mass failure process.

A simple assessment is to examine the cumulative density functions for p-parameters (right) and K-parameters (left) with respect to the classifications for the response-blasting relationship (**Figure 168**). The *local and immediate* response exhibits lower K-parameters and higher p-parameters with respect to other responses. These parameters indicate that these responses are less productive and decay more rapidly. In contrast, *remote and delayed* responses are more productive (higher K-parameters) and slower to decay (low p-parameters). It is recognised that *remote and delayed* responses inevitably contain time-independent seismicity that will contribute to the underestimation of p-parameters and overestimate of K-parameters (Section 5.9.5). The parameters will reflect the composite processes that contribute to seismic responses and biased proportionally to the rate of time-independent seismicity.

*Local and delayed* responses have insufficient observations for a confident assessment, although, these responses appear to share similar parameters to *local and immediate* responses. A two-sample Kolmogorov Smirnov test indicates that the maximum allowable differences in cumulative distributions for a 99% confidence interval are critical values of 0.10 for *local and immediate* versus *remote and delayed* responses, 0.11 for *remote and delayed* versus *remote and immediate*, and 0.12 for *remote and immediate* versus *local and immediate*. These critical values indicate that for the distribution of *remote and immediate* parameters the p-parameter distribution has an underlying difference in distributions to *local and immediate*, and *remote and delayed* responses. For the K-parameter distribution there is an underlying difference to *local and immediate* parameters, however, no significant difference to *remote and delayed* parameters is found. These critical values indicate that for the distribution of *local and immediate* parameters both K-parameter and p-parameter distributions are fundamentally different to distributions for *remote and immediate* and *remote and delayed* responses.



**Figure 168** CDFs per response-blasting relationships for the K-parameter (left) and p-parameter (right).

Parameter distributions appear to be characteristic of different response-blasting relationships. The previous figure failed to provide insight into how these responses evolve over time. **Figure 169** addresses this deficiency in assessment by considering a 30-day moving average of the K-parameter (left) and p-parameter (right) with a minimum of 10 responses per temporal bin. The moving average is plotted with respect to the progressive number of undercut blasts and blasting-response relationships. *Local and delayed* responses are not considered in this assessment due to a lack of observations. **Figure 170** shows a plan view of undercutting blasting development. Shown left are the blasts coloured by progressive count and the directional progression undercutting. Shown right is the response-blast relationship for the closest response in space and time. Black markers are used if no response occurs within the 0.5 h or 50 m classification thresholds, i.e., *remote and delayed* responses are not allocated to a blast. The same spatial plots are shown in **Figure 171**, although, plot the K-parameter (left) and p-parameter (right) for each blast.

The undercut blasts are coloured by K-parameters (left) and p-parameters (right) of the associated responses. **Figure 169**, **Figure 170**, and **Figure 171** show three periods of responses:

Period 1 (1-1000 blasts): exclusively *local and immediate* responses to blasting.

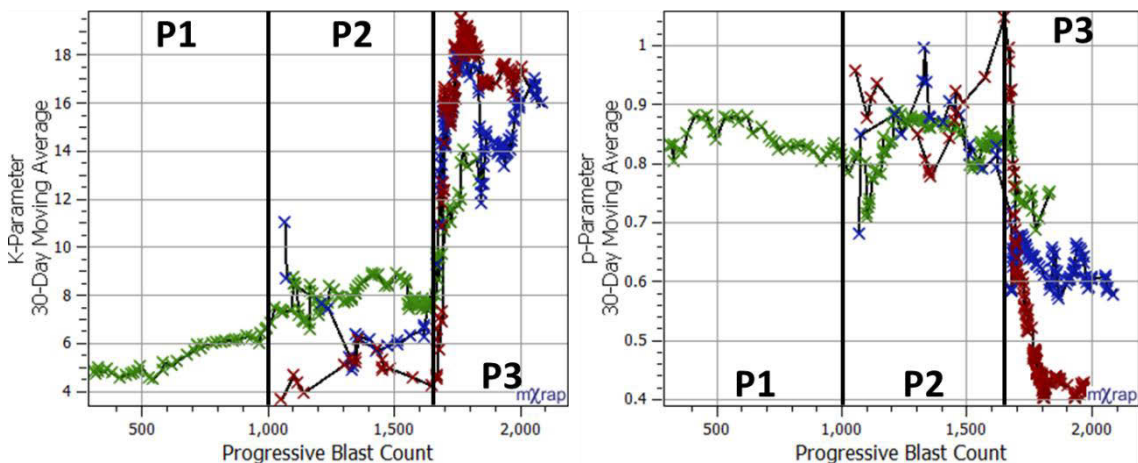
- Slightly increasing in K-parameter and decreasing in p-parameter.

Period 2 (1001-1650 blasts): *local and immediate*, and *remote and delayed* responses.

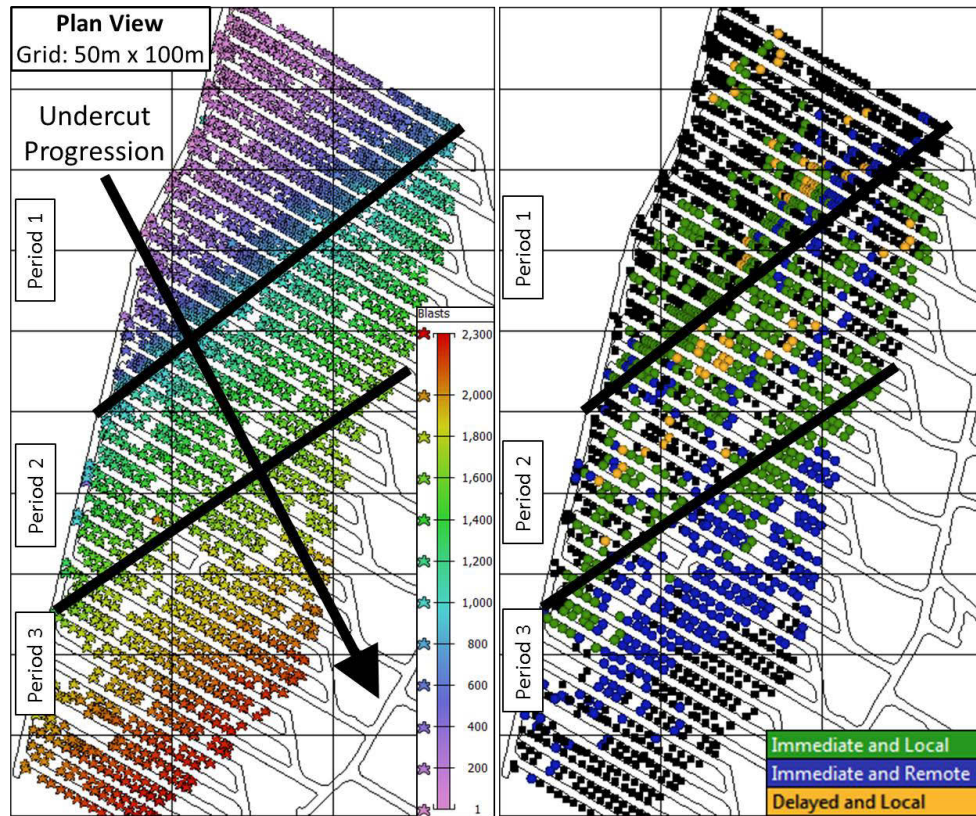
- K-parameter and p-parameter are erratic but consistent over the period;
- Additional sources of seismicity contribute to time-dependent responses that are spatially offset and sometimes temporally offset from blasting; and
- Remote or delayed responses have lower K-parameters than *local and immediate* responses.

Period 3 (1651-2200 blasts): the occurrence of *local and immediate* response diminishes.

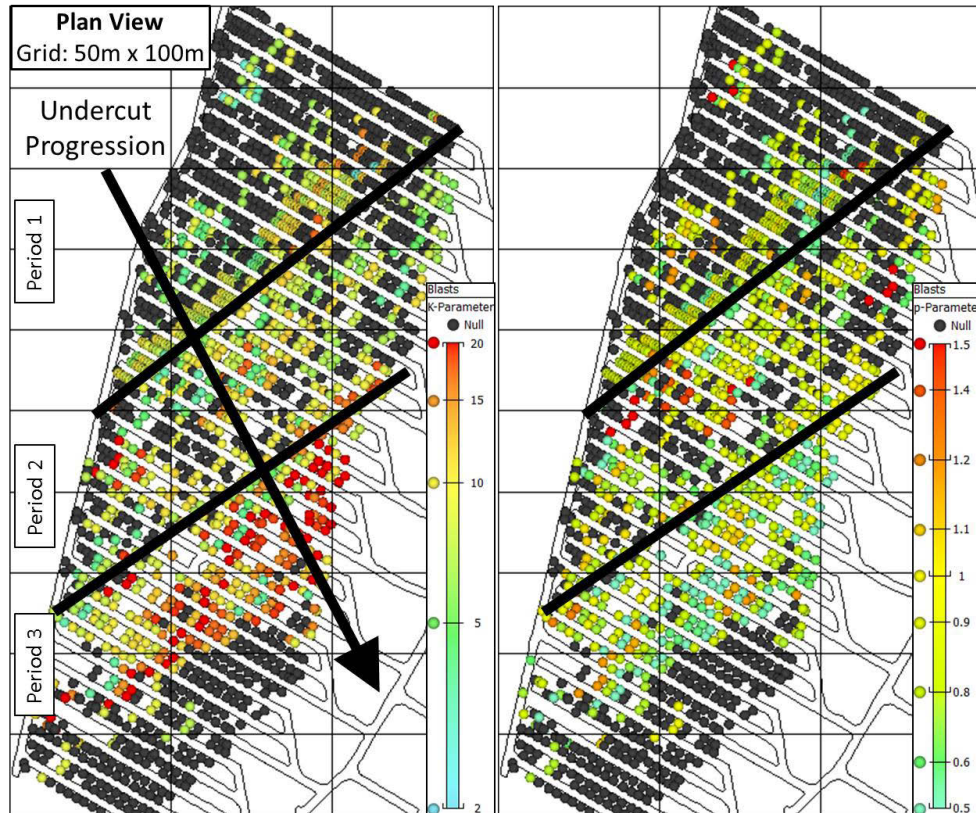
- The vast majority of responses are spatially remote and temporally immediate or delayed and have significantly higher K-parameters and lower p-parameters; and
- Immediate and remote responses have higher p-parameters than unrelated responses.



**Figure 169** Thirty day moving averages of K-parameter (left) and p-parameter (right) with respect to progressive undercut blasting. A series is plotted for each response-blasting relationship.



**Figure 170** Plan views of the progress of undercutting and the space-time relationship between blasting to closest seismic response. Blasts that do not have responses allocated are coloured black.



**Figure 171** The K-parameter (left) and p-parameter (right) allocated from the closest seismic response in space and time to each blast. Blasts that do not have responses allocated are coloured black.

The quantification of the responses and the relationships to blasting provides insight into the caving process. The initial period indicates that blasting has a greater influence on seismicity as undercutting progresses (responses become more productive and are slower to decay).

Responses become less consistent in the second period with limited cases not directly related to blasting. In comparison to those related to blasting during this period, these responses have low productivities and sporadic decay rates. A response not directly related to blasting indicates that more complex sources of seismicity develop, although, these responses do not significantly contribute to the generation of seismicity. During the second period, blasting remains as the dominate causation process for time-dependent seismicity.

The caving process is inferred during the third period due to the dramatic increase in productivity and slower decaying responses that are not directly associated with blasting. These responses are likely to include an increased portion of spatially and temporally superimposed time-independent seismicity that will bias underlying parameters. Despite the bias of parameters, the significantly contrasting values to the previously observed *local and immediate* responses indicate a clear transition in dominant seismic source mechanism.

Applying the STIDSR method to the seismicity associated with a block cave mining environment allows for the spatial and temporal evaluation of different rock mass failure mechanisms. Furthermore, seismic responses and their relationship to blasting can be quantified over time and provide insight into the development of seismic sources to mining. This section shows the applicability of the STIDSR method to large datasets that contain responses with a range of different spatial and temporal characteristics, highlights that the STIDSR method can consistently achieve thesis outcomes.

## 6.7 Seismic Response Hazard

This section shows the applicability of the STIDSR method when assessing mining induced seismic response hazard. Seismic hazard associated with mining induced seismicity considers the probability that an event will exceed certain magnitude within a specific spatial and temporal interval. Seismic hazard assessment generally considers an event magnitude that is able to induce sufficient dynamic ground motion to damage excavations (Potvin, Wesseloo & Heal 2010; Mendecki 2013). Within the context of this thesis, response hazard focuses on the temporal scale of hours for specific seismic response. The application of time-dependent hazard assumes that temporal event occurrence can be suitably modelled by the MOL, spatial occurrence is confined to the volume of the response, and the magnitude distribution follows a consistent magnitude-frequency relationship.

This section comprises of three subsections that build towards the assessment of individual seismic responses relative to historical responses. Firstly, a discussion of the determination of seismic hazard for responses provides context for the subsequent sections. Secondly, analysis allows seismic responses to be retrospectively parameterised and allows a historical reference to be established for the geotechnical domains within the mine. Thirdly, the hazard associated with individual seismic responses is assessed with respect to an area specific history, temporal modelling of the entire interval, and a hazard estimation using a partial modelling interval.

### 6.7.1 Determination of Seismic Response Hazard

The seismic hazard for an individual response developed within this section assumes there is a temporal decay in event rate and that b-values found from the magnitude-frequency relationship are constant. Given these two assumptions, the instantaneous seismic hazard for a response decreases over time. A relative reference of seismic hazard is estimated by an instantaneous approximation of the likelihood that a spatially constrained response will generate an event exceeding a certain magnitude for a given time interval. The b-values throughout this section and following sections (6.7.2 and 6.7.3) are determined from the magnitude-frequency relationship using the method proposed by Wesseloo (2014).

An established current time-dependent hazard model is the Reasenber-Jones Model and has been applied to earthquake aftershocks in order address to seismic response hazard (Reasenber & Jones 1989; Gasperini & Lolli 2006). The Reasenber-Jones Model also assumes that the number of aftershocks is related to the magnitude of a mainshock. This is a consistent relationship observed for aftershocks, e.g., Felzer, Abercrombie and Ekström (2004). While this relationship has been observed for mining induced seismic responses following large events (Kgarume, Spottiswoode & Durrheim 2010b), it is not generally applicable to mining induced

seismic responses due to the influence of blasting. While the magnitude of a blast can be estimated by seismic monitoring, this approximation is questionable due to factors such as the superimposition of blast waveform coda and the detection of the variable number of individual blasting rings that contribute to a single excavation blast.

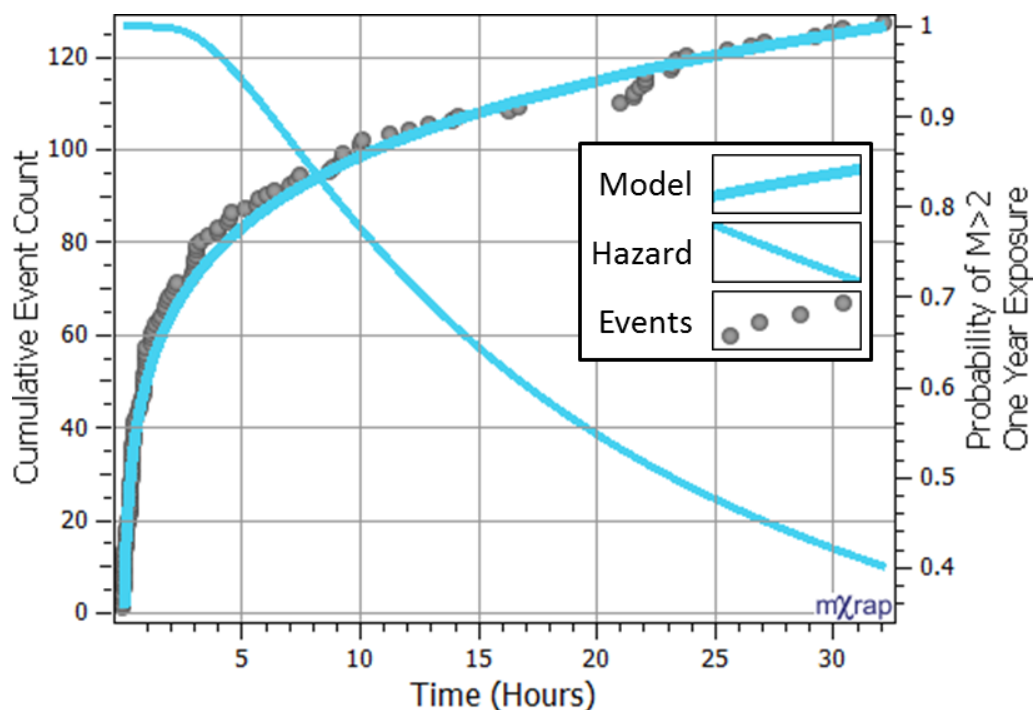
Time-dependent models for earthquake aftershocks are limited when applied to mining induced seismicity and, therefore, an approach is implemented that only considers historical magnitude-frequency relationships and a forward estimate of number of events within a spatial and temporal interval. A major advantage of the delineation of individual seismic responses is that a spatial interval is defined, i.e., considering hazard within the spatial extent of a seismic response. This is important when considering re-entry protocols, e.g., sparse responses may require restrictions to entire sections of an orebody, while localised responses may allow mining to resume outside of volumes directly affected by mining. It is important to acknowledge that multiple individual seismic responses may contribute to the total hazard associated with any specific excavation and, as a result, holistic assessment must consider composite seismic hazard models. This section focuses on the hazard associated with individual responses and while this forms the basis for a composite model, this aspect of seismic hazard is not addressed within this thesis.

The analysis interval is limited by the duration of responses that has been suitably modelled and is typically interrupted by the initiation of a new response to routine blasting. It is important to acknowledge that the hazard from preceding responses does not cease because the response cannot be modelled. It is ambiguous whether the seismic contribution of the preceding time-dependent failure process is diminished, constant, or increased given that additional blasting sufficiently alters rock mass failure to create a new dominant failure process. This assessment captures the cumulative effects of time-dependent failure processes by the quantification of individual responses, i.e., if cumulative processes result in increased seismic productivity, then this is reflected by increased productivity of individual responses irrespective of preceding response quantification.

The magnitude of significant hazard is arbitrarily chosen for the purpose of this thesis ( $2.0M_L$ ). In practice, this magnitude reflects site-specific considerations. The length of the hazard period does not influence the relative assessment of event probabilities. The selection of a small hazard period causes absolute probabilities to be small. Small hazard periods are difficult to interpret and typically result in an under appreciation of the true likelihood of experiencing a large event (Wesseloo 2013), given that routine blasting typically occurs twice a day, for the entire life of the mine (in the order of years). This section expresses hazard as a “yearly

hazard” (proposed by Wesseloo (2013)), hazard is normalised to an equivalent exposure period of year. Refer to Appendix B: Applying Hazard to Mining Induced Seismic Responses.

A length of one year is arbitrarily chosen to provide probabilities relatable to the context of mining induced seismic hazard. The equivalent probability of exceeding a magnitude  $2.0M_L$ , given a one year exposure period, is referred to as  $P(>2M_L | 1Y)$ . **Figure 172** provides an example of the  $P(>2M_L | 1Y)$  for a seismic response. The cumulative MOL model (left y-axis) and corresponding hazard model (right y-axis) are plotted with respect to time. The b-value for this response was determined from historical seismic responses in the location of the response. For early time intervals when activity rates are high, the  $P(>2M_L | 1Y)$  approaches a probability of 1 (almost certain that an event exceeding  $2.0M_L$  will occur if this hazard was sustained for one year). The  $P(>2M_L | 1Y)$  decreases to a probability of 40% by the end of the analysis interval.



**Figure 172** The cumulative event count and MOL model (left y-axis) along with the corresponding hazard model (right y-axis) plotted with respect to time.

The analysis of seismic hazard associated with individual responses is enabled by the application of the STIDSR method to seismicity. The quantification of seismic responses improves the objective understanding of conditions resulting in high and low seismic hazard. Quantification is achieved by addressing the thesis objectives (Section 1.3) and problem defined by this thesis (Section 1.2). It is important to reiterate that the scope of this section is to illustrate the thesis objectives achieved by the STIDSR method within the context of seismic response hazard. The method for assessing seismic response hazard presented within this section is not comprehensive.

### 6.7.2 Retrospective Parameterisation of Responses

The STIDSR method is used for retrospective response assessment to establish characteristic parameters and seismic hazard for different mining conditions. This assessment evaluates the temporal components that contribute to hazard, specifically, K-parameters, p-parameters, c-parameter, b-values, and modelling intervals.

The identification and delineation of seismic responses was applied to a dataset containing 360,000 events using the parameters specified in **Table 40**. These parameters are calibrated by the assessment of a number of 3-day intervals of typical time-dependent seismicity. Calibration involves visually inspecting responses to ensure reasonable solutions are found, optimisation of the CVNN index to determine optimal spatial parameters, and assessment of the quality of temporal modelling outcomes. These parameters were then applied to the entire dataset.

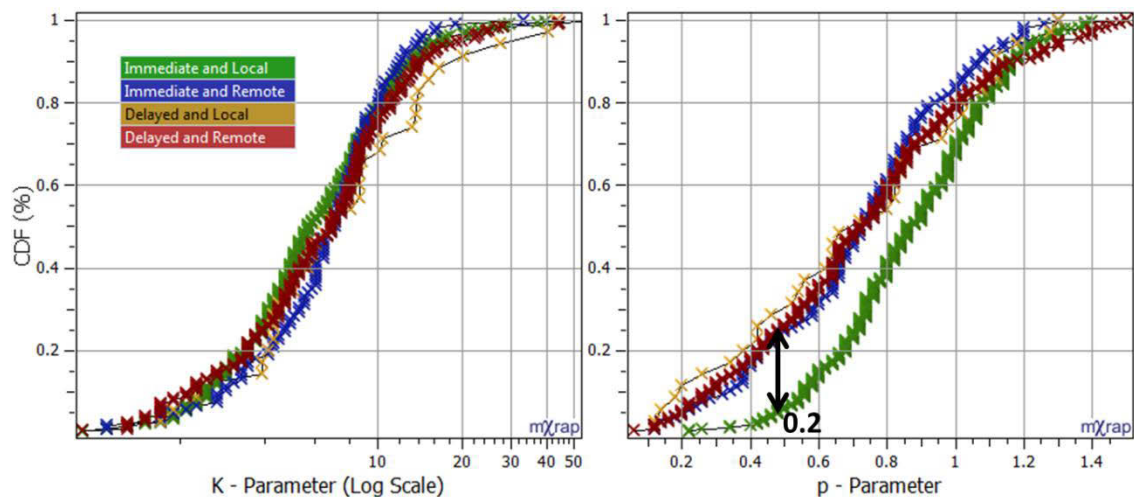
The STIDSR method finds 1,559 responses containing 96,000 events ( $\approx 25\%$  of all events). Only responses with reasonable parameters were considered in subsequent analysis by removing responses that were unsuitably modelled by the MOL, unreasonably short, exhibited high uncertainty in parameters, or had high c-parameters. Quantity exclusion thresholds are based on the assessment of temporal errors (Section 5.9.4) and acceptable values reported in literature (Section 2.5.). This filtering removed 8,500 events contained in 190 responses from further consideration.

**Table 40** Identification and delineation parameters used for the retrospective response quantification.

Identification and Delineation Parameters	Initial Value	Iteration Increment
Spatial Window (m)	20	+20
Spatial Density Tolerance (%)	10	Constant
Temporal Window (h)	0.25	Constant
Lower Count Threshold (proportional method)	80% and >10 events	Constant
Temporal Modelling Window (h)	48	Constant

The expected response parameters for different mining conditions were approached by considering the relationship between quality seismic responses and blasting. These classifications follow the method presented in Section 6.5.1. Spatial and temporal classifications used 0.5 h and 50 m thresholds for remote and delayed responses. The relationship between seismic responses and blasting, and parameters is assessed by plotting the cumulative density functions of each classifications (**Figure 173**). With one exception, this broad assessment indicates that there is no significant difference in the distribution of these

parameters when grouped by response-blasting relationships. The exception is the generally higher distribution of p-parameters for *local and immediate* responses and this indicates that these responses have quicker decays in event rates. This result is expected, as *local and immediate* responses are more likely to be associated with localised rock mass failure on smaller spatial and temporal scales. These observations are supported by a two-sample Kolmogorov Smirnov test that assesses if two distributions are fundamentally different. A general scope of testing is considered given that results are dependent on an arbitrarily selected significance level. This test specifies that the maximum allowable difference in the smallest cumulative distributions (critical values) for 99% significance level is 0.12. **Figure 173** shows that distributions are within the allowable range of each other, although, the maximum separation of the *local and immediate* p-parameter distribution (0.2) is greater than the critical value (0.12) for 99% significance level.



**Figure 173** CDFs per response-blasting relationships for K-parameter (left) and p-parameter (right).

The lack of separation in parameter distributions for response-blasting relationships are indicative of a mining environment with multiple, varied sources of seismicity. The sources of seismicity have a greater influence on the decay and productivity of seismic responses and, therefore, spatial and temporal relationships to blasting are not able to provide characteristic separations in parameters. Time-dependent responses from sources of seismicity are spatially controlled by the characteristics of mining, stress conditions, and rock mass strength. It is sensible to consider the variation of parameters within different geotechnical domains due to the spatial dependency of seismic sources within this mining environment.

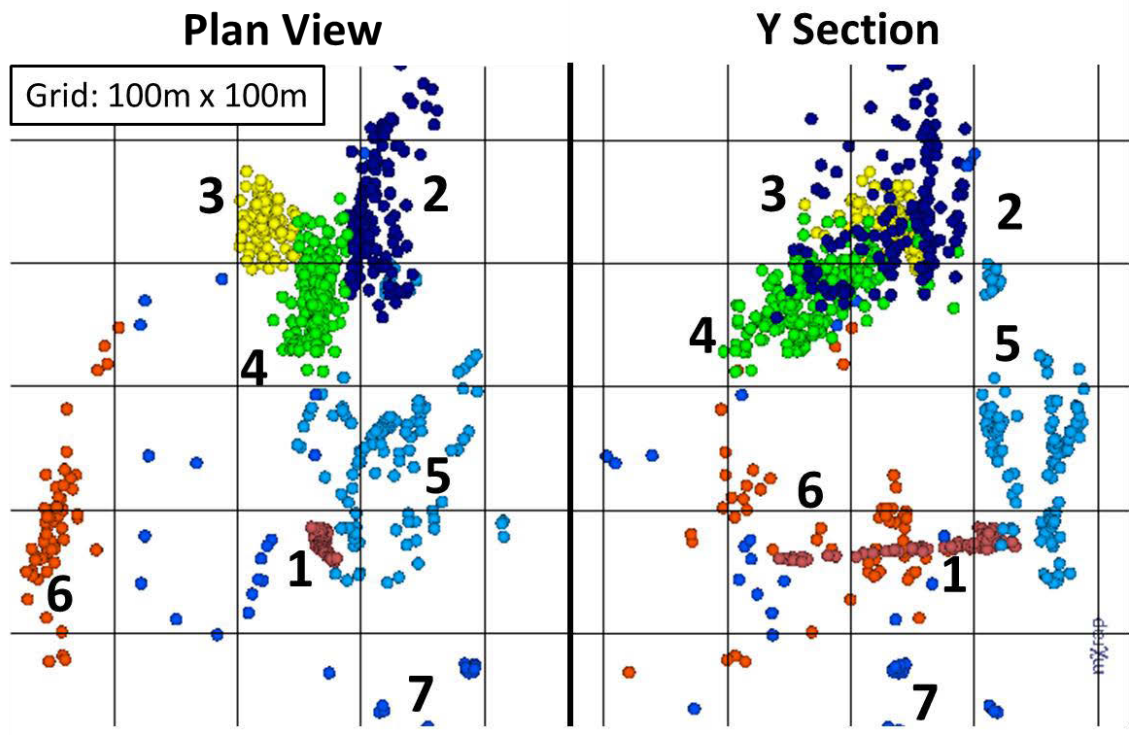
Geotechnical domains are given an arbitrary numerical ID in **Table 41** that corresponds to the associated figures. This table provides quantification of mean parameters from temporal modelling. Each spatial geotechnical domain has distinctly coloured markers in **Figure 174** and is annotated by the corresponding numerical ID (Left: Plan view, Right: Y section). The same marker colours correspond to the cumulative density functions of K-parameters (left) and p-parameters (right) for each geotechnical domain (**Figure 175**).

The geotechnical domains shown in **Figure 174** are described by the following qualitative mining characteristics:

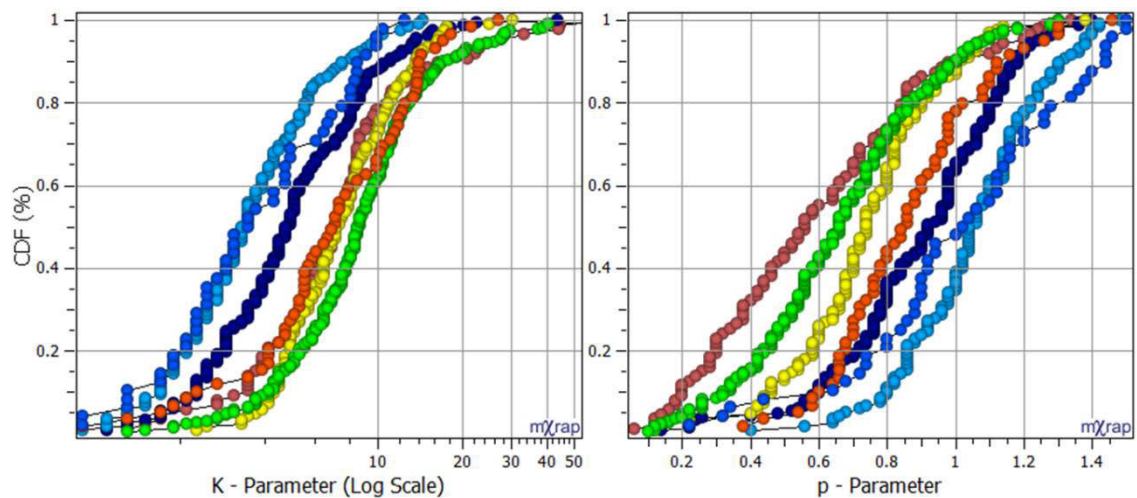
1. Raise bore development under high stress conditions;
2. Development blasting, faulting, and contrasting rock properties;
3. Development and production blasting, and geologically controlled stress conditions;
4. Development blasting, production blasting, significant geological features, and mining that cross cuts major principal stresses;
5. Development blasting under high stress conditions due to increased mining depth;
6. Development and production blasting, geological features, and varied stress conditions; and
7. Isolated responses to development blasting.

**Table 41** The geotechnical domain ID, characteristics and relevant mean parameters for temporal quantification. The *b*-value of each domain is also calculated.

ID	#Responses	$T_s$	$T_E$	$p(\pm)$	$K(\pm)$	$c(\pm)$	$b(\pm)$
1	136	0.032	12.7	0.65(0.38)	11.1(11.8)	0.00(0.01)	1.40(0.02)
2	315	0.019	11.6	0.86(0.29)	7.3(5.8)	0.01(0.02)	0.99(0.02)
3	205	0.020	19.0	0.74(0.27)	8.4(4.2)	0.01(0.02)	1.00(0.01)
4	420	0.023	20.0	0.64(0.29)	11.6(10.0)	0.01(0.02)	1.21(0.01)
5	297	0.015	9.2	0.99(0.28)	5.6(4.1)	0.01(0.02)	1.42(0.03)
6	91	0.013	13.7	0.86(0.26)	9.0(7.0)	0.01(0.03)	0.99(0.02)
7	95	0.027	9.7	0.95(0.32)	5.4(3.8)	0.00(0.01)	1.35(0.05)



**Figure 174** Spatial locations of geotechnical domains are shown on a Plan View (left) and Y Section (right). Each sphere is an individual seismic response.



**Figure 175** Cumulative density functions per geotechnical domain for the K-parameter (left) and p-parameter (right). Markers are coloured corresponding to the spatial plot.

A generalised two-sample Kolmogorov Smirnov test considered again, as results are dependent on an arbitrary selected significance level. Testing indicates the majority of distributions presented in **Figure 175** are fundamentally different, although, may be visually similar, e.g., K-parameter distributions for domains three (yellow) and four (green). The maximum allowable difference in cumulative distributions for a 99% significance level ranges from 0.07, when comparing large distributions, to 0.14 when comparing small distributions.

These critical values are surpassed convincingly for the majority of K-parameter distributions and all p-parameter distributions and although fundamentally different, these distributions can be similar within the context of distributions associated with all domains.

Considering specific geotechnical domains allows the following qualitative observations:

- Seismicity associated with raise boring has distinctive low p-parameters and a distribution of K-parameters comparable to the most productive responses;
- Domains that only contain development blasting result in higher p-parameters and lower K-parameters (light blue, blue, and dark blue);
- Geotechnical domains with high stress conditions, i.e., deeper in the mine (light blue), or cross cutting principal stress directions (green), and has a relatively higher b-value;
- Domains with lower b-values are likely influenced by geological features (Legge & Spottiswoode 1987) and also have lower p-parameters, and higher K-parameters (dark blue versus light blue); and
- Domains that likely contain a mixture of influences (stress concentration, geology, production, and development blasting) have lower p-parameters and higher K-parameters (green, yellow, orange).

Quantifying the evolution of the mining environment is essential to the appropriate management of seismic hazard. The identification and delineation of seismic responses provides historical characterisations of geotechnical domains and provides guidance for future responses in these regions. When geology begins to influence seismicity that is associated with lower development (light blue) as future production levels are mined, it can be expected that the productivity of responses will increase, the temporal decay of event occurrence will decrease, and the b-value will decrease (more large events relative to small events).

This example begins to address the issues outlined in Section 6.2 that formed the motivation for assessing seismic hazard associated with seismic response. Firstly, the quantification of seismic responses within the mining environment limits the degree that human judgement may influence the assessment of seismic hazard. Furthermore, quantification of seismic hazard objectively guides the management of low and high hazard environments with respect to the portion of time-dependent and independent seismic responses. The retrospective quantification of parameters contributing to seismic hazard is a major component to removing the subjectivity and increasing the transparency of engineering decisions. These decisions can have significant positive and negative political, social, and economic implications for the mine and associated stakeholders.

This section applied the STIDSR method to a large dataset containing seismic responses that ranged in attributes and reiterates the ability of the method to address thesis outcomes. The application of the STIDSR method enables the temporal behaviour of seismic responses to be characterised and used as a reference for the behaviour of future responses.

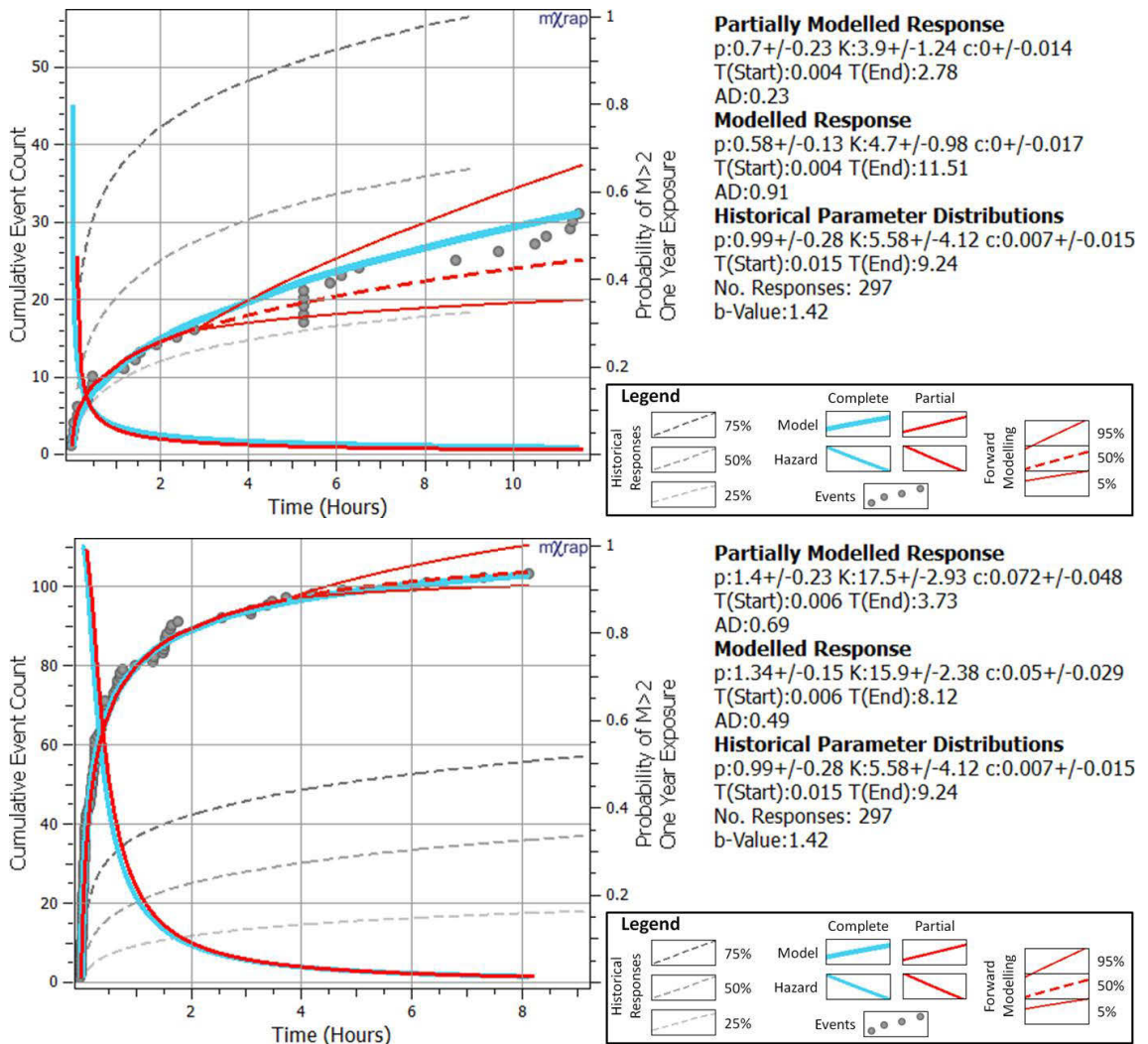
### 6.7.3 Current Seismic Response Hazard

The ability to characterise historical responses and link observations to general conditions is important for current operations. The distribution of parameters provides an indication if an observed response is abnormally large or small with respect to the number of events observed. To reflect the variability and average historical responses within a geotechnical domain, Monte Carlo simulations are used to develop a reference for the expected cumulative number of events. The mean and standard deviation of these parameter distributions are found from responses in the geotechnical domain of interest. Section 6.7.2 showed that these distributions are well populated and contain between 91 and 420 responses. Based on work Vallejos and McKinnon (2010a) and Vallejos and McKinnon (2010b), the p-parameter is assumed to follow a normal distribution, and the K-parameter and c-parameter are assumed to follow a log-normal distribution.

The assessment of current seismic hazard also considers partially modelled responses. Partially modelled responses replicate operational conditions whereby only a portion of a seismic response has occurred. Time-dependent hazard is determined for a partial fit and projected for the length of the analysis interval by assuming that future events are suitably modelled by current MOL parameters. Monte Carlo simulations use the mean and standard error of current parameters to determine the 5% and 95% cumulative event intervals for future projections under the assumption that the standard error in MOL parameter represents the uncertainty in future response behaviour. The future cumulative event intervals are intended to provide guidelines for extreme response behaviour given the current uncertainty. High uncertainties in MOL parameters indicate that the response should be modelled over a longer interval before projecting event occurrence. The subsequent figures contain the following information:

- 25, 50, and 75% cumulative event intervals for historical responses (grey dashed lines).
- For the complete time interval: cumulative seismic events (grey spheres), cumulative MOL model (blue line, left y-axis), and hazard model (blue line, right y-axis).
- For the partially fitted time interval: MOL model (red line, left y-axis), 5 and 95% cumulative uncertainty intervals (thin red line, left y-axis), projected MOL (red dashed line, left y-axis), and partially fitted and projected hazard model (red line, right y-axis).

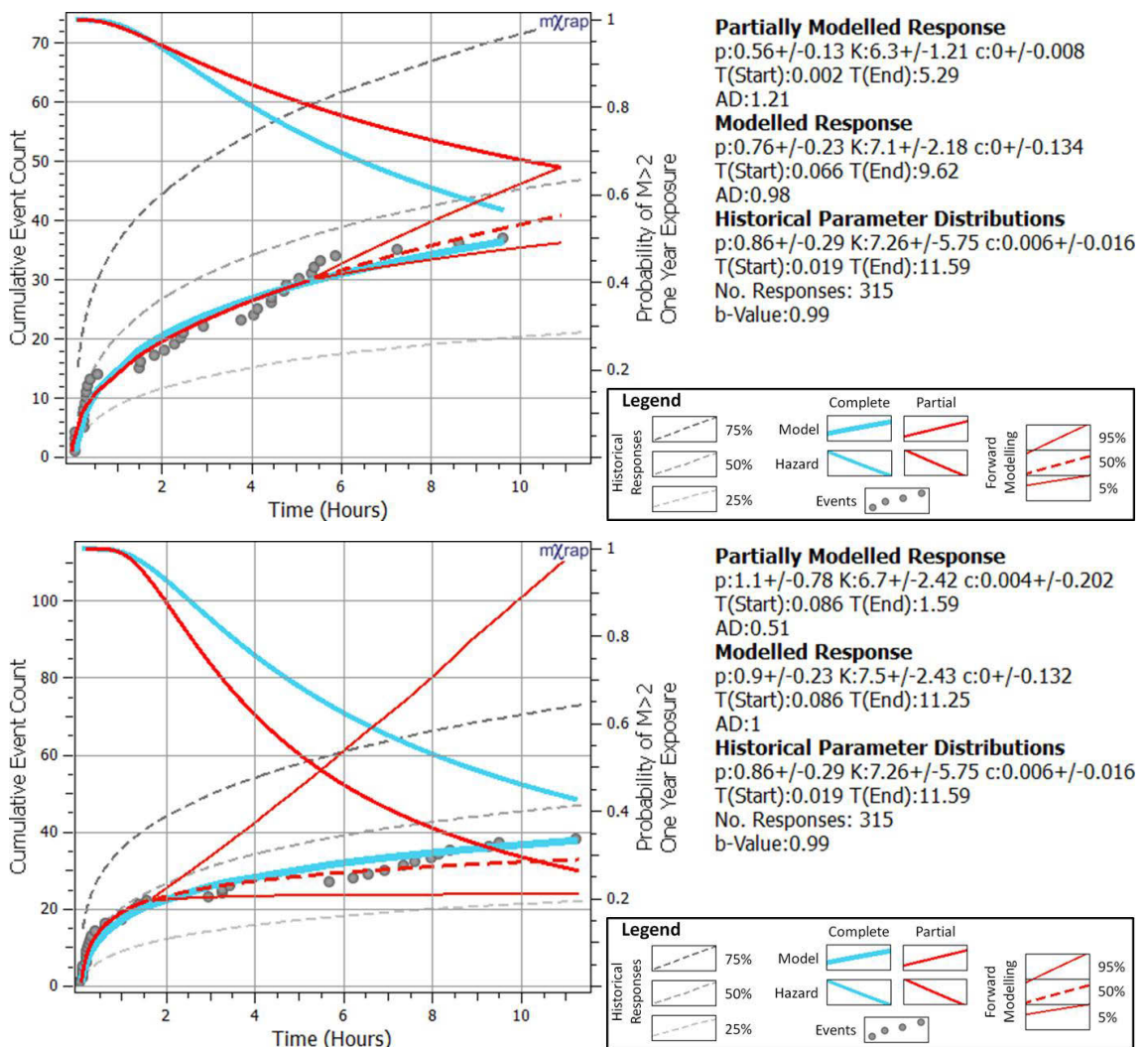
**Figure 176** shows two seismic responses with contrasting MOL parameters, although both occur within a geotechnical domain that is characterised by a relatively high b-value (1.42). The response shown top generates a less than average number of seismic events, while the response shown bottom generates significantly more events than historical responses. After modelling three hours of the top response, the partially fitted model provides a reasonable representation of seismicity over the time interval given the uncertainty in MOL parameters. Despite the projected response underestimating the hazard model for the complete interval there is a negligible impact on the low  $P(>2M_L | 1Y)$  values. This result is similar to that obtained for a more productive response (bottom) with partially modelled projections matching hazard modelling for the interval. The hazard model for both of these responses quickly reduces following initiation. Trends in the hazard model are created by low productivity and high b-values for the top response. For the bottom response, the trends in hazard model are due to a high decay rate and high b-value.



**Figure 176** Two contrasting seismic responses that occur within the same geotechnical domain

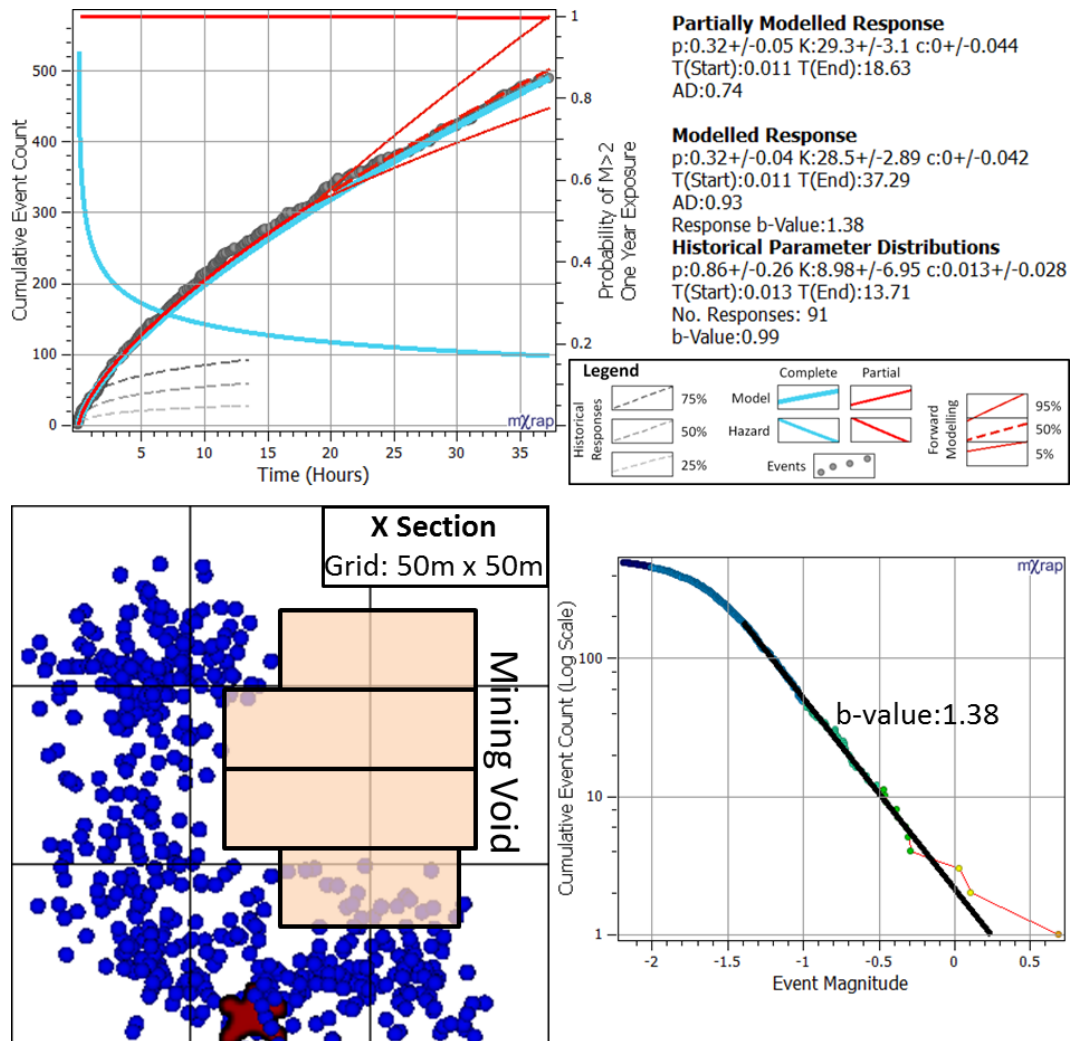
characterised by a high b-value. Top: Low p-parameter and low K-parameter. Bottom: High p-parameter and high K-parameters.

**Figure 177** shows two seismic responses with similar MOL parameters, although responses are partially modelled with significantly different p-parameters. Seismic responses within this geotechnical domain are historically characterised by a lower b-value (0.99). For the response bottom, partial modelling causes high uncertainties and is reflected in a wide range between the 5-95% uncertainty intervals. Despite high uncertainties, both the top and bottom responses have projected MOL models that are reasonably close to the number of events observed. Despite the relative accuracy of partial models, there is a relatively large discrepancy in the hazard model for both responses. Lower b-values cause the hazard model to be sensitive to event occurrence and, hence, small changes in parameters can cause large discrepancies in the hazard model. For these examples, the absolute  $P(>2M_L | 1Y)$  estimations are significantly higher in contrast with **Figure 176**. This difference in absolute hazard highlights the sensitivity of  $P(>2M_L | 1Y)$  to changes in event rates when b-values are low. Longer modelling intervals are required to establish confidence in results when considering low b-value responses.



**Figure 177** Similar complete seismic responses despite being partially modelled with significantly different p-parameters. The slight discrepancy in cumulative event occurrence translates to a significant different  $P(>2M_L | 1Y)$  for low b-values.

Seismic responses characterised by low p-parameters, high K-parameters, and low b-values result in the highest estimations of  $P(>2M_L | 1Y)$ . These responses combine slow decay, high productivity, and a high proportion of larger events relative to smaller events. While these responses can dominate seismic hazard, a large number of events allows the refinement of hazard modelling. **Figure 178** provides an example of the most productive seismic response within a geotechnical domain. The partial model of this response accurately forecasts the temporal occurrence of seismicity and considers a historical b-value (0.99). For this hazard model, the  $P(>2M_L | 1Y)$  is practically certain irrespective of the modelling interval (top). The magnitude-frequency relationship can be assessed independently of historical responses given the quantity of events (bottom right). The adjusted b-value (1.38) greatly diminishes the estimated hazard despite being extremely productive. The spatial plot of this response indicate that these events surround the mining void (bottom left) and, hence, may be more likely to be due to localised fracturing rather than more hazardous failure processes.



**Figure 178** Top: Seismic hazard plot for a highly productive, slowly decaying response. Bottom right: Magnitude-frequency distribution for all response events. Bottom left: Spatial view.

Establishing a relative reference for current seismic hazard is enabled by the application of the STIDSR method to assess a large dataset retrospectively. In addition to achieving thesis objectives, this method enables the consistent assessment for current and historical responses and, hence, facilitates a relative comparison between responses. While not explicitly addressed in this section, the STIDSR method also enables the incorporation of the spatial component of seismic responses and has important implications when considering what rock mass failure processes contribute to time-dependent event occurrence, the magnitude-frequency relationship of events, and seismic response hazard. This section highlights the applicability of the STIDSR method to the retrospective assessment of large datasets while also considering single seismic responses. In both applications, the STIDSR method consistently achieves thesis objectives (Section 1.3) for a range of responses with different spatial and temporal characteristics.

## 6.8 Chapter Summary

This chapter showed the ability of the STIDSR method to address the problem defined by this thesis (Section 1.2) through achieving the required objectives (Section 1.3) for a range of mining environments. This is illustrated by utilising the STIDSR method to evaluate the relationship between seismic responses and blasting, the evolution of seismic responses, and seismic response hazard. The STIDSR method answers the fundamental questions for mining induced responses:

1. Identification: Where and when responses occur; and
2. Delineation: The spatial and temporal extent of responses.

Furthermore, the STIDSR method considers and addresses the following requirements:

1. To only use the spatial and temporal characteristics of seismicity;
2. To identify responses superimposed in space and/or time;
3. The ability to perform for a range of event densities; and
4. The practical application to a large dataset while minimising subjective decisions.

This method is suitable for various applications and the outcomes of the method enable subsequent analysis that would not have been possible with existing methods. The analysis within this chapter that utilises the outcomes of the STIDSR method represents a significant contribution to the analysis of time-dependent seismicity by enabling:

- Retrospective assessment of the relationship between responses and blasts;
- Evaluating how the relationship between responses and blasting evolves over time;
- Quantifying seismic responses with respect to their relationship to blasting;
- Temporally quantifying the evolution of seismic responses as mining progresses;
- Temporally quantifying seismic responses for geotechnical domains; and
- Assessment of the partial and complete seismic hazard for individual responses.

## 7 Conclusions

Many specific and detailed conclusions were drawn from the work presented in Chapters 2, 3, 4, 5, and 6. These conclusions are summarised in Appendix C: Complete List of Conclusions, and will not be discussed further in this chapter. This chapter will present a holistic discussion of conclusions with relation to the problem and the objectives defined in Section 2.7.

The concluding discussion focuses on the three fundamental research questions that were addressed by the comprehensive methodology that identified and delineated individual seismic responses. The three fundamental research questions (repeated for convenience) are:

1. Identification of seismic responses: Where and when do responses occur?
2. Spatial delineation of related seismicity: What is the extent of responses in space?
3. Temporal delineation of related seismicity: When do responses start and finish?

The ability of the thesis to answer the three fundamental research questions successfully is underpinned by the ability of the STIDSR (spatially and temporally, identified and delineated, seismic responses) method to address the challenges associated with mining induced seismic responses. The challenges (repeated for convenience) were:

- The identification of seismic responses using only spatial and temporal parameters;
- The superimposition of responses in space and/or time;
- Responses with a range of spatial and temporal densities; and
- Practical application to a large dataset while minimising subjective decisions.

Chapter 3 developed an iterative method for the identification of seismic responses that answered the research question: Where and when do responses occur? This method is effective in determining the initiation time and approximate centre of seismic responses. This structured approach addresses challenges that are specific to mining induced seismicity by utilising only spatial and temporal parameters to identify responses of various event densities, temporal and spatial scales, and spatially or temporally superimposed responses. The method is insensitive to manual parameter selection as response delineation refines identification outcomes and the spatial and temporal distinction that typically exists between responses. An initial manual estimate of temporal and spatial scales appears to be sufficient given that these scales are refined and validated by a combination of subjective and objective considerations.

Chapter 4 developed a method for the spatial delineation of mining induced seismic responses and answered the research question: What is the extent of responses in space? The procedure

only considers the location of events and delineates a single spatial cluster for each identified response before refinement by temporal modelling. The refinement of associated events addressed the temporal superimposition of mining induced responses. This method performs adequately for a range of synthetic and real scenarios. The spatial scale of rock mass failure is the most distinct feature of seismic responses and, therefore, the comprehensive assessment of clustered seismicity is essential for achieving suitable response delineation. Density-based clustering is an ideal non-parametric method due to a range of relevant advantages, e.g., the ability to cluster arbitrary shapes. Practical implementation of density-based clustering required a number of disadvantages associated with this method to be addressed, e.g., outcomes are sensitive to clustering parameters. Disadvantages are minimised by clustering only one spatial cluster of consistent density per iteration and the use of information initially provided by the iterative identification of responses. These adjustments to the density-based clustering method improve its performance and it successfully delineates a range of spatial and temporal densities while minimising subjective decisions for synthetic and real seismic data.

External clustering validation was achieved by clustering synthetic response scenarios for a range of relative separation and scale characteristics. The performance of clustering is adequately measured by the Matthews Correlation Coefficient that summarised truth class labels determined from prior knowledge of the synthetic dataset. Internal validation utilised the CVNN index that agrees with external validation and is able to reproduce the optimal clustering parameters for medium to high cluster separations. The CVNN index provides insight into the relationship between optimal clustering parameters and the spatial characteristics of real seismic responses. Although a component of subjectivity remains in spatial assessments due to inherently ambiguous clustering decisions, the CVNN index is able to provide guidance for the optimal selection of clustering parameters.

Chapter 5 developed a straightforward and versatile method for the temporal delineation of mining induced seismic responses and answered the research question: When do responses start and finish in time? The initiation of a seismic response is typically unambiguous although there is no clear cessation of event occurrence. Temporal modelling delineated and quantified time-dependent seismicity by only considering the time of event occurrence. Furthermore, the modelling incorporated essential considerations such as the suitability of fit and parametric uncertainties. Quantitative modelling minimises the subjective decisions associated with temporal delineation. Modelling applicable to mining induced responses is enabled by the implementation of the Modified Omori Law (MOL) with a variable  $c$ -parameter and a method

that also allows for the redefinition of individual response event times relative to a variable initiation of the response.

Temporal modelling delineated a response by overestimating response length and subsequently removing events that do not follow consistent temporal observations. The assessment of consistent temporal observations is essential to delineate large datasets of spatially superimposed responses. Temporal intervals were selected by the optimisation of a weighted Maximum Likelihood Estimate (MLE) that considers relevant quantification and delineation objectives. The metric allows for the assessment of responses with a range of temporal densities while additionally minimising subjective modelling decisions. The optimised metric accurately recovers parameters and delineates a range of synthetically generated scenarios that represent simple and challenging cases of mining induced responses. Parameter recovery and delineation errors occur when there is an insufficient contrast in temporal behaviour to distinguish between the linear variation and response events, responses of short durations, and time-independent seismicity that is superimposed with responses.

The case studies presented in Chapter 6 demonstrated the ability of the STIDSR method to account for the challenges associated with mining induced seismicity and address the problem defined by this thesis (Section 2.7). A range of mining environments was assessed within this chapter and analysis outcomes were utilised to develop an objective understanding of time-dependent seismicity. The STIDSR method outcomes reduce the subjectivity and increase the transparency of engineering decisions that strive to minimise seismic risk. The case studies adopted two modes of assessing mine wide seismicity using the STIDSR method. Firstly, specific assessments focused on select seismic responses to blasting and/or large events. Secondly, comprehensive retrospective analysis considered large datasets that contained a range of spatial and temporal response characteristics for an entire seismic history.

The STIDSR method provides insight into aspects of seismic hazard and fundamental rock mechanics by objectively assessing time-dependent seismicity for a range of spatial scales with respect to blasting and large seismic events. Objective assessment of seismic responses and likely causation processes allows for improvements to interpretations of rock mass failure mechanisms, e.g., fault deformation or the initiation of caving. An outcome of the STIDSR method is the temporal quantification of seismic responses that allow for the assessment of factors that may influence seismicity and subsequent seismic response hazard. The quantification results suggest that distinct rock mass failure processes influence the productivity and decay rate of seismic responses. Significant differences in response quantification exist for varied relationships between blasting and geotechnical domains.

Additionally, seismic response quantification allows for the parameterisation of historical and partially observed responses and enables the estimation of time-dependent response hazard.

In addition to identifying and delineating seismic responses, the case studies presented in each section in Chapter 6 (**Table 42** row headings) demonstrated the ability of the STIDSR method to address the challenges associated with mining induced responses (**Table 42** column headings). The emphasised challenges for each of these sections is summarised by using two qualitative classes. A major emphasis addresses the specific challenge associated with mining induced responses that enables the fundamental research questions to be answered. A minor emphasis considers the specific challenge, although, it is not a major consideration or focus.

**Table 42** A summary of thesis objectives that the STIDSR method achieves throughout Chapter 6.

	Only spatial and temporal parameters	Spatial superimposition	Temporal superimposition	A range of event densities	Large datasets minimising subjectivity
<b>6.4 General Application</b>					
6.4.1 Seismic Responses to Routine Blasting	Major	Major	Major	Major	Minor
6.4.2 Response to a Large Seismic Event	Major	Major	Major	Major	Minor
6.4.3 Complex Response to Mining	Major	Minor	Major	Major	Minor
<b>6.5 Seismic Responses and Blasting</b>					
6.5.1 Classification of Responses and Blasting Relationship *	Major	Major	Major	Minor	Major
6.5.2 Responses Remote from Blasting	Major	Minor	Major	Minor	Major
6.5.3 Responses Delayed from Blasting	Major	Major	Minor	Minor	Major
6.5.4 Proportionality of Response Classifications	Major	Minor	Minor	Minor	Major
6.5.5 Temporal Evolution of Response Classifications	Major	Minor	Minor	Minor	Major
<b>6.6 Seismic Responses Evolution *</b>					
6.6.1 General Response Assessment	Minor	Minor	Minor	Minor	Major
6.6.2 Seismic Response and Undercut Blasting	Major	Minor	Major	Major	Major
6.6.3 Quantified Seismic Responses and Blasting Relationship	Major	Minor	Major	Major	Major
<b>6.7 Seismic Response Hazard</b>					
6.7.1 Determination of Seismic Response Hazard	Minor	Minor	Minor	Minor	Minor
6.7.2 Retrospective Parameterisation of Responses	Minor	Minor	Minor	Minor	Major
6.7.3 Current Seismic Response Hazard	Minor	Minor	Minor	Minor	Major

\*Abbreviated headings.

Minor: Considers the specific challenge, although, it is not a major consideration or focus.

Major: Addresses the specific challenge that enables the fundamental research questions to be answered.

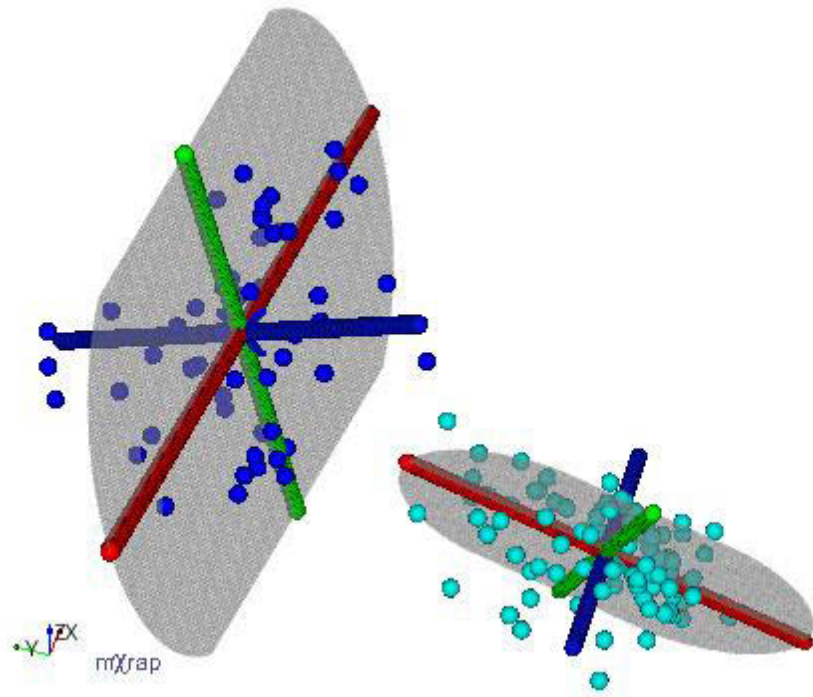
## 8 Recommendations for Future Work

Recommendations for future work fall into two main categories. Firstly, while the iterative identification and delineation of seismic responses achieved its objectives given the scope of this thesis, future work can improve this (or similar) method. Secondly, there are general areas of future work that will improve the current understanding of time-dependent and time-independent seismicity induced by mining. General future work aims to develop the current understanding and methods used to assess seismic hazard to further minimise seismic risk within mines.

### 8.1 Recommendations for the Identification and Delineation of Seismic Responses

The current implementation of the algorithm that identifies and delineates seismic responses can be improved by further developing the spatial aspects of analysis. The selection of spatial clustering parameters requires manual consideration of the spatial scales of seismicity. The current implementation is adequate as choices can be guided by internal performance measures (Section 4.5.5) and is particularly successful when applied to small datasets as these measures can be consistently optimised, e.g., a few days. Before these parameters can be applied to an entire dataset, spatial clustering must be calibrated using typical seismic responses. Spatial clustering can be improved by assessing the spatial properties of seismicity within the temporal modelling window. Further developments could automatically optimise spatial parameters by assessing quality measures during the delineation of seismic responses.

It is recommended that future work develops a method of describing spatial characteristics of seismic responses that is relatable to seismic and non-seismic quantities. This would allow spatial characteristics to be linked to temporal quantities to test hypothesis of rock mass failure processes. While many potential methods exist that can quantify spatial characteristics, an example of further spatial assessment is Principal Component Analysis (PCA). Preliminary work was conducted to quantify spatial clusters through eigenvectors and eigenvalues associated with the PCA method. **Figure 179** shows the primary (red), secondary (green), and tertiary (blue) axis that maximise spatial event variation.



**Figure 179** PCA applied to mining induced seismic responses. Shown are the primary (red), secondary (green), and tertiary (blue) axis of maximum spatial variation.

## 8.2 General Recommendations

### 8.2.1 Seismic Source Mechanism

The characteristics of seismic responses are intrinsically linked to the source of seismicity that arises during the mining. Aspects associated with the mining process can be described with relatively high confidence (e.g., geometry, rates, and volumes). In contrast, other aspects of the mining environment, such as mechanical rock mass properties and stress conditions, are challenging to describe.

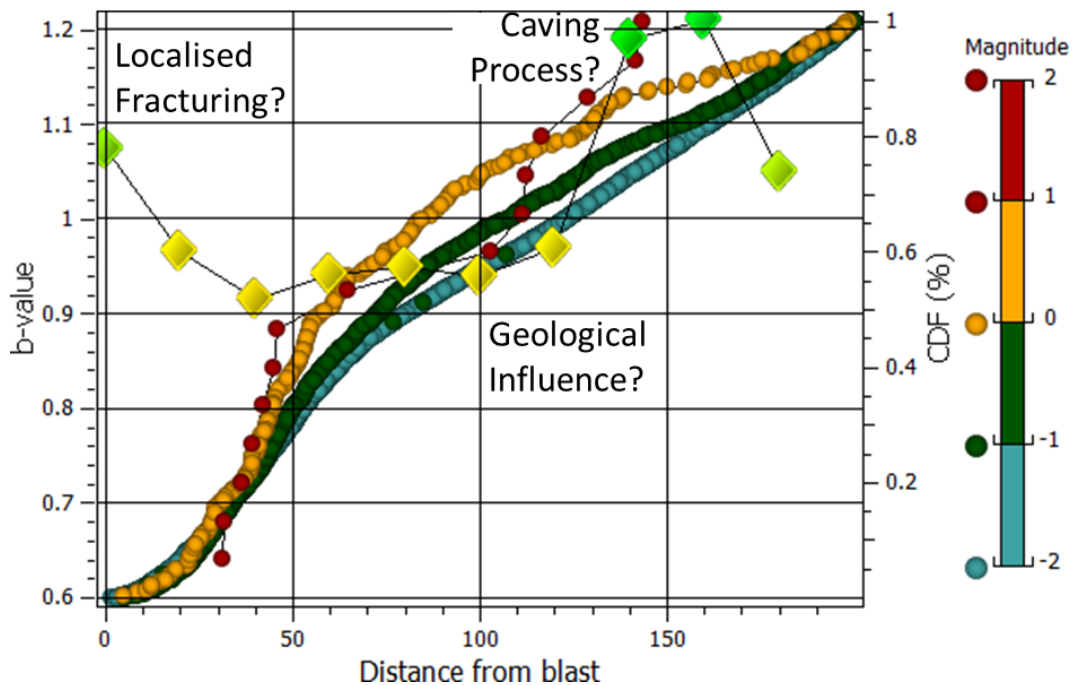
It is recommended that additional seismic and non-seismic information is considered in conjunction with qualitative and quantitative STIDSR (spatially and temporally, identified and delineated, seismic responses) results. Additional information can provide insight and increase confidence in the relationship between seismic responses and causative sources. Additional information includes (but is not limited to):

- Seismic source parameters, e.g. energy and moment along with derivative measures such as stress drop, energy index, and apparent volume;
- Seismic moment tensors;
- Numerical modelling;
- Non-seismic monitoring, e.g. extensometers and stress cells;
- Geotechnical aspects, e.g. faulting and geological contacts along with rock mass characteristics such as joint sets, strength, and brittleness; and
- Mining aspects, e.g. geometry, rates, and volumes.

The b-value is of particular importance when inferring seismic source mechanisms as this statistic has significant implications for seismic hazard (Section 6.7). A limitation to assessing the b-value is the quantity of seismic events needed to establish a magnitude-frequency relationship. The need for a large quantity of data results in responses being grouped spatially or temporally and this inevitably, leads to a combination of seismicity resulting from different rock mass failure processes. The ability to assess the contribution of different rock mass processes that result in contrasting magnitude-frequency distributions depends on the ability of assessment to create relevant groups of seismicity, i.e., groups of seismicity generated by similar failure processes. The ability to assess spatially or temporally superimposed seismic responses allows for the evaluation of b-values associated with time-dependent seismicity that exhibits similar spatial and temporal characteristics. The capability to investigate the magnitude-frequency relationship further, allows for a more complete understanding of

seismic hazard to be developed and, therefore, an improved management of seismic hazard. It is recommended that further work investigate the relationship between the spatial and temporal characteristics of seismic responses and b-values.

**Figure 180** illustrates the relationship between b-values and spatially controlled sources of seismicity in a sublevel caving environment. The b-value is high (1.09) for seismicity close to the location of blasting (<20 m) before reducing to 0.95 for intermediate distances (20 to 140 m) within and closely surrounding the cave. Higher b-values (1.05-1.2) are found for distances (>140 m) due to the inclusion of caving seismicity. The cumulative count distributions show that relatively few events occur within the first 30 m to blasting with the vast majority of large and significant events occurring between 30 and 140 m. Cumulative distributions exhibit a strong spatial relation to blasting, particularly the significant events ( $0 < M_L < 1$ ).



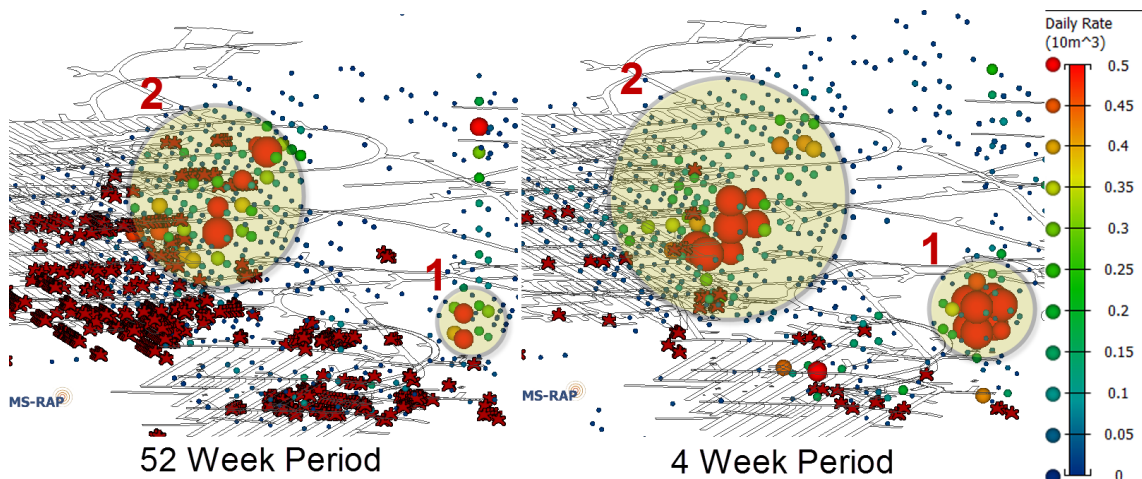
**Figure 180** Initially b-values are elevated (1.09), before falling and remaining constant (0.95) up to a radius of 140 m, and then rising (1.05-1.2) with the inclusion of caving seismicity (diamond series). Cumulative count distributions are strongly related to blasting with the majority of large and significant events at a distance between 30 and 140 m (spherical series).

### 8.2.2 Time-Independent Rates of Seismicity

The identification and delineation of seismic responses allows for assessment of the spatial and temporal characteristics of the remaining and presumably time-independent seismicity. Further work should develop analysis of time-independent rates of seismicity to understand the scales of spatial and temporal event occurrence.

Time-independent events are intrinsically linked to sources of seismicity and, therefore, are sensitive to the spatial and temporal aspects of analysis. The most obvious manifestation of this is when a source of seismicity is newly established. Using a longer period will average out the temporal occurrence of these events resulting in a lower time-independent rate of seismicity when compared to results using a shorter analysis period. Volumetric event rates (daily events per  $10\text{m}^3$ ) shown in Area 1 (**Figure 181**) provide a clear example of when a newly established source of seismicity becomes active. The significantly increased time-independent rate associated with this feature is less obvious over a 52-week period (left) in comparison to a 4-week period (right).

Less obvious cases of spatial and temporal variation in time-independent rates are potentially more relevant as they may go unnoticed. When a rock mass experiences relatively small incremental changes to stress conditions, in comparison to the existing stress state, the occurrence of time-independent seismicity may appear consistent, yet slowly increase. When blasting has a significant influence on seismicity, time-independent rates may be subject to significant variation. The latter case is particularly sensitive to the selection of the analysis period. Area 2 in **Figure 181** shows that the abutment has reasonably consistent time-independent seismicity ( $0.1\text{--}0.3$  daily rate per  $10\text{m}^3$ ). The highest volumetric rates of time-independent seismicity occur with the abutment ( $>0.4$  daily rate per  $10\text{m}^3$ ). High rates associated with recent blasting are averaged out over a longer analysis period (52-weeks). A shorter analysis period reveals high rates are closely associated with recent blasting (4-weeks).



**Figure 181** Comparison of volumetric time-independent event rates calculated using 52-week (left) and 4-week (right) periods. Shown is a new source of seismicity (area 1) and an abutment (area 2) along with blasting during these periods.

### **8.2.3 Comprehensive Seismic Hazard**

The generalised seismic response hazard presented in this thesis (Section 6.7) examines an individual seismic response. Further work is required to transfer this generalise simple approach into a more comprehensive seismic hazard. Further work should develop a hazard model that is temporally continuous and considers time-dependent and time-independent spatial sources of seismicity. Furthermore, it is recommended that future work ensure that b-values used by the seismic hazard model are representative of the spatially and temporally active sources of seismicity.

The model of seismic hazard forms an essential component for the assessment seismic risk. Basic seismic hazard experienced by a specific excavation depends on the magnitude of a seismic event and the distance to the seismic source. A significant amount of future work is required to develop a reliable model that considers spatial and temporal sources of time-dependent and independent seismicity. Such a model can significantly benefit the mining industry by allowing engineering decisions to be based on an accurate quantification of seismic hazard.

## 9 References

- Akaike, H. 1974, 'A New Look at the Statistical Model Identification', *IEEE Transactions on Automatic Control*, vol. 19, no. 6, pp. 716-723.
- Aliguliyev, R.M. 2009, 'Performance Evaluation of Density-Based Clustering Methods', *Information Sciences*, vol. 179, no. 20, pp. 3583-3602.
- Amelung, F. & King, G. 1997, 'Earthquake Scaling Laws for Creeping and Non-Creeping Faults', *Geophysical Research Letters*, vol. 24, no. 5, pp. 507-510.
- Anagnos, T. & Kiremidjian, A.S. 1988, 'A Review of Earthquake Occurrence Models for Seismic Hazard Analysis', *Probabilistic Engineering Mechanics*, vol. 3, no. 1, pp. 3-11.
- Anderson, T.W. & Darling, D.A. 1954, 'A Test of Goodness of Fit', *American Statistical Association*, vol. 49, no. 268, pp. 765-769.
- Ankerst, M., Breunig, M., Kriegel, H. & Sander, J. 1999, 'Optics: Ordering Points to Identify the Clustering Structure', in *ACM SIGMOD International Conference on Management of Data ACM*, Philadelphia, Pennsylvania, pp. 49-60.
- Arbi, H., Riyanto, E., Rabbani, R. & Meiharrik, L. 2012, 'Shear Slip Indication at Big Gossan Mine', in *6th International Seminar on Deep and High Stress Mining*, ed. Y. Potvin, Australia Centre for Geomechanics, Perth, Australia, pp. 189-200.
- Arora, S.K., Willy, Y.A., Srinivasan, C. & Benady, S. 2001, 'Local Seismicity Due to Rockbursts and near-Field Attenuation of Ground Motion in the Kolar Gold Mining Region, India', *International Journal of Rock Mechanics and Mining Sciences*, vol. 38, no. 5, pp. 711-719.
- Baiesi, M. & Paczuski, M. 2004, 'Scale-Free Networks of Earthquakes and Aftershocks', *Physical Review E*, vol. 69, no. 6, p. 066106.
- Baldi, P., Brunak, S., Chauvin, Y., Andersen, C.A.F. & Nielsen, H. 2000, 'Assessing the Accuracy of Prediction Algorithms for Classification: An Overview', *Bioinformatics*, vol. 16, no. 5, pp. 412-424.
- Bohnenstiehl, D.R., Tolstoy, M., Dziak, R.P., Fox, C.G. & Smith, D.K. 2002, 'Aftershock Sequences in the Mid-Ocean Ridge Environment: An Analysis Using Hydroacoustic Data', *Tectonophysics*, vol. 354, no. 1, pp. 49-70.
- Bottiglieri, M., Lippiello, E., Godano, C. & de Arcangelis, L. 2009, 'Identification and Spatiotemporal Organization of Aftershocks', *Geophysical Research: Solid Earth (1978–2012)*, vol. 114, no. B3, p. B03303.
- Butt, S.D., Calder, P.N. & Apel, D.B. 1998, 'The Use of High Frequency and Mine-Wide Microseismic Systems to Monitor the Movement of Blasting Induced Stresses', *CIM bulletin*, vol. 93, no. 1040, pp. 90-95.
- Cho, N.F., Tiampo, K.F., McKinnon, S.D., Vallejos, J.A., Klein, W. & Dominguez, R. 2010, 'A Simple Metric to Quantify Seismicity Clustering', *Nonlinear Processes in Geophysics*, vol. 17, no. 4, pp. 293-302.
- Cook, N.G.W. 1976, 'Seismicity Associated with Mining', *Engineering Geology*, vol. 10, no. 2, pp. 99-122.
- Creamer, F.H. 1994, The Relation between Temperature and Earthquake Aftershock Decay for Aftershock Sequences near Japan, PhD Thesis, University of Colorado.

- Davis, S.D. & Frohlich, C. 1991a, 'Single-Link Cluster Analysis of Earthquake Aftershocks: Decay Laws and Regional Variations', *Geophysical Research: Solid Earth (1978–2012)*, vol. 96, no. B4, pp. 6335-6350.
- Davis, S.D. & Frohlich, C. 1991b, 'Single-Link Cluster Analysis, Synthetic Earthquake Catalogues, and Aftershock Identification', *Geophysical Journal International*, vol. 104, no. 2, pp. 289-306.
- Deborah, L.J., Baskaran, R. & Kannan, A. 2010, 'A Survey on Internal Validity Measure for Cluster Validation', *International Journal of Computer Science & Engineering Survey*, vol. 1, no. 2, pp. 85-102.
- Dieterich, J. 1994, 'A Constitutive Law for Rate of Earthquake Production and Its Application to Earthquake Clustering', *Geophysical Research: Solid Earth (1978–2012)*, vol. 99, no. B2, pp. 2601-2618.
- Disley, N.V. 2014, 'Seismic Risk and Hazard Management at Kidd Mine', in *Deep Mining 2014*, eds M. Hudyma & Y. Potvin, Australian Centre for Geomechanics, Sudbury, Canada, pp. 107-121.
- Dunlop, R.E. & Gaete, S.B. 2001, 'Induced Seismicity at El Teniente Mine: The Esmeralda Sector Case History', in *5th International Symposium on Rockbursts and Seismicity in Mines* South African Institute of Mining and Metallurgy, South Africa, pp. 287-292.
- Duplancic, P. 2001, Characterisation of Caving Mechanisms through Analysis of Stress and Seismicity, PhD Thesis, University of Western Australia.
- Enescu, B., Mori, J., Miyazawa, M. & Kano, Y. 2009, 'Omori-Utsu Law C-Values Associated with Recent Moderate Earthquakes in Japan', *Bulletin of the Seismological Society of America*, vol. 99, no. 2A, pp. 884-891.
- Eremenko, V.A., Eremenko, A.A., Rasheva, S.V. & Turuntaev, S.B. 2009, 'Blasting and the Man-Made Seismicity in the Tashtagol Mining Area', *Mining Science*, vol. 45, no. 5, pp. 468-474.
- Ertöz, L., Steinbach, M. & Kumar, V. 2003, 'Finding Clusters of Different Sizes, Shapes, and Densities in Noisy, High Dimensional Data', in *SIAM International Conference on Data Mining*, Society for Industrial and Applied Mathematics, San Francisco, California, pp. 47-58.
- Ester, M., Kriegel, H.-P., Sander, J. & Xu, X. 1996, 'A Density-Based Algorithm for Discovering Clusters in Large Spatial Databases with Noise', *Knowledge Discovery and Data Mining*, vol. 96, no. 34, pp. 226-231.
- Falmagne, V. 2001, Quantification of Rock Mass Degradation Using Micro-Seismic Monitoring and Applications for Mine Design, PhD Thesis, Queen's University.
- Fawzy, M., Badr, A., Reda, M. & Farag, I. 2013, 'Dbclum: Density-Based Clustering and Merging Algorithm', *International Journal of Computer Applications*, vol. 79, no. 14, pp. 1-6.
- Felzer, K.R., Abercrombie, R.E. & Ekström, G. 2004, 'A Common Origin for Aftershocks, Foreshocks, and Multiplets', *Bulletin of the Seismological Society of America*, vol. 94, no. 1, pp. 88-98.
- Felzer, K.R. & Brodsky, E.E. 2006, 'Decay of Aftershock Density with Distance Indicates Triggering by Dynamic Stress', *Nature*, vol. 441, no. 7094, pp. 735-738.
- Finnie, G.J. 1999, 'Using Neural Networks to Discriminate between Genuine and Spurious Seismic Events in Mines', *Pure and Applied Geophysics*, vol. 154, no. 1, pp. 41-56.
- Frohlich, C. & Davis, S.D. 1985, 'Identification of Aftershocks of Deep Earthquakes by a New Ratios Method', *Geophysical Research Letters*, vol. 12, no. 10, pp. 713-716.
- Frohlich, C. & Davis, S.D. 1990, 'Single-Link Cluster Analysis as a Method to Evaluate Spatial and Temporal Properties of Earthquake Catalogues', *Geophysical Journal International*, vol. 100, no. 1, pp. 19-32.

- Gardner, J.K. & Knopoff, L. 1974, 'Is the Sequence of Earthquakes in Southern California, with Aftershocks Removed, Poissonian?', *Bulletin of the Seismological Society of America*, vol. 64, no. 5, pp. 1363-1367.
- Gasperini, P. & Lolli, B. 2006, 'Correlation between the Parameters of the Aftershock Rate Equation: Implications for the Forecasting of Future Sequences', *Physics of the Earth and Planetary Interiors*, vol. 156, no. 1, pp. 41-58.
- Gasperini, P. & Lolli, B. 2009, 'An Empirical Comparison among Aftershock Decay Models', *Physics of the Earth and Planetary Interiors*, vol. 175, no. 3, pp. 183-193.
- Gibowicz, S.J. 1990, 'Seismicity Induced by Mining', *Advances in Geophysics*, vol. 32, pp. 1-74.
- Gibowicz, S.J. & Kijko, A. 1994, 'An Introduction to Mining Seismology', in, vol. 55, Academic Press, San Diego.
- Gibowicz, S.J. & Lasocki, S. 2001, 'Seismicity Induced by Mining: Ten Years Later', *Advances in Geophysics*, vol. 44, pp. 39-181.
- Gross, S.J. & Kisslinger, C. 1994, 'Tests of Models of Aftershock Rate Decay', *Bulletin of the Seismological Society of America*, vol. 84, no. 5, pp. 1571-1579.
- Guha, S., Rastogi, R. & Shim, K. 1998, 'Cure: An Efficient Clustering Algorithm for Large Databases', in *ACM Sigmod Record*, ACM, pp. 73-84.
- Gutenberg, B. & Richter, C.F. 1944, 'Frequency of Earthquakes in California.', *Bulletin of the Seismological Society of America*, vol. 34, no. 4, pp. 185-188.
- Halkidi, M., Batistakis, Y. & Vazirgiannis, M. 2002, 'Clustering Validity Checking Methods: Part 2', *ACM Sigmod Record*, vol. 31, no. 3, pp. 19-27.
- Halkidi, M. & Vazirgiannis, M. 2001, 'Clustering Validity Assessment: Finding the Optimal Partitioning of a Data Set', in *IEEE International Conference on Data Mining*, IEEE, pp. 187-194.
- Hasegawa, H.S., Wetmiller, R.J. & Gendzwil, D.J. 1989, 'Induced Seismicity in Mines in Canada—an Overview', *Pure and Applied Geophysics*, vol. 129, no. 3-4, pp. 423-453.
- Heal, D. 2007, *Perilya Broken Hill - Investigation of Re-Entry Times Following Production Blasts*, Australian Centre for Geomechanics, Perth.
- Heal, D., Hudyma, M. & Vezina, F. 2005, 'Seismic Hazard at Agnico-Eagle's Laronde Mine Using Ms-Rap', in *CIM Maintenance Engineering and Mine Operators Conference*, Canadian Institute of Mining, Sudbury, Canada.
- Hedley, D.G.F. & Udd, J.E. 1989, 'The Canada-Ontario-Industry Rockburst Project', in *Seismicity in Mines*, vol. 129, ed. S.J. Gibowicz, Birkhäuser Basel, pp. 661-672.
- Helmstetter, A., Kagan, Y.Y. & Jackson, D.D. 2005, 'Importance of Small Earthquakes for Stress Transfers and Earthquake Triggering', *Geophysical Research: Solid Earth (1978–2012)*, vol. 110, no. B5, pp. 1-13.
- Helmstetter, A. & Sornette, D. 2002, 'Subcritical and Supercritical Regimes in Epidemic Models of Earthquake Aftershocks', *Geophysical Research: Solid Earth (1978–2012)*, vol. 107, no. B10, pp. 1-21.
- Hill, D.P. & Prejean, S.G. 2007, 'Dynamic Triggering', in *Earthquake Seismology* vol. 4, ed. H. Kanamori, Elsevier, Amsterdam, pp. 258-288.
- Hills, P.B. & Penney, A.R. 2008, 'Management of Seismicity at the Beaconsfield Gold Mine, Tasmania', in *10th Underground Operators' Conference*, Australasian Institute of Mining and Metallurgy, Launceston, Tasmania, Australia, pp. 157-170.

- Hinneburg, A. & Keim, D.A. 1998, 'An Efficient Approach to Clustering in Large Multimedia Databases with Noise', in *The Fourth International Conference on Knowledge Discovery and Data Mining*, eds R. Agrawal & P. Stolorz, AAAI Press, Menlo Park, California, pp. 58-65.
- Hofmann, G.F. & Murphy, S.K. 2007, 'Coulomb Stress Triggering in the Underground Mining Environment', in *1st Canada - U.S. Rock Mechanics Symposium*, eds E. Eberhardt, D. Stead & T. Morrison, Taylor & Francis 2007, Vancouver, Canada, pp. 1415-1422.
- Hudyma, M. 2008, Analysis and Interpretation of Clusters of Seismic Events in Mines, PhD Thesis, University of Western Australia.
- Hudyma, M., Beneteau, D. & Potvin, M. 2012, 'Evaluating Seismic Source Mechanism with Phasor Analysis', *Geotechnique Letters*, vol. 2, pp. 3-7.
- Hudyma, M., Heal, D. & Mikula, P. 2003, 'Seismic Monitoring in Mines - Old Technology - New Applications', in *1st Australasian Ground Control in Mining Conference*, ed. B.K. Hebblewhite, UNSW School of Mining Engineering, Sydney, Australia, pp. 201-218.
- Hudyma, M., Mikula, P. & Owen, M. 2002, 'Seismic Hazard Mapping at Mt. Charlotte Mine', in *5th North American Rock Mechanics Symposium*, eds R. Hammah, W. Bawden, J. Curran & M. Telesnicki, University of Toronto Press, Toronto, Ontario, Canada, pp. 1087 - 1094.
- Hudyma, M. & Potvin, Y. 2008, 'Characterizing Caving Induced Seismicity at Ridgeway Gold Mine', in *5th International Conference and Exhibition on Mass Mining*, eds H. Schunnesson & E. Nordlund, Luleå University of Technology, Luleå, pp. 931-942.
- Hudyma, M. & Potvin, Y. 2010, 'An Engineering Approach to Seismic Risk Management in Hardrock Mines', *Rock Mechanics and Rock Engineering*, vol. 43, no. 6, pp. 891-906. Available from: ProQuest Science Journals.
- Ishimoto, M. & Iida, K. 1939, 'Observations of Earthquakes Registered with the Microseismograph Constructed Recently', *Bulletin of the Earthquake Research Institute*, vol. 17, pp. 443-478.
- Jain, A.K., Murty, M.N. & Flynn, P.J. 1999, 'Data Clustering: A Review', *ACM Computing Surveys*, vol. 31, no. 3, pp. 264-323.
- Kagan, Y.Y. 2004, 'Short-Term Properties of Earthquake Catalogs and Models of Earthquake Source', *Bulletin of the Seismological Society of America*, vol. 94, no. 4, pp. 1207-1228.
- Kagan, Y.Y. 2006, 'Why Does Theoretical Physics Fail to Explain and Predict Earthquake Occurrence?', in *Modelling Critical and Catastrophic Phenomena in Geoscience: A Statistical Physics Approach*, vol. 705, eds P. Bhattacharyya & B.K. Chakrabarti, Springer-Verlag Berlin Heidelberg, pp. 303-359.
- Kagan, Y.Y. & Jackson, D.D. 1991, 'Long-Term Earthquake Clustering', *Geophysical Journal International*, vol. 104, no. 1, pp. 117-133.
- Kagan, Y.Y. & Knopoff, L. 1981, 'Stochastic Synthesis of Earthquake Catalogs', *Geophysical Research: Solid Earth (1978-2012)*, vol. 86, no. B4, pp. 2853-2862.
- Kagan, Y.Y. & Knopoff, L. 1987, 'Statistical Short-Term Earthquake Prediction', *Science*, vol. 236, no. 4808, pp. 1563-1567.
- Karypis, G., Han, E.-H. & Kumar, V. 1999, 'Chameleon: Hierarchical Clustering Using Dynamic Modeling', *Computer*, vol. 32, no. 8, pp. 68-75.
- Kgarume, T. 2010, Mine Aftershocks and Implications for Seismic Hazard Assessment, MSc Thesis, University of the Witwatersrand.
- Kgarume, T., Spottiswoode, S. & Durrheim, R. 2010a, 'Statistical Properties of Mine Tremor Aftershocks', *Pure and Applied Geophysics*, vol. 167, no. 1, pp. 107-117.

- Kgarume, T.E., Spottiswoode, S.M. & Durrheim, R.J. 2010b, 'Deterministic Properties of Mine Tremor Aftershocks', in *5th International Seminar on Deep and High Stress Mining*, eds M. Van Sint Jan & Y. Potvin, Australian Centre for Geomechanics, Santiago, Chile, pp. 227-237.
- Kijko, A. & Funk, C.W. 1996, 'Space-Time Interaction Amongst Clusters of Mining Induced Seismicity', *Pure and Applied Geophysics*, vol. 147, no. 2, pp. 277-288.
- Kisslinger, C. 1993, 'The Stretched Exponential Function as an Alternative Model for Aftershock Decay Rate', *Geophysical Research: Solid Earth (1978–2012)*, vol. 98, no. B2, pp. 1913-1921.
- Kisslinger, C. & Jones, L.M. 1991, 'Properties of Aftershock Sequences in Southern California', *Geophysical Research: Solid Earth (1978–2012)*, vol. 96, no. B7, pp. 11947-11958.
- Klein, F.W., Wright, T. & Nakata, J. 2006, 'Aftershock Decay, Productivity, and Stress Rates in Hawaii: Indicators of Temperature and Stress from Magma Sources', *Geophysical Research: Solid Earth (1978–2012)*, vol. 111, no. B7, p. B07307.
- Knopoff, L., Kagan, Y.Y. & Knopoff, R. 1982, 'B Values for Foreshocks and Aftershocks in Real and Simulated Earthquake Sequences', *Bulletin of the Seismological Society of America*, vol. 72, no. 5, pp. 1663-1676.
- Kriegel, H.-P., Kröger, P., Sander, J. & Zimek, A. 2011, 'Density-Based Clustering', *Wiley Interdisciplinary Reviews: Data Mining and Knowledge Discovery*, vol. 1, no. 3, pp. 231-240.
- Kulhanek, O. 2005, *Seminar on B-Value*, Prague Centre of Mathematical Geophysics, Meteorology, and their Applications Dept. of Geophysics, Charles University, Prague.
- Kwiatek, G. 2004, 'A Search for Sequences of Mining-Induced Seismic Events at the Rudna Copper Mine in Poland', *Acta Geophysica Polonica*, vol. 52, no. 2.
- Larsson, K. 2004, Mining Induced Seismicity in Sweden, Licentiate Thesis, Luleå University of Technology.
- Legge, N.B. & Spottiswoode, S.M. 1987, 'Fracturing and Microseismicity Ahead of a Deep Gold Mine Stope in the Pre-Remnant and Remnant Stages of Mining', in *6th International Conference on Rock Mechanics*, A A Balkema, Montreal, Canada, pp. 1071-1077.
- Lewis, P.A.W. 1961, 'Distribution of the Anderson-Darling Statistic', *The Annals of Mathematical Statistics*, vol. 32, no. 4, pp. 1118-1124.
- Li, T., Cai, M.F. & Cai, M. 2007, 'A Review of Mining-Induced Seismicity in China', *International Journal of Rock Mechanics and Mining Sciences*, vol. 44, no. 8, pp. 1149-1171.
- Liu, Y., Li, Z., Xiong, H., Gao, X. & Wu, J. 2010, 'Understanding of Internal Clustering Validation Measures', in *10th International Conference on Data Mining*, IEEE, pp. 911-916.
- Liu, Y., Li, Z., Xiong, H., Gao, X., Wu, J. & Wu, S. 2013, 'Understanding and Enhancement of Internal Clustering Validation Measures', *IEEE Transactions on Cybernetics*, vol. 43, no. 3, pp. 982-994.
- Lolli, B., Boschi, E. & Gasperini, P. 2009, 'A Comparative Analysis of Different Models of Aftershock Rate Decay by Maximum Likelihood Estimation of Simulated Sequences', *Geophysical Research: Solid Earth (1978–2012)*, vol. 114, no. B1, p. B01305.
- Malek, F. & Leslie, I.S. 2006, 'Using Seismic Data for Rockburst Re-Entry Protocol at Inco's Copper Cliff North Mine', in *The 41st U.S. Symposium on Rock Mechanics*, American Rock Mechanics Association, Golden, Colorado pp. 06-1163.
- Matsumura, S. 1984, 'A One-Parameter Expression of Seismicity Patterns in Space and Time', *Bulletin of the Seismological Society of America*, vol. 74, no. 6, pp. 2559-2576.

- Matthews, B.W. 1975, 'Comparison of the Predicted and Observed Secondary Structure of T4 Phage Lysozyme', *Biochimica et Biophysica Acta (BBA) - Protein Structure*, vol. 405, no. 2, pp. 442-451.
- McGarr, A. & Simpson, D. 1997, 'Keynote Lecture: A Broad Look at Induced and Triggered Seismicity', in *4th International Symposium on Rock bursts and Seismicity in Mines*, eds S.J. Gibowicz & S. Lasocki, A.A. Balkema, Poland, pp. 385-396.
- McGarr, A., Simpson, D. & Seeber, L. 2002, 'Case Histories of Induced and Triggered Seismicity', in *International Handbook of Earthquake and Engineering Seismology Part a (International Geophysics)*, vol. 81 A, eds H.K. William, H. Kanamori, P.C. Jennings & C. Kisslinger, Academic Press, International Geophysics, pp. 647-661.
- McKinnon, S.D. 2006, 'Triggering of Seismicity Remote from Active Mining Excavations', *Rock Mechanics and Rock Engineering*, vol. 39, no. 3, pp. 255-279.
- Melick, A.G. 2007, *Beaconsfield Investigation Report*, Tasmanian Government, [http://www.magistratescourt.tas.gov.au/coronial/mellick\\_report](http://www.magistratescourt.tas.gov.au/coronial/mellick_report)
- Mendecki, A. 2005, 'Persistence of Seismic Rock Mass Response to Mining', in *6th International Symposium on Rockburst and Seismicity in Mines*, eds Y. Potvin & M. Hudyma, Perth, Australia, pp. 97-105.
- Mendecki, A.J. 2008, 'Keynote Address: Forecasting Seismic Hazard in Mines', in *1st Southern Hemisphere International Rock Mechanics Symposium*, eds Y. Potvin, J. Carter, A. Dyskin & R. Jeffrey, Perth, Australia, p. 17.
- Mendecki, A.J. 2013, 'Characteristics of Seismic Hazard in Mines: Keynote Lecture', in *8th International Symposium on Rockbursts and Seismicity in Mines*, eds A. Malovichko & D. Malovichko, Geophysical Survey of Russian Academy of Sciences, Petersburg-Moscow, Russia, pp. 275-292.
- Mendecki, A.J. & Lynch, R.A. 2004, *Experimental and Theoretical Investigations of Fundamental Processes in Mining Induced Fracturing and Rock Instability Close to Excavations*, ISS International Limited, Johannesburg.
- Mendecki, A.J., van Aswegen, G. & Mountfort, G.v. 1999, 'A Guide to Routine Seismic Monitoring in Mines', in *A Handbook on Rock Engineering Practice for Tabular Hard Rock Mines*, eds J. Ryder & A. Jager, Creda Communications, Cape Town.
- Mogi, K. 1962, 'Magnitude-Frequency Relationship for Elastic Shocks Accompanying Fractures of Various Materials and Some Related Problems in Earthquakes ', *Bulletin of the Earthquake Research Institute*, vol. 40, pp. 831-883.
- Molchan, G.M. & Dmitrieva, O.E. 1992, 'Aftershock Identification - Methods and New Approaches', *Geophysical Journal International*, vol. 109, no. 3, pp. 501-516.
- Mollison, L., Sweby, G. & Potvin, Y. 2003, 'Changes in Mine Seismicity Following a Mine Shutdown', in *1st Australasian Ground Control in Mining Conference*, ed. B.K. Hebblewhite, UNSW School of Mining Engineering, Sydney, pp. 181-191.
- Morrison, D.M., Blake, W. & Hedley, D.G.F. 2002, '100 Years of Rockbursting in North American Hard Rock Mines', in *1st International Seminar on Deep and High Stress Mining*, Australian Centre for Geomechanics, Perth, Australia, p. Section 2.
- Naoi, M., Nakatani, M., Yabe, Y., Kwiatak, G., Igarashi, T. & Plenkens, K. 2011, 'Twenty Thousand Aftershocks of a Very Small (M 2) Earthquake and Their Relation to the Mainshock Rupture and Geological Structures', *Bulletin of the Seismological Society of America*, vol. 101, no. 5, pp. 2399-2407.

- Narteau, C., Shebalin, P. & Holschneider, M. 2002, 'Temporal Limits of the Power Law Aftershock Decay Rate', *Geophysical Research: Solid Earth (1978–2012)*, vol. 107, no. B12, pp. ESE-12.
- Nyffenegger, P. 1998, Aftershock Occurrence Rate Decay for Individual Sequences and Catalogs, PhD Thesis, University of Texas at Austin
- Nyffenegger, P. & Frohlich, C. 1998, 'Recommendations for Determining P Values for Aftershock Sequences and Catalogs', *Bulletin of the Seismological Society of America*, vol. 88, no. 5, pp. 1144-1154.
- Nyffenegger, P. & Frohlich, C. 2000, 'Aftershock Occurrence Rate Decay Properties for Intermediate and Deep Earthquake Sequences', *Geophysical Research Letters*, vol. 27, no. 8, pp. 1215-1218.
- Ogata, Y. 1983, 'Estimation of the Parameters in the Modified Omori Formula for Aftershock Frequencies by the Maximum Likelihood Procedure. ', *Physics of the Earth*, vol. 31, no. 2.
- Ogata, Y. 1988, 'Statistical Models for Earthquake Occurrences and Residual Analysis for Point Processes', *American Statistical Association*, vol. 83, no. 401, pp. 9-27.
- Ogata, Y., Utsu, T. & Katsura, K. 1996, 'Statistical Discrimination of Foreshocks from Other Earthquake Clusters', *Geophysical Journal International*, vol. 127, no. 1, pp. 17-30.
- Omori, F. 1894a, 'On after-Shocks', *Seismological Journal of Japan*, vol. 19, pp. 71-80.
- Omori, F. 1894b, 'On the after-Shocks of Earthquakes', *College of Science, Imperial University of Tokyo*, vol. 7, no. 2, pp. 111-200.
- Orlecka-Sikora, B. 2010, 'The Role of Static Stress Transfer in Mining Induced Seismic Events Occurrence, a Case Study of the Rudna Mine in the Legnica-Glogow Copper District in Poland', *Geophysical Journal International*, vol. 182, no. 2, pp. 1087-1095.
- Ortlepp, W.D. 1999, 'Stress and How It Leads to Seismicity', in *ACG Workshop on Mine Seismicity and Rockburst Risk Management in Underground Mines*, Australian Centre for Geomechanics, Perth, Australia.
- Ortlepp, W.D. 2005, 'Rasim Comes of Age — a Review of the Contribution to the Understanding and Control of Mine Rockbursts', in *6th International Symposium on Rockburst and Seismicity in Mines*, eds Y. Potvin & M. Hudyma, Australian Centre for Geomechanics, Perth, Western Australia, Australia, pp. 9-11.
- Parker, C. 2011, 'An Analysis of Performance Measures for Binary Classifiers', in *11th International Conference on Data Mining*, pp. 517-526.
- Pei, T., Jasra, A., Hand, D., Zhu, A.X. & Zhou, C. 2009, 'Decode: A New Method for Discovering Clusters of Different Densities in Spatial Data', *Data Mining and Knowledge Discovery*, vol. 18, no. 3, pp. 337-369.
- Peng, Z., Vidale, J.E. & Houston, H. 2006, 'Anomalous Early Aftershock Decay Rate of the 2004 Mw6.0 Parkfield, California, Earthquake', *Geophysical Research Letters*, vol. 33, no. 17, p. L17307.
- Penney, A.R. 2011, Development of Re-Entry Guidelines and Exclusion Zones at the Tasmania Gold Mine, MSc Thesis, Curtin University of Technology.
- Phillips, W.S., Pearson, D.C., Edwards, C.L. & Stump, W.B. 1997, 'Microseismicity Induced by a Controlled, Mine Collapse at White Pine, Michigan', *International Journal of Rock Mechanics and Mining Sciences*, vol. 34, no. 3, pp. 246-e1.
- Plenkers, K., Kwiatek, G., Nakatani, M. & Dresen, G. 2010, 'Observation of Seismic Events with Frequencies  $F > 25$  Khz at Mponeng Deep Gold Mine, South Africa', *Seismological Research Letters*, vol. 81, no. 3, pp. 467-479.

- Potvin, Y. 2009, 'Strategies and Tactics to Control Seismic Risks in Mines', *Journal of the South African Institute of Mining and Metallurgy*, vol. 109, no. 3, pp. 177-186.
- Potvin, Y., Wesseloo, J. & Heal, D. 2010, 'An Interpretation of Ground Support Capacity Submitted to Dynamic Loading', *Mining Technology*, vol. 119, no. 4, pp. 233-245.
- Reasenber, P. 1985, 'Second-Order Moment of Central California Seismicity, 1969–1982', *Geophysical Research: Solid Earth (1978–2012)*, vol. 90, no. B7, pp. 5479-5495.
- Reasenber, P.A. & Jones, L.M. 1989, 'Earthquake Hazard after a Mainshock in California', *Science*, vol. 243, no. 4895, pp. 1173-1176.
- Rebuli, D.B. & Kohler, S.J. 2014, 'Using Clustering Algorithms to Assist Short-Term Seismic Hazard Analysis in Deep South African Mines', in *Deep Mining 2014*, eds M. Hudyma & Y. Potvin, Australian Centre for Geomechanics, Sudbury, Canada, pp. 107-121.
- Reimnitz, M. 2004, Shear-Slip Induced Seismic Activity in Underground Mines: A Case Study in Western Australia, MSc Thesis, University of Western Australia.
- Ryder, J.A. 1988, 'Excess Shear Stress in the Assessment of Geologically Hazardous Situations', *Journal of the South African Institute of Mining and Metallurgy*, vol. 88, no. 1, p. 14.
- Saichev, A. & Sornette, D. 2007, 'Power Law Distributions of Seismic Rates', *Tectonophysics*, vol. 431, no. 1, pp. 7-13.
- Sander, J., Ester, M., Kriegel, H.-P. & Xu, X. 1998, 'Density-Based Clustering in Spatial Databases: The Algorithm Gdbscan and Its Applications', *Data Mining and Knowledge Discovery*, vol. 2, no. 2, pp. 169-194.
- Scholz, C.H. 1968, 'The Frequency-Magnitude Relation of Microfracturing in Rock and Its Relation to Earthquakes', *Bulletin of the Seismological Society of America*, vol. 58, no. 1, pp. 399-415.
- Shilen, S. & Toksöz, M.N. 1974, 'A Statistical Method of Identifying Dependent Events and Earthquake Aftershocks', *Seismological Research Letters*, vol. 45, no. 3, pp. 3-16.
- Shlien, S. & Nafi Toksöz, M. 1970, 'A Clustering Model for Earthquake Occurrences', *Bulletin of the Seismological Society of America*, vol. 60, no. 6, pp. 1765-1787.
- Sokolova, M. & Lapalme, G. 2009, 'A Systematic Analysis of Performance Measures for Classification Tasks', *Information Processing & Management*, vol. 45, no. 4, pp. 427-437.
- Spottiswoode, S.M. 2000, 'Aftershocks and Foreshocks of Mine Seismic Events', in *3rd International Workshop on the Application of Geophysics to Rock and Soil Engineering*, ISRM, Melbourne, Australia, p. 82.
- Sweby, G. 2002, 'Kambalda Nickel Operations Mining in High-Stress, Seismically Active Conditions', in *1st International Seminar on Deep and High Stress Mining*, Australian Centre for Geomechanics, Perth, Australia, p. Section 15.
- Thirumalai, D. & Mountain, R.D. 1993, 'Activated Dynamics, Loss of Ergodicity, and Transport in Supercooled Liquids', *Physical Review E*, vol. 47, no. 1, pp. 479-489.
- Tiampo, K.F. & Shcherbakov, R. 2012, 'Seismicity-Based Earthquake Forecasting Techniques: Ten Years of Progress', *Tectonophysics*, vol. 522–523, no. 0, pp. 89-121.
- Trifu, C.-I. & Urbancic, T.I. 1996, 'Fracture Coalescence as a Mechanism for Earthquakes: Observations Based on Mining Induced Microseismicity', *Tectonophysics*, vol. 261, no. 1, pp. 193-207.
- Urbancic, T.I. 1991, Source Studies of Mining - Induced Microseismicity at Strathcona Mine, Sudbury, Canada: A Spatial and Temporal Analysis, PhD Thesis, Queen's University.

- Urbancic, T.I. & Trifu, C.I. 1995, 'Remote Triggering of Large Seismic Events in Mines: Evidence Based on the Spatial and Temporal Migration of Microseismic Events Along Increasing Stress Gradients', *Earthquakes Induced by Underground Nuclear Explosions: Environmental and Ecological Problems. NATO ASI Series*, vol. 2, no. 4, pp. 353-374.
- Urbancic, T.I. & Trifu, C.I. 1996, 'Microseismic Identification of Stress Transfer as Related to Rockburst Occurrences', in *6th Conference on Acoustic Emission/Microseismic Activity in Geological Structures and Materials*, Trans Tech Publications, Pennsylvania State University, University Park, Pennsylvania, pp. 358-369.
- Urbancic, T.I., Trifu, C.I., Long, J.M. & Young, R.P. 1992, 'Space-Time Correlations of B Values with Stress Release', *Pure and Applied Geophysics*, vol. 139, no. 3-4, pp. 449-462.
- Utsu, T. 1957, 'Magnitude of Earthquakes and Occurrence of Their Aftershocks', *Seismological Society of Japan*, vol. 2, no. 10, pp. 35-45.
- Utsu, T. 1961, 'A Statistical Study of the Occurrence of Aftershocks', *Geophysical Magazine*, vol. 30, no. 4.
- Utsu, T. 1999, 'Representation and Analysis of the Earthquake Size Distribution: A Historical Review and Some New Approaches', *Pure and Applied Geophysics*, vol. 155, no. 2, pp. 509-535.
- Utsu, T. 2002, 'Statistical Features of Seismicity', *International Geophysics Series*, vol. 81, no. A, pp. 719-732.
- Utsu, T., Ogata, Y. & Matsu'ura, R.S. 1995, 'The Centenary of the Omori Formula for a Decay Law of Aftershock Activity', *Physics of the Earth*, vol. 43, no. 1, pp. 1-33.
- Vallejos, J.A. & McKinnon, S.D. 2008, 'Guidelines for Development of Re-Entry Protocols in Seismically Active Mines', in *42nd U.S. Symposium on Rock Mechanics*, American Rock Mechanics Association, San Francisco, pp. 8-97.
- Vallejos, J.A. & McKinnon, S.D. 2010a, 'Omori's Law Applied to Mining-Induced Seismicity and Re-Entry Protocol Development', *Pure and Applied Geophysics*, vol. 167, no. 1-2, pp. 91-106.
- Vallejos, J.A. & McKinnon, S.D. 2010b, 'Temporal Evolution of Aftershock Sequences for Re-Entry Protocol Development in Seismically Active Mines', in *5th International Seminar on Deep and High Stress Mining*, eds M. Van Sint Jan & Y. Potvin, Australian Centre for Geomechanics, Santiago, Chile, pp. 199-214.
- Vallejos, J.A. & McKinnon, S.D. 2011, 'Correlations between Mining and Seismicity for Re-Entry Protocol Development', *International Journal of Rock Mechanics and Mining Sciences*, vol. 48, no. 4, pp. 616-625.
- Varden, R. & Esterhuizen, H. 2012, 'Kanowna Belle - Evolution of Seismicity with Increasing Depth in an Ageing Mine', in *6th International Seminar on Deep and High Stress Mining*, ed. Y. Potvin, Australia Centre for Geomechanics, Perth, Australia, pp. 211-227.
- Wesseloo, J. 2013, 'Towards Real-Time Probabilistic Hazard Assessment of the Current Hazard State', in *8th International Symposium on Rockbursts and Seismicity in Mines*, eds A. Malovichko & D. Malovichko, Geophysical Survey of Russian Academy of Sciences, Petersburg-Moscow, Russia, pp. 307-312.
- Wesseloo, J. 2014, 'Evaluation of the Spatial Variation of the B-Value', *South African Institute of Mining and Metallurgy*, vol. 114, no. October, pp. 823-828.
- Wiemer, S., McNutt, S.R. & Wyss, M. 1998, 'Temporal and Three-Dimensional Spatial Analyses of the Frequency-Magnitude Distribution near Long Valley Caldera, California', *Geophysical Journal International*, vol. 134, no. 2, pp. 409-421.
- Wiemer, S. & Wyss, M. 2002, 'Mapping Spatial Variability of the Frequency-Magnitude Distribution of Earthquakes', *Advances in Geophysics*, vol. 45, pp. 259-302.

- Wyss, M. 1973, 'Towards a Physical Understanding of the Earthquake Frequency Distribution', *Geophysical Journal International*, vol. 31, no. 4, pp. 341-359.
- Wyss, M., Shimazaki, K. & Wiemer, S. 1997, 'Mapping Active Magma Chambers by B Values beneath the Off-Ito Volcano, Japan', *Geophysical Research: Solid Earth (1978–2012)*, vol. 102, no. B9, pp. 20413-20422.
- Xu, R. & Wunsch, D. 2005, 'Survey of Clustering Algorithms', *IEEE Transactions on Neural Networks*, vol. 16, no. 3, pp. 645-678.
- Xu, X., Ester, M., Kriegel, H.-P. & Sander, J. 1998, 'A Distribution-Based Clustering Algorithm for Mining in Large Spatial Databases', in *14th International Conference on Data Engineering*, IEEE, pp. 324-331.

## 10 Appendix

### Appendix A: Generation of Synthetic Seismic Responses

The synthetic generation of seismic responses allows for the testing of the ability of the modelling procedure to recover synthetic parameters under different scenarios. This procedure is used throughout Chapter 5. The Modified Omori Law (MOL) is used to replicate time-dependent event occurrence as this law is also used to model seismic responses. The methodology used to generate responses follows the method presented by Nyffenegger and Frohlich (1998). Two key differences are that the c-parameter is allowed to vary and the K-parameter is specified rather than the number of response events. These changes ensure that the parameters used to create the response are directly relatable to MOL modelling results. The procedure used to generate synthetic responses is summarised by five steps.

**Table 43** provides a simple example of two, unrealistically small responses to illustrate the outcomes of each procedural step (after step 1: specification of the required parameters). Uniformly randomly sampled numbers on the interval  $[0, 1]$  ( $u_i$ ) are generated for each of the four events within each response. These samples are used to calculate the relative times ( $t_i$ ). The final times ( $t$ ) are found by applying a 12 h offset ( $T_O$ ) for the second response.

**Table 43** The outcomes of each procedural step are tabulated for two unrealistically small responses to illustrate the outcomes of each procedural step.

Step 2	Step 3	Step 4	Step 5
$i \in [1, N]$	$u_i$	$t_i$	$t$
1	0.012	0.011	0.011
2	0.417	0.024	0.024
3	0.720	0.239	0.239
4	0.933	1.198	1.198
1	0.013	0.009	12.009
2	0.417	0.024	12.024
3	0.720	0.239	12.239
4	0.933	1.198	13.198

**Step One:** Specify parameter required.

- MOL parameters (p, K, c,)
- Relative time interval (S, T)
- Absolute time offset (T<sub>o</sub>)

**Step Two:** The MOL parameters and relative time interval specify the number of events (*N*) within the seismic response (**Equation 22**).

$$N = \begin{cases} K[\ln(T + c) - \ln(S + c)] & \text{for } p = 1 \\ K \left[ \frac{(T + c)^{(1-p)} - (S + c)^{(1-p)}}{(1-p)} \right] & \text{for } p \neq 1 \end{cases} \quad \text{Equation 22}$$

Where;

*N*: Number of response events

*S*: Start of time interval

*T*: End of time interval

*p*: Constant (decay)

*K*: Constant (productivity)

*c*: Constant (time offset)

**Step Three:** Randomly uniformly sampled (*N*) times over the interval [0,1]. The samples provide the cumulative density positions for events:  $u_i = (u_1, u_2, u_3, \dots, u_N)$ .

**Step Four:** Calculate the relative time of event occurrence ( $t_i$ ) for each cumulative density position( $u_i$ ) (**Equation 23**).

$$t_i = \begin{cases} \exp[\ln(S + c) + u_i\{\ln(T + c) - \ln(S + c)\}] & p = 1 \\ [(S + c)^{(1-p)} + u_i\{(T + c)^{(1-p)} - (S + c)^{(1-p)}\}]^{1/(1-p)} & p \neq 1 \end{cases} \quad \text{Equation 23}$$

Where;

$t_i$ : Relative occurrence time of the  $i^{th}$  event

$u_i$ : MOL cumulative density function

*S*: Start of time interval

*T*: End of time interval

*p*: Constant (decay)

*c*: Constant (time offset)

**Step Five:** The event times are adjusted based of the number of responses and specific scenario. Relative times  $t_i$  are offset by  $T_0$  to construct a continuous dataset of events (**Equation 24**).

$$t = t_i + T_0 \quad \text{Equation 24}$$

Where;

$t$ : Absolute occurrence time of the  $i^{\text{th}}$  event

$t_i$ : Relative occurrence time of the  $i^{\text{th}}$  event

$T_0$ : Absolute time offset



## Appendix B: Applying Hazard to Mining Induced Seismic Responses

The mathematical foundation for time-dependent seismic hazard follows the work presented by Gibowicz and Kijko (1994), and Utsu (2002). The truncated magnitude-frequency relationship in the form of a cumulative density function is expressed as **Equation 25**:

$$F(m) = \begin{cases} 0 & \text{for } m < M_C \\ \frac{1 - e^{-\beta(m-M_C)}}{1 - e^{-\beta(M_{Max}-M_C)}} & \text{for } M_C \leq m \leq M_{Max} \\ 1 & \text{for } m > M_{Max} \end{cases} \quad \text{Equation 25}$$

Where;

$\beta$ : Power law exponent

$M_C$ : Magnitude of completeness

$M_{Max}$ : Magnitude of relationship truncation

$m$ : Event magnitude

The probability distribution of the largest event for a given number of events is an extreme value distribution. The cumulative probability function of the largest event in a set of  $n$  events is specified by **Equation 26**:

$$F_{max}(m) = P(M_1 \leq m, M_2 \leq m, \dots, M_n \leq m) = [F(m)]^n \quad \text{Equation 26}$$

Where;

$F_{max}(m)$ : Cumulative probability function of event size

$m$ : Magnitude

$M_i$ : Magnitude of event  $i$

$n$ : Number of events

For forecasting future hazard, the uncertainty in the number of events in the future time interval ( $\Delta t$ ), needs to be taken into account (**Equation 27**):

$$F_{max}(m|\Delta t) = \sum_{n=0}^{\infty} P(n|\Delta t)[F(m)]^n \quad \text{Equation 27}$$

Where;

$[F(m)]^n$ : Cumulative probability function for event magnitude

$P(n|\Delta t)$ : Probability of observing  $n$  events given a time interval

$\Delta t$ : Time interval

$n$ : Number of seismic events

Defining the probability distribution  $P(n|\Delta t)$  falls outside of the scope of this thesis that focuses on the identification and delineation of seismic responses. The definition of the cumulative magnitude density function is limited to **Equation 26**.

Given the cumulative magnitude density function  $F_{\max}(m)$ , the probability of at least one event out of a total of  $n$  events having a magnitude ( $m$ ), exceeding ( $M$ ), is given by **Equation 28**. Note that the sample number of events is calculated from the event rate for an interval adjusted by a hazard period.

$$P(m > M|n) = 1 - [F(m)]^n \quad \text{Equation 28}$$

Where;

$$n = \frac{\Delta n}{\Delta t} T$$

$\Delta t$ : Time interval

$\Delta n$ : Number of events during interval

$T$ : Hazard time period

$m_o$ : Maximum magnitude observed

$M$ : Magnitude of significant hazard

## Appendix C: Complete List of Conclusions

### Chapter 2: Literature Review

The following conclusions are drawn from the review of the spatial and temporal characteristics of mining induced seismicity, the analysis of spatial and temporal clustering seismicity, and applicable scaling laws (Chapter 2). The reviewed literature provides a foundation for understanding the spatial and temporal characteristics of seismicity that is essential for the effective management of mining induced seismic hazard.

#### Spatial Characteristics of Mining Induced Seismicity

- Seismicity results from various rock mass failure mechanisms for mining environments.
- Rock mass failure mechanisms are broadly considered as seismic source mechanisms characterised by conditions resulting in seismicity.
- While classification schemes for seismic source mechanisms vary based on the scope and context of the studies, general source mechanism classifications are analogous throughout literature, e.g., volumetric and shear failure.
- Sources of seismicity are spatially controlled by factors including, but, not limited to:
  - Excavation geometry (development, stoping, pillars, abutments etc.);
  - Geological features (faulting, dykes, etc.); and
  - Rock mass properties (rock strength, frequency of discontinuities, etc.).
- Sources of seismicity are temporally influenced by factors that evolve over time.
- The potential for large seismic events is controlled by failure mechanisms and, therefore, delineating sources of seismicity is an important component to understanding seismic hazard.
- Considering sources of seismicity has practical benefits by simplifying seismic analysis.
- Magnitude-frequency relationships are widely applicable to the mining environment and are consistent for sources of seismicity.
- Magnitude-frequency relationships quantify the limits of seismic monitoring (magnitude of completeness  $M_c$ ) and the distribution of event magnitudes (b-value).
- b-values have been used to characterise spatially and temporally constrained sources of seismicity.

- Consistent magnitude-frequency relationships support the spatial and temporal characteristics for self-similar sources of seismicity.

### **Temporal Characteristics of Mining Induced Seismicity**

- There is significant uncertainty surrounding the factors that contribute to the temporal attributes of mining induced seismicity.
- Temporal characteristics of seismicity are analogous to the temporal characteristics of earthquakes and are considered with respect to two broad categories:
  - Time-independent seismicity (background) that typically follows a stationary Poisson process; and
  - Time-dependent seismicity (seismic responses) that typically follows a non-stationary Poisson process.
- No definitive theoretical foundation exists for the occurrence of background seismicity or seismic responses.
- Time-independent seismicity is considered as temporally independent and weakly spatially clustered. This seismicity is temporally represented by a single rate parameter that is synonymous with a stationary Poisson model.
- Accurate quantification of time-independent seismicity is important as these events are a major consideration for the management of seismic hazard with respect to:
  - Short-term re-entry decisions: When has a seismic response decayed to pre-existing conditions?
  - Long-term decisions: What portion of seismic hazard can only be managed using long-term strategies?
- Background seismicity is dependent on source mechanisms.
- Background seismicity is assessed by two general approaches:
  - The quantification of seismicity not associated with seismic responses. This method will typically result in an overestimation of background seismicity due to the inability of current methods to delineate seismic responses spatially and temporally.
  - The quantification of seismicity associated with periods of mining cessation. This method will typically result in an underestimation of background seismicity as routine mining activities no longer influence stress conditions.

- The study and outcome of seismic responses in the mining environment is similar to earthquake mainshock-aftershock responses.
- Seismic responses contribute to the timing, location, and magnitude of seismic hazard and, therefore, are an important consideration in the management of seismic risk.
- There is significant variation in the characteristics of seismic responses following blasting or large seismic events.
- The spatial and temporal characteristics of seismic responses are related to sources of seismicity, although, are only tentatively related to factors that contribute to rock mass failure.
- Isolated case studies show that time-dependent responses are intrinsically related to stress transfer mechanisms and can be generalised by two types of seismic responses:
  - Induced seismicity: The observed seismic response is greater than, or proportional to, a causative stress change.
  - Triggered seismicity: The causative stress changes are significantly less than the observed seismic response.

### **Analysis of Spatially and Temporally Clustered Seismicity**

- It is impossible to identify and delineate events that are associated with background or response seismicity without error.
- Routine activities in the mining environment may result in the spatial or temporal superimposition of seismic responses.
- There are limited studies that attempt to quantify temporal characteristics of spatially constrained responses and assess spatial and temporal relationships between responses and routine mining activities.
- The study of time-dependent seismicity comprises of three main components and aims to address three broad research questions:
  1. Response identification: Where and when do responses occur?
  2. Spatial delineation: Where do responses occur?
  3. Temporal delineation: When do responses start and when do they finish?
- The outcomes of reviewed studies dictate if identification or delineation of responses is considered by assessing various combinations of the spatial, temporal, or magnitude attributes of time-dependent seismicity.

- The study of time-dependent earthquake occurrence explores a wider range of approaches. The majority of these methods employ assumptions that are not suitable for mining induced seismicity due to:
  - The reliance on magnitude of events for response identification;
  - Inability to account for superimposition of responses in space or time; or
  - The use of constants that inhibit the assessment of contrasting spatial and temporal densities associated with varied sources of mining induced seismicity.
- Quantification of mining induced seismic responses is limited, with the majority of studies focused on determining appropriate re-entry protocol criteria.
- For mining induced seismicity, temporal and spatial delineation are generally limited by arbitrarily defined space-time windows around blasting or large events. Methods have addressed aspects of response identification, temporal delineation, or spatial delineation.
- The temporal characteristics of mining induced seismicity are generally studied independently of spatial aspects and vice versa.
- Studies of mining induced seismicity do not provide a comprehensive method for the spatial and temporal, identification and delineation of mining induced seismic responses.

### **Modified Omori Law**

- The Modified Omori Law (MOL) has been extensively applied to the study of earthquakes. Well-established methods exist to estimate the law's parameters and parameter uncertainty, and quantify the suitability of fit between the model and observations.
- A wide range of mining induced seismic responses has been modelled by the MOL.
- Other temporal models have been applied to mining induced seismicity and earthquake aftershocks. In comparison to the MOL, none of these models has been shown to be consistently and significantly more representative of time-dependent behaviour.
- There is not a complete understanding of the relationship between MOL parameters and a physical processes for mining induced seismicity:

*Appendix C: Complete List of Conclusions*

- Decay rate (p-parameter): No clear relationships, although tentatively related to rate of rock mass relaxation.
- Productivity (K-parameter): Parameter has been related to mainshock magnitude, volume of blasted rock, and depth of mining.
- Time-offset (c-parameter): It is well accepted that the parameter is related to limitations of seismic monitoring and potentially related to the breakdown in power-law behaviour soon after response initiation.
- There is a range of approaches implemented for selecting a modelling time interval for mining induced seismicity and earthquakes.
- No single methodology is consistently applied to model spatially and temporally delineated seismic responses using the MOL.

## **Chapter 3: Iterative Approach to the Identification of Mining Induced Seismic Responses**

Chapter 3 presented an iterative method to identify seismic responses specifically addressing the challenges associated with mining induced seismicity and the shortcomings of existing methods. The following conclusions are drawn from the work presented in Chapter 3.

### **Iterative Methodology**

- The initiation of a seismic response is identified if the number of subsequent and neighbouring events within the spatial and temporal window, for a seismic event, is above a threshold. This method is effective in determining the initiation time and approximate centre of a seismic response.
- An iterative method that considers characteristic identification parameters is able to identify the time and location of responses of individual scales within the mining environment.
- To identify spatially or temporally superimposed responses of varying scales, smaller scales must be identified and delineated prior to large scales.
- An iterative method using this structured approach is able to evaluate when and where spatially or temporally superimposed seismic responses of various temporal and spatial scales occur.
- The scale specific seismic responses can be represented by response scale sets that comprise of a spatial window, temporal window, count threshold, and temporal modelling window.
- The estimation of response scale sets is validated by visual inspection to identify obvious errors and quantitative measures. The manual estimation of each one of these parameters is sufficient to identify responses reliably and consistently.

### **Iterative Parameters**

- The following conclusions are made specifically for the spatial window:
  - The physical scale is the most distinct feature of responses;
  - The definition of the spatial window has the greatest impact on analysis;
  - The spatial window is the focus of qualitative and quantitative validation of response scale sets; and

- Subsequent spatial modelling reduces the sensitivity of analysis to selecting an appropriate spatial window.
- The following conclusions are made specifically for the temporal window:
  - The temporal window represents the time scale of response initiation and occurs on a consistent order of magnitude (minutes);
  - Temporal modelling reduces the sensitivity of outcomes to the definition of a temporal window by allowing for the adjustment of the response initiation; and
  - Selecting an appropriate temporal window to represent an optimal time scale is not a major consideration due to the insensitivity of outcomes and consistency of scale.
- The following conclusions are made specifically for the count threshold:
  - A threshold for the lowest spatial and temporal event density is required to define the initiation of a response;
  - Threshold values represent a trade-off between identifying small responses and falsely identifying stochastic event occurrence;
  - Large responses are identified for any reasonable threshold;
  - The identification of small stochastic responses has the smallest impact on outcomes; and
  - The definition of a count threshold is not a significant consideration for analysis due to outcomes being insensitive to parameter selection.
- The following conclusions are made specifically for the temporal modelling window:
  - A temporal window is used to delineate potentially related events following the identification of a seismic response. This approach is sufficient to delineate a subset of potentially related events to be refined by spatial and temporal modelling;
  - The duration of the seismic response is unknown as there is no clear cessation of event occurrence;
  - Response duration may be approximated by a fixed period between known changes to stress conditions, i.e., time between blasting. This is the optimal approach when:

*Appendix C: Complete List of Conclusions*

- Computational constraints must be managed; or
  - There is a significant influence from temporally independent processes.
- The best general estimation of response duration can be achieved by a significant overestimation that is refined by temporal modelling; and
  - Outcomes are insensitive to the selection of the modelling time window due to the spatial and temporal distinction that typically exists between individual seismic responses.

## **Chapter 4: Spatial Delineation of Mining Induced Seismic Responses**

Chapter 4 documents the development and validation of a generalised method for the spatial delineation of mining induced seismic responses. This method fulfils requirements of the iterative evaluation framework and creates a subset of spatially clustered seismicity to be refined by temporal modelling.

- Spatial characteristics of mining induced seismicity are controlled by sources of seismicity caused by rock mass failure.
- Inherent spatial characteristics guide the attributes of an ideal clustering methodology.
- This method should be able to objectively cluster events and must be flexible with respect to geometries and densities in three-dimensional space.

### **Delineation Methodology**

- Density-based clustering is a non-parametric method (DBSCAN) with advantages including:
  - Class identification, i.e., each event belongs to a unique cluster;
  - Minimal requirements for existing database knowledge;
  - The ability to discover arbitrary shapes;
  - Resistant to noise; and
  - The ability to discover high-density clusters within low-density clusters.
- Density-based methods have a number of shortcomings:
  - Difficulty in finding suitable clustering parameters;
  - Poor performance for datasets with varying element densities; and
  - Sensitive to the selection clustering parameters.
- Specialised approaches address the problem-specific limitations of density-based clustering. In the context of iterative response assessment, density-based clustering limitations are addressed by considering:
  - Only one spatial cluster of consistent density per iteration;
  - Initial identification that approximates the centre of the seismic response and allowing for the estimation of spatial event density;

- Refinement of the density estimation during the clustering procedure; and
- The implementation of a density tolerance.
- A four-step spatial clustering procedure classifies elements by considering the number of neighbouring elements within a search distance, with respect to an initially estimated number of events and a given count tolerance. This procedure is able to delineate a single spatial cluster associated with the initial response identified.

### **Spatial Delineation Validation**

- Synthetic data validates the clustering approach and assesses the influence on classification errors by considering numerous scenarios.
- A range of results are developed by creating a synthetic dataset with small incremental changes for numerous scenarios and clustering using a procedure with constant parameters, or a constant individual scenario that is repeatedly clustered for a range of parameters.
- Clustering results are summarised by truth class label, e.g., correctly clustered events are true positives. External cluster validation can evaluate the performance of the clustering method by using a synthetic dataset.
- Truth class labels are summarised by the Matthews Correlation Coefficient (MCC) for a simplified interpretation of classifications. The MCC is able to represent errors associated with a range of relative separation and scale response characteristics.
- External validation benchmarks internal validation that quantifies errors without prior knowledge of the dataset.
- Internal clustering validation can evaluate the performance of the clustering method by considering the similarity of density and the separation of clusters.
- Two internal clustering validation measures are considered and compared. The SDbw index and CVNN index share the same conceptual basis and measure intra-cluster variance in densities and inter-cluster separation.
- The CVNN and SDbw indices indicate that parameter ranges that result in a single cluster are optimal when cluster scales and separations are relatively similar.

- If a sufficient difference exists in response scale or separation, the CVNN index is preferable to the SDbw index when identifying appropriate search distances and spatial density tolerances.
- The internal validation (CVNN) agrees with external validation (MCC) on optimal solutions and reproduces the optimal clustering parameters for medium to high cluster separation.
- It is concluded from the analysis of real seismic responses containing a range of shapes, densities, and configurations that the CVNN index:
  - Provides insight into the relationship between parameter selection and spatial characteristics of clusters;
  - Provides guidance for the selection of optimal parameters for the range of response scales considered by clustering;
  - Shows the clustering procedure is insensitive to parameter selection; and
  - Can be minimised to find optimal search distances and tolerances.
- Despite optimisation of the CVNN index, a component of subjectivity remains due to inherently ambiguous clustering decisions.

## Chapter 5: Temporal Delineation of Mining Induced Seismic Responses

Chapter 5 documents the development and validation of a methodology that is able to temporally delineate and quantify mining induced seismic responses from a subset of spatially clustered seismicity. This methodology assumes temporal event occurrence follows a power law decay and fulfils the requirements for an iterative approach.

- Temporal modelling is required to:
  - Consistently delineate partially temporally superimposed responses;
  - Optimise delineation and quantification objectives; and
  - Integrate within the context of iterative assessment.
- MOL implementation is required to address:
  - The selection of a modelling interval based only on temporal attributes;
  - Minimise the interdependency between the p-parameter and c-parameter; and
  - Quantify the quality of modelling results.

### Implementation of the MOL

- Possible modes for implementing the MOL are based on if the c-parameter is fixed to zero or variable, and the definition of relative event times:
  - The Principal Event Fixed (PEF) approach does not allow relative times to be redefined if the interval start is redefined; and
  - The Principal Event Adjusted (PEA) approach allows relative times to be redefined.
- Synthetic generated responses represent commonly observed challenging scenarios. These cases are investigated for different implementation modes:
  - Simple responses;
  - Simple responses with early variation;
  - Late superimposed responses with early variation; and
  - Early superimposed responses with early variation.
- For a simple response:

- *Mode 4* (PEF  $c=0$ ) provides the most accurate parameter recovery, although, it requires the exclusion of early events.
- *Mode 1* (PEA  $c \geq 0$ ) and *Mode 2* (PEF  $c \geq 0$ ) consistently recover parameters and while K-parameters are accurately recovered, p-parameters are slightly overestimated.
- For simple responses with early variation, late superimposed responses, and early superimposed responses, *Mode 1* (PEA  $c \geq 0$ ) provides the most representative solution space of p-parameters and K-parameters and is the optimal approach. While a variable c-parameter is interdependent with the p-parameter, it must be used to achieve consistent quantification and delineation.
- *Mode 2* (PEF  $c \geq 0$ ), *Mode 3* (PEA  $c=0$ ), and *Mode 4* (PEF  $c=0$ ) were associated with erroneous parameter recovery. This was due to:
  - A fixed c-parameter equal to zero that required the exclusion of early events to recover parameters consistently; and
  - The PEF approach that was not able to delineate a response that did not correspond to the start of the interval.

### **Delineation Methodology**

- Maximum Likelihood Estimate (MLE) is the historical basis for statistical modelling selection, although, can lead to erroneous selection of modelling intervals. Additional considerations are required to optimally quantify and delineate seismic responses using the MOL.
- Quantification and delineation objectives are optimised by minimising the c-parameter, parametric standard error, and Anderson-Darling statistic, along with maximising the MLE and number of events.
- Relative measures can be modified by a piecewise linear weighting function to include additional information such as:
  - The acceptable range of parameter values;
  - An increased emphasis for ideal solutions;
  - A lessened emphasis for poor solutions; and
  - Appropriate scaling within a range of marginal parameter values.

- A multiplicative function is able to combine weighted factors, the MLE, and number of events into a metric. The metric captures desirable parametric attributes and is simple in construction, application, and interpretation.
- Four synthetically generated configurations of time-dependent seismicity represent commonly observed challenging scenarios. The weighted metric is used to optimise temporal interval selection and compared to the optimal MLE solution for:
  - Simple responses;
  - Simple responses with early variation;
  - Late superimposed responses with early variation; and
  - Early superimposed responses with early variation.
- For all response scenarios, the optimal weighted MLE metric solution excludes early variation, accurately quantifies, and accurately delineates the largest individual response.
- For a simple response, the optimal weighted MLE metric solution is not significantly different to the MLE solution and both solutions quantify and delineate the response accurately.
- For simple responses with early variation, late superimposed responses, and early superimposed responses, the MLE solution cannot accurately quantify and delineate responses. The MLE solution favours the inclusion of additional events and results in an unsuitable modelling fit with a significant negative impact on quantification accuracy.
- $SE_w$ ,  $c_w$ ,  $AD_w$ , MLE, and  $N_{Events}$  are essential for selecting a modelling interval that meets quantification and delineation objectives:
  - The MLE and  $N_{Events}$  contribute to delineation objectives of modelling;
  - While the  $SE_w$  does not significantly assist in the exclusion of erroneous events, it contributes to quality objectives and does not negatively weigh desirable solutions;
  - The  $c_w$  excludes early variation and minimises the interdependence between the p-parameter and the c-parameter; and
  - $AD_w$  provides a clear indication of appropriate intervals that are suitably modelled by the MOL, specifically, excluding early variation and additional responses.

- The method of temporal modelling meets iterative assessment requirements by:
  - Refining the time interval for temporally misidentified responses;
  - Refining an overestimated modelling window to model an individual response; and
  - Quantifying and delineating the remainder of late and early superimposed responses in subsequent iterations.

### **Temporal Delineation Errors**

- Mining induced seismic responses are typically well modelled by the MOL by similar ranges of parameters and, therefore, there is relatively high confidence in inherent structural and parametric uncertainties associated with the applicability of this law.
- Synthetic seismic responses are generated to evaluate a dataset with known temporal attributes. The errors associated with synthetic data generation can be quantified by considering sampling methods that introduce different degrees of randomness.
- The assessment of errors associated with synthetic data generation allow the following conclusions to be drawn:
  - Small errors are associated with fitting the MOL to non-sampled data and are due to interval selection and the modelling resolution;
  - While uniform random sampling represents the stochastic nature of seismicity, this method of synthetic data generation significantly influences modelling results and prevents the reliable assessment of modelling errors; and
  - 20% quota sampling reduces random errors and represents a reasonable trade-off between replicating inherent uncertainty and enabling the consistent assessment of modelling errors.
- 20% quota sampling is used to generate synthetic scenarios that embody characteristics of mining responses. Scenarios consider responses with early variation, short responses, and responses with independent events for a range of productivity and decay rates.
- Error analysis focuses on the accuracy and precision of parameter recovery of the modelling procedure that uses the weighted MLE metric.
- Conclusions drawn from the iterative assessment of responses with early variation:

- For a temporal modelling window that is overestimated, the weighted MLE metric can delineate the interval for each response within a continuous dataset;
- Quantification of responses is generally accurate. There is a small increase to standard deviation of error and the p-parameters are slightly underestimated;
- The delineation of responses is generally accurate ( $\approx 95\%$  of responses is within  $\pm 5\%$  error in recovered events); and
- For a small population of responses with low p-parameters and low K-parameters, there is insufficient contrast to distinguish between the linear variation and response events. Errors have a small impact as they:
  - Are a small portion of responses;
  - Contain relatively few events; and
  - Are distinguishable by high uncertainty in parameters.
- Conclusions drawn from the iterative assessment of short responses:
  - The delineation of responses is accurate and the quantification of responses is generally accurate. Short responses are associated with:
    - An increase in the standard deviation of modelling errors;
    - An overestimation of the p-parameter; and
    - An underestimation of the K-parameter.
  - Errors rapidly decrease for increasing response durations; and
  - The recovery of the K-parameter is more sensitive in comparison to p-parameters.
- Conclusions drawn from the iterative assessment of responses with independent events:
  - Errors increase for higher rates of time-independent seismicity;
  - The inclusion of time-independent seismicity causes the p-parameter to be consistently underestimated and the K-parameter to be consistently overestimated;
  - If there is sufficient contrast between time-dependent and independent processes, then modelling can delineate when the time-dependent process ceases to dominate event generation; and

*Appendix C: Complete List of Conclusions*

- Response separation occurs when the synthetic p-parameter is high and results in shorter response durations and more accurate parameter recovery.

## Chapter 6: Assessment of Mining Induced Seismic Responses

This chapter focused on the relationship between seismic responses and routine blasting for a range of mining environments. This chapter examined the ability for the STIDSR method (spatially and temporally, identified and delineated, seismic responses) to provide insight into optimal seismic hazard management and fundamental rock mechanics associated with mining induced seismicity.

- The management of time-dependent seismic hazard relies significantly on subjective site-specific experience of personnel and has inherent limitations associated with interpretation, and motivational bias.
- Identification and delineation of seismic responses allows for the development of an objective understanding of time-dependent seismic hazard that removes subjectivity and increases the transparency of engineering decisions.
- The STIDSR method can be applied to a range of bulk and selective mining methods.
- The STIDSR method can examine seismicity recorded by monitoring systems that are average to excellent in quality.
- The method is not sensitive to erroneous events that do not typically spatially cluster. Furthermore, clustered seismic noise has a negligible impact on analysis as it is spatially confined to known locations, e.g., crusher noise, ore passes, etc.
- Quality of responses can be ensured by post analysis filtering of responses that are:
  - Unreasonably short;
  - Modelled by erroneous parameters; or
  - Unsuitably represented by the MOL.
- Post analysis filtering is only required to remove a small number of responses ( $\approx 10\%$ ) and, therefore, seismic responses are suitably modelled by the MOL.

### General Application

The methods presented in this thesis reduce the subjectivity associated with previous methods. Some subjectivity remains in parameter selection for temporal and count thresholds. User defined spatial parameters are the most subjective and are the main consideration for the practical application of the STIDSR method. The following conclusions results from the practical application of the STIDSR method in Chapter 6:

- Spatial parameters require user interpretation to define a reasonable spatial scale;

- Subjectivity is reduced by optimising the CVNN index for a reasonable parameters;
- While responses with ambiguous spatial distributions are more sensitive to user decisions, this ambiguity also reduces the ability of users to preconceive clusters;
- Optimising the CVNN index is particularly important for ambiguous spatial distributions; and
- While not optimal, it appears to be sufficient for practical purposes to calibrate the method of large datasets using short intervals of typical seismic responses.

The following conclusions are drawn from applying the method to seismicity associated with immediate and localised redistribution of stress caused by routine blasting in an open stoping mine. The STIDSR method is able to:

- Quantify responses by p-parameters and K-parameters within reported ranges, and c-parameters equalling zero (except one response);
- Quantify seismic hazard associated with routine operations;
- Develop an objective seismic response history to blasting and delineate time-independent seismicity; and
- Establish a context to identify alternative rock mass failure processes as mining progresses.

The following conclusions are drawn from applying the method to seismicity before and after the occurrence of a relatively large seismic event. The STIDSR method is able to:

- Identify, delineate, and quantify an initial response prior to the event, two dense responses immediately after and close to the large event, and one sparse regional response;
- Provide insight into the fundamental rock mechanics associated with the time-dependent deformation of a fault and the regional redistribution of stress; and
- Provide insight into seismic hazard associated with a faulting causation process that is elevated prior to and following the large event, along with a more ambiguous mine wide elevated seismic hazard.

The following conclusions are drawn from applying the method to number of spatial clusters in an open stoping mine that were simultaneously caused by two blasts and a delayed large seismic event. The STIDSR method is able to:

- Temporally and spatially model all responses suitably;

- Contrast processes related to blasting with similar parameters, and a sparser response that is less productive and slower to decay;
- Provide insight into the rock mass failure processes related directly and indirectly to causation processes (large event and blasting); and
- Quantify seismic responses associated with different rock mass failure processes that can be related to seismic hazard.

### Seismic Responses and Blasting

The STIDSR method identifies seismic responses by only spatial and temporal seismic parameters and, therefore, allows for the classification of the relationship between individual responses and blasting. The following conclusions are drawn for the analysis of response-blast classifications:

- Comprehensive retrospective analysis is enabled by the method and is applicable to large datasets and a range of different spatial and temporal characteristics.
- The classification scheme enables the consistent assessment of the spatial and temporal relationship between seismic responses and blasting by defining four classes:
  - Responses *local and immediate* to blasting;
  - Responses *local and delayed* to blasting;
  - Responses *remote and immediate* to blasting; and
  - Responses *remote and delayed* to blasting.
- Considerations for setting the thresholds used to define classification are:
  - Spatial influence of blasting;
  - Spatial scale of responses;
  - The timing and location accuracy of blast records; and
  - The performance of the seismic array.
- The STIDSR method, in conjunction with the response-blast classification scheme, enables objective analysis and allows for the development of confidence in unexpected results.
- Remote responses are a contentious issue due to uncertainty surrounding the mechanism of stress transfer that creates rock mass instability and has significant implications for the management of seismic hazard.

- The STIDSR method and response-blast classification scheme identify an unambiguous example showing mining induced seismicity remotely triggered by blasting.
- Delayed responses caused by renewed rates of seismicity are contentious and have significant implications for the management of seismic hazard.
- Delayed responses are evaluated objectively by incorporating modelling suitability (Anderson-Darling statistic) to decide if the variability is too great to be associated with an initial response.
- The practical management of seismic hazard associated with *remote and delayed* responses requires an increased emphasis on seismic hazard management of time-independent processes and consideration to employing re-entry protocols outside of blasting times.
- Proportionality of response-blast classifications provides insight into the mining environment. A greater proportion of responses that are remote and/or delayed to blasting are observed for relatively more complex conditions contributing to seismicity.
- Proportionality of *local and immediate* and *remote and delayed* classifications is influenced by the evolution of the mining environment over time and infers how the rock mass is responding to the progression of mining.
- The proportionality of seismicity associated with blasting has implications for the effectiveness of current and future seismic hazard management strategies.

### Evolution of Seismic Responses

The following conclusions are drawn from analysis of seismicity in a block caving mine. The progressive nature of undercut blasting results in a systematic increase in stress conditions and a distinct evolution in rock mass failure mechanisms that results in a structured seismic dataset.

- Seismic responses to blasting are *local and immediate* during the early undercutting and indicate that the caving process has not been initiated.
- As undercut blasting continues, seismic responses are increasingly associated with the cave back as various combinations of spatially separate but temporally superimposed responses.

- The cave back dictates the spatial location and orientation of responses and shows that if rock mass is sufficiently close to failure, time-dependent seismicity can be caused by blasting despite being a significant distance away.
- For undercut blasting *local and immediate* responses are:
  - Relatively less productive and quicker to decay; and
  - More productive and slower to decay as blasting progresses;
- For undercut blasting *remote and delayed* responses are:
  - More productive and slower to decay;
  - Likely to contain time-independent seismicity and as a result the p-parameter will be underestimated and the K-parameter overestimated; and
  - An indication of the transition in dominant source mechanism, as this type of response has a significantly different MOL parameter in comparison to *local and immediate* responses.
- Application of the STIDSR method and response-blast classifications provides insight into caving process by showing that blasting has a greater influence on seismicity as undercutting increases stress conditions.
- Caving initiation is inferred from a significant increase in productivity and slower decaying responses that are not associated with blasting.

### Seismic Response Hazard

The following conclusions are drawn from the application of the STIDSR method to assess seismic response hazard. This section considered the determination of seismic response hazard, the retrospective parameterisation of responses, and current response hazard.

- Seismic hazard associated with a seismic response can be represented by the probability that an event will exceed certain magnitude within a specific spatial and temporal interval given the assumptions:
  - Temporal event occurrence can be suitably modelled by the MOL;
  - Spatial occurrence is confined to the volume of the response; and
  - Magnitude distribution follows a consistent magnitude-frequency relationship.
- The STIDSR method allows the spatial delineation of individual seismic responses and, therefore, allows for a spatially constrained hazard.

- Seismic hazard can be expressed by the instantaneous approximation of the likelihood that a spatially constrained response will generate an event exceeding a certain magnitude for a given time interval assuming a historical magnitude-frequency relationship.
- The STIDSR method allows seismic responses to be retrospectively parameterised and a historical reference to be established for geotechnical domains. This assessment characterises parameters:
  - Modelling intervals (response durations);
  - K-parameters (productivity);
  - p-parameters (decay rate);
  - c-parameters (time offset); and
  - b-values (magnitude-frequency relationship).
- To assess seismic hazard for different mining conditions, geotechnical domains need to be considered due to variable:
  - Stress conditions;
  - Rock mass strength;
  - Mining characteristics; and
  - Dominate sources of seismicity.
- For individual geotechnical domains, there is a statistically significant difference between the majority of K-parameter distributions and all p-parameter distributions, although, the distributions are generally similar for all domains.
- Quantifying the characteristics of seismic responses has important implications for the management of seismic hazard and includes:
  - Providing guidance for future responses in these domains;
  - Objective management of low and high seismic hazard environments with respect to the portion of time-dependent and independent seismicity;
  - Increasing the transparency of engineering decisions; and
  - Limiting the influence of subjective human judgement in hazard assessment.
- The STIDSR method allows individual seismic response hazard to consider:
  - A seismic hazard estimation of the seismic response modelling interval;

- A seismic hazard estimation of a partially modelled response, replicating operational re-entry decisions when a response has partially occurred; and
  - The ability to compare historical responses to individual responses, which is important to provide an indication if an observed response is abnormal.
- The STIDSR method assessing seismic response hazard results in the following conclusions:
  - Partially modelled intervals are representative for entire response models;
  - Small discrepancies between partial and entire MOL models and the disparity between seismic hazard models are inversely proportion to the b-values;
  - Seismic hazard is related to event rates (MOL model) and b-values;
  - Hazard models rapidly reduce for responses with high b-values and p-parameters following initiation and are slow to diminish for low b-values and p-parameters;
  - Longer modelling intervals are required to establish confidence in hazard results when considering seismicity with low b-values; and
  - The b-value can be refined for large responses and has the potential to significantly changes seismic hazard.
- The contribution of the preceding time-dependent failure processes is ambiguous given that blasting alters rock mass failure sufficiently to create a new dominant failure process. As a result, the STIDSR method captures the cumulative effects of time-dependent failure processes.
- Future holistic assessment must consider composite seismic hazard models as multiple individual seismic responses that may contribute to the total hazard for any specific excavation.